Université de Montréal

Fonctions antitumorales de la voie ERK/MAPK et développement rationnel de nouvelles stratégies thérapeutiques

par
Xavier Deschênes-Simard

Département de biochimie et médecine moléculaire
Faculté de médecine

Thèse présentée à la Faculté de médecine
en vue de l'obtention du grade de Philosophiae Doctor (Ph.D.)
en biochimie

Juin, 2014

Université de Montréal
Faculté des études supérieures et postdoctorales

Cette thèse intitulée :

Fonctions antitumorales de la voie ERK/MAPK et développement rationnel de nouvelles stratégies thérapeutiques

Présentée par :

Xavier Deschênes-Simard

a été évaluée par un jury composé des personnes suivantes :

Sylvie Mader, présidente-rapporteur
Gerardo Ferbeyre, directeur de recherche
Marc Therrien, membre du jury
Maxime Bouchard, examinateur externe
Guillaume Lettre, représentant du doyen de la FES

Résumé

Les kinases régulées par les signaux extracellulaires (ERK1/2) régulent une multitude de processus cellulaires, incluant la prolifération, la survie et la différenciation. Ces kinases représentent l'élément terminal de la voie ERK/MAPK, laquelle est activée dans près de 30% de tous les cancers humains et donc généralement perçue comme étant un effecteur critique de la progression tumorale. Cependant, une accumulation d'observations suggèrent que les kinases ERK pourraient également induire la suppression tumorale.

Le but premier de cette thèse est de démontrer comment la signalisation par ERK peut contribuer à la suppression tumorale et de concilier les mécanismes impliqués avec son rôle dans la progression du cancer. Puisque nos travaux ont une incidence sur les bénéfices attendus de certaines thérapies actuellement en développement, le deuxième objectif de la thèse est de proposer de nouvelles stratégies thérapeutiques pour combattre le cancer.

Nous avons démontré qu'une hyperactivation des kinases ERK induit la sénescence cellulaire. Le mécanisme implique la dégradation sélective et dépendante du protéasome de nombreuses protéines, ce que nous avons nommé le SAPD (*Senescence-Associated Protein Degradation*). Ce processus cible des protéines requises pour différentes fonctions cellulaires, incluant la progression du cycle cellulaire, les fonctions mitochondriales et la biogenèse des ribosomes. Ensuite, nos résultats montrent qu'en plus d'inhiber l'établissement de la sénescence, une diminution de la signalisation par les kinases ERK favorise la reprogrammation cellulaire, laquelle permet aux cellules précancéreuses de développer leur tumorigénicité et aux cellules cancéreuses d'acquérir des propriétés attribuables aux cellules souches. Ces observations suggèrent que les mécanismes qui inhibent la voie ERK/MAPK pourraient favoriser l'initiation du cancer, la formation de métastases et la résistance à diverses thérapies. Enfin, nous avons démontré que la metformine, utilisée pour le traitement du diabète, inhibe le facteur de transcription NF-κB. Ce dernier joue un rôle central dans la reprogrammation cellulaire et dans la production de cytokines pro-inflammatoires nocives par les cellules sénescentes. Ainsi, nous émettons l'hypothèse que la metformine pourrait être

utilisée en combinaison avec certaines thérapies afin d'éviter les effets secondaires tant d'une inhibition des kinases ERK que d'une hyperactivation.

Globalement, les résultats présentés démontrent que l'effet de la voie ERK/MAPK dépend de la force de son activation. Alors qu'une activation modérée peut contribuer à la prolifération de la plupart des cellules, une forte activation induit la sénescence tandis qu'au contraire, une faible activation favorise la reprogrammation des cellules cancéreuses et donc une augmentation de l'agressivité de la tumeur. Cette polyvalence de la voie suggère une certaine prudence face à l'usage des inhibiteurs de la voie ERK/MAPK. Cependant, elle nous motive à travailler au développement de nouvelles stratégies thérapeutiques, lesquelles pourraient inclure la metformine.

Mots-clés : Cancer, ERK, suppression tumorale, senescence cellulaire, dégradation protéique, SAPD, SASP, reprogrammation cellulaire, NF-κB, metformine

Abstract

The Extracellular Signal-Regulated Kinases (ERK1/2) regulate multiple cellular processes such as proliferation, survival and differentiation. These kinases are the last component of the ERK/MAPK pathway, which is activated in about 30% of all human cancers. Therefore, current thinking proposes that the ERK/MAPK pathway is a critical mediator of tumor progression. However, a steadily growing number of observations suggest that ERK kinases could trigger tumor suppression as well.

The first aim of this thesis is to determine how ERK signaling triggers tumor suppression and to try to reconcile these mechanisms with its putative contribution to tumor progression. Since our work has a profound impact on the value of some therapies currently in development, the second aim of the thesis is to propose new strategies to fight cancer.

We found that hyperactivation of the ERK kinases induces cellular senescence. Mechanistically, this involves selective proteasome-dependent protein degradation. This "Senescence-Associated Protein Degradation" (SAPD) targets proteins required for several cellular functions, including cell cycle progression, mitochondrial functions and ribosome biogenesis. Furthermore, our results showed that downregulation of ERK signaling not only inhibits the establishment of senescence but promotes cellular reprogramming, thereby allowing precancerous cells to gain tumorigenicity and cancer cells to acquire stem cell-like properties. These results suggest that mechanisms downregulating the ERK/MAPK pathway could promote cancer initiation, metastasis and resistance to multiple therapies. Finally, we demonstrated that the antidiabetic drug metformin targets the transcription factor NF-κB. The latter plays a central role in reprogramming, but also in the generation of deleterious pro-inflammatory cytokines by senescent cells. Hence, we suggest that metformin could be used in combination with other therapies to avoid the side effects of either downregulating or overactivating ERK signaling.

Taken together, the results presented in this thesis demonstrate that the outcome of the ERK/MAPK pathway activity depends on signaling strength. While a moderate activation of the pathway may contribute to cell proliferation, a strong activation induces senescence and,

conversely, a low activation promotes cancer cell reprogramming. This versatility of the pathway suggests caution with the use of ERK/MAPK pathway inhibitors, but motivates us to develop new therapeutic strategies, which could include metformin.

Keywords: Cancer, ERK, tumor suppression, cellular senescence, protein degradation, SAPD, SASP, cellular reprogramming, NF-κB, metformin

Table des matières

Liste des tableaux

Chapitre 2 – Article 1

Chapitre 2 – Article 2

Chapitre 3 – Article 4

Chapitre 4 – Article 5

Liste des figures

Chapitre 1 - Introduction

Chapitre 2 – Article 1

Chapitre 2 – Article 3

Chapitre 3 – Article 4

Chapitre 4 – Article 5

Chapitre 4 – Article 6

Chapitre 6 - Discussion

Liste des abréviations

ACN	*Acetonitrile*
ACVRL1	*Activin A receptor type II-like 1*
ADM	*Acinar-to-ductal metaplasia*
ADN	*Acide désoxyribonucléique*
AKT	*Ak strain transforming*
AMEM	*Alpha Modification of Eagle's Medium*
AML	*Acute myeloid leukemia*
AMPK (PRKAA1)	*5' AMP-activated protein kinase*
APC	*Anaphase-promoting complex*
AP-1	*Activator protein 1*
ARAF	*v-raf murine sarcoma 3611 viral oncogene homolog*
ARF (p19ARF)	*Alternative reading frame protein*
ARN	*Acide ribonucléique*
ARNm	*ARN messager*
ATCC	*American Type Culture Collection*
ATG	*Autophagy related*
ATM	*Ataxia telangiectasia mutated*
ATP	*Adenosine triphosphate*
ATP5B	*ATP synthase subunit beta, mitochondrial*
BALB/c	*Bagg Albino/c mouse strain*
BCA	*Bicinchoninic acid*
BCR	*Biochemical relapse*
BDKRB1	*Bradykinin receptor B1*
BECN1	*Beclin 1, autophagy related*
BIF-1 (SH3GLB1)	*SH3-domain GRB2-like endophilin B1*
BPE	*Bovine pituitary extract*
BPH	*Benign prostatic hyperplasia*
BRAF	*v-Raf murine sarcoma viral oncogene homolog B*
BRCA1/2	*Breast cancer 1 and 2*

BrdU	*Bromodeoxyuridine*
BSA	*Bovine serum albumin*
BTB domain	(*BR-C, TTK and BAB) domain*
c-CBL	*Casitas B-lineage lymphoma E3 ubiquitin ligase*
CCDC6	*Coiled-coil domain containing 6*
CDC6	*Cell division cycle 6*
CDC25A	*Cell division cycle 25 homolog A*
CDEA	*Comité de déontologie de l'expérimentation sur les animaux*
CDK	*Cyclin-dependent kinase*
CDKI	*Cyclin-dependent kinase inhibitor*
CDKN1A (p21)	*Cyclin-dependent kinase inhibitor 1A*
CDKN2A (p16)	*Cyclin-dependent kinase inhibitor 2A*
cDNA	*Complementary DNA*
C/EBPβ,δ	*CCAAT-enhancer-binding proteins beta or delta*
CHIP	*Carboxy terminus of Hsp70p-interacting protein*
CHK2 (CHEK2)	*Checkpoint kinase 2*
CHX	*Cycloheximide*
CIC	*Cancer-initiating cell*
CiPSC	*Chemically induced pluripotent stem cell*
CIP1	*Cdk interacting protein 1*
CM	*Conditioned medium*
CMML	*Chronic myelomonocytic leukemia*
CMT	*MGH Center for Molecular Therapeutics*
COT	*Carnitine octanoyltransferase*
CRAF (RAF1)	*v-raf-1 murine leukemia viral oncogene homolog 1*
CREBBP (CBP)	*CREB binding protein*
CRL	*Cullin-RING ligase*
CSC	*Cancer stem cell*
CTNNB1	*Catenin (cadherin-associated protein), beta 1, 88kDa*
CUL	*Cullin*
CXCL5	*Chemokine (C-X-C motif) ligand 5*
DAPI	*4',6-diamidino-2-phenylindole*

DBA	*Dolichos Biflorus Agglutinin*
DDB1/2	*Damage-specific DNA binding protein 1 or 2*
DDR	*DNA damage response*
DDX21/51	*DEAD (Asp-Glu-Ala-Asp) box helicase 21 or 51*
DEC1	*Deleted in esophageal cancer 1*
DEF domain	*Docking site for ERK and FXFP domain*
DEJL motif	*Docking site for ERK and JNK, LXL motif*
DHE	*Dihydroethidium*
DMEM	*Dulbecco's Modified Eagle Medium*
DMSO	*Dimethyl sulfoxide*
DNA	*Deoxyribonucleic acid*
DTT	*Dithiothreitol*
DUB	*Deubiquitinase*
DUSP	*Dual-specificity phosphatase*
ECL	*Enhanced chemiluminescence*
EDTA	*Ethylenediaminetetraacetic acid*
EGF	*Epidermal growth factor*
EGFR	*EGF receptor*
EGTA	*Ethylene glycol tetraacetic acid*
eIF4E	*Eukaryotic translation initiation factor 4E*
ELK1	*ELK1, member of ETS oncogene family*
EMT	*Epithelial-mesenchymal transition*
EpiSC	*Epiblast-derived stem cell*
ERBB	*Avian erythroblastosis oncogene B*
ERK	*Extracellular signal-regulated kinase*
ESC	*Embryonic stem cell*
E1A	*Adenovirus early region 1A*
E2F	*E2 promoter binding factor*
FACS	*Fluorescence-activated cell sorting*
FAK (PTK2)	*Focal Adhesion Kinase*
FANC	*Fanconi anaemia complementation group*
FBS	*Fetal bovine serum*

FBW7	*F-box and WD repeat domain containing 7, E3 ubiquitin protein ligase*
FBXL11 (KDM2A)	*F-box and leucine-rich repeat protein 11*
FDR	*False discovery rate*
FGF	*Fibroblast growth factor*
FITC	*Fluorescein isothiocyanate*
FOS (c-FOS)	*Finkel–Biskis–Jinkins murine osteogenic sarcoma virus*
GADD45a	*Growth arrest and DNA damage-inducible 45a*
GAP	*GTPase-activating protein*
GDP	*Guanosine diphosphate*
GEF	*Guanine nucleotide exchange factor*
GEO	*Gene Expression Omnibus*
GFP	*Green fluorescent protein*
GLB1	*Galactosidase, beta 1*
GO	*Gene ontology*
GPAM (GPAT)	*Glycerol-3-phosphate acyltransferase, mitochondrial*
GP130	*Glycoprotein 130*
GRIM-19 (NDUFA13)	*NADH dehydrogenase (ubiquinone) 1 alpha subcomplex, 13*
GSEA	*Gene set enrichment analysis*
GSK3	*Glycogen synthase kinase 3*
GTP	*Guanosine triphosphate*
G0	*Gap 0*
G1	*Gap 1*
G2	*Gap 2*
HBSS	*Hank's balanced salt solution*
HCC	*Hepatocellular carcinoma*
HDAC	*Histone déacétylase*
HE (H&E)	*Hematoxylin and eosin*
HECT	*Homologous to the E6AP Carboxyl Terminus*
hEGF	*Human EGF*
HEK	*Human embryonic kidney cell*
HER2	*Human epidermal growth factor receptor 2*

hESC	*Human ESC*
HIPK2	*Homeodomain interacting protein kinase 2*
HIRA	*Histone repressor A*
HMBS	*Hydroxymethylbilane synthase*
HMEC	*Human mammary epithelial cell*
HMGB1	*High mobility group box 1*
HNF4α	*Hepatocyte nuclear factor 4, alpha*
HOXA4	*Homeobox A4*
HPDE	*Human pancreatic duct epithelial*
HP1	*Heterochromatin protein 1*
HRAS (H-RAS; HA-RAS)	*Harvey RAS viral oncogene homolog*
HRP	*Horseradish peroxidase*
HSP	*Heat shock protein*
HSPA1A (HSP70)	*Heat shock 70kDa protein 1A*
HSPA5	*Heat shock 70kDa protein 5 (glucose-regulated protein, 78kDa)*
HSPA7	*Heat shock 70kDa protein 7 (HSP70B)*
HSPA8	*Heat shock 70kDa protein 8*
HSPA9	*Heat shock 70kDa protein 9 (mortalin)*
HSPB1 (HSP27)	*Heat shock 27kDa protein 1*
HSPD1 (HSP60)	*Heat shock 60kDa protein 1 (chaperonin)*
HSP90AB1	*Heat shock protein 90kDa alpha (cytosolic), class B member 1*
hTERT	*Human telomerase reverse transcriptase*
H3	*Histone H3*
IEG	*Immediate early gene*
IFNB1	*Interferon, beta 1*
IHC	*Immunohistochemistry*
IKKα, β, γ	*IκB kinase alpha, beta or gamma*
IL	*Interleukine*
INK4A	*Inhibitor of CDK 4A*
IPI	*International Protein Index*
iPSC	*Induced pluripotent stem cell*
IRF3/7	*Interferon regulatory factor 3 or 7*

IRIC	*Institut de recherche en immunologie et en cancérologie*
IκBα (NFKBIA)	*Nuclear factor of kappa light polypeptide gene enhancer in B-cells inhibitor, alpha*
JAK	*Janus kinase*
JARID1B	*Jumonji AT-rich interactive domain 1B*
JNK	*c-Jun N-terminal kinase*
JUN (c-JUN)	*Jun proto-oncogene*
KAP1	*KRAB-associated protein 1*
KDM5B	*Lysine-specific demethylase 5B*
KEGG	*Kyoto Encyclopedia of Genes and Genomes*
KLF4	*Kruppel-like factor 4 (gut)*
KRAS (K-RAS)	*Kirsten RAS viral oncogene homolog*
KYNU	*Kynureninase*
LC-MS/MS	*Liquid chromatography-tandem mass spectrometry*
LIF	*Leukemia inhibitory factor*
LPS	*Lipopolysaccharide*
LRR	*Leucine-rich repeat*
LRWD1 (ORCA)	*Leucine-rich repeats and WD repeat domain containing 1*
LT	*Large T antigen*
MAGE	*Melanoma antigen*
MAPK	*Mitogen-activated protein kinase*
MAP2K (MAPKK)	*MAPK Kinase Kinase*
MAP3K (MAPKKK)	*MAPK kinase kinase kinase*
MAX	*MYC associated factor X*
MCM	*Minichromosome maintenance complex component*
MDM2 (HDM2)	*MDM2 oncogene, E3 ubiquitin protein ligase*
MDMX (MDM4)	*MDM4, p53 regulator*
MEF	*Mouse embryonic fibroblast*
mEGF	*Mouse EGF*
MEGM	*Mammary Epithelial Cell Growth Medium*
MEK	*Mitogen-activated protein kinase/ERK kinase*
mEpiSC	*Mouse epiblast-derived stem cell*

mESC	*Mouse ESC*
MGH	*Massachusetts General Hospital*
MKP	*MAPK phosphatase*
M phase	*Mitosis phase*
mRNA	*Messenger RNA*
mTOR	*Mammalian target of rapamycin*
MYC (c-MYC)	*v-myc avian myelocytomatosis viral oncogene homolog*
NAD	*Nicotinamide adenine dinucleotide*
NCL	*Nucleolin*
NEMO	*NF-kB Essential Modulator*
NES	*Normalized enrichment score*
NF-κB (NFKB)	*Nuclear factor kappa-light-chain-enhancer of activated B cells*
NF1	*Neurofibromin 1*
NHEJ	*Non-homologous end joining*
NK	*Natural killer*
NOC2L (NIR)	*Nucleolar complex associated 2 homolog*
NOLC1	*Nucleolar and coiled-body phosphoprotein 1*
NOL6 (NRAP)	*Nucleolar protein 6 (RNA-associated)*
NOP56	*NOP56 ribonucleoprotein*
NOP58	*NOP58 ribonucleoprotein*
NOT4 (CNOT4)	*CCR4-NOT transcription complex, subunit 4*
NPM1 (B23)	*Nucleophosmin (nucleolar phosphoprotein B23, numatrin)*
NRAS (N-RAS)	*Neuroblastoma RAS viral oncogene homolog*
NRF2 (NFE2L2)	*Nuclear factor, erythroid 2-like 2*
NS	*Nucleostemin*
NSCLC	*Non-small-cell lung carcinoma*
N4BP1	*NEDD4 binding protein 1*
OCT1 (POU2F1)	*Organic cation transporter 1*
OCT4 (POU5F1)	*Octamer-binding transcription factor 4*
OD	*Optical density*
OIS	*Oncogene-induced senescence*
ORC	*Origin recognition complex*

PAI-1	*Plasminogen activator inhibitor-1*
PAMP	*Pathogen-associated molecular pattern*
PanIN	*Pancreatic intraepithelial neoplasia*
PBS	*Phosphate buffered saline*
PBS-T	*PBS-Tween 20*
PCR	*Polymerase chain reaction*
PDAC	*Pancreatic ductal adenocarcinoma*
PDGFRA	*Platelet-derived growth factor receptor, alpha polypeptide*
PDK1	*Phosphoinositide-dependent kinase-1*
PDL	*Population doubling*
pH	*Potentiel hydrogène*
PHD	*Plant Homeodomain*
PIN	*Prostatic intraepithelial neoplasia*
PI3K	*Phosphoinositide 3 -kinase*
PI3KCA	*Constitutively active PI3K*
PLD	*Phospholipase D*
PML	*Promyelocytic leukemia protein*
PML-NB	*PML nuclear body*
PPase	*Phosphatase*
PolI	*RNA Polymerase 1*
pre-RC	*Pre-replication complex*
PTC	*Papillary thyroid carcinoma*
PTEN	*Phosphatase and tensin homolog*
PTGS2 (COX-2)	*Prostaglandin-endoperoxide synthase 2 (prostaglandin G/H synthase and cyclooxygenase)*
P/S	*Penicillin G/Streptomycin sulfate*
PSA	*Prostate specific antigen*
p38MAPK	*p38 Mitogen-activated protein kinase*
p90RSK (RPS6KA1-3)	*90 kDa ribosomal S6 kinase*
qPCR	*Quantitative polymerase chain reaction*
QPRT	*Quinolinate phosphorybosyl transferase*
RAF	*Rapidly growing fibrosarcomas kinase*

RAL	*RAS-like small GTPase*
RALGEF	*Guanine nucleotide exchange factor of the RALs*
RANTES	*Regulated on activation normal T-cell expressed and secreted*
RAS	*Rat sarcoma viral oncogene homolog*
RASGRF	*RAS protein-specific guanine nucleotide-releasing factor*
RASGRP	*RAS guanyl releasing protein*
RB	*Retinoblastoma protein*
RBBP6	*Retinoblastoma binding protein 6*
rDNA	*Ribosomal DNA*
REL (c-REL)	*v-rel avian reticuloendotheliosis viral oncogene homolog*
RELA (p65)	*v-rel avian reticuloendotheliosis viral oncogene homolog A*
RELB	*v-rel avian reticuloendotheliosis viral oncogene homolog B*
rESC	*Rat ESC*
RFU	*Relative fluorescence unit*
RIN	*RNA Integrity Number*
RING	*Really Interesting New Gene*
RIPA	*Radioimmunoprecipitation assay*
RIP1 (RIPK1)	*Receptor-interacting protein 1*
RKIP	*RAF kinase inhibitory protein*
RMA	*Robust Multi-array Average algorithm*
RNA	*Ribonucleic acid*
RNAi	*RNA interference*
RNF4	*Ring finger protein 4*
ROS	*Reactive oxygen species*
RP	*Ribosomal protein*
RPLP1	*Ribosomal protein, large, P1*
RPL23	*Ribosomal protein L23*
RPM	*Rotation per minute*
RPMI	*Roswell Park Memorial Institute medium*
rRNA	*Ribosomal RNA*
RSD	*Relative standard deviation*
RSL1D1 (CSIG)	*Ribosomal L1 domain containing 1*

RSV	*Rous sarcoma virus*
RTK	*Récepteur tyrosine kinase*
SAHF	*Senescence-associated heterochromatic foci*
SAPD	*Senescence-associated protein degradation*
SASP	*Senescence-associated secretory phenotype*
SA-β-Gal	*Senescence-associated β-galactosidase*
SCC	*Squamous cell carcinoma*
SCID	*Severe combined immunodeficiency*
SCF	*SKP, Cullin, F-Box containing complex*
SD	*Standard deviation*
SDS	*Sodium dodecyl sulfate*
Ser	*Serine*
shRNA	*Short hairpin RNA*
shCTR	*Control shRNA (nontargeting)*
SH2B3 (LNK)	*SH2B adaptor protein 3*
SIM	*SUMO-interacting motif*
SKP2	*S-phase kinase-associated protein 2, E3 ubiquitin protein ligase*
SMF	*Serum-free media*
snoRNA	*Small nucleolar RNA*
snoRNP	*Small nucleolar ribonucleoprotein*
SOCS	*Suppressor of cytokine signaling*
SOD1	*Superoxide dismutase 1, soluble*
SOS	*Son of sevenless homologue*
SOX2	*SRY (sex determining region Y)-box 2*
SPEED	*Signaling Pathway Enrichment using Experimental Datasets*
S Phase	*Synthesis phase*
SPRED1	*Sprouty-related protein with EVH-1*
SPRY	*Sprouty*
SRm160/300 (SRRM1/2)	*Ser/Arg-related nuclear matrix protein 160 or 300*
ST	*Small t antigen*
STAT3	*Signal transducer and activator of transcription 3*
STUbL	*SUMO-targeted ubiquitin ligase*

SV40 ER	*Simian virus 40 early region*
TAK1 (MAP3K7)	*Transforming growth factor beta activated kinase-1*
TBS	*Tris-buffered saline*
TBS-T	*TBS-Tween 20*
TBX2	*T-box 2*
TBP	*TATA box binding protein*
TCEP	*Tris (2-chloroethyl) phosphine*
TCF4	*Transcription factor 4*
TER	*Termination regions*
TERF2IP	*Telomeric repeat binding factor 2, interacting protein*
TF	*Transcription factor*
TFA	*Trifluoroacetic acid*
Thr	*Threonine*
TIC	*Tumor-initiating cell*
TIF	*Telomere dysfunction-induced foci*
TLR	*Toll-like receptor*
TMA	*Tissue micro arrays*
TMEFF2	*Transmembrane protein with EGF-like and two follistatin-like domains 2*
TNF	*Tumor necrosis factor*
TOMM34	*Translocase of outer mitochondrial membrane 34*
TOMM70A	*Translocase of outer mitochondrial membrane 70 homolog A*
TOPBP1	*Topoisomerase (DNA) II binding protein 1*
TOP2 (TOP2A)	*DNA topoisomerase 2*
TP53 (p53)	*Tumor protein p53*
TRCP (BTRC)	*Beta-transducin repeat containing E3 ubiquitin protein ligase*
TRED	*Transcriptional Regulatory Element Database*
TRIM28	*Tripartite motif-containing 28*
TRUSS (TRPC4AP)	*(TNF-R)-associated ubiquitous scaffolding and signaling protein*
TTF-1	*Transcription termination factor, RNA polymerase I*
Tyr	*Tyrosine*
UBE2L3	*Ubiquitin-conjugating enzyme E2 L3*

UBF	*Upstream binding factor*
UPP	*Ubiquitin-proteasome pathway*
UVRAG	*UV radiation resistance associated*
VHL	*von Hippel-Lindau tumor suppressor, E3 ubiquitin protein ligase*
v-src	*Viral-Src*
WNT	*Wingless-type MMTV integration site family*
WT	*Wild type*
X-Gal	*5-bromo-4-chloro-3-indolyl-β-D-galactopyranoside*
YAP1	*Yes-associated protein 1*
YB-1 (YBX1)	*Y box binding protein 1*
γH2AX	*H2A histone family, member X – phosphorylated*
53BP1	*p53-binding protein 1*

Notes importantes :

1. Tout au long du texte, les noms de protéines et de gènes humains sont écrits à l'aide de lettres majuscules, alors que les minuscules sont utilisées pour les autres espèces.

2. Les noms de gènes sont écrits en italique afin de les distinguer des protéines.

3. Les préfixes «p-» et «phospho-» indiquent la phosphorylation d'une protéine.

En vos noms chers grands parents, car vous m'avez transmis l'énergie

Pour toi mon fils, pour m'avoir donné la motivation

Remerciements

Cette thèse est l'aboutissement d'un long parcours, qui a pris racine bien avant le début du doctorat. Ces racines viennent d'une semence, bien arrosée, bichonnée et aimée. Elle a grandi sous les soins attentionnés de nombreuses personnes, pour donner ce que je suis, pour justifier ce que je fais. Sans vous, je n'aurais jamais accompli cette thèse. Écrire les lignes qui suivront est pour moi une façon d'immortaliser l'importance que vous avez eue; de rendre le mérite qui vous revient.

Laboratoire Ferbeyre

Plus de sept années se sont écoulées depuis mon arrivée au sein du laboratoire. Sur l'échelle d'une vie humaine, c'est significatif. Non seulement j'ai grandi professionnellement durant ces années, mais j'ai aussi énormément évolué en tant qu'individu. J'ai appris bien au-delà de la dimension purement scientifique. Toute cette évolution, je la dois à tous ceux et celles qui ont partagé un passage de leur vie avec nous. Le temps passe vite, très vite, peut-être même trop vite.

Gerardo, je me souviens du temps où je cherchais un stage en ne connaissant pas trop les laboratoires du département de biochimie. En tombant sur le site du labo, non seulement le sujet correspondait à ce que je cherchais, mais je décelais entre les lignes quelqu'un d'humain. Après notre première réunion, j'en étais convaincu et le temps me l'aura confirmé. Merci de m'avoir accueilli, de m'avoir transmis le maximum que vous pouviez, de m'avoir supporté et de m'avoir laissé beaucoup de liberté. J'ai apprécié votre patience, votre ouverture d'esprit et votre approche de psychologie positive. Par contre, ce que j'ai apprécié par-dessus tout c'est votre passion pour la recherche. C'est une passion contagieuse, qui pourrait motiver n'importe qui. Juste pour cette raison, je peux sans le moindre doute affirmer que j'ai fait un excellent choix en postulant pour votre laboratoire. Ce fut un privilège d'assister à son évolution et d'avoir pu y prendre part. J'espère que nous aurons la chance de collaborer dans le futur, de partager à nouveau notre passion pour la science, et aussi d'apprendre à se connaître au-delà du contexte professionnel.

Viviane, ma première complice de laboratoire. J'ai un souvenir très net de cette première journée au A533, à t'aider dans tes immunoprécipitations, tout en apprenant à se connaître. Tu es celle qui m'a appris le travail de terrain et qui a eu la patience de tout m'expliquer. Considérant ton souci du détail, ton désir de bien faire et ton professionnalisme, tu ne pouvais que me donner une excellente formation. Merci de la confiance que tu m'as accordée et merci de ta grande intégrité. J'ai adoré travailler avec toi et apprécié nos discussions matinales. J'aurais aimé pouvoir te connaître encore plus, mais le contexte du travail impose parfois ses limites. J'espère bien que nous pourrons échanger à nouveau dans le futur, dans un tout autre contexte, car je sais que tu mérites à être connue.

Marie-France, ma chère Marie. Nous pourrions qualifier ces années d'une épopée. De grandes années et d'autres terribles. Des échecs et de belles réussites. De l'extérieur, on pourrait presque se demander comment se fait-il que nous ayons survécu et surtout, comment pouvons-nous autant nous apprécier maintenant. Le travail, la pression, les échecs à répétition, ça impose parfois une dynamique. Si on combine tout ça à une bonne dose de ce que nous qualifierons «d'autres choses»…l'énergie peut devenir difficile à trouver et c'est normal. Le plus important c'est d'être assez intelligent pour réaliser, une fois la tempête terminée, à quel point la vie peut parfois sembler absurde, mais que nous pouvons agir de façon tout aussi absurde. Surtout, il faut être assez sage pour reconnaître que les dommages causés par une tempête sont toujours réparables. Pour les quelques taches qui ne veulent pas partir, quelle importance! Cela nous fait quelque chose à conter et ça nous fait apprécier la vie encore plus. Cela nous fait aussi réaliser toute l'importance des gens qui nous entourent et des liens particuliers se tissent avec ceux qui ont traversé la tempête avec nous. Tu es une personne particulièrement forte, qui sait rebondir et qui fait preuve de beaucoup d'humilité et de bonté. Ça me fait tellement plaisir de te voir aujourd'hui t'épanouir dans quelque chose que tu aimes, que tu fais par pure conviction et dans lequel tu excelles. Je ne suis pas inquiet pour ton avenir. Merci pour ces belles années, j'ai beaucoup grandi.

Ольга, научной базой этой диссертации во многом послужила ваша работа. Экран, который вы сделали, позволяет предположить, что если сбить ERK, то можно обойти PAH-индуцированное старение. Таким образом, я действительно благодарен вам

за возможность, которую вы мне предоставили. Я также ценю то время, когда мы работали вместе над проектом метформина. Вы много работаете, и вы заслуживаете, чтобы вы получили признание за все усилия, которые вы вкладываете в исследования. Я не могу пожелать вам ничего лучшего, чем быть счастливой, быть в гармонии с жизнью и чтобы исполнились ваши желания.

Véronique, merci pour les centaines de qPCR que tu as faites. Le qualificatif qui te décrit le mieux est «compétente». Tu es une excellente scientifique et nous pouvons toujours avoir confiance aux résultats que tu obtiens. Tes idées sont précieuses et il n'y a pas un projet dans le laboratoire qui n'en profite pas.

Geneviève, nous sommes arrivés presque le même jour au laboratoire et nous avons traversé toute cette époque ensemble. Nous avons eu la chance de nous voir évoluer mutuellement…et dans les deux cas nos vies sont biens différentes maintenant! J'ai trois mots pour te décrire : simple, humaine et intègre. Merci pour ce que tu es, merci de ton amitié sincère tout au long de ce parcours. Merci d'écouter tes valeurs profondes et de ne pas tomber dans le jeu des uns et le jeu des autres. Enfin, merci d'accepter les gens tels qu'ils sont, de ne pas souffrir de prétention, de sentiment d'infériorité et ne pas sombrer dans les procès d'intention. Ça fait toujours du bien d'avoir une personne simple, à qui on peut dire à peu près n'importe quoi et ce, sans trop faire attention aux mots utilisés! Toi et Jordan, vous avez une grande et belle intelligence sociale. Marie-Ève et moi, on vous apprécie énormément et, définitivement, vous avez une philosophie de vie à laquelle nous adhérons. On espère bien garder contact; une philosophie ça se transmet à des enfants et les enfants apprennent par l'exemple.

Vickram, véritable lanterne dans la noirceur. Peu importe ce que les uns et les autres peuvent penser, tu es l'une des personnes les plus positives que j'ai rencontrées dans ce laboratoire. Quand j'avais l'impression que le seul fait de respirer perturbait l'univers, tu étais là pour sourire, blaguer, parler de science, mais aussi de vie. Tu t'intéressais à mon projet, tu voulais m'aider et tu souhaitais mon succès. Travailler avec toi était simple, par moment ressourçant. Ton départ aura été un jour triste, surtout que ton remplaçant a été pendant un certain temps le son de l'agitateur. Ce sera un grand plaisir de te revoir bientôt cher ami!

Vincent, hyperactif certes, mais quelle belle énergie positive. Je vais me souvenir de la musique à fond…surtout la fois où tu as convaincu Olga d'écouter une chanson «tranquille» de Billy Talent. Non mais, quelle arnaque…c'est nous qui avons dû subir son comportement totalement réfractaire à tout son sortant de la radio…et ce jusqu'à tout récemment! Sans rancune cher ami, ça fait partie des situations mémorables du labo! Merci pour le positivisme que tu avais et merci pour ta bench!

Frédéric, le remplaçant du son de l'agitateur. Sans blague, quelle joie ce fut d'avoir quelqu'un pour mettre de la vie dans ce petit labo qui s'était vidé après l'ouverture du grand! Fred, je ne sais pas comment je pourrais te remercier. Non seulement tu m'as apporté une aide précieuse pour terminer le Genes & Dev, mais tu as apporté un souffle de renouveau dans mon doctorat. Tu m'as permis de travailler en équipe, de partager librement mes idées et en retour, tu en faisais tout autant. Bref, ce fut le réel commencement de ce que j'avais imaginé pour mon doctorat. Merci pour l'absence de compétition, d'une quelconque forme de jalousie face aux autres et de considérer tes collègues comme des alter egos. Merci pour la belle camaraderie que tu as permise. Merci pour toutes tes blagues, parfois à la limite de la décence. C'est incroyable comment le ridicule et le fait de ne pas trop se prendre au sérieux peut faire du bien! Mon homme, tu as de belles motivations qui te poussent à faire de la recherche et je suis convaincu que tu vas aller loin. Les qualités que j'ai décrites te seront des outils précieux. Tu peux d'ailleurs compter sur mon support dans ce que tu entreprendras; je te suis redevable.

Mathieu, le boute-en-train du labo. Comment mieux te décrire, définitivement tu aimes faire la fête. Tu auras été mon premier acolyte dans le laboratoire. Nous avons eu de belles soirées et avons été complices dans des situations que peu peuvent prétendre avoir vécues. Nous pourrons les conter à nos enfants quand ils seront vieux…question de leur faire comprendre que leur père n'a pas toujours été sage! Merci pour ces bons souvenirs. Je sais que tu vas aller loin en recherche; tu es prêt à faire beaucoup pour atteindre tes objectifs.

Mariana, eres parte de la gente siempre positiva, siempre de buen humor. Tú eres muy trabajadora, siempre organizada y nunca te desanimas. Eres inspiracion en un laboratorio, especialmente cuando los resultados positivos son raros. Fue un honor trabajar contigo. También es un gran privilegio compartir este momento tan especial de nuestras vidas, de dar

vida a un nuevo ser humano. Con las pocas semanas que nos separarán, no tengo ninguna duda de que vamos a tener una hermosa complicidad!

Emmanuelle, toi aussi tu es une personne déterminée. Avec Mathieu, vous formez un team d'enfer! La question sera où allez-vous faire votre recherche…pas trop loin j'espère, car je veux voir la tronche de vos enfants! Plus sérieusement, merci pour l'aide que tu as apportée sur le dernier projet, mais aussi sur le projet metformine. Tu as le souci du travail bien fait et c'est une qualité que j'apprécie particulièrement.

Lian, petit rayon de soleil de l'aile A. Tu fais partie de ces personnes qui sourient toujours et SVP, ne change jamais. C'est le plus simple, mais le plus beau cadeau que tu peux faire à autrui. Si tu savais le nombre de fois que je me suis passé le commentaire à savoir à quel point c'est agréable de te croiser le matin. Ça donne une petite dose d'énergie de plus que la caféine. Je te souhaite du succès et beaucoup de plaisir dans la poursuite de ton Ph.D, tu le mérites.

Sebastian, es gehört viel Mut dazu in einem Land seine Dissertation zu schreiben in dem die Dauer, statt festgesetzten drei Jahren, unbestimmt lang zu sein scheint. Außerdem ist es beeindruckend sich für einen bezahlten Bildungsweg zu entscheiden, wo doch Bildung in deiner Heimat gebührenfrei ist. All dies ehrt dich sehr und zeigt einmal mehr wie stark du dich reinhängst für deine Ziele und Sehnsüchte. Ich hatte die Ehre dich als Praktikanten betreuen zu dürfen und wurde somit Zeuge deines stetigen Engagements. Wenn du dir einmal etwas in den Kopf gesetzt hast, kann man sich sicher sein, dass du nicht mehr locker lässt. Immer weiter so Sébas, du entwickelst dich mit rasanter Geschwindigkeit. Man kann Großes von dir erwarten! Und wie immer wirst du unsere Erwartungen noch weit übertreffen.

Alexandra, tu es une de ces rares personnes étant totalement dépourvue de malice. Tu avais toujours de bons mots pour tout le monde, tu as su mettre un peu de couleur dans le laboratoire et tu avais de belles petites attentions pour nous. Merci pour ta volonté de rendre ton entourage heureux. Ton rayonnement nous a fait du bien. Travailler avec toi a été un grand plaisir.

Karine, tu es l'une des personnes que j'ai vues le plus évoluer. J'ai eu le privilège de t'enseigner dès ta première année de baccalauréat et de te suivre jusqu'à ton doctorat. C'est un sentiment très valorisant. Gerardo peut bien adorer ce qu'il fait! Tu es très talentueuse, tu apprends vite. Je n'ai donc pas trop à me justifier en disant que tu devrais t'en sortir avec de belles réalisations. N'oublie juste pas une chose, réponds aux courriels, surtout quand je voudrai prendre de tes nouvelles! Je veux aussi te remercier pour l'aide que tu apportes au projet en cours. Avec la période très TRÈS intense que je viens de traverser, cette aide a été des plus précieuses.

Neylen, gracias por la sonrisa que tienes. Una sonrisa espontánea, sincera y amigable. Tenemos la capacidad de sonreír. Es muy fácil y realmente vale la pena. Es increíble lo que tan pequeño gesto puede hacer a los demás y a nosotros mismos. Nos motiva en nuestro trabajo, transforma las semillas de energía negativa en una fuente de energía positiva. Se llena una necesidad básica de todo ser humano: el sentido de pertenencia. A pesar de todos los beneficios de este gesto, no todas las personas pueden brindarla. Tú, sabes cómo; Nunca cambies.

Marienieve, algo de lo que puedo tener certeza es tu vitalidad y entusiasmo ante de la vida, los cuales serán un ejemplo a seguir. Por siempre recordaré esa noche loca en San Diego; continúa disfrutando de la vida siempre. Agradezco profundamente por la ayuda que aportaste para el diseño del plasmido. Finalmente ese día llego y este es el resultado de tu duro trabajo durante varios meses!

Enfin, un merci à tous les autres membres du laboratoire que j'ai moins eu la chance de connaître, mais qui ont contribué à cette belle aventure. Merci Frédérick, Frédérique, Antoine, Catherine, David, Virginie, Malik, Benjamin.

Bardeesy laboratory

Many thanks for all of you guys. I was really fortunate to have this opportunity to work in your lab. Not only did I learn a lot, but I made new friends. I especially appreciated your openness, your willingness to collaborate and share ideas, and your desire to take pleasure in doing your work. I felt welcomed into your group; I never felt like a threat; you never showed

the slightest sign of a willingness to compete; you never wanted to judge me. It was amazing to feel integrated, a part of the group, and this, so quickly. Here are the keywords describing your lab: sharing, collaboration, esteem, confidence, competence. This is exactly the kind of environment where we can give the best of ourselves. Thus, it was more difficult than expected to decide not to join the team for a post-doc. Nevertheless, I am pretty sure to see you in the future, perhaps collaborate with you again; it is a question of time.

Nabeel, I will repeat it again. You did a lot, and I will never forget. You did not hesitate to welcome me in your lab. You gave me access to you resources and all the liberty to pursue my research. You accepted to take me for a post-doc without guaranty, knowing that my first choice was to go back to the school bench. You wrote so many recommendation and assessment letters for me. You shared ideas, contacts, tools and expertise. You gave me the chance to present my results to the MGH Annual Retreat. You were always involved in the project. Considering the fact that you have many obligations, I appreciate even more all the time you invested in me.

Filippos, I could not have gotten a better lab partner. You were really involved and always there for me, and this not only in the lab. I had such a nice time in your home. Popi, Katerina and you form a beautiful little family. Thanks also to you Popi, for welcoming me so warmly. For you dear Katerina, if by any chance you read these lines in a few years, I can vouch for all the love your parents have for you. I wish my son will be friend with you, and this even as teenagers! Don't forget dear friends, you have a home here in Québec.

Nicole, to live the playoff series in your presence …with the Bruins at the Stanley Cup finals, in addition to seeing Canada eliminate the United States during the Olympic Games... has been a memorable experience. Unfortunately I missed your reaction after the elimination of the Bruins by the Habs this year. I cannot do anything Nicole, I love you all the same! I will always have a thought for you when I watch hockey games.

Thanks to all the other lab members (Rushika, Julien, Yusuke, Supriya, Christine, Krishna, Krushna, Svetlana, Julia, and Mortada) for all the reasons mentioned in the first

paragraph. Yusuke, a special thanks for the time you took to show me how to do surgery on mice.

Il en est de même pour toi, Julien. Les injections IV sont quelque chose de plutôt ardu à effectuer au début. Tes trucs ont vraiment été utiles et ton savoir servira maintenant à plusieurs personnes dans le laboratoire de Gerardo. N'abandonne pas ta mission face à nos chers États-Uniens!

Thanks also to the administrative staff, which did A LOT of things for me. Christin and Justine you are amazing! Everything is fast and well done with you. Furthermore, you always seem happy to do it. Please consider teaching your skills.

Mostoslavsky laboratory

The Spanish teem of MGH! It is really great to work just beside your group. You always have fun, share everything and give nice feedback on our projects. I also appreciated the opportunity to practice my Spanish a bit! I wish to give a special thanks to Sita and Jean-Pierre. We have some "sunny persons" in our university. I mean those persons that have the faculty to make you happy whatever the situation. You fall into this category of persons. Sita, I will never forget your smile every morning when I entered the lab. And you JP, your positive energy is like a kind of drug. Stay as you are; smart, but simple and human.

Laboratoire Roy

Stéphane, mille mercis pour l'opportunité que tu m'as offerte d'utiliser tes installations de culture cellulaire. Sans cette générosité, je serais encore en train de faire de la culture et j'en aurais pour quelques années. Merci aussi pour les nombreuses lettres de référence, ton enthousiasme et ta bonne humeur. Merci également à tous les membres du labo (Mathieu, Jean-Charles, Éric, Samuel, Étienne, Jean-François), pour m'avoir enduré en quasi permanence dans la salle de culture! Sérieusement, ce fut un plaisir de travailler avec vous. J'ai d'ailleurs passé plus de temps avec certains d'entre vous qu'avec quelques membres de mon propre laboratoire.

Laboratoires Desgroseillers, Chartrand et Michnick

Avec les membres de notre laboratoire, vous avez formé le microcosme de l'aile A. Il s'agit de l'un des endroits où j'ai passé le plus de temps dans les 7 dernières années. Il est donc clair que vous avez tous eu un impact dans ma vie. Je dirais que la dynamique est particulièrement agréable depuis quelques temps. Une belle chimie entre les labos s'est installée. Merci de partager l'équipement et de dépanner sans hésitation. De savoir que l'on peut compter sur l'ensemble de nos collègues est non seulement rassurant, mais très motivant. Rémy, Élizabeth, Sami, Karen, Amélie, Anik, Jacqueline, Emmanuelle, Louis-Pilippe, Lara, Mohan, Vincent, Po Hien et Arturo merci pour votre bonne humeur. Rémy, quel sera le nom du prochain chapitre? Karine, Véronique, Emmanuelle, merci pour les millions de fois que je vous ai dérangées pour emprunter du matériel!

Laboratoire d'enseignement

Le désir de servir mon prochain est parmi les sources de motivation les plus importantes ayant guidé mes choix. Ainsi, je voulais faire de la recherche pour faire avancer notre société, nous donner de nouveaux outils pour vivre mieux, pour vivre heureux. Bien que j'adhère toujours à cette philosophie, le travail au sein du laboratoire ne me permettait pas d'être en contact avec la source première de ma motivation, c'est-à-dire les gens. Merci de m'avoir donné l'opportunité d'enseigner, de transmettre quelque chose directement à autrui. Vous m'avez permis de combler un grand besoin et d'avoir une expérience complète et enrichissante au cours de mon doctorat.

Merci Daniel pour ta confiance et toutes les opportunités que tu m'as offertes. Merci Nathalie pour ton énergie, ta complicité et ton implication. Merci André, Nicole et Jacques pour votre sourire, votre travail impeccable et votre bonne compagnie. Merci Shona (alias SchyzophReine) pour ta folie, ta bonté et ta simplicité. Discuter avec toi est toujours thérapeutique et j'espère pouvoir bénéficier encore de cette thérapie. Merci Audrey pour ta complicité, ton support et ta bonne humeur. J'ai adoré travailler avec toi autant lors des démonstrations que lors de la gestion des rapports de stage. En passant, félicitations…je n'ai aucun doute que tu es une super maman! Philipe, merci pour ton leadership, ton énergie

positive et ton humanité. Tu es un membre précieux du département, de par ton implication dans tous les projets, ton professionnalisme, ta capacité de rassembler les gens, ton écoute, ton charisme et surtout, ta constante bonne humeur qui nous assure de passer une bonne journée. Tu as compris l'importance de la collégialité et tout le positif qui en découle. Il s'agit en effet de l'un des moteurs les plus puissants pour assurer le rayonnement d'une institution.

Madame Brakier-Gingras

Léa, ce fut un honneur de pouvoir vous côtoyer durant ces dernières années. Je me souviens des cours que vous m'avez donnés au baccalauréat. J'avais été impressionné par la clarté de vos propos, mais surtout, de l'aura que vous avez. Cette impression est encore plus forte maintenant. Vous dégagez à la fois intelligence, calme, sagesse, bonté et humanité. Vous êtes une inspiration pour plusieurs et un modèle pour nous tous.

Personnel du département

Christian, la gestion du département est assurément un art complexe. Je vous félicite pour vos réalisations et vous remercie pour tout votre investissement afin d'assurer le succès de la petite communauté que nous formons. Linda, Yves, Lorraine, Dominique, Élaine et Patrick, merci pour votre travail précieux et impeccable. Merci Ernest pour toute la vaisselle que tu as lavée pour nous…Je ne peux que m'excuser pour les lundis matin et les retours de vacances avec des montagnes de vaisselle. Ton travail est tellement apprécié. Monique, merci pour ta disponibilité, le plaisir que tu prends à nous aider et tout ce que tu m'as appris. Louise, merci pour ton aide avec la culture cellulaire et toutes les bombonnes que tu as changées !

Sylvie, je te consacre un paragraphe. Tu es une véritable perle pour le département. Nous pouvons toujours compter sur ton aide et nous avons toujours l'assurance que tu le feras avec plaisir. Tu aimes ce que tu fais et ça se voit; tu rayonnes de positivisme. Les couloirs gris du pavillon Roger-Gaudry sont une partie importante de l'environnement de vie des étudiants et employés du département. Pouvoir y croiser des gens dévoués, qui vont au-delà de l'accomplissement de leurs tâches professionnelles, fait toute la différence sur notre épanouissement et notre sentiment d'appartenance. Nous en oublions ainsi la couleur des murs et en retenons le rayonnement des gens qui leur font face.

Comité de thèse et jury

Nathalie et Alain, j'ai été choyé de vous avoir sur mon comité de thèse. J'ai grandement apprécié chacune de nos rencontres. Nous avions toujours des échanges d'idées enrichissants et vous aviez une attitude très positive face au projet. J'espère que nous aurons l'opportunité d'échanger à nouveau. Je remercie également les membres du jury de thèse qui ont accepté d'évaluer l'ouvrage durant l'été, et ce, avec une contrainte de temps. Je perçois votre geste comme une belle considération pour autrui; une volonté d'aider, en quelque sorte, un futur collègue. Je vous en suis reconnaissant.

Hommage aux charpentiers

Aussi inattendu que cela puisse paraître, je souhaite prendre quelques lignes pour souligner l'importance de deux personnes toutes particulières. Enfant, je ne peux pas dire que j'aimais beaucoup l'école. S'il pouvait y avoir un prétexte pour manquer quelques minutes de classe, celui-ci faisait mon bonheur. On n'avait pas encore su allumer en moi la soif d'apprendre, du moins d'apprendre ce qui était inscrit au programme. Sans aucunement vouloir porter d'accusations, même avec du recul, j'ai de la difficulté à concevoir comment j'aurais pu apprécier l'école durant les premières années. Pourtant, c'est à cette époque que l'on édifie la fondation de ce que nous serons, la charpente de notre capacité à apprendre, et surtout, notre motivation à persévérer. Heureusement, il y a eu Diane Gilbert et André Ouimet, deux enseignants exceptionnels. Vous m'avez appris à aimer apprendre. En toute simplicité, vous m'avez montré toute la satisfaction que l'on peut tirer de maîtriser des connaissances et de pouvoir les mettre en application. C'est ce qu'on devrait montrer à tous les enfants. J'espère que les miens auront cette chance. Cette thèse est dédiée à bien des gens, mais vous êtes parmi les tous premiers instigateurs. Sans le cadeau dont vous m'avez fait, jamais elle n'aurait vu le jour. Je me souviens, telle est ma devise.

Famille

À mes parents, Colette et Marc-André

Chers parents, une phrase que vous avez répétée à quelques reprises : la réussite d'un enfant vient de beaucoup d'efforts de sa part, mais aussi un peu des parents. Elle est trop humble à mon avis. Il est clair que l'éducation que vous nous avez transmise a joué un rôle déterminant dans ce que nous sommes et dans ce que nous faisons. Vous nous avez appris la valeur du travail. Certes, il était pénible de passer des journées à arracher des choux gras, de l'amarante, sans compter le souchet!!! Je ne connais pas beaucoup d'autres personnes qui peuvent dire qu'ils ont désherbé un champ de maïs à la main…et j'en passe. Vous nous avez appris l'endurance et la persévérance.

J'ai eu une mère qui s'est réorientée à 40 ans, en droit. Retour à l'Université de Montréal alors qu'elle a 4 enfants, dont deux en bas âge (moi-même ayant que quelques années de vie)…alors que nous vivions près de Mont-Laurier. Un père qui travaille dur pour faire vivre tout le monde et une mère qui assure son rôle de mère à toutes les fins de semaine et qui retourne en ville la semaine pour ses études. Vous avez survécu, nous n'en avons pas tant souffert. Vous nous avez appris que tout est possible.

Vous nous avez appris tellement de choses qui ne s'apprennent pas à l'école. Nous savons reconnaitre les espèces d'arbres, les champignons, les plantes sauvages; nous savons comment utiliser nos mains. La tête c'est bien, mais les deux c'est mieux. Quoiqu'il arrive, nous serons outillés. Merci pour avoir élargi notre esprit hors du contexte préétabli par le système de l'éducation.

Enfin, le plus important de tout, vous nous avez appris l'ouverture à l'autre. Oui travailler, persévérer, mais le faire pour soi et pour les autres, mais pas pour recevoir des autres et surtout pas contre les autres. Je comprends aujourd'hui toute la valeur de ce principe. L'ouverture à l'autre est le meilleur moyen pour s'épanouir et progresser intellectuellement. C'est la forme d'intelligence qui ouvre la porte aux autres. Merci de nous avoir donné une telle vision de la vie. Elle confronte certaines personnes. Les gens avec une éducation essentiellement basée sur la compétition ne la comprennent pas et interprètent nos agissements

à leur façon, voire la jugent. Il faut juste apprendre à ne pas s'en préoccuper et à ne surtout pas changer. Nous ne pouvons qu'espérer qu'un jour, plus de gens la partageront.

À mon frère, Benoît

Grand frère, mais tu es aussi mon meilleur ami. Nous pouvons tous deux constater la chance que nous avons eu de recevoir cette éducation. Il faut toutefois admettre que nous avons dû nous serrer les coudes par moment. Merci d'avoir été là, toujours. Nous étions jeunes, mais je me souviens très bien du moment où nous avons eu cette discussion d'adulte. Nous avons signé un pacte qui nous aura permis d'affronter tous les tourments; un pacte qui nous aura permis d'être heureux peu importe ce qui se passait. Il n'est pas nécessaire d'en dire plus, ce pacte ne prendra jamais fin.

À mes demi-frères, Serge et Simon

Nous n'avons grandi que partiellement ensemble. Évidemment, bien des choses nous distinguent, mais bien d'autres nous rassemblent. Je le répète et je l'immortalise, moi c'est une chose, mais mes enfants c'est autre chose. Vous êtes des gens formidables et vous avez beaucoup à offrir. Malgré la complexité apparente de notre famille, elle a une grande force, c'est sa diversité. Parmi les plus beaux cadeaux que je pourrai donner à mes enfants, c'est de pouvoir bénéficier de cette belle diversité et d'avoir une famille qui les aime. J'aimerais qu'ils connaissent bien leur famille. J'aimerais qu'ils apprennent de vous et de mes beaux-frères/belles-sœurs également. Vous savez que je vous adore Maryse et Charles.

À ma demi-soeur

Je te connais encore trop peu, mais c'est tout de même impressionnant comment un lien s'est tissé rapidement. Je vais toujours me souvenir de la première fois que je t'ai rencontrée, du moins que je pouvais en avoir conscience. Aucune gêne, juste une grande joie d'enfin nous voir. Tu as une magnifique personnalité. Malgré que je ne comprendrai jamais pourquoi il aura fallu attendre tant d'années pour nous retrouver, je regarde en avant et je compte bien reprendre le temps perdu. Félix aura une matante formidable.

À Gilbert

Cher beau-père, les choses n'arrivent jamais pour rien. Nous avons une mère heureuse et un beau-père formidable. Tu nous ouvres ta porte et tu nous offres de l'aide (et des arbres…!) comme si nous étions tes fils. Nous sommes choyés de t'avoir. Bourré de connaissances générales, agréable à discuter, juste un peu espiègle et toujours partant pour une descente du Massif en luge, que demander de mieux!

À ma belle-famille paternelle

Nicole, nous ne pouvions espérer mieux pour notre père. Merci de le rendre heureux, merci de ta simplicité. Nous t'avons immédiatement adoptée, tu es une source inépuisable de bonté. Tes deux enfants, qui commencent à être pas mal grands, font tout autant partie de notre famille. Nous pourrions nous connaître davantage, mais ils ont leur place assurée à titre de demi-frères!

À ma deuxième mère, Odette

Ahhh Odette, je t'ai gardée pour la fin et ce n'est pas pour rien. Je ne sais pas si tu réalises l'importance que tu as eue dans ma vie. C'est toi qui me faisais faire mes devoirs et qui devais subir mes «écœurantites» aiguës des dictées. Tu vivais mes peines, mes joies et mes colères. Tu étais toujours là pour moi et mon frère. Quelle patience, quelle belle personnalité et quelle simplicité. Tu es, et j'insiste, totalement unique. Tu as une bonté en toi que je n'ai jamais vu égalée chez une autre personne. Tu es une inspiration, un modèle. Je me considère tellement privilégié de t'avoir eue dans ma vie et une grande partie de ce que je suis découle de ce que tu es. Je ne t'oublie pas; ne l'oublie pas.

Belle-famille

Je ne vous oublie pas. Merci de votre accueil chaleureux. Je me suis senti le bienvenu au sein de votre famille dès le premier jour. Vous êtes une belle famille tissée serrée; c'est un beau succès. Marie-France et Daniel, vous avez transmis de superbes valeurs à vos enfants. Jolyanne, Steve, Pierre-Émile, Émilie, Marc-Olivier, Lore, Louis-Xavier: merci de m'avoir considéré des vôtres. J'espère que cette belle chimie perdurera et que rien, n'y personne, ne

viendra la briser. Il faut se souvenir qu'aucun motif valable ne justifierait de mettre un terme à quelque chose d'aussi beau.

À vous chers amis

Cette section des remerciements pourrait devenir beaucoup plus longue que la thèse en soit. Je ne peux malheureusement pas mentionner tous les noms pour qui j'ai une pensée. Sachez cependant, que même si votre nom n'y figure pas, je n'oublie pas l'impact que vous avez eu dans ma vie.

Je tiens néanmoins à souligner les noms d'un petit groupe de personnes à qui je dois beaucoup de choses : Cynthia, Benoit, Cynthia (alias Maurice), Sonia, Étienne, Maryse, Sylvain. Merci de considérer les gens pour ce qu'ils sont, de vous ouvrir si naturellement et de les intégrer. L'image qui suivra est anodine, mais on ne peut plus claire. Que fait-on avec la fleur qui dépasse de la plate-bande? On l'admire et elle porte ainsi ombrage aux autres; on la coupe pour la rentrer à l'intérieur, comme ça plus besoin de sortir pour voir les autres; elle dérange et on l'élimine; ou on la replace tout naturellement afin de créer une harmonie avec l'ensemble. Vous êtes formidables, car vous avez cette faculté de choisir spontanément cette dernière option dans vos interactions avec les gens. Il s'agit d'une grande force, d'une grande intelligence. Cette qualité fait de vous des amis indéfectibles. Nous partageons nos vies depuis de nombreuses années, on se supporte, on rit, on s'apprécie. À force de vous fréquenter, vous m'avez enseigné que ce sont les gens comme vous qui, pour moi, méritent qu'on investisse dans la relation. Vous m'apprenez à prendre le bon côté des gens et à faire fi du mauvais. Merci, vous m'aurez grandement aidé à franchir toute ces étapes qui m'ont mené à la fin de ce doctorat. De plus, vous me transmettez un outil pour être heureux dans la vie, peu importe la situation et, être heureux n'est-elle pas la plus belle raison d'une vie.

À toi Marie-Ève

Non seulement ce qui est dit dans la section précédente te concerne, mais il manquerait de mots pour la compléter. Tu as d'abord été une amie, ensuite une compagne. Ce qui fait de toi la personne qui me connait le mieux au monde. La complicité que nous avons est sans limite. Ce qu'il y a de plus beau, c'est qu'elle est toute naturelle. Nous n'avons rien à dire, rien

à faire pour se comprendre. Tu dis souvent que nous formons une super équipe; c'est plus qu'une équipe, c'est une unité. Merci d'être dans ma vie; Merci d'être la mère de ce petit homme en devenir; je serai toujours là pour vous. Je t'aime.

À toi Félix

La fin de ce doctorat coïncide avec le début d'une autre belle aventure, mais une aventure pour la vie. Il s'agit de ta venue mon cher Félix. Nous t'attendons tous avec beaucoup d'amour en réserve et nous souhaitons fortement pouvoir te transmettre beaucoup plus que ton nom, c'est-à-dire toute sa signification. Nous espérons ainsi que ce nom reflétera ta vie, une vie remplie de bonheur. Tu es l'ouverture sur l'avenir, petit homme.

Avant-propos

Cancer

Un mot si court, un mot si simple, un mot que tout le monde connait. Un mot par contre, que personne ne comprend réellement, ou plutôt, un mot que nous ne pouvons que comprendre à notre façon. Un mot qui éveille en nous tout ce qu'il peut y avoir d'humanité. La seule idée d'y penser fait peur. Non seulement ce mot fait peur, mais il peut faire mal, il peut rendre triste. Il peut aussi, étonnamment, nous rassembler et nous motiver. Nous motiver dans une cause; une cause générant un espoir. Une grande lutte qui a le mérite de chercher le bien de tous, car non seulement le cancer ne dort jamais, mais il ne discrimine personne. Cette grande lutte mène à des succès, des petits pas vers une victoire qui savent faire émerger une joie, un sentiment d'accomplissement, voire une fierté, et toujours, un espoir.

Il est clair que le cancer implique des sphères philosophiques, émotionnelles; humaines. Pour ces raisons, nos sociétés investissent énergie et volonté dans la lutte contre cette maladie. Le monde scientifique moderne a le mérite de donner des outils précieux pour avancer dans ce combat. Nous avons, à titre de scientifiques, le grand privilège de pouvoir les utiliser. Chaque petit grain d'idée que nous apportons, chaque petit grain de faits que nous confirmons et chaque individu qui en profitera, sont pour nous une source de gratification qui n'a d'autre mesure. Aujourd'hui, cher lecteur, j'aimerais vous présenter en toute humilité ce petit grain de sable, que j'ai eu le privilège de déposer au sein de ce tout qui nous fait tant espérer.

1. Introduction

1.1 Introduction au cancer

1.1.1 L'origine du cancer

Le comportement des cellules au sein d'un organisme dépend d'un réseau complexe de signaux intra et intercellulaires. Ce réseau assure une coordination des fonctions et de la destinée des différentes cellules, et il s'avère essentiel au bon fonctionnement de l'organisme. L'information qui dicte le maintien de cette homéostasie se trouve encodée dans le génome. Par conséquent, les mutations que subissent chaque jour de nombreuses cellules du corps humain sont susceptibles de rompre l'équilibre en place. L'ADN est une vaste molécule et la plupart des mutations sont distribuées de façon plus ou moins aléatoire. Dans la grande majorité des cas, les mutations ont peu d'effets, voire aucun effet, survenant dans une région silencieuse du génome ou ne changeant pas l'identité du message qui s'y trouve. D'autres mutations peuvent affecter une fonction critique à la survie cellulaire, conduisant à la mort de la cellule. Enfin, certaines peuvent conférer un comportement invasif à une cellule, initiant ainsi le processus de la transformation maligne, laquelle est à l'origine du développement d'un cancer (1).

Le caractère génétique du cancer a émergé au début du XIX^{e} siècle lorsque Theodor Boveri a proposé que cette maladie découle d'anomalies chromosomiques (2, 3). Depuis, selon une logique darwinienne, Peter Nowell a énoncé le modèle de l'évolution clonale du cancer (4). La transformation d'une cellule normale à l'état tumoral a été décrite comme étant un processus progressif, nécessitant l'accumulation de plusieurs défauts génétiques. Ces derniers sont en partie le résultat de l'infidélité intrinsèque de la machinerie de réplication de l'ADN, qui est mise à profit lors de la prolifération cellulaire (5, 6). Ils sont aussi une conséquence des bris de l'ADN imposés par des facteurs mutagènes de l'environnement et de l'interaction de l'ADN avec des agents réactifs dérivés du métabolisme cellulaire. Enfin, ils peuvent être favorisés par des défauts au niveau des mécanismes de réparation de l'ADN (5, 6). Les aberrations génétiques ainsi induites sont également de nature variée, incluant : la substitution de nucléotides dans l'ADN; l'insertion ou la délétion de fragments d'ADN; les réarrangements chromosomiques; l'augmentation ou la réduction du nombre de copies d'un gène; et l'insertion d'ADN viral (7, 8). Ces défauts s'additionnent aux altérations épigénétiques qui, sans affecter l'intégrité de la molécule d'ADN, affectent l'expression du

génome (9, 10). Selon le modèle de l'évolution clonale du cancer, ces diverses altérations génomiques doivent avoir un point en commun, soit de conférer un avantage sélectif à une cellule par rapport aux cellules environnantes. Ainsi, à l'image du processus de la sélection naturelle, cette cellule pourra se diviser plus vigoureusement que les autres, ce qui cause la propagation de l'altération génomique au sein d'une lignée cellulaire dite clonale (11, 12). Chaque cellule fille peut ensuite subir de nouvelles mutations génétiques ou modifications épigénétiques. Il en résulte une population cellulaire hétérogène où la pression de sélection propre au microenvironnement d'un tissu donné favorise les cellules avec le plus grand potentiel prolifératif (12). Ainsi, au cours de la vie d'un individu et au sein d'une même lignée cellulaire, l'acquisition d'une combinaison fortuite et unique de perturbations génomiques peut aboutir à la transformation maligne.

1.1.2 La progression tumorale

Le modèle de l'évolution clonale du cancer se reflète au niveau histologique. Bien que l'identification de la nature exacte de la cellule d'origine d'un cancer est une tâche à laquelle nous ne parvenons toujours pas (13), la caractérisation de lésions macroscopiques a été informative afin de comprendre l'évolution de la maladie. En règle générale, les cellules portant les premières anomalies génomiques favorisant le cancer prolifèrent afin de former des lésions précancéreuses (12). La progression des tumeurs ainsi formées, qualifiées de bénignes, est alors limitée par des processus de suppression tumorale (14), dont nous discuterons ultérieurement dans le présent ouvrage. Suite à une période de latence souvent prolongée, de nouvelles anomalies génomiques au sein des cellules précancéreuses peuvent initier la transformation maligne et, par conséquent, entraîner une progression vers le stade de tumeur maligne non invasive (tumeur *in situ*) (12). Toujours selon la même logique, de nouvelles anomalies permettent de gagner en agressivité. Une tumeur acquiert ainsi la capacité d'envahir les tissus environnants et de métastaser. Cet état est donc l'aboutissement d'une accumulation progressive et généralement lente de propriétés conférant un avantage prolifératif (14). En bref, ces propriétés incluent une insensibilité aux signaux normaux de restriction de la

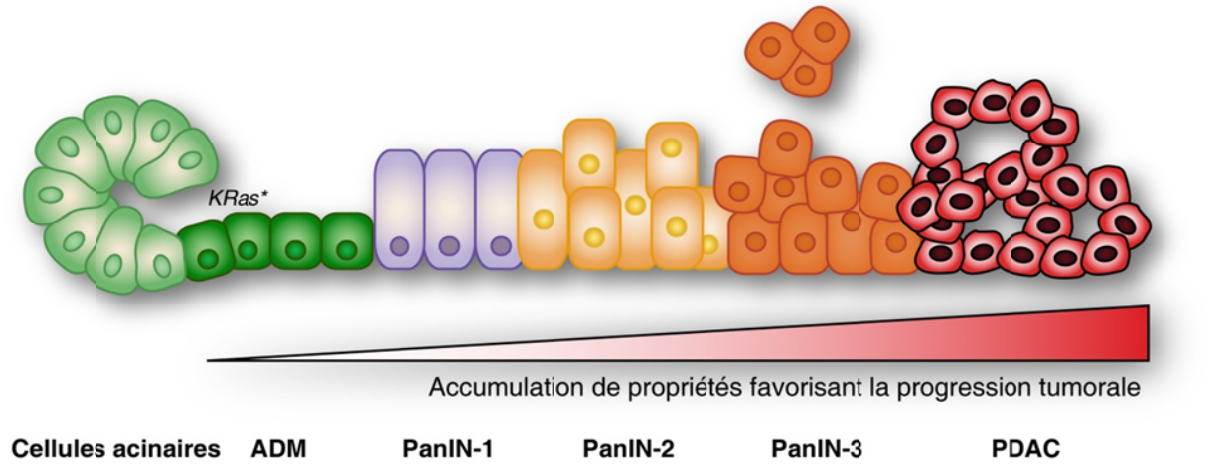

Figure 1. Modèle de la progression tumorale lors de l'initiation du PDAC
L'initiation d'un adénocarcinome canalaire pancréatique (PDAC) suit une succession d'étapes bien définies. Les premières cellules acinaires s'étant multipliées suite à l'acquisition d'un défaut génétique procancéreux subissent une métaplasie vers un état semblable aux cellules canalaires (*acinar-to-ductal metaplasia*; ADM). L'acquisition de défauts génétiques et/ou épigénétiques supplémentaires permettent une progression à travers d'autres stades précancéreux, à savoir les néoplasies intraépithéliales pancréatiques (*pancreatic intraepithelial neoplasia*; PanIN) de type 1 et de type 2. Lorsque les conditions sont rencontrées, la transformation maligne survient et permet l'établissement d'une tumeur *in situ* (PanIN-3) qui peut progresser vers une tumeur invasive (PDAC).

prolifération cellulaire combinée à une stimulation constitutive du processus, une résistance aux mécanismes de suppression tumorale, la capacité d'induire l'angiogenèse et enfin, le pouvoir de coloniser des tissus normalement réservés à d'autres cellules (14).

La progression tumorale séquentielle décrite ci-haut est particulièrement vraie en ce qui concerne les cancers solides. Nous pouvons à titre d'exemple citer l'adénocarcinome canalaire pancréatique (*pancreatic ductal adenocarcinoma*; PDAC), pour lequel ces étapes sont assez bien caractérisées (Figure 1) (15-22). En général, elles impliquent une succession de lésions précancéreuses. Plus précisément, les cellules acinaires du pancréas exocrine qui acquièrent les premières anomalies génomiques subissent une métaplasie vers des cellules canalaires (*acinar-to-ductal metaplasia*; ADM) (16-18). Ces lésions évoluent vers l'état de néoplasie intraépithéliale pancréatique (*pancreatic intraepithelial neoplasia*; PanIN) de type 1, puis de type 2. Ces types de PanIN sont peu prolifératifs et se distinguent par une désorganisation tissulaire plus prononcée pour le type 2 (19, 20). Enfin, la transformation

maligne permet la progression vers le stade de PanIN de type 3, qui correspond à un carcinome *in situ* (19, 20). L'acquisition subséquente de la capacité d'invasion tissulaire provoque la transition vers le PDAC (21, 22), qui représente de loin la forme la plus commune et mortelle des cancers pancréatiques (23, 24).

1.2 Les oncogènes

1.2.1 Mise en contexte

Parmi les altérations génétiques que doit subir une cellule durant le processus de la sélection clonale, certaines affectent des régulateurs positifs de la prolifération. En d'autres mots, des modifications du génome peuvent conduire à l'hyperactivation des fonctions de certains gènes, les proto-oncogènes, qui assurent l'exécution des signaux mitogéniques. L'existence de tels gènes mutés engendrant l'expression de protéines hyperactives, alors qualifiés d'oncogènes, a d'abord été montrée à l'intérieur de génomes viraux. En effet, *v-src* est le tout premier oncogène à avoir été identifié en 1970 par Peter Duesberg et Peter Vogt (25, 26). Sa séquence, qui confère le pouvoir transformant au Rous sarcoma virus (RSV), a ensuite été identifiée comme étant homologue à un gène au sein de l'ADN normal de l'hôte (27). Cette découverte de Vogt *et al.* a ainsi pavé la voie à la notion de proto-oncogènes à titre de précurseurs des oncogènes. Finalement, ce n'est qu'en 1982 que le premier oncogène humain, *RAS (Rat sarcoma viral oncogene homolog),* a été isolé et caractérisé grâce aux travaux conjoints des laboratoires de Robert Weinberg, Michael Wigler, Mariano Barbacid et Geoffrey Cooper (28-39). La découverte du potentiel oncogénique de *MYC* a rapidement suivi (40-42), et depuis, plus d'une quarantaine d'oncogènes ont été confirmés chez l'humain (43).

1.2.2 L'exemple de l'oncogène *RAS*

Les travaux que nous aborderons dans le présent ouvrage sont particulièrement pertinents en ce qui concerne le rôle de l'oncogène *RAS* dans la transformation maligne. Celui-ci est retrouvé dans environ 30% de tous les cancers humains, ce qui en fait l'oncogène le plus commun (44). En outre, son rôle semble particulièrement déterminant quant à l'initiation des PDAC puisqu'il s'y retrouve à une fréquence d'environ 95% des cas (22, 45).

Il existe 4 isoformes du proto-oncogène *RAS*, généralement désignées sous trois appellations, à savoir *NRAS*, *HRAS* et *KRAS* (regroupant les isoformes 4A et 4B) (28, 44). Les 85 premiers acides aminés sont identiques pour toutes les isoformes. Ils contiennent un site de liaison au GTP (la boucle P), ainsi que les éléments nécessaires aux interactions avec les régulateurs et les effecteurs de la protéine (les motifs Switch I et II) (44). Conséquemment, la régulation de l'activité des différentes protéines RAS s'effectue de manière très similaire. Localisées au niveau de différents compartiments membranaires, mais principalement recrutées à la membrane plasmique (46), les protéines RAS répondent à divers signaux extracellulaires suite à l'activation de récepteurs à la surface cellulaire (28, 47). Elles sont de petites GTPases monomériques qui se retrouvent sous une conformation active lorsque liées au GTP et inactive lorsque liées au GDP (Figure 2) (47). L'activation d'un récepteur membranaire, par exemple un récepteur tyrosine kinase (RTK), assure le recrutement de protéines adaptatrices et de facteurs d'échange du nucléotide guanine (*guanine nucleotide exchange factors*; GEF), tels que SOS (*son of sevenless homologue*), les RASGRFs (*RAS protein-specific guanine nucleotide-releasing factors*) et les RASGRPs (*RAS guanyl releasing proteins*) (28, 47). Ces facteurs permettent l'élimination du GDP et, par conséquent, l'activation de la protéine RAS par la liaison passive au GTP qui se trouve en abondance dans le cytoplasme (Figure 2) (47, 48). À l'inverse, les protéines activatrices des GTPases (*GTPase-activating proteins*; GAP), comme NF1 (*neurofibromin 1*), stimulent l'hydrolyse du GTP afin de mettre fin à l'activation des protéines RAS (Figure 2) (47, 48).

Les substitutions d'acides aminés qui interfèrent avec l'hydrolyse du GTP sont les principales causes expliquant l'activation oncogénique des protéines RAS. Ainsi, une substitution au niveau des résidus glycine 12 et 13 (G12, G13) prévient le changement de conformation normalement imposé lors de l'interaction avec les GAP, ce qui se solde par une diminution prononcée de l'hydrolyse du GTP. De plus, une substitution de la glutamine 61 (Q61) affecte la capacité intrinsèque des protéines RAS à hydrolyser le GTP (49). Les protéines mutantes demeurent donc liées au GTP, ce qui conduit à une activation aberrante des voies de signalisation en aval.

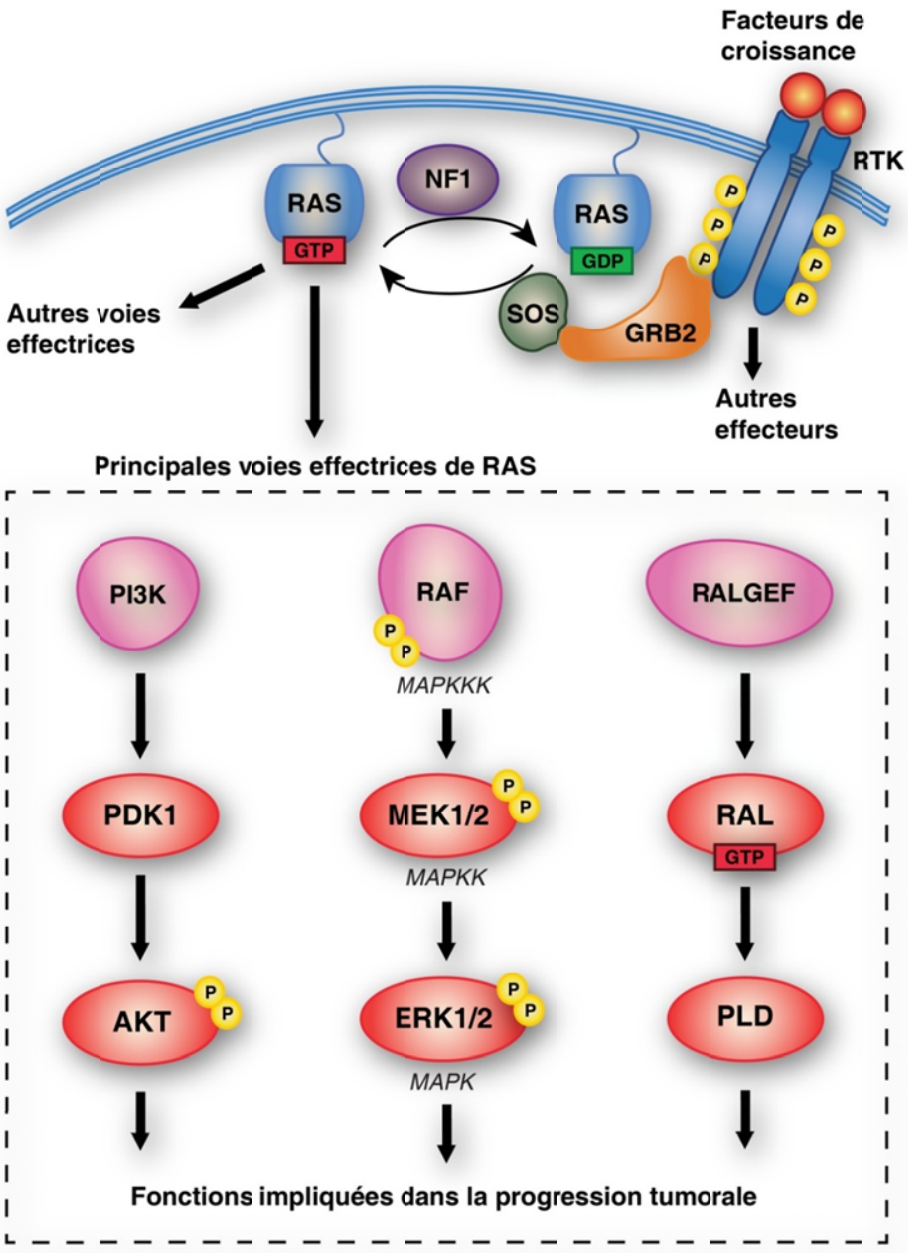

Figure 2. La transduction des signaux par les GTPases RAS

Les protéines RAS permettent la transduction du signal acheminé par divers facteurs extracellulaires, tels que les facteurs de croissance. Suite à l'activation d'un récepteur membranaire, par exemple un récepteur tyrosine kinase (RTK), un complexe adaptateur se forme et permet le recrutement d'un facteur d'échange du nucléotide guanine (GEF), comme une protéine SOS. Celui-ci permet l'activation d'une GTPase RAS en favorisant l'échange d'un GDP par un GTP. RAS active alors plusieurs voies de signalisation afin de réguler une multitude de processus cellulaires. Les mieux caractérisées sont représentées, soit les voies ERK/MAPK, PI3K/AKT et RALGEFs/RAL. Les protéines RAS sont inactivées suite à l'hydrolyse du GTP, une réaction qui est favorisée par l'interaction avec une protéine activatrice des GTPases (GAP), telle que NF1. P, phosphorylation.

Bien que des fonctions non redondantes ont été suggérées pour les différentes isoformes de RAS (50), elles ont la caractéristique commune de réguler une multitude de processus cellulaires via l'activation de nombreuses voies de signalisation (Figure 2) (28, 49). Parmi celles-ci, les mieux caractérisées sont la voie ERK/MAPK (*extracellular signal-regulated kinase/ mitogen-activated protein kinase*), la voie PI3K/AKT (*phosphoinositide 3 - kinase/ Ak strain transforming*) et la voie RALGEFs/RAL (*guanine nucleotide exchange factors of the RAS-like small GTPases*/ *RAS-like protein*) (Figure 2) (28). Ces trois voies de signalisation ont des rôles établis dans la transformation maligne ainsi que dans la progression tumorale, mais nos travaux porteront une attention particulière sur la voie ERK/MAPK. Pour cette raison, une revue de la littérature sur cette voie de signalisation est disponible un peu plus loin.

1.3 La suppression tumorale

1.3.1 Les gènes suppresseurs de tumeurs

Le processus de la sélection clonale ne favorise pas uniquement les cellules portant des mutations oncogéniques. Il sélectionne tout aussi bien les événements génétiques qui conduisent à la perte de mécanismes freinant la transformation maligne (51). Précisons que dans ce cas, contrairement aux oncogènes, c'est l'inactivation de la fonction d'un gène qui confère l'avantage sélectif. Ces gènes qui s'opposent au cancer, ainsi qualifiés de gènes suppresseurs de tumeurs, se regroupent en deux grandes familles (52-54). La première, les gènes de maintenance (*caretakers*), inclut les gènes responsables du maintien de l'intégrité du génome (55). Ces gènes assurent la stabilité génomique et la réparation de l'ADN endommagé afin d'éviter une accumulation accélérée de mutations et, conséquemment, un risque accru de cancer. Ils jouent donc un rôle préventif de premier plan en limitant la cause moléculaire du cancer, c'est-à-dire l'accumulation de défauts génétiques. Cependant, l'activation de tels gènes au sein de cellules cancéreuses ne peut renverser le phénotype tumoral. Les gènes *BRCA1/2* (*breast cancer 1 and 2*) et *ATM* (*ataxia telangiectasia mutated*) sont des exemples classiques du groupe des gènes de maintenance (55). La seconde famille, les gènes garde-barrières (*gatekeepers*), concerne plutôt les gènes qui assurent un contrôle négatif de la prolifération et qui permettent les processus de mort cellulaire (52, 54). La perte de tels gènes confère

directement un avantage prolifératif qui contribue à la progression tumorale. Conséquemment, leur réactivation dans les cellules cancéreuses limite, voire renverse, le phénotype tumoral. C'est à ce groupe qu'appartiennent les gènes suppresseurs de tumeurs *TP53* (*tumor protein p53*) (56), *RB* (*retinoblastoma protein*) (57) et *PTEN* (*phosphatase and tensin homolog*) (58).

1.3.2 Les mécanismes de suppression tumorale

Les cellules subissent plusieurs stress inhérents à leur fonctionnement, tels que le raccourcissement des télomères et le stress oxydatif. De plus, elles sont exposées à une multitude de stress environnementaux, tels que certains virus, différentes formes de radiations et des carcinogènes chimiques. Ces stress peuvent endommager l'ADN et, en conséquence, favoriser l'apparition des mutations requises pour la transformation maligne (59, 60). Néanmoins, l'évolution a permis la sélection de mécanismes de défense afin de restreindre l'accumulation de telles mutations. Ces mécanismes sollicitent les gènes suppresseurs de tumeurs pour rétablir l'intégrité du bagage génétique, voire induire un arrêt transitoire de la prolifération afin d'octroyer le temps nécessaire aux cellules pour réparer les dommages subis et éviter une propagation de cellules mutantes (59, 60). Cependant, si les dommages sont trop importants et que l'état normal des cellules est compromis, par exemple suite à l'activation d'un oncogène, des mécanismes de suppression tumorale visant à bloquer de façon permanente la prolifération cellulaire sont engagés. Il s'agit soit de l'apoptose ou de la sénescence cellulaire (53, 59). Les gènes suppresseurs de tumeurs *RB* et *TP53* jouent des rôles clefs dans la mise en place de telles défenses (56, 57, 60). La fréquence de leur inactivation dans les cancers humains souligne d'ailleurs leur importance dans la suppression tumorale (57, 61, 62). À titre d'exemple, les mutations qui inactivent *TP53*, aussi nommé le gardien du génome, sont trouvées dans plus de 50% de tous les cancers humains, ce qui en fait l'altération génétique la plus commune (61, 62). L'induction de l'apoptose, qui implique principalement *TP53*, vise l'élimination des cellules anormales. En bref, elle correspond à une mort cellulaire programmée, à l'image d'un suicide cellulaire. Elle se distingue de la nécrose par le fait qu'elle s'effectue d'une façon à prévenir les dommages aux cellules avoisinantes (61). Étant donné l'importance de la sénescence cellulaire au sein des travaux présentés dans cette thèse, nous y apporterons une attention plus approfondie dans les sections qui suivent.

1.3.3 La sénescence cellulaire

La notion de sénescence cellulaire a été introduite par Hayflick en 1965 suite à l'observation d'un arrêt de la prolifération des fibroblastes humains normaux ayant subi de nombreux cycles de division en culture (63, 64). Elle avait alors été définie comme étant une perte stable et à long terme de la capacité de prolifération, malgré le maintien de la viabilité et de l'activité métabolique (64). Ce n'est que plusieurs années plus tard, en 1990, que la cause moléculaire de ce phénotype a été identifiée. L'arrêt de la prolifération cellulaire est associé à l'érosion des télomères au fil des cycles de réplication de l'ADN, résultant de l'incapacité de l'ADN polymérase à répliquer complètement les extrémités des chromosomes (65). De plus, les cellules somatiques humaines n'expriment pas la télomérase et, en conséquence, ne peuvent pas allonger leurs télomères pour compenser cette incapacité de l'ADN polymérase (66-68). Ainsi, les télomères raccourcissent à chaque cycle de division cellulaire, jusqu'à l'atteinte d'une limite, appelée la limite de Hayflick, où la cellule ne peut plus continuer à proliférer (64, 67). Cet état cellulaire est maintenant connu sous le nom de sénescence réplicative.

Divers stress en mesure d'induire la sénescence cellulaire autres que le raccourcissement des télomères ont été identifiés, ce qui permet aujourd'hui de distinguer différentes classes de sénescence (67, 69, 70). Le phénotype sénescent imposé par ces stress est alors qualifié de sénescence prématurée puisqu'elle survient avant l'atteinte de la limite de Hayflick. Ce qualificatif couvre large et peut être sous-divisé en deux grands types de sénescence selon la source du stress (67). Tout d'abord, la sénescence induite par le stress fait référence au phénotype sénescent engendré par les stress environnementaux, tels que des conditions de culture inadéquates, le stress oxydatif et les agents qui endommagent l'ADN. La sénescence induite par les oncogènes (*Oncogene-induced senescence*; OIS) qualifie plutôt les cellules dont l'entrée en sénescence est provoquée par l'activation d'un oncogène ou la perte d'un suppresseur de tumeur (67, 69).

La grande majorité des connaissances que nous possédons sur les cellules sénescentes découlent de travaux sur des cellules en culture. Un questionnement sur la pertinence *in vivo* du phénotype a donc longtemps perduré. Cependant, au cours des dernières années, plusieurs

rapports ont montré son importance *in vivo* et ont identifié une série de modèles permettant de l'étudier (71-73). Chez l'humain, les cellules sénescentes ont été identifiées dans divers tissus, surtout ceux possédant une capacité de régénération (72) ou certaines hyperplasies bénignes, telle que l'hyperplasie bénigne de la prostate (*benign prostatic hyperplasia*; BPH) (74, 75). En accord avec la notion de sénescence réplicative, ces cellules s'accumulent dans les tissus âgés et plusieurs montrent des défauts au niveau de leurs télomères (72, 76, 77) et ce, autant chez l'humain que la souris (78, 79). Appuyant l'importance de l'OIS à titre de mécanisme antitumoral, les cellules sénescentes ont aussi été identifiées dans une série de lésions prénéoplasiques humaines portant des mutations oncogéniques, comme les neavi mélanocytaires (71, 80). Des cellules sénescentes ont aussi été rapportées au niveau de lésions prémalignes qui résultent de l'activation d'oncogènes au sein de modèles murins (71), tels que dans les PanIN (81) et les adénomes pulmonaires (82). Enfin, l'inactivation de régulateurs importants de la sénescence, comme TP53 et $p16^{INK4A}$, facilite la transformation maligne par les oncogènes *in vivo* (71, 83-88), alors que la réactivation de tels régulateurs peut induire la sénescence au sein de tumeurs malignes (89, 90). Confronté à l'ensemble de ces observations, le rôle que joue la sénescence cellulaire dans la suppression tumorale apparaît maintenant bien établi.

1.3.4 Les caractéristiques et mécanismes effecteurs de la sénescence

Les cellules sénescentes se caractérisent par un large éventail de biomarqueurs et de mécanismes effecteurs qui peuvent varier selon la cause du phénotype et le type cellulaire (Figure 3). Outre cette hétérogénéité, les marqueurs de la sénescence ne sont généralement pas spécifiques à cet état cellulaire (67, 73). Pour ces raisons, la définition exacte de la sénescence est parfois ambiguë et l'étude du phénotype requiert l'analyse d'une combinaison de caractéristiques attribuables aux cellules sénescentes. Parmi celles-ci, l'arrêt permanent de la prolifération, dû à un blocage en phase G1 du cycle cellulaire, est considéré comme la caractéristique au centre de la définition de la sénescence cellulaire (67). C'est d'ailleurs l'arrêt permanent en phase G1 du cycle cellulaire qui distingue la sénescence de l'état de quiescence, lequel correspond plutôt à un arrêt réversible qualifié de retrait en phase G0 (69).

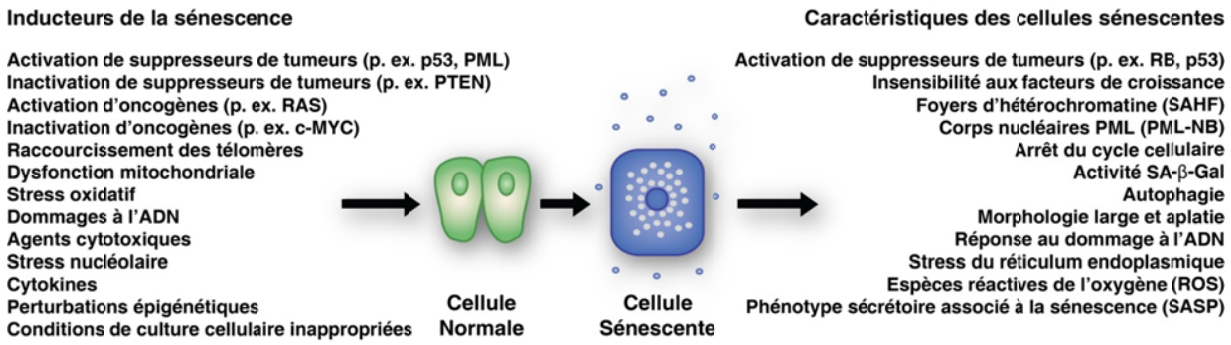

Figure 3. Inducteurs et caractéristiques de la sénescence cellulaire

La sénescence cellulaire est un phénotype complexe aux multiples facettes. La figure résume les principaux stress connus pour induire ce phénotype et les principales caractéristiques des cellules sénescentes (67, 73). Il est à noter que ces propriétés ne sont pas exclusives aux cellules sénescentes ni universelles. Un type de sénescence se caractérise donc par une combinaison donnée de ces marqueurs.

Les cellules sénescentes se caractérisent ensuite par une série de changements morphologiques, incluant un aspect élargi et aplati, ainsi qu'une apparence souvent multinuclée. Dans le cas de la sénescence induite par l'oncogène *RAS* se retrouve également une accumulation de nombreuses vacuoles (67, 91).

À ces changements s'ajoute une activité β-galactosidase lysosomiale élevée qui résulte de l'augmentation de l'expression du gène *GLB1* (*galactosidase, beta 1*) (76, 92, 93). Cette propriété est appelée l'activité β-galactosidase associée à la sénescence (*senescence-associated beta-galactosidase*; SA-β-Gal). La mesure de l'activité SA-β-Gal est couramment utilisée puisqu'elle permet une identification simple et rapide des cellules sénescentes. En effet, celles-ci sont en mesure d'hydrolyser le X-Gal (5-bromo-4-chloro-3-indolyl-β-D-galactopyranoside) en un précipité bleu insoluble (5,5'-dibromo-4,4'-dichloro-indigo) à un pH acide sous-optimal (pH 6,0), ce qui leur confère une coloration bleue (76, 94). L'activité SA-β-Gal n'est pas requise pour la sénescence, mais pourrait être le reflet d'une augmentation de l'autophagie puisque celle-ci requiert la fonction des lysosomes (73, 95). Un nombre croissant d'observations indiquent que l'autophagie est associée à la sénescence cellulaire et qu'elle pourrait y jouer un rôle important (73). À titre d'exemple, le laboratoire de Masashi Narita a démontré que son inhibition retardait l'établissement du phénotype sénescent (96). Nous approfondirons ce sujet dans l'article 2 du chapitre 2 de cette thèse (97).

Les autres caractéristiques des cellules sénescentes incluent la formation de foyers d'hétérochromatine associés à la sénescence (*senescence-associated heterochromatic foci*; SAHF) (98, 99), de même que des corps nucléaires PML (*promyelocytic leukemia protein*) (100-102). Les deux structures jouent un rôle important dans l'inhibition de l'expression des gènes permettant la progression du cycle cellulaire, tels que les gènes cibles des facteurs de transcription E2F (*E2 promoter binding factors*) (98, 103). D'ailleurs, une accumulation d'observations suggère un lien étroit entre les deux structures. Plus précisément, les corps nucléaires de PML pourraient servir de site où la formation des SAHF est initiée. Effectivement, les travaux du laboratoire de Peter D. Adams ont montré que la translocation de la protéine HIRA (*histone repressor A*) via les corps nucléaires PML est requise pour la formation des SAHF (99, 104). Ceci s'ajoute au fait que les corps de PML contiennent des médiateurs de l'hétérochromatine, comme la protéine de l'hétérochromatine 1 (*heterochromatin protein 1*; HP1) (99, 105) et des histones déacétylases (HDAC) (106). De plus, la protéine PML interagit avec le complexe formé du suppresseur de tumeur RB et des E2F (103, 107), suggérant son recrutement au niveau du promoteur des gènes cibles des E2F. Il faut savoir que les SAHF se forment au niveau du promoteur de ces gènes lors du recrutement de RB (98).

Un autre aspect des cellules sénescentes consiste en d'importants changements métaboliques (73). Outre la dégradation des protéines par autophagie, le métabolisme mitochondrial semble jouer un rôle clef. Cependant, les changements observés peuvent sembler contradictoires. En effet, des études récentes ont rapporté qu'une augmentation du métabolisme oxydatif serait essentielle à l'établissement du phénotype sénescent (108, 109). À l'opposé, des études antérieures ont montré une dysfonction des mitochondries dans les cellules sénescentes (110, 111). Ces différences pourraient s'expliquer par des systèmes expérimentaux divergents ou l'analyse de la sénescence à des temps distincts. Néanmoins, il y a un point de convergence pour toutes ces études; dans tous les cas, une augmentation de la production d'espèces réactives de l'oxygène (*reactive oxygen species*; ROS) est détectée (108-111), lesquelles sont connues pour contribuer à l'initiation de la sénescence (110, 112, 113).

Les ROS participent à l'établissement de la sénescence, du moins en partie, de par les dommages à l'ADN qu'ils imposent (110, 114). Lors de l'OIS, ces dommages s'additionnent à ceux produits par le stress réplicatif, qui consiste en l'accumulation d'intermédiaires de réplication incomplets suite à une hyperstimulation de la réplication de l'ADN par les oncogènes (115, 116). Ainsi, dans plusieurs types de sénescence, les cellules accumulent les brisures au sein de l'ADN et ne parviennent pas à réparer les dommages infligés. Ce phénomène est observable par la formation de nombreux foyers de dommage à l'ADN, caractérisés par une accumulation de protéines telles que le variant de l'histone H2A phosphorylé γH2AX (*H2A histone family, member X - phosphorylated*), la protéine 53BP1 (*p53-binding protein 1*) et la protéine ATM phosphorylée. Les cellules subissent alors une réponse au dommage à l'ADN (*DNA damage response*; DDR) permanente (73). Dans ces types de sénescence, incluant différents cas d'OIS et la sénescence réplicative, la DDR a été montrée comme étant un mécanisme contribuant significativement à l'arrêt du cycle cellulaire (115-124).

L'impact de la DDR sur le cycle cellulaire implique principalement l'activation du suppresseur de tumeur TP53, aussi nommé p53. Ce facteur de transcription induit l'expression de différents gènes ayant des rôles établis dans la sénescence cellulaire, tels que PML (100, 125), PAI-1 (*plasminogen activator inhibitor-1*) (126), GADD45a (*growth arrest and DNA damage-inducible 45a*) (127), DEC1 (*Deleted in esophageal cancer 1*) (128) et E2F7 (129). Cependant, l'induction de l'inhibiteur des CDK (*cyclin-dependent kinase inhibitor*; CDKI) $p21^{CIP1}$, aussi appelé CDKN1A (*cyclin-dependent kinase inhibitor 1A*), est probablement le mécanisme le mieux décrit afin d'expliquer le rôle de p53 dans l'arrêt du cycle cellulaire associé à la sénescence (130-132). En plus de $p21^{CIP1}$, un autre CDKI, mais régulé de manière indépendante de p53, est fréquemment induit dans les cellules sénescentes, à savoir la protéine $p16^{INK4A}$ (*cyclin-dependent kinase inhibitor 2A*; CDKN2A) (133). Ces CDKI convergent vers un même mécanisme qui consiste en l'inhibition des CDK (*cyclin-dependent kinase*) (73). Lors de la phase G1 du cycle cellulaire, les CDK (principalement 4 et 6) forment des complexes avec les cycles de type D. Ces complexes assurent la phosphorylation de RB sur plusieurs résidus et, par conséquent, conduisent à son inactivation (134, 135). Cependant, lorsque les CDK sont inactivées par $p21^{CIP1}$ ou $p16^{INK4A}$, RB demeure actif et est en mesure d'interagir avec les facteurs de transcription E2F pour empêcher l'induction de leurs gènes

cibles. Puisque l'activité transcriptionnelle des E2F est requise pour l'entrée en phase S, le cycle cellulaire est alors bloqué en phase G1 (134, 135).

Considérant l'ensemble des mécanismes contribuant à la sénescence cellulaire, il est évident qu'elle implique des changements profonds au niveau du patron d'expression des gènes. Malgré le fait que les changements observés varient grandement d'un type cellulaire à l'autre (136, 137), certaines signatures caractérisant les cellules sénescentes ont été mises au jour. Entre autres, la répression d'un groupe de gènes associés à la progression du cycle cellulaire est unique à la sénescence, ce qui permet de la distinguer de la quiescence (138). De plus, diverses analyses ont révélé une forte expression des gènes pro-inflammatoires, particulièrement ceux sous le contrôle du facteur de transcription NF-κB (*nuclear factor kappa-light-chain-enhancer of activated B cells*) (136, 139-141). Ce dernier aspect est particulièrement important en ce qui concerne le rôle de la sénescence cellulaire dans la physiopathologie de plusieurs contextes. Nous y consacrerons donc la prochaine section.

1.3.5 Le phénotype sécrétoire associé à la sénescence cellulaire

La capacité des cellules sénescentes à sécréter une variété de protéines, principalement des cytokines, des chimiokines et des protéases, est reconnue depuis longtemps (73, 139, 142, 143). Ce phénotype sécrétoire associé à la sénescence (*senescence-associated secretory phenotype*; SASP) résulte de l'activation d'un réseau de signalisation complexe qui converge principalement vers l'activation des facteurs de transcription NF-κB et C/EBPβ (*CCAAT-enhancer-binding proteins beta*) (73, 140, 144, 145). Les protéines alors induites et sécrétées peuvent influencer le comportement des cellules environnantes et contribuer à la physiopathologie de diverses maladies. Cependant, son rôle peut être très diversifié, pouvant être bénéfique ou délétère pour l'organisme, selon le contexte dans lequel il est impliqué et l'identité de la cellule sur laquelle il agit (Figure 4) (72, 146, 147).

Tout d'abord, le SASP peut être bénéfique en contribuant à la suppression tumorale. Certaines cytokines peuvent renforcer le phénotype sénescent par un processus autocrine (144, 145, 148), voire propager la sénescence aux cellules environnantes via un processus paracrine

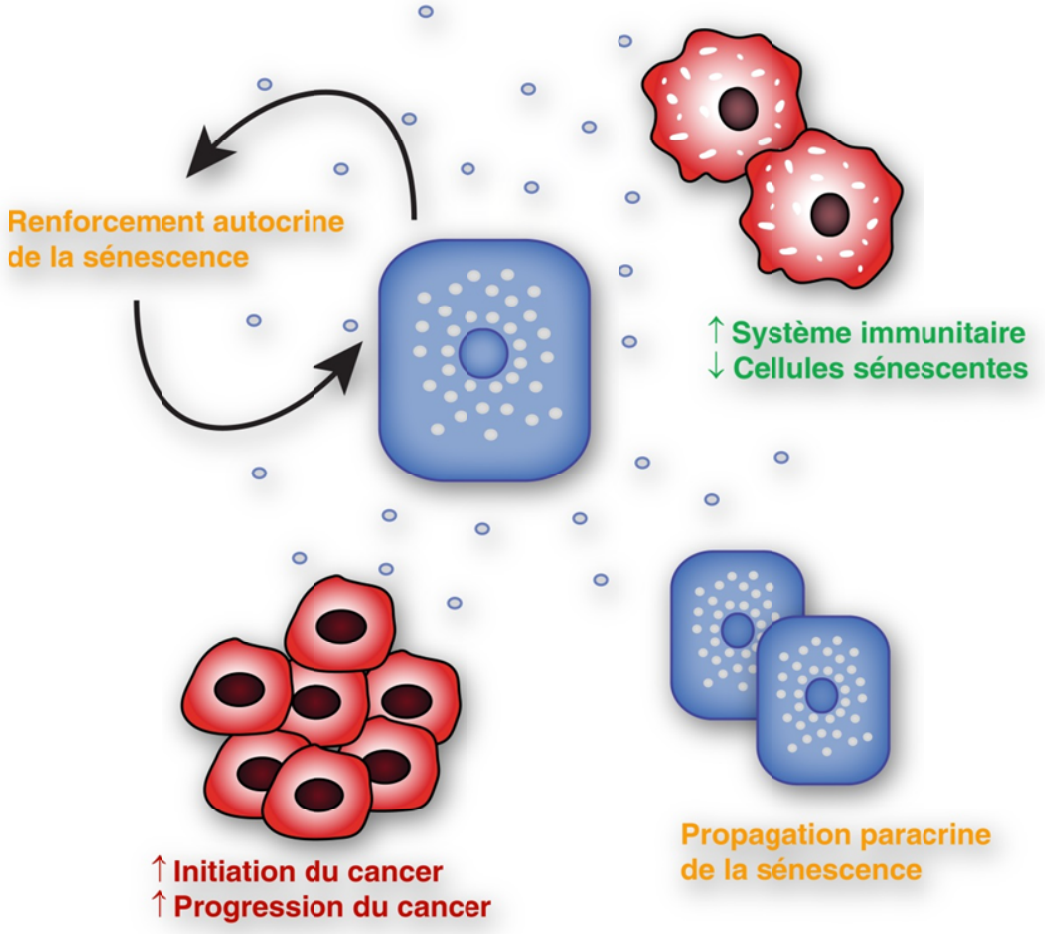

Figure 4. Effet du phénotype sécrétoire associé à la sénescence (SASP)
Le SASP a des effets à la fois procancéreux (identifiés en rouge) et antitumoraux (identifiés en vert). En effet, le SASP active le système immunitaire, ce qui permet l'élimination des cellules sénescentes. D'un autre côté, il favorise la transformation maligne et la prolifération des cellules cancéreuses. Il permet également un renforcement autocrine de la sénescence et la propagation du phénotype à d'autres cellules par une signalisation paracrine. Étant donné les bénéfices et les effets délétères du SASP, sa contribution à la sénescence est perçue comme bonne ou mauvaise selon le contexte (identifications en jaune).

(Figure 4) (149, 150). Ceci pourrait donc contribuer à la robustesse de l'arrêt prolifératif au niveau d'une lésion précancéreuse. De plus, le SASP favorise le recrutement de cellules spécialisées du système immunitaire, comme les cellules NK (*natural killer*), les lymphocytes T $CD4^+$ et les macrophages de type M1 (Figure 4). Conséquemment, ces cellules permettent l'élimination des cellules sénescentes (89, 151-154). Une telle fonction pourrait, au même titre

que l'apoptose, être d'une grande importance afin d'éliminer les cellules portant des anomalies procancéreuses.

Malgré les fonctions bénéfiques du SASP que nous venons de présenter, son effet est tout autre lorsqu'il agit sur des cellules cancéreuses ou ayant déjà franchi certaines étapes clefs dans le processus de la sélection clonale. En effet, certaines cytokines favorisent la prolifération des cellules cancéreuses et peuvent contribuer au processus de la transformation maligne, stimulant ainsi la progression tumorale (Figure 4) (72, 147, 155-157). De plus, certaines protéines sécrétées modifient l'intégrité des tissus environnants et créent un microenvironnement propice à l'angiogenèse et à l'invasion (72, 139, 147, 158).

Outre le rôle protumoral que peut jouer le SASP, il pourrait aussi contribuer à la physiopathologie du vieillissement (72, 159). Depuis longtemps, la sénescence cellulaire est suspectée de contribuer au vieillissement des organismes, du moins aux pathologies qui lui sont associées (160, 161). Certaines études ont d'ailleurs apporté un appui à cette hypothèse. Par exemple, les populations de diverses cellules progénitrices déclinent avec l'âge et ce phénomène dépend de l'activation du facteur prosénescence $p16^{INK4A}$ (162-164). De même, une déficience en $p16^{INK4A}$ ou l'élimination des cellules sénescentes au sein de modèles murins atténuent le vieillissement des tissus, voire prolongent la durée de vie (165, 166). En plus de compromettre la capacité régénérative des tissus par la diminution du réservoir de cellules progénitrices, la sénescence pourrait participer au vieillissement en créant un contexte inflammatoire pathologique (72, 159). L'inflammation chronique contribue en effet à plusieurs pathologies associées au vieillissement, telles que l'athérosclérose, arthrose et le diabète (72, 167, 168). Une activation anormale des cellules du système immunitaire au cours du vieillissement explique en partie l'inflammation chronique. Cependant, une augmentation de la sécrétion de cytokines pro-inflammatoires par le SASP, due à une accumulation de cellules sénescentes au fil du temps, pourrait aussi contribuer au contexte inflammatoire (72, 76, 77, 161). Il est d'ailleurs à noter que la présence de cellules sénescentes est souvent observée aux sites associés aux pathologies en question (72, 169-171).

En résumé, la sénescence, et particulièrement le SASP, apparaissent comme des armes à double tranchant (Figure 4). Bien qu'ils puissent protéger l'organisme à court terme grâce à

leur rôle antitumoral, une accumulation de cellules sénescentes avec le temps pourrait devenir néfaste pour l'organisme. Est-ce qu'il s'agirait d'un exemple de la pléiotropie antagoniste (172-174), qui stipule que la sélection naturelle a sélectionné des mécanismes assurant la survie jusqu'à l'âge de la reproduction, mais qu'aucune pression de sélection n'ait pu s'exercer sur les dommages collatéraux que causent ces mécanismes à plus long terme? Il s'agit probablement de l'explication la plus populaire. Cependant, il est en réalité difficile d'expliquer le paradoxe et surtout, nous ne comprenons pas ce qui pourrait justifier que certaines cellules sénescentes soient éliminées par le système immunitaire, alors que d'autres persistent dans l'organisme.

1.4 L'initiation et la progression du cancer

1.4.1 La reprogrammation cellulaire et l'initiation du cancer

À travers les deux sections précédentes, nous avons mis en évidence le rôle joué par les deux grands types d'altérations génétiques contribuant à l'initiation du cancer : l'activation d'oncogènes et la perte de suppresseurs de tumeurs. Le modèle de la sélection clonale pourrait laisser sous-entendre que la transformation maligne résulte d'une simple addition de telles altérations (12). En fait, le processus est beaucoup plus complexe. Certes, l'acquisition de mutations oncogéniques et la perte des défenses antitumorales intrinsèques d'une cellule sont requises. Cependant, la cellule doit également acquérir une propriété essentielle, soit la tumorigénicité, laquelle correspond à la capacité d'initier la formation d'une tumeur maligne. L'acquisition de cette propriété requiert un changement d'identité cellulaire important, parfois qualifié de reprogrammation maligne (175-177). Les cellules qui en découlent, désignées sous l'appellation de cellules initiatrices de tumeurs (*tumor-initiating cells*; TIC) ou cellules initiatrices de cancers (*cancer-initiating cells*; CIC), possèdent un certain nombre de propriétés normalement attribuables aux cellules progénitrices, ou cellules souches, telle que la capacité d'auto-renouvellement cellulaire (13, 178).

La transformation maligne d'une cellule différenciée inclut donc un certain niveau de dédifférenciation (13, 178, 179). Ce processus ne dépend pas uniquement des défauts génétiques acquis; il dépend aussi de changements épigénétiques importants (175, 178, 180).

À titre d'exemple, les cellules transformées montrent souvent une hypométhylation globale de l'ADN (181), ce qui pourrait réactiver certains gènes dont l'expression est normalement réservée aux cellules souches. À l'inverse, l'hyperméthylation des îlots CpG de l'ADN peut mener à l'inactivation de régulateurs négatifs des voies qui contribuent à l'acquisition de propriétés associées aux cellules progénitrices (175), telle que la voie de WNT (*wingless-type MMTV integration site family*) (182, 183).

Les changements épigénétiques ne sont pas nécessairement la conséquence de mutations; ils peuvent être influencés par le microenvironnement (184-186). Il est effectivement reconnu qu'un contexte inflammatoire soutenu peut contribuer à l'étiologie de plusieurs cancers (14, 187, 188). Cependant, les mécanismes liant le microenvironnement au remodelage de la chromatine sont loin d'être compris. Ils pourraient néanmoins inclure l'activation de facteurs intimement liés à la plasticité cellulaire, laquelle correspond à la capacité de changer d'identité, en réponse aux éléments caractérisant un microenvironnement pathologique (187, 188). Ces facteurs pourraient inclure, à titre d'exemple, l'activation de STAT3 (*signal transducer and activator of transcription 3*) et de la voie de NF-κB, puisque les deux ont des rôles connus à la fois dans la reprogrammation cellulaire et dans le processus de la transformation maligne (179, 187-190).

Le PDAC est un exemple de cancer illustrant bien l'importance du microenvironnement et de la reprogrammation cellulaire dans le processus menant à la transformation maligne (191, 192). L'induction d'une pancréatite chronique semble d'ailleurs requise pour le développement du PDAC chez les modèles murins qui expriment l'oncogène *KRas* (18). Non seulement l'inflammation chronique contribue au contournement de la sénescence cellulaire, mais elle favorise également l'ADM, une étape de transdifférenciation qui initie la progression tumorale (Figures 1 et 5) (81, 192). Les cellules qui résultent de l'ADM présentent certaines caractéristiques des cellules progénitrices du pancréas, suggérant un processus de dédifférenciation partielle (192, 193). Les facteurs de transcription STAT3 et NF-κB sont activés par des cytokines produites par les cellules du système immunitaire et jouent un rôle critique dans cette étape de reprogrammation (194-197), de même que pour l'initiation du PDAC (Figure 5) (192, 198-200).

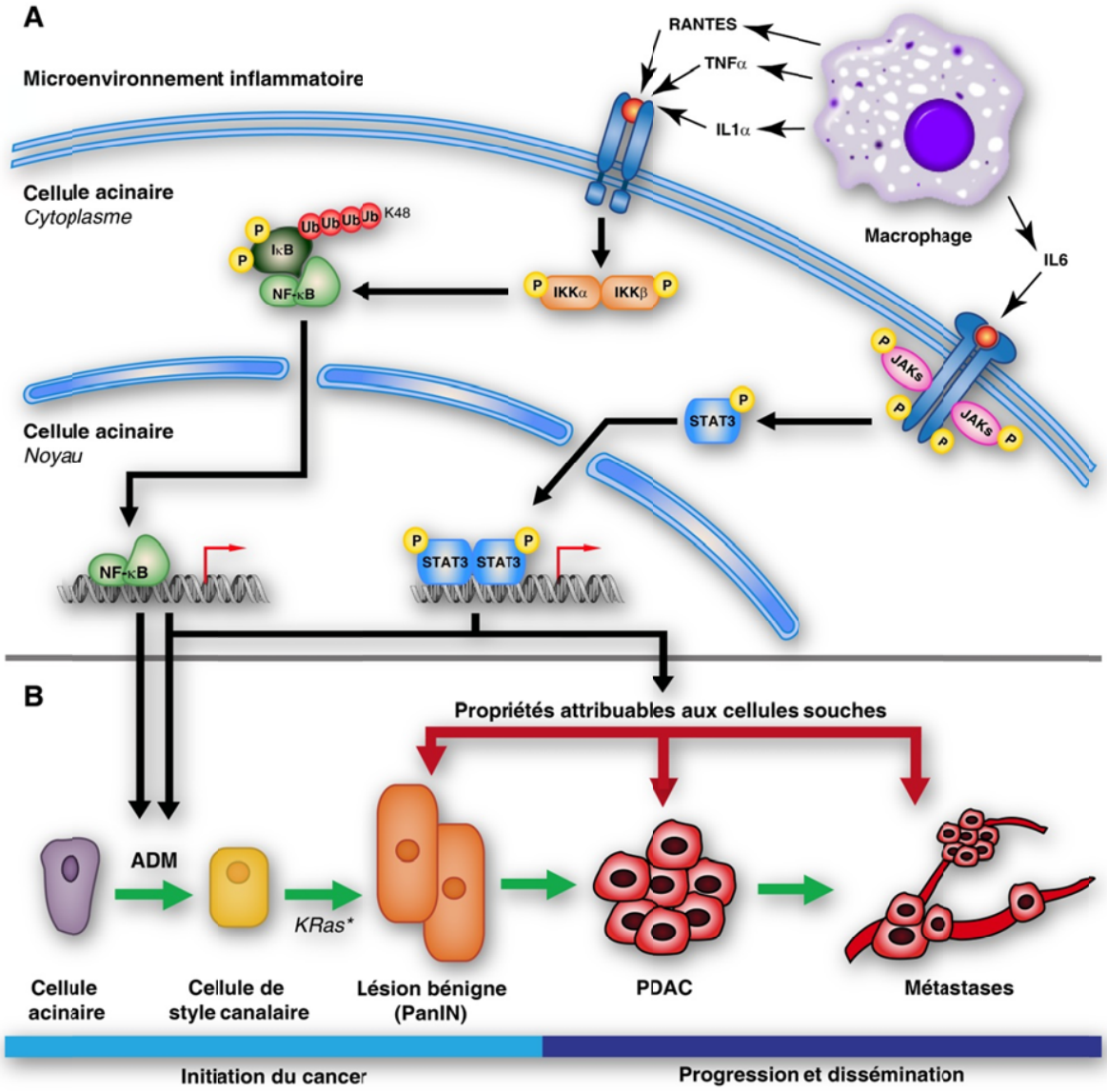

Figure 5. Effet de l'inflammation sur l'évolution du cancer pancréatique

(***A***) Les voies de signalisation activées au sein des cellules acinaires du pancréas par le microenvironnement inflammatoire sont illustrées. Par exemple, les macrophages produisent RANTES, le TNFα et l'IL1α, lesquels activent la voie de NF-κB (196, 197). De plus, ils produisent l'IL6 qui permet l'activation des protéines JAK, lesquelles activent STAT3 par phosphorylation (198). (***B***) Les facteurs de transcription NF-κB et STAT3 stimulent une métaplasie des cellules acinaires vers un état semblable aux cellules canalaires (ADM) (194, 195, 197). Ces lésions progressent vers les néoplasies intraépithéliales pancréatiques (PanIN), puis vers l'adénocarcinome canalaire pancréatique (PDAC). Les protéines NF-κB et STAT3 favoriseraient l'acquisition de propriétés associées aux cellules souches à différents stades de la progression tumorale (195, 198, 200, 201). Ub, ubiquitine; P, phosphorylation; *, activation de l'oncogène *KRas*; adapté de Deschênes-Simard *et al.* (2013) (192).

1.4.2 Les cellules souches cancéreuses et la progression du cancer

Nous pourrions croire qu'une tumeur contient une population homogène de cellules cancéreuses. Cependant, tout comme le processus de la sélection clonale est à l'image de la sélection naturelle, la tumeur est à l'image d'un écosystème. En d'autres mots, il s'agit généralement d'un mélange hétérogène de cellules cancéreuses qui interagissent entre elles et avec les cellules «saines» du microenvironnement (202-204). L'hétérogénéité des tumeurs est interprétée depuis longtemps comme étant une extension de la sélection clonale menant à l'initiation du cancer. Ainsi, des événements génétiques aléatoires au sein de la population de cellules cancéreuses donnent naissance à des sous-populations, lesquelles prennent une importance relative en fonction des avantages que peuvent conférer les nouvelles mutations ou altérations épigénétiques (4, 175, 202-204). L'instabilité génomique associée à de nombreuses cellules cancéreuses donne d'ailleurs un argument important en faveur de ce modèle d'évolution clonale du cancer (203, 205). Cependant, les différents microenvironnements au sein d'une tumeur peuvent aussi contribuer à des changements de phénotypes, voire épigénétiques, au niveau de populations localisées de cellules (202-204, 206, 207). Enfin, la présence de cellules cancéreuses pluripotentes capables de se différencier en une diversité de cellules tumorales est un autre modèle proposé pour expliquer l'hétérogénéité des tumeurs (202, 204).

Au cours des dernières années, de nombreuses études ont identifié des sous-populations de cellules cancéreuses ayant des caractéristiques attribuables aux cellules souches, désignées comme étant des cellules souches cancéreuses (*cancer stem cells*; CSC) (176, 184). Étant donné leur présence dans une grande diversité de tumeurs, autant liquides que solides (208-210), le modèle de l'hétérogénéité découlant de la plasticité des cellules cancéreuses gagne en popularité (211). Ce modèle voudrait que les sous-populations de CSC, aussi petites soient-elles (212), puissent supporter la maintenance et le développement des tumeurs (213). Effectivement, ces cellules seraient hautement tumorigéniques, alors que les autres cellules de la tumeur résulteraient de leur différenciation et pourraient avoir perdu cette faculté (202). De plus, les CSC pourraient répondre au microenvironnement afin d'assurer une descendance adaptée au contexte (176, 214). Pour cette raison, les CSC sont soupçonnées de

jouer un rôle important dans l'établissement des métastases et dans la résistance à plusieurs thérapies (176, 213). De plus, certaines propriétés associées aux cellules souches, telle qu'une plus grande capacité d'expulsion de divers agents chimiques, expliqueraient la résistance intrinsèque des CSC face à diverses stratégies thérapeutiques (176).

L'identité exacte des CSC, et surtout leur origine, demeurent controversées. Bien qu'elles partagent des caractéristiques avec les cellules souches, elles ne dérivent pas nécessairement de cellules progénitrices. Des évidences suggèrent plutôt qu'elles résulteraient de la dédifférenciation de cellules cancéreuses «différenciées» (179, 213, 215). Cette logique n'est pas sans rappeler la reprogrammation cellulaire contribuant à la transformation maligne. Les CSC résultent-elles simplement de la propagation des TIC, par exemple, via une division asymétrique de ces cellules? Bien que cette possibilité ne soit pas totalement exclue, elle demeure spéculative et ne serait pas nécessairement la norme. Premièrement, le niveau de dédifférenciation des TIC comparativement au CSC n'est pas défini. Étant donné les difficultés qui découlent de l'isolation et de l'analyse des cellules d'origine d'un cancer, il n'est pas clair pour le moment si les TIC représentent un stade transitoire de dédifférenciation ou un stade analogue aux CSC. En effet, elles pourraient avoir acquis quelques propriétés des cellules progénitrices, comme la capacité d'auto-renouvellement, ce qui conférerait la tumorigénicité. Cependant, contrairement aux CSC, elles n'auraient peut-être pas la capacité de différenciation et les marqueurs classiques de la pluripotence (216, 217). Une reprogrammation supplémentaire des TIC serait peut-être nécessaire afin de permettre l'apparition d'une réelle sous-population de CSC. Deuxièmement, une plasticité bidirectionnelle pourrait exister au sein d'une tumeur (184, 211, 214). En d'autres termes, les cellules cancéreuses différenciées pourraient se dédifférencier à nouveau afin de contribuer à la population de CSC. Les principes gouvernant la reprogrammation de ces cellules pourraient néanmoins être similaires à ceux évoqués pour les TIC, avec un rôle clef des changements épigénétiques et du microenvironnement (Figure 5) (218). Ceci pourrait expliquer pourquoi les sous-populations de CSC sont parfois hétérogènes au sein d'une même tumeur (176, 214).

Étant donné le flou qui existe entre la définition des TIC et celle des CSC, une grande ambiguïté dans la terminologie utilisée est observable dans la littérature. Les deux termes sont

souvent interchangés, alors considérés comme synonymes. Néanmoins, certains groupes proposent l'utilisation du terme TIC afin de désigner les toutes premières cellules ayant subi la transformation maligne. Les CSC représentent alors les cellules reprogrammées au sein d'une tumeur déjà établie (13, 184). Tout au long de cet ouvrage, nous avons appliqué cette logique.

En résumé, les tumeurs malignes sont hétérogènes et dynamiques. La reprogrammation cellulaire est un processus qui assure la plasticité des cellules cancéreuses, ce qui contribue significativement à l'hétérogénéité et à l'évolution de la tumeur. C'est cette capacité d'évoluer et de s'adapter aux restrictions qu'impose l'environnement qu'un cancer gagne en agressivité et qu'il peut éventuellement résister aux outils thérapeutiques dont nous disposons.

1.5 La voie de signalisation ERK/MAPK

1.5.1 Mise en contexte

La première composante de la voie ERK/MAPK, soit la kinase ERK1, fut isolée en 1986 par Thomas W. Sturgill et Bryan Ray (219, 220). L'époque qui suivit fut charnière pour notre compréhension de la signalisation cellulaire. C'est effectivement au début des années 1990 que l'organisation de la voie ERK/MAPK fut mise au jour (219, 221-225). C'est aussi à cette époque, en 1992, que le lien entre l'activation de RAS et la signalisation via cette voie a été établi (226-231). La voie ERK/MAPK est alors devenue un paradigme pour expliquer le fonctionnement d'autres voies MAPK, telles que les voies de JNK (*c-Jun N-terminal kinases*) et de p38 (232, 233).

La voie ERK/MAPK est une cascade de trois protéines kinases qui s'activent successivement par phosphorylation (Figures 2 et 6). En amont de la voie se trouvent les sérine/thréonine kinases RAF (nom dérivé de : *rapidly growing fibrosarcomas*), qui agissent ainsi à titre de MAP3K (MAPK kinase kinase kinase) (234). Trois isoformes de ces protéines existent chez l'humain, soit ARAF, BRAF et CRAF (RAF1), mais toutes sont en mesure d'activer les éléments en aval de la voie ERK/MAPK (234). Les kinases RAF sont recrutées au niveau de la membrane plasmique en interagissant avec les GTPases RAS actives (235-241). Elles y subissent un processus d'activation complexe et encore mal compris (242, 243),

qui implique une série de phosphorylations/déphosphorylations (242, 244), la dissociation de la protéine inhibitrice RKIP (*RAF kinase inhibitory protein*) (242, 245), la formation d'homo ou d'hétérodimères (244, 246-249) et l'interaction avec divers partenaires, incluant des protéines d'échafaudage (244, 250). Les protéines RAF activent ensuite les kinases MEK1/2 (*Mitogen-activated protein kinase/ERK kinase 1 and 2*) par phosphorylation (242). Ces kinases à double spécificité (tyrosine et sérine/thréonine) représentent la composante MAP2K (*MAPK kinase kinase*; MAP2K1/2) de la voie (233). À leur tour, elles transmettent le signal en activant leurs seuls substrats connus, les sérine/thréonine kinases ERK1/2, par la phosphorylation d'un motif thréonine/acide glutamique/tyrosine (TEY) conservé (251-253). Ces dernières constituent l'élément terminal de la voie linéaire et, par conséquent, elles sont aussi connues sous le nom de MAPK3 et MAPK1 respectivement (254).

Les deux kinases ERK partagent une homologie de séquence de 84% et possèdent des fonctions redondantes (255). Bien qu'un débat concernant des rôles distincts attribuables à chacune des isoformes perdure (255), les données actuelles indiquent que leur niveau d'expression différent pourrait expliquer la plupart des supposées divergences fonctionnelles observées lors de leur ablation spécifique (255-257). Le niveau d'activation total des kinases ERK1/2 apparait donc comme étant un paramètre déterminant afin de spécifier différentes réponses cellulaires suite à l'activation de la voie ERK/MAPK (255, 258). Il est à noter que nos travaux abondent dans ce sens et qu'à des fins de simplification, nous utilisons généralement l'appellation ERK afin d'inclure les deux isoformes.

1.5.2 Une voie, plusieurs fonctions

Les kinases ERK sont des régulateurs ubiquitaires d'une multitude de processus cellulaires, parfois même contradictoires. Ceux-ci incluent, à titre d'exemples, la prolifération, la survie, l'apoptose, la différenciation, la motilité, le remodelage de la chromatine et le métabolisme (253-255). Cette variété de fonctions s'explique par une grande diversité de substrats (Figure 6) (259). En effet, les kinases ERK phosphorylent plusieurs centaines de protéines (259-264), tant cytoplasmiques que nucléaires (255). Ces substrats ont tous la particularité de contenir un motif minimal de phosphorylation serine/thréonine-proline (S/T-P) (265, 266) et un domaine d'interaction D (motif DEJL) ou DEF (motif FxFP) (253, 267, 268).

La phosphorylation d'un ensemble spécifique de substrats et, conséquemment, la régulation d'un processus cellulaire particulier, dépend de plusieurs facteurs.

Au-delà du protéome qui diverge d'un type cellulaire à l'autre, la sélection des substrats s'explique en partie par la compartimentalisation de la voie ERK/MAPK. Ce phénomène peut être causé par l'interaction des composantes de la voie avec une protéine d'échafaudage (255). De telles protéines assurent l'efficacité de la signalisation ainsi que son acheminement à des endroits spécifiques de la cellule, voire sélectionnent directement un nombre limité de substrats (269-273). Les protéines d'ancrage jouent aussi un rôle critique dans la localisation cellulaire de l'activité des ERK (255). Au contraire des protéines d'échafaudage, elles interagissent uniquement avec les kinases ERK, et ne peuvent donc pas contribuer directement à la sélection des substrats. Cependant, elles restreignent la localisation des ERK à des compartiments cellulaires spécifiques, limitant ainsi l'accès à des ensembles de substrats différents (254, 271, 273). Plus d'une cinquantaine de protéines d'ancrage et d'échafaudage ont été associées au contrôle de la localisation de l'activité des kinases ERK (254, 255, 274-276). Il est donc évident que la régulation de ces protéines a une grande influence sur l'effet qui découle de la voie ERK/MAPK.

La cinétique d'activation de la voie est un autre paramètre déterminant dans le choix d'une réponse cellulaire spécifique. Celui-ci inclut l'intensité, la durée et l'oscillation de la signalisation (273). Notre compréhension de l'impact de la dynamique temporelle du signal sur le comportement cellulaire demeure limitée. Néanmoins, ces dynamiques impliquent un couplage étroit entre la signalisation et la régulation de l'activité transcriptionnelle (277). Par exemple, la voie ERK/MAPK active rapidement une série de facteurs de transcription qui induisent l'expression des gènes immédiats-précoces (*immediate early genes*; IEG) (277-279). Parmi les protéines nouvellement synthétisées, certaines sont des substrats des kinases ERK. Elles sont donc régulées par la voie ERK/MAPK uniquement si la signalisation est suffisamment prolongée afin de permettre leur expression et ensuite leur phosphorylation. De plus, des IEG peuvent coder pour de nouveaux facteurs de transcription, dont l'activation dépend de la phosphorylation par les kinases ERK. Une signalisation prolongée peut ainsi engendrer l'expression d'une seconde vague de gènes, et ainsi de suite (254, 277, 280).

L'intensité et la durée de la signalisation peuvent aussi influencer la stabilité des substrats. L'ubiquitination de plusieurs protéines, laquelle conduit à leur dégradation subséquente par le protéasome, est contrôlée par la présence d'un phosphodégron (281). De telles séquences contiennent généralement plus d'un site de phosphorylation. Les phosphates peuvent être ajoutés séquentiellement par une même kinase ou par des kinases différentes. La phosphorylation d'un premier site est souvent un prérequis pour la phosphorylation d'un second site. Par exemple, elle permet la formation d'un motif d'interaction pour une kinase différente ou assure l'exposition du second résidu qui doit être phosphorylé (281, 282). Ainsi, une activation modérée de la voie ERK/MAPK peut conduire à l'activation, voire la stabilisation, de plusieurs substrats. À l'opposé, l'on peut supposer qu'une accumulation de kinases ERK actives due à une signalisation forte ou prolongée favorise la phosphorylation de phosphodégrons et, subséquemment, la dégradation d'une série de substrats (282). Cet aspect est d'ailleurs approfondi dans l'article 2 présenté au chapitre 2 de cette thèse (97). En résumé, la cinétique de l'activation de la voie ERK/MAPK influence grandement le patron des effecteurs pouvant répondre à la voie et ce, via un ensemble de processus transcriptionnels et post-traductionnels.

En constatant l'importance de la dynamique de la signalisation, une question émerge. Comment la cinétique d'activation de la voie ERK/MAPK peut-elle autant diverger selon le contexte? Malgré la simplicité apparente de la voie due à sa linéarité, le contrôle de son activité est complexe. La voie est impliquée dans une série de mécanismes de rétrocontrôle, à la fois négatifs et positifs, et elle interagit avec d'autres cascades de signalisation (254, 271, 273, 277). À défaut de couvrir l'ensemble de ces mécanismes, mentionnons l'importance que jouent plusieurs membres de la grande famille des phosphatases à double spécificité (*dual-specificity phosphatases*; DUSP), aussi connues sous le nom de phosphatases des MAPK (*MAPK phosphatases*; MKP) (255, 283-285). Plusieurs membres de cette famille sont induits transcriptionnellement en réponse à l'activation de la voie ERK/MAPK (286, 287). Ils enclenchent ensuite une boucle de rétrocontrôle négatif en déphosphorant les kinases ERK (Figure 6) (255, 271, 283). D'autres joueurs importants qui méritent une mention sont les membres de la famille des protéines sprouty (SPRY) (288-290). Leur expression est également

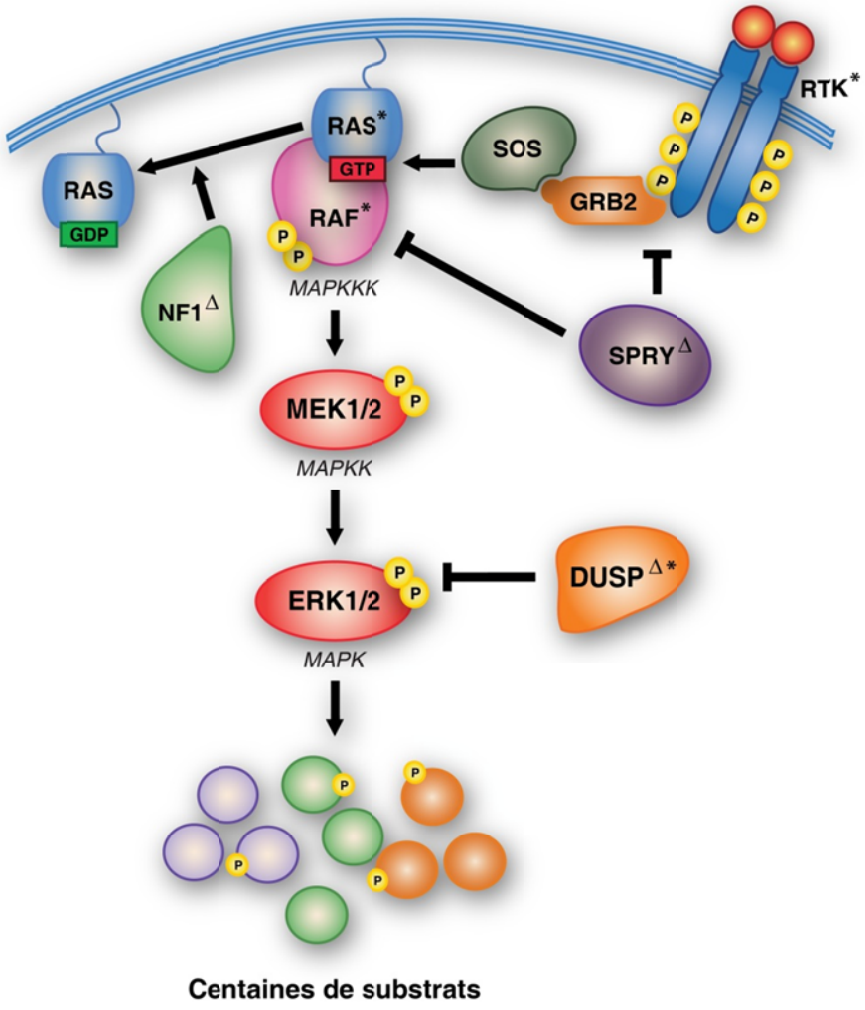

Figure 6. La voie ERK/MAPK

Une simplification de la voie et de ses régulateurs est illustrée. Le noyau de la voie est constitué des kinases RAF (MAPKKK), MEK (MAPKK) et ERK (MAPK). La voie est activée par RAS lorsqu'il est lié au GTP. Ce dernier répond aux facteurs extracellulaires suite à l'activation de récepteurs membranaires, tels que les récepteurs tyrosines kinases (RTK). Sa liaison au GTP dépend de l'action des GEF (p. ex. SOS) et des GAP (p. ex. NF1). Les protéines SPRY et les phosphatases DUSP sont des régulateurs négatifs importants de la voie. *, activation oncogénique rapportée dans les cancers; Δ, délétion rapportée dans les cancers; P, phosphorylation.

induite par la voie ERK/MAPK, mais ils peuvent avoir un effet positif ou négatif sur la voie dépendamment du contexte (289, 290). En effet, les protéines SPRY sont principalement connues pour interférer avec l'activation de la voie ERK/MAPK par les récepteurs RTK (291).

Pour ce faire, elles agissent à plus d'un niveau (Figure 6) (289, 290). Entre autres, les protéines phosphorylées inhibent l'activation de RAS (292, 293), alors que les protéines déphosphorylées interagissent avec RAF et empêchent son activation (294-296). D'autre part, des études ont montré que les protéines SPRY pouvaient augmenter l'activation de la voie ERK/MAPK en réponse au facteur de croissance épidermique (*epidermal growth factor*; EGF) dans un certain nombre de types cellulaires (297-299). Cet effet s'expliquerait par la capacité de SPRY à séquestrer la protéine E3 ubiquitine ligase c-CBL (*casitas B-lineage lymphoma*) (290), responsable de la dégradation des récepteurs à l'EGF (*EGF receptors*; EGFR) suite à leur activation (300). Les protéines SPRY seraient donc des régulateurs polyvalents de la voie ERK/MAPK, qui pourraient distinguer différents stimuli ou contextes afin d'apporter une modulation appropriée de la signalisation.

En conclusion, la voie ERK/MAPK apparaît aujourd'hui comme bien plus qu'un simple circuit linéaire assurant la transmission d'un signal. Il s'agit plutôt d'un noyau important, voire central, d'un vaste réseau de protéines régulatrices. Ce n'est que par une combinaison bien spécifique d'événements au sein de ce réseau que la voie ERK/MAPK peut induire une réponse cellulaire donnée. Pour cette raison, malgré des dizaines de milliers de publications au sujet de cette voie de signalisation au cours des trois dernières décennies, l'étude de son rôle dans divers phénotypes cellulaires ainsi que dans plusieurs pathologies humaines demeure un champ de recherche très actif.

1.5.3 La voie ERK/MAPK et la progression tumorale

Les mutations oncogéniques au niveau de régulateurs en amont de la voie ERK/MAPK sont nombreuses (Figure 6). Non seulement *RAS* est l'oncogène le plus fréquemment retrouvé dans l'ensemble des cancers humains, mais en outre, les mutations au niveau de *RAF* sont fréquentes (44, 255, 301, 302). Les formes oncogéniques de *BRAF* sont d'ailleurs particulièrement récurrentes dans les mélanomes, puisqu'elles s'y retrouvent dans environ 50% des cas (303). Des membres de la famille ERBB (nom dérivé de : *avian erythroblastosis oncogene B*) des RTK sont aussi impliqués dans de nombreux cancers (304). À titre d'exemple, ERBB1/EGFR est surexprimé dans environ 60% des carcinomes du poumon non à petites cellules (*non-small-cell lung carcinomas*; NSCLC) (305, 306), tandis qu'une

surexpression de ERBB2/HER2 (*human epidermal growth factor receptor 2*) est observée dans approximativement 20% de tous les cancers du sein (307). Enfin, certains cancers sont associés à la perte ou à une activité diminuée de différents régulateurs négatifs de la voie ERK/MAPK, tels que NF1 (308-310), SPRY1/2 (290, 311) et certaines protéines DUSP (Figure 6) (283, 312, 313). Collectivement, ces observations suggèrent qu'une activation anormale de la voie ERK/MAPK pourrait être le point convergeant de nombreuses anomalies favorisant la progression tumorale. Cette supposition est appuyée par l'observation que la voie est activée dans environ 30% de toutes les tumeurs humaines (314, 315).

L'idée d'une contribution importante de la voie ERK/MAPK au phénotype agressif des cellules cancéreuses est davantage confortée par sa capacité à promouvoir divers processus intimement liés à la physiopathologie du cancer. Entre autres, une accumulation nucléaire anormale des kinases ERK actives peut conduire à une instabilité génomique, ce qui pourrait favoriser l'accumulation de lésions génétiques associées à la progression tumorale (159, 160). De plus, l'activation des kinases ERK peut favoriser la biosynthèse de macromolécules afin de supporter la croissance et la prolifération cellulaire (316-319). Parallèlement, elle peut stimuler la synthèse protéique en augmentant la signalisation via mTOR (*mammalian target of rapamycin*) (316, 320, 321), soit un régulateur critique de la traduction (322), ou en stimulant la biogenèse des ribosomes. Ce dernier aspect impliquerait une activation de la transcription des gènes ribosomiques suite à la phosphorylation d'UBF (*upstream binding factor*) (323), ainsi que l'induction de diverses protéines ribosomiques par c-MYC suite à sa stabilisation (40, 324-326). Ensuite, l'activation des kinases ERK peut favoriser la migration cellulaire (327, 328) et prévenir l'apoptose (242, 329), ce qui, en plus de conférer un avantage prolifératif, pourrait contribuer à la résistance à certains agents thérapeutiques (242). Finalement, l'effet le plus documenté de la voie ERK/MAPK est sa capacité à engager la progression du cycle cellulaire (316).

Malgré le fait que certains travaux suggèrent que la voie ERK/MAPK pourrait promouvoir la transition de la phase G2 du cycle cellulaire à la mitose (transition G2/M) (147), le rôle le plus évident de la voie est la promotion de la transition G1/S. En effet, les kinases ERK activent une série de facteurs de transcription (254), incluant ELK1 (330), c-FOS

(278), c-JUN (331) et c-MYC (325, 326). Ces derniers contribuent à la progression du cycle cellulaire en induisant l'expression des cyclines de type D (316). L'exemple le mieux caractérisé est l'induction de la cycline D1 par le facteur de transcription hétérodimérique AP-1 (*activator protein 1*), formé par l'association de c-FOS et c-JUN (316, 332, 333). La phosphorylation d'eIF4E (*eukaryotic translation initiation factor 4E*) suite à l'activation de la voie ERK/MAPK favoriserait également l'export nucléaire de l'ARNm de la cycline D1 afin de favoriser sa traduction (316, 334). Enfin, c-MYC joue un rôle majeur dans la promotion de la prolifération, non seulement en induisant la cycline D2 (335), mais aussi en induisant d'autres composantes contribuant à la progression du cycle cellulaire, tels que CDK4 (336) et CDC25A (*cell division cycle 25 homolog A*) (337). L'ensemble des facteurs énoncés ci-haut favorise la formation de complexes CDK-cyclines au cours de la phase G1 du cycle cellulaire afin d'initier la transition vers la phase S (134, 338). Cette fonction de la voie ERK/MAPK s'additionne à sa capacité d'inhiber l'expression de certains régulateurs négatifs de la transition G1/S (339).

Au-delà des fonctions que possède la voie ERK/MAPK pouvant expliquer le comportement des cellules cancéreuses, divers appuis expérimentaux soutiennent son rôle dans la progression tumorale. En effet, la surexpression de formes constitutivement actives de Raf (302, 340), de Mek (341-343) et de Erk (344), a été montrée en mesure d'induire la transformation de cellules murines. À l'opposé, l'expression de formes dominantes négatives de Raf (345, 346), de Mek (347) et de Erk (345, 348), limitait ou inhibait la transformation de ces cellules par l'oncogène *Ras*. Ces observations suggéraient un rôle critique de la voie ERK/MAPK dans le processus de la transformation maligne. Ce rôle a été évalué dans plusieurs modèles murins génétiquement modifiés. Au sein des modèles portant une activation oncogénique de *KRas*, le développement de certains cancers corrèle avec une activation des kinases Erk. Une revue de la littérature à ce sujet est d'ailleurs effectuée dans l'article 3 présenté au chapitre 2 de cette thèse (349). De plus, l'ablation génétique des kinases Erk ou Mek supprime l'initiation des NSCLC par la protéine oncogénique KRas (350). La voie Erk/Mapk semble aussi contribuer au développement de cancers murins découlant de l'activation des oncogènes *HRas*, *NRas* et *BRaf*, tels que les carcinomes cellulaires squameux (*squamous cell carcinomas*; SCC) (351), les carcinomes de la vessie (352), les mélanomes

(84), les leucémies myélomonocytiques chroniques (*chronic myelomonocytic leukemias*; CMML), les leucémies myéloïdes aiguës (*acute myeloid leukemias*; AML) (353, 354), ainsi que les carcinomes papillaires de la thyroïde (*papillary thyroid carcinomas*; PTC) (355). Chez l'humain, l'étude du rôle de la voie ERK/MAPK dans la transformation maligne a été difficile étant donné la résistance des cellules humaines à la transformation *in vitro* (356). Ce n'est que par la combinaison de différents facteurs, tels que l'expression ectopique de la sous-unité catalytique de la télomérase (*human telomerase reverse transcriptase*; hTERT), de l'antigène T (*large T antigen*; LT) de la région précoce du virus SV40 (*simian virus 40 early region;* SV40 ER) et de l'oncogène *Ras*, que les cellules pouvaient être transformées (357-359). De telles approches ont cependant été peu informatives sur l'importance de l'activation de la voie ERK/MAPK dans le processus puisqu'elles n'ont pas permis de démontrer systématiquement le pouvoir transformant de chaque membre de la voie. Des évidences suggérant un rôle dans la transformation maligne ou la progression du cancer ont néanmoins été obtenues grâce à l'usage d'inhibiteurs pharmacologiques ciblant RAF et MEK (360). L'article 3 présenté au chapitre 2 couvre également ce volet (349).

Pour toutes les raisons évoquées jusqu'à maintenant, l'activation de la voie ERK/MAPK est traditionnellement perçue comme étant une composante clef de la progression tumorale, voire comme un prérequis à la transformation maligne et ce, pour divers types de cancers.

1.6 Problématiques et objectif de la thèse

1.6.1 Un rôle de la voie ERK/MAPK dans la suppression tumorale?

Une accumulation d'études vient confronter le dogme attribuant un rôle essentiellement protumoral à la voie ERK/MAPK. Effectivement, un certain nombre d'observations cliniques suggèrent que l'importance de la voie dans l'évolution du cancer serait beaucoup plus dépendante du contexte tel qu'imaginé à l'origine.

L'analyse des niveaux des kinases ERK activées (p-ERK) dans les tumeurs humaines, ainsi que des corrélations avec divers paramètres cliniques, ont généré des conclusions

contradictoires. Par exemple, les niveaux de p-ERK sont généralement élevés dans les cancers du sein (361), ce qui a été initialement associé à un plus grand risque de rechute thérapeutique (362). Suite à l'analyse de nouvelles cohortes de patients, l'activation des kinases ERK a plutôt été corrélée avec les stades précoces de la maladie, un risque réduit de rechute thérapeutique et un meilleur pronostic (363, 364). De telles corrélations contradictoires entre les niveaux de pERK et l'agressivité de la maladie ont aussi été observées dans divers autres cancers, tels que les glioblastomes (365-367), les cancers rénaux (368-370), les carcinomes hépatocellulaires (*hepatocellular carcinoma*; HCC) (371, 372) et les cancers colorectaux (373-375). De plus, bien que la progression du NSCLC corrèle généralement avec de hauts niveaux de p-ERK (376), d'autres cancers intimement liés à la présence d'oncogènes en amont de la voie ERK/MAPK présentent un patron d'activation de la voie hétérogène. Ces cancers, incluant l'AML (377-379) et les mélanomes (380-382), ne montrent pas de corrélation entre la présence de tels oncogènes (p.ex. *NRAS* et *BRAF*) et une augmentation de p-ERK. Cette observation remet donc en doute la nécessité de l'activation de la voie ERK/MAPK par ces oncogènes afin de promouvoir la progression tumorale. Elle suggère l'implication d'autres voies de signalisation ou mécanismes. Les cas de PDAC illustrent particulièrement bien cette idée. Effectivement, les mutations au niveau de *KRAS* sont quasi présentes dans la totalité des tumeurs, alors qu'une élévation des niveaux de p-ERK est souvent absente ou négligeable (383, 384). Dans des cas où une augmentation significative de p-ERK a été rapportée, des niveaux également élevés ont été observés au sein des cellules normales des tissus adjacents (385), suggérant un effet du microenvironnement plutôt qu'une activation spécifique par KRAS. De plus, ces cas ne seraient pas nécessairement associés à un pire pronostic (386).

Les ambiguïtés qui découlent des observations décrites ci-haut questionnent le rôle critique de la voie ERK/MAPK dans la progression tumorale. Par ailleurs, d'autres études suggèrent même que l'activation de la voie pourrait s'opposer au processus. Encore une fois, des observations cliniques supportent cette hypothèse. Un des exemples les plus révélateurs concerne les cancers de la prostate. Les premières analyses immunohistochimiques ont montré des niveaux plus élevés de p-ERK au sein des tumeurs comparativement aux tissus normaux (387, 388). Par contre, une analyse subséquente plus approfondie de la progression tumorale a révélé des niveaux plus importants de p-ERK dans les tissus normaux, les hyperplasies et dans

les néoplasies intraépithéliales prostatiques (*prostatic intraepithelial neoplasia*s; PIN). Les niveaux de p-ERK déclinaient par la suite avec la progression du cancer et ce, pour atteindre les niveaux les plus faibles dans les stades les plus agressifs de la maladie (389, 390). Cette diminution de l'activation des kinases ERK suggère que des mécanismes régulant négativement la voie ERK/MAPK soient sélectionnés au cours de la progression du cancer de la prostate. En accord avec cette présomption, une fusion entre la protéine E2 ubiquitine ligase UBE2L3 (*ubiquitin-conjugating enzyme E2 L3*) et KRAS inhibe l'activation des kinases ERK. Cette protéine a été identifiée dans des cellules prostatiques métastatiques et s'avère requise pour le maintien du phénotype tumoral (391). D'autre part, la protéine transmembranaire TMEFF2 (*transmembrane protein with EGF-like and two follistatin-like domains 2*) joue un rôle de suppresseur de tumeurs et active la voie ERK/MAPK, alors que sa troncation conduit à une forme oncogénique de la protéine inhibant l'activation des kinases ERK (392). Enfin, la phosphatase DUSP1 est surexprimée dans certaines tumeurs prostatiques, pouvant ainsi contribuer à la diminution des niveaux de p-ERK (Figure 6) (393).

Il est à noter qu'une augmentation de l'expression des phosphatases DUSP n'est pas exclusive au cancer de la prostate et est souvent associée à la progression tumorale ou à un mauvais pronostic (312, 394-402). De plus, un certain nombre d'études ont montré que ces phosphatases contribuent à l'agressivité des cellules cancéreuses (397-400, 403). Ceci restreint la possibilité que leur surexpression dans le cancer ne soit que purement corrélative, soit uniquement le reflet de leur induction par une voie ERK/MAPK hyperactivée. Alors, en supposant un rôle critique de l'hyperactivation de la voie ERK/MAPK dans la progression tumorale, pourquoi l'expression des phosphatases responsables de la déphosphorylation des kinases ERK est-elle augmentée dans plusieurs cancers? Les mécanismes favorisant spécifiquement l'activation de la voie, incluant l'inactivation des DUSP, ne devraient-ils pas être sélectionnés durant le processus de la sélection clonale?

En résumé, la réduction de l'activité des kinases ERK au cours de la progression tumorale suggère qu'une forte signalisation via la voie ERK/MAPK pourrait activer des mécanismes antitumoraux. En plus des corrélations observées entre de mauvais pronostics et l'extinction de la voie, cette supposition remet en doute le dogme souvent véhiculé selon

lequel la voie est essentiellement protumorigénique. Pourtant, elle appuie des travaux importants des laboratoires de Mariano Barbacid et de Tyler Jacks sur l'oncogenèse par Ras au sein de modèles murins génétiquement modifiés, où la transformation cellulaire impliquait une activité réduite de la voie Erk/Mapk (404, 405).

1.6.2 La voie ERK/MAPK; un effecteur de la sénescence cellulaire?

Afin de discriminer le rôle protumoral de la capacité antitumorale de la voie ERK/MAPK, il importe de comprendre les mécanismes par lesquels une activation de la voie peut s'opposer à la progression du cancer. La sénescence cellulaire pourrait-elle être l'un de ces mécanismes? Certaines observations cliniques le suggèrent. Par exemple, des niveaux élevés de p-ERK ont été montrés dans certaines lésions bénignes, tels que les nævi de Spitz (406) et les astrocytomes pilocytiques (407, 408), et corrèlent avec l'induction de la sénescence cellulaire (406-408). Toutefois, une telle hypothèse serait surtout conforme avec ce qui caractérise la sénescence cellulaire *in vitro* observée suite à l'expression de l'oncogène *RAS* dans des cellules humaines normales (409). Cette forme de sénescence implique une signalisation constitutive via la voie ERK/MAPK. Celle-ci semble contribuer à l'induction du phénotype puisque l'expression d'une forme mutante de RAS activant sélectivement la voie ERK/MAPK, soit HRASV12/S35, conduit à la sénescence cellulaire (410). En outre, les formes constitutivement actives des kinases RAF et MEK induisent également le phénotype (410-412), alors que l'inhibition pharmacologique des kinases MEK prévient son établissement (410).

De nombreuses évidences *in vivo*, quoique corrélatives, supportent aussi un rôle de la voie ERK dans l'induction de l'OIS. Des modèles de souris portant une mutation oncogénique au niveau de *KRas* développent différentes lésions bénignes associées à des niveaux élevés de p-ERK et à des marqueurs de la sénescence (voir l'article 3 du chapitre 2 pour une revue de la littérature à ce sujet) (349). Des résultats similaires ont été obtenus lors de l'activation oncogénique de *HRas*, *NRas* et *BRaf*. Par exemple, l'oncogène *HRas* au niveau des mélanocytes n'est pas suffisant pour générer des mélanomes. Il provoque plutôt l'apparition de lésions bénignes associées avec des marqueurs de l'OIS (352, 413). Seule la perte d'effecteurs clefs de la sénescence permet une progression vers des tumeurs malignes (83).

Les résultats obtenus avec les oncogènes *Raf* sont encore plus révélateurs puisqu'ils activent plus spécifiquement la voie Erk/Mapk que les oncogènes *Ras*. Étonnamment, les souris portant une mutation oncogénique de *Raf* développent rarement des tumeurs malignes. Les oncogènes *Raf* induisent plutôt diverses lésions bénignes qui corrèlent avec l'activation des kinases ERK et des caractéristiques attribuables aux cellules sénescentes (86, 87, 340, 414-417).

Malgré les observations que nous venons de mentionner, l'implication des kinases ERK dans l'établissement de la sénescence cellulaire a longtemps été controversée. Ceci s'explique en partie par l'absence de démonstration liant directement les kinases ERK à l'induction du phénotype sénescent. En effet, les données antérieures découlaient de l'activation ou de l'inhibition d'éléments en amont de la voie ERK/MAPK et, par conséquent, elles ne permettaient pas d'exclure l'activation de mécanismes indépendants des kinases ERK. De plus, les substrats pouvant expliquer le rôle de ces kinases dans l'induction des diverses propriétés des cellules sénescentes étaient largement méconnus.

Les travaux présentés au second chapitre de cette thèse ont adressé cette problématique. Dans un premier temps, nous avons démontré l'importance des kinases ERK dans l'induction de la sénescence cellulaire. Ensuite, nous avons identifié un mécanisme impliquant une dégradation massive et spécifique de protéines, qui pourrait expliquer comment la voie ERK/MAPK contribue à l'établissement de la sénescence. Globalement, nos résultats suggèrent un modèle où une activation modérée des kinases ERK serait permissive à la transformation maligne et à la prolifération des cellules cancéreuses, alors qu'une forte activation induirait la sénescence cellulaire. Ce modèle a des implications importantes en ce qui concerne l'utilisation des inhibiteurs de la voie ERK/MAPK pour traiter le cancer.

1.6.3 La voie ERK/MAPK; un frein à la reprogrammation des cellules cancéreuses?

Les CSC et les cellules souches embryonnaires (*embryonic stem cells*; ESC) partagent de nombreuses similitudes. Il est donc intéressant de noter que l'inhibition de la voie ERK/MAPK supporte la capacité d'auto-renouvellement des ESC (418-423). À l'inverse, une activation soutenue de la voie est bien connue pour induire la différenciation cellulaire (424-430). Les oncogènes en amont de la voie ERK/MAPK, tel que l'oncogène *RAS*, n'induisent-ils

pas une activation forte et soutenue de la voie? Ceci pourrait-il contribuer à la différenciation des CSC?

De nombreux parallèles peuvent également être établis entre l'acquisition de la tumorigénicité, les CSC et la reprogrammation *in vitro* des cellules somatiques en cellules souches pluripotentes induites (*induced pluripotent stem cells*; iPSCs) (431-433). Par exemple, les transgènes utilisés pour reprogrammer les cellules somatiques ont presque tous un rôle connu dans l'acquisition de la tumorigénicité (213). De manière analogue, les oncogènes *RAS* et *c-MYC* favorisent la reprogrammation cellulaire, et par conséquent, la plasticité des cellules cancéreuses (434). Ces analogies suggèrent que les processus de reprogrammation cellulaire menant aux iPSC, aux TIC et aux CSC pourraient partager de nombreuses similitudes. L'étude de la reprogrammation des cellules cancéreuses est un domaine émergent de l'oncologie moléculaire et notre compréhension du processus est très fragmentaire. Cependant, l'étude de la reprogrammation des cellules somatiques *in vitro* a été prolifique au cours des dernières années. Il apparait clair que la voie ERK/MAPK s'oppose à ce processus. Non seulement l'inhibition de la voie augmente l'efficacité de la reprogrammation par l'expression des transgènes classiques du cocktail de Yamanaka, c'est-à-dire *OCT4*, *SOX2*, *KLF4*, and *c-MYC* (435-438), mais elle permet la substitution de certains de ces facteurs (439, 440). La voie ERK/MAPK serait-elle une barrière générale à la reprogrammation cellulaire? S'opposerait-elle ainsi à la reprogrammation nécessaire à l'acquisition de la tumorigénicité et à l'apparition des CSC?

Cette dernière question a été abordée au sein du troisième chapitre de cette thèse. Nous avons d'abord observé que l'initiation du PDAC corrèle avec une diminution significative des niveaux de p-ERK, de même qu'avec l'apparition de propriétés associées aux cellules souches. Nos résultats suggèrent aussi que de manière générale, une réduction de la signalisation par la voie ERK/MAPK est requise pour la reprogrammation conférant la tumorigénicité et permettant le maintien d'une sous-population de cellules semblables aux cellules souches. Ainsi, bien que la majorité des cellules d'une tumeur puissent se caractériser par une activation significative de la voie ERK/MAPK, les TIC et les sous-populations de CSC pourraient plutôt être associées à une faible activité de la voie.

1.6.4 La metformine : une solution à de nouveaux défis thérapeutiques?

Étant donné les fonctions de la voie ERK/MAPK qui peuvent contribuer à la prolifération des cellules cancéreuses et à la progression tumorale, beaucoup d'efforts sont investis dans le développement d'inhibiteurs pharmacologiques de la voie. Ce volet est d'ailleurs détaillé dans l'article 3 du second chapitre de la thèse (349). Cependant, les processus qui interfèrent avec l'activation des kinases ERK pourraient non seulement limiter l'induction de la sénescence cellulaire, mais aussi favoriser la sous-population de CSC au sein d'une tumeur. Ainsi, un effet indésirable des inhibiteurs de la voie ERK/MAPK pourrait être de limiter la capacité de suppression tumorale intrinsèque des cellules face à l'activation d'oncogènes en amont de la voie. De plus, ils pourraient favoriser la sous-population de CSC, lesquelles ont une résistance accrue aux thérapies conventionnelles et la capacité de reconstituer une nouvelle tumeur. Nous posons ainsi l'hypothèse que ces effets indésirables de l'inhibition de la voie ERK/MAPK pourraient expliquer un certain nombre de rechutes thérapeutiques et de cas de résistance (349). Les fonctions antitumorales qui s'additionnent aux fonctions protumorales des kinases ERK posent donc un sérieux défi thérapeutique.

Nos résultats qui associent la reprogrammation cellulaire et les CSC à une faible activité de la voie ERK/MAPK montrent l'importance de cibler les cellules cancéreuses avec de faibles niveaux de p-ERK. En combinaison avec des inhibiteurs de la voie ERK/MAPK, une telle stratégie pourrait éviter la reprogrammation de cellules précancéreuses en TIC ou de cellules cancéreuses en CSC, tout en conservant l'inhibition des fonctions protumorales de la voie dans les autres cellules constituant la tumeur. À cet effet, la metformine pourrait être un agent thérapeutique envisageable.

La metformine est un biguanide utilisé depuis longtemps pour traiter le diabète et le syndrome des ovaires polykystiques (441). Cependant, au cours de la dernière décennie, une série de rapports ont associé l'usage de la metformine à une diminution significative du risque de développer un cancer (441-444). Depuis, la communauté scientifique démontre un vif intérêt pour la compréhension de son mécanisme d'action et de nombreuses possibilités sont évoquées (441, 445). Parmi celles-ci, la metformine semble cibler les sous-populations de CSC (441, 446). Cet effet pourrait s'expliquer par la capacité de la metformine à interférer

avec plusieurs effecteurs de la reprogrammation cellulaire, tels que STAT3 (447, 448) et c-MYC (449, 450). Cependant, suite à des traitements avec la metformine afin de vérifier sa capacité à cibler les CSC avec de faibles niveaux de p-ERK (voir chapitre 3), nous avons constaté qu'elle semblait inhiber le facteur de transcription NF-κB. Un tel effet pourrait avoir un impact thérapeutique considérable. Effectivement, la protéine NF-κB est impliquée dans le processus de la reprogrammation cellulaire associé aux TIC et aux CSC (179, 190), mais à la fois dans l'induction de nombreuses cytokines pro-inflammatoires associées au SASP (140, 144). En plus de contribuer à éliminer les sous-populations de CSC, la metformine pourrait donc restreindre les effets délétères du SASP. En d'autres mots, elle pourrait réduire les effets procancéreux d'une accumulation de cellules sénescentes induites par une hyperactivation de la voie ERK/MAPK.

La démonstration de la capacité de la metformine à inhiber le facteur de transcription NF-κB fait donc l'objet du chapitre 4 de cette thèse. Nous avons tiré avantage de la sénescence induite par l'oncogène *RAS* étant donné le rôle clef que joue NF-κB dans le SASP. Conformément à l'hypothèse émise ci-haut, la metformine permet une inhibition importante de la production des cytokines pro-inflammatoires. L'impact thérapeutique potentiel d'un tel effet est discuté et les différents avantages que l'inhibition de NF-κB par la metformine pourrait apporter sont approfondis dans la discussion de la thèse se trouvant au chapitre 5.

2. Rôle suppresseur de tumeur de la voie ERK/MAPK par la promotion d'une dégradation protéique spécifique

2.1 Mise en contexte de l'article 1

L'origine du projet dont découle cet article, et on pourrait dire cette thèse, est un criblage génétique à l'aide de petits ARN interférents en épingles à cheveux (*short hairpin RNA*; shRNA) exprimés de manière stable dans des cellules normales exprimant également l'oncogène *RAS*. L'objectif de ce criblage était d'identifier des gènes critiques pour l'établissement de l'OIS par *RAS*. Cette approche a mené à l'identification récurrente de shRNA ciblant les kinases ERK. Ainsi, les travaux présentés dans l'article qui suit avaient pour but de confirmer l'importance des kinases ERK dans l'induction de l'OIS par l'oncogène *RAS*.

Afin d'y parvenir, nous avons manipulé directement les niveaux d'expression des kinases ERK en tirant avantage d'interventions génétiques et ce, dans divers systèmes de cellules en culture. Non seulement nos résultats ont apporté une démonstration directe du rôle des kinases ERK dans l'induction de l'OIS, mais ils ont aussi montré l'importance de leur hyperactivation afin de freiner la transformation maligne.

Nous avons ensuite voulu déterminer le mécanisme par lequel la voie ERK/MAPK contribue à la suppression tumorale. Par une approche protéomique, nous avons montré qu'une hyperactivation de la voie conduit à une dégradation dépendante du protéasome de nombreuses protéines requises pour l'homéostasie cellulaire. Nous avons nommé ce phénomène la dégradation protéique associée à la sénescence (*senescence-associated protein degradation*; SAPD). La dégradation de ces protéines pourrait contribuer à différentes caractéristiques des cellules sénescentes, et serait possiblement critique pour la suppression tumorale. Afin de vérifier la capacité des kinases ERK à induire la sénescence et le SAPD dans un contexte n'impliquant pas la surexpression de l'oncogène *RAS*, nous avons tiré avantage de la sénescence réplicative, laquelle a été associée à une activation constitutive de la voie ERK/MAPK (451). Enfin, pour évaluer si nos résultats possédaient une certaine pertinence *in vivo*, nous avons corrélé nos résultats clefs avec des observations obtenues à partir de tissus prostatiques. Les tissus provenant de BPH ont été choisis comme modèle de sénescence *in vivo* étant donné leur association étroite avec les marqueurs de la sénescence (74, 75, 103). Ils représentent

d'ailleurs un exemple de sénescence stable *in vivo*, étant donné l'absence de progression vers le cancer de la prostate, ce qui les distingue des PIN (452, 453).

Dans leur ensemble, les résultats présentés au sein de l'article 1 suggèrent un modèle où une activation modérée des kinases ERK favoriserait la prolifération des cellules cancéreuses, alors qu'une forte activation induirait la suppression tumorale. De plus, ils proposent que la dégradation protéique puisse être un puissant mécanisme de rétrocontrôle négatif sur les fonctions de la voie ERK/MAPK lorsque son activation est aberrante.

2.2 Contribution à l'article 1

Pour cet article, j'ai partagé la gestion du projet avec Marie-France Gaumont-Leclerc. J'ai effectué la majorité des expériences *in vitro* et chez la souris. Plus précisément, j'ai effectué l'ensemble des travaux pour les figures 1 A, C-G; 2 A, D, H-K, O-P; 3 B-C; 4 A, D; 5; 6 A, E-F, H, J-L; 7 A, E-F; S1 A-G; S2 A-D, F, J-L; S3 A, C-K; S4; S5; S8 J et S9 A-B. J'ai effectué les travaux en collaboration avec les autres auteurs du manuscrit pour les figures 1 B; 2 B-C, E-G, I, L-N; 3 A, D-E; 4 B-C, E-H; 6 B-D, G, I; 7 B-D; S1 H-L; S2 E, G-I, M-N; S3 B; S6; S7; S8 A-I, K; S9 C-H et S11. Marie-France Gaumont-Leclerc a effectué l'ensemble des immunohistochimies et les expériences de spectrométrie de masse. Véronique Bourdeau a effectué la plupart des réactions de PCR quantitatif.

Au niveau de l'écriture, j'ai conçu l'ensemble des figures et rédigé les légendes, la section matériel et méthodes, ainsi que le matériel supplémentaire. Gerardo Ferbeyre a rédigé les autres sections. Conjointement avec Marie-France Gaumont-Leclerc et Gerardo Ferbeyre, j'ai contribué à la révision de l'ensemble du manuscrit.

2.3 Article 1

Tumor suppressor activity of the ERK/MAPK pathway by promoting selective protein degradation

Xavier Deschênes-Simard[1]*, Marie-France Gaumont-Leclerc[1]*, Véronique Bourdeau[1], Fréderic Lessard[1], Olga Moiseeva[1], Valérie Forest[2], Sebastian Igelmann[1], Frédérick A. Mallette[1], Marc K. Saba-El-Leil[3], Sylvain Meloche[3], Fred Saad[2], Anne-Marie Mes-Masson[2] and Gerardo Ferbeyre[1]

Genes & Development, 2013 April 15, 27 (8): 900-15

1) Département de Biochimie, Université de Montréal, Montréal, Québec H3C 3J7, Canada
2) CHUM, Université de Montréal, Montréal, Québec H2L 4M1, Canada
3) Department of Pharmacology and Program in Molecular Biology, Institut de Recherche en Immunologie et Cancérologie, Université de Montréal, Montréal, Québec H3C 3J7, Canada

* These authors contributed equally to this work

Running title: Senescence-associated protein degradation

Keywords: ERK; benign prostatic hyperplasia; oncogenic *ras*; proteasome; senescence

Correspondence to: Gerardo Ferbeyre

2.3.1 Summary

Constitutive activation of growth factor signaling pathways paradoxically triggers a cell cycle arrest known as cellular senescence. In primary cells expressing oncogenic *ras*, this mechanism effectively prevents cell transformation. Surprisingly, attenuation of ERK/MAP kinase signaling by genetic inactivation of Erk2, RNAi-mediated knockdown of ERK1 or ERK2 or MEK inhibitors prevented the activation of the senescence mechanism, allowing oncogenic *ras* to transform primary cells. Mechanistically, ERK-mediated senescence involved the proteasome-dependent degradation of proteins required for cell cycle progression, mitochondrial functions, cell migration, RNA metabolism and cell signaling. This senescence-associated protein degradation (SAPD) was observed not only in cells expressing ectopic *ras*, but also in cells that senesced due to short telomeres. Individual RNAi-mediated inactivation of SAPD targets was sufficient to restore senescence in cells transformed by oncogenic *ras* or trigger senescence in normal cells. Conversely, the anti-senescence viral oncoproteins E1A, E6 and E7 prevented SAPD. In human prostate neoplasms, high levels of phosphorylated ERK were found in benign lesions, correlating with other senescence markers and low levels of STAT3, one of the SAPD targets. We thus identified a mechanism that links aberrant activation of growth signaling pathways and short telomeres to protein degradation and cellular senescence.

2.3.2 Introduction

Normal mammalian cells respond to oncogenic threats by triggering intrinsic tumor suppression mechanisms that curtail cell cycle progression and execute cell death or permanent cell cycle arrest (59). These outcomes were originally discovered by studying the response of normal cells to Myc overexpression, which induces apoptosis (454), or Ras overexpression, which induces a terminal cell cycle arrest known as cellular senescence (455). Subsequently, these mechanisms have been demonstrated in animal models expressing these oncogenes (85, 456-458). Apoptosis is a programmed response where proteolytic enzymes digest selective cellular targets, leading to a non-inflammatory cell death process and eventually the engulfing of apoptotic cells by the immune system (459). The effector mechanism of senescence remains unknown, although these cells seem to be also programmed to interact with the immune system, secreting large amounts of cytokines (147) and being the target of immune mediated clearance (89, 152).

Ras-induced senescence depends on the concerted action of the p53, $p16^{INK4a}$/RB and PML tumor suppressor pathways (100, 455). The activation of p53 by *ras* and other oncogenes involves the DNA damage response (DDR) (115, 116, 120), a consequence of DNA damage triggered by oncogenic activity. This DNA damage could be the result of a replication stress induced by aberrant activation of replication forks or the increased production of mitochondrial reactive oxygen species (ROS) (121). However there is still a gap between our current view of oncogene signaling and the molecular events leading to DNA damage. In addition, senescence can occurs in the absence of DNA damage. For example, in normal fibroblasts expressing oncogenic *ras*, the inactivation of the DDR was not sufficient to bypass senescence (120), and in mice, there is no evidence linking DNA damage to Ras-induced senescence (460). Other effects of oncogenic activity have been proposed as mediators of senescence and may compensate for or cooperate with the DDR. These include $p19^{ARF}$ expression (461), autophagy (96), mitochondrial dysfunction (110), cytokines (147), PML bodies (103) and heterochromatin formation (462). However, it remains puzzling why constitutive growth factor signaling pathways and the Ras/ERK pathway trigger these proliferation barriers in normal cells.

Here we performed an unbiased screen using shRNA libraries to discover genes required for oncogenic *ras* to regulate senescence in human normal fibroblasts. We identified the ERK/MAPKs as essential mediators of senescence and surprisingly found that attenuating ERK expression in human or mouse primary fibroblasts allowed their transformation by oncogenic *ras*. We also found that aberrant Ras/ERK signaling led to a proteasome-dependent protein degradation process targeting proteins required for cell cycle progression, cell migration, mitochondrial functions, RNA metabolism and cell signaling. These findings were validated in cells with short telomeres and in human prostate benign neoplasms where we found expression of senescence markers, high levels of phospho-ERK, and low levels of STAT3, one of the targets of the senescence-associated protein degradation (SAPD) process.

2.3.3 Results

ERK/MAPKs are required for Ras-induced senescence in human fibroblasts

In order to identify genes that contribute to oncogene-induced senescence (OIS), we performed RNAi screening looking for shRNAs able to bypass Ras-induced senescence in human fibroblasts (Figure S1A). shRNAs targeting *ERK2* (*MAPK1*) and *HMGB1* were recovered from the screening. We confirmed the senescence bypass using several shRNAs against *ERK1* and *ERK2* that were all capable of inhibiting RasV12-induced senescence (Figure S1B). We found a good correlation between the degree of total ERK inhibition and the bypass of senescence (Figure S1B). More important, since several shRNAs against *ERK1* or *ERK2* bypassed Ras-induced senescence, it is very unlikely that off-target effects of shRNAs were responsible for the bypass. To further characterize the consequences of ERK inhibition for RAS-signaling, we then used one shRNA that efficiently inhibited *ERK2*, the more abundant ERK isoform in fibroblasts. This shRNA did not inhibit the members of the pathway upstream of ERK (RAS, RAF and MEK) (Figure 7A) but efficiently inhibited the expression of several transcriptional targets of the ERK pathway (Figure 7B) (463). Interestingly, the phosphorylation of p90RSK at Ser380 did not decrease upon inhibition of ERK2 (Figure 7A), suggesting that another kinase activated by RasV12 can catalyze this event or that the remaining levels of phospho-ERK in cells expressing shERK are sufficient to do it.

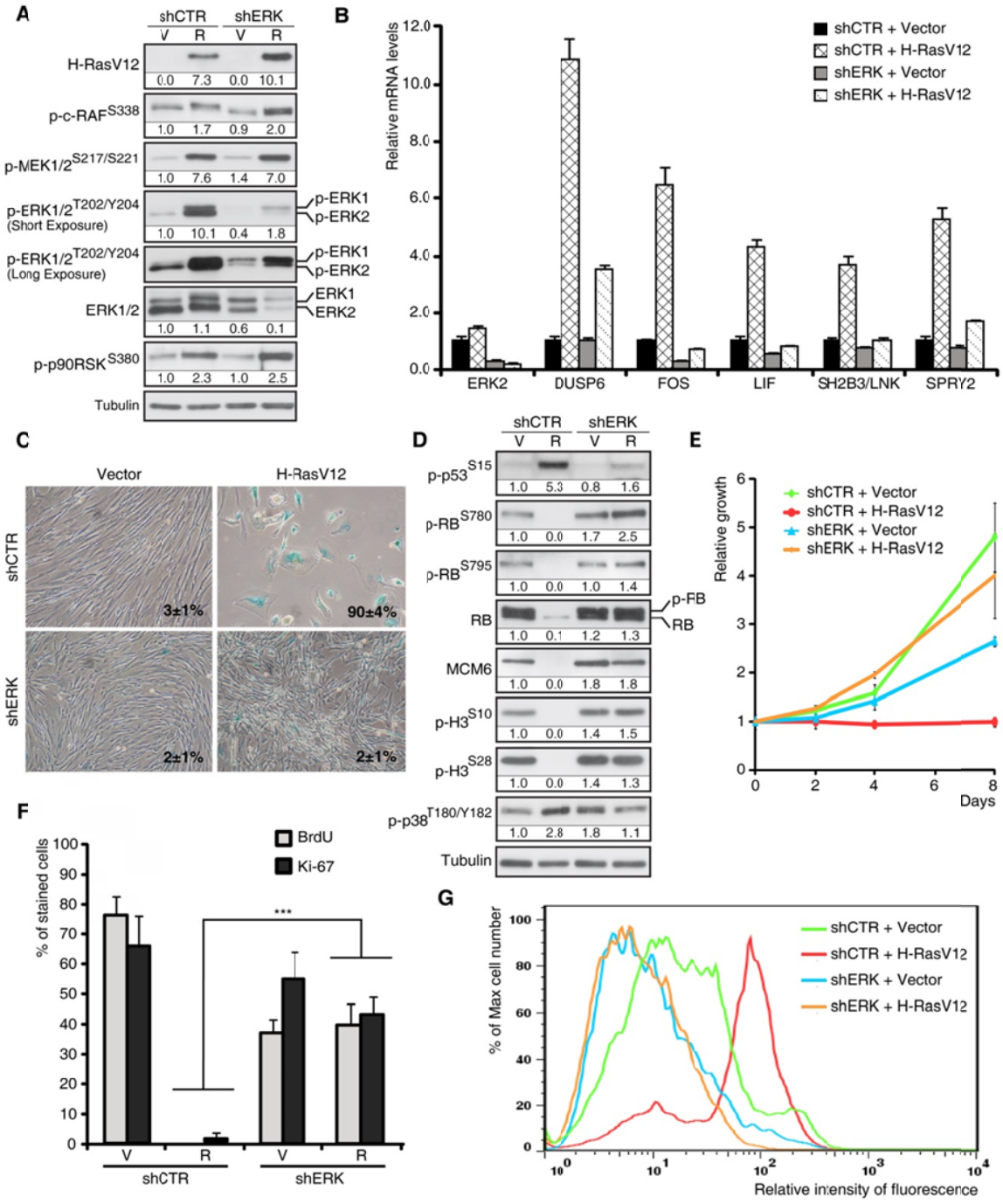

Figure 7. ERK/MAPK inhibition bypasses Ras-induced senescence

(***A***) Immunoblots for proteins in the ERK pathway using extracts from fibroblasts expressing H-RasV12 (R) or an empty vector (V) and shRNA against *ERK2* (shERK) or a nontargeting shRNA (shCTR) obtained from cells 14 d after infection. (***B***) Quantitative PCR (qPCR) for *ERK2* mRNA and mRNAs encoded by ERK-stimulated genes in cells as in (*A*). (***C***) SA-β-Gal of cells as in (*A*). Data were quantified from 100 cell counts in triplicate and are presented as the mean percentage of positive cells ± standard deviation (SD). (***D***) Immunoblots for cell cycle-regulated proteins in cells as in (*A*).

(***E***) Growth curves started with cells as in A. Data are presented as mean ± SD of triplicates. (***F***) Quantitation of BrdU incorporation (2 h of incubation with 10 μM BrdU) and KI-67 staining in cells as in (*A*). Data were quantified from 100 cells counts in triplicate and are presented as the mean of positive cells ± SD. (***) $P < 0.0005$, two-sample *t*-test. (***G***) Superoxide levels in cells as before, measured by flow cytometry (FACS) after staining with 1 μM fluorescent probe dihydroethidium (DHE) during 1 h. The results are expressed as the percentage of maximum cell number. The maximum cell number is the number of cells for the most-represented fluorescence intensity in the cell population of a condition and is expressed as 100%. All experiments were performed a minimum of three times.

ERK2 knockdown in cells expressing RasV12 inhibited the induction of senescence-associated β-galactosidase (SA-β-Gal) (Figure 7C), PML bodies and DNA damage foci (Figure S1C-G). Oncogenic *ras* engaged the p53/p21, $p16^{INK4a}$/RB and p38MAPK pathways in primary cells, and this was efficiently prevented by knockdown of *ERK2* (Figures 7D and S1H, I). The induction of several senescence-associated cytokine genes by RasV12 was also efficiently blocked by *ERK2* knockdown (Figure S1J-L). The inhibition of Ras-induced senescence by several shERKs was accompanied by the adoption of distinctive cell morphology of small cells growing sometimes on top of each other (Figure 7C), a complete rescue of the proliferation arrest (Figure 7E), a stimulation of DNA synthesis as measured by BrdU incorporation and KI-67 staining (Figure 7F), and the expression of mitotic markers such as phospho-$H3^{S10}$ or phospho-$H3^{S28}$ (Figure 7D). Moreover, the high levels of ROS known to contribute to DNA damage during Ras-induced senescence (110) were decreased in cells depleted of ERK2 (Figure 7G). Taken together, the results indicate that reducing ERK levels shuts down the senescence tumor suppression response to oncogenic *ras* in normal human fibroblasts.

To assess the generality of these findings, we next studied the induction of senescence by oncogenic *ras* in primary human mammary epithelial cells (HMECs). Introduction of oncogenic *ras* by retroviral gene transfer in these cells induced a senescent phenotype, characterized by induction of PML bodies, DNA damage foci, and cell cycle arrest (Figure S2A-D). We also noticed that in cultures of HMECs expressing RasV12, some cells spontaneously escaped from senescence and started proliferating as small cells. All of these cells turned out to express very low levels of RasGTP and phospho-ERK (Figure S2E),

consistent with the requirement for strong ERK/MAPK kinase signaling to sustain Ras-induced senescence. Then, we studied the effect of ERK2 knockdown on Ras-induced senescence in HMECs. As described for human fibroblasts, shERK2 (Figure 8A) reduced the expression of ERK-dependent targets (Figure 8B) and restored cell proliferation (Figure 8C) and the expression of the mitotic markers phospho-$H3^{S10}$ and phospho-$H3^{S28}$. shERK2 allowed RB phosphorylation in HMECs expressing oncogenic *ras*, and the expression of E2F target genes such as MCM6 (Figure 8D). shERK2 also prevented the induction of p53 target genes and cytokines by oncogenic *ras* in HMECs (Figure 8E). The senescent phenotype was bypassed by shERK2 with a frequency several times higher than the spontaneous escape from senescence mentioned above (Figure 8F, G).

To demonstrate that reducing ERK levels in a genetic model also prevents Ras-induced senescence, we used mouse embryonic fibroblasts (MEFs) from Erk2 knockout mice (257). In wild-type MEFs, oncogenic *ras* induced Erk1/2 phosphorylation (Figure 8H) and the expression of Erk target genes (Figure 8I). The oncoprotein E1A, able to bypass Ras-induced senescence (455), reduced Erk1/2 activation and also the expression of Erk target genes (Figure 8H, I). In *Erk2*$^{-/-}$ MEFs, oncogenic Ras induced Erk1 but not Erk2 phosphorylation (Figure 8H). This reduction in overall Erk activity was translated in a reduced induction of Erk target genes (Figure 8I). More important, oncogenic Ras failed to induce growth arrest, p53, and senescence in *Erk2*$^{-/-}$ MEFs, in clear contrast to its effects in wild-type MEFs (Figure 8J-O). In fact, *Erk2*$^{-/-}$ MEFs had a response to oncogenic *ras* similar to that of wild type MEFs expressing E1A (Figure 8J). We also looked at the expression of the tumor suppressor $p19^{ARF}$ in Erk2-null cells expressing RasV12. We found that RasV12 still induced $p19^{ARF}$ in these cells (Figure 8O), but obviously, this was not sufficient to trigger senescence. We also found that p53 was stabilized and phosphorylated at Ser15 after treatment of Erk2$^{-/-}$ MEFs with doxorubicin, indicating that their resistance to Ras-induced senescence was not the result of an accidental loss in p53 (Figure 8P).

Finally, we studied whether inhibition of ERK activity, not levels, was also sufficient to bypass RasV12-induced senescence. We used the MEK inhibitors U0126 and AZD6244,

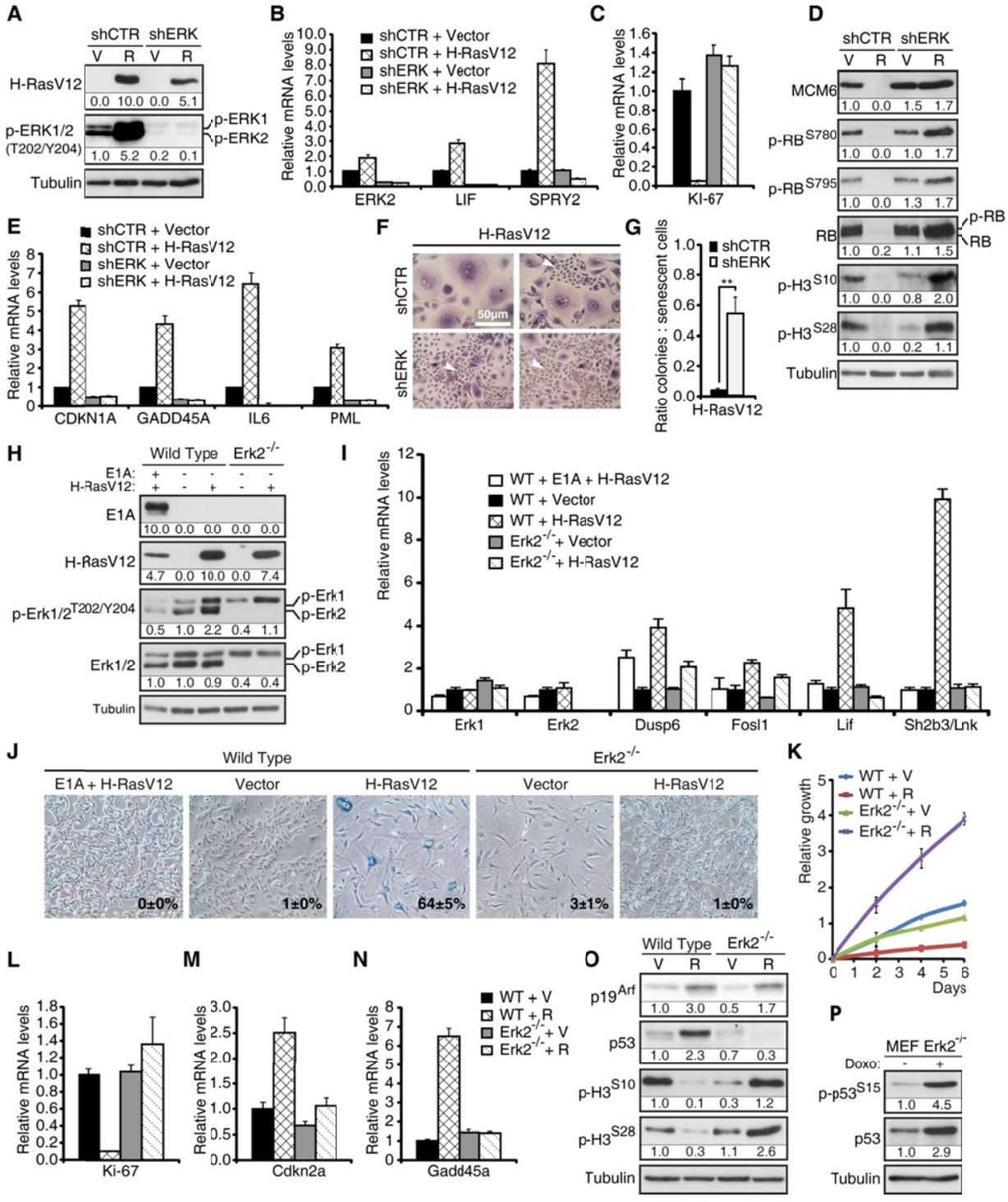

Figure 8. ERK/MAP kinases play a general role in cellular senescence

(***A-G***) Role of ERK/MAPK in H-RasV12-induced senescence in primary HMECs. (***A***) Immunoblots to confirm ERK knockdown and expression levels of H-RasV12 in extracts obtained 14 d after infection. (***B***) qPCR for ERK target genes to confirm the biological effect of ERK knockdown in cells expressing

the indicated vectors. (***C***) qPCR for KI-67, a proliferation marker, in cells as in (*A*). (***D***) Immunoblots for proteins in the RB pathway and mitosis markers in cells as in (*A*). (***E***) qPCR for senescence markers in cells as in (*A*). (***F***) Morphology of HMECs expressing H-RasV12-ER and shRNA against *ERK2* (shERK) or a nontargeting shRNA (shCTR). Note the large size and vacuolated cytoplasm of senescent cells in contrast with the small growing cells that escape from senescence (arrows) due to low phospho-ERK levels. (***G***) Quantification of the bypass from senescence between cells with shControl (shCTR) and shERK2. Error bars represent SD. (**) $P < 0.005$, two-sample *t*-test. (***H-P***) Genetic inactivation of Erk2 bypasses Ras-induced senescence in MEFs. (***H***) Immunoblots for the indicated proteins in wild-type and $Erk2^{-/-}$ MEFs expressing H-RasV12, a vector control, or H-RasV12 + E1A 14 d after infection. (***I***) qPCR for Erk target genes in cells as in (*H*). (***J***) SA-β-Gal markers in cells as in (*H*). Data were quantified from 100 cell counts in triplicate and are presented as the mean percentage of positive cells ± SD. (***K***) Growth curves started with MEFs from wild-type and $Erk2^{-/-}$ animals expressing H-RasV12 or a vector control 14 d after infection. Data are presented as the mean ± SD of triplicates. (***L-N***) qPCR for the indicated genes in cells as in (*H*). (***O***) Immunoblots for the indicated senescence markers in cells as in (*H*). (***P***) Immunoblots against p53 and $p53^{S15}$ from $Erk2^{-/-}$ MEFs treated 24 h with doxorubicin (300 ng/mL) or vehicle. Experiments were performed $n \geq 3$.

which inhibited ERK phosphorylation induced by RasV12 in human fibroblasts in a dose-dependent manner (Figure S2F) without altering ERK mRNA levels (Figure S2G). MEK inhibitors also prevented the induction of ERK target genes (Figure S2H, I) and restored RB phosphorylation and the expression of E2F targets in cells expressing RasV12 (Figure S2F). In agreement with previous results (464), MEK inhibitors blocked Ras-induced senescence (Figure S2J), growth arrest (Figure S2K-M), and the induction of the senescence genes CDKN1A and CDKN2A (Figure S2N). We thus conclude that reducing ERK activity by different manipulations in both human and mouse primary cells compromises Ras-induced senescence, preventing the induction of several tumor suppressor pathways. Next, we asked whether oncogenic *ras* was capable of transforming cells where reduced ERK levels prevented the activation of tumor suppressors.

ERK/MAPK knockdown facilitates Ras-dependent transformation of primary human cells

To investigate the effect of ERK inhibition in *ras*-dependent transformation, we first used the experimental system where RasV12 cooperates with hTERT and SV40 early region to transform normal human fibroblasts (465). We reasoned that ERK2 inhibition could be genetically equivalent to SV40 early region, which also inhibits the activation of p53 and RB

by RasV12 (465). We first prepared IMR90 cells expressing hTERT using a lentiviral vector. Then, we introduced vectors expressing shERK2 and RasV12 or the corresponding control vectors and confirmed the knockdown of ERK in these cells and the expression of oncogenic *ras* (Figure S3A). We found that ERK inhibition by shERK2 in RasV12-expressing cells enabled colony formation in soft agar (Figure 9A, top) and inhibited the process of contact inhibition, as seen in a focus assay (Figure 9A, middle). These two assays are strong indications of the transformation of normal cells into cancer cells. Consistent with these ex-vivo models, primary human fibroblasts expressing hTERT, RasV12 and shERK2 formed tumors in nude mice (Figure 9A [bottom], E). Upon histological examination, these tumors were characterized by large nuclei, abundant mitotic images, many blood vessels, and very low levels of phospho-ERK in the tumor cells (Figure S3B). These low levels of ERK were confirmed by immunoblots from tumor cell extracts (Figure S3C) or in cell lines established from the tumors (Figure S3D). We also found that adding c-MYC to the cells expressing hTERT, RasV12 and shERK2 further enhanced their transformation (Figure 9A, E). When tested for their ability to grow on a monolayer of normal fibroblasts, cells recovered from these tumors formed as many colonies in focus assays as the parent populations (Figure S3E). In conjunction, these results suggest that cells expressing oncogenic *ras* and shERK2 did not undergo additional genetic changes in vivo that would have further enhanced their transformed phenotype. As shown before for the senescence bypass, a different anti-ERK shRNA cooperated with oncogenic *ras* to transform primary human fibroblasts or HMECs (Figure S3F-I).

Finally, we observed that oncogenic *ras* was able to transform primary MEFs from Erk2 knockout animals without the need to express any other cooperating oncogene (Figure 9B-E). As shown for human fibroblasts, the ability of cells transformed by oncogenic *ras* in Erk2 knockout MEFs to form colonies in soft agar was the same before and after forming tumors in mice, suggesting that no other genetic modifications occurred in vivo to further transform these cells (Figure S3J, K). As shown before (455), oncogenic *ras* cooperated with E1A to transform primary rodent cells (Figure 9B-E). In E1A-expressing MEFs, both

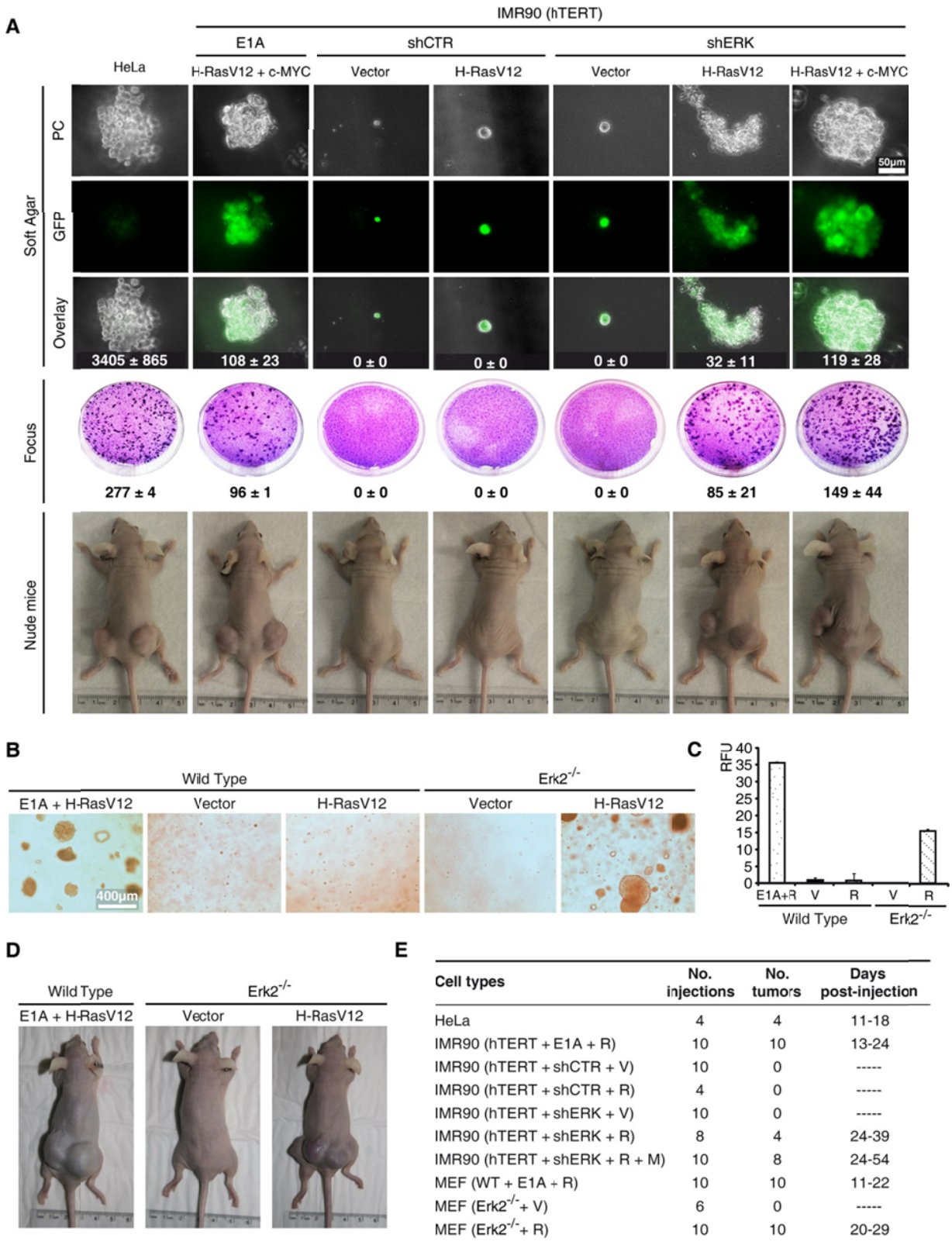

E

Cell types	No. injections	No. tumors	Days post-injection
HeLa	4	4	11-18
IMR90 (hTERT + E1A + R)	10	10	13-24
IMR90 (hTERT + shCTR + V)	10	0	-----
IMR90 (hTERT + shCTR + R)	4	0	-----
IMR90 (hTERT + shERK + V)	10	0	-----
IMR90 (hTERT + shERK + R)	8	4	24-39
IMR90 (hTERT + shERK + R + M)	10	8	24-54
MEF (WT + E1A + R)	10	10	11-22
MEF (Erk2$^{-/-}$ + V)	6	0	-----
MEF (Erk2$^{-/-}$ + R)	10	10	20-29

Figure 9. ERK/MAPK inhibition promotes Ras-induced transformation

(***A, top***) Soft agar assay with HeLa cells or IMR90 fibroblasts expressing the indicated vectors. Representative GFP-positive colonies are shown. A focus-forming assay (***A, middle***) and tumor formation in nude mice (***A, bottom***) were performed with cells as *above*. Numbers of colonies in soft agar and focus-forming assays are expressed as the mean ± SD of triplicates. (***B***) Soft agar assay with wild-type and Erk2$^{-/-}$ MEFs expressing the indicated vectors. (***C***) Quantification of (*B*) using the CyQuant GR Dye. (RFU) Relative fluorescence units (a measure of growth in soft agar). Data are presented as the mean ± SD of triplicates. (***D***) Tumor formation in nude mice of wild-type (WT) and Erk2$^{-/-}$ MEFs expressing the indicated vectors. (***E***) Quantification of tumor formation in nude mice. The number of injections that generated tumors and the time taken by the tumors to reach the threshold of significance (0.2 cm^3) are shown.

phospho-Erk1 and phospho-Erk2 were reduced (Figure 8H). The same was noticed in human cells (Figure S3A, C, D). Since decreasing ERK activity is sufficient to bypass Ras-induced senescence and promote transformation, these results suggest a novel mechanism by which E1A cooperates with oncogenic *ras* to transform primary cells. Taken together, these results reveal a tumor suppressor function of the ERK kinases in normal cells and dissociation between the transforming functions of *ras,* which do not require high ERK activity, and its ability to induce senescence, which requires high ERK activity.

Selective ERK-dependent protein degradation characterizes cellular senescence

Next we addressed the mechanism by which the strength of ERK activation induces the stress signaling pathways leading to senescence. We used vectors able to drive either high or low expression levels of RasV12. As expected, high levels of RasV12 led to higher phosphorylation of ERK1/2 and some ERK targets such as ELK^{S383} and FAK^{S910} (Figure S4A). Low levels of RasV12 slightly stimulated ERK phosphorylation and p53 target gene expression (Figure S4A, B) but did not engage the RB tumor suppressor pathway (Figure S4B) and also failed to induce growth arrest, the DDR, and senescence (Figure S4C-H). We used these vectors and a battery of phospho-specific antibodies (Kinexus) to profile the state of ERK phosphorylation targets depending on the strength of Ras signaling. We found, as anticipated, that some ERK targets were highly phosphorylated in cells expressing high levels of RasV12. However, we also found unexpectedly that some phospho-ERK targets were less phosphorylated (Figure 10A). Intriguingly, the reduction in phosphorylation of STAT3^{S727} and

Caldesmon^{S789} in cells expressing high levels of Ras was also observed at the level of total protein (Figure S4I). As protein phosphorylation and protein degradation are often linked (281), we thought that one mechanism connecting high ERK signaling to senescence might involve the degradation of phosphorylated proteins due to aberrant ERK signaling.

To support the model that increased ERK signaling leads to proteasome-dependent protein degradation in senescent cells, we used large-scale proteomics to look for phosphoproteins stabilized by the proteasome inhibitor MG132 in senescent cells. We identified an enrichment of nearly 3000 phosphopeptides from 1018 proteins. Most of the phosphorylation sites identified consisted of serine/threonine adjacent to a proline, consistent with ERK/MAPK phosphorylation sites (Figure 10B; Table SI). We also identified stabilized phosphopeptides where the phosphorylated residues were not part of the ERK consensus site that may be targets of ERK-regulated kinases. Motif analysis of the phosphopeptides revealed phosphorylation motifs for Proline–directed kinases but also basophilic and acidophilic kinases (Figure S5). We analyzed the proteomics data using a FatiGO single enrichment from the bioinformatics platform Babelomics 4.3. We found that in senescent cells, phosphoproteins that control the response to growth factor stimulation and tumor progression are unstable. Hence, the degradation pattern may favor senescence and inhibit transformation (Figure 10C). In Table SI, we present a summary of the proteomics data with references to the implication of the proteins in cell senescence and cancer pathways, and in Figure S6, we present the most significant functional categories affected by the degradation process. For example, the proteins FBXL11 (466), HSP70 (467), RSL1D1 (468), and TBX2 (469) have been previously linked to the control of senescence, validating our results. In addition, the presence of multiple proteins linked to pseudopods, cell migration, and RNA metabolism (Table SI) suggests that these pathways are targeted by a SAPD process.

We characterized in detail the degradation of c-MYC, HSP27, HSP70, KAP1, RSL1D1, and STAT3. The total level of these proteins was down-regulated in senescent cells, and all but HSP27 were restored by treatment with the proteasome inhibitor MG132,

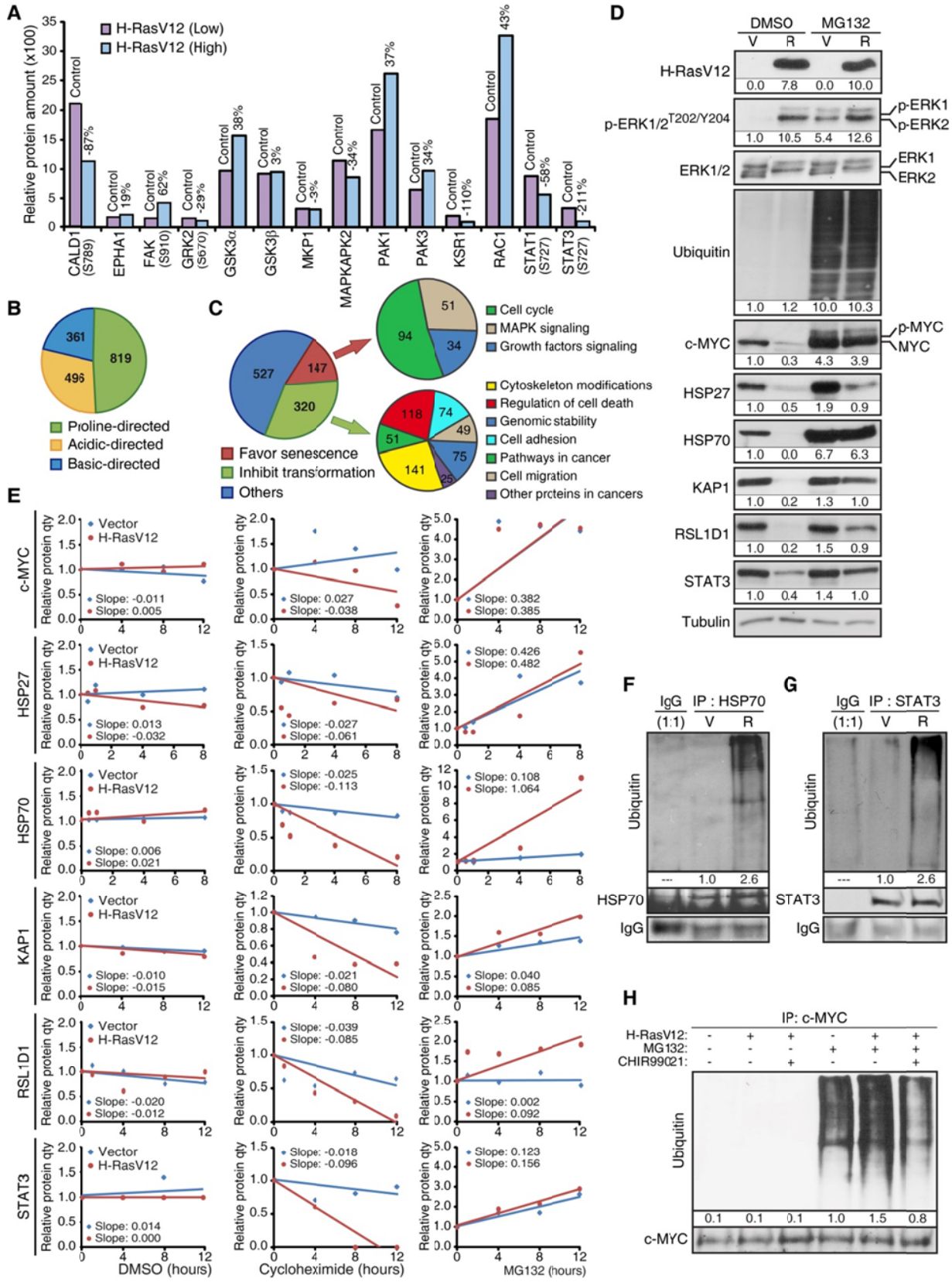
A
H-RasV12 (Low)
H-RasV12 (High)
Relative protein amount (x100)
CALD1 (S789)
EPHA1
FAK (S910)
GRK2 (S670)
GSK3α
GSK3β
MKP1
MAPKAPK2
PAK1
PAK3
KSR1
RAC1
STAT1 (S727)
STAT3 (S727)
B
Proline-directed
Acidic-directed
Basic-directed
C
Favor senescence
Inhibit transformation
Others
Cell cycle
MAPK signaling
Growth factors signaling
Cytoskeleton modifications
Regulation of cell death
Genomic stability
Cell adhesion
Pathways in cancer
Cell migration
Other proteins in cancers
D
DMSO
MG132
H-RasV12
p-ERK1/2T202/Y204
p-ERK1
p-ERK2
ERK1/2
ERK1
ERK2
Ubiquitin
c-MYC
p-MYC
MYC
HSP27
HSP70
KAP1
RSL1D1
STAT3
Tubulin
E
Vector
H-RasV12
Relative protein qty
c-MYC
HSP27
HSP70
KAP1
RSL1D1
STAT3
DMSO (hours)
Cycloheximide (hours)
MG132 (hours)
F
IgG (1:1)
IP : HSP70
Ubiquitin
HSP70
IgG
G
IgG (1:1)
IP : STAT3
Ubiquitin
STAT3
IgG
H
IP: c-MYC
H-RasV12:
MG132:
CHIR99021:
Ubiquitin
c-MYC

Figure 10. Selective and proteasome-dependent protein degradation characterizes Ras-induced senescence

(***A***) Summary of proteomics data obtained from cell lysates of IMR90 fibroblasts expressing a low level (LR) or high level (HR) of oncogenic *ras*. Cells were harvested 14 d after infection. Data show phosphorylation levels of 14 ERK targets measured by Western blot with phospho-specific antibodies by Kinexus (n = 1). The difference in the relative protein amount in cells that express HR is presented as a percentage of the relative protein amount in LR-expressing cells set as a reference (control). (***B***) Frequencies of phosphorylation motifs in phosphopeptides stabilized by MG132. Ras senescent cells (10 d after infection with H-RasV12) were treated 18 h with DMSO (control) or 20 μM MG132. Then, cells were harvested, and protein extracts were analysed by liquid chromatography-tandem mass spectrometry (LC-MS/MS) for phosphoproteomics (n = 2, in triplicate each time). Phosphopeptides enriched in cells treated with MG132 were analysed with the Motif-X software tool. Three motif families were identified (acidic, basic, and proline-directed), and almost half the phosphopeptides with an enriched motif have a proline-directed motif. (***C***) FatiGO single-enrichment analysis of phosphopeptides enriched in Ras-senescent cells, treated with MG132, with the Babelomics 4.3 platform. This platform was used to identify *Gene Ontology* (GO), *Kyoto Encyclopedia of Genes and Genomes* (KEGG), and *Reactome* terms that were significantly enriched (Figure S5B). Then, these terms and their associated peptides were grouped in the indicated general categories. These categories were also classified according to their predicted ability to induce senescence or limit transformation when they are decreased. (***D***) Immunoblots for the indicated proteins and total ubiquitinylated proteins from fibroblasts expressing oncogenic *ras* or an empty vector (10 d after infection) and treated 18 h with 20μM MG132 or DMSO as control (n = 3). (***E***) Protein stability assays for the indicated proteins in cells as in (*D*). Cells were treated with DMSO, 10 μg/mL cycloheximide, or 20 μM MG132 for the indicated times. The relative protein quantity was evaluated by immunoblotting and quantification with Adobe Photoshop CS4 or Image Lab 4.0 ($n \geq 2$). (***F, G***) Immunoprecipitation of HSP70 or STAT3 in extracts from IMR90 cells expressing H-RasV12 or an empty vector 10 d after infection and treated 18 h with 20μM MG132 and immunoblotted against mono- and polyubiquitinylated conjugates ($n \geq 2$). (***H***) Immunoprecipitation of c-MYC in extracts from cells expressing H-RasV12 or an empty vector (10 d after infection) and treated for 18 h with 20 μM MG132 and/or GSK3 inhibitor CHIR99021 (3 μM) and immunoblotted against mono- and polyubiquitinylated conjugates.

consistent with the anticipated role of the proteasome in SAPD (Figure 10D). This proteasome-dependent degradation seems to be selective because total levels of ubiquitinated proteins did not change significantly in cells expressing RasV12 (Figure 10D). We also evaluated the half-life of several of these proteins after inhibition of protein synthesis with cycloheximide. As expected, c-MYC, HSP70, KAP1, RSL1D1, and STAT3 had a reduced half-life that was restored by the proteasome inhibitor MG132 in primary fibroblasts expressing RasV12 (Figure 10E). In addition, in RasV12-expressing cells treated with

MG132, the levels of ubiquitinated HSP70 and STAT3 were increased (Figure 10F, G). Together, the results are consistent with a model of selective protein degradation triggered by aberrant ERK signaling during Ras-induced senescence. However, not all phosphoproteins found unstable in our proteomic analysis are expected to be depleted in senescent cells, since their reduction will depend on the extent of phosphorylation of each protein pool and compensatory biosynthesis and the degradation rate for each protein in normal conditions. In addition, although most phosphoproteins contain candidate ERK phosphorylation sites, others do not, suggesting that other kinases may be engaged by ERK in the process. The case of c-MYC illustrates this point. c-MYC is phosphorylated by ERK at Ser62, and this phosphorylation facilitates phosphorylation at Thr58 by GSK3; it is this latter event that targets c-MYC to the proteasome (470). In agreement with this model, the GSK3 inhibitor CHIR99021 inhibited the ubiquitination of c-MYC in Ras-expressing cells (Figure 10H). Nevertheless, the levels of c-MYC, HSP27, HSP70, KAP1, RSL1D1, and STAT3 were restored by shERK2 in Ras-expressing IMR90 cells (Figure 11A) or HMECs (Figure 11B), indicating that ERK signaling, directly or indirectly, triggers their degradation. In MEFs, we also observed a decrease in levels of Hsp70, Kap1, and Stat3, but not c-Myc, in response to RasV12, and this down-regulation did not occur in $Erk2^{-/-}$ MEFs (Figure 11C). In all cell types, the ERK-dependent decrease in c-MYC, HSP70, KAP1, RSL1D1, and STAT3 could not be explained by a reduction in their mRNA levels (Figure S7A-C). However, HSP27 levels were reduced at the mRNA level by an ERK-independent mechanism, explaining why its levels could not be restored by MG132 (Figure S7A, B). Of note, RasV12 induced RSL1D1 mRNA levels in human cells, perhaps as a feedback response to the reduction in protein levels (Figure S7A, B). To investigate whether protein degradation is dependent on ERK levels only or ERK signaling, we used MEK inhibitors. Both AZD6244 and U0126 restored the levels of selected proteins in RasV12-expressing cells (Figure 11D) without corresponding changes in mRNA levels (Figure S7D-I), consistent with their ability to bypass RasV12-induced senescence (Figure S2F-N).

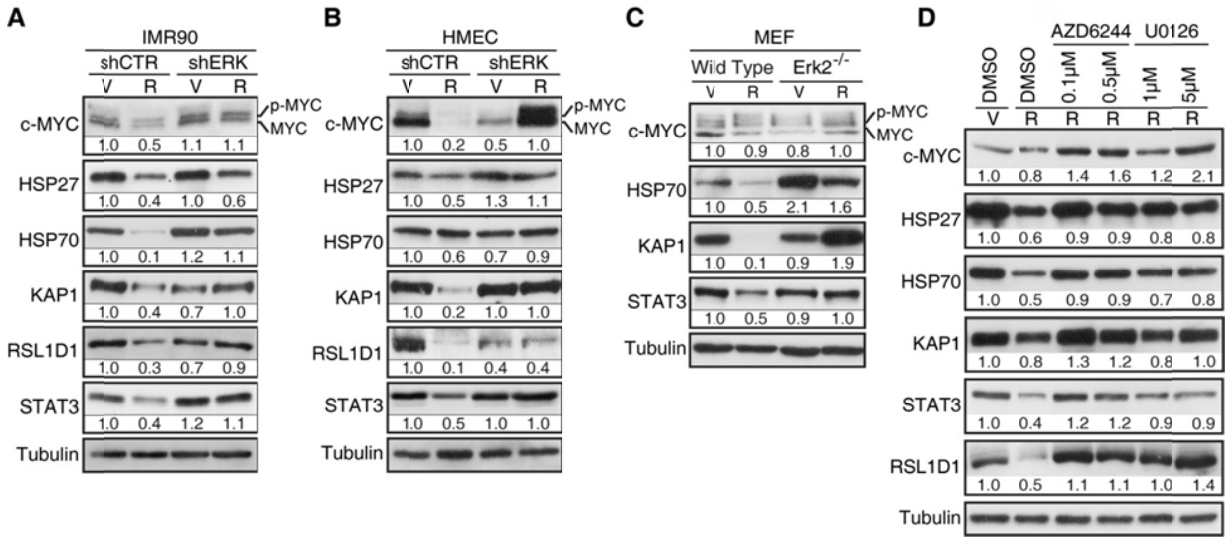

Figure 11. Role of ERK kinases in SAPD

(***A***) Immunoblots showing the levels of the indicated proteins in IMR90 cells expressing H-RasV12 (R) or a vector control (V) and shERK2 or a control shRNA (shCTR) 14 d after infection ($n \geq 3$). (***B***) Immunoblots for proteins and conditions as in *A* but for HMECs ($n = 3$). (***C***) Immunoblots showing the levels of the indicated proteins in wild-type or Erk2$^{-/-}$ MEFs expressing oncogenic *ras* or a vector control 14 d after infection ($n = 3$). (***D***) Immunoblots for the indicated proteins in IMR90 cells with a vector control (V) or H-RasV12 (R) and treated with the indicated chemicals. The treatments started immediately after infection, and the medium was changed every 2 d. Cells were harvested 10 d after infection ($n = 2$).

Cell senescence can also be induced by other stresses, such as radiation and short telomeres (replicative senescence). These situations commonly trigger a persistent DDR (118), mitochondrial dysfunction, accumulation of ROS (111), and a constitutive ERK activation (451). We thus reasoned that sustained ERK activation may accelerate protein degradation during replicative senescence and contribute to the establishment and maintenance of this phenotype. We cultured young normal human fibroblasts until their replicative senescence in the presence of two concentrations of the MEK inhibitors AZD6244 and U0126. We confirmed that senescent (old) fibroblasts displayed a constitutive high ERK activity, but MEK inhibitors reduced this trait almost to young levels (Figure 12A). This inhibition of phospho-ERK levels translated in a decrease of p53 phosphorylation at Ser15 and an increase in RB phosphorylation, indicating a cell cycle pattern of young healthy cells (Figure 12A). In

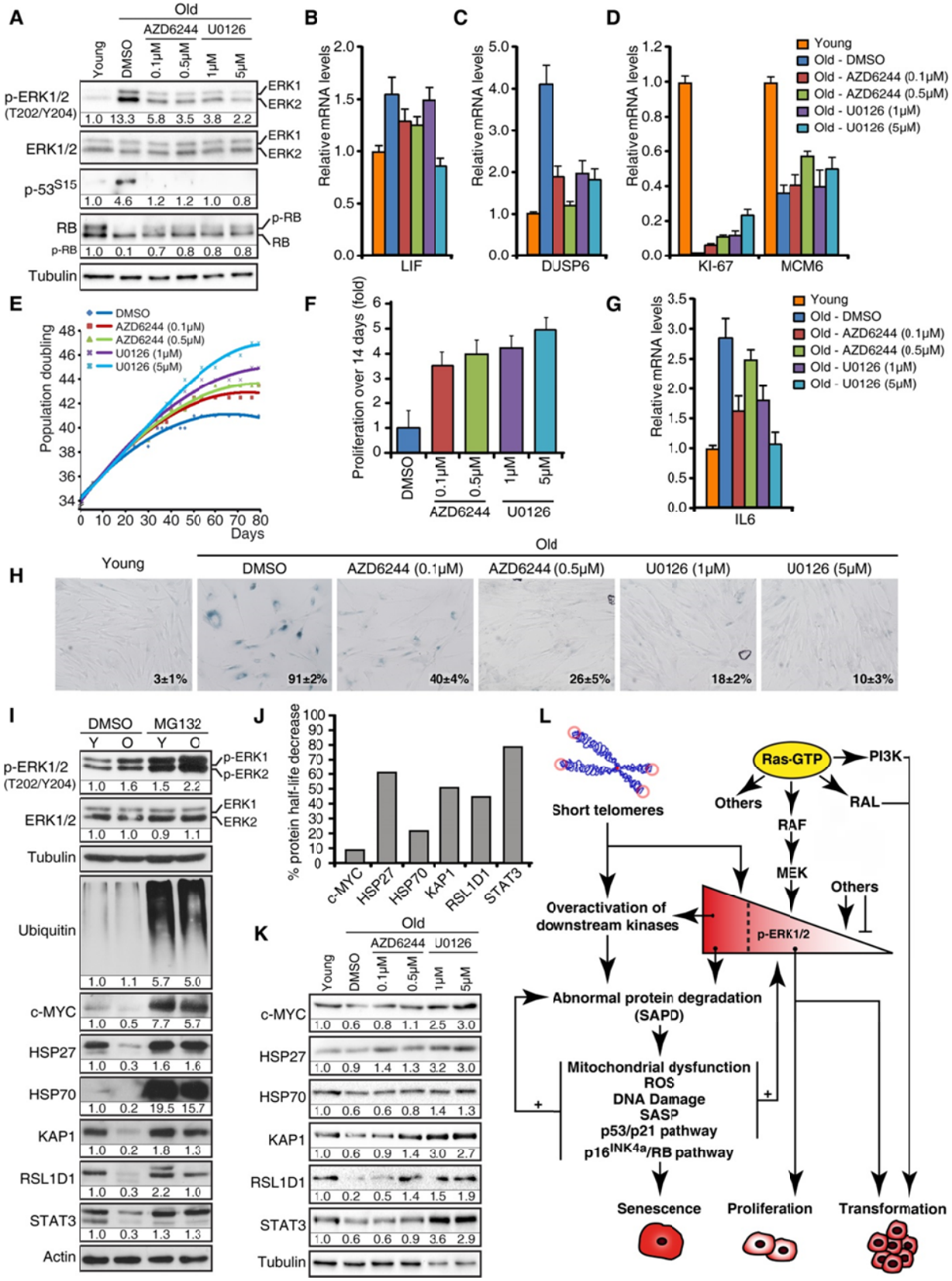
A
Old
AZD6244
U0126
Young
DMSO
0.1μM
0.5μM
1μM
5μM
p-ERK1/2 (T202/Y204)
1.0 13.3 5.8 3.5 3.8 2.2
ERK1/2
p-53S15
1.0 4.6 1.2 1.2 1.0 0.8
RB
p-RB
1.0 0.1 0.7 0.8 0.8 0.8
Tubulin
ERK1
ERK2
p-RB
RB
B
Relative mRNA levels
LIF
C
DJSP6
D
KI-67
MCM6
Young
Old - DMSO
Old - AZD6244 (0.1μM)
Old - AZD6244 (0.5μM)
Old - U0126 (1μM)
Old - U0126 (5μM)
E
Population doubling
Days
F
Proliferation over 14 days (fold)
G
IL6
H
3±1%
91±2%
40±4%
26±5%
18±2%
10±3%
I
DMSO
MG132
Y O Y C
p-ERK1/2 (T202/Y204)
1.0 1.6 1.5 2.2
ERK1/2
1.0 1.0 0.9 1.1
Tubulin
Ubiquitin
1.0 1.1 5.7 5.0
c-MYC
1.0 0.5 7.7 5.7
HSP27
1.0 0.3 1.6 1.6
HSP70
1.0 0.2 19.5 15.7
KAP1
1.0 0.2 1.8 1.3
RSL1D1
1.0 0.3 2.2 1.0
STAT3
1.0 0.3 1.3 1.3
Actin
p-ERK1
p-ERK2
J
% protein half-life decrease
c-MYC
HSP27
HSP70
KAP1
RSL1D1
STAT3
K
c-MYC
1.0 0.6 0.8 1.1 2.5 3.0
HSP27
1.0 0.9 1.4 1.3 3.2 3.0
HSP70
1.0 0.6 0.6 0.8 1.4 1.3
KAP1
1.0 0.6 0.9 1.4 3.0 2.7
RSL1D1
1.0 0.2 0.5 1.4 1.5 1.9
STAT3
1.0 0.6 0.6 0.9 3.6 2.9
Tubulin
L
Short telomeres
Ras-GTP
PI3K
Others
RAL
RAF
MEK
Others
Overactivation of downstream kinases
p-ERK1/2
Abnormal protein degradation (SAPD)
Mitochondrial dysfunction
ROS
DNA Damage
SASP
p53/p21 pathway
p16INK4a/RB pathway
Senescence
Proliferation
Transformation

Figure 12. ERK and the SAPD during replicative senescence

(***A***) Immunoblots for the indicated proteins in young (population doublings [PDL] = 21.5) and old (PDL ≥ 40) IMR90 cells treated with the indicated concentrations of MEK inhibitors or DMSO as control for 27 d. Fresh medium and inhibitors were added every 2 d. (***B-D***) qPCR for mRNAs encoded by ERK-stimulated genes and proliferation markers in cells as in (*A*). (***E***) PDL of normal human fibroblasts in the presence of the indicated concentrations of MEK inhibitors or vehicle during 80 d. The experiment was started with 1 x 10^6 of middle-age (PDL = 34) IMR90 cells for each condition. (***F***) Relative growth of late-passage human fibroblasts (PDL ≥ 41) after 60 d of treatments with MEK inhibitors or vehicle evaluated by a crystal violet assay. (***G***) qPCR for IL6 in cells as in (*A*). (***H***) SA-β-Gal of cells as before after 40 d of treatments. Data were quantified from 100 cell counts in triplicate and are presented as the mean percentage of positive cells ± SD (shown in the *bottom right* of every panel). (***I***) Immunoblots for the indicated proteins in young (Y) (PDL = 21.5) and old (O) (PDL = 40) IMR90 cells treated with 20 μM MG132 or vehicle (n = 2). (***J***) Relative decrease of half-lives for the indicated proteins calculated from cycloheximide stability assays as presented in Figure 10E. (***K***) Immunoblots for the indicated proteins in cells as in (*A)*. (***L***) High-strength ERK signals or short telomeres lead to protein degradation, which in turn activate multiple stress responses that characterize cellular senescence. Note that the process could be self-sustained by multiple positive feedback loops. Lower levels of ERK signaling are permissive for Ras-dependent transformation in cooperation with other signals stimulated by oncogenic *ras*.

addition, the levels of ERK target genes LIF and DUSP6 increased with replicative senescence and were decreased by MEK inhibitors (Figure 12B, C). MEK inhibitors improved cell proliferation and the life span of normal human fibroblasts according to several criteria. First, they increased the expression of the proliferation markers KI-67 and MCM6 (Figure 12D). Second, they increased the number of passages upon serial culture of normal human fibroblasts (Figure 12E). Third, in a proliferation assay performed over 14 d, cells from late-passage cultures proliferated faster if they were previously treated with MEK inhibitors (Figure 12F). Finally, since the loss of proliferation potential of normal human fibroblasts upon serial culturing is due to cellular senescence, we measured the senescence markers IL6 (part of the senescence-associated secretory phenotype) and SA-β-gal. MEK inhibitors reduced significantly the accumulation of both markers in late-passage cultures (Figure 12G, H). Taken together, our data indicate that ERK signaling is required for both replicative senescence and OIS and raise the question of whether the SAPD phenotype is also relevant for replicative senescence.

To investigate whether the proteins that we found down-regulated in Ras-induced senescence were also reduced during replicative senescence, we measured their levels in old and young cultures by immunoblotting. Again, we characterized these cells for a variety of cell cycle and senescence markers (Figure S8A-H). We found that c-MYC, HSP27, HSP70, KAP1, RSL1D1, and STAT3 were all found down-regulated in replicative senescence, and their levels were restored by the proteasome inhibitor MG132 (Figure 12I). The mRNAs coding for these proteins were not down-regulated in senescent cells, and some of them were found slightly increased (Figure S8I). The half-life of all of these proteins was decreased in senescent cells (Figure 12J) and restored by MG132 (Figure S8J). Culturing cells with MEK inhibitors prevented the proteasome-dependent down-regulation of these proteins (Figure 12K), and the mRNAs for all of them but HSP27 were not changed (Figure S8K). Altogether, the results indicate that replicative senescence and OIS involve a proteasome-dependent degradation of multiple proteins (SAPD), which can potentially explain the activation of many stress signaling pathways in senescent cells and their resistance to proliferating stimuli (Figure 12L). The mechanistic connections between the SAPD and the stresses that characterize senescence suggest multiple positive feedback loops in the process that may contribute to the robustness of senescence as a tumor suppressor mechanism.

If SAPD is important for senescence, it should be possible to induce senescence by mimicking the process and bypass senescence by inhibiting it. We tested this idea first by using shRNAs against HSP27, HSP70, KAP1, RSL1D1, and STAT3 (Figure S9A, B), and, as expected, the individual knockdown of these proteins triggers cellular senescence in both primary fibroblasts and IMR90 cells transformed by hTERT, RasV12, and shERK2 (Figures 13A and S9A, B). Unfortunately, we could not rescue senescence with proteasome inhibitors because they stabilize multiple tumor suppressors upon long-term incubation, leading to cell death. On the other hand, ectopic expression of the viral oncoproteins E1A and E6/E7 (Figure 13B-D) restored cell proliferation and inhibited senescence (Figures 13E and S9C-E). The expression of all tested SAPD targets — c-MYC, HSP27, HSP70, KAP1, RSL1D1, and STAT3 — was restored by these viral oncoproteins (Figure 13F), while the expression of their mRNAs was not generally increased (Figure S9F-H), indicating a close correlation between SAPD inhibition and bypass of senescence.

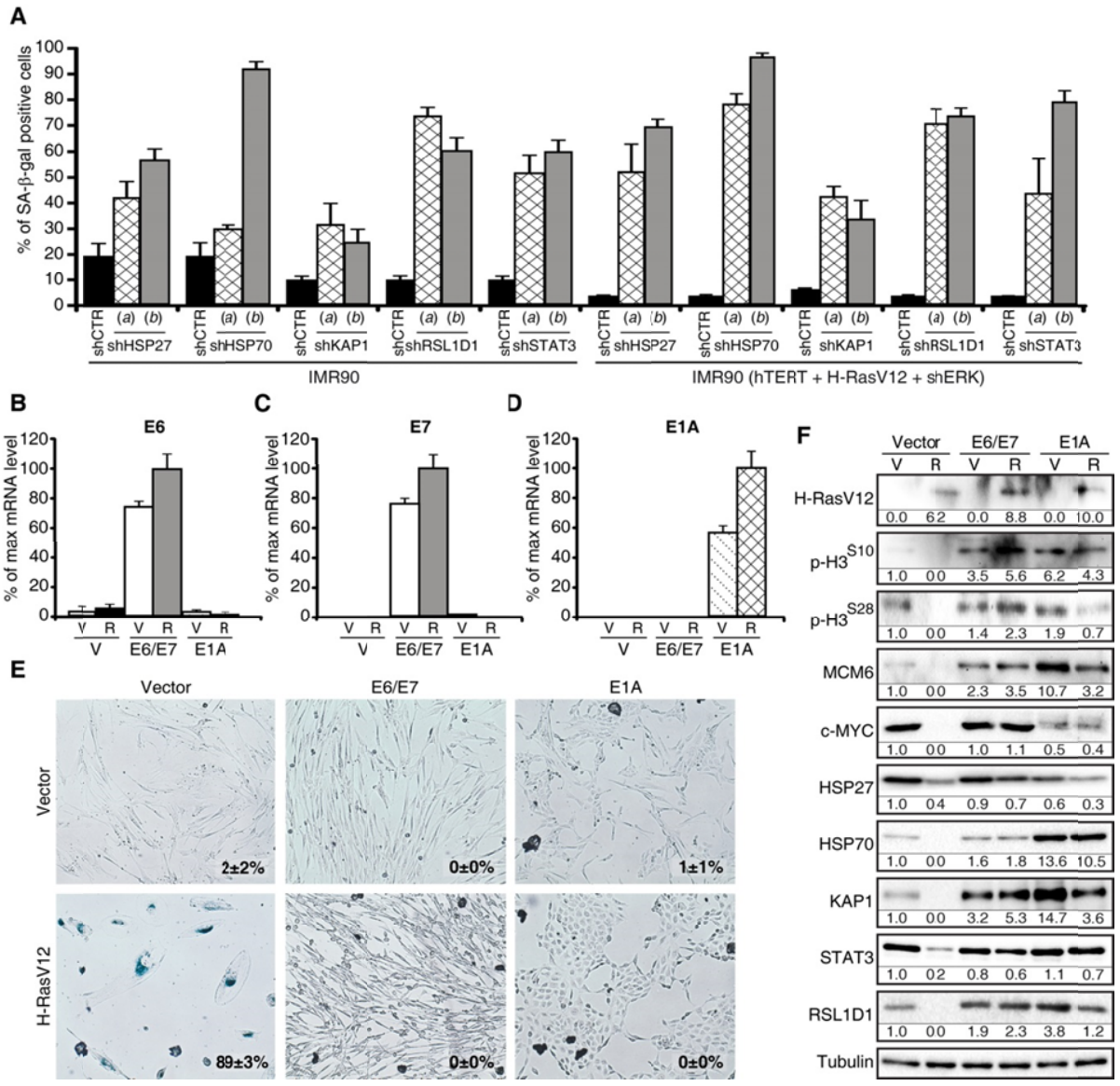

Figure 13. Inactivation and stabilization of targets of SAPD

(***A***) SA-β-Gal of wild-type IMR90 cells or transformed IMR90 cells (hTERT, H-RasV12, shERK2) expressing the indicated shRNA expression vectors fixed 10 d after infection. Data were quantified from 100 cell counts in triplicate and are presented as the mean percentage of positive cells ± SD. These experiments were done in triplicate and at least two times. (***B-D***) qPCR for the viral oncoproteins E6, E7, and E1A expressed from retroviral vectors in IMR90 cells. (***E***) SA-β-Gal of IMR90 fibroblasts expressing an empty vector, the human papillomavirus E6/E7 oncoproteins, or the adenovirus E1A oncoproteins together with H-RasV12 or an empty vector. SA-β-Gal activity was measured 14 d after infection. Data were quantified from 100 cell counts in triplicate and are presented as the mean percentage of positive cells ± SD. (***F***) Immunoblots for cell cycle-regulated proteins and SAPD targets using extracts from cells as in (*E)*.

High levels of ERK/MAPK activation characterize benign prostate tumors and predict a better outcome in malignant tumors

To confirm the biological and clinical importance of senescence stimulated by hyperactivation of ERK and the SAPD process, we next investigated several prostate tumors. In cases of benign prostatic hyperplasia (BPH), which can be considered senescent lesions (103, 471), we found very high levels of phospho-ERK as well as the senescence markers $p16^{INK4a}$ and PML in epithelial cells of prostate acini (Figures 14A, B and S10A, B). In prostate carcinomas, ERK activation was never seen as high as in BPH (Figure 14A, B vs. C). Moreover, in epithelial cells, nuclear phospho-ERK levels had an inverse correlation with the Gleason pattern ($P < 0.05$) (Figure S10C) and a positive correlation with the presence of regions of BPH in the same prostate ($P < 0.05$) (Figure S10D). We also found a negative correlation between phospho-ERK staining in the nucleus of the tumor cells or in the tissue adjacent to the tumor and patients' biochemical relapse (measured by their prostate-specific antigen [PSA] levels; $P < 0.06$) (Figure 14C, D). Consistent with our results, ERK activation is rare in human pancreatic cancers, where *ras* mutations occur in ~90% of the cases (384), and correlations between ERK activation and good prognosis were previously reported in prostate (389) and breast cancer patients (363).

We also stained sections of normal prostate, BPH, and prostate cancer for one of the targets of SAPD, STAT3. Consistent with the results shown above characterizing BPH as senescent benign lesions with high levels of phospho-ERK, STAT3 was found down-regulated in BPH when compared to normal tissues, while most malignant tumors displayed high levels of STAT3 (Figure 14E).

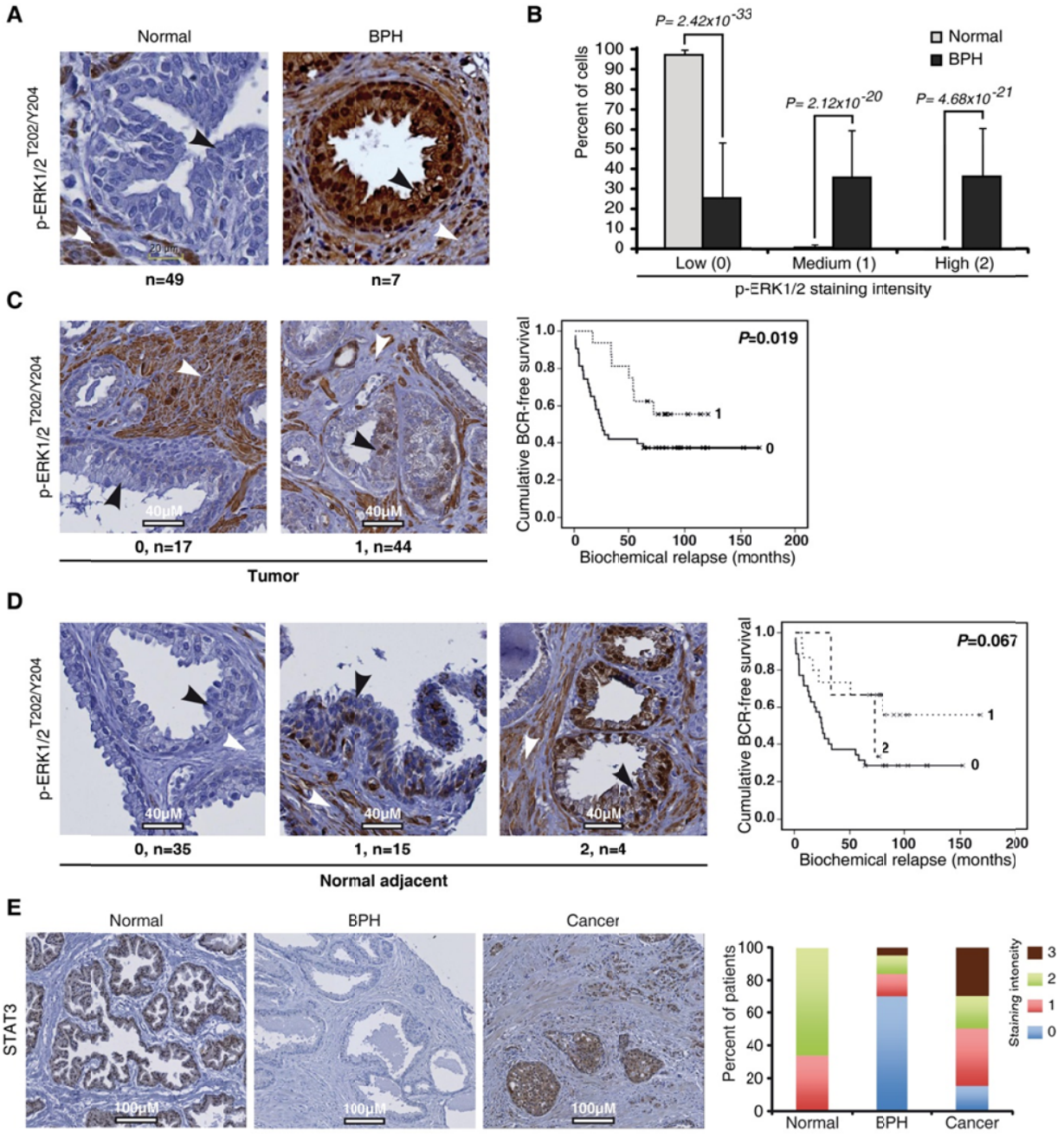

Figure 14. Phospho-ERK and STAT3 in the normal prostate and BPH

(***A***) Phospho-ERK staining in samples from patients with BPH or normal controls. White arrows point the stroma, and black arrows point to epithelial cells. (***B***) Quantification of phospho-ERK data in normal and BPH patients according to three degrees of staining intensity (none, 0; moderate, 1; and high, 2). The differences between normal tissues and BPH were evaluated with the nonparametric Mann-Whitney *U*-test. (***C***) Degrees of phospho-ERK staining (0, 1 and 2) in prostate cancer. The survival Kaplan-Meier curves describe the time for biochemical relapse (BCR) in patients with different levels of staining. (***D***) Degrees of phospho-ERK staining (0, 1, and 2) in normal tissue

adjacent to prostate cancer and survival Kaplan-Meier curves as in *C*. (***E***) STAT3 staining in samples from patients with BPH ($n = 43$) or normal controls ($n = 3$) or cancer patients ($n = 20$). The percentage of patients with a STAT3 staining of four different degrees of intensity (none, 0; low, 1; moderate, 2; and high,3) is shown in the *right* panel. The differences between normal and tumor tissues versus BPH were evaluated with the nonparametric Mann-Whitney *U*-test, $P = 0.0003$.

2.3.4 Discussion

We show here that the outcome of the stimulation of the ERK/MAP kinases depends on the expression levels and activity of ERK1/2. In normal cells, high levels of stimulation led to cellular senescence. In contrast, reducing ERK levels and, as a consequence, its activity rescued cells from senescence and facilitated cell transformation by oncogenic *ras*. Our results are consistent with previous data showing that MEK inhibitors can bypass Ras-induced senescence (464) and that shRNAs against MEK increased tumor formation in Myc-expressing cells (472). Collectively, these studies reveal a tumor suppressor role for the ERK/MAP kinase pathway, which depends on the strength of its activation, and anticipate that molecular mechanisms controlling ERK kinase levels and activity are critical for tumor suppression and are likely targets of the transformation process.

Most functions of the ERK/MAP kinase pathway depend on the ability of the ERK kinases to phosphorylate multiple target proteins. How, then, do these kinases stimulate or inhibit cell proliferation, depending on the strength of their activity? An unbiased proteomics study comparing the levels and phosphorylation of several ERK targets in conditions of high or moderate activity led to the identification of a selective and ERK-dependent protein degradation process in senescent cells that we named SAPD. SAPD provides a direct mechanism to explain the anti-proliferative prosenescence functions of the ERK/MAP kinase pathway because phosphorylation and protein degradation are tightly linked (281). During normal signaling, this process will only reduce a minor fraction of every ERK target protein because only a minor fraction of each protein is phosphorylated (473). However, aberrant ERK signaling can effectively deplete some ERK targets because the fraction of phosphorylation will be dramatically increased (Figure S11). SAPD also explains the inability of cells with activated oncogenes to proliferate despite activation of growth signaling pathways. Analysis of individual SAPD targets likely explains many traits of senescence,

including the cell cycle arrest, DDR, telomere dysfunction, and cell motility defects (Table SI). For example, the down-regulation of c-MYC or HSP70 were reported to be sufficient to trigger senescence (467, 474, 475), and the down-regulation of STAT3 and several mitochondrial import proteins could account for the mitochondrial dysfunction associated with Ras-induced senescence (110, 476). Interestingly, both c-MYC and STAT3 cooperate with oncogenic *ras* to transform primary cells (476, 477) and are targets of ERK-dependent protein degradation. Remarkably, the oncoprotein E1A cooperates with *ras* for transformation, but it is not clear how E1A may block p53 functions or stabilize c-MYC. We show now that by reducing overall ERK phosphorylation, perhaps via the induction of ERK-specific phosphatases (478), E1A can cooperate with RasV12 as ERK knockdown or the SV40 early region.

The mechanistic links between ERK activity and protein degradation will require further studies. However, most phosphopeptides stabilized by proteasome inhibitors in Ras senescent cells contained serine or threonine residues adjacent to proline (Figure 10B; Table SI), a characteristic of ERK phosphorylation sites. However, not all phosphoproteins stabilized by proteasome inhibitors in senescent cells were recognized ERK targets or contained ERK phosphorylation sites. This suggests that other kinases downstream of ERK or the DDR may provide signals for phosphorylation-dependent protein degradation, leading to senescence. In addition, an overall reduction of phosphatase activity in senescent cells due to ROS may also contribute to phosphorylation-dependent protein degradation and likely explains why SAPD is also observed in cells with short telomeres, which are characterized by mitochondrial dysfunction and oxidative stress (111, 479).

The increase in phospho-ERK levels during replicative senescence and the increase in the life span of normal human fibroblasts after using inhibitors of the ERK pathway suggest a role for ERK signaling in the activation of the senescence program by short telomeres. We found that the phosphorylation of p53 at Ser15, a hallmark of the DDR, was prevented by MEK inhibitors. This observation is consistent with results showing that inhibition of the DDR can restore cell cycle progression despite telomere shortening (118). In some contexts, preventing telomere shortening by expressing telomerase can delay aging in mice (480, 481).

Since MEK inhibitors were able to extend the replicative life span of normal human fibroblasts, which is normally limited by short telomeres, they could be tested to mitigate signals from short telomeres during aging or age-related diseases.

Clinical studies in a variety of cancers indicate that in some tumors, phospho-ERK levels are remarkably low. The most compelling example of phospho-ERK down-regulation was described in pancreatic tumors where *ras* mutations occur frequently (384). Presumably, pancreatic carcinogenesis selects early for events that down-regulate ERK levels/activity to avoid senescence and other anti-proliferative consequences of high ERK activity. Interestingly, patients with pancreatic tumors with high ERK levels had better survival and responded better to treatment (482), suggesting that some of the tumor suppressor functions of the ERK pathway could be reactivated in cancer patients. Likewise, in mammary carcinomas, phospho-ERK levels correlated with good prognosis and a less aggressive phenotype (363, 364), and similar correlations were found in brain tumors as well (483, 484). We extend these observations here by showing that phospho-ERK levels were remarkably low in the most aggressive prostate tumors. Also, patients with tumors having high phospho-ERK levels had a better prognosis. In agreement with our findings, it has been reported that advanced prostate cancer correlates with low phospho-ERK and high AKT levels (389). It has been reported as well that, in some tumors, phospho-ERK levels are very high and that MEK inhibitors may have therapeutic value (485). We anticipate that such tumors contain genetic or epigenetic lesions that inactivate the protein degradation mechanism acting downstream from ERK to mediate tumor suppression.

Astonishingly, we found a dramatic increase in phospho-ERK staining along with the senescence markers PML and $p16^{INK4a}$ in BPH. Senescent cells have been also observed in benign human nevi, which, like BPH, rarely progress into malignant melanomas (80). On the other hand, in some mouse models of prostate cancer, premalignant lesions (prostatic intraepithelial neoplasias [PIN]) display some markers of senescence in association with less aggressive but detectable tumor progression (457). It will be very important to characterize which traits associated with senescence determine the reversibility of the cell cycle arrest and the potential for further tumor progression. The incidence of both prostate cancer and BPH

increases with age, and both require androgens for growth, but unlike PIN, BPH is not a premalignant lesion (486). Comparison of lesions that do not progress, such as BPH, and lesions that eventually become malignant tumors, such as PIN (487), can help us understand how senescence prevents tumor formation in vivo. One such factors is the presence of PML bodies, which accumulate in an ERK-dependent manner during OIS in cell culture and are highly expressed in BPH but absent in PIN lesions (103). To circumvent ERK-dependent tumor suppression, some tumors may select for a reduction of ERK levels/activity, while others may disable the SAPD mechanism. The relationship between ERK levels, senescence, and transformation is also relevant for anti-cancer therapeutics, as drugs that inhibit the pathway may inhibit tumor suppression in some contexts, while drugs increasing ERK activity beyond the threshold required for senescence may have anti-tumor effects. In conclusion, we describe a plausible mechanism linking hyperactivation of signaling pathways with protein degradation and the cellular defects and malfunctions associated with cellular senescence, suggesting that attenuation of excessive or aberrant signaling can have anti-aging effects by preventing cellular senescence.

2.3.5 Materials and methods

Mice and cells

All mouse experiments were conducted in accordance with institutional and national guidelines and regulations. Conditional *Erk2*$^{flox/flox}$ female mice (257) were crossed with male mice carrying a Cre-expressing transgene under the control of a Sox2 promoter (488) to generate heterozygous *Erk2*$^{-/+}$ animals. Erk2 knockout embryos (*Erk2*$^{-/-}$) were obtained in normal Mendelian frequencies when male *Sox2-Cre*; *Erk2*$^{-/+}$ mice were crossed to *Erk2*$^{flox/flox}$ females. Sox2-mediated excision by the Cre recombinase permitted the rescue of the otherwise embryonic-lethal phenotype caused by the absence of Erk2 by specifically excising *Erk2* floxed alleles in the epiblast and maintaining functional floxed alleles in the extraembryonic tissues of the embryo. MEFs were prepared at embryonic day 14.5 (E14.5) as previously reported (257).

For xenografts, BALB/c 6-wk-old nude mice (Charles River) were injected subcutaneously in both flanks with 10^6 cells resuspended in 250 µL of PBS mixed with 250 µL of Matrigel (BD Biosciences) at 4°C. Tumor formation was evaluated over a period of 60 d. Tumors >0.2 cm^3 were counted, and mice were euthanized before the end point of the experiment when tumor volume reached 2 cm^3.

Cell lines, reagents, plasmids, quantitative PCR (qPCR), cell growth analysis, soft agar, focus-forming assay, and protein analysis (immunoblotting and immunofluorescence) are described in the Supplemental Material.

Immunohistochemistry

We used samples from seven patients diagnosed with BPH and five different tissue microarrays (TMAs) (489). The first is comprised of 49 normal prostate specimens from autopsies. The four others contain tissues obtained from 64 patients with primary prostate cancer. They are comprised of related nonneoplasic tissues adjacent to prostate cancer and cancerous tissues from 64 patients who underwent radical prostatectomy. Regions of normal, intraepithelial neoplasia or cancerous epithelial tissue were identified by two pathologists and subsequently spotted on TMAs (489). Specimens were obtained from consenting patients, and the institutional ethics review committee approved the study. We also purchased TMAs from Biochain Institute (catalog no. Z5070001). They comprised 63 cores, with 43 cases of BPH and 16 cases of adenocarcinomas. Normal prostate samples were obtained from BioChain Institute.

Tissue sections and TMAs were stained with a mouse monoclonal anti-phospho-ERK1/2$^{T202/Y204}$ (1:175; clone E10, no. 9106, Cell Signaling Technology), anti-PML antibody (1:300; clone PG-M3, Sc-966, Santa Cruz Biotechnology), and anti-p16^{INK4a} (1:25; clone F-12, Sc-1661, Santa Cruz Biotechnology). Primary antibody detection was carried out using the LSAB 2 peroxidase system from DAKO. Briefly, tissue samples were deparaffinized, rehydrated, and treated with 0.3% H_2O_2 in methanol to eliminate endogenous peroxidase activity. Antigen epitope retrieval was performed by heating for 15 min at 95°C in Tris–EDTA buffer (10 mM Tris Base, 1 mM EDTA solution, pH 8.0) for phospho-ERK and PML or 10

mM citrate buffer (pH 6.0) for $p16^{INK4a}$. All subsequent steps were done at room temperature. The sections were blocked with a protein-blocking serum-free reagent (DAKO) and incubated with primary antibody for 60 min followed by a 20-min treatment with the secondary biotinylated antibody (DAKO) and then incubated for 20 min with streptavidin-peroxidase label (DAKO). Reaction products were developed with diaminobenzidine (DAKO) containing 0.3% H_2O_2 as a substrate for peroxidase. Nuclei were counterstained with Harris hematoxylin (Sigma-Aldrich).

Statistics

Statistical analysis was performed using SPSS software 16.0 (SPSS, Inc.). The expression level of phosphorylated ERK1/2 was evaluated on a scale of 0 (for no expression) to 2 (strong expression) in both the epithelial cells (nucleus and cytoplasm) and the stroma of normal prostate samples, normal adjacent tissues, prostate tumor tissues, and BPH. The nonparametric Mann-Whitney *U*-test was used to show significant differences between the normal, normal adjacent, PIN, tumor, and BPH groups. Correlations in expression between cell types and/or subcellular expression levels were done using the nonparametric Spearman's rank correlation coefficient or the Pearson χ^2 analysis

2.3.6 Acknowledgments

We thank James R. Davie, Elliot Drobetsky, Philippe Roux, Patrick J. Padisson, Peiqing Sun, Stéphane Roy, Jacques Landry, and Jason C. Young for critical reading, reagents and/or support. We thank Éric Bonneil and the Institut de Recherche en Immunologie et Cancérologie (IRIC) proteomic service for the phosphopeptide analysis and identification, and Louise Cournoyer, Catherine Ménard, and Frédérique Badeaux for technical assistance. This work was supported by grants from the Canadian Institute of Health and Research (CIHR) to G.F. and S.M. G.F. is a FRSQ senior fellow. S.M. holds the Canada Research Chair in Cellular Signaling. X.D.-S. is a fellow of the Vanier Canada Graduate Scholarships Program. M.-F.G.-L. is a CIHR fellow.

2.3.7 Supplemental Material

2.3.7.1 Supplemental Results

Table SI. Senescence-associated phosphoprotein degradation (SAPD)

Protein	Peptide/ (Phospho SitePlus)	Fold	Functions
AF4	SSSPGKPQAVSSLNSSHSR	3	RNA pol II transcription (PMID 21574958).
AHNAK	TVIRLPSGSGAASPTGSAVDIR (S210-p) LKSEDGVEGDLGETQSR (S135-p)	14	Calcium and PKC signaling (PMID: 19497879) Actin cytoskeleton dynamics and pseudopodia formation (PMID: 20388789).
AKT1S1	SSDEENGPPSSPDLDR (S212-p)	2.36	AKT/Tor signaling, (PMID: 18372248)
ARHGEF12	IYLEENPEKSETIQDTDTQSLVGSPSTR (S341-p) HLSTPSSVSPEPQDSAK (S637)	1.4	Cell motility and invasion, (PMID: 17575049)
ARHGAP1	SSSPELVTHLK (S51-p)	1.8	Cdc42 and Rho signaling, (PMID: 16157885)
ARHGAP17	SPSPPTQHTGQPPGQPSAPSQLSAPR (S676)	2.3	Rho signaling and cell polarity, (PMID: 16678097)
BAG3	VPPAPVPCPPPSPGPSAVPSSPKSVATEER (S377-p, S386-p) SSTPLHSPSPIR (T285-p, S291) AASPFR (S264)	9.2	Chaperone in complex with Hsp70, (PMID: 12750378), mediates ERK inactivation by DUSP6, (PMID: 22310281)
BRD2	KADTTTPTPTAILAPGSPASPPGSLEPK (S298-p)	*	Bind acetylated histones and stimulate transcription (PMID: 18406326)
CALD1	RGSIGENQGEEK (S202-p)	1.9	Cell migration and lamellipodia (PMID:16800003)
CCDC6	ILQEKLDQPVSAPPSPR (S240-p, S244-p)	2.9	Genomic stability, (PMID: 22363533). ERK target at S244) (PMID: 14712216)
CCDC86	ALVEFESNPEETREPGSPPSVQR (S47-p) RLGGLRPESPESLTSVSR (S18-p) AGLGSPERPPK (S58-p)	6.2	Nucleolar protein with coiled coil domain, (PMID: 17300783)
CD44	LVINSGNGAVEDR (S686-p) LVINSGNGAVEDRKPSGLNGEASK (S697-p) LVINSGNGAVEDRKPSGLNGEASK (S704-p) KPSGLNGEASKSQEMVHLVNK (S706-p) KPSGLNGEASKSQEMVHLVNK (S697-p, S706-p)	9	Cell migration and lamellipodia component PMID: 12145196
Cortactin	TQTPPVSPAPQPTEERLPSSPVYEDAASFK (T401-p, S405-p)	4.4	Cytoskeletal protein, cell motility, (PMID: 18406052), ERK1/2 target (S405), lamellipodia and N-WASP regulator, (PMID: 21079800)
CYBRD1	NLALDEAGQRSTM (T285-p)	3.0	Iron metabolism (PMID: 18194661).
DDX21	LKNGFPHPEPDCNPSEAASEESNSEIEQEIPVEQK (S171-p) VTKNEEPSEEEIDAPKPK (S121-p)	12.3	Nucleolar RNA helicase, pre-rRNA processing, (PMID: 19106111)
DDX24	SPGKAEAESDALPDDTVIESEALPSDIAAEAR (S287-p) AQAVSEEEEEEGK (S82-p)	13.0	RNA helicase

DDX42	YMAENPTAGVVQEEEEDNLEYDSDGNPIAPTKK (S185-p)	1.7	RNA helicase
DDX51	RVNDAEPGSPEAPQGK (S83-p)	2.6	Nucleolar component. Ribosomal RNA maturation, (PMID: 20404093)
EGFR	MHLPSPTDSNFYR (S991-p), GSHQISLDNPDYQQDFFPK (S1166-p) GSHQISLDNPDYQQDFFPK (S1162-p)	10	Growth factor signaling
EIF3G	GIPLATGDTSPEPELLPGAPLPPPKEVINGNIK (S42-p)	3.9	Translation initiation, (PMID: 17094969)
EIF3B	TEPAAEAEAASGPSESPSPPAAEELPGSHAEPPVPAQGEAPGEQA RDER (S85-p) TEPAAEAEAASGPSESPSPPAAEELPGSHAEPPVPAQGEAPGEQA RDER (S81-p)	10	Translation initiation
EIF4G1	SFSKEVEER (S1185-p), SFSKEVEER (S1187-p) EAALPPVSPLK (S1231-p)	2.4	Protein synthesis (PMID: 9418880).
EIF4G2	TQTPPLGQTPQLGLK (T506-p)	1.3	Protein synthesis
FAK/PTK2	LQPQEISPPPTANLDR (S910-p)	2.3	Signaling and cell motility, S910 is phosphorylated by ERK, (PMID: 12692126), pseudopodia protein (PMID: 15985431)
FBXL11	KMEESDEEAVQAK (S692-p) SCDEPLTPPPHSPTSMLQLIHDPVSPR (T713-p, S718-p)	9.5	Histone demethylase of K36H3, knockdown induces senescence (PMID: 18836456)
FLNB	LVSPGSANETSSILVESVTR (S-2478-p)	12	Actin binding protein, RalA effector to induce filopodia, (PMID: 10051605)
G3BP2	NLEELEEKSTTPPPAEPVSLPQEPPKPR (T227-p)	12	hnRNA-binding protein, Ras and NF-κB signaling (PMID: 10969074)
HDGF2	ARGDSEALDEES (S664-p)	1.7	Nuclear protein, Methyl lysine histone binding (PMID: 19162039)
HSPA1A	GGSGSGPTIEEVD (S631-p)	14.8	Stabilizes proteins against aggregation during cellular stress and mediate the folding of newly translated polypeptides (PMID: 21874533). Controls OIS (PMID: 19001088).
HSPB1	AQLGGPEAAKSDETAAK (S199-p) QLSSGVSEIR (S82-p) GPSWDPFRDWYPHSR (S15-p)	48.2	Involved in stress resistance, actin organization (PMID: 19593530) and mitochondrial quality control (PMID: 21641551). Phosphorylated by MAPKAP kinase 2 at S15 and S82, (PMID: 1332886)
IGF2BP1	QGSPVAAGAPAK (S181-p)	1.5	Involved in translational control, mRNA localization and cell migration (PMID: 22279049

ILF3/NF90	DSSKGEDSAEETEAKPAVVAPAPVVEAVSTPSAAFPSDATAEQG PILTK (S482-p) RPMEEDGEEKSPSK (S382-p)	2.3	RNA binding protein, nucleolar protein, CDK2 target at S382) (PMID: 18847512), regulates DNA damage repair and non-homologous end joining, (PMID: 21969602)
IGF2R/M6PR	LVSFHDDSDEDLLHI (S2484-p) TVSSTKLVSFHDDSDEDLLHI (S2484-p)	2.6	Involved in the transport of phosphorylated lysosomal enzymes from the Golgi and the cell surface to lysosomes (PMID: 20615935, 11058096, 2541923).
IRF2BP2	RKPSPEPEGEVGPPK (S360-p)	*	Transcriptional repressor of IRF-2, (PMID: 12799427)
ITGA2	NPDEIDETTELSS (S1180-p)	1.7	Involved in cell adhesion to collagens, modulation of collagen and collagenase gene expression. It regulates generation and organization of newly synthesized extracellular matrix (PMID: 2545729).
JUN	LASPELER (S73-p)	25	Transcription factor (PMID: 20132737).
JunB	SRDATPPVSPINMEDQER (T255-p)	1.4	Transcription factor (PMID: 20132737).
KAP1	SRSGEGEVSGLMR (S473-p) STAPSAAASASASAAASSPAGGGAEALELLEHCGVCR (S50-p)	7	Heterochromatin and gene repression (PMID: 8769649).
LIMA1/EPLIN	ETPHSPGVEDAPIAK (S490-p) SEVQQPVHPKPLSPDSR (S362-p) ASSLSESSPPK (S374-p)	5	Cytoskeletal protein, ERK target at S360, cell motility, (PMID: 17875928)
LMO7	ATLSSTSGLDLMSESGEGEISPQREVSR (S1026-p) EVAATEEDVTRLPSPTSPFSSLSQDQAATSK (T990-p, S991-p) EVAATEEDVTRLPSPTSPFSSLSQDQAATSK (S988) SHSPSASQSGSQLR (S1593-p)	15	Nucleocytoplasmic shuttling protein (PMID: 17067998), cell migration, (PMID: 21670154)
LRWD1	ANSPEKPPEAGAAHKPR (S212-p)	*	Origin of replication, (PMID: 20932478)
MAP1A	CLSPDDSTVK (S986-p) MASPPPSGPPSATHTPFHQSPVEEKSEPQDFQEADSWGDTK (S1013-p) WPEVSPEDTQSLSLSEESPSKETSLDVSSK (S1203-p) QLSPESLGTLQFGELNLGK (S1218-p) YLPGAITSPDEHILTPDSSFSK (S1311-p) WLAESPVGLPPEEEDKLTR (S1776-p) SPFEIISPPASPPEMVGQR (S1797-p, S1801-p) SPFEIISPPASPPEMVGQRVPSAPGQESPIPDPK (S1801-p) VPSAPGQESPIPDPK (S1818) NTSAEKELSSPISPK (S2019-p, S2022-p) GELSPSFLNPPLPPSIDDR (S2449-p) SPTPGKGPADR (S2629-p)	14	Structural protein that interacts with MAPK (PMID: 20936779).
MAP1B	DVMSDETNNEETESPSQEFVNITK (S1154-p) SPSLSPSPPSPLEK (S1262-p) SPSLSPSPPSPLEK (S1265-p)	6	Cytoskeleton (PMID: 17292797)

	VSAEAEVAPVSPEVTQEVVEEHCASPEDK (S1298-p) ASVSPMDEPVPDSESPIEK (S1378-p, S1389-p) GAESPFEEKSGK (S1427) QGSPDQVSPVSEMTSTSLYQDKQEGK (S1438-p, S1443-p) KLGDVSPTQIDVSQFGSFK (S1501) VQSLEGEKLSPK (S1779-p) SDISPLTPR (S185) ESSPLYSPTFSDSTSAVKEK (S1793-p) ESSPLYSPTFSDSTSAVKEK (S1797-p) TATCHSSSSPPIDAASAEPYGFR (S1819-p)		
MAP4	DMESPTKLDVTLAK (S280-p) DMESPTKLDVTLAK (T282-p) DMSPLSETEMALGKDVTPPPETEVVLIK (S507-p) DMSPLSETEMALGKDVTPPPETEVVLIK (S510-p) DVTPPPETEVVLIK (T521-p) GISEDSHLESLQDVGQSAAPTFMISPETITGTGKK (S624-p) KCSLPAEEDSVLEK (S636-p) RASPSKPASAPASR (S793-p, S797-p) VGSTENIKHQPGGGR (S941-p)	29	Microtubules dynamics, (PMID:15840946)
MARCKSL1	AAATPESQEPQAK (T148-p) GDVTAEEAAGASPAKANGQENGHVK (S22-p)	15	PKC signaling
MVP	RVASGPSPGEGISPQSAQAPQAPGDNHVVPVLR (S873-p) RVASGPSPGEGISPQSAQAPQAPGDNHVVPVLR (S867-p, S876-p)	3	Vault ribonucleoproteins
Nestin	TLLEAENSRLQTPGGGSK (T315-p) QEASTGQSPEDHASLAPPLSPDHSSLEAK (S471-p) TPTLASTPIPPTPQAPSPAVDAEIR (S398-p) ENQEPLRSPEVGDEEALRPLTK (S680-p) WEDTVEKDQELAQESPPGMAGVENEDEAELNLR (S965-p)	19	Cancer Stem cell marker (PMID: 20429619)
NOC2L	EAARSPDKPGGSPSASR (S49-p) EAARSPDKPGGSPSASR (S49-p, S56-p)	10	Nucleolar protein, p53 inhibitor, (PMID: 16322561)
NOLC1	GGSISVQVNSIKFDSE (S698-p)	28	Pol1 coactivator, nucleologenesis (PMID: 7657714)
NOL6/NRAP	GQSPAGDGSPEPPTPR (S283-p)	7.5	Nucleolar protein (PMID: 11895476)
NOP5	HIKEEPLSEEEPCTSTAIASPEK (S502-p)	23	Nucleolar protein, 60S biogenesis, (PMID: 11583964)
NOP56	FSKEEPVSSGPEEAVGK (S570-p)	21	Nucleolar protein, 60S biogenesis, snoRNP biogenesis, (PMID: 19620283)
Nucleolin	VVVSPTKK (S67-p) LELQGPRGSPNAR (S563-p)	20	Nucleolar protein and pol I cofactor, (PMID: 17130237), p53 inhibitor, (PMID: 22013067)
NUP188	GAPSSPATGVLPSPQGK (S1708-p, S1717-p)	1.5	Nuclear pore, (PMID: 20566687)
ODZ2	SLMYWMTVQYDSMGRVIK (S2181)	54	Tenascin family

PDLIM4	IHIDPEIQDGSPTTSR (S112-p)	22	Cytoskeletal protein.
PHLDA2	TAPAAPAEDAVAAAAAAPSEPSEPSRPSPQPKPRTP (S144-p) TAPAAPAEDAVAAAAAAPSEPSEPSRPSPQPKPRTP (T160-p)	9.6	Competes with other PH domain-containing proteins to prevent their binding to membrane lipids (PMID: 9403053).
PRKAR2A	VADAKGDSESEEDEDLEVPVPSR (S78-p, S80-p) RVSVCAETYNPDEEEEDTDPR (S99-p)	11	Regulatory subunit of cAMP-regulated kinase
RPLP1	KEESEESDDDMGFGLFD (S104-p) KEESEESDDDMGFGLFD (S101-p)	3.4 54.7	Structural component of ribosome (PMID: 16572171), bypass senescence (PMID: 19233166).
RPL23	IRTSPTFR (S43-p)	35	Ribosomal protein Actin cytoskeleton dynamics and pseudopodia formation (PMID: 20388789).
RRBP1	SHVEDGDIAGAPASSPEAPPAEQDPVQLK (S1277-p)	6	Binding of ribosomes to the ER, (PMID: 22156060)
RSL1D1 (CSIG) IPI00642046	ATNESEDEIPQLVPIGK (S361-p)	2.4	Nucleolar protein. Inhibits PTEN and p27 and is downregulated in replicative senescence (PMID: 18678645). Regulates nucleostemin localization (PMID: 17158916).
SCAMP2	AASSAAQGAFQGN (S319-p)	10	Secretory pathway, (PMID:17713930)
SEC22B	NLGSINTELQDVQR (S137-p)	16	Vesicle mediated transport
SEPT9	HVDSLSQRSPK (S85-p)	2.7	Actin cytoskeleton dynamics and pseudopodia formation (PMID: 20388789).
SLC4A2	RRPGASPTGETPTIEEGEEDEDEASEAEGAR (S113-p) RRPGASPTGETPTIEEGEEDEDEASEAEGAR (T115-p)	2.2	Anion exchange protein (PMID: 16239253)
SLC20A1	EIKCSPSESPLMEK (S265-p) EIKCSPSESPLMEK (S267-p)	11	Phosphate transport, (PMID: 12759754)
SLC35B2	AVPVESPVQKV (S427-p)	4	Protein sulfation and synthesis of proteoglycans (PMID: 12716889).
SRRM1/SRm160	EKTPELPEPSVK (T220-p) VPKPEPIPEPKEPSPEK (S260-p) RLSPSASPPR (S389-p, S393-p) TRHSPTPQQSNR (T416-p) VSVSPGRTSGK (S431-p) RESPSPAPKPR (S450-p. S452-p) YSPPIQR (S597-p) RYSPSPPPK (S605-p, S607-p) TASPPPPPKR (T614-p, S616-p) RASPSPPPK (S626-p, S628-p) RVSHSPPPK (S636-p, S638-p) APQTSSSPPPVR (S694-p, S696-p) RQSPSPSTRPIR (S713-p, T718-p) VSRTPEPK (T727-p) AASPSPQSVR (S738-p) AASPSPQSVR (S738-p, S740-p) SVSGSPEPAAK (S756-p) KPPAPPSPVQSQSPSTNWSPAVPVKK (S769-p. S775-p)	5.4	Splicing regulation (PMID: 16354706), (PMID: 9531537), Exon junction complex and mRNA export, (PMID: 12624182)

SRRM2	THTTALAGRSPSPASGR (S295-p, S297-p) SATRPSPSPERSSTGPEPPAPTPLLAER (S353-p, S357-p) SATRPSPSPERSSTGPEPPAPTPLLAER (T348-p, S351-p) EISSSPTSKNR (S455-p, S456-p) SLSGSSPCPK (S778-p) SCFESSPDPELKSR (S876-p) SRSVSPCSNVESR (S952-p, S954-p) VKPETPPR (T983-p) AQTPPGPSLSGSKSPCPQEK (T1003-p) AQTPPGPSLSGSKSPCPQEK (S1014-p) AQTPPGPSLSGSKSPCPQEK (T1003-p, S1014-p) SSTPPGESYFGVSSLQLK (T1043-p) QSHSESPSLQSK (S1083-p) SSSPVTELASR (S1103-p) GEFSASPMLK (S1124-p) SGMSPEQSR (S1132-p) MALPPQEDATASPPRQK (S1179-p) ELSNSPLRENSFGSPLEFR (S1320-p) SSGHSSSELSPDAVEK (S1382-p, S1387-p) AGMSSNQSISSPVLDAVPR (S1404-p) GRSECDSSPEPK (S1482-p, S1483-p) ALPQTPRPR (T1492-p) SSRSSPELTR (S1693-p, S1694-p) SRTPPVTR (S1925-p, T1927-p) SRTSPITR (S1975-p) SRSPLAIR (S2044-p, S2046-p) SLTRSPPAIR (T2069-p, S2071-p) NHSGSRTPPVALNSSR (S2100-p, S2102-p, T2104-p) MSCFSRPSMSPTPLDR (S2121-p, S2123-p) TPAAAAAMNLASPR (S2272-p) VSGRTSPPLLDR (S2398-p) SRTPPSAPSQSR (T2409-p) MTSERAPSPSSR (S2426-p) MGQAPSQSLLPPAQDQPRSPVPSAFSDQSR (S2449-p) RVPSPTPAPK (S2581-p) KPIDSLRDSR (S2688-p) SLSYSPVER (S2692-p, S2694-p)	8.6	Splicing regulation, (PMID: 10668804), (PMID: 9531537)
STIM1	SHSPSSPDPDTPSPVGDSR (S611-p) SHSPSSPDPDTPSPVGDSR (S613-p) SHSPSSPDPDTPSPVGDSR (S616-p)	2.5	Calcium metabolism and proapoptotic ERKsignaling (PMID: 21441934).
S100A11	ISSPTETER (S6-p)	2.8	Actin cytoskeleton dynamics and pseudopodia formation (PMID: 20388789).
TBX2	SPAPDSASPTRLTEPER (S386-p) ALSPGRESPK (S705-p, S710-p)	1.39	Repress PML functions and senescence (PMID: 22002537)
TERF2IP	YLLGDAPVSPSSQK (S213-p)	3.9	Telomere biology, (PMID: 10850490)

TFPT/FB1	TPAPPEPGSPAPGEGPSGR (S180-p)	*	Nuclear protein, target of CDK1 and recruited to actin filaments by Par4 (PMID: 16229834)
TNKS1BP1	WLDDLLASPPPSGGGAR (S494-p) TEAQDLCRASPEPPGPESSSR (S672-p) YESQEPLAGQESPLPLATR (S601-p)	3.6	Bind tankyrase (PMID: 11854288)
TOM1	AADRLPNLSSPSAEGPPGPPSGPAPR (S461-p)	6.7	Intracellular trafficking (PMID: 20604899)
TOMM70A	ASPAPGSGHPEGPGAHLDMNSLDR (S91-p)	5.1	Mitochondrial protein import acting in coordination with Hsp70 and Hsp90 chaperones, (PMID: 12526792)
TOMM34	NRVPSAGDVEK (S186-p)	8.6	Cytosolic cochaperone of Hsp90/Hsp70 complex involved in mitochondrial protein import (PMID: 22178133)
YAP1	QASTDAGTAGALTPQHVR (S109-p) SQLPTLEQDGGTQNPVSSPGMSQELR (S367-p) AHSSPASLQLGAVSPGTLTPTGVVSGPAATPTAQHLR (S131-p, S138-p)	9.5	Coactivator, inhibits senescence (PMID: 20677011)
YBX1	AADPPAENSSAPEAEQGGAE (S313-p)	21.7	Regulates splicing, translation and mRNA stability (PMID: 12815724)
ZC3HC1/NIPA	SQDATFSPGSEQAEKSPGPIVSR (S344-p) SMGTGDTPGLEVPSSPLRK (S395-p)	3.6	Mitosis entry, (PMID: 16009132)

Note: LC-MS/MS analysis on total protein extracts from RasV12-expressing cells treated with MG132 (20μM) or vehicle for 18 h. The protein extracts were sent to the Proteomics Core Facility of the Institute for Research in Immunology and Cancer (IRIC, Montreal, Canada; www.iric.ca) for analysis. The fold indicates the enrichment for the most abundant peptides found and * denotes that the peptide was not detected in the control cells without MG132 and no ratio was calculated.

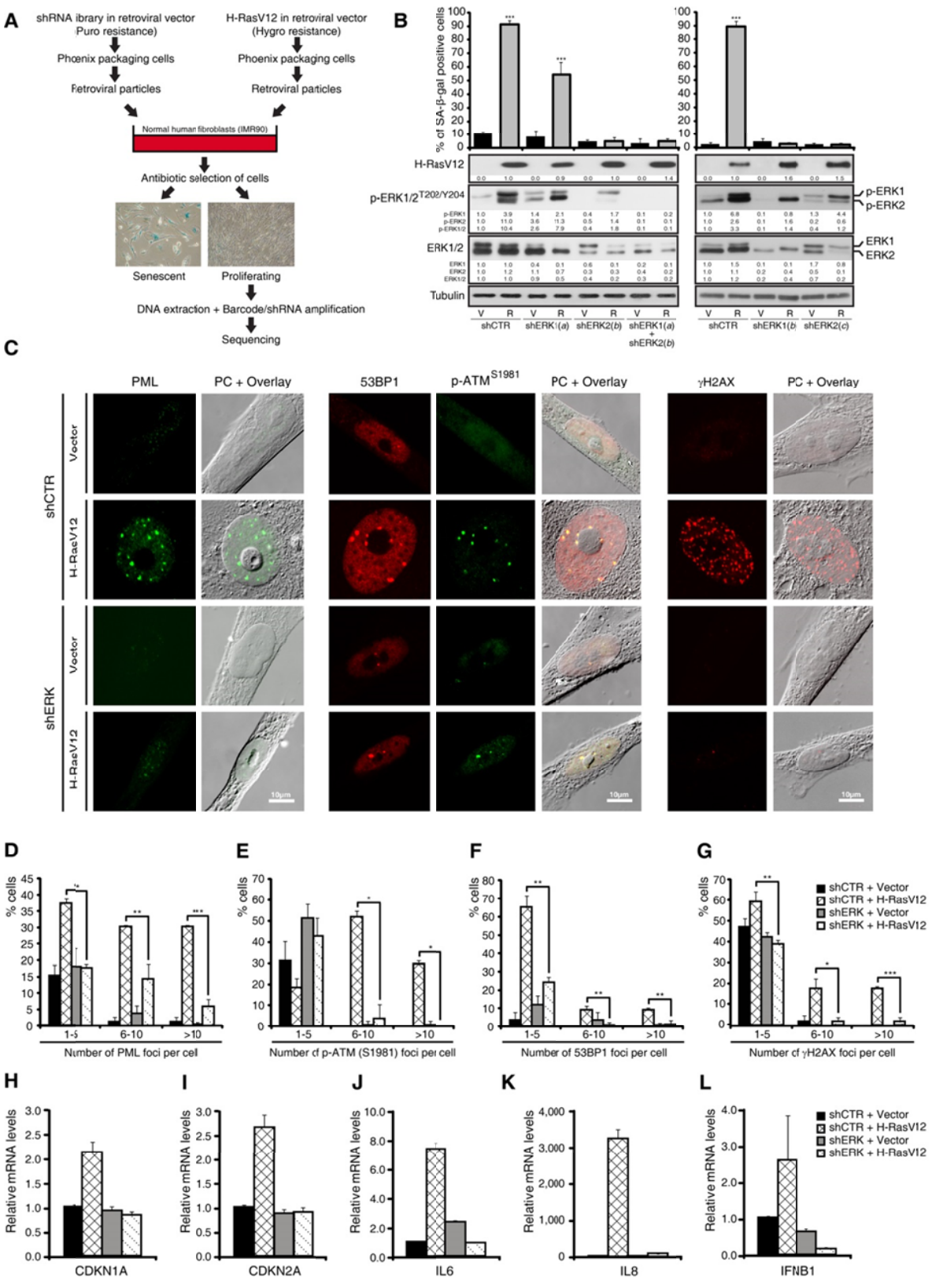
A
shRNA library in retroviral vector (Puro resistance)
H-RasV12 in retroviral vector (Hygro resistance)
Phoenix packaging cells
Phoenix packaging cells
Retroviral particles
Retroviral particles
Normal human fibroblasts (IMR90)
Antibiotic selection of cells
Senescent
Proliferating
DNA extraction + Barcode/shRNA amplification
Sequencing
B
% of SA-β-gal positive cells
H-RasV12
p-ERK1/2 T202/Y204
p-ERK1
p-ERK2
ERK1/2
ERK1
ERK2
Tubulin
shCTR
shERK1(a)
shERK2(b)
shERK1(a) + shERK2(b)
shERK1(b)
shERK2(c)
C
PML
PC + Overlay
53BP1
p-ATM S1981
γH2AX
shCTR
shERK
Vector
H-RasV12
10μm
D
% cells
Number of PML foci per cell
E
Number of p-ATM (S1981) foci per cell
F
Number of 53BP1 foci per cell
G
Number of γH2AX foci per cell
shCTR + Vector
shCTR + H-RasV12
shERK + Vector
shERK + H-RasV12
H
Relative mRNA levels
CDKN1A
I
CDKN2A
J
IL6
K
IL8
L
IFNB1

Figure S1. ERK/MAPK inhibition required for Ras-induced senescence

(***A***) Library of shRNAs containing hairpins against 2000 cancer related genes in the human genome was constructed in the retroviral vector MLP (a gift from Scott W. Lowe, Memorial Sloan-Kettering Cancer Center). The library was introduced into normal human fibroblasts (IMR90) by retroviral gene transfer followed by selection with puromycin. Then cells were infected with another retrovirus expressing H-RasV12 and conferring resistance to hygromycin. Most cells senesced (*left*), but colonies of cells escaping senescence emerged after one week (*right*). shRNAs sequences in those colonies were amplified by PCR, re-cloned into the original retroviral vector and sequenced. Once we identified shRNAs that bypass senescence we proceeded to the validation process. First, the newly subcloned shRNAs were re-tested to confirm that they were able to bypass H-RasV12-induced senescence. Then, additional shRNAs against the same gene were tested to eliminate the possibility of off-target effects of the original shRNA. Finally the ability of each shRNA to downregulate its target was evaluated by qPCR and immunoblots. Two genes identified in this screening were validated with independent shRNAs: ERK2 and HMGB1. (***B***) ERK knockdown inhibits Ras-induced senescence. A collection of shRNAs targeting *ERK1* or *ERK2* with different efficiencies inhibited Ras-induced senescence showing a correlation between the degree of ERK inhibition and the bypass of senescence as measured using the SA-β-Gal assay. Left panel represents retroviral constructs while the right panel corresponds to lentiviral constructs. Extracts for Immunoblots were done 14 d after infection with H-RasV12 (R) or an empty vector (V) and the indicated shRNA. Data from the SA-β-Gal assays were quantified from 100 cells counts in triplicate and presented as the mean percentage of positive cells ± SD. (***C***) Indirect immunofluorescence for PML bodies and several components of DNA damage foci (phospho-p53BP1, phospho-ATM and γH2AX) followed by laser-scanning confocal microscopy. IMR90 fibroblasts expressing oncogenic *ras* (R) or an empty vector (V) and shRNA against *ERK2* (shERK) or a non-targeting shRNA (shCTR) fixed 14 d after selection. PC is phase contrast. (***D-G***) Quantification of the data on (*C)*. For each condition, 100 cells were analyzed in three different experiments. Histograms indicate the percentage of cells containing 1 to 5, 6 to 10, and >10 foci. Error bars represent SD. (*) $P < 0.05$, (**) $P < 0.005$, (***) $P < 0.0005$, two-sample *t*-test. (***H-L***) qPCR for expression of CDKN1A (p21) and CDKN2A (p16Ink4a), IL-6, IL-8, and IFN-β1 using total RNA from IMR90 fibroblasts expressing the indicated vectors and extracted 14 d after selection ($n \geq 3$).

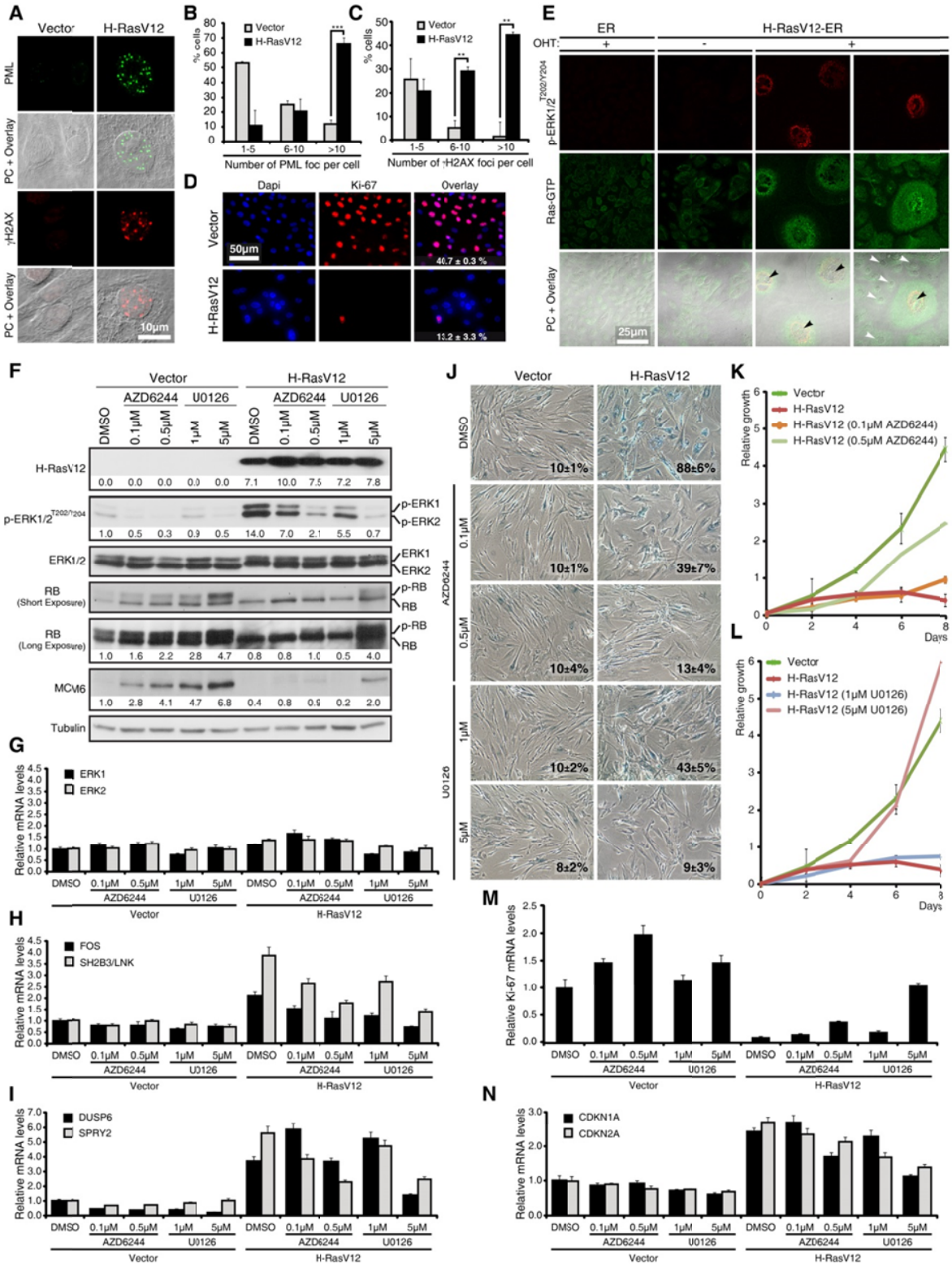
A
Vector
H-RasV12
PML
PC + Overlay
γH2AX
PC + Overlay
10μm
B
Vector
H-RasV12
% cells
1-5
6-10
>10
Number of PML foc per cell
C
Vector
H-RasV12
% cells
1-5
6-10
>10
Number of γH2AX foci per cell
D
Dapi
Ki-67
Overlay
Vector
H-RasV12
50μm
40.7 ± 0.3 %
13.2 ± 3.3 %
E
ER
H-RasV12-ER
OHT:
+
-
+
p-ERK1/2T202/Y204
Ras-GTP
PC + Overlay
25μm
F
Vector
H-RasV12
AZD6244
U0126
DMSO
0.1μM
0.5μM
1μM
5μM
H-RasV12
p-ERK1/2T202/Y204
p-ERK1
p-ERK2
ERK1/2
ERK1
ERK2
RB
(Short Exposure)
RB
(Long Exposure)
p-RB
RB
MCM6
Tubulin
G
ERK1
ERK2
Relative mRNA levels
H
FOS
SH2B3/LNK
Relative mRNA levels
I
DUSP6
SPRY2
Relative mRNA levels
J
Vector
H-RasV12
DMSO
0.1μM
0.5μM
1μM
5μM
AZD6244
U0126
10±1%
88±6%
10±1%
39±7%
10±4%
13±4%
10±2%
43±5%
8±2%
9±3%
K
Vector
H-RasV12
H-RasV12 (0.1μM AZD6244)
H-RasV12 (0.5μM AZD6244)
Relative growth
Days
L
Vector
H-RasV12
H-RasV12 (1μM U0126)
H-RasV12 (5μM U0126)
Relative growth
Days
M
Relative Ki-67 mRNA levels
N
CDKN1A
CDKN2A
Relative mRNA levels

Figure S2. Additional contexts for ERK-dependent senescence

(***A-E***) Ras-induced senescence in HMECs. (***A***) Immunofluorescence images for senescence markers. HMECs expressing hTERT were subsequently modified by retroviruses expressing H-RasV12 or an empty vector. Then, they were fixed 14 d after infection. Indirect immunofluorescence for PML bodies and γH2AX followed by laser-scanning confocal microscopy. PC is phase contrast. (***B-C***) Quantification of the data on (*A*). For each condition 3 x 100 cells were analyzed and the data were expressed as the percentage of cells containing 1 to 5, 6 to 10, and >10 foci ± SD. (**) $P < 0.005$, (***) $P < 0.0005$, two-sample *t*-test ($n = 3$). (***D***) Indirect immunofluorescence of KI-67 expression in cells as in (*A*). Cells were fixed 14 d after infection with the indicated vectors and co-stained with 300 nM DAPI. Data were quantified from 100 cells counts in triplicate and presented as the mean of positive cells ± SD. (***E***) Immunofluorescence showing that HMECs escaping spontaneously from Ras-induced senescence have reduced levels of phospho-ERK1/2. Black arrows indicate large senescent cells expressing both H-RasV12 and phospho-ERK1/2. White arrows indicate small non-senescent cells expressing H-RasV12 but little phospho-ERK1/2. HMECs were infected with retroviral vectors expressing H-RasV12-ER or empty vectors and were then treated with 4-hydroxy-tamoxifen (100 nM) or vehicle ($n = 3$). (*F-N*) Bypass of Ras-induced senescence with MEK inhibitors. (***F***) Immunoblots for the indicated proteins in IMR90 cells with vectors control or H-RasV12 and treated with the indicated chemicals. The treatments started immediately after infection and the medium was changed every 2 d. Cells were harvested 10 d after infection. (***G-I***) qPCR for the indicated mRNAs in cells as in (*F*). (***J***) SA-β-Gal of cells as in (*F*); the percentage of positive cells is indicated at the *bottom* of each panel together with SD of three replicates. (***K-L***) Growth curves of IMR90 cells expressing a vector control or H-RasV12 and treated with DMSO compared to IMR90 expressing H-RasV12 and treated with the indicated concentrations of AZD6244 (*K*) or U0126 (*L*). (***M-N***) qPCR for the indicated mRNAs in cells as in (*F*) ($n \geq 3$).

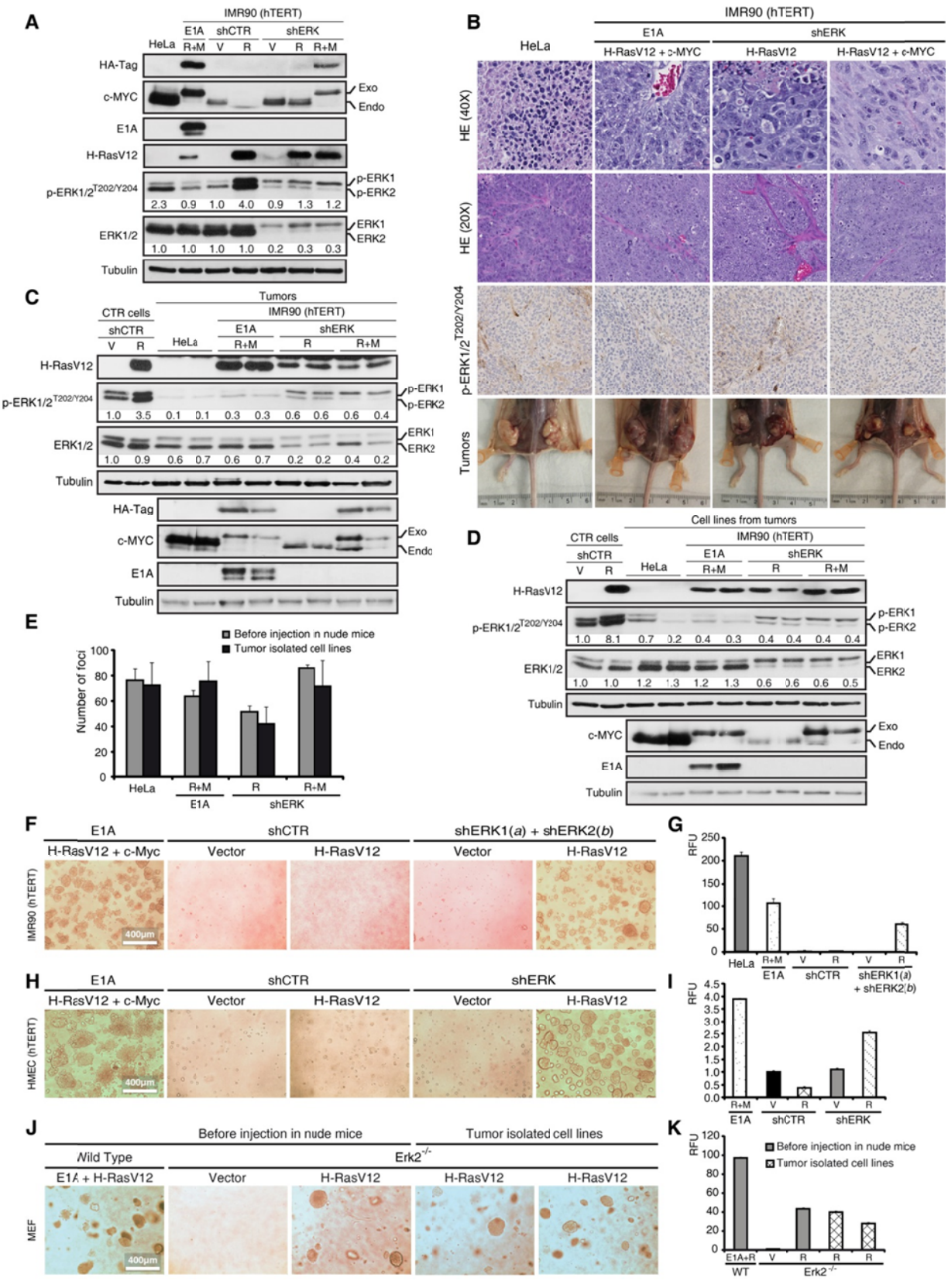
A
IMR90 (hTERT)
E1A
shCTR
shERK
HeLa
R+M
V
R
V
R
R+M
HA-Tag
c-MYC
Exo
Endo
E1A
H-RasV12
p-ERK1/2T202/Y204
p-ERK1
p-ERK2
2.3 0.9 1.0 4.0 0.9 1.3 1.2
ERK1/2
ERK1
ERK2
1.0 1.0 1.0 1.0 0.2 0.3 0.3
Tubulin
B
IMR90 (hTERT)
HeLa
E1A
shERK
H-RasV12 + c-MYC
H-RasV12
H-RasV12 + c-MYC
HE (40X)
HE (20X)
p-ERK1/2T202/Y204
Tumors
C
Tumors
CTR cells
shCTR
IMR90 (hTERT)
HeLa
E1A
shERK
V
R
R+M
R
R+M
H-RasV12
p-ERK1/2T202/Y204
p-ERK1
p-ERK2
1.0 3.5 0.1 0.1 0.3 0.3 0.6 0.6 0.6 0.4
ERK1/2
ERK1
ERK2
1.0 0.9 0.6 0.7 0.6 0.7 0.2 0.2 0.4 0.2
Tubulin
HA-Tag
c-MYC
Exo
Endo
E1A
Tubulin
D
Cell lines from tumors
CTR cells
shCTR
IMR90 (hTERT)
HeLa
E1A
shERK
V
R
R+M
R
R+M
H-RasV12
p-ERK1/2T202/Y204
p-ERK1
p-ERK2
1.0 8.1 0.7 0.2 0.4 0.3 0.4 0.4 0.4 0.4
ERK1/2
ERK1
ERK2
1.0 1.0 1.2 1.3 1.2 1.3 0.6 0.6 0.6 0.5
Tubulin
c-MYC
Exo
Endo
E1A
Tubulin
E
Before injection in nude mice
Tumor isolated cell lines
Number of foci
100
80
60
40
20
0
HeLa
R+M
R
R+M
E1A
shERK
F
E1A
shCTR
shERK1(a) + shERK2(b)
H-RasV12 + c-Myc
Vector
H-RasV12
Vector
H-RasV12
IMR90 (hTERT)
400μm
G
RFU
250
200
150
100
50
0
HeLa
R+M
V
R
V
R
E1A
shCTR
shERK1(a) + shERK2(b)
H
E1A
shCTR
shERK
H-RasV12 + c-Myc
Vector
H-RasV12
Vector
H-RasV12
HMEC (hTERT)
400μm
I
RFU
4.5
4.0
3.5
3.0
2.5
2.0
1.5
1.0
0.5
0.0
R+M
V
R
V
R
E1A
shCTR
shERK
J
Before injection in nude mice
Tumor isolated cell lines
Wild Type
Erk2-/-
E1A + H-RasV12
Vector
H-RasV12
H-RasV12
H-RasV12
MEF
400μm
K
RFU
120
100
80
60
40
20
0
Before injection in nude mice
Tumor isolated cell lines
E1A+R
V
R
R
R
WT
Erk2-/-

Figure S3. Characterization of the transformation promoted by ERK/MAPK inhibition in oncogenic *ras*-expressing cells

(***A***) Hematoxylin/eosin (HE) staining of sections from tumors formed in nude mice and expressing the indicated vectors. These sections were also stained for phospho-ERK. Representative tumors are shown at the *bottom*. (***B***) Immunoblots for the indicated proteins in cells before injection in nude mice. (***C***) Immunoblots for the indicated proteins in tumor cell extracts. Results for two representative tumors of each condition are shown. (***D***) Immunoblots for the indicated proteins in cells isolated from tumors (two representative cell lines by condition are shown). (***E***) Focus-forming assay with cells expressing the indicated vectors. We compared cells before injection into nude mice or isolated from tumors. Two hundred cells were mixed with normal IMR90 fibroblasts, grown to confluence in 6 cm tissue culture dishes and foci were scored after 14 d. Numbers of foci per dish are presented as the mean ± SD of triplicates. The cells expressed H-RasV12 (R) or c-MYC (M). (***F***) Representative images of a soft agar colony formation assay of IMR90 cells to show that different shERKs (shERK1[a] + shERK2[b]) can cooperate with H-RasV12 to bypass senescence and transform primary human cells. (***G***) Quantification of several experiments ($n = 3$) as in (*F*) using the CyQuant GR Dye. (RFU) Relative fluorescence units and data are presented as the mean ± SD of triplicates. (***H***) Representative images of soft agar colony formation assay of HMECs expressing the indicated vectors. (***I***) Quantification of (*H*) as described in (*G*). (***J***) Focus-forming assay with MEFs expressing the indicated vectors to compare cells before injection into nude mice or isolated from tumors. (***K***) Quantification of (*I*) as described in (*G*).

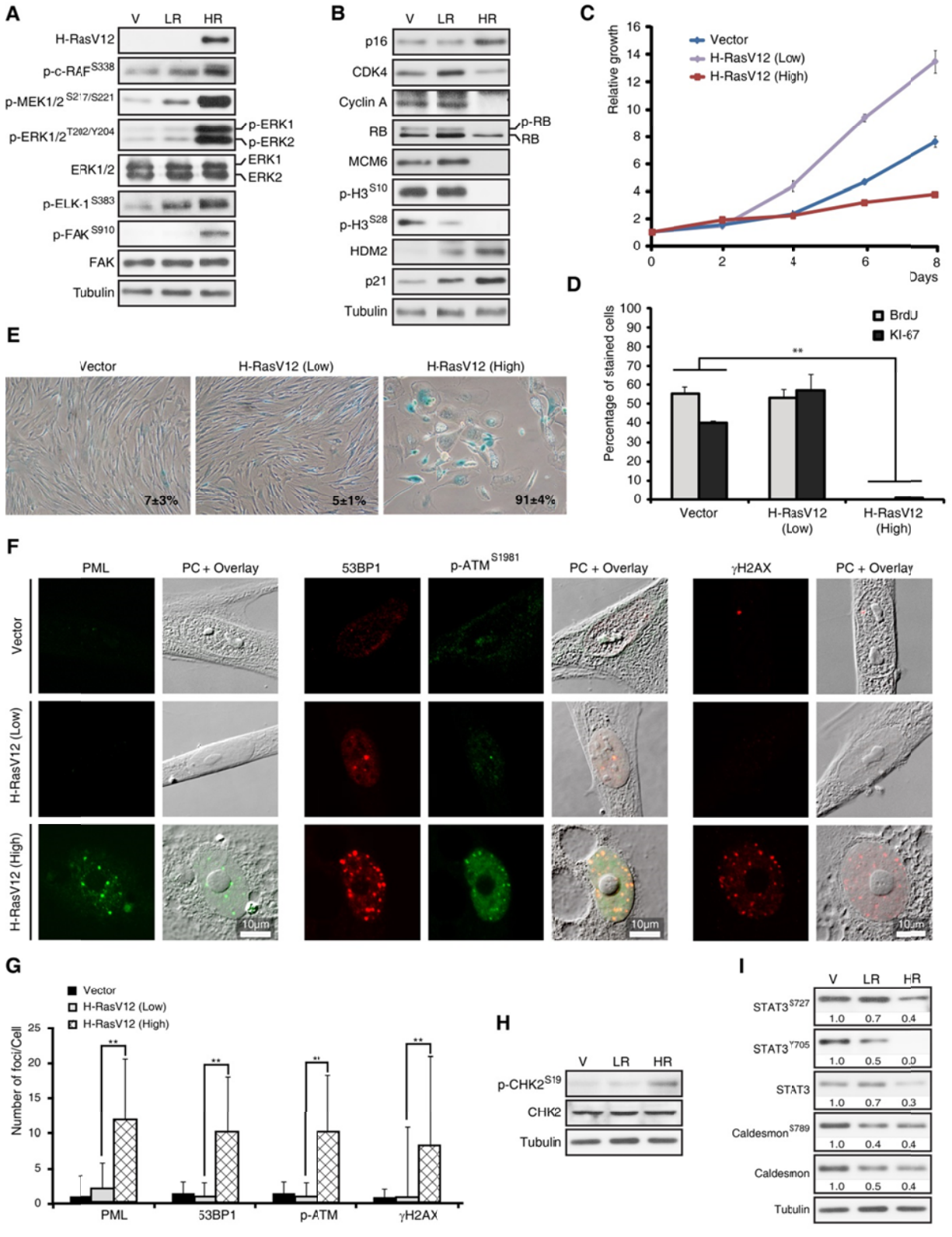
A
V
LR
HR
H-RasV12
p-c-RAF S338
p-MEK1/2 S217/S221
p-ERK1/2 T202/Y204
p-ERK1
p-ERK2
ERK1/2
ERK1
ERK2
p-ELK-1 S383
p-FAK S910
FAK
Tubulin
B
V
LR
HR
p16
CDK4
Cyclin A
RB
p-RB
RB
MCM6
p-H3 S10
p-H3 S28
HDM2
p21
Tubulin
C
Relative growth
Vector
H-RasV12 (Low)
H-RasV12 (High)
Days
D
Percentage of stained cells
BrdU
KI-67
**
Vector
H-RasV12 (Low)
H-RasV12 (High)
E
Vector
H-RasV12 (Low)
H-RasV12 (High)
7±3%
5±1%
91±4%
F
PML
PC + Overlay
53BP1
p-ATM S1981
PC + Overlay
γH2AX
PC + Overlay
Vector
H-RasV12 (Low)
H-RasV12 (High)
10μm
10μm
10μm
G
Vector
H-RasV12 (Low)
H-RasV12 (High)
Number of foci/Cell
**
PML
53BP1
p-ATM
γH2AX
H
V
LR
HR
p-CHK2 S19
CHK2
Tubulin
I
V
LR
HR
STAT3 S727
1.0 0.7 0.4
STAT3 Y705
1.0 0.5 0.0
STAT3
1.0 0.7 0.3
Caldesmon S789
1.0 0.4 0.4
Caldesmon
1.0 0.5 0.4
Tubulin

Figure S4. Growth and senescence markers in cells expressing high or low levels of H-RasV12

(***A***) Immunoblots for proteins in the ERK/MAPK pathway and ERK targets using protein extracts from IMR90 fibroblasts expressing low levels of oncogenic *ras* (LR) or high levels (HR) or an empty vector (V). Cells were harvested 14 d after infection. (***B***) Immunoblots for components of the p53/p21 and $p16^{INK4a}$/Rb pathways and cell cycle-regulated proteins in cells as in (*A*). (***C***) Growth curves started with cells as in (*A*). Data are presented as the mean ± SD of triplicates. (***D***) BrdU incorporation (2 h of incubation with 10 µM BrdU) and Ki-67 staining from cells as in (*A*). Data were quantified from 100 cells counts in triplicate and presented as the mean of positive cells ± SD. Asterisks represent a significant change according to the two-sample *t*-test. (**) $P < 0.005$. (***E***) SA-ß-Gal with cells as in (*A*). Data were quantified from 100 cells counts in triplicate and presented as the mean percentage of positive cells ± SD. (***F***) Indirect immunofluorescence for PML bodies and several components of DNA damage foci (phospho-ATM, phospho-p53BP1 and γH2AX) in cells as in (*A*). The phase contrast (PC) is shown. (***G***) Quantification of the data on (*F*). For each condition the number of foci was evaluated in 100 cells and in three different experiments. Histogram indicates the mean number of foci per cell. Error bars represent the SD. (**) $P < 0.005$ according to the two-sample *t*-test. (***H***) Immunoblots for phosphorylated and total CHK2 in cells as in (*A*). (***I***) Immunoblots showing two ERK targets identified in the Kinexus analysis and for which the level is decreased in fibroblasts as in (*A*). All experiments were done at least three times.

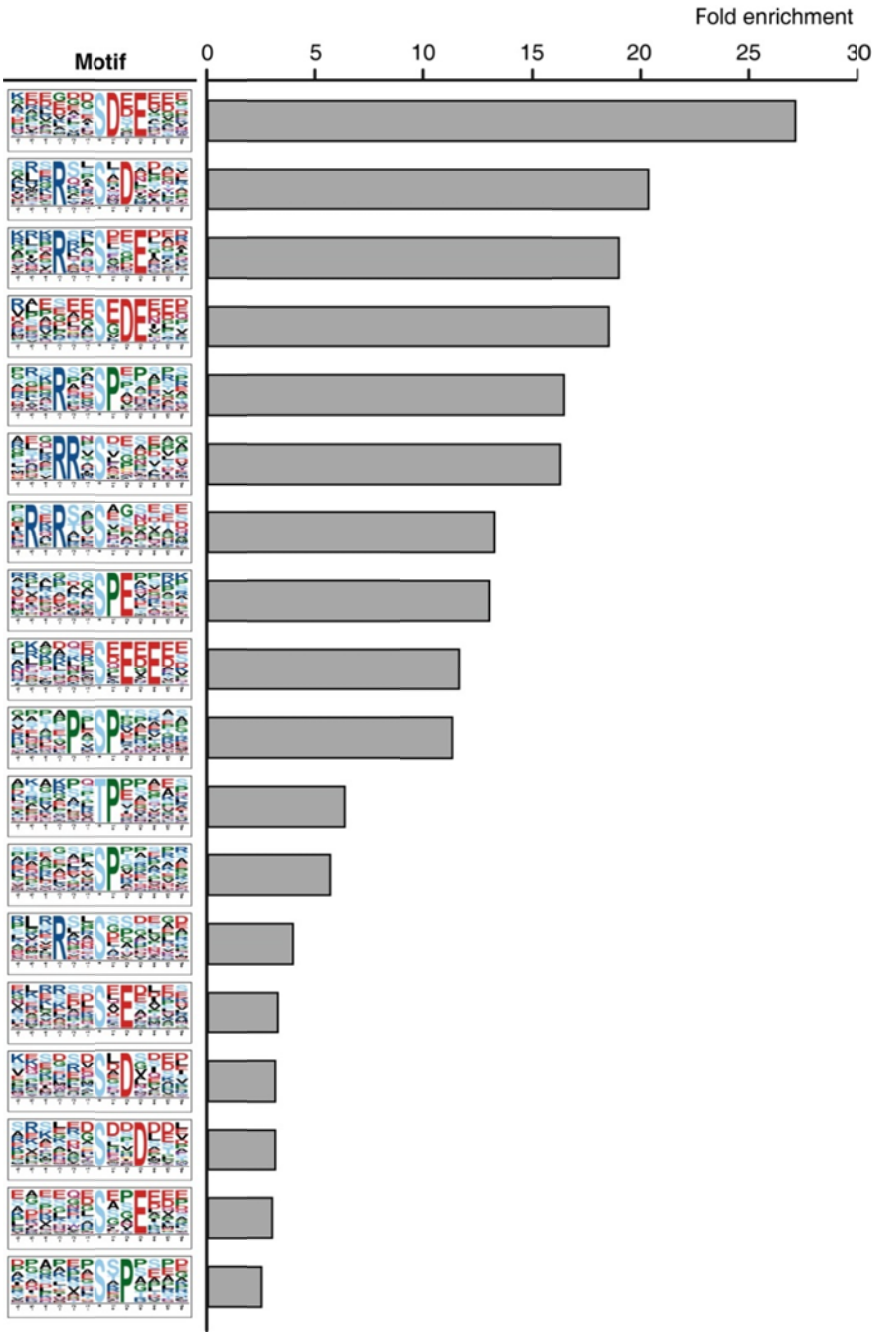

Figure S5. Phosphorylation motifs enriched among unstable phosphopeptides in Ras senescent cells

IMR90 fibroblasts were infected with H-RasV12. When cells were fully senescent, 10 d after infection, they were treated 18 h with DMSO (control) or 20 μM MG132 and then harvested. Protein extracts were analysed by LC-tandem mass spectrometry (LC-MS/MS) for phosphoproteomics (n = 2, in triplicate each time). Phosphopeptides enriched in MG132-treated cells were analysed with Motif-X (490) to allow identification of overrepresented phosphorylation motifs. The motifs found and their fold enrichment is shown. The enrichment is based on the frequency of each motif in the phosphoproteome.

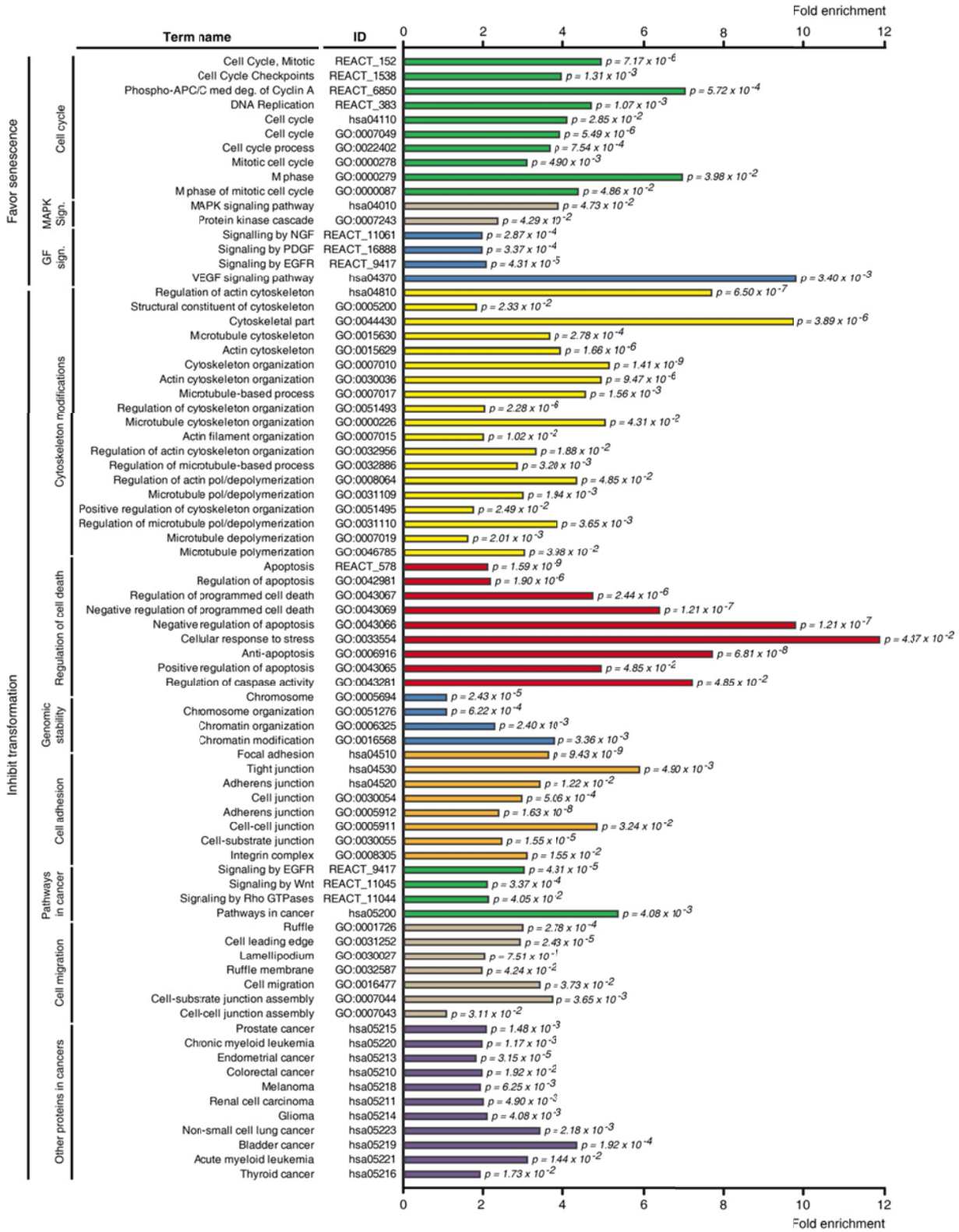
Fold enrichment
Term name
ID
0
2
4
6
8
10
12
Favor senescence
Inhibit transformation
Cell cycle
MAPK Sign.
GF sign.
Cytoskeleton modifications
Regulation of cell death
Genomic stability
Cell adhesion
Pathways in cancer
Cell migration
Other proteins in cancers
Cell Cycle, Mitotic REACT_152 p = 7.17 x 10-6
Cell Cycle Checkpoints REACT_1538 p = 1.31 x 10-3
Phospho-APC/C med deg. of Cyclin A REACT_6850 p = 5.72 x 10-4
DNA Replication REACT_383 p = 1.07 x 10-3
Cell cycle hsa04110 p = 2.85 x 10-2
Cell cycle GO:0007049 p = 5.49 x 10-6
Cell cycle process GO:0022402 p = 7.54 x 10-4
Mitotic cell cycle GO:0000278 p = 4.90 x 10-3
M phase GO:0000279 p = 3.98 x 10-2
M phase of mitotic cell cycle GO:0000087 p = 4.86 x 10-2
MAPK signaling pathway hsa04010 p = 4.73 x 10-2
Protein kinase cascade GO:0007243 p = 4.29 x 10-2
Signalling by NGF REACT_11061 p = 2.87 x 10-4
Signaling by PDGF REACT_16888 p = 3.37 x 10-4
Signaling by EGFR REACT_9417 p = 4.31 x 10-5
VEGF signaling pathway hsa04370 p = 3.40 x 10-3
Regulation of actin cytoskeleton hsa04810 p = 6.50 x 10-7
Structural constituent of cytoskeleton GO:0005200 p = 2.33 x 10-2
Cytoskeletal part GO:0044430 p = 3.89 x 10-6
Microtubule cytoskeleton GO:0015630 p = 2.78 x 10-4
Actin cytoskeleton GO:0015629 p = 1.66 x 10-6
Cytoskeleton organization GO:0007010 p = 1.41 x 10-9
Actin cytoskeleton organization GO:0030036 p = 9.47 x 10-6
Microtubule-based process GO:0007017 p = 1.56 x 10-3
Regulation of cytoskeleton organization GO:0051493 p = 2.28 x 10-6
Microtubule cytoskeleton organization GO:0000226 p = 4.31 x 10-2
Actin filament organization GO:0007015 p = 1.02 x 10-2
Regulation of actin cytoskeleton organization GO:0032956 p = 1.88 x 10-2
Regulation of microtubule-based process GO:0032886 p = 3.20 x 10-3
Regulation of actin pol/depolymerization GO:0008064 p = 4.85 x 10-2
Microtubule pol/depolymerization GO:0031109 p = 1.94 x 10-3
Positive regulation of cytoskeleton organization GO:0051495 p = 2.49 x 10-2
Regulation of microtubule pol/depolymerization GO:0031110 p = 3.65 x 10-3
Microtubule depolymerization GO:0007019 p = 2.01 x 10-3
Microtubule polymerization GO:0046785 p = 3.98 x 10-2
Apoptosis REACT_578 p = 1.59 x 10-9
Regulation of apoptosis GO:0042981 p = 1.90 x 10-6
Regulation of programmed cell death GO:0043067 p = 2.44 x 10-6
Negative regulation of programmed cell death GO:0043069 p = 1.21 x 10-7
Negative regulation of apoptosis GO:0043066 p = 1.21 x 10-7
Cellular response to stress GO:0033554 p = 4.37 x 10-2
Anti-apoptosis GO:0006916 p = 6.81 x 10-8
Positive regulation of apoptosis GO:0043065 p = 4.85 x 10-2
Regulation of caspase activity GO:0043281 p = 4.85 x 10-2
Chromosome GO:0005694 p = 2.43 x 10-5
Chromosome organization GO:0051276 p = 6.22 x 10-4
Chromatin organization GO:0006325 p = 2.40 x 10-3
Chromatin modification GO:0016568 p = 3.36 x 10-3
Focal adhesion hsa04510 p = 9.43 x 10-9
Tight junction hsa04530 p = 4.90 x 10-3
Adherens junction hsa04520 p = 1.22 x 10-2
Cell junction GO:0030054 p = 5.06 x 10-4
Adherens junction GO:0005912 p = 1.63 x 10-8
Cell-cell junction GO:0005911 p = 3.24 x 10-2
Cell-substrate junction GO:0030055 p = 1.55 x 10-5
Integrin complex GO:0008305 p = 1.55 x 10-2
Signaling by EGFR REACT_9417 p = 4.31 x 10-5
Signaling by Wnt REACT_11045 p = 3.37 x 10-4
Signaling by Rho GTPases REACT_11044 p = 4.05 x 10-2
Pathways in cancer hsa05200 p = 4.08 x 10-3
Ruffle GO:0001726 p = 2.78 x 10-4
Cell leading edge GO:0031252 p = 2.43 x 10-5
Lamellipodium GO:0030027 p = 7.51 x 10-1
Ruffle membrane GO:0032587 p = 4.24 x 10-2
Cell migration GO:0016477 p = 3.73 x 10-2
Cell-substrate junction assembly GO:0007044 p = 3.65 x 10-3
Cell-cell junction assembly GO:0007043 p = 3.11 x 10-2
Prostate cancer hsa05215 p = 1.48 x 10-3
Chronic myeloid leukemia hsa05220 p = 1.17 x 10-3
Endometrial cancer hsa05213 p = 3.15 x 10-5
Colorectal cancer hsa05210 p = 1.92 x 10-2
Melanoma hsa05218 p = 6.25 x 10-3
Renal cell carcinoma hsa05211 p = 4.90 x 10-3
Glioma hsa05214 p = 4.08 x 10-3
Non-small cell lung cancer hsa05223 p = 2.18 x 10-3
Bladder cancer hsa05219 p = 1.92 x 10-4
Acute myeloid leukemia hsa05221 p = 1.44 x 10-2
Thyroid cancer hsa05216 p = 1.73 x 10-2
0
2
4
6
8
10
12
Fold enrichment

Figure S6. Biological function analysis of phosphoproteomics data obtained from oncogenic *ras* senescent cells treated with MG132

FatiGO single enrichment analysis of phosphopeptides enriched in Ras senescent cells, treated with MG132, with the Babelomics 4.3 platform. The significant *Gene Ontology* (GO), *Kyoto Encyclopedia of Genes and Genomes* (KEGG), and *Reactome* term names associated to senescence and transformation phenotypes according to the literature were extracted. For each term, an adjusted *P*-value was calculated by the methodology implemented in the Babelomics 4.3 platform. The terms were then grouped in more general categories for simplification. These categories are based on knowledge and literature.

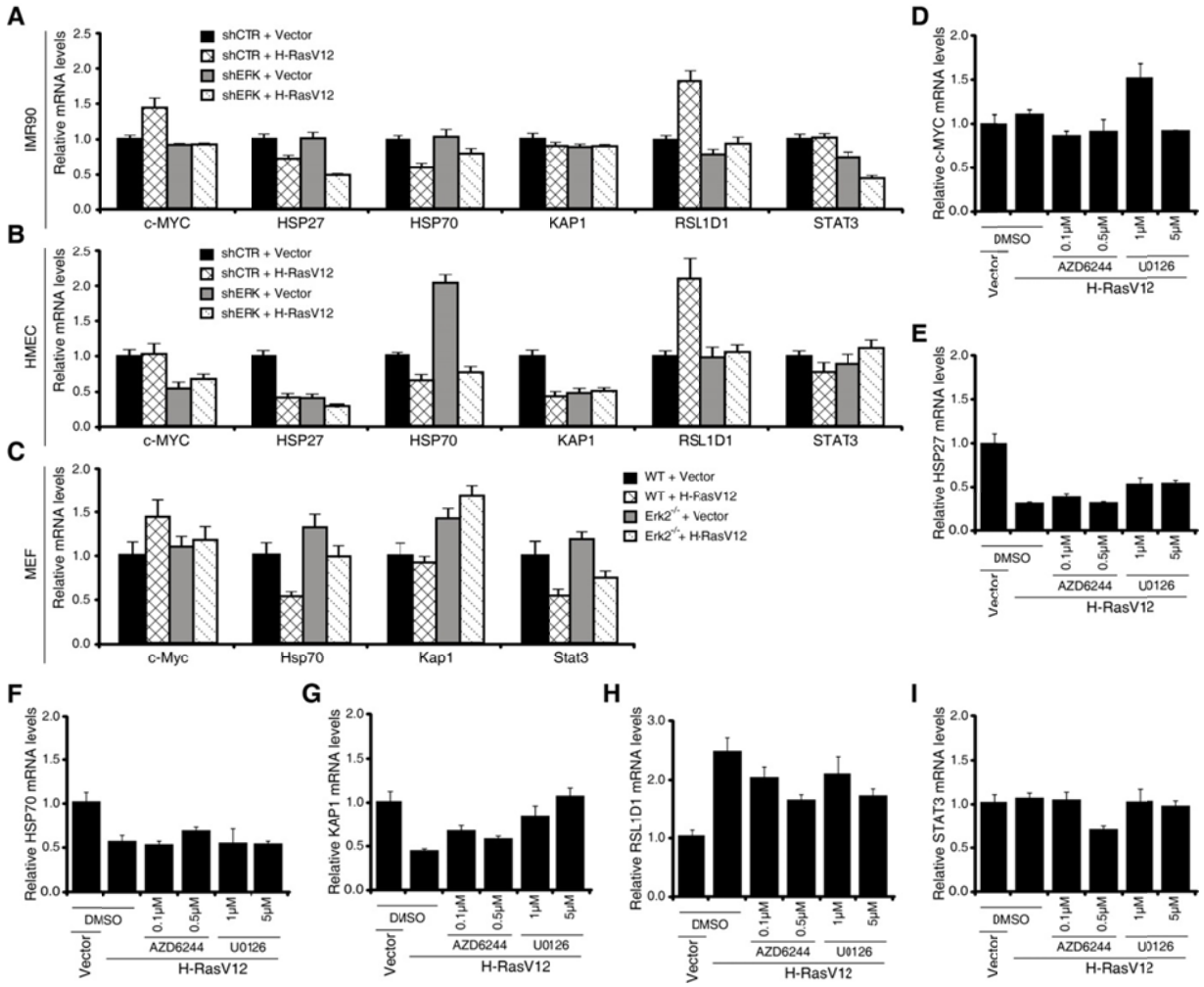

Figure S7. mRNA levels of proteins found degraded in an ERK-dependent manner during Ras-induced senescence

(***A***) qPCRs showing the levels of the indicated mRNAs in IMR90 cells expressing H-RasV12 (R) or a vector control (V) and shERK2 or a control shRNA (shCTR) 14 d after infection. (***B***) qPCRs for mRNAs and conditions as in (*A*) but for HMECs. (***C***) qPCRs showing the levels of the indicated mRNA in wild type or Erk2$^{-/-}$ MEFs expressing oncogenic *ras* or a vector control 14 d after infection. (***D-I***) qPCRs for the indicated mRNAs in IMR90 cells with a control vector (V) or H-RasV12 (R) and treated with the indicated chemicals. The treatments started immediately after infection and the medium was changed every 2 d. Cells were harvested 10 days after infection. All experiments $n \geq 2$.

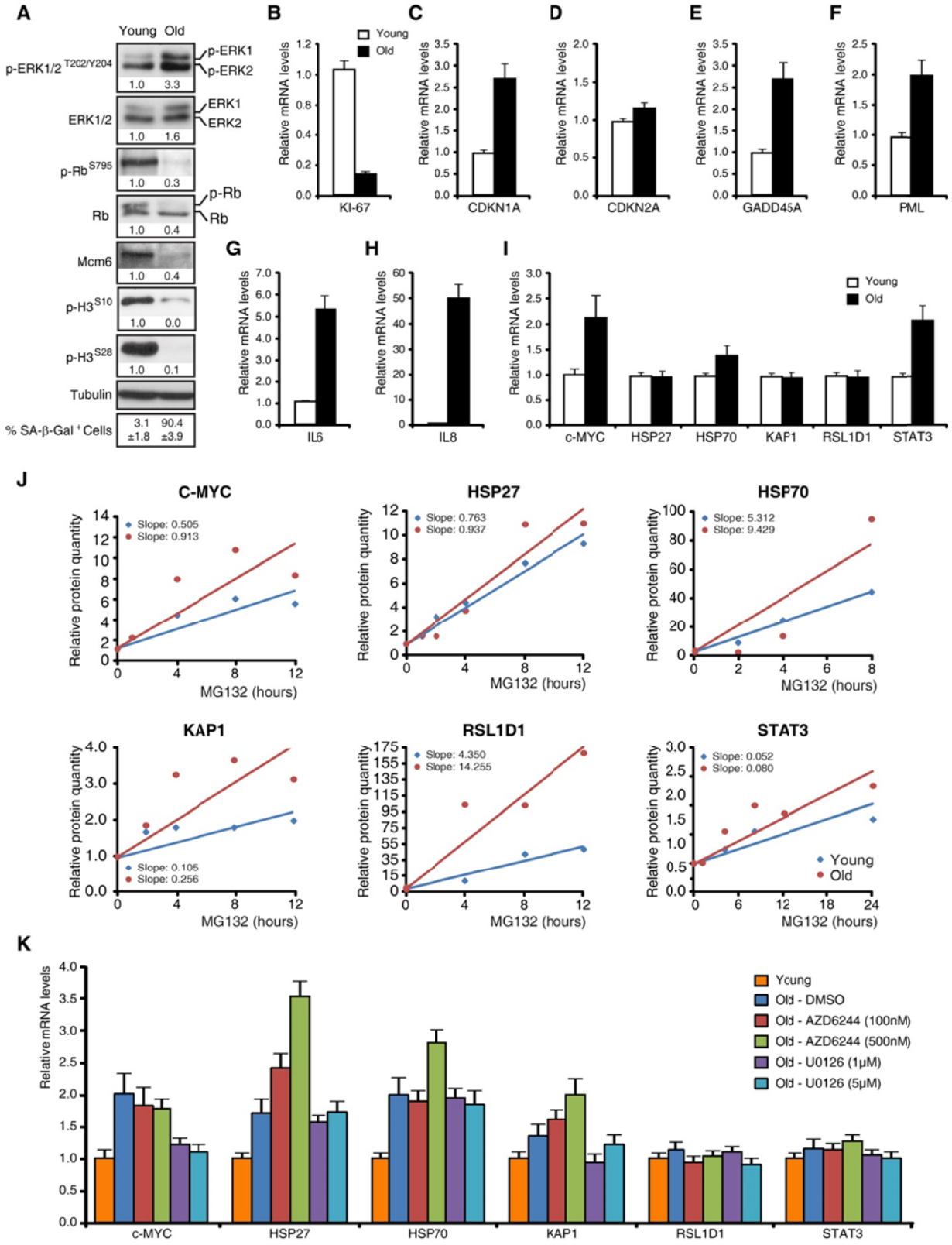
A
Young Old
p-ERK1/2 T202/Y204
p-ERK1
p-ERK2
1.0 3.3
ERK1/2
ERK1
ERK2
1.0 1.6
p-Rb S795
1.0 0.3
Rb
p-Rb
Rb
1.0 0.4
Mcm6
1.0 0.4
p-H3 S10
1.0 0.0
p-H3 S28
1.0 0.1
Tubulin
% SA-β-Gal + Cells
3.1 ±1.8
90.4 ±3.9
B
Young
Old
Relative mRNA levels
KI-67
C
CDKN1A
D
CDKN2A
E
GADD45A
F
PML
G
IL6
H
IL8
I
c-MYC
HSP27
HSP70
KAP1
RSL1D1
STAT3
J
C-MYC
Slope: 0.505
Slope: 0.913
HSP27
Slope: 0.763
Slope: 0.937
HSP70
Slope: 5.312
Slope: 9.429
KAP1
Slope: 0.105
Slope: 0.256
RSL1D1
Slope: 4.350
Slope: 14.255
STAT3
Slope: 0.052
Slope: 0.080
Young
Old
Relative protein quantity
MG132 (hours)
K
Young
Old - DMSO
Old - AZD6244 (100nM)
Old - AZD6244 (500nM)
Old - U0126 (1μM)
Old - U0126 (5μM)
Relative mRNA levels
c-MYC
HSP27
HSP70
KAP1
RSL1D1
STAT3

Figure S8. Senescence markers and mRNA levels of proteins found degraded in an ERK-dependent manner during replicative senescence

(***A***) Immunoblots for ERK and cell cycle regulators in young (PDL = 21.5) and old IMR90 fibroblasts (PDL = 40) (*n* = 3). (***B-I***) qPCR for the indicated mRNAs in young and old cells obtained as in (*A*) (*n* = 2). (***J***) Protein stability assays for the indicated proteins obtained from young or old cells as in (*A*). Cells were treated with 20 μM MG132 for the indicated time. The relative protein quantity was evaluated by immunoblotting and quantification was carried out with Image Lab 4.0. (***K***) qPCR for the indicated mRNAs in young (PDL = 21.5) and old (PDL ≥ 40) IMR90 cells treated with the indicated MEK inhibitors for 27 d. Fresh medium and inhibitors were added every 2 d.

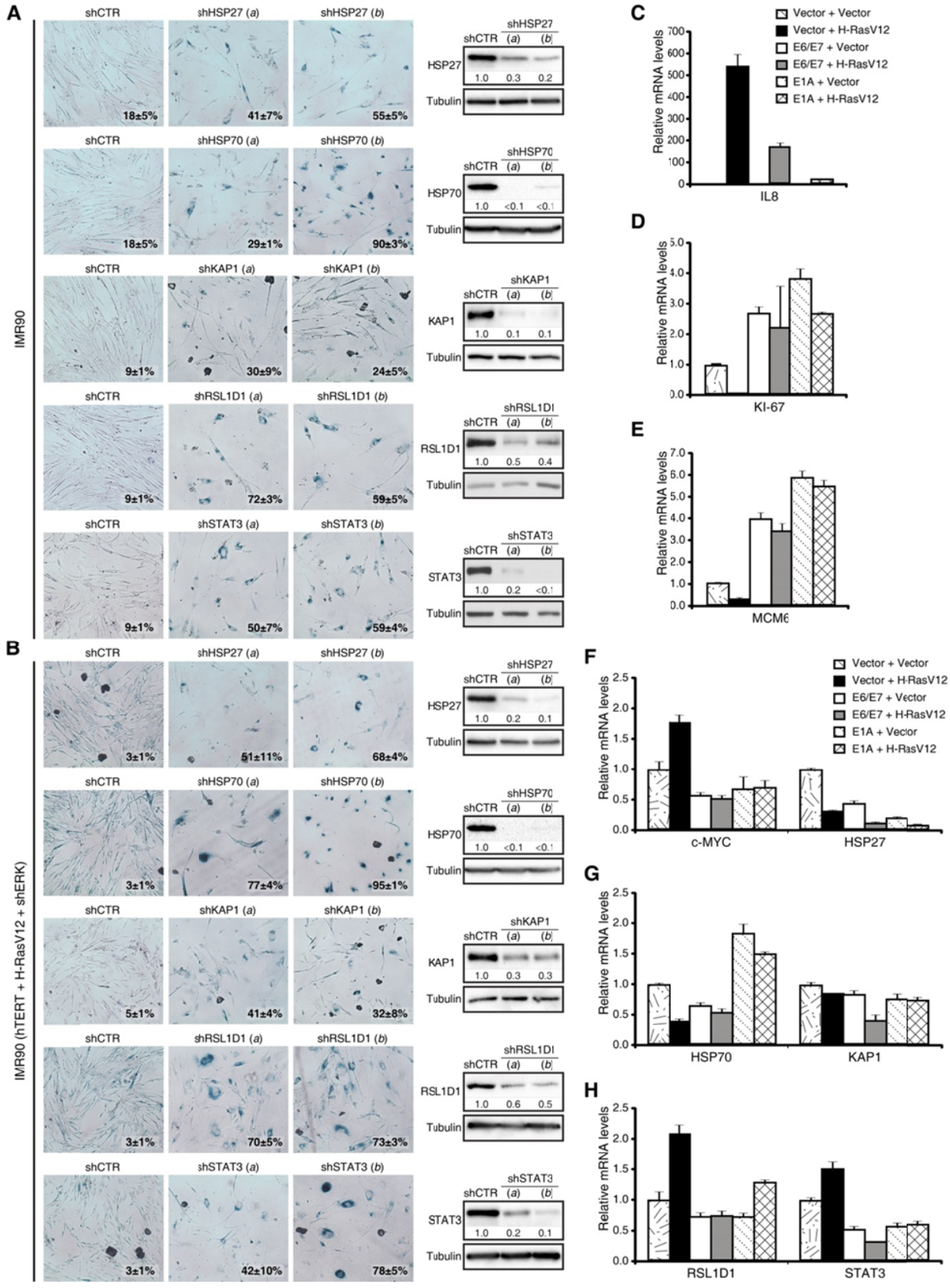
A
IMR90
shCTR
shHSP27 (a)
shHSP27 (b)
18±5%
41±7%
55±5%
shHSP70 (a)
shHSP70 (b)
18±5%
29±1%
90±3%
shKAP1 (a)
shKAP1 (b)
9±1%
30±9%
24±5%
shRSL1D1 (a)
shRSL1D1 (b)
9±1%
72±3%
59±5%
shSTAT3 (a)
shSTAT3 (b)
9±1%
50±7%
59±4%
HSP27
1.0 0.3 0.2
HSP70
1.0 <0.1 <0.1
KAP1
1.0 0.1 0.1
RSL1D1
1.0 0.5 0.4
STAT3
1.0 0.2 <0.1
Tubulin
B
IMR90 (hTERT + H-RasV12 + shERK)
3±1%
51±11%
68±4%
3±1%
77±4%
95±1%
5±1%
41±4%
32±8%
3±1%
70±5%
73±3%
3±1%
42±10%
78±5%
HSP27
1.0 0.2 0.1
HSP70
1.0 <0.1 <0.1
KAP1
1.0 0.3 0.3
RSL1D1
1.0 0.6 0.5
STAT3
1.0 0.2 0.1
C
Vector + Vector
Vector + H-RasV12
E6/E7 + Vector
E6/E7 + H-RasV12
E1A + Vector
E1A + H-RasV12
Relative mRNA levels
IL8
D
KI-67
E
MCM6
F
c-MYC
HSP27
G
HSP70
KAP1
H
RSL1D1
STAT3

Figure S9. Knockdown of SAPD targets induces senescence

(***A, B***) SA-β-Gal of normal (*A*) or transformed (hTERT + H-RasV12 + shERK2) (*B*) IMR90 cells expressing the indicated shRNA, fixed 10 d after infection. Data were quantified from 100 cell counts in triplicate and presented as the mean percentage of positive cells ± SD (shown in the *bottom right* of every picture). The immunoblots shown on the *right* indicate the efficiency of the knockdown. These experiments were done in triplicate and at least 2 times. (***C-E***) qPCR for senescence markers in IMR90 fibroblasts expressing an empty vector or the human papillomavirus E6/E7 oncoproteins or the adenovirus E1A oncoproteins, and then coinfected with H-RasV12 or an empty vector. (***F-H***) qPCR for the indicated mRNAs in cells and in (*C-E*).

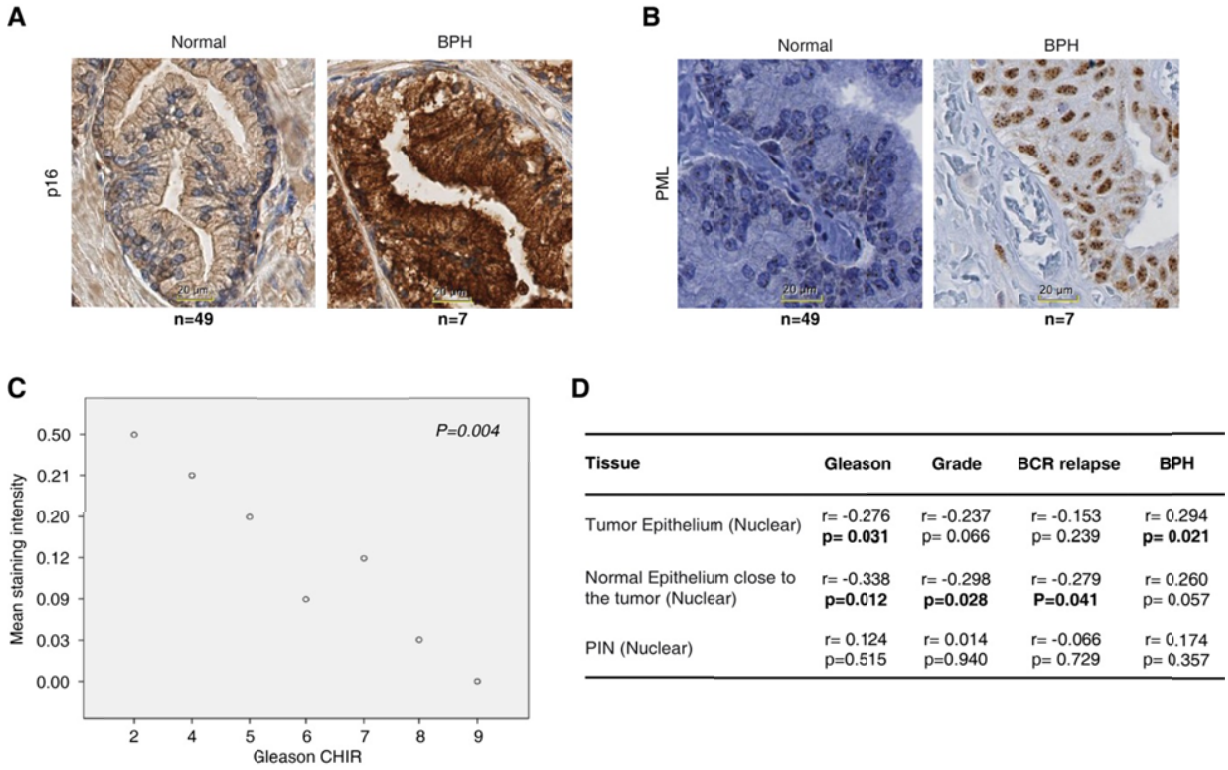

Tissue	Gleason	Grade	BCR relapse	BPH
Tumor Epithelium (Nuclear)	r= -0.276 **p= 0.031**	r= -0.237 p= 0.066	r= -0.153 p= 0.239	r= 0.294 **p= 0.021**
Normal Epithelium close to the tumor (Nuclear)	r= -0.338 **p=0.012**	r= -0.298 **p=0.028**	r= -0.279 **P=0.041**	r= 0.260 p= 0.057
PIN (Nuclear)	r= 0.124 p=0.515	r= 0.014 p=0.940	r= -0.066 p= 0.729	r= 0.174 p= 0.357

Figure S10. Senescence markers and phospho-ERK in prostate tumors

(***A***) Immunochemistry for p16INK4a in benign prostatic hyperplasia compared to normal prostate tissues. (***B***) Immunochemistry for PML in benign prostatic hyperplasia compared to normal prostate tissues. (***C***) Phospho-ERK staining is lower in patients with high Gleason score. Summary point plot showing the relationship between the mean intensity of phospho-ERK labeling in tissue microarrays with samples taken from prostate cancer patients and the Gleason pattern of the patients. χ^2 analysis revealed statistically significant differences in phospho-ERK staining according to the Gleason pattern, $P = 0.004$. (***D***) Spearmans correlation coefficients (r) and P-values for correlations between phospho-ERK staining and clinical parameters of prostate cancer patients ($n = 64$).

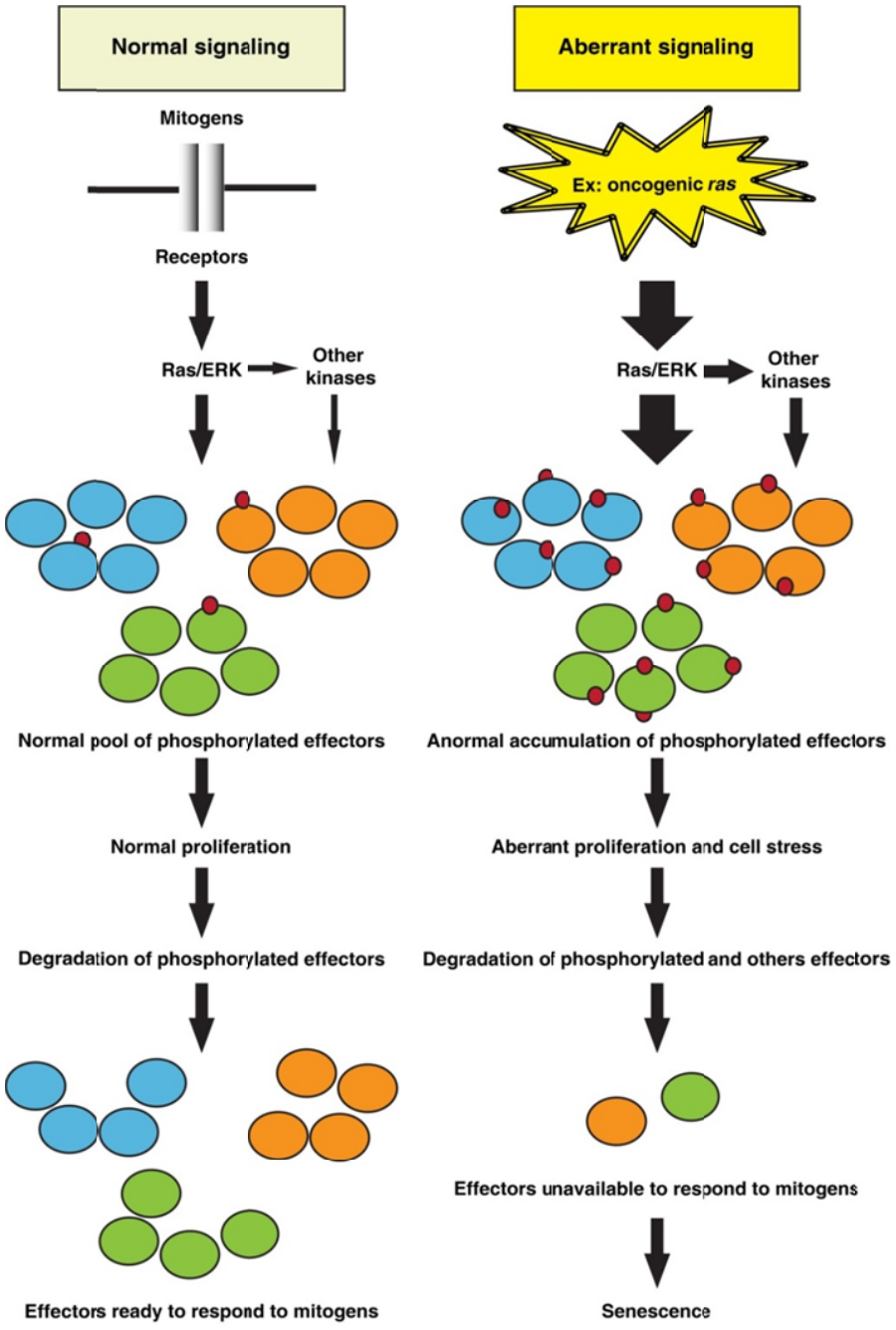

Figure S11. Model of phosphorylation-dependent protein degradation during senescence
We propose that aberrant signaling stimulated by oncogenic *ras* or short telomeres leads to the phosphorylation of a larger fraction of direct or indirect targets of ERK signalling, while normal signaling would engage the phosphorylation of a minor fraction of each protein. Some of these targets will undergo phosphorylation-dependent ubiquitination and proteasome-dependent degradation. As a consequence, aberrant ERK signaling can effectively deplete some critical targets of signalling pathways involving phosphorylation.

2.3.7.2 Supplemental materials and methods

Reagents and plasmids

The proteasome inhibitor MG132 and the protein synthesis inhibitor cycloheximide were from Sigma-Aldrich (Oakville, ON). The GSK3β inhibitor CHIR99021 was from BioVision (Mountain View, CA), the MEK inhibitor AZD6244 was from Symansis (Shanghai, China) and the MEK inhibitor U0126 was from Calbiochem EMD Millipore (Billerica, MA).

Retroviruses pWZL and pWZL-H-RasV12 were described in Ferbeyre *et al.* (2000) (100). pLPC-E1A, pLPC-MYC-HA, pBabe-ER, pBabe-H-RasV12-ER and pLXSN-E6/E7 were a gift from the laboratory of Dr. Scott W. Lowe (Memorial Sloan-Kettering Cancer Center, New-York, NY). To express a low level of oncogenic *ras* we use pWZL-H-RasV12 under the control of the PGK promoter (491). Lentivirus pFG12-CMV-hTERT-IRES-GFP was described before (492). The shRNA library was cloned in the backbone of the retroviral vector pMLP. The shERK1(*a*), shERK2(*a*) shERK2(*b*) and one shCTR were cloned in pMLPX (pMLP without GFP reporter). Lentiviruses pLKO expressing shERK1(*b*), shERK2(*c*), shHSP27(*a*), shHSP27(*b*), shHSP70(*a*), shHSP70(*b*), shKAP1(*a*), shKAP1(*b*) shRSL1D1(*a*), shRSL1D1(*b*), shSTAT3(*a*), shSTAT3(*b*) and shCTR were from Sigma-Aldrich (#6152, #10041, #352750, #11466, #8756, #8758, #18001, #199141, #159162, #159486, #20840, #20842, and SHC002). shRNA target sequences (sense strand) are presented in the Table SII.

Table SII. Description of the shRNAs used

Name	Vector	Sequence
shCTR	pMLPX	CGCGAAGTCTGTACTCTTG
shCTR	pLKO	CAACAAGATGAAGAGCACCAA
shERK1 (*a*)	pMLPX	CATGAAGGCCCGAAACTAC
shERK1 (*b*)	pLKO	CTATACCAAGTCCATCGACAT
shERK2 (*a*)	pMLPX	CCAGATCCTCAGAGGGTTAAA
shERK2 (*b*)	pMLPX	GCGCTTCAGACATGAGAAC
shERK2 (*c*)	pLKO	GACATTATTCGAGCACCAACC
shHSP27 (*a*)	pLKO	AGGAGTGGTCGCAGTGGTTAG
shHSP27 (*b*)	pLKO	CCCGGACGAGCTGACGGTCAA
shHSP70 (*a*)	pLKO	GCCATGACGAAAGACAACAAT
shHSP70 (*b*)	pLKO	CGTGGAGGAGTTCAAGAGAAA
shKAP1 (*a*)	pLKO	CTGAGACCAAACCTGTGCTTA
shKAP1 (*b*)	pLKO	CTCTGTTCTCTGTCCTGTCAC
shRSL1D1 (*a*)	pLKO	GCCTTTGTAACCTTCTCTAAA
shRSL1D1 (*b*)	pLKO	CAAGAGAGATCAATGACTGTA
shSTAT3 (*a*)	pLKO	GCTGACCAACAATCCCAAGAA
shSTAT3 (*b*)	pLKO	GCACAATCTACGAAGAATCAA

Cells and viral-mediated gene transfer

Phoenix ampho packaging cells were a gift from S. W. Lowe. Human embryonic kidney (HEK) 293t cells, HeLa cells and normal human diploid fibroblasts (IMR90) were obtained from American Type Culture Collection (ATCC, Manassas, VA). Cells were cultured in Dulbecco's modified Eagle medium (DMEM; Wisent, Montréal, QC) supplemented with 10% fetal bovine serum (FBS; Wisent) and 1% penicillin G/streptomycin sulfate (Wisent). HMECs (Human Mammary Epithelial Cells) were obtained from Lonza (Basel, Switzerland) and grown in 90% MEGM (Mammary Epithelial Growth Medium) completed with Bovine Pituitary Extract (BPE), human recombinant Epidermal Growth Factor (hEGF), Insulin, Hydrocortisone and Gentamicin/Amphotericin as provided in the MEGM Bullet kit (CC-3150; Lonza) and 10% DMEM (Wisent) supplemented with 10% FBS (Wisent).

Retroviral-mediated gene transfer was done as described previously (100). Briefly, 5 x 10^6 Phoenix Ampho packaging cells were seeded in a 10 cm petri dish, incubated 24 h, and then transiently transfected using calcium phosphate method with 20 µg of a retroviral plasmid and 10 µg of the 4070A amphotropic envelope protein expression plasmid pAMPHO. After 18 h, transfected cells were treated with 10 mM sodium butyrate (Sigma-Aldrich) for 12 h, and then the medium was changed. The virus-containing supernatants were collected 48 to 72 h after transfection, filtered through a 0.45 µM filter (Sarstedt, Montréal, QC), supplemented with 4 µg/mL polybrene (Sigma-Aldrich) and added on target cells. These cells were divided the day before to ensure that they can proliferate throughout the period of infection. Target cells were infected with two viral soups for 6 h at 37°C each time.

For lentiviral transduction, 5 x 10^6 HEK 293t cells were seeded in 10 cm tissue culture dishes and grown for 24 h. Then, cells were transiently transfected using calcium phosphate method with 6 µg of a lentiviral expression vector, 3 µg of the VSV-G envelope protein expression plasmid pMD2, 1.5 µg of the regulator of virion expression (REV) expression plasmid pRSV and 1.5 µg of gag/pol elements expression plasmid pMDLg/pRRE. The medium was changed after 24 h incubation. Supernatants from the transfected plates were collected 48 to 72 h after transfection. The viral soups were filtered through a 0.45µm filter, supplemented with 4 µg/mL polybrene and then added on target cells.

Finally, 12 h after the last infection, infected cell population were selected using 2.5 µg/mL puromycin (Wisent) and/or 75 µg/mL hygromycin (Wisent) and/or 400 µg/mL G418 (Wisent).

Cells proliferation and senescence analysis

Growth curves were obtained from estimations of cell numbers according to a crystal violet retention assay (100). KI-67 expression was evaluated by immunofluorescence staining with a mouse monoclonal anti-KI-67 primary antibody (1:150; clone MIB-1, M7240, DAKO, Carpinteria, CA) and a donkey anti-mouse secondary antibody (1:1500; AlexaFluor 594, A-21203, Molecular Probes, Invitrogen, Logan, UT). BrdU incorporation in subconfluent cultures was evaluated by immunofluorescence after a 2 h incubation with 10 µM BrdU (Cell

proliferation kit, Amersham Pharmacia Biotech., Baie d'Urfe, QC), fixation of cells and staining with a mouse monoclonal anti-BrdU antibody conjugated with AlexaFluor 594 (1:150; clone PRB-1, A-21304, Molecular Probes). To evaluate senescence, SA-β-Gal activity was assayed as described before (100). For KI-67 expression, BrdU incorporation and SA-β-Gal, data were quantified from 100 cells counts in triplicate in at least three independent experiments.

Flow Cytometry

To measure superoxide production, subconfluent cells were incubated with 1 μM dihydroethidium (DHE; Molecular Probes) during 1 h. Cells were washed with Hanks' balanced salt solution (HBSS; Invitrogen) and the fluorescent probes were detected by a FACSort flow cytometer (BD Biosciences, San Jose, CA). The results are expressed as the percent of maximum cell number according to fluorescence intensity. This percentage is achieved by normalizing to the cell number at mode of the distribution. Thus, the maximum cell number on the Y axis for each experimental condition becomes 100% of total.

Soft Agar assays

For the soft agar assays shown in Figure 9A, 1 x 10^4 cells in 2.5 mL of DMEM containing 0.3% low-melting agarose (Wisent) and 10% fetal bovine serum (FBS) were seeded in 6 cm tissue culture dishes with a basal layer of 3 mL 0.5% low-melting agarose containing 10% FBS. Cells were maintained at 37°C and were fed every 4 d by adding 1 mL of DMEM supplemented with 10% FBS on top of the soft agar. After three weeks of culture, the colonies with a diameter greater than 100 μm were counted and GFP-positive colonies were confirmed by inverted fluorescence microscopy.

For other figures, soft agar assays with IMR90-derivated cells were done on 96-well flat-bottom microplate by using the CytoSelect™ 96-Well Cell Transformation Assay kit (Cell Biolabs, San Diego, CA). 5000 cells were seeded per well and 100 μL of complete DMEM was added. Cells were maintained at 37°C during 8 d and fresh medium was added after 4 d. The quantification of anchorage independent growth was done by measuring the fluorescence emitted by the CyQuant GR Dye (485/520 nm) according to manufacturer's instructions.

Soft agar assays with HMEC-derivated cells were done on 96-well flat-bottom microplate. 5000 cells in 75µL of 0.92X MEGM/DMEM medium (90% complete MEGM + 10% DMEM supplemented with 10% FBS) containing 0.4% low-melting agarose were seeded per well on a basal layer of 50µL of 0.88X MEGM/DMEM containing 0.5% low-melting agarose. 100µL of 1X MEGM/DMEM medium was added in each well. Cells were maintained at 37^{o}C during 8 d and fresh medium was added after 4 d. The quantification of colony proliferation was carried out using the CyQuant GR Dye as before.

Focus-forming assay (contact inhibition assay)

For focus-forming assay, 500 cells (or 200 cells) were mixed with a high concentration of normal IMR90 fibroblasts and grown to confluence in 10 cm (or 6 cm) tissue culture dishes. Cell medium was changed every 4 d. After 14 d of culture in a confluent state, cells were fixed using 1% glutaraldehyde (Sigma-Aldrich) in PBS for 15 min at room temperature. Then, cells were stained 30 min with crystal violet, washed with water, and foci were scored. Numbers of foci per dish are presented as the means ± SD of triplicates.

Immunofluorescence

Immunofluorescence images were performed as described before (100). Images were captured with an Olympus FV300 confocal laser microscope and were processed with Metamorph and Image J. Primary antibodies used were: anti-phopho-ATM^{S1981} (1:150; clone 10H11.E12, #4526, Cell Signaling Technology, Pickering, ON), anti-phospho-ERK1/2$^{T202/Y204}$ (1:200; clone D13.14.4E, #4370, Cell Signaling Technology), anti-phospho-Histone H2AX^{S134} (1:200; clone JBW301, #05-636, Millipore, Bedford, MA), anti-PML (1:400; clone PG-M3, Sc-966, Santa Cruz Biotechnology, Santa Cruz, CA), anti-RasGTP (1:200; #26909, NewEast Biosciences, Malvern, PA) and anti-53BP1 (1:200; PC712, Calbiochem, EMD Biosciences, San Diego, CA). Appropriate secondary antibodies were used: goat anti-mouse AlexaFluor 568 (1:1000; A-11004, Molecular Probes), goat anti-rabbit AlexaFluor 568 (1:1000; A-11011, Molecular Probes) and goat anti-mouse AlexaFluor 488 (1:1000; A-11001, Molecular Probes).

Immunoblotting

Primary antibodies used were: anti-Caldesmon (1:10000; ab32330, Abcam, Cambridge, MA), anti-phospho-Caldesmon^{S789} (1:10000; clone E89, #1089-1, Epitomics Inc., Burlingame, CA), anti-CDK4 (1:1500; clone DCS156, #2906, Cell Signaling Technology), anti-CHK2 (1:800; #2662, Cell Signaling Technology), anti-phospho-CHK2^{S19} (1:800; #2666, Cell Signaling Technology), anti-c-MYC (1:1000; clone D84C12, #5605, Cell Signaling Technology), anti-phospho-c-RAF^{S338} (1:1000; clone 56A6, #9427, Cell Signaling Technology), anti-Cyclin A (1:800; Sc-596 (C-19), Santa Cruz Biotechnology), anti-phospho-ELK-1^{S383} (1:1000; #9181, Cell Signaling Technology), anti-ERK1/2 (1:400; Sc-94 (K-23), Santa Cruz Biotechnology), anti-phospho-ERK1/2$^{T202/Y204}$ (1:2000; clone D13.14.4E, #4370, Cell Signaling Technology), anti-E1A (1:400; clone 0.N.7, ab33183, Abcam), anti-FAK (1:1000; clone EP1831Y, ab76496, Abcam), anti-phospho-FAK^{S910} (1:1000; 44-596G, Biosource, Invitrogen), anti-HA-tag (1:1000; clone 6E2, #2367, Cell Signaling Technology), anti-phospho-Histone H3^{S10} (1:1000; #06-570, Millipore), anti-phospho-Histone H3^{S28} (1:1000; #07-145, Millipore), anti-HSP27 (1:15 000, gift from Dr. Jacques Landry, CRC of Laval University, Québec, QC), anti-HSP70 (1:5000; clone C92F3A-5, SMC-100A/B, StressMarq Biosciences, Victoria, BC), anti-H-Ras (1:250; clone F235, Sc-29, Santa Cruz Biotechnology), anti-KAP1 (1:1000, A300-274, Bethyl Laboratories, Montgomery, TX), anti-MCM6 (1:100; clone W817, gift from Dr. Hans-Jürgen Heidebrecht, University of Kiel, Germany), anti-MDM2 (1:200; clone 2A10, Sc-56153, Santa Cruz Biotechnology), anti-phospho-MEK1/2$^{S217/S221}$ (1:1000; clone 41G9, #9154, Cell Signaling Technology), anti-p16^{INK4a} (1:500; clone F-12, Sc-1661, Santa Cruz Biotechnology), anti-p19^{Arf} (1:500, clone 5-C3-1, Sc-32748, Santa Cruz Biotechnology), anti-p21 (1:750; Sc-397 (C-19), Santa Cruz Biotechnology), anti-phospho-p38$^{T180/Y182}$ (1:800; clone 3D7, #9215, Cell Signaling Technology), anti-p53 (1:400, NCL-p53-CM5p, NovoCastra Laboratories, Newcastle upon Tyne, UK), anti-phospho-p53^{S15} (1:800; #9284, Cell Signaling Technology), anti-phospho-p90RSK^{S380} (1:1500; AF889, R&D Systems, Minneapolis, MN), anti-RB (1:250; clone G3-245, #554136, BD Pharmingen, San Diego, CA), anti-phospho-RB^{S780} (1:1000; #9307, Cell Signaling Technology), anti-phospho-RB^{S795} (1:1000; #9301, Cell Signaling Technology), anti-RSL1D1 (1:1000; GTX88161, GeneTex, San Antonio, TX), anti-STAT3 (1:800; clone

124H6, #9139, Cell Signaling Technology), anti-phospho-STAT3^{S727} (1:800; #9134, Cell Signaling Technology), anti-phospho-STAT3^{Y705} (1:800; #9131, Cell Signaling Technology), anti-Mono and polyubiquitinylated conjugates (1:1000; clone FK2, BML-PW8810, Enzo Life sciences, Farmingdale, NY) and anti-α-Tubulin (1:20000; clone B-5-1-2, T6074, Sigma-Aldrich).

Immunoblotting by Kinexus

Total cell lysates from IMR90 fibroblasts expressing low levels (LR) or high levels (HR) of oncogenic *ras* were prepared according to the instructions from Kinexus and were processed for Kinexus phosphorylation site version 1.0 (KCPS-1.0), which tracks for phosphorylation levels of 14 ERK targets with antibodies against specific epitopes. Kinexus Corp. (Vancouver, BC) uses a highly sensitive imaging system with a 16-bit camera (Bio-Rad, Fluor-S Max Multi-Imager) in combination with quantification software (Bio-Rad, Quantity One) to quantify the chemiluminescent samples. The resulting trace quantity for each band was quantified as counts per minute (relative protein amount).

Immunoprecipitation

Cells were scraped into IP buffer (50 mM Tris-HCl, pH 7.9, 1 mM EDTA, 0.1 mM EGTA, 12.5 mM $MgCl_2$, 400 mM NaCl, 20% glycerol, 1% Triton X-100 [BioShop, Burlington, ON], 0.1% SDS and 1X Complete-EDTA free protease inhibitor cocktail [Roche Applied Science, Laval, QC]). Cell lysates were kept on ice for 15 min, and then sonicated 40 sec at the lowest intensity. Cell lysates were cleared by centrifugation at 13 000 RPM for 1 min, and the immunoprecipitations were performed with 1 or 2 mg of total cell proteins 2 h at 4^{o}C with a suitable antibody. The antibodies used for immunoprecipitation were anti-c-MYC (1:200; clone D84C12, #5605, Cell Signaling Technology), anti-HSP70 (1:300, clone C92F3A-5, SMC-100A/B, StressMarq Biosciences), anti-STAT3 (1:1600; clone 124H6, #9139, Cell Signaling Technology). Control immunoprecipitations were done with normal mouse IgG (10400C, Invitrogen) in a mixture 1:1 of cell lysates. Protein A/G-Sepharose beads (Amersham/GE Healthcare, Baie d'Urfe, QC) were blocked 1 h at 4^{o}C in IP buffer containing 2.5% BSA, 0.16 µg/µL salmon sperm DNA (Sigma-Aldrich) and 0.16 µg/µL E.coli tRNA

(Sigma-Aldrich). Immunoprecipitates were recovered after 30 min of incubation at 4°C with beads and washed three times in IP buffer. Proteins of immunoprecipitates and total cell lysates were separated by SDS-PAGE and transferred to nitrocellulose membranes (Bio-Rad Laboratories) and analyzed by Western blotting with the antibodies described in the section Immunoblotting of Supplemental materials and methods.

Phosphoproteomics

Sample preparation and protein digestion

A total of 40 15-cm plates of IMR90 fibroblasts were infected with pWZL-H-RasV12. 10 d after infection when the whole population was fully senescent, 20 plates of cells were treated with 20 μM MG132 (Sigma-Aldrich) or DMSO for 18 h. Cells were collected on PBS containing 1X Complete-EDTA free protease inhibitor cocktail and 1X PhoStop phosphatase inhibitor cocktail (Roche Applied Science), pelleted and snap frozen on liquid nitrogen. These were then resuspended in the same buffer and sonicated. The extracts were next digested with trypsin as follows. Proteins in extraction buffer were reduced in 50 mM ammonium bicarbonate containing 0.5 mM TCEP and 1% SDS for 20 min at 37°C, then alkylated in 5 mM iodoacetamide for 20 min at 37°C. 5 mM DTT was added to the protein solution to react with excess iodoacetamide. After dilution with 50 mM ammonium bicarbonate, protein digestion was performed in 0.1% SDS with sequencing grade modified trypsin (enzyme/protein ratio: 1/50) overnight at 37 ºC and under high agitation speed. The digest mixture was acidified with Trifluoroacetic acid (TFA) and then evaporated to dryness in a SpeedVac.

Phosphopeptides isolation

For the TiO_2 enrichment procedure, sample loading, washing and elution were performed by spinning the micro-column at 8 000 RPM at 4°C in a regular Eppendorf microcentrifuge. The spinning time and speed were adjusted in function of the elution rate. 6 mg of titanium dioxide phase was packed in a tip. After drying, the digest mixture was dissolved in 400 μL of lactic acid (250 mM final in 3% TFA/70% ACN), centrifuged 5 min at 13 000 RPM and the soluble supernatant was loaded on a micro-column previously

equilibrated with 100 µL of 3% TFA/70% ACN. Each micro-column was washed with 100 µL of lactic acid solution followed by 200 µL of 3% TFA/70% ACN to remove non-specific binding peptides. Phosphopeptides were eluted with 200 µL of 1% NH_4OH pH 10 in water and acidified with 7 µL of TFA. Samples were dried down in a SpeedVac and resuspended in 25 µL of 0.2% formic acid/2% ACN for 2D-LC-MS/MS experiments on the LTQ-Orbitrap mass spectrometer (Thermo Fisher Scientific, Bremen, Germany).

Liquid Chromatography

For LC experiments, protein digests were separated using a home-made 10 cm x 150 µm i.d. analytical column and a 4 mm length, 360 µm i.d. trap column packed with 3 µm C_{18} particles (Jupiter 300 Å, Phenomenex, Torrance, CA). Tryptic digests (200 ng loading unless otherwise specified) were injected on the column and elution was achieved using a linear gradient of 5-40% acetonitrile (0.2% formic acid) during 51 min with a flow rate of 600 nL/min.

Mass spectrometry

All MS analyses were performed using an LTQ-Orbitrap XL hybrid mass spectrometer with a nanoelectrospray ion source coupled to a LC system (Eksigent, Dublin, CA) equipped with a Finnigan AS autosampler (Thermo Fisher Scientific). The conventional MS spectra (survey scan) were acquired at high resolution (M/ΔM: 60 000 full width half maximum) over the acquisition range of *m/z* 400-1600. Unless otherwise indicated, MS/MS spectra were collected using data-dependent acquisition for multiply charged ions exceeding a threshold of 10 000 counts.

Database searching and phosphoproteomic analyses

MS data were analyzed using the Xcalibur software (version 2.0.7). Peak lists were then generated using the Mascot distiller software (version 2.3.2.0, Matrix science), where MS processing was carried out using the LCQ_plus_zoom script. Database searches were performed using the search engine Mascot (version 2.3.0, Matrix Science, London, UK). For all protein analyses, searches were conducted using the International Protein Index (IPI)

mouse forward reverse database containing 111974 entries (version 3.54, released January 2009). The error window for experimental peptide mass values and MS^2 fragment ion mass values were set to +/- 15 ppm and 0.5 Da, respectively. The number of allowed missed cleavage sites for trypsin was set to 1 and phosphorylation (STY), oxidation (M) and deamidation (NQ) were all selected as variable modifications. No fixed modification was included in the search. A cut-off score threshold was established for a false-discovery rate of less than 2% ($P < 0.02$).

Peptide detection, clustering and validation

The comparison of peptide abundances across different experimental paradigms was achieved using label free quantitative proteomics. Briefly, raw data files (.raw) from the Xcalibur software were converted into peptide map files representing all ions according to their corresponding *m/z* values, retention time, intensity and charge state. Intensity values above a threshold of typically 10 000 counts were considered for further analysis. Clustering of peptide maps across different sample sets were performed on peptides associated to a Mascot entry using hierarchical clustering with tolerances of ± 15 ppm and ±1 min for peptide mass and retention time, respectively. Normalization of retention time is then performed on the initial peptide cluster list using a dynamic and nonlinear correction which confines the retention time distribution to less than 0.1 min (<0.3% relative standard deviation [RSD]) on average. Reproducible changes in abundance across conditions were determined using a two-tail homoscedastic *t*-test on sample replicates to identify peptide clusters with *P*-values < 0.05 with fold change greater than 7 standard deviations. Peptide clusters fulfilling these selection criteria were inspected manually to validate identification and changes in abundance.

Bioinformatic analyses of phosphoproteomics data

The Motif-X software tool was used to extract overrepresented phosphorylation motif from the phosphopeptides enriched in cells treated with MG132 (http://motif-x.med.harvard.edu/) (490). The software uses an iterative strategy to build successive motifs through comparison to a dynamic statistical background. For our analysis, we used an

occurrence threshold of 20 (minimum number of times each of the extracted motif occurs in the data set) and a significance threshold of $P < 0.000001$.

Phosphopeptides were associated to biological functions by a FatiGO single enrichment analysis using the Babelomics 4.3 platform (http://babelomics.bioinfo.cipf.es/) (493). The databases used were GO biological process, GO molecular function, GO cellular component, KEGG pathways and Reactome. The input data list was compared to the complete human genome reference and significance was determined using a two-tailed Fisher's exact test. The GO, KEGG and Reactome terms and their associated peptides were grouped into general categories based on knowledge and literature

Real-time PCR

Total mRNA extracts were prepared in TRIzol (Invitrogen) according to the manufacturer's instructions. Total RNA was reverse transcribed and gene expression level was determined with a lightCycler 480 Real-Time PCR System (Roche Applied Science) and using the SYBR Green or TaqMan technologies as described before (103). The relative quantification of target genes was determined by using the ΔΔCT method.

The primers used for qPCR with the SYBR Green technology were designed with the Universal Probe Library Assay Design Center (https://www.roche-applied-science.com/sis/rtpcr/upl/index.jsp), except for DUSP6 and KI-67, which were taken from Engelbrecht *et al.* (2003) (494) and from PrimerBank (ID: 19923217a1) respectively. (http://pga.mgh.harvard.edu/primerbank/index.html). The primers are presented in the Table SIII.

The primers used for qPCR with the TaqMan technology were provided by the genomics platform of the Institute for Research in Immunology and Cancer (IRIC, Montréal, QC). The primers are presented in the Table SIV.

Table SIII. List of primers used for qPCR with the SYBR Green technology

Target	Forward (5'→3')	Reverse (5'→3')
CDKN1A	ACCCTTGTGCCTCGCTCAGG	GCGTTTGGAGTGGTAGAAATCTGT
CDKN2A	GCTGAGGAGCTGGGCCATCG	CTGGTTCTTTCAATCGGGGATG
c-MYC	ACCACCAGCAGCGACTCTGA	GGCTGTGAGGAGGTTTGCTGTG
DUSP6	ACACCCCTCCTTGCTGGAAT	CACACACAAAGAAAGCAGCCC
ERK1	CAGGAGACAGCACGCTTCCAG	TCTAACAGTCTGGCGGGAGAGG
ERK2	CAACCCACACAAGAGGATTGAA	GTCGAACTTGAATGGTGCTTCG
FOS	ACCACTCACCCGCAGACTCC	CCAGGTCCGTGCAGAAGTCCT
GADD45a	TTGCAATATGACTTTGGAGGAA	CATCCCCCACCTTATCCAT
HSP27 (HSPB1)	CCCTGGATGTCAACCACTTCG	AGATGTAGCCATGCTCGTCCTG
HSP70 (HSPA1A)	CAAGATCACCATCACCAACG	TCGTCCTCCGCTTTGTACTT
KAP1 (TRIM28)	GGCATGGCCATTGTCAAGGA	GCCATAAGCACAGGTTTGGTCTC
IL6	CCAGGAGCCCAGCTATGAACTC	AAGGCAGCAGGCAACACCAG
KI-67	AGAAGACAGTACCGCAGATGA	CGGCTCACTAATTTAACGCTGG
LIF	CCCTCTGAAGTGCAGCCCATAAT	TTTCCAGTGCAGAACCAACAGC
PML	TGCATCACCCAGGGGAAAGA	ATAGGGTCCCTGGGAGTGCTG
RSL1D1	TCCCACAGCTGGTACCAATAGGA	TCCTGTGGCATGTTTTTGAATCTC
SH2B3/LNK	GCTCTTCGACCCACCCAAGA	CAGGCATCTCAAGCCGTGTG
SPRY2	AGAATCCAAGGGAGAGGGGTTG	CCATCAGGTCTTGGAAGTGTGGT
STAT3	GCCTAGATCGGCTAGAAAACTGGA	CCCCTTTGTAGGAAACTTTTTGCTG

Table SIV. List of primers used for qPCR with the TaqMan technology

Target	Forward (5'→3')	Reverse (5'→3')	Probe UPL
CDKN1A	CGAAGTCAGTTCCTTGTGGAG	CATGGGTTCTGACGGACAT	82
CDKN2A	GTGGACCTGGCTGAGGAG	CTTTCAATCGGGGATGTCTG	34
Cdkn2a	GGGTTTTCTTGGTGAAGTTCG	TTGCCCATCATCATCACCT	106
c-Myc	TTTGTCTATTTGGGGACAGTGTT	CATCGTCGTGGCTGTCTG	34
Dusp6	GCAGCGACTGGAATGAGAAC	GAACTTACTGAAGCCACCTTCC	22
Erk1	CCTCAAGTATATACACTCAGCCAATG	CAGGCCAAAATCACAGATCTTA	97
Erk2	ACCGTGACCTCAAGCCTTC	TGATCTGGATCTGCAACACG	18
Fosl1	TGCAGAAACCGAAGAAAGGA	TTCTCATCCTCCAATTTGTCG	4
Gadd45a	GCAGAGCAGAAGACCGAAAG	GTAATGGTGCGCTGACTCC	69
Hsp70 (Hspa1b)	ATGACGGCGCTCATCAAG	CCGAGTAGGTGGTGAAGGTC	22
Ki-67	AGGGTAACTCGTGGAACCAA	TTAACTTCTTGGTGCATACAATGTC	88
IL6	GATGAGTACAAAAGTCCTGATCCA	CTGCAGCCACTGGTTCTGT	40
IL8	AGACAGCAGAGCACACAAGC	ATGGTTCCTTCCGGTGGT	72
INFB1	CGACACTGTTCGTGTTGTCA	GAAGCACAACAGGAGAGCAA	25
Kap1 (Trim28)	TGGTCAATGATGCCCAGA	TTGGTCATGGTCCAGTGCT	18
Lif	TGAAAACGGCCTGCATCTA	AGCAGCAGTAAGGGCACAAT	25
Sh2b3/Lnk	GTGCGGCAGAGTGAGTCC	CACCAGGCGTAAGTGCTTG	91
Stat3	AGTCTCGCCTCCTCCAGAC	GCTGCTTCTCTGTCACTACGG	26

2.4 Mise en contexte de l'article 2

Cet article avait pour but d'approfondir la discussion sur nos résultats présentés au sein de la publication précédente. Nous avons ainsi clarifié qu'en plus de l'autophagie (73, 96), la voie de dégradation dépendante de l'ubiquitination des protéines et du protéasome (*ubiquitin-proteasome pathway*; UPP) pourrait avoir un rôle de premier plan dans l'établissement du phénotype sénescent. En s'appuyant sur nos résultats, nous avons spéculé quant à l'impact que pourrait avoir le SAPD sur les différents mécanismes effecteurs de la sénescence. Nous avons également discuté des limites actuelles du modèle et des questions clefs auxquelles nous devrons répondre dans les prochaines années. Nous avons aussi tenté de concilier le SAPD avec les patrons de dégradation protéiques souvent observés dans les cellules cancéreuses. Enfin, nous avons inscrit notre discussion dans un contexte plus global. Plus précisément, nous avons avancé un modèle qui intègre les différents avantages que pourrait apporter le SAPD à une cellule sénescente afin de lui permettre d'accomplir sa fonction première, c'est-à-dire de protéger l'organisme contre le cancer.

2.5 Contribution à l'article 2

Cet article contient quelques résultats originaux. J'ai réalisé les expériences présentées à la figure 15. Marie-France Gaumont-Leclerc était en charge des expériences de spectrométrie de masse, pour lesquelles j'ai ensuite analysé les résultats obtenus. Ces résultats sont présentés aux figures 16 et 17, ainsi qu'au tableau I.

En ce qui concerne l'écriture, j'ai rédigé la majorité de l'article et conçu les figures. Gerardo Ferbeyre a rédigé une partie de l'introduction et a contribué aux sections suivantes : *Mitochondrial dysfunction*; *DNA damage response*; *Cell cycle arrest*; *Impaired mRNA metabolism and translation*. Frédérique Lessard a rédigé la section *Dysfunction in nucleolar and ribosome biogenesis*. La révision du manuscrit a été effectuée par l'ensemble des auteurs.

2.6 Article 2

Cellular senescence and protein degradation: breaking down cancer

Xavier Deschênes-Simard[1], Frédéric Lessard[1], Marie-France Gaumont-Leclerc[1], Nabeel Bardeesy[2] and Gerardo Ferbeyre[1]

Cell Cycle, 2014 June 15, 13 (12): 1840-58

1) Department of Biochemistry and Molecular Medicine, Université de Montréal, Montréal, Québec H3C 3J7, Canada
2) Massachusetts General Hospital Cancer Center, Harvard Medical School, Boston, MA 02114, USA

Running title: Cellular senescence and protein degradation

Keywords: E3 ligases; ERK kinases; Ras oncogene; ubiquitin; SASP

Correspondence to: Gerardo Ferbeyre

2.6.1 Summary

Autophagy and the ubiquitin-proteasome pathway (UPP) are the major protein degradation systems in eukaryotic cells. Whereas the former mediate a bulk nonspecific degradation, the UPP allows a rapid degradation of specific proteins. Both systems have been shown to play a role in tumorigenesis and the interest in developing therapeutic agents inhibiting protein degradation is steadily growing. However, emerging data point to a critical role for autophagy in cellular senescence, an established tumor suppressor mechanism. Recently, a selective protein degradation process mediated by the UPP was also shown to contribute to the senescence phenotype. This process is tightly regulated by E3 ubiquitin ligases, deubiquitinases and several post-translational modifications of target proteins. Illustrating the complexity of UPP, more than 600 human genes have been shown to encode E3 ubiquitin ligases, a number which exceeds that of the protein kinases. Nevertheless, our knowledge of proteasome-dependent protein degradation as a regulated process in cellular contexts such as cancer and senescence remains very limited. Here we discuss the implications of protein degradation in senescence and attempt to relate this function to the protein degradation pattern observed in cancer cells.

2.6.2 Introduction to cellular senescence

The long lifespan and constant cell turnover of complex organisms pose the challenge of dealing with the inevitable accumulation of DNA damage and gene mutations that drive carcinogenesis. Fortunately, multiple mechanisms have evolved to detect DNA aberrations and oncogenic stress, and protect against the initiation and progression of neoplastic growth. Among these, cellular senescence is a stable cell cycle arrest triggered by a variety of insults including short telomeres, activated oncogenes, DNA damage and reactive oxygen species (73). However, how these stresses converge to regulate a common cellular state is not currently well understood. Senescence is a complex multifaceted cellular phenotype, without an exclusive hallmark, with a broad range of proposed effector mechanisms, and still, with an ambiguous definition. Indeed, different senescent cells are characterized by a wide range of biomarkers (67, 73), many of which are neither exclusive to senescence nor universally present in senescent cells. Because of this phenotypic heterogeneity and often imprecise definition, the assessment of senescence should be carefully addressed and should attempt to rigorously define a combination of senescence-associated features. Moreover, it needs to recognize that this diversity in the phenotypic traits could reflect a concomitant heterogeneity at the level of the effector programs.

At the molecular level, senescence triggers important changes in gene expression patterns, but there is little overlap between different cell types (136). For example, a comparison between young and senescent human fibroblasts and mammary epithelial cells (HMEC) revealed a transcriptional fingerprint unique to senescence, but limited similarity between the two cell lineages (137). Other gene expression analyses have revealed a proinflammatory gene profile in senescent cells under the regulation of the NF-kB transcription factor (139-141) or a downregulation of E2F target genes under the regulation of the retinoblastoma tumor suppressor (RB) (103, 138). However, cells with inactivation in NF-kB or RB can senesce in response to multiple stressors (103, 138-141), indicating that the programs they control are not essential for the initiation of the process. Several target genes of the tumor suppressor p53 (TP53) were also reported to mediate senescence, such as p21 (CDKN1A) (130-132), the tumor suppressor promyelocytic leukemia (PML) (100, 125), the

plasminogen activator inhibitor-1 (PAI-1) (126), DEC1 and E2F7 (129). Again, a p53-dependent transcriptional pattern is not a prerequisite for senescence, and its relative contribution to the process depends on the cell type and the status of the $p16^{INK4A}$–RB pathway (495). Our current knowledge thus suggests that senescence is consistent with distinct gene expression profiles and a variety of effector mechanisms, depending on the triggers, cell types and cellular context.

Beyond transcriptional regulatory networks that characterize senescence, direct control of protein levels also appears strikingly affected. This involves the regulation of mRNA translation and protein stability of specific senescence mediators, such as p53 (496-498) and PML (499-501). In addition, it is thought that a global upregulation of translation may contribute to senescence since the key regulator of protein synthesis, mTOR, has been shown to favor senescence in different contexts (73) and that total protein synthesis is increased in Ras-induced senescent cells (96). Similarly, a more general function of protein degradation now emerges as critical to reorganize the proteome of cells undergoing senescence. Here, we will discuss the impact of protein degradation on the senescence-associated proteome and how this mechanism could contribute to the onset of cellular senescence. Thus, we will effectively address the question: how does a pre-neoplastic cell destroy the machinery required for its subsequent progression to a cancer?

2.6.3 Protein degradation and senescence

The lysosomal degradation pathway is the principal system used by eukaryotic cells to degrade and recycle cytosolic components and organelles. A cytoplasmic cargo is engulfed into vesicles and delivered to the lysosome by the process of autophagy, which can be divided into three classes: 1) chaperone-mediated autophagy; 2) microautophagy; and 3) macroautophagy (502). The latter is mainly a nonspecific cytoplasmic degradation mechanism that has been shown to support tumorigenesis in Ras-expressing cancer cells (503), pancreatic tumors (504), lymphomas (505) and breast cancer (506). Macroautophagy is required to eliminate abnormal mitochondria, reduce the production of reactive oxygen species and replenish tricarboxylic acid (TCA) cycle metabolites (503, 504). Given its catabolic capacity, macroautophagy improves the survival of both normal and cancer cells under metabolic stress

by maintaining the availability of building blocks in order to preserve essential cellular functions (507).

It is now appreciated that in addition to supporting cell viability in established tumors, macroautophagy has context-specific tumor suppressor functions. The first evidence of such a function came from the discovery that the haploinsufficiency of the autophagy-related gene Beclin1 (BECN1) leads to cancer predisposition in mice (508). Moreover, many effectors of macroautophagy, including Atg5 (509), Atg7 (509, 510), Atg4C (511), Bif-1 (512) and UVRAG (513, 514), have been linked to tumor suppression, further supporting its importance in anticancer mechanisms. Mechanistically, macroautophagy may circumvent malignant transformation by inducing autophagic cell death (515) or cellular senescence (96) in the context of oncogenic stress. Despite the demonstration that chaperone-mediated autophagy is downregulated in senescent cells (516) and that macroautophagy may prevent senescence in some contexts (517), a growing number of observations show a correlation between markers of autophagy and the senescence phenotype (95, 518, 519). Also, numerous studies have now demonstrated the critical role of macroautophagy during the establishment of senescence triggered by various stresses (96, 520-525). Interestingly, some recent work suggests an intimate relationship between macroautophagy and the senescence-associated secretory phenotype (SASP) (109, 526). These studies propose that macroautophagy is required to attenuate the proteotoxic stress induced by the high protein synthesis rate involved in the SASP and to supply the process with building blocks and energy (502, 527). The SASP has been linked to the deleterious effects of senescence (139, 147), but also to the auto/paracrine reinforcement of the phenotype (140, 144, 145, 528) and to the immune clearance of senescent cells (89, 151, 152, 154), thereby suggesting that autophagy might play a central function to explain the pathophysiological relevance of senescence.

During the molecular characterization of the role of the ERK kinases in Ras-induced senescence in human fibroblasts, our group discovered that senescence depends on high-strength ERK signals. In this context, we serendipitously found that some ERK targets were degraded. This initial observation lead to the identification of multiple actively degraded

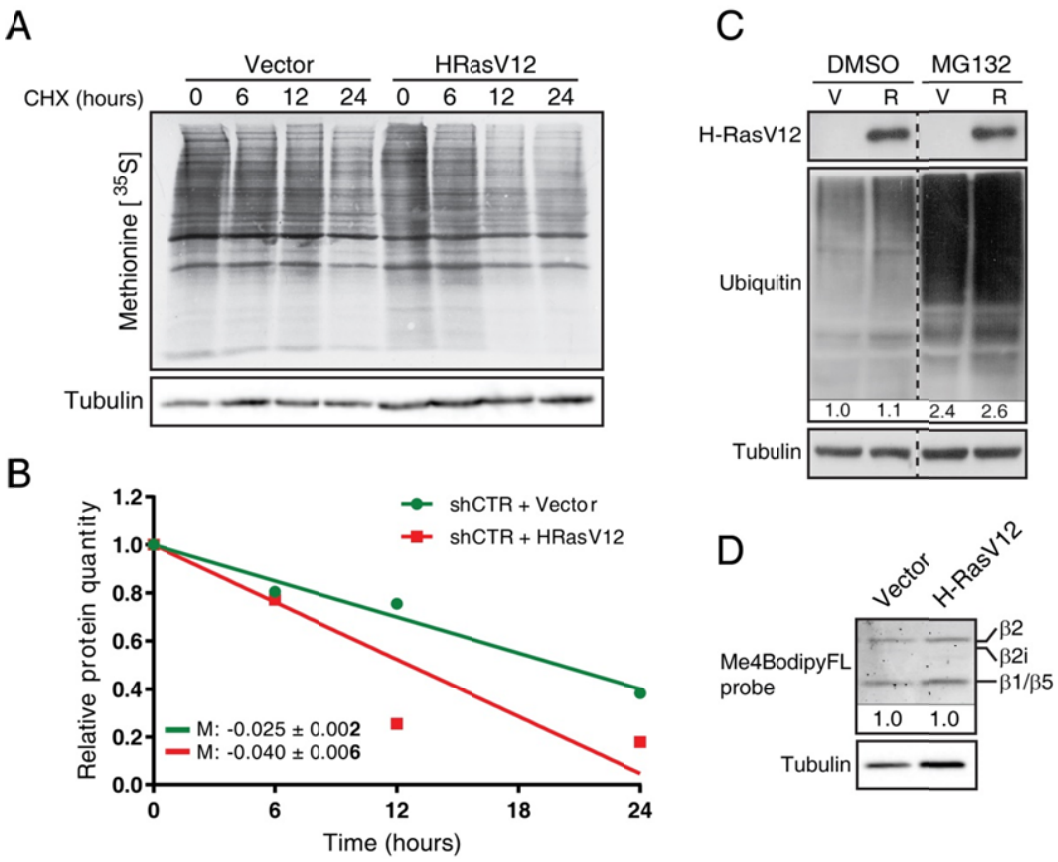

Figure 15. Oncogenic Ras increases overall protein degradation, but does not increase proteasome activity

(***A***) Normal human fibroblasts (IMR90; from ATCC) cultured in Dulbecco's modified Eagle medium (DMEM; Wisent) and expressing oncogenic Ras (R) or an empty pWZL vector (V), 10 d after retroviral infection. Total protein extracts after a pulse with 0.5 µCi [35S]-methionine for 2 h, followed by a treatment with 75 µg/mL cycloheximide (CHX; Sigma-Aldrich) for the indicated times. (***B***) Bands were quantitated using Image Lab 4.0 (M = slope). An immunoblot for α-tubulin (1:5000; clone B-5-1-2, T6074, Sigma-Aldrich) was used for normalization. (***C***) Immunoblots for HRas (1:250; clone F235, Sc-29, Santa Cruz), α-tubulin and mono-polyubiquitylated conjugates (1:1000; clone FK2, BML-PW8810, Enzo Life sciences). Protein extracts from IMR90 cells as in (*A*), but treated with DMSO or 20 µM MG132 (Sigma-Aldrich) for 18 h. (***D***) Fibroblasts as in (*A*) were treated with 500 nM of the proteasome activity probe Me4BodipyFL-Ahx3Leu3VS (Boston Biochem, I-190) for 1 h. Total protein extracts were subjected to SDS-PAGE, and fluorescence was analyzed on a ChemiDoc™ MP System (Bio-Rad). Multiple catalytic subunits are visible (β1, 2 and 5).

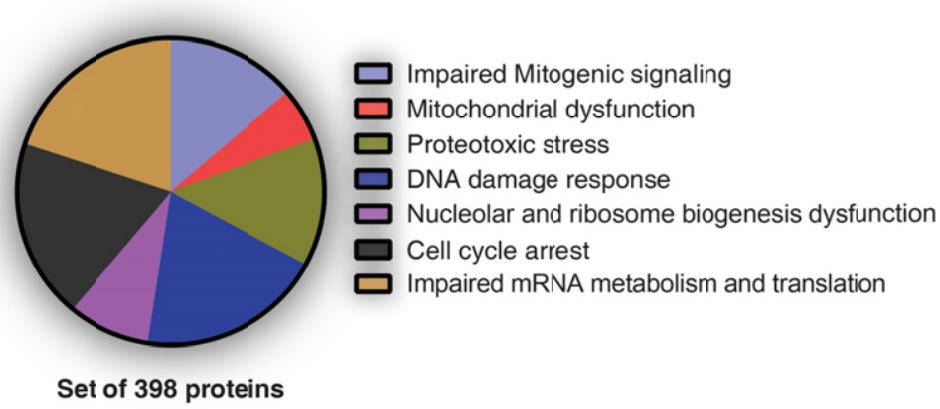

Figure 16. Senescence-associated phenotypes likely regulated by SAPD targets
Normal human fibroblasts, 10 d after infection with H-RasV12, were treated 18 h with DMSO (control) or 20 µM MG132 (Sigma-Aldrich). Then, cells were harvested and protein extracts were analysed by liquid chromatography-tandem mass spectrometry (LC-MS/MS) for phosphoproteomics. Almost 3000 phosphopeptides from 1018 proteins were enriched. A FatiGO single enrichment analysis with the Babelomics 4.3 platform was perform in order to identify *Gene Ontology* (GO), *Kyoto Encyclopedia of Genes and Genomes* (KEGG) and *Reactome* terms significantly enriched. The terms related to a senescence phenotype and their associated peptides (398 proteins) were grouped into the indicated phenotypes.

phosphoproteins during Ras-induced senescence (390). Consistent with increased macroautophagy during senescence, we observed an increase in overall protein degradation in oncogenic Ras-expressing senescent cells (Figure 15A, B), but no increase in the total amount of polyubiquitinated conjugates (Figure 15C) or upregulation of the proteasome activity as measured with the proteasome activity probe Me4BodipyFL-Ahx3Leu3VS (Figure 15D) (529). However, by in-depth characterization of an array of proteins that we found to be degraded, we discovered that the degradation process involved ubiquitination and the proteasome. This senescence-associated degradation program was conserved in multiple contexts, including mouse fibroblasts and human mammary epithelial cells expressing oncogenic Ras and in human fibroblasts with short telomeres. Thus, the second major degradation system used by eukaryotic cells, the selective degradation by the ubiquitin-proteasome pathway (UPP), is also engaged in senescent cells and allows the degradation of specific proteins. We called the process senescence-associated protein degradation or SAPD

Table I. Potential SAPD targets and the senescence-associated phenotypes they could regulate

Phenotypes	Proteins	Functions
Mitochondrial dysfunction	**ATP5B**	β-Subunit of the ATP synthase catalytic core (F1); ATP synthesis (530)
	STAT3	Modulates respiration via complex I and II (531, 532)
	HSP1A1 (HSP70)	Component of the TOM complex; import of matrix mitochondrial proteins (533)
	TOMM70A	Component of the TOM complex; import of matrix mitochondrial proteins (533)
	TOMM34	Component of the TOM complex; import of matrix mitochondrial proteins (533)
Proteotoxic stress	**HSPA1A (HSP70)**	Protein refolding under stress conditions; supports oncogenesis (534, 535)
	HSPA5,7,8 and 9	Protein refolding under stress conditions; supports oncogenesis (534, 535)
	HSPB1 (HSP27)	Protein refolding under stress conditions; suppresses cellular senescence (534-536)
	HSPD1 (HSP60)	Protein refolding under stress conditions (534, 535)
	HSP90AB1	Protein refolding under stress conditions; supports oncogenesis (534, 535)
DNA damage response	**CCDC6**	DNA damage checkpoints and DNA repair (537, 538)
	SOD1	Superoxide detoxification (113, 539)
	TOP2	Relaxes topological constraints during DNA replication; chromosomes segregation (540)
	TERF2IP	Component of the telosome; tethering telomeres to the nuclear envelope; protect telomere ends from NHEJ and HDR (541-546)
Nucleolar and ribosome biogenesis dysfunction	**NOLC1**	Polymerase I coactivator; scaffold protein for nucleolar assembly (547, 548)
	NOP56 and 58	Components of the box C/D snoRNPs (549)
	DDX51	RNA helicase; processing of the 3' end of the 28S rRNA (550)
	NOL6	Processing of the 18S rRNA (551)
	NOC2L	Processing of the 18S, 28S and 5.8S rRNAs (552)
	NCL	Polymerase I transcription; rRNA processing; ribosome assembly and transport (553)

	RPLP1	Translational elongation; overexpression bypasses replicative senescence (554)
	RSL1D1	Regulates the nucleolar localization of nucleostemin; rRNA processing (555, 556)
	NPM1	Processing of the 32S pre-rRNA to the mature 28S rRNA(557, 558)
Cell cycle arrest	**YAP1**	Regulates apoptosis; regulates organ size; liver oncogene (559, 560)
	MCM2	Initiation and progression of DNA replication (561)
	LRWD1 (ORCA)	stabilizes the origin recognition complex (ORC) to chromatin (562)
	MYC	Promotes DNA replication (40)
	JUN	Promotes G1-to-S-phase progression (563)
	KAP1 (TRIM28)	Destabilized the tumor suppressor p53 (564-566)
	TBX2	Repression of P19ARF; repression of the CDK inhibitors p21 and p27 (567-569)
Impaired mRNA metabolism and translation	**YB-1 (YBX1)**	mRNA stability, mRNA packaging, splicing and translational initiation; oncogene (570, 571)
	SRm160 (SRRM1)	Coactivator for exonic splicing enhancers and for 3'-end processing of specific pre-mRNAs (572-575)
	SRm300 (SRRM2)	Coactivator for exonic splicing enhancers and for 3'-end processing of specific pre-mRNAs (572-574)

(390). Although its exact contribution to senescence needs further study, depletion of some individual SAPD targets was sufficient to trigger senescence, thereby illustrating the relevance of this mechanism for the onset and/or maintenance of senescence. We hypothesized that under mitogenic stress, such as conferred by hyperactivation of the ERK/MAPK pathway, the downstream effectors of mitogenic signaling undergo proteasome-dependent degradation and that their depletion accounts for different characteristics of senescent cells (349). Consistent with this model, a phosphoproteomic analysis of Ras-expressing senescent cells treated with the proteasome inhibitor MG132 revealed many proteasome targets whose downregulation can contribute to senescence (Figure 16; Table I). We will thus discuss the features of senescence that are most likely to be induced or affected by the SAPD.

2.6.4 SAPD and the senescent phenotype

Mitochondrial dysfunction

Mitochondria are dysfunctional in senescent cells (110, 111), but the mechanism explaining their alterations is unknown. The ATP synthase enzyme uses the proton gradient generated by the electron transport chain in inner mitochondrial membrane to catalyze ATP production (530). The ATP synthase subunit ATP5B is degraded by the proteasome in Ras-induced senescence (Table I), and an increase of its turnover might explain the drop in ATP levels in senescent cells reported in some studies (110, 576, 577). This might contribute to senescence since inhibition of ATP synthase with oligomycin has been shown to induce a partial senescence phenotype (110).

The signal transducer and activator of transcription 3 (STAT3) is a transcription factor activated by the JAK receptors in response to cytokines. However, a pool of this protein has been shown to be imported into mitochondria and incorporated to complex I via GRIM-19 (532). Mitochondrial STAT3 modulates respiration, mainly by promoting the activity of complex I and II of the electron transport chain (531). This function of STAT3 appears to support RAS-driven transformation and ensures the proper functioning of mitochondria (476). Indeed, impaired levels or regulation of STAT3 have been shown to induce mitochondrial dysfunction and ROS production (578, 579). Interestingly, STAT3 is a confirmed SAPD target and its degradation may thus link senescence to mitochondrial dysfunction (Table I) (390).

In addition, three components of the TOM complex were found to be unstable during Ras-induced senescence: HSP70 (HSP1A1), TOMM70A and TOMM34 (Table I) (390). The TOM complex is responsible for the import of matrix mitochondrial proteins involved in the TCA cycle and β-oxidation (533). This complex is assisted by the chaperone ATPase HSP70 which is very unstable in senescent cells (390). It is thus possible that defects in mitochondrial protein import due to degradation of TOM complex components contribute to the mitochondrial dysfunction observed in senescent cells. It is known that the TOM complex is regulated by phosphorylation (580) and we found phosphorylation of serine 91 of TOMM70A and serine 186 of TOMM34 in Ras-induced senescence. It will be of considerable interest to

address whether these sites are phosphorylated by the ERKs or other kinases and mediate recognition of E3 ligases. Of note, HSP70 regulates oncogene-induced senescence (OIS) and knockdown of this protein is associated to an increase in ERK activity (467), perhaps creating a positive feedback loop that plays a role in maintaining OIS.

Proteotoxic stress

Accumulation of damaged and misfolded proteins leads to chronic proteotoxic stress, which is intimately linked to organismal aging and associated pathologies (581). The oxidative stress resulting from either mitochondrial dysfunction (110, 582) or upregulation of oxidative metabolism (108, 109) can promote protein oxidation (583, 584), thereby leading to protein misfolding (534, 535). Also, it is proposed that the high production of secreted cytokines in the SASP overcomes the cellular capacity for accurate protein synthesis and thus produces improper proteins and proteotoxic stress (109). Interestingly, we found that the main housekeeping system to maintain protein homeostasis, the heat-shock proteins (HSPs), is also downregulated in senescence (390). Indeed, the proteasomal degradation of HSP70 has been confirmed and an impressive number of HSP proteins are unstable in Ras-induced senescence (Table I). This is consistent with the demonstration that chaperone-mediated autophagy, but not macroautophagy, is downregulated in senescent cells (516). Further supporting our observations, several reports have shown either a decrease in HSPs during senescence or a direct function of these proteins in opposing the induction of senescence (467, 536, 585-589). Conversely, high levels of HSPs support tumorigenesis by circumventing a toxic accumulation of misfolded proteins in cancer cells which frequently experience proteotoxic stress, suggesting a widespread vulnerability that can be targeted therapeutically (534, 590-593). Taken together, the observations discussed above strongly suggest that a breakdown of protein homeostasis is an important feature of cellular senescence and therefore of tumor suppression.

Beyond these correlative findings, we are tempted to speculate that downregulation of HSP activity might have a primary and critical role during the establishment of a senescent program. First, the reduction of protein refolding might stimulate abnormal protein clearance by degradation, either by macroautophagy or proteasomal-dependent degradation (502, 594-596). Notably, a decrease in HSP levels correlates with an elevated activity of the CHIP ligase

during senescence, suggesting that this E3 ligase could play a pivotal role in targeting misfolded proteins to the UPP (597). Somehow, the directed degradation of HSPs could reinforce the main cellular protein degradation mechanisms in order to eliminate dysfunctional proteins instead of investing too much energy in protein repair. Senescent cells use energy to support production of signaling molecules and secretion products. Protein degradation produces amino acids used as building blocks and substrates to feed the TCA cycle, thereby supporting metabolite synthesis and energy production (502). Perhaps, protein degradation is a better investment than protein repair to support the SASP. This could be particularly true if low-cost degradation processes are favored during senescence. In this regard, it has been reported that ubiquitin and ATP-independent proteasomal degradation, accomplished by the 20S proteasomes, is the predominant mechanism to remove damaged proteins in oxidative contexts (598), as is the case in senescent cells. If this speculation proves true, this is maybe the designated route to optimize production of building blocks and energy saving.

DNA damage response

Cellular senescence induced by various stresses is characterized by an inability to properly repair DNA breaks and thus by a permanent DNA damage response (DDR) (117, 122-124). The latter is thought to contribute to both the induction and maintenance of senescence (115, 116, 118-121). The coiled-coil domain containing protein 6 (CCDC6) is a component of the DNA damage checkpoint machinery, and its corresponding gene is rearranged in 20% of papillary thyroid carcinomas (537). During DDR, CCDC6 is stabilized by ATM and contributes to proper DNA repair (538). Interestingly, we found that CCDC6 is unstable in Ras-induced senescence (Table I), and its degradation may thus contribute to the persistent DDR observed in senescent cells (115, 116, 118-120, 122-124). Moreover, this protein is a target for the tumor suppressor E3 ligase SCF-FBW7, suggesting a role of this E3 ligase in SAPD (538).

In addition to limiting proper DNA repair, the SAPD could itself promote DNA damage. The DNA breaks that underlie senescence can be triggered by different stresses. One of these is the increase in reactive oxygen species (ROS) (112, 113, 599), resulting from abnormal mitochondrial activities during senescence as discussed previously. Surprisingly, we

found that the copper zinc superoxide dismutase 1 (SOD1) is unstable in Ras-dependent senescent cells (Table I). Since this enzyme metabolizes superoxide radicals to molecular oxygen and hydrogen peroxide and therefore is a major component of the antioxidant defences within the cell (113, 539), SOD1 depletion could cooperate with mitochondrial generation of ROS to increase the total amount of these reactive ions and concomitant DNA damage. Further supporting this conjecture, SOD1 deficiency has been shown to induce persistent DNA damage in mice (600) and senescence in human fibroblasts (601). In addition to increased ROS levels, oncogenic activation drives an initial phase of DNA hyper-replication leading to premature termination of replication forks, thereby producing DNA damage that triggers senescence (115, 116). Intriguingly, another candidate target of SAPD identified by proteomics is TOP2 (Table I), which is known to relax topological constraints during DNA replication and to allow chromosome segregation (540). Accordingly, a deficiency in this topoisomerase could increase fork collapses by preventing their progression, causing aberrant replication intermediates and the activation of DDR (602). Also, a lack in TOP2 can impair completion of DNA replication by interfering with the proper resolution of replication forks at chromosomal termination regions (TERs) (603, 604), thus generating DNA damage at TERs and even more when cells undergo mitosis (604-606). Furthermore, TOP2 has been shown to play an architectural function at intergenic regions adjacent to transcribed genes during S phase, and this seems to protect against collisions between replication forks and transcription sites. This role appears critical to avoid replication-induced DNA damage since cells deficient in TOP2 experience DNA breaks at normally TOP2-bound regions (607). Taken together, the functions of TOP2 suggest that it plays a critical role to maintain genome integrity in cycling cells, and that its depletion in cells experiencing hyper-replication is likely to trigger DNA damage-promoted senescence. Finally, another proposed source of DNA damage leading to senescence is telomere dysfunction, which leads to telomere dysfunction-induced foci (TIF) (117, 119). The shelterin complex (telosome) associates with telomeres and protects chromosome ends (542). The human orthologue of the yeast telomere binding protein Rap1, TERF2IP (543), is part of the complex and has been shown to play a role in tethering telomeres to the nuclear envelope (541) and to protect telomere ends from non-homologous end joining (NHEJ) (544, 608). TERF2IP downregulation may trigger telomere dysfunction-induced DNA damage (Table I), which contributes to DDR in OIS (124, 609, 610).

Interestingly, TERF2IP interacts with PML (611), a protein forming PML nuclear bodies (PML-NBs) during senescence and that has been implicated in protein degradation (612-615). This suggests that senescence-associated PML-NBs could be a specialized compartment where nuclear proteins are degraded during SAPD.

Dysfunction in nucleolar and ribosome biogenesis

The nucleolus is the principal site of ribosome synthesis where the RNA polymerase I (PolI) transcribes the ribosomal RNA genes (rDNA) to produce the 47S ribosomal RNA (rRNA) precursor. The 47S precursor is cleaved and modified by 2'-O-methylation and pseudouridylation of specific nucleotides to form the mature 18S and 28S rRNAs. These processes are guided by small nucleolar RNAs (snoRNAs) assembled into RNA/protein complexes called small nucleolar ribonucleoproteins (snoRNPs). Mature rRNAs are assembled with ribosomal proteins (RPs), inside the nucleolus, to produce the 40S and 60S ribosomal subunits, which then migrate toward the cytoplasm (616). Approximately 50% of the energy of proliferating eukaryotic cells is dedicated to ribosome biogenesis and the process requires approximately 200 snoRNAs, more than 80 RPs and hundreds of accessory proteins (616). We found that many proteins implicated in rRNA transcription and maturation are unstable in Ras-induced senescence, such as NOLC1 (547, 548), NOP58, NOP56 (549), DDX51 (550), NOL6 (551) and NOC2L (390, 552). We also found unstable proteins which are implicated in late steps of ribosome synthesis, such as nucleolin (NCL) (553), the ribosomal protein P1 (RPLP1) (554) and the ribosomal protein L23 (RPL23) (Table I). Although we do not know yet whether the instability of the proteins discussed above causes a decrease in their levels in senescent cells, such a reduction may lead to defects in ribosome biogenesis or may simply be part of a compensatory mechanism that degrades these proteins when ribosome biogenesis is reduced.

We confirmed the proteasome-dependent degradation of the Ribosomal L1 domain-containing 1 protein (RSL1D1 or CSIG) and its decrease in Ras-induced senescence (Table I) (390). Interestingly, this protein was previously found downregulated in senescent cells (468). RSL1D1 regulates the nucleolar localization of nucleostemin (NS), which in turn regulates the nucleolar localization of DDX21 (555). Nucleostemin and DDX21 have been shown to be

important for the processing of pre-rRNA (617, 618). Using RNAi screening, a role in rRNA processing was also shown for RSL1D1 together with NOP56, DDX51, NOL6/NRAP, NOC2L/NIR and nucleolin (NCL) (556). We knocked-down the expression of this protein in normal human fibroblasts and this resulted in the induction of the senescent phenotype (390). Hence, a reduction in RSL1D1 can be causative for senescence and its role in ribosomal biogenesis suggests that defects in this process may be another effector mechanism of senescence.

It has been shown that the alternative reading frame protein (ARF, also known as p19ARF), a well-known inducer of senescence, stabilizes p53 by inhibiting the E3 ubiquitin ligase MDM2 (HDM2) (461, 619, 620). However, ARF also inhibits cell proliferation by targeting nucleophosmin (NPM1/B23) for sumoylation and degradation and in this way regulates the processing of the 32S pre-rRNA to the mature 28S rRNA (557, 558). Furthermore, ARF and NPM1 control the sub-nuclear localization of the transcription termination factor I (TTF-1), which has been shown to regulate PolI transcription initiation/termination and rRNA processing (621). Therefore, in addition to inducing the senescence phenotype through the MDM2-p53 axis, ARF affects ribosome biogenesis, and we can hypothesize that this function may also reinforce the senescence program. Supporting this, we found that NPM1 is unstable in Ras-induced senescence (Table I).

In light of the results presented above, it is tempting to suggest that defects in ribosome biogenesis can be an important mediator of senescence. This is in agreement with recent reports showing that CX-5461, an inhibitor of rRNA synthesis, induces cellular senescence in solid tumor cell lines (622, 623). However, a defect in ribosome biogenesis may appear contradictory to the increased global translation reported in senescent cells (96), which could result from the activation of TOR signaling (624). Indeed, this pathway has been shown important to convert cells from a reversible quiescent state to a permanent senescent phenotype (625-628), a phenomenon called geroconversion by Blagosklonny and colleagues (629), and this could be in part due to the translational effects of TOR (630). Although further work will be required to explain how senescent cells can increase translation despite less

ribosome biogenesis, it is likely that ribosome turnover decreases in these cells forcing them to use "old" ribosomes to make proteins.

Cell cycle arrest

Impaired proliferation, mainly by an arrest in the G1 phase of the cell cycle, is an established senescence feature, and the SAPD may be an important player in this process. During G1, the D-type cyclins bind the cyclin-dependent kinase (CDK) 4 and 6, and this stimulates the progression towards initiation of S phase (134). We found that the transcription coactivator Yes-associated protein YAP1 has a high turnover in Ras-expressing senescent cells (Table I) (390). Later, it was found reduced by another group during replicative senescence as well (631). YAP1 localizes to PML bodies and can regulate apoptosis via p73 (559). In addition, YAP1 is the orthologue of Drosophila Yorkie that regulates organ size as part of the Hippo pathway and acts as a liver oncogene in mammals (632). Interestingly, it appears that YAP1 can circumvent senescence in some contexts by inducing the transcription of CDK6 (631). Despite the fact that CDK4/6 have been shown not to be essential for proliferation, unlike CDK1 (134), their downregulation in YAP1-deficient cells might interfere with cell cycle progression in a subset of specialized cells or YAP1 might play a more broad effect on CDKs. The identification of YAP1 as a potential SAPD target also suggests a role for more E3 ligases in this process. YAP1 degradation depends on a phosphodegron recognized by the E3 ligase SCF-β-TRCP (633) and can also be triggered by the E3 ligase NOT4 (634).

The G1 to S phase transition is ensured by the formation of the pre-replication complexes (pre-RCs) on chromatin, which depends on the sequential recruitment of the origin recognition complexes (ORCs), CDC6 and MCM proteins (635). The DNA replication licencing factor MCM2 is an important component of the pre-RCs and has been found unstable in Ras-induced senescence (Table I). Accordingly, degradation of MCM2 could limit the initiation of DNA replication and the progression of the cell cycle (561). In addition, LRWD1/ORCA is a protein that stabilizes the origin recognition complex (ORC) on chromatin (562). LRWD1/ORCA degradation that could occur in Ras-triggered senescence (Table I) is likely to abrogate the binding of the ORC to chromatin, consequently arresting the

cells in G1. Interestingly, this protein is suspected to be polyubiquitinated by the E3 ligase complex CUL4A-DDB1 (636), which has already been linked to $p16^{INK4A}$ upregulation in senescence (637). Hence, we can add CUL4A-DDB1 to the list of E3 ligase candidates that promote SAPD.

Since CUL4A-DDB1 has also been shown to promote proteasome-dependent degradation of MYC via the substrate receptor TRUSS (TRPC4AP) (638), a role of this E3 ligase in cell cycle arrest and senescence is even more consistent considering our observation of MYC degradation in Ras-induced senescent cells (Table I) (390). MYC promotes DNA replication and is a master regulator of many cellular programs, including proliferation (40). Its downregulation is reported to contribute to senescence (475, 639), and its overexpression cooperates with different oncogenes to transform cells by inhibiting cellular senescence (639-641). The downregulation of MYC levels in order to shut down the cell cycle is thus possibly at the crossroads of several senescence promoting pathways. This not only suggests a role for the CUL4A-DDB1-TRUSS ligase in senescence, but also supports the investigation of the multiple other E3 ligases reported to target MYC to the proteasome, such as SCF-FBW7 (642, 643), SCF-SKP2 (644, 645), CHIP (646), the Mule complex (Mule/Huwe1/Arf-BP1) (647), and the suggested CUL2/F-Box hybrid complex ElonginBC-CUL2-SKP2 (648). Similar to MYC, JUN is another classic regulator of cell proliferation found unstable in Ras-senescent cells (563). Its downregulation may contribute to a block in G1-to-S-phase progression by decreasing the expression of cyclin D1 (649) and elevating the expression of p53 and p21 (650).

The degradation of the KRAB-associated protein 1 (KAP1, also known as TRIM28 or TIF1β) (Table I), a validated SAPD target (390), may block the cell cycle by different mechanisms. First, KAP1 is known to destabilize p53, possibly explaining why high levels of KAP1 are associated with poor prognosis in gastric cancers (564). KAP1 binds and cooperates with the E3 ligase MDM2 to drive p53 degradation (565). Furthermore, the melanoma antigen (MAGE) proteins interact with KAP1 and stimulate its own E3 ligase activity to allow p53 ubiquitination and degradation in a MDM2-independent manner (566). Accordingly,

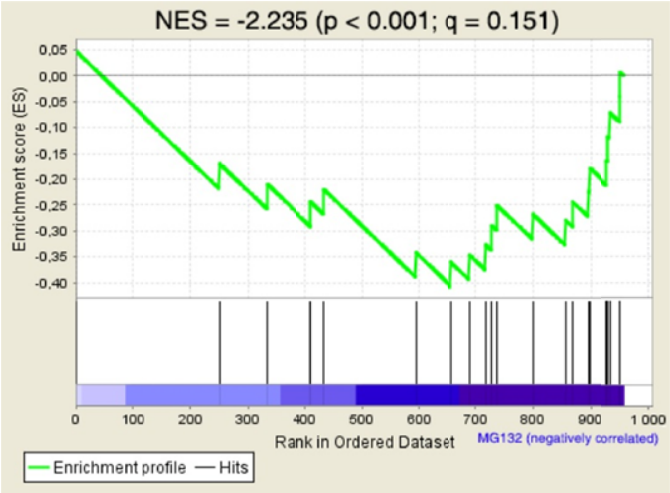

Figure 17. The proteins corresponding to the genes downregulated by RB1 in Ras-induced senescent fibroblasts are also unstable

Unbiased Gene Set Enrichment Analysis (GSEA) of the proteomic data as in figure 16. The gene set CHICAS_RB1_TARGETS_SENESCENT (Systematic name: M2125) was the second most significant result among the proteins stabilized by MG132 in Ras-induced senescent cells. The Normalized Enrichment Score (NES), the nominal *P*-value determined by an empirical phenotype-based permutation test procedure and the false discovery rate (FDR; q-value) are shown.

downregulation of KAP1 is likely to stabilize p53, allowing the expression of key cell cycle inhibitors (651). Secondly, the degradation of KAP1 may relieve its transcriptional repression functions, which have been shown to directly inhibit the transcription of p53-target genes, such as the CDK inhibitor p21 (652, 653). Thirdly, KAP1 depletion increases the number of PML-NBs (654). These senescence-associated nuclear structures inhibit E2F target gene expression. The latter are critical to initiate DNA synthesis, and inhibiting their transcription arrests cell proliferation (103).

The T-box protein 2 (TBX2) is linked to repression of p19ARF gene expression, thereby promoting the MDM2-mediated degradation of p53 and cellular senescence suppression (567). TBX2 further antagonizes senescence by repressing the CDK inhibitors p21 and p27 (CDKN1B) (568, 569). Finally, TBX2 is reported to be an E2F-target gene repressed by PML, and its repression stimulates the pro-senescence functions of PML (469). Collectively, these results suggest that degradation of TBX2 (Table I) could initiate the cell

cycle arrest characterizing senescence, and then reinforce the phenotype by activating a positive loop via the inhibition of its own transcription by PML.

According to a FatiGO single enrichment analysis of proteomics data with the bioinformatics platform Babelomics, the regulation of proliferation is one of the biological functions that is most enriched among unstable proteins in Ras-induced senescence (Figure 16) (390). Here, we have discussed the implication of just a few of the possible SAPD targets involved in cell proliferation. Surprisingly, after further analysis of the proteomics data, we found that the proteins corresponding to the genes identified by Chicas et al. (2010) as downregulated by RB1 in Ras-senescent fibroblasts are also unstable (Figure 17) (138). In this context, RB1 predominantly represses the E2F target genes implicated in DNA replication. Although this idea will need further investigation, our results suggest that bulk degradation of the same E2F-induced proteins could cooperate with transcriptional repression to safeguard cell cycle arrest. Does the SAPD cooperate with RB1 and PML-NBs to ensure a rapid and potent shutdown of E2F target genes?

Impaired mRNA metabolism and translation

The Y-Box binding protein 1 (YB-1 or YBX1) is also unstable in Ras-senescent cells (Table I) and its downregulation has been linked to the senescence phenotype (655), whereas its overexpression strongly correlates with aggressive tumors (570). However, YB-1 is a multifunctional protein and we are still far from understanding how its functions could oppose senescence. One hypothesis is that YB-1 could stimulate the transcription of E2F-target genes by binding to multiple E2F promoters (656). Conversely, it could act as a transcriptional repressor of p53 (657). These scenarios suggest that depletion of YB-1 could have a relatively direct effect on cell cycle as discussed in the previous section. Nonetheless, direct evidence also highlights critical functions in mRNA metabolism, including mRNA stability, mRNA packaging, splicing and translational initiation (570, 571). Does the regulation of p53 and E2F-target genes result from these activities? Although the answer is not clear, this could be the case at least for p53. The DNA-damaging stresses prevent YB-1-mediated splicing of MDM2, leading to an mRNA molecule lacking several exons, and resulting in a non-functional protein (658). This regulation of MDM2 may contribute to the stabilisation of p53

in senescent cells experiencing DDR. Because YB-1 is a putative general regulator of mRNA maturation and translation for mRNAs with YB-1 binding sites (571), we hypothesize that suppression of these functions could promote senescence by affecting the expression of several proteins. In senescence, the YB-1 functions could be abrogated by its degradation, possibly catalyzed by the E3 ligase activity of RBBP6 (659).

Two other splicing regulators have an increased turnover in Ras-induced senescence (Table I). SRm160 (SRRM1) and SRm300 (SRRM2) are splicing coactivators required for the functions of exonic splicing enhancers and for 3'-end processing of specific pre-mRNAs (572-575). These proteins are phosphorylated at multiple distinct S/T-P phosphorylation sites in senescent cells, suggesting that they may act as a sensor of ERK signaling strength (390). Perhaps an accumulation of phosphorylated sites over a given threshold controls the interaction with E3 ligases, promoting the ubiquitination and degradation of hyperphosphorylated SRm160/300 in response to oncogenic stress. Such degradation could consequently promote senescence by impeding normal mRNA maturation of a specific set of genes, including critical regulators of normal cell functions.

2.6.5 Key remaining questions

Targeting protein to SAPD: Where?

Proteasomes are widespread in cells, but can interact with some specific cellular structures. In the cytoplasm, proteasomes can bind the cytoskeleton, the outer surface of the endoplasmic reticulum and the centrosomes (660-662). They are also found throughout the nucleoplasm, but interestingly, they have been shown to be concentrated in PML-NBs (660, 663-666), nucleoplasmic speckles (665, 667) and other focal subdomains (665, 668). In some particular contexts, proteasomes can also accumulate in nucleoli (668, 669). Thus, the degradation of SAPD targets could use specific "proteolytic centers". For example, Wójcik and DeMartino (2003) proposed that cytosolic proteins targeted for degradation are delivered to a master proteolytic complex located at the centrosome via microtubule-mediated transport (660). Similarly, PML-NBs and nuclear speckles could act as the proteolytic complexes for nucleoplasmic SAPD targets. Speckles are enriched in splicing factors and may thus be the

proteolytic center for these proteins we found unstable during Ras-induced senescence, including YBX1, SRm160 and 300 (Table I) (670, 671). Also, PML-NBs might be a specialised structure for short proteins destined to be degraded versus these that should not, thereby representing the so-called clastosome previously described as nuclear bodies enriched in proteasome-dependent degradation effectors (672). Consistent with this idea, several potential and validated SAPD targets colocalize with PML-NBs, including TERF2IP (611), YAP1 (559), MYC (613, 639, 673) and STAT3 (674, 675). Furthermore, PML-NBs have been shown to be involved in the degradation of factors for which downregulation is known to mediate a senescence program, such as CREBBP (CBP) (676, 677) and MYC (475, 613, 639). Conversely, PML-NBs might also play an active role in protecting other proteins from degradation, like HIPK2 (678), p73 (679), TOPBP1 (680), and p53 (681). Thus, PML may be critical for the specificity of SAPD.

Targeting protein to SAPD: How?

The pattern of proteins degraded by the proteasome seems dramatically changed during senescence, while there is no apparent modification in total proteasome activity (Figure 15D). Also, even if there is a large amount of unstable proteins, other key senescence mediators are stabilized (e.g. p53). These observations suggest two principal mechanisms explaining the proteasome-dependent degradation of a large subset of specific proteins in senescence: the upregulation of specific E3 ligases activity and the targeting of specific proteins for SAPD. Previous work and our recent observations strongly propose that post-translational modifications of proteins play a central role in SAPD. Because PML-NBs could be involved in SAPD target degradation, sumoylation is a candidate modification of particular interest. Indeed, PML-NBs are among the principal sites of sumoylation in cells since they interact with many SUMO ligases and sumoylated proteins (666). Furthermore, sumoylation is known to lead to the subsequent ubiquitination and degradation of particular proteins (682, 683). There is now accumulating evidence that sumoylation at PML-NBs is coupled with the UPP, the SUMO-dependent degradation of N4BP1 (615) and NRF2 (684) being examples. Of note, the degradation of the latter in PML-NBs could limit ROS detoxification, thereby contributing to the induction of senescence (458). Senescent cells experience oxidative stress, suggesting

that protein carbonylation may serve as another modification to distinguish SAPD targets (685). This modification marks oxidized proteins for degradation, mostly via the 20S proteasome and in an ATP and ubiquitin-independent manner (686). Despite the fact that carbonyl-mediated degradation exhibits a certain level of specificity, depending on the intrinsic susceptibility of a protein to oxidative carbonylation, this mechanism is rather unspecific and hardly explains the global proteome of senescent cells (685).

Our group identified a remarkable number of phosphopeptides from proteins degraded by the proteasome in Ras-senescent cells, suggesting that phosphorylation is an important protein modification triggering SAPD (390). Further strengthening this hypothesis, protein phosphorylation and ubiquitination-dependent degradation are tightly linked (281). Phosphorylation can drive ubiquitination either by regulating the subcellular localization of target proteins, thereby eliminating a spatial separation between the substrate and its E3 ligase, or by creating a docking site for an E3 ligase (281). In replicative and Ras-induced senescence, hyperactivation of the ERK/MAPK pathway is essential to mediate SAPD and to maintain the senescent phenotype (390). This suggests a model where the hyperphosphorylated ERK targets are degraded, creating a negative feedback to mitogenic signaling that promotes senescence (349). In this model, the sustained phosphorylation of ERK targets is suspected to increase the chance of an interaction with an E3 ligase or to activate a phosphodegron. However, we cannot exclude that other kinases play a role in ERK-mediated SAPD. Such kinases could be either hyperactivated downstream of the ERK/MAPK pathway or contribute to the full activation of phosphodegrons. The SAPD candidates MYC and JUN are two examples of proteins regulated by a phosphodegron implicating multiple kinases. Both are first phosphorylated by the ERK kinases, which primes them for further phosphorylation by the GSK3 kinase that is the final act in order to recruit the E3 ligase SCF-FBW7 (281, 563, 687). Supporting an important role for GSK3 in mediating activation of phosphodegrons during SAPD, its inhibition leads to a reduction of MYC ubiquitination (390). Furthermore, another SAPD candidate in Ras-induced senescence, namely β-catenin (CTNNB1), is a well-known protein undergoing degradation following GSK3-mediated phosphodegron activation (281). Considering that GSK3 is inactivated by the PI3K/AKT pathway (687), buffering AKT activity is maybe an important strategy employed to promote

SAPD in Ras-senescent cells. This could explain, at less in part, why activation of AKT contributes to circumvent RAF and RAS-induced senescence (688, 689). Nevertheless, we can speculate that hyperactivation of different kinases, including AKT, could also engage the degradation of their targets and thus promote a different pattern of SAPD, but with senescence as a common phenotypic output. SAPD could be a universal response to "phosphorylation stress" to avoid cellular transformation in the context of abnormal mitogenic signaling.

Kinases vs phosphatases and E3 ligases vs deubiquitinases: different weapons, same fight?

When we address proteasome-dependent protein degradation, we naturally think of E3 ubiquitin ligases. However, the global picture is much more complicated and involves several players. Proteins can be dynamically ubiquitinated by E3 ligases and deubiquitinated by deubiquitinases. As we discussed in the previous section, ubiquitination can depend on phosphorylation (281). In this situation, protein degradation is also regulated by kinases and dephosphorylation by phosphatases. We can thus simplify the situation by presenting kinases and E3 ubiquitin ligases as collaborating to favor protein degradation, whereas phosphatases and deubiquitinases are their respective opponents. A similar logic can be applied for SUMO-dependent ubiquitination; while SUMO E3 ligases cooperate with E3 ubiquitin ligases, deSUMOylases antagonize the process (683). In normal conditions, a subtle equilibrium between all the players impacting on protein stability ensures determined levels for a specific protein (Figure 18A). During SAPD, the equilibrium is displaced to favor an increased turnover leading to reduced levels of the same protein. What exactly leads to the displacement of the equilibrium? For a given protein, the process can be mediated mostly by: 1) an increased activity of its kinases/SUMO E3 ligases (Figure 18B); 2) an increased activity of its E3 ubiquitin ligases (Figure 18C); 3) both 1 and 2 (Figure 18D); 4) a decreased activity of its phosphatases/deSUMOylases (Figure 18E); 5) a decreased activity of its deubiquitinases (Figure 18F); 6) both 4 and 5 (Figure 18G); 7) different combinations of 2 to 6. One challenge for the coming years will be to determine how these regulators interact to affect the steady state and what the resulting dynamic is. Is the equilibrium displaced linearly or does the collaboration between different SAPD mediators rather promote switch-like mechanisms?

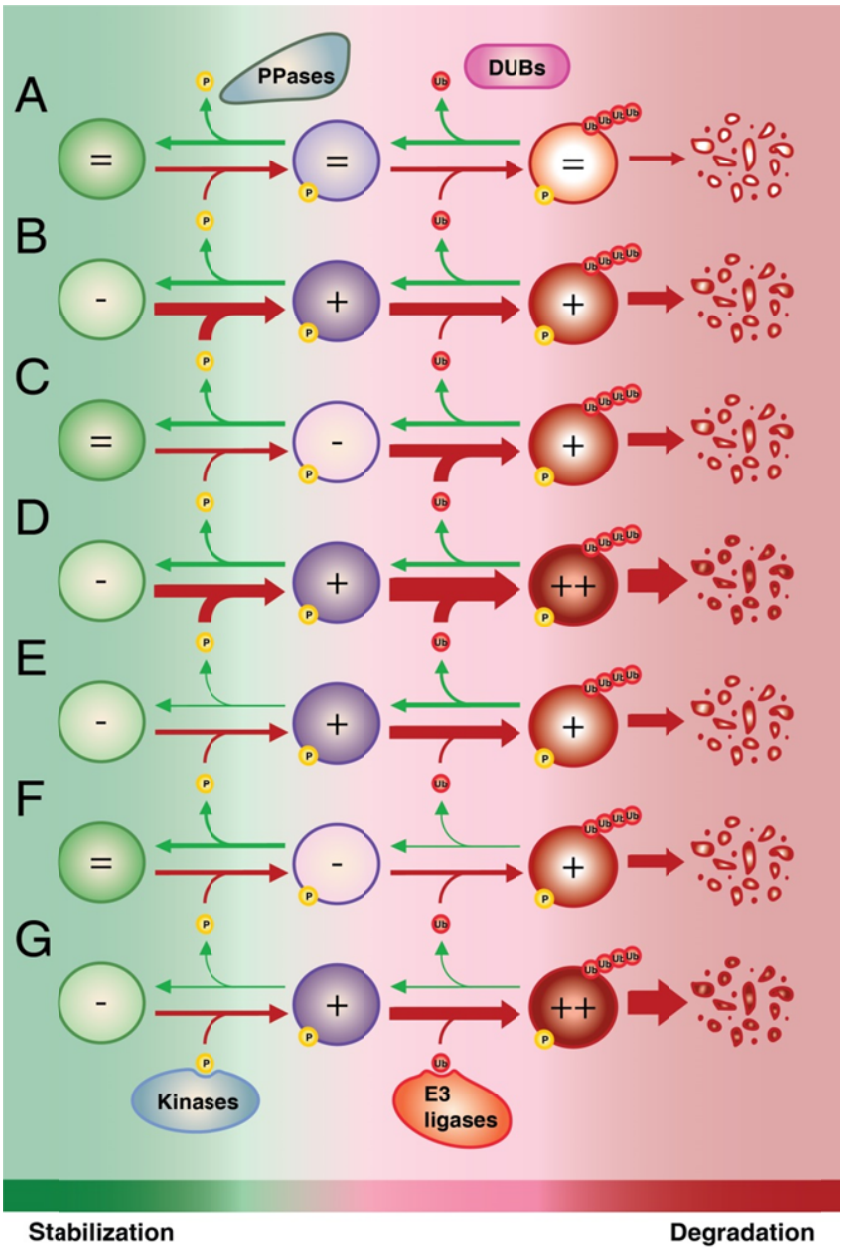

Figure 18. Modulation of protein stability for proteins regulated by phosphorylation-driven ubiquitination and proteasome-dependent degradation

(***A***) Under normal conditions, competition between the activity of kinases vs phosphatases (PPases) and E3 ubiquitin ligases vs deubiquitinases (DUBs) ensures the maintenance of appropriate levels of a specific protein. The turnover of this protein can be increased by: (***B***) increasing the activity of its kinases; (***C***) increasing the activity of its E3 ubiquitin ligases; (***D***) both (B) and (C); (***E***) decreasing the activity of its PPases; (***F***) decreasing the activity of its DUBs; (***G***) both (E) and (F). Of note, different combinations of (B) to (G) can be involved. Also, a similar scenario can be applied for SUMO-dependent ubiquitination; kinases and PPases can be substituted by SUMO E3 ligases and deSUMOylase. Ub, ubiquitin; P, phosphorylation.

Such switch-like responses could point to competition between regulators with opposite effects on the substrate, which has been shown in the control of the orthologous yeast ERK/MAPK pathway (690). Finally, another challenge is to evaluate whether there are master regulators of protein degradation in SAPD, allowing opportunities to target the phenotype, or whether each protein or subset of proteins is regulated via distinct machinery.

Is there a master senescence-associated E3 ligase?

The specificity of the UPP is conferred by E3 ubiquitin ligases, a large and complex group of proteins, with an estimated 600 to 1000 members in the human proteome (691). Based on the structure of their catalytic domain, the E3 ubiquitin ligases are generally classified into four main categories: the RING-finger type (692, 693), the HECT type (694), the U-box type (695, 696) and the less characterized PHD domain-containing type (692, 697). The former is by far the most abundant and is further subdivided as single unit or multiple subunit RING-finger E3 ligases. The latter form complexes grouped into two principal families, the anaphase-promoting complex (APC) and the cullin-RING ligase (CRL) superfamily (692). There are seven cullins expressed in human cells (CUL1, 2, 3, 4A, 4B, 5 and 7) and they interact with specific receptor proteins which provide target specificity, including proteins harboring F-box, SOCS-box, VHL-box and BTB domains (698, 699). These complexes are referred to by various names [reviewed in ref. (699)], but the most common appellation is probably SCF for the classic complex containing CUL1 and SCF2-5 and 7 for complexes containing the corresponding cullins.

In the simplest scenario, one or few E3 ubiquitin ligases could be responsible for SAPD. Such a possibility would likely involve the regulation of the activity of specific E3 ligases. However, current evidence reviewed above points the specificity being conferred by upstream steps targeting designated proteins for degradation. Considering these data as well as the complexity of the E3 ubiquitin ligase superfamily, we favour the view that SAPD is likely regulated by several E3 ligases, each catalyzing the ubiquitination of its specific targets. However, this more complex picture does not exclude the possibility that some E3 ligases could play a more critical role in the senescent phenotype. Indeed, as discussed previously, SCF-FBW7 is a well-known tumor suppressor and has been recently shown to contribute to

senescence (687, 691, 700), and correspondingly many FBW7 targets are degraded in SAPD. The CUL4A-DDB1 (SCF4) complex and its interacting receptor protein DDB2 are also strong candidates since both have been shown to drive senescence (637, 701). Furthermore, the fact that phosphorylation could be a mark to distinguish SAPD targets highlights the interest in investigating the roles of the SCF complexes in senescence. Indeed, this subfamily of E3 ubiquitin ligases is primarily responsible for serine/threonine phosphorylation-dependent ubiquitination. Two classes of F-box proteins are specialized to recognize phosphodegrons, namely the WD40 F-box proteins (e.g. FBW7 and β-TRCP1/2) and leucine-rich repeat (LRR) F-box proteins (e.g. SKP2) (281). The proposed involvement of PML-NBs and SUMO-dependent degradation in SAPD also increases the interest in studying the contribution of the SUMO-targeted ubiquitin ligase (STUbL) family in senescence (702), such as RNF4 that contains a SUMO-interacting motif (SIM) (703).

Although many E3 ubiquitin ligases have tumor suppressive functions, including APC, SCF-FBW7, BRCA1, VHL and FANC, several others are clearly oncogenic and can oppose senescence (692). For example, MDM2 and MDMX are bona fide oncogenes and limit senescence by catalyzing ubiquitination and degradation of p53 (620, 692). Senescence is also limited by the oncogene SCF-SKP2 that targets p27 and p21 in a p53-independent manner (704). The potential role in cancer of E3 ligases that have a complex array of targets including both tumor suppressors and oncogenes is more difficult to ascertain. This is the case for SCF-β-TRCP, functioning primarily as an oncogene by targeting apoptotic proteins, but showing tumor suppressive activities in some contexts (692). Since SCF-β-TRCP targets preferentially phosphorylated proteins (281), whether it acts as an oncogene or as a tumor suppressor may depend on the pool of phosphorylated substrates in a given context. In light of these dissimilar functions in tumorigenesis, it seems obvious that different members of the large family of E3 ubiquitin ligases use the UPP to compete in opposite directions. We can thus compare the effect of the E3 ligases on cell fate to a delicate balance, where the equilibrium between the activities of oncogenic versus tumor suppressive E3 ligases is critical to maintain cells in a normal state (Figure 19). Under oncogenic stress, depending on whether the balance is tipped in one direction or the other, the UPP could favor transformation into cancer cells or tumor suppression respectively.

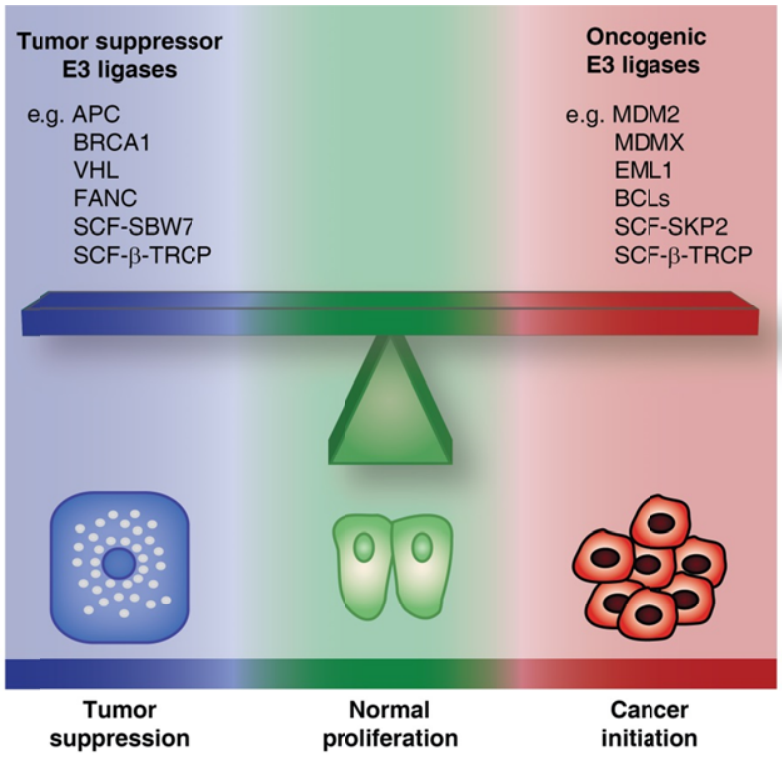

Figure 19. The balance of oncogenic versus tumor suppressor E3 ubiquitin ligases
The activities of oncogenic versus tumor suppressor E3 ligases are in equilibrium to maintain cells in a normal state. Tipping the balance in one direction or the other can be critical for determining whether a cell under oncogenic stress will undergo tumor suppression or neoplastic transformation.

SAPD: a coordinated proteome reprogramming?

The answer to this question first depends on how senescence should be seen. Is it a totally abnormal and non-functional cellular state initiated in response to stress, which is basically avoided in normal organisms? Is it rather one of the fundamental tools that evolution has provided as a defense against the insults inherent to organismal life? The prevailing view at present favors that latter paradigm. Indeed, not only is senescence a gatekeeper response that is acutely triggered by stress stimuli, but it now appears that the process can have important functions in non-stressed conditions, namely in embryonic patterning (705, 706). Hence, considering senescence as a "normal" adaptive state, the question is now: what is the fundamental role of SAPD in senescence and why it was selected during evolution?

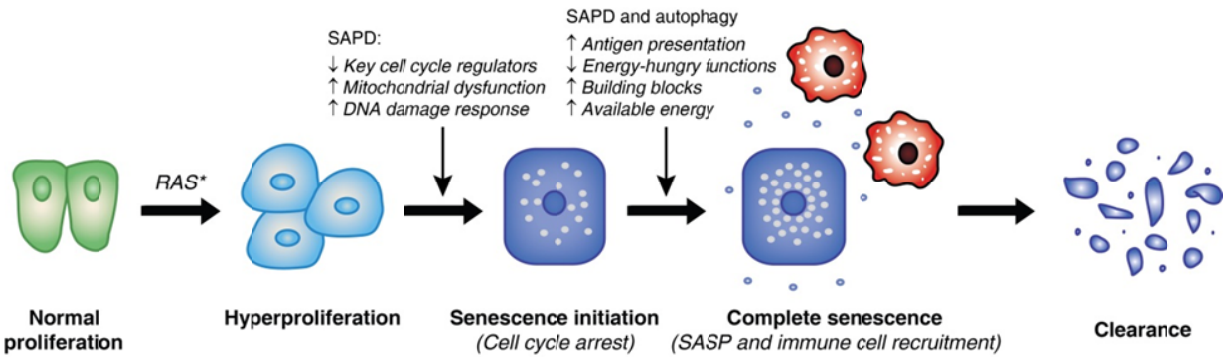

Figure 20. Theoretical purpose of oncogene-induced senescence and contribution of protein degradation

Increasing evidence suggests that the destiny of senescent cells in many organs is clearance by the immune system. This implies a central role for the cytokine production characteristic of the SASP in the recruitment of immune cells (in red). Specific protein degradation (SAPD) may contribute directly and/or indirectly to the initial cell cycle arrest, but may also cooperate with macroautophagy to produce antigenic peptides and to support the SASP. Proteolysis may redistribute cellular energy to the SASP and may supply nutrient building blocks for biosynthetic reactions.

Cellular senescence was first thought to underlie organismal aging, and this hypothesis steadily gained experimental support (161). The deleterious effects of senescence are caused by the accumulation of senescent cells in aging organisms. However, it is possible that this accumulation is rather the result of an abnormal senescence program and that evolution has selected a mechanism to avoid the accumulation of senescent cells. The recent literature suggests that this mechanism may be the clearance of senescent cells by the immune system (89, 151, 152, 154). The SASP seems critical to activate the immune response by signaling the presence of senescent cells and attracting destructive immune cells (140). If the ultimate destiny of senescent cells is their elimination, the production of signaling molecules during the SASP appears central to ensure a complete and effective senescence phenotype (Figure 20). An abnormal SASP pattern or a defect in the capacity of the immune system to eliminate senescent cells could thus be the basis of an "abnormal" accumulation of senescent cells and age-related pathologies (161).

The SASP is a costly anabolic process and senescent cells have to deal with the limited availability of building blocks and energy to support the process. Thus, we can suppose that

cells reorganize the distribution of these resources in order to favor the synthesis of cytokines. Does reorganizing the proteome mean reallocating resources? Such a link between autophagy and SASP has already been proposed (109, 502, 527). Is the SAPD part of this reorganization? The degradation of specific proteins by the UPP could shut down highly energy-consuming functions, such as protein repair, DNA repair, synthesis of new ribosomes and DNA synthesis. Since senescent cells are destined for clearance, these functions are dispensable for senescent cells, and their inhibition allows more resources to support the SASP (Figure 20). Protein degradation by UPP consumes ATP, but the resulting amino acids can be used to obtain energy or supply building blocks for anabolic reactions. Overall, the SAPD could be a better investment for senescent cells whose final destiny is to be eliminated.

Breaking down cancer?

Although SAPD could be a powerful mechanism to mediate senescence and tumor suppression, it raises many new questions for further research. The exact contribution of protein degradation to senescence, including SAPD and autophagy, is still mostly speculative. Perhaps it simply brings a balance to cells unable to divide but making more proteins. However, catabolic processes may take a central place to induce cell cycle arrest of premalignant cells and to trigger their elimination by the immune system. Not only could proteolysis redistribute the resources to support the production of cytokines by oncogene-expressing cells, but it could also generate peptides for antigen presentation to ensure their specific recognition and destruction by immune cells (Figure 20) (707, 708). This may involve the production of an abnormal quantity of a self-antigen or the generation of abnormal antigens, such as pieces of activated oncogenes or damaged proteins.

A better understanding of the senescence degradome appears essential to have a more global picture of how anabolic and catabolic changes are linked together to trigger a complete senescence phenotype. This could provide insights into how cancer cells circumvent senescence and the role of metabolic changes in this process, thereby suggesting new therapeutic strategies. Targeting components of UPP and autophagy with small-molecule inhibitors is an emerging area for the treatment of cancer (709). The clinical potential of this strategy has been highlighted by the success of the proteasome inhibitor bortezomib for the

treatment of myeloma and lymphoma. Currently, most of the efforts are invested in the development of proteasome inhibitors, which have a global, and thus non-specific, effect on the UPP-mediated degradome. Such an approach can preferentially affect cancer cells where the pattern of E3 ubiquitin ligase activities and UPP-targeted substrates clearly support tumorigenesis and cancer progression (Figure 19). However, the UPP has a fundamental role in normal cellular functions and in tumor suppression as well. This suggests caution in the clinical use of proteasome inhibitors and may explain the toxicity associated with these compounds (709). A better comprehension of SAPD and its dysfunction in cancer cells will certainly uncover new pharmacologic vulnerabilities to allow the rational development of new targeted therapies. Can we restore the advantages given by the SAPD, such as the elimination of precancerous cells by the immune system, and at the same time inhibit UPP-driven oncogenesis? In other words, can we tip the balance of protein breakdown to break down cancer?

2.6.6 Acknowledgments

X. Deschênes-Simard is a fellow of the Vanier Canada Graduate Scholarships Program and Michael Smith Foreign Study Supplements Program. F. Lessard is a fellow of FRQS (Fonds de recherche du Québec - Santé). N. Bardeesy is supported by grants from the National Institutes of Health (R01 CA133557-05 and P01 CA117969-07) and the Linda J. Verville Cancer Research Foundation. G. Ferbeyre is a FRSQ national research fellow.

2.7 Mise en contexte de l'article 3

Le présent article a permis d'approfondir et de mettre en évidence un autre aspect important découlant des travaux présentés à l'article 1. Plus précisément, nous avons effectué une revue de la littérature afin de confronter le rôle suppresseur de tumeurs versus oncogénique de la voie ERK/MAPK. Pour ce faire, nous avons utilisé une série d'observations venant des animaux modifiés génétiquement permettant l'étude des mutations oncogéniques en amont de la voie. À partir de ces observations, nous avons établi 3 modèles généraux pouvant expliquer la suppression tumorale induite par la voie ERK/MAPK et le contournement de cette barrière afin d'initier la transformation maligne. Une constante émerge de ces modèles : la suppression tumorale dépend d'une hyperactivation de la voie. Cette conclusion a d'importantes répercussions sur l'usage des inhibiteurs de la voie ERK/MAPK en clinique. Nous avons donc effectué un survol des résultats obtenus avec les inhibiteurs de RAF et de MEK. Sans exclure un bénéfice thérapeutique de ces inhibiteurs, nous avons apporté un regard critique sur leur utilisation. Nous approfondissons aussi la discussion concernant l'acquisition de résistance à ces inhibiteurs. La réactivation de l'activité des kinases ERK a été proposée pour expliquer une telle résistance. Nous démontrons qu'elle pourrait aussi s'expliquer par une série d'effets indépendants de ces kinases. Cette conclusion vient relativiser l'idée d'un rôle central des kinases ERK dans la progression tumorale et met en évidence le besoin de cibler d'autres voies de signalisation protumorigéniques. Dans son ensemble, cet article s'inscrit dans une volonté d'offrir des pistes de solution pour adapter l'usage des inhibiteurs de la voie ERK/MAPK au contexte. Le but étant d'éviter la perte des avantages conférés par le pouvoir suppresseur de tumeurs de la voie et l'acquisition de résistance via l'activation de mécanismes protumoraux indépendants des kinases ERK.

2.8 Contribution à l'article 3

Cet article a été écrit en étroite collaboration avec Gerardo Ferbeyre et nous avons une contribution sensiblement équivalente. J'ai conçu la figure. Les autres auteurs ont contribué à la révision du manuscrit.

2.9 Article 3

ERKs in cancer: friends or foes?

Xavier Deschênes-Simard[1, 3], Filippos Kottakis[3], Sylvain Meloche[2] and Gerardo Ferbeyre[1]

Cancer Research, 2014 January 15, 74 (2): 412-19

1) Département de Biochimie et Médecine Moléculaire, Université de Montréal, Montréal, Québec H3C 3J7, Canada
2) Department of Pharmacology and Program in Molecular Biology, Institut de Recherche en Immunologie et Cancérologie, Université de Montréal, Montréal, Québec H3C 3J7, Canada
3) Massachusetts General Hospital Cancer Center, Harvard Medical School, Boston, MA 02114, USA

Running title: ERK and Cancer

Keywords: ERK; cancer; tumor suppression; MAPK inhibitors, mouse models

Correspondence to: Gerardo Ferbeyre

2.9.1 Summary

The extracellular signal-regulated kinase ERK1 and ERK2 (ERK1/2) cascade regulates a variety of cellular processes by phosphorylating multiple target proteins. The outcome of its activation ranges from stimulation of cell survival and proliferation to triggering tumor suppressor responses such as cell differentiation, cell senescence, and apoptosis. This pathway is intimately linked to cancer as several of its upstream activators are frequently mutated in human disease and are shown to accelerate tumorigenesis when engineered in the mouse genome. However, measurement of activated ERKs in human cancers or mouse models does not always support a role in tumorigenesis, and data consistent with a role in tumor suppression have been reported as well. The intensity of ERK signaling, negative feedback loops that regulate the pathway, and cross-talks with other signaling pathways, seem to be of primary importance in determining the final cellular outcome. Cell senescence, a putative tumor-suppression mechanism, depends on high-intensity ERK signals that trigger phosphorylation-dependent protein degradation of multiple proteins required for cell-cycle progression. This response may be circumvented during carcinogenesis by a variety of mechanisms, some of them yet to be discovered, which in essence turn ERK functions from tumor suppression to tumor promotion. The use of pharmacologic inhibitors targeting this pathway must be carefully evaluated so they are applied to cases in which ERKs are mainly oncogenic.

2.9.2 Introduction

The extracellular signal-regulated kinases (ERK1/2; MAPK3/1) are ubiquitous regulators of multiple cellular processes such as proliferation, differentiation, survival, and transformation. These kinases are the last components of a signaling module composed of the small GTPase RAS and the protein kinases RAF and MEK1/2 [MAP2K1/2; (28)]. With an overall mutation incidence of up to 30% in human cancer, mutant RAS is among the most common human oncogenes (44). RAF mutations are also frequent, particularly in melanoma (301), but MAP-ERK kinase (MEK) mutations are rare and ERK mutations have never been reported as drivers in human cancers. Nevertheless, current thinking proposes that both RAS and RAF oncogenes promote human cancers by activating the ERK kinases (44, 485). Consistent with this idea is the fact that ERK kinases positively regulate the cell cycle by increasing the availability of building blocks for cell growth (319), by stimulating the cyclin-dependent kinase (CDK)-cyclin complexes required for cell-cycle progression (338), and by preventing cell death (329). In addition, deregulated nuclear accumulation of activated ERKs (pERK) can lead to genomic instability and subsequent tumor progression (710). On the other hand, recent results indicate that the ERK kinases may trigger tumor suppressor pathways as well (390, 472) and that this activity depends on the strength of their activation (390). Hence, the role of ERK kinases in human cancers appears to be context dependent and more complex than originally suspected, reflecting its involvement in both oncogenesis and tumor suppression.

Clinical studies indicate a variable association between ERK activation and human cancers, consistent with either an oncogenic or a tumor-suppressing role. Consequently, ERK activation in human cancers has been linked to either good or bad prognosis. Otherwise, ERKs might be required in cancer cells for proliferation and survival, but their activation could be transient because of the activation of negative feedback mechanisms still not understood (273). Therefore, it is unclear whether sustained ERK hyperphosphorylation is an obligate prerequisite of cancer initiation or progression despite activated oncogenes upstream of the pathway. There are also confounding issues in clinical studies that use immunohistochemistry (IHC) to determine the status of ERK signaling. Detection of phosphoepitopes depends on the

quality of the antibody chosen and the time taken to fix tissues after obtaining them from patients (711). Furthermore, the most critical issue is the definition of high and low staining. Most studies use internal scoring systems and report relative levels. Only a few reports include downstream components of the pathway such as ERK targets or gene expression signatures that could give a better assessment of signaling strength. We are thus left with only a qualitative assessment of ERK signaling and therefore we can hardly make conclusions about outputs of this pathway that depend on signaling strength.

In mice, ERK kinases are essential for survival, complicating the efforts of testing their role in tumorigenesis (350). Interestingly, in KRAS-driven lung cancer, decreasing the total ERK amount by genetic ablation of ERK1 or ERK2 had no significant effect on tumor development. However, eliminating both ERK isoforms abrogated tumor development, suggesting that a minimal amount of ERKs is still required (350). The authors also evaluated the effect of total ERK deletion in the whole animal and observed rapid death. Consequently, can the need for the ERK kinases in tumors be explained by a general requirement for cell viability, or rather by a specific role in neoplastic transformation?

2.9.3 Lessons from ERK pathway inhibitors

Given the difficulties in evaluating the role of ERK kinases in human and mouse cancers using IHC data, studies using inhibitors of the pathway may shed additional light into their function. Many studies have been conducted with BRAF and MEK inhibitors. It is usually assumed that RAF, MEK, and ERK act in a linear signaling pathway, so the results of using these inhibitors are interpreted as an inhibition of the ERK kinases. However, there is evidence that RAF (712) and MEK kinases (713) exert ERK-independent functions and therefore results obtained with the use of these inhibitors may not exclusively reflect the involvement of ERK.

MEK inhibitors (AZD6244 or selumetinib and PD0325901) reduced tumor formation in mouse xenograft models (714) and achieved stable disease in phase II trials in patients with advanced cancer (715, 716). However, they were not superior to conventional cytotoxic chemotherapy in patients with advanced melanoma (717) and failed to improve liver cancer

patients' outcomes despite reducing pERK levels (718). Intriguingly, using anchorage-independent growth as an *in vitro* surrogate of transformation, ERK activation was shown to be a poor predictor of sensitivity to MEK inhibitors (719, 720). Several studies reported that inhibition of ERKs by MEK inhibitors may be compensated by phosphoinositide 3-kinase (PI3K)/AKT pathway activation (721) and numerous mechanisms have been proposed to explain this effect. These include the relief of an ERK-dependent negative feedback loop on receptor tyrosine kinase (RTK) activation (722, 723) and a dynamic reprogramming of the kinome due to MYC degradation and subsequent induction of RTKs (724). Thus, combining MEK inhibitors with AKT pathway inhibitors could improve anticancer activity, a concept that has been validated in murine models (725).

In patients with melanoma, the BRAF inhibitor vemurafenib (PLX4032) induces partial or complete tumor regression, and this correlates with inhibition of cytoplasmic ERK activation (726). However, patients develop resistance to vemurafenib within 6 months of treatment, and analysis of their tumors revealed changes that reactivate the ERK pathway (727) or increase signaling through RTKs in an ERK-independent manner (728). In cells expressing BRAFV600E, negative feedback mechanisms activated by pERKs suppress RTK-dependent RAS activation. The SPRY proteins are in part responsible for this process (729). BRAF inhibitors relieve this feedback mechanism and thereby improve the cell response to RTK ligands and signaling through RAS and CRAF (RAF1), possibly explaining the ERK reactivation (728, 729). On the basis of the latter hypothesis, clinical trials that combine BRAF and MEK inhibitors in patients with melanoma have been designed to overcome the development of resistance to BRAF inhibitors (730). This combination proved to be moderately better than individual treatments (730, 731), supporting the proposition that the rebound in pERKs is most likely related to BRAF inhibitor resistance. However, it was not demonstrated that MEK inhibitors acted specifically on the ERK kinases and some results indicate that MEK may have other targets (713, 732). Another important concern is that the combination of a BRAF inhibitor with a MEK inhibitor improves survival but does not cure patients. Moreover, in patients with melanoma who were not selected according to BRAF status, MEK inhibitors did not improve progression-free survival and induced significant toxicity (717). In the context of a combination therapy, the acquisition of simultaneous BRAF

and MEK inhibitor resistance is a plausible explanation for a treatment failure. Reactivation of ERKs by COT-mediated MEK-independent ERK phosphorylation is a candidate mechanism allowing this dual resistance (733). This hypothesis raised the interest in developing ERK inhibitors to circumvent resistance to BRAF and MEK inhibitors. Although *in vivo* and long-term experiments are still needed to reach conclusions on their value, selective pyrimidylpyrrole ERK inhibitors have been shown to inhibit cell proliferation of some MEK inhibitor-resistant cancer cell lines (734). However, the failure of BRAF/MEK inhibitors in therapies is also consistent with the idea that ERK-independent pathways (728) may contribute to tumor progression in melanoma. Melanoma cell lines resistant to BRAF inhibitors are often resistant to MEK inhibitors but sensitive to inhibition of AKT. These cells also display persistent AKT activation (735), indicating again that combining AKT pathway inhibitors with RAF/MEK inhibitors may achieve better clinical response.

Some patients with melanoma treated with the BRAF inhibitor vemurafenib develop new nonmelanoma skin cancers in the first few weeks after the start of therapy, and many of these lesions display mutations in the RAS oncogene (736). Also, at least one case of leukemia with RAS mutations has been reported in patients with melanoma undergoing BRAF inhibitor treatment (737). Vemurafenib probably stimulates the growth of preexisting lesions rather than causing them directly, and that is likely why this phenomenon is not observed in every patient. In a mouse model of skin carcinogenesis known to induce RAS mutations, vemurafenib reduced tumor latency (736). Accordingly, the authors of the study proposed that the treatment led to a paradoxical increase in ERK activation and accelerated tumor progression (736). A proposed mechanism to explain this paradox is an unexpected ability of the inhibited BRAF isoform to heterodimerize with CRAF to increase its activation by the RAS oncogene (738). However, because treatment with these inhibitors also reduced ERK activation (726), it remains a challenge to determine the context and kinetics of ERK inhibition and ERK activation by BRAF inhibitors.

2.9.4 Models emerging from genetically engineered mice

Studies in genetically engineered mouse models for activated oncogenes upstream of the ERK/mitogen-activated protein kinase (MAPK) pathway have provided conflicting insights about the role of ERK kinases in cancer, just like the clinical data. KRAS is the most frequent mutational target upstream of ERK kinases in human cancers, and diverse mouse models have been generated to study its functions [reviewed in (739)]. Mice with mutant HRAS, NRAS, and RAF were also developed and provided similar observations.

An increase of pERKs was demonstrated in multiple KRAS-driven benign neoplasms, each showing a correlation with elevated levels of pERKs and markers of cellular senescence, such as $p16^{ink4a}$ (CDKN2A/p16), $p19^{Arf}$ (CDKN2A/p19), p53 (TP53), and promyelocytic leukemia protein [PML; (740)]. These observations suggest that the ERK kinases engage tumor-suppressor genes, and that abrogation of these genes must be performed for tumor initiation from cells with elevated pERK levels (Figure 21A). This model shows agreement with the observations reported for colonic serrated adenocarcinoma in which KRAS induces oncogene-induced senescence (OIS) and the ERK/MAPK pathway but not the other effectors of RAS, such as the AKT and RAL pathways. The loss of Ink4a in this context circumvented OIS and allowed the hyperplastic lesions to progress into serrated cancers (741).

On the other hand, even if the activation of the KRAS oncogene in the lung was shown sufficient to promote pulmonary adenocarcinoma (742), no IHC evidence of increased pERK levels was initially found during cancer initiation or in most tumors (405). Only a subset of late-stage tumors in the context of a p53 loss showed activation of these kinases (743). In this context, elevated ERK phosphorylation tightly correlated with $p19^{Arf}$ upregulation, a potent activator of the tumor suppressor p53 in mice (744). Likely, p53 loss abrogated this ERK-mediated tumor suppression axis. Intriguingly, CRAF, but not BRAF, was found critical for lung cancer initiation in KRASG12D mice. Nonetheless, lack of CRAF was shown to have no significant effect on pERK levels, whereas BRAF ablation does (745). It is possible that CRAF regulates an ERK-independent pathway essential for tumor initiation, possibly, the reported inhibition of the Rokα kinase pathway in skin carcinogenesis (712). In other malignant lesions or hyperproliferative disorders, such as adenocarcinomas of the colon and a

myeloproliferative disorder resembling chronic myelogenous leukemia, the pERKs were again not significantly upregulated by oncogenic KRAS (50, 746, 747). These reports suggest that negative regulators of the ERK/MAPK pathway may be involved to limit its activation by oncogenic KRAS in certain cellular contexts and raise questions about the importance of the pathway in these cancers. As observed in mouse embryonic fibroblasts (MEF) derived from mice expressing endogenous levels of KRASG12D (405), such inhibition of the pathway may circumvent high ERK signaling-induced senescence to allow tumor initiation (Figure 21B).

In pancreatic cancers, the role of the ERK/MAPK pathway is still controversial. Elevated levels of pERKs were found in pancreatic premalignant lesions and in pancreatic ductal adenocarcinoma (PDAC) cells (748, 749). The MEK inhibitor PD325901 inhibited tumor growth in orthotropic xenografts of mouse PDA-derived cell lines, suggesting a role for ERK in tumor progression (750). In addition, the genetic ablation of the EGF receptor (EGFR) was shown to compromise pancreatic tumorigenesis in mice expressing oncogenic KRAS (751, 752). This dependency can be explained by induction of a robust RAS-RAF-MEK-ERK pathway activity, further suggesting its requirement for transformation. However, treatment with the EGFR inhibitor erlotinib in this context resulted in strong inactivation of the PI3K/AKT pathway (751). Furthermore, another study published simultaneously has revealed that either treatment with erlotinib or genetic ablation of EGFR in pancreas expressing KRASG12D caused a robust inhibition of the PI3K/AKT pathway, but had no effect on pERK levels (752). In this regard, the PI3K/AKT pathway, but not CRAF, was shown to be genetically essential for KRAS-induced PDAC initiation, thereby suggesting that the activation of AKT rather than a hyperactivation of the ERK kinases is critical for tumor initiation in this cancer (753). Overall, these observations suggest that the PI3K/AKT pathway could play a critical role in RAS-driven cancers and raises questions about the relative contribution of a hyperactivation of the ERK pathway in this process.

OIS markers have been found in preneoplasms during the early stages of PDAC tumorigenesis (81, 754). The activation of the PI3K/AKT pathway was shown to antagonize this state and resulted in rapid development of PDAC (689, 755), providing a mechanistic explanation for its critical role in PDAC onset. Although the capacity of AKT signaling to

inhibit senescence in lung premalignant lesions has not yet been demonstrated, accumulating observations suggest such a mechanism. Premalignant lung adenomas were shown to be positive for senescence markers (82), and activation of AKT by PTEN loss accelerates KRAS-initiated tumorigenesis (756). Furthermore, a point mutation in the p110α catalytic PI3K subunit (PI3KCA) introduced to inhibit its interaction with RAS in a KRAS-driven lung adenocarcinoma model abrogated signaling to AKT, but not ERKs, and strongly reduced tumor formation (757). The critical role of AKT signaling in KRAS-driven lung cancer onset was then confirmed by genetic deletion of the p85 PI3K regulatory subunit (758). The molecular mechanisms explaining the capacity of the PI3K/AKT pathway to circumvent tumor suppression will need further investigation, but may include inactivation of tumor-suppressor mechanisms induced by high ERK signaling or inhibition of the ERK/MAPK pathway (Figure 21A, B).

The ERK pathway has been also studied in mouse models for loss of function of negative regulators of the pathway. The genetic ablation of both *Spry1* and *Spry2* alleles, which are negative regulators of RTK signaling, leads to the expected increase in pERK levels, but no significant regulation of AKT signaling was observed in the prostate. This context induced frequent ductal hyperplasia, occasionally progressing into low-grade prostatic intraepithelial neoplasia (PIN) lesions (759). These lesions were previously shown to display markers of senescence (760). However, when the *Spry* alleles are deleted in the context of heterozygosity for a *Pten* null allele, the development of high-grade PINs is promoted and evidence of neoplastic invasion is observed (759). Interestingly, the loss of Sprouty function cooperates with the loss of one allele of the *Pten* gene to promote AKT activation. Reciprocally, overexpression of *Spry2* in *Pten* null animals inhibited the hyperactivation of AKT and suppressed *Pten* ablation-driven tumorigenesis (759). Overall, this study may suggest that a loss of function of Sprouty promotes prostatic cancer initiation by the release of a negative regulation on the AKT pathway rather than (or in addition to) a negative feedback on the ERK/MAPK pathway. Such a conclusion suggests again that the PI3K/AKT pathway could circumvent ERK-induced OIS. Loss of function of another negative regulator of the ERK/MAPK pathway, the RAS-GAP neurofibromatosis type 1 (NF1), was also studied in mice and showed dissimilarities according to the ERK status in tumorigenesis. A lack of NF1

has been shown to drive benign lesions, such as plexiform neurofibromas (761) and gastric hyperplasia, in conjunction with hyperactivation of RAS and the ERKs (762). Inactivation of tumor-suppressor genes in addition to *Nf1* inactivation leads to diverse frank malignant tumors (761, 763, 764), including astrocytomas (765). These observations are consistent with a model in which abrogation of tumor-suppressor genes is a prerequisite for malignant lesion initiation with elevated pERK levels (Figure 1A).

An important limitation with the classic genetically engineered mouse models is that the genetic modifications are applied to the whole animal, the whole organ, or all the cells of a specific lineage. Such an approach greatly increases the penetrance because the chances that a cell with the prerequisite to transform is being affected by the desired genetic modification are high. These tools are helpful to study the initiation of malignancy from the emerging lesions and then cancer progression and maintenance. However, those models do not allow an accurate study of the cell of origin. Evidence suggests tissue- and context-specific differences in ERK regulation, thereby reflecting a different role of the pathway in the context of oncogenic RAS and likely explaining divergent propensities to undergo neoplastic transformation (740). If high ERK activity has a ubiquitous role in promoting tumor suppression, we can speculate that tissues with a higher subpopulation of cells with increased capacity to buffer the activation of the ERK/MAPK pathway could develop malignant tumors more frequently in the context of spontaneous and random mutations in upstream regulators of the pathway. In mice engineered to allow spontaneous expression of mutant KRAS in different tissues, mainly lung tumors were observed. Intriguingly, tumors of the pancreas and colon, in which RAS mutations are frequent in humans, were not observed (766). It is possible that these differences are due to differences between humans and mice, but we suggest that the mouse lung may contain more transformation-permissive cells with the capacity to reduce ERK activation. Such a speculation is consistent with the reported low pERK levels found during KRAS-driven initiation of lung adenocarcinoma in mice (405).

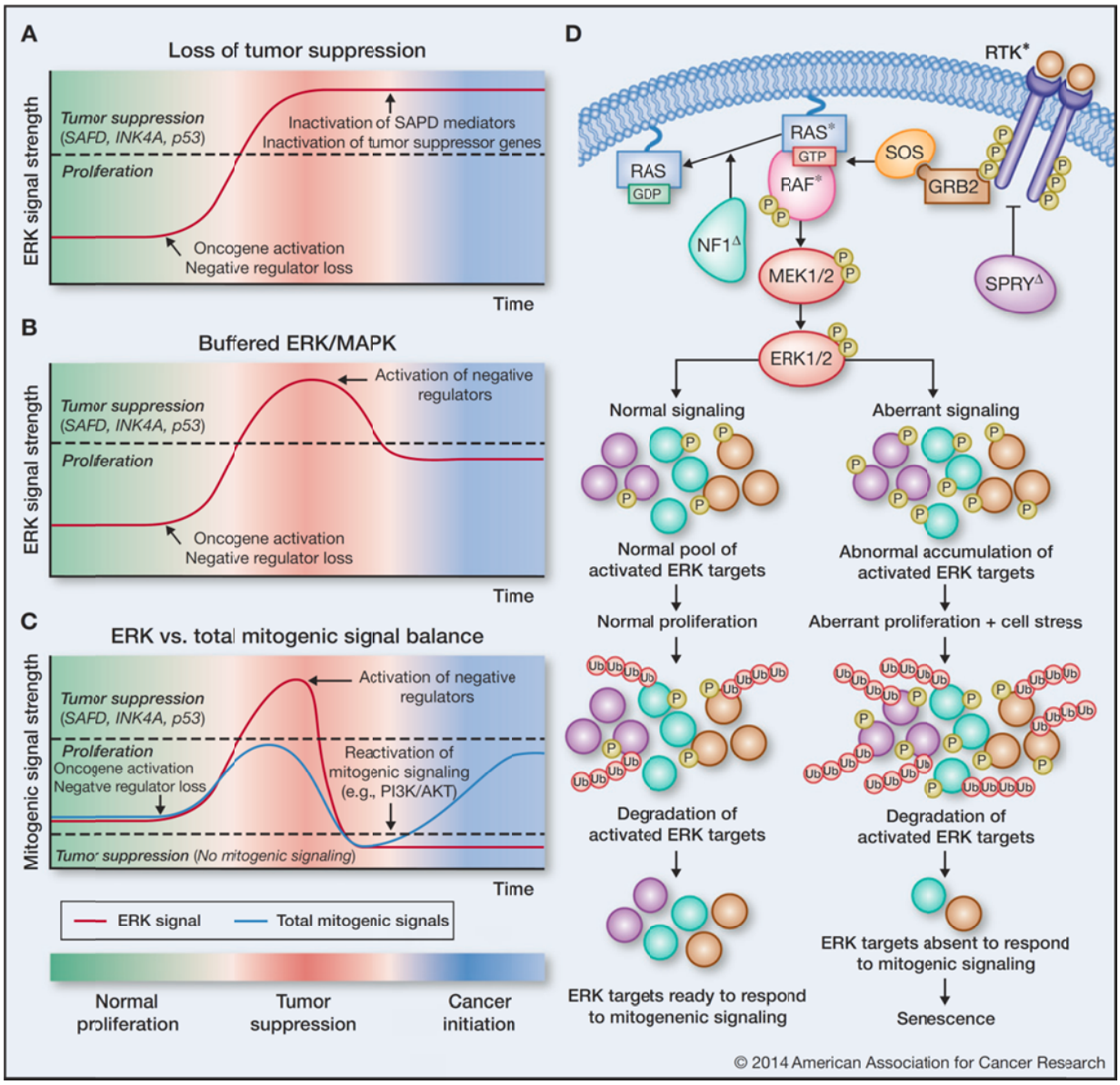

Figure 21. Modeling ERK signaling intensity in tumor suppression and cancer initiation

(***A***) High ERK/MAPK pathway activity mediates tumor suppression by inducing the senescence-associated protein degradation (SAPD) of targets of ERK signaling (direct or indirect). Loss-of-function of tumor suppressors or SAPD effectors (i.e. E3 ligases) may allow bypass of senescence and cancer initiation. (***B***) High ERK signaling induces tumor suppression as described before. The activation of negative regulators of the ERK/MAPK pathway buffer its activation below the threshold required for tumor suppression. (***C***) After activation of tumor suppression as previously, hyperactivated ERK induces strong negative feedback mechanisms, reducing mitogenic signaling below the minimal threshold required for proliferation. Reactivation of other mitogenic signaling pathways may thus enable proliferation and cancer initiation. A moderate activation of the ERK/MAPK pathway is not excluded. (***D***) simplified model of ERK-mediated SAPD. Aberrant ERK activity leads to the direct or

indirect phosphorylation of a larger fraction of targets, whereas normal signaling engages the phosphorylation of a minor fraction. Some of these targets with sustained phosphorylation undergo phosphorylation-dependant ubiquitination and proteasome-dependent degradation. *, oncogenic activation reported; Δ, negative regulator loss reported; Ub, Ubiquitin; P, Phosphorylation.

2.9.5 ERKs, protein degradation and tumor suppression

Tumor suppressor pathways have necessarily evolved to respond to oncogenic threats. Consequently, these pathways must be intrinsically wired to respond to aberrant growth factor signaling. The ERK kinases are at the center of multiple signaling pathways activated by growth factor receptors and other proliferation stimuli. Hence, tumor-suppressor pathways might have evolved to recognize aberrant ERK signaling. Regarding the response to ERK signaling intensity, studies in genetically engineered mouse models proposed so far two models in which high ERK activity mediates senescence and tumors arise after inactivating the senescence program (Figure 21A) or downregulation of prosenescent high ERK activation (Figure 21B). However, in some contexts, senescent cells and lesions correlate with extinction of the ERK/MAPK pathway (528, 767). These studies have shown that the mechanisms involve negative feedbacks affecting upstream activators of RAS, and thereby inhibiting signaling by the latter, including the PI3K and the RAL pathways. It is thus likely that senescence in this case is maintained by the downregulation of multiple mitogenic signaling pathways and not only the ERK pathway (Figure 21C).

The ERK kinases transduce their signals by phosphorylating multiple targets, which for the most part, execute cell growth signals. During RAS-induced senescence, aberrant signaling through ERK kinases led to the proteasome-dependent degradation of multiple phosphoproteins required for cell growth and cell-cycle progression (390). The degradation of these phosphorylated proteins is suspected to contribute to cellular stresses associated with senescence, including mitochondrial dysfunction, telomere dysfunction, and DNA damage. This process was named senescence-associated protein degradation or SAPD (Figure 21D). SAPD depended on ERK activation and was also observed during senescence triggered by short telomeres. Although SAPD may require specific E3 ligases activated by the senescence program, it is the aberrant phosphorylation triggered by high ERK signaling that renders

multiple proteins sensitive to depletion by this mechanism. Lowering the strength of ERK activity with pharmacological inhibitors of the pathway or RNA interference (RNAi) prevented protein degradation and allowed RAS-expressing cells to become malignant (390). The mechanistic details of this tumor-suppression pathway will be the focus of future studies, but it can be anticipated that it involves novel functions of the ubiquitin-dependent proteasome pathway (390) and a tumor-suppressive role for E3 ligases mediating the recognition of phosphorylated proteins. Of note, PML, which is important for OIS, plays a role in the degradation of MYC (613) and could be implicated in the degradation of other targets of the SAPD.

Recognizing the tumor-suppressive function of the ERK kinases and the characterization of the molecular mechanisms implicated will allow a better assessment of the role of the ERK kinases in human tumors. Cancers may avoid the barrier for proliferation provided by the SAPD in diverse manners. In some situations, the SAPD mechanisms and the tumor suppressors activated as a consequence of the stress generated by ERK signaling are disabled, allowing cells with high ERK levels to become malignant (Figure 21A). Other tumors will simply buffer ERK to levels that are not sufficient to trigger tumor suppression. This could be achieved by, for example, overexpression of ERK phosphatases (DUSP; Figure 21B and Supplementary Data). It has been also observed that activation of the ERK pathway can trigger a negative feedback mechanism on the ERK and other mitogenic pathways preventing cell growth with features of senescence (767). It is not known whether the initial high ERK activity was sufficient to trigger a SAPD process in this context, but tumors could arise in these cells if they manage to reactivate mitogenic signaling by mutations or epigenetic mechanisms (Figure 21C).

These models of tumor progression create a framework to target the use of ERK pathway inhibitors. They could be more effective in tumors where the ERK pathway is highly active and the tumor-suppressor responses downstream of ERKs are inactivated during the carcinogenesis process (Figure 21A). In tumors where ERK activity is low, it is likely that ERK-dependent tumor suppression has not been mutationally inactivated and ERK pathway inhibitors are anticipated to be less effective. In this context, novel anticancer drugs that

increase ERK activity over the threshold required to activate tumor suppression could be used. We must keep in mind that tumors resist any attempt to simplify them into clear categories and within the same tumor we can probably find cells with high or low ERK levels with likely different histories of tumor progression. Proper drug combinations should be identified to target these tumors.

Another important active debate about the ERK kinases in cancer is the attribution of nonredundant functions to the two isoforms. Again, conflicting results can be found in the recent literature. Genetic studies in fibroblast cells using quantitative assays of ERK activity have provided compelling evidence for a redundant role of the two ERK isoforms in cell proliferation (256, 257). Conversely, ERK2 but not ERK1 was shown to contribute to cancer progression by promoting epithelial-mesenchymal transition (768) and by inducing the cytokine receptor subunit gp130 (769). Also, ERK2 but not ERK1 has been recently proposed as a critical mediator of RAS-induced senescence in mouse fibroblasts (770), whereas our work in human cells suggested that the two isoforms may contribute to senescence (390). The outcome of inactivating one specific isoform may be influenced by the cellular context and the relative expression of ERK1 versus ERK2. Senescence depends on the strength of global ERK activation (390), indicating that in tissues where one isoform predominates, its role in senescence will be more important.

In the end, whether ERK signaling is friend or foe will depend on the context, but evolutionary biology indicates that tumor suppression can be adaptive, whereas cancer formation is not for the individual. Therefore, in broad strokes we can theorize that in normal cells with intact tumor suppression modules ERK activity will protect from tumorigenesis, but in altered or mutated cells where some of these modules are disabled the ERKs will promote the cancer phenotype.

2.9.6 Acknowledgments

We would like to thank Nabeel Bardeesy for comments on the manuscript. X. Deschênes-Simard is a fellow of the Vanier Canada Graduate Scholarships Program and Michael Smith Foreign Study Supplements Program. G. Ferbeyre and S. Meloche are supported by grants from the Canadian Institute of Health and Research (CIHR). G. Ferbeyre is a FRSQ national research fellow (Fonds de la recherche en santé du Québec). S. Meloche holds the Canada Research Chair in Cellular Signaling.

3. Rôle suppresseur de tumeur de la voie ERK/MAPK par l'inhibition de la reprogrammation cellulaire

3.1 Mise en contexte de l'article 4

Ce quatrième article ouvre un nouveau volet de la thèse. En effet, il introduit l'étude d'une autre fonction antitumorale potentielle de la voie ERK/MAPK, soit sa capacité à favoriser la stabilité d'un état différencié. En s'inspirant de la biologie des cellules souches normales, nous avons voulu déterminer si la signalisation par la voie ERK/MAPK s'oppose à la reprogrammation nécessaire à l'acquisition de la tumorigénicité et à l'apparition des CSC.

Pour ce projet, plusieurs raisons nous ont motivés à tirer avantage du modèle de la progression du PDAC. D'abord, les étapes de la progression tumorale sont bien établies pour ce cancer. Ainsi, nous avons été en mesure d'évaluer les niveaux de p-ERK aux différents stades menant à la transformation maligne et donc, à l'acquisition de la tumorigénicité. De plus, puisque 95% des cas de PDAC présentent une mutation oncogénique au niveau de *RAS*, ce modèle est particulièrement approprié pour l'étude du rôle de la voie ERK/MAPK dans la réponse aux oncogènes (22, 45). Enfin, il s'agit d'un cancer pour lequel des sous-populations de CSC ont déjà été mises en évidence (771-773). Afin de faciliter l'étude du rôle des kinases ERK lors de la reprogrammation des cellules cancéreuses et d'élargir la portée des résultats au-delà du cancer pancréatique, nous avons également utilisé une série de modèles de cellules en culture.

Globalement, nos résultats suggèrent qu'une réduction de la signalisation par la voie ERK/MAPK est requise pour la reprogrammation conférant la tumorigénicité et favoriserait le maintien des sous-populations de CSC. Ces résultats mettent en évidence l'importance de cibler les cellules reprogrammées avec une faible activité de la voie ERK/MAPK. Pour ce faire, nous suggérons la metformine, laquelle semble posséder une activité anti-CSC.

Il est important de noter que l'article présenté ci-dessous est en fait un manuscrit en préparation. Il n'a encore jamais été soumis à un comité de pairs. Nous espérons soumettre le manuscrit d'ici la fin de l'année 2014 au journal *Cell Stem Cell*. Plusieurs expériences contrôles sont en cours et d'autres expériences sont prévues. Nous discuterons plus en détails des limites du manuscrit actuel dans la discussion.

3.2 Contribution à l'article 4

J'ai été l'investigateur principal des travaux présentés dans ce manuscrit, ce qui inclut les immunohistochimies, la plupart des expériences de culture cellulaires et d'analyse biochimique, les xénogreffes sous-cutanées et les analyses par puce à ADN. Filippos Kottakis a contribué aux résultats obtenus par xénogreffes et a assuré la validation des résultats d'immunohistochimie auprès du service de pathologie du MGH. Il a également assuré la coordination du projet au sein du laboratoire du Dr. Bardeesy suite à mon départ. Emmanuelle Saint-Germain a contribué aux expériences de formation de sphères tumorales (Figures 26 et S17). Karine Moineau-Vallée a contribué à l'obtention des résultats des figures 27D et S18, ainsi qu'à la quantification des immunohistochimies (Figure 22C, D; Figure 23B, C). L'équipe du Dr. Bardeesy a contribué à l'obtention des échantillons pour les immunohistochimies, à l'établissement de lignées cellulaires, ainsi qu'aux injections orthotopiques et intraveineuses. Marie-France Gaumont-Leclerc a effectué l'immunohistochimie de la figure 26D.

J'ai rédigé le manuscrit et conçu les figures. Celui-ci a été révisé par Marie-France Gaumont-Leclerc, Frédéric Lessard, Filippos Kottakis, Nabeel Bardeesy et Gerardo Ferbeyre.

3.3 Article 4

Tumor suppressor activity of ERK/MAPK signaling by inhibiting cellular reprogramming

Xavier Deschênes-Simard[1], Filippos Kottakis[2], Emmanuelle Saint-Germain[1], Karine Moineau-Vallée[1], Rushika M. Perera[2], Yusuke Mizukami[2], Julien Fitamant[2], Marie-France Gaumont-Leclerc[1], Frédéric Lessard[1], Nabeel Bardeesy[2] and Gerardo Ferbeyre[1]

Manuscript in preparation for submission to Cell Stem Cell

1) Department of Biochemistry and Molecular Medicine; Université de Montréal, Montréal, Québec H3C 3J7, Canada
2) Massachusetts General Hospital Cancer Center, Harvard Medical School, Boston, MA 02114, USA

Running title: ERK signaling inhibits cancer cell reprogramming

Keywords: ERK; reprogramming; cancer stem cells; cancer; tumor suppression

Correspondence to: Gerardo Ferbeyre and Nabeel Bardeesy

3.3.1 Summary

Cancer cell reprogramming into a stem cell-like state has been established as a mechanism that contributes to tumor initiation, heterogeneity, metastasis and resistance to cancer therapies. Studies on embryonic stem cells (ESCs) and induced pluripotent stem cells (iPSCs) have shown that ERK signaling circumvents pluripotency. Here, we show that the ERK/MAPK pathway plays a similar role in cancer stem cells (CSCs). Accordingly, a downregulation of the pathway is observed during the transition from pancreatic benign neoplasms to aggressive pancreatic ductal adenocarcinoma, and this correlates with the acquisition of stem cell-like properties. Furthermore, reduced ERK signaling is critical for cancer cell reprogramming since hyperactivation of the pathway abrogates the stem cell-like phenotype. Conversely, the inhibition of ERK signaling allows Ras-mediated reprogramming *in vitro*. Sphere-forming tumor cells with low ERK signaling were sensitive to metformin, suggesting that this drug can be combined with other therapies that target the bulk of the tumor but not the "cancer stem cells".

3.3.2 Highlights

Decreased p-ERK levels correlate with initiation of pancreatic cancer

Cancer cells with low p-ERK levels are associated with markers of dedifferentiation

The stem cell-like phenotype depends on low p-ERK levels

Metformin targets cancer stem cell-like with low p-ERK levels

3.3.3 Introduction

The regulation of the ERK/MAPK signaling pathway is complex and its biological outcomes depend on the spatiotemporal dynamics of ERK activation, including kinetics, strength, duration and subcellular localization (273). A well-known example illustrating this versatility of the ERK pathway is the induction of cell proliferation by transient signaling, while a sustained ERK activation promotes differentiation (424). In agreement with a role in lineage commitment, the suppression of ERK signaling supports self-renewal of embryonic stem cells from mice (mESCs) (418, 419) and rats (rESCs) (420, 421). Furthermore, activation of this pathway in ESCs and mouse embryos has been shown to trigger loss of pluripotency and lineage priming (425-430). In contrast, ERK signaling promotes self-renewal of the first pluripotent cell lines derived from human blastocysts and described as ESC (hESCs) (774-777). However, these cells have been subsequently shown to be analogous to the rodent epiblast-derived stem cells (EpiSCs), which represent a primed state for lineage specification characterising post-implantation epiblasts (427, 778-780). Accumulating evidence suggests that ERK signaling promotes the transition from the less differentiated mESCs, representing a naïve pluripotent state, to mEpiSCs and stabilizes this primed state (777), perhaps explaining the role of ERK in the first isolated human embryonic stem cell lines. Indeed, ERK inhibition promotes dedifferentiation of mEpiSCs to mESC (781, 782). Following these observations, conventional hESCs have been rewired into a more dedifferentiated state highly similar to the naïve mESCs (783, 784), and naïve hESCs have been isolated from blastocysts (422, 423). In all cases, the maintenance of these naïve hESCs was strictly dependant on ERK inhibition.

Further evidence of a critical role of ERK signaling in the regulation of cell fate determination and plasticity comes from the development of reprogramming technologies. Since the first generation of induced pluripotent stem cells (iPSCs) from somatic cells using ectopic expression of reprogramming factors (431-433), several laboratories have tried to increase the efficiency of the process and to mimic the effect of the required transgenes using small chemical compounds. The use of ERK/MAPK pathway inhibitors has first been shown to strikingly increase the efficiency of reprogramming by the four classical reprogramming factors (*OCT4*, *SOX2*, *KLF4*, and *c-MYC*) (435-438), and to favor the conversion of human

iPSCs to ground state naïve pluripotency (422, 783). Then, the classical 2i inhibitor combination (GSK3-β and ERK/MAPK inhibitors) has been shown to functionally replace exogenous reprogramming genes, thereby contributing to reprogramming with exogenous expression of only *OCT4* (439). Recently, Hou and colleagues succeeded for the first time in reprogramming somatic cells using chemical agents only. They called these cells chemically induced pluripotent stem cells (CiPSCs) (440). The procedure involved an initial treatment with a combination of 6 chemical compounds (VC6TFZ), which activated the expression of *Oct4*, but failed to strongly induce the expression of the other pluripotency genes. A subsequent treatment including an inhibitor of the ERK/MAPK pathway was required for the establishment of the pluripotency circuitry (440). Taken together, these reports suggest that ERK signaling not only promotes differentiation of naïve stem cells, but also stabilizes the specialized phenotypes of differentiated cells to circumvent reprogramming into pluripotent cells.

An emerging area in cancer biology research is the reprogramming of cancer cells into a stem-cell like state. Heterogeneity is a hallmark of several cancers and a growing body of studies has shown that a subpopulation of self-renewing cancer stem cells (CSCs) exists among the distinct subpopulations of neoplastic cells within the same tumor (176, 184). These cells have first been identified in blood cancers (208, 209), but subsequently found in breast tumors (785), brain tumors (786), and then in a variety of other solid tumors (210). Although these cells represent a very small subpopulation within a tumor (212), they are thought to contribute to tumor maintenance, heterogeneity, metastasis and resistance to multiple cancer therapies (213). The CSCs share several gene expression pathways and regulators with ESCs (787, 788), but they are not necessarily derived from normal stem cells nor do they represent the cell of origin, which is the first cell receiving oncogenic hits (13). The current thinking is rather that CSCs arise from dedifferentiation of more specialized cells or cancer cells (179, 213, 215). Interestingly, there are many parallels between the cellular reprogramming leading to CSCs and tumorigenesis and the molecular process leading to iPSCs. Indeed, a role in tumorigenesis has been established for almost all the genes used to generate iPSCs (213). Also, the most frequently activated oncogene in human cancers, *Ras*, has been shown to increase cell plasticity and predispose to reprogramming into stem cell-like cells (434).

Therefore, the similarities presented above suggest that several mechanisms found important in stem cell biology could be transposed to the reprogramming into CSCs. Our actual knowledge suggests that inhibition of ERK/MAPK signaling could play a positive role in the generation and maintenance of CSCs. However, this assumption is paradoxical according to the well-established role of this pathway in cancer progression (349). Nevertheless, recent studies have shown that ERK signaling can promote tumor suppression as well, depending on the context and the signaling strength (390, 472). Moreover, it is not excluded that the effect of ERK signaling is as heterogeneous as are the tumor cells, perhaps required for the proliferation of bulk tumor cells, but detrimental to the maintenance of a small pool of CSCs.

The purpose of the research presented herein was to evaluate the role of ERK signaling on cancer cell reprogramming. Overall, our results indicate that downregulation of the ERK/MAPK pathway favors the acquisition of CSC properties. We also propose that metformin could be used to curb propagation of CSCs with low levels of activated ERK.

3.3.4 Results

Low ERK signaling correlates with initiation of human and mouse pancreatic cancer

According to the cancer stem cell model, reprogramming into dedifferentiated cancer cells is required during tumorigenesis (202, 211). Supporting this concept, it has been shown that oncogenic *Ras* drives reprogramming and dedifferentiation in early steps of pancreatic tumor initiation (434, 771, 789). To address if low ERK activity is associated with tumor initiation *in vivo*, and thus with the appearance of cancer stem cell-like cells (CSC-like cells), we assessed the status of ERK activation by immunochemistry in tissues recapitulating multistage pancreatic cancer initiation. In general, this process is clearly defined by sequential premalignant steps, which are acinar-to-ductal metaplasia (ADM) and pancreatic intraepithelial lesions from grade 1 to 3 (PanIN-1 to 3), and then initiation of pancreatic ductal adenocarcinoma (PDAC) (22). In human pancreatic tissues, we found that p-ERK levels are modestly increased in ADM compared to normal tissues and correlate with hyperproliferation

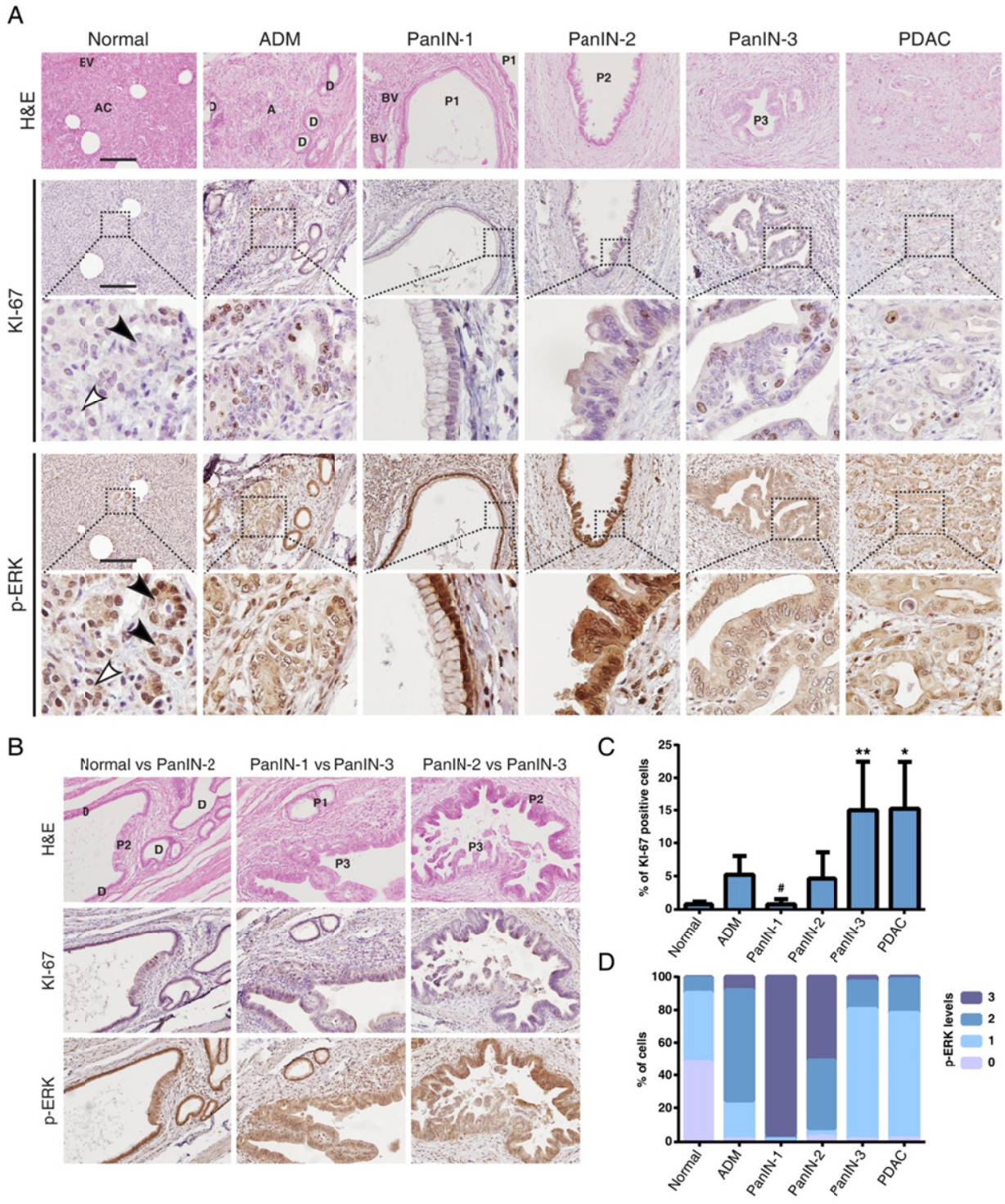

Figure 22. Decreased p-ERK levels correlate with initiation of human pancreatic cancer

(*A*) Immunohistochemical staining with anti-p-ERK and anti-KI-67 antibodies of human tissues representing normal pancreas and the stages of pancreatic cancer progression. Insets: higher magnification of representative regions. ADM, acinar-to-ductal metaplasia; PanIN-1 to 3, pancreatic

intraepithelial lesions (grades 1 to 3); PDAC, pancreatic ductal adenocarcinoma; H&E, hematoxylin and eosin; BV, blood vessel; AC, acinar cells; D, normal duct; A, ADM; P1-3, PanIN-1 to 3; black arrows, normal ducts; white arrows, acinar cells; scale bars = 100μm. (***B***) Staining as in (*A*), but fields showing two different types of pancreatic lesions allowing direct comparison. (***C***) Quantification of KI-67-positive epithelial cells in (*A-B*). Data are presented as the average percentage of positive cells ± SD. n = 16 patients; (#) $P < 0.05$ compared to ADM, two-sample t-test; (*) $P < 0.01$, (**) $P < 0.005$ compared to PanIN-1, two-sample t-test. (***D***) Quantification of p-ERK staining of epithelial cells in (*A-B*) according to four intensity of staining (none, 0; low, 1; moderate, 2; high, 3). The average percentage of cells for each staining intensity is shown. Patients as in (*C*); PanIN-1 vs ADM $P < 0.001$, PanIN-3 vs PanIN-2 $P < 0.05$, PanIN-3 vs PanIN-1 $P < 0.001$, PDAC vs PanIN-1 $P < 0.001$, two-sample t-test. See also Figure S12.

in these lesions (Figures 22 and S12). However, the levels of p-ERK are much higher in PanIN-1 and 2, which are mainly non-proliferative lesions (Figures 22 and S12). Then p-ERK levels are significantly decreased in PanIN-3 and PDAC, and this correlates with hyperproliferation (Figures 22 and S12). PanIN-1 and 2 are frequently found in patient older than 40 years old and are of little clinical significance. However, PanIN-3 are referred to as carcinoma-in-situ, which represent fully developed but non-invasive neoplastic lesions, and demonstrate a high potential to progress to invasive PDAC (20, 790). Thus, our results suggest that downregulation of the ERK pathway is associated with complete neoplastic transformation of human pancreatic cells.

To evaluate whether inhibition of ERK activation during tumor initiation also occurs in genetically engineered mouse models recapitulating the stepwise initiation of pancreatic cancer, we measured p-Erk levels in tissues from *Pdx1-Cre;LSL-KRas^{G12D}* mice. The pattern of p-Erk was similar to the one observed in human tissues, with moderate levels in the proliferative ADM lesions compared to normal tissues, higher levels in the non-proliferative PanIN-1 and 2 and low levels in the highly proliferative PanIN-3 lesions and PDAC (Figures 23A-C and S13A). To simplify the characterisation of the role of Erk signaling during the development of tumorigenicity in pancreatic cells, we took advantage of ductal cell lines established from *Pdx1-Cre;LSL-KRas^{G12D}* mice pancreas enriched for ADM/PanIN-1 lesions versus pancreas with PDAC (Figure 23D). The ADM/PanIN-1-derived cell lines were clearly non-tumorigenic while the PDAC-derived cell lines had greater proliferative potential

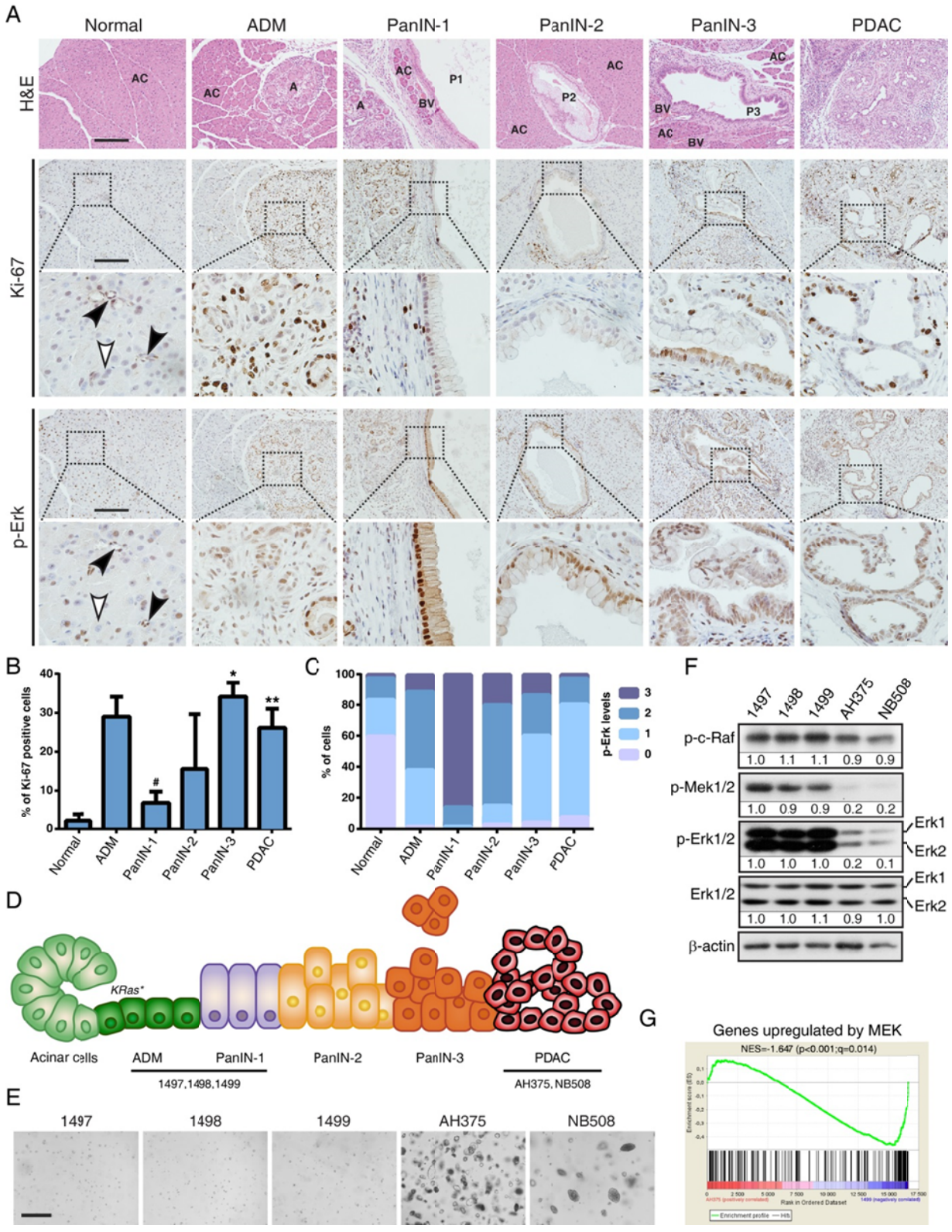
A
Normal
ADM
PanIN-1
PanIN-2
PanIN-3
PDAC
H&E
Ki-67
p-Erk
AC
A
BV
P1
P2
P3
B
% of Ki-67 positive cells
C
% of cells
p-Erk levels
D
KRas*
Acinar cells
ADM
PanIN-1
PanIN-2
PanIN-3
PDAC
1497,1498,1499
AH375, NB508
E
1497
1498
1499
AH375
NB508
F
p-c-Raf
p-Mek1/2
p-Erk1/2
Erk1/2
β-actin
Erk1
Erk2
G
Genes upregulated by MEK
NES=-1.647 (p<0.001;q=0.014)

Figure 23. Decreased p-ERK levels correlate with tumor initiation in a KRas-driven mouse model of pancreatic cancer

(***A***) Immunohistochemical staining (p-Erk and Ki-67 antibodies) of pancreatic tissues from *Pdx1-Cre;LSL-KRas*^{G12D} mice. Normal pancreatic tissues, acinar-to-ductal metaplasia (ADM) lesions, pancreatic intraepithelial lesions (PanIN; grades 1 to 3) and pancreatic ductal adenocarcinoma (PDAC) are shown. Insets: higher magnification of representative regions. H&E, hematoxylin and eosin; BV, blood vessel; AC, acinar cells; A, ADM; P1-3, PanIN-1 to 3; black arrows, normal duct; white arrows, acinar cells; scale bars = 100μm. (***B***) Quantification of Ki-67-positive epithelial cells in (*A-B*). Data are presented as the average percentage of positive cells ± SD. n = 14 mice; (#) $P < 0.05$ compared to ADM, two-sample t-test; (*) $P < 0.05$, (**) $P < 0.01$ compared to PanIN-1, two-sample t-test. (***C***) Quantification of p-Erk staining of epithelial cells in (*A-B*) according to four intensity of staining (none, 0; low, 1; moderate, 2; high, 3). The average percentage of cells for each staining intensity is shown. Mice as in (*B*); PanIN-1 vs ADM $P < 0.001$, PanIN-3 vs PanIN-1 $P < 0.005$, PDAC vs PanIN-1 $P < 0.001$, two-sample t-test. (***D***) Schema of the multistage pancreatic cancer progression after oncogenic *ras* activation (KRas*). Mouse pancreatic ductal cell lines were established from the indicated lesions in *Pdx1-Cre;LSL-KRas*^{G12D} mice. (***E***) Cell lines from PDAC form colonies in soft agar, but not cell lines from ADM/PanIN-1 lesions. Scale bar = 400μm. (***F***) Immunoblots for the indicated proteins in cell lines as in (*D-E*). The ERK/MAPK pathway is downregulated in PDAC cell lines. (***G***) RNA from 1499 and AH375 cells was collected for microarray gene expression analysis (GEO accession number: GSE57566). Gene Set Enrichment Analysis (GSEA) revealed a gene expression signature of MEK activation in 1499 cells (MEK_UP.V1_UP; M2725). See also Figure S13.

(Figure S13B) and formed colonies in soft agar (Figures 23E and S13C). In agreement with our observation in tissues, the Erk pathway and the expression of its transcriptional targets were strikingly downregulated in the PDAC-derived tumorigenic cell lines (Figures 23F, G and S13D-F). Collectively, these results suggest that a decrease in Erk activation associated with pancreatic tumor formation is a shared phenomenon between mouse and human.

Initiation of pancreatic cancer is associated with acquisition of stem cell-like properties

To investigate the mechanisms susceptible to explain the transition from a non-transformed phenotype correlating with high p-Erk levels to a low-p-Erk-associated transformed phenotype, we proceeded to study the gene expression profile of these two conditions. For this purpose, we used RNA extracts from the 1499 ADM/PanIN-1-derived cell line, which is non-tumorigenic, and RNA extracts from the AH375 PDAC-derived cell line, which forms tumors following subcutaneous or orthotopic injection into SCID mice (Figure

24A-D). To infer the biological functions significantly altered between both cell lines, we did a FatiGO single enrichment of microarray data using the Babelomics 4.3 platform. Among the general biological function categories that were associated with cellular transformation, the most important change was found in genes regulating cell differentiation (Figure 24E). This may reflect a reprogramming of AH375 cells into less differentiated cells since the 1499 cell line is significantly associated with several gene expression signatures suggesting differentiation and loss of stem cell properties (Figures 24F, G and S14C). Conversely, the AH375 cells significantly express multiple gene expression modules reflecting stem cell properties (Figure S14A, C). A close relationship between the transdifferentiation process of epithelial-mesenchymal transition (EMT) and the acquisition of stem cell traits was previously demonstrated (791). Our findings agree with these observations since the gene expression profiles we compared have revealed regular epithelial characteristics in 1499 cells, while many significant gene expression signatures suggest that AH375 cells have undergone EMT (Figures 24H and S14B, D). Overall, our analysis suggests that tumorigenicity in pancreatic cells correlates with a reprogrammed gene expression profile associated with dedifferentiation.

To determine if our findings at the gene expression levels are transposable to a phenotype of CSC-like cells, we tested the capacity of the mouse ductal cell lines derived from the different pancreatic lesions to form free-floating tumor spheres. While no spheroid formation was observed in ADM/PanIN-1-derived cell lines, there were multiple ones in PDAC-derived cells, thereby showing the presence of an important subpopulation of tumor-initiating cells in these cell lines (Figure 24I, J). Because EMT has been shown to play a critical role in promoting dissemination of cancer cells (792) and a steadily growing number of studies suggest a role for CSCs in metastatic colonization (176, 793, 794), we tested the metastatic potential of the AH375 cells. Following tail vein injection of SCID mice, these cells showed a strong potential to metastasize in multiple organs, with an elevated number of metastasis in the lungs (Figure 24K and data not shown). Interestingly, these metastatic cells maintained low levels of p-Erk, which were lower than in the surrounding normal lung tissue, and strongly expressed the c-Myc transcription factor (Figure 24L). The latter has been shown to be a potential master regulator of the ESC-like transcriptional program, allowing

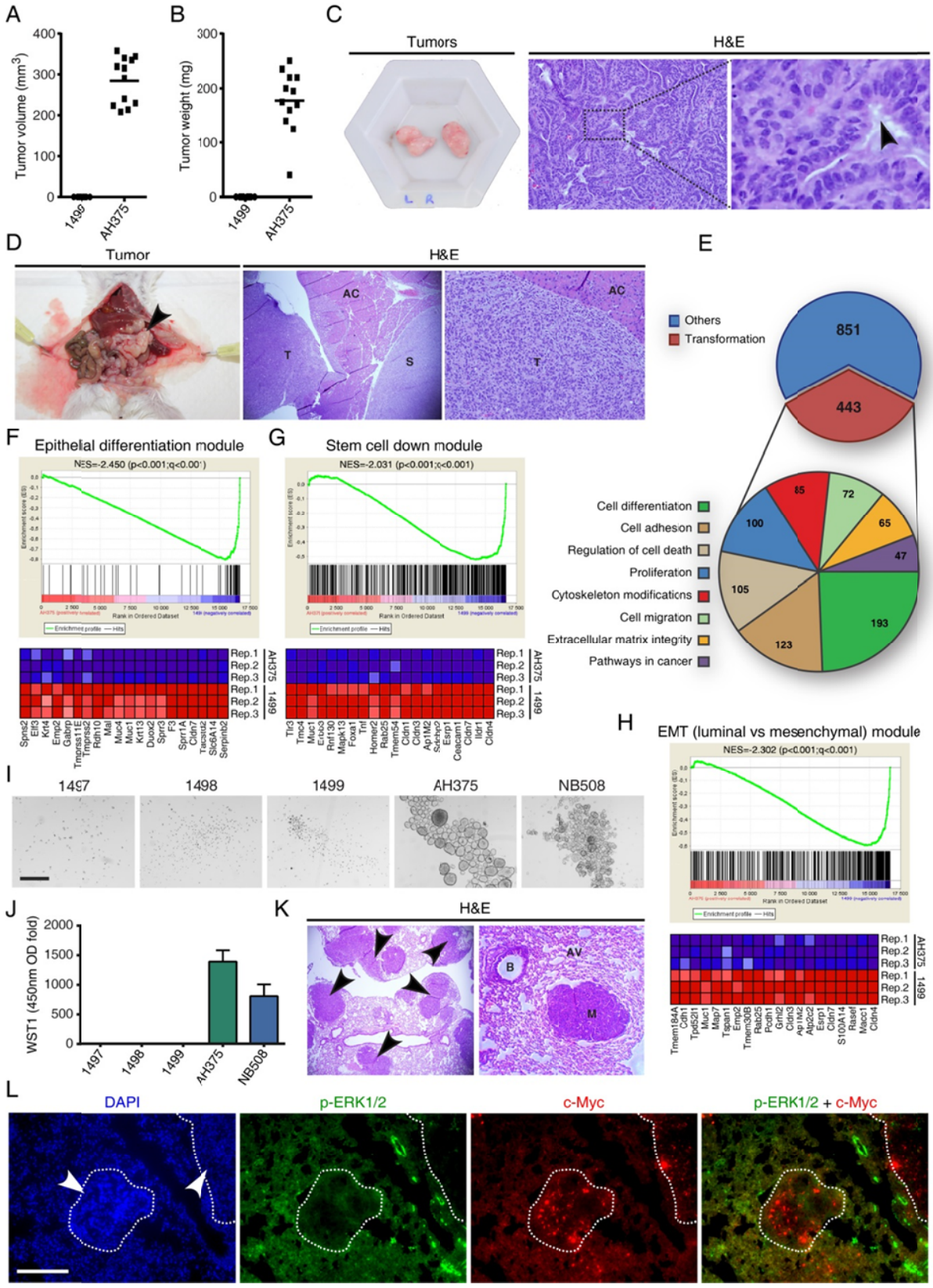
A
Tumor volume (mm3)
400
300
200
100
0
1499
AH375
B
Tumor weight (mg)
300
200
100
0
1499
AH375
C
Tumors
H&E
D
Tumor
H&E
AC
T
S
AC
T
E
Others
Transformation
851
443
Cell differentiation
Cell adhesion
Regulation of cell death
Proliferation
Cytoskeleton modifications
Cell migration
Extracellular matrix integrity
Pathways in cancer
85
72
100
65
47
105
193
123
F
Epithelial differentiation module
NES=-2.450 (p<0.001;q<0.001)
Enrichment score (ES)
Rank in Ordered Dataset
Enrichment profile
Hits
Rep.1
Rep.2
Rep.3
AH375
1499
Spns2
Elf3
Krt4
Emp2
Gabrp
Tmprss11E
Tmprss2
Rdh10
Mal
Muc4
Muc1
Krt13
Duox2
Spn3
F3
Sprr1a
Cldn7
Tacstd2
Slc8A14
Serpinb2
G
Stem cell down module
NES=-2.031 (p<0.001;q<0.001)
Enrichment score (ES)
Rank in Ordered Dataset
Enrichment profile
Hits
Rep.1
Rep.2
Rep.3
AH375
1499
Tlr3
Tmc4
Muc1
Erbb3
Pnf130
Mapk13
Foxa1
Tnf
Homer2
Rab25
Tmem54
Cldn1
Cldn3
Ap1M2
Sdcbp2
Esrp1
Ceacam1
Cldn7
Vdr
Cldn4
H
EMT (luminal vs mesenchymal) module
NES=-2.302 (p<0.001;q<0.001)
Enrichment score (ES)
Rank in Ordered Dataset
Enrichment profile
Hits
Rep.1
Rep.2
Rep.3
AH375
1499
Tmem184A
Cdh1
Tpd52l1
Muc1
Map7
Tspan1
Emp2
Tmem30B
Rab25
Pcdh1
Grhl2
Cldn3
Ap1M2
Atp2c2
Esrp1
Cldn7
S100A14
Rasef
Macc1
Cldn4
I
1497
1498
1499
AH375
NB508
J
WST1 (450nm OD fold)
2000
1500
1000
500
0
1497
1498
1499
AH375
NB508
K
H&E
AV
B
M
L
DAPI
p-ERK1/2
c-Myc
p-ERK1/2 + c-Myc

Figure 24. Pancreatic cancer initiation is associated with markers of dedifferentiation
(***A, B***) Tumor volume (*A*) and weight (*B*) 15 days after subcutaneous injection of $5x10^5$ 1499 or AH375 cells into SCID mice. Only AH375 cells form tumors. (***C***) Phenotype and histology of subcutaneous tumors formed by AH375 cells as in (*A-B*). H&E, hematoxylin and eosin. (***D***) Phenotype and histology of tumors formed following orthotopic injection of AH375 cells into the pancreas of SCID mice. H&E, hematoxylin and eosin; AC, normal acinar cells; S, spleen; T, tumor. (***E***) Microarray gene expression analysis using RNA from 1499 and AH375 cells (GEO accession number: GSE57566). A total of 1365 transcripts with a fold change higher or equal to 2 and a $p < 0.05$ according to a two-sample Student's t-test were used for a FatiGO single enrichment analysis with the Babelomics 4.3 platform. The terms obtained which may explain the transformed phenotype of AH375 cells and their associated transcripts are grouped in the indicated general categories. The number of transcripts in each category is indicated. (***F***) Gene Set Enrichment Analysis (GSEA) of microarray data as in (*E*) revealed several gene expression signatures of differentiation in 1499 cells. The most significant is shown (BOSCO_EPITHELIAL_DIFFERENTIATION_MODULE; M2533). (***G***) Several stem cell gene expression signatures showing dedifferentiation in AH375 cells were revealed by GSEA. The most significant is shown (LIM_MAMMARY_STEM_CELL_DN; M2574). (***H***) Numerous gene expression signatures suggest epithelial-mesenchymal transition (EMT) in AH375 cells. The most significant is shown (CHARAFE_BREAST_CANCER_LUMINAL_VS_MESENCHYMAL_UP; M17299). (***I***) Cell lines from PDAC form free-floating tumor spheres, but not cell lines from ADM/PanIN-1 lesions. Scale bar = 400μm. (***J***) Quantification of cell proliferation in (*I*) with the WST-1 cell proliferation assay. The fold of absorbance at 450 nm over a period of 14 days is shown. Average of triplicates ± SD. (***K***) Histology of lung metastasis formed after tail vein injection of $1x10^6$ AH375 cells into SCID mice. B, bronchiole; AV, alveolus; M and black arrows, metastasis. (***L***) Indirect immunofluorescence staining with the indicated antibodies of mouse lung tissues containing metastasis as in (*K*). White arrows, metastasis; scale bar = 100μm. See also Figures S14 and S15.

dedifferentiation and promotion of metastatic pancreatic cancer cells (434, 788). Taken together, our results provide evidence that initiation of pancreatic cancer not only correlates with lower p-Erk levels but is also associated with the acquisition of stem cell-like properties.

Reprogramming into cancer cells with a stem cell-like phenotype depends on low p-ERK levels

In order to evaluate the mechanisms involved in the reprogramming of mouse PDAC-derived cells, we evaluated the transcription factors that could be responsible for the stem cell-like transcriptional profile displayed by AH375 cells. Thus, the promoters of the significantly regulated transcripts in our microarray data were analysed for known transcription factor binding sites with the DIRE platform. Strikingly, several transcription factors with reported

role in development or stemness were found among the most significant candidates (Figure 25A), such as STAT3 (795), NF-κB (201, 796), OCT1 (797), HOXA4 (798), HNF4α (799) and c-MYC/MAX (40). Also, significant gene expression signatures suggesting upregulation of STAT3 and c-MYC in AH375 cells were found, further strengthening a role for these two transcription factors (Figure 25B, C). Notably, other significant gene expression signatures suggest the implication of key signaling pathways associated with stem cells and regulation of c-MYC and STAT3, including WNT signaling (Figure S15A, B) (183, 800), the LIF/STAT3 pathway (Figure S15C) (795) and the NF-kB pathway (Figure S15D) (801). According to the well documented importance of c-MYC and STAT3 in cellular reprogramming, we confirmed that an increased expression of these proteins characterises the PDAC-derived cell lines (Figure 25D). We next addressed whether the molecular and cellular stem cell-like features of the PDAC-derived cell lines depend on low ERK signaling. To hyperactivate the pathway, we took advantage of a dual-specificity phosphatases (DUSPs) inhibitor, BCI (802), which induces a potent activation of ERK signaling. Treatment of the AH375 or NB508 CSC-like cells with 20 μM BCI caused a strong inhibition of tumorigenicity, as shown by inhibition of colony formation in soft agar (Figures 25E, G and S15E, G) and tumor sphere formation (Figures 25F, G and S15F, G). Consistently, decreased Stat3 and c-Myc levels at this concentration correlate with a drastic increase in p-ERK levels (Figures 25H and S15H). Hence, our data suggest that hyperactivation of the ERK kinases circumvents tumorigenicity by restricting the maintenance of stem cell-like properties.

To better characterize the importance of low ERK signaling in the acquisition of a stem cell-like phenotype, we used an *in vitro* model to generate transformed cells with stem cell properties. It was previously reported that the stable expression of hTERT, $HRas^{G12V}$ and two oncoproteins of the Simian Virus 40 Early Region (SV40 ER), namely the large T antigen (LT) and the small t antigen (ST), could induce reprogramming of primary fibroblasts into CSC-like cells (803). Recently, ERK inhibition was shown as being a surrogate for the components of the SV40 ER in hTERT/$HRas^{G12V}$-induced transformation of primary cells (390). Therefore, we reasoned that ERK inhibition could eliminate the barrier against Ras-mediated reprogramming, thereby playing the same role as in conventional production of non-

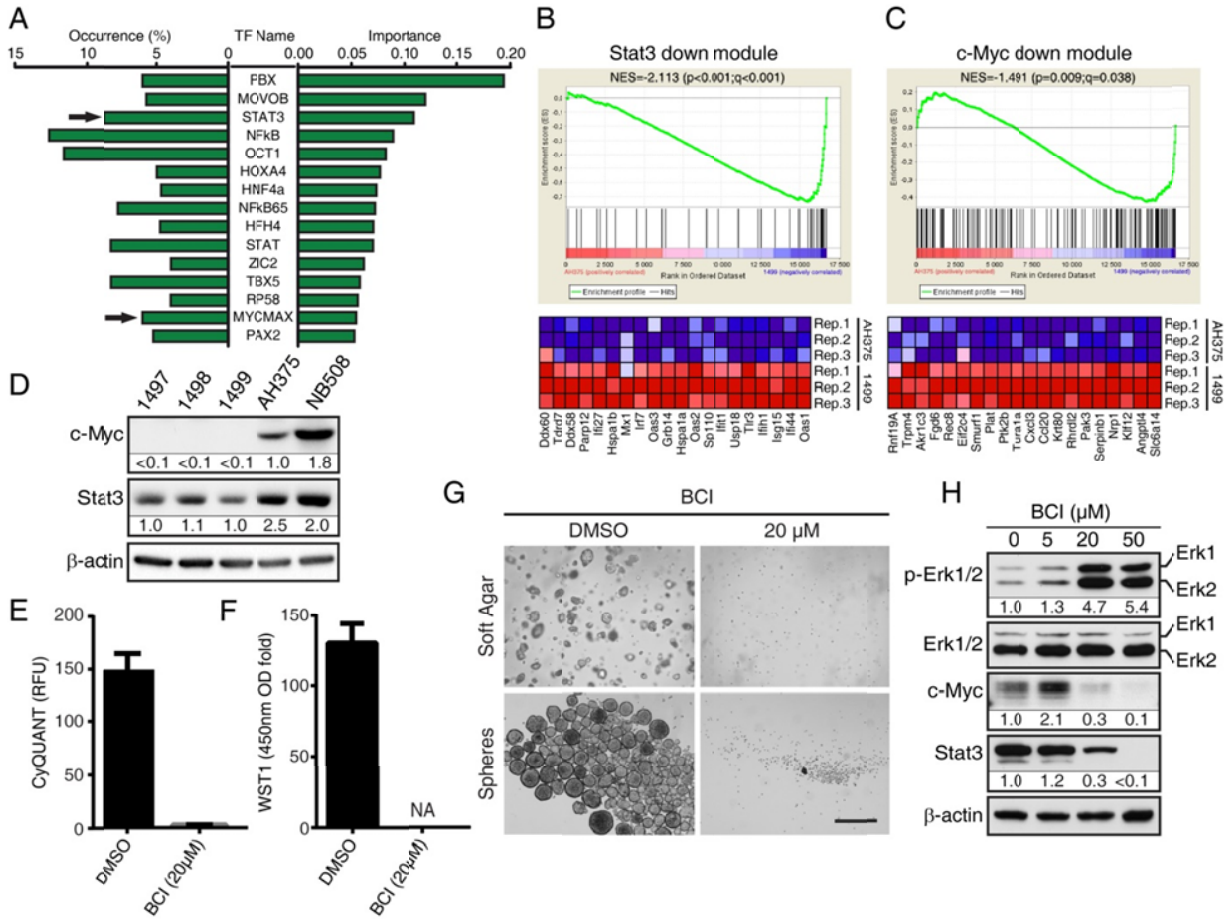

Figure 25. The stem cell-like phenotype depends on low p-ERK levels

(***A***) DIRE prediction of upregulated transcription factors (TFs) in AH375 cells from microarray data as in Figure 24. The percentage of target genes found in the submitted list of transcripts is shown for each potential TF (occurrence). The importance indicates the product of a TF occurrence with is weight in the database. (***B, C***) GSEA found gene expression signatures suggesting upregulation of Stat3 (DAUER_STAT3_TARGETS_DN; M13696) (*A*) and c-Myc (MYC_UP.V1_DN; M2708) (*B*) in AH375 cells. (***D***) Immunoblots with anti-Stat3 and anti-c-Myc antibodies on extracts from the indicated cell lines. (***E***) The DUSP1/6 inhibitor BCI inhibits the capacity of AH375 cells to form colonies in soft agar. Proliferation over a period of 7 days was quantitated using the CyQuant GR dye and expressed as relative fluorescence unit (RFU) at 520 nm. Average of triplicates ± SD. (***F***) The DUSP1/6 inhibitor BCI inhibits the tumor sphere-forming capacity of AH375 cells. Proliferation was quantitated with the WST-1 cell proliferation assay. The fold of absorbance at 450 nm over a period of 7 days is shown. Average of triplicates ± SD. (***G***) Phenotype of colonies in soft agar (top) and tumor spheres (bottom) of cells in (*E-F*). Scale bar = 400μm. (***H***) Immunoblots for the indicated proteins in extracts from AH375 cells treated with the indicated concentration of BCI. Loss of stem cell-like properties correlates with hyperactivation of the ERK/MAP pathway. See also Figure S15.

transformed iPSCs. Combined with the transforming potential of oncogenic *Ras*, the elimination of such a barrier could allow the formation of CSC-like cells and the initiation of tumorigenicity. To reduce the overall ERK activity, we first used Erk2-null MEFs. As shown in a previous report, the expression of oncogenic *Ras* in these cells is sufficient to drive tumorigenesis (Figure 26A) (390). Then, to assess the effect of ERK downregulation in human cells expressing oncogenic *Ras*, we used hTERT-immortalized mammary epithelial cells (HMEC) and fetal lung fibroblasts (IMR90) transduced with a vector expressing an shRNA against ERK2. As already reported, these cells are tumorigenic (Figure 26B, C) (390). Although transformed HMECs formed cystic tumors filled with abundant necrotic cells in nude mice (data not shown), transformed IMR90 formed dense solid tumors. The latter showed the maintenance of low p-ERK levels, proving the stable expression of the shRNA against ERK *in vivo* (Figure 26D). Consistent with the presence of a sub-population of CSC-like cells in the whole population of transformed cells described above, they all formed spheroids, unlike the negative controls (Figure 26E-I). The conditions used as controls of transformation expressed the oncoprotein E1A, which was shown to reduce ERK activity, explaining its ability to promote spheroid formation (390). These results suggest that downregulating ERK signaling allows tumorigenicity of oncogenic *Ras*-expressing cells and promotes the acquisition of a stem cell-like phenotype.

We next evaluated if the phenotype of free-floating tumor spheres reflects a Ras-mediated reprogramming of the gene expression profile consistent with dedifferentiation when the ERK pathway is downregulated. Thus, we profiled and compared the transcriptomes of the low-p-ERK transformed IMR90 cells with a negative control expressing oncogenic *Ras* but a non-targeting shRNA, namely the hTERT/HRas^{G12V}/shERK-expressing cells versus the hTERT/HRas^{G12V}/shCTR-expressing cells. The analysis of the microarray data first revealed gene expression signatures clearly showing a decrease of the ERK pathway activity in hTERT/HRas^{G12V}/shERK-expressing cells, providing compelling evidence that manipulating ERK levels greatly affects the output of ERK signaling (Figure 26J, K). We next performed a FatiGO single enrichment analysis on the microarray data to infer the biological functions significantly altered between the two conditions. Obviously, many of the significantly

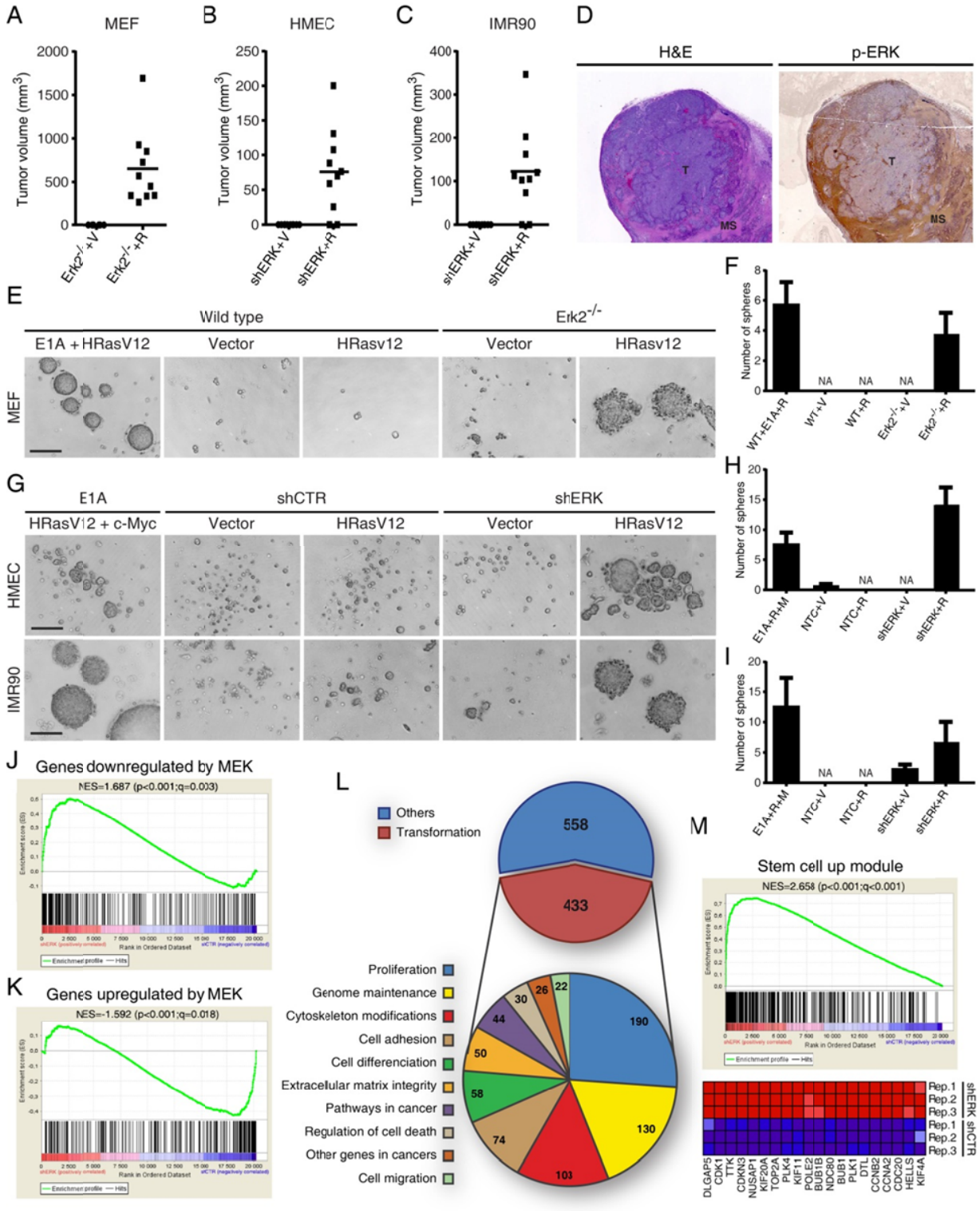
A
MEF
Tumor volume (mm3)
2000
1500
1000
500
0
Erk2-/- +V
Erk2-/- +R
B
HMEC
Tumor volume (mm3)
250
200
150
100
50
0
shERK+V
shERK+R
C
IMR90
Tumor volume (mm3)
400
300
200
100
0
shERK+V
shERK+R
D
H&E
p-ERK
T
MS
T
MS
E
Wild type
Erk2-/-
E1A + HRasV12
Vector
HRasv12
Vector
HRasv12
MEF
F
Number of spheres
8
6
4
2
0
NA
NA
NA
WT+E1A+R
WT+V
WT+R
Erk2-/- +V
Erk2-/- +R
G
E1A
shCTR
shERK
HRasV12 + c-Myc
Vector
HRasV12
Vector
HRasV12
HMEC
IMR90
H
Number of spheres
20
15
10
5
0
NA
NA
E1A+R+M
NTC+V
NTC+R
shERK+V
shERK+R
I
Number of spheres
20
15
10
5
0
NA
NA
E1A+R+M
NTC+V
NTC+R
shERK+V
shERK+R
J
Genes downregulated by MEK
NES=1.687 (p<0.001;q=0.003)
Enrichment score (ES)
Rank in Ordered Dataset
shERK (positively correlated)
shCTR (negatively correlated)
Enrichment profile
Hits
K
Genes upregulated by MEK
NES=-1.592 (p<0.001;q=0.018)
Enrichment score (ES)
Rank in Ordered Dataset
shERK (positively correlated)
shCTR (negatively correlated)
Enrichment profile
Hits
L
Others
Transformation
558
433
Proliferation
Genome maintenance
Cytoskeleton modifications
Cell adhesion
Cell differenciation
Extracellular matrix integrity
Pathways in cancer
Regulation of cell death
Other genes in cancers
Cell migration
190
130
103
74
58
50
44
30
26
22
M
Stem cell up module
NES=2.658 (p<0.001;q<0.001)
Enrichment score (ES)
Rank in Ordered Dataset
shERK (positively correlated)
shCTR (negatively correlated)
Enrichment profile
Hits
Rep.1
Rep.2
Rep.3
shERK
Rep.1
Rep.2
Rep.3
shCTR
DLGAP5
CDK1
TTK
CDKN3
NUSAP1
KIF20A
TOP2A
PLK4
KIF11
POLE2
BUB1B
NDC80
BUB1
PLK1
DTL
CCNB2
CCNA2
CDC20
HELLS
KIF4A

Figure 26. Low p-ERK levels promote stem cell-like properties in Ras-induced transformation of primary cells

(***A***) Volume of solid tumors 32 days after subcutaneous injection of $1x10^6$ Erk2-null mouse embryonic fibroblasts (MEF) transduced with an empty vector (V) or a vector to express $HRas^{G12V}$ (R) into BALB/c nude mice. (***B***) Volume of cystic tumors 32 days after subcutaneous injection of $1x10^6$ normal human mammary epithelial cells (HMEC) transduced with an shRNA targeting ERK2 (shERK), a vector to express hTERT and an empty vector (V) or a vector to express $HRas^{G12V}$ (R) into BALB/c nude mice. (***C***) Volume of solid tumors 32 days after subcutaneous injection of $1x10^6$ normal human fibroblasts from the lung (IMR90) transduced as in (*B*) into BALB/c nude mice. (***D***) Representative immunohistochemical staining with anti-p-ERK of tumors as in (*C*). (***E***) Tumor sphere formation assay with wild type or Erk2-null MEF expressing the indicated vectors. Scale bar = 200μm. (***F***) Number of spheres from an initial plating of 1000 cells as in (*E*). Average of triplicates ± SD. (***G***) Tumor sphere formation assay with HMEC and IMR90 cells expressing hTERT and the indicated vectors. Scale bar = 200μm. (***H, I***) Number of spheres from an initial plating of 1000 HMEC (*H*) or IMR90 (*I*) cells as in (*G*). Average of triplicates ± SD. (***J, K***) RNA from IMR90 cells stably expressing hTERT, $HRas^{G12V}$ and shRNA against ERK2 (shERK) or a non-targeting shRNA (shCTR) was collected for microarray gene expression analysis (GEO accession number: GSE33613). GSEA revealed gene expression signatures of genes known as downregulated by active MEK in cells expressing an shERK2 (MEK_UP.V1_DN; M2724) (*J*) and genes known as upregulated by active MEK in cells expressing an shCTR (MEK_UP.V1_UP; M2725) (*K*). (***L***) A total of 1048 transcripts [microarray as in (*J*)] with a fold change higher or equal to 2 and a $p < 0.05$ according to a two-sample Student's t-test were used for a FatiGO single enrichment analysis with the Babelomics 4.3 platform. The terms obtained which may explain the transformed phenotype of the IMR90 hTERT/ $HRas^{G12V}$/shERK-expressing cells and their associated transcripts are grouped in the indicated general categories. The number of transcripts in each category is indicated. (***M***) Several stem cell gene expression signatures showing dedifferentiation in IMR90 hTERT/ $HRas^{G12V}$/shERK-expressing cells were revealed by GSEA. The most significant is shown (WONG_EMBRYONIC_STEM_CELL_CORE; M7079). See also Figure S16.

regulated genes can have roles in the process of cellular transformation, and these can be classified in general subcategories (Figure 26L). However, many of these genes and the function they mediate, such as the genes involved in proliferation and genome maintenance, may reflect the bypass of Ras-induced cellular senescence reported previously (Figure S16A) (390). Indeed, several gene expression signatures indicate a bypass of senescence (Figure S16B, C) and of its associated phenotypes (Figure S16D-H). Nevertheless, regulation of the genes affecting differentiation is among one of the most important changes that are less likely to overlap with a bypass of senescence (Figure 26L). As further support for reprogramming into a gene expression profile conductive to dedifferentiation, multiple gene expression modules associated with stemness were significantly enriched in hTERT/$HRas^{G12V}$/shERK-

expressing cells (Figure S16I). Also, we found that similarly to the PDAC-derived stem-like cells and in agreement with previous observations, the Ras-transformed IMR90 cells with low p-ERK levels exhibited higher levels of STAT3 and c-MYC than the Ras-senescent IMR90 cells with high p-ERK levels (Figure S16J-L) (390). Taken together, our results suggest that ERK signaling prevents Ras-mediated reprogramming into a tumorigenic stem-like state.

To ascertain that the presence of CSC-like cells with low ERK signaling is an observable phenomenon in human cancers, we first screened multiple human cancer cell lines, from various cancer types, for the capacity to form tumor spheres (Table SV). The majority of the cell lines tested were able to proliferate in tumor sphere-forming conditions (Figure S17A). However, this proliferative potential was not necessarily associated with the capacity to form tumor spheres (Figure S17B). Indeed, some cell lines were able to proliferate in suspension as single detached cells or in agglomeration of easily distinguishable cells. Only the cell lines forming well-defined spheres with indistinguishable individual cells were considered positive for tumor sphere formation (Figure S17C). We selected two tumor sphere-forming cell lines, the pancreatic cancer cell line HPAF-II and the lung cancer cell line NCI-H1299. In order to evaluate if the subpopulation of tumor sphere-initiating cells exhibits lower levels of p-ERK than the other cells in these cell lines, we first amplified the population of CSC-like cells. Thus, we cultivated the cells in the same CSC medium, but in adherent condition (2D culture) or in non-adherent condition in order to allow only proliferation of the CSC-like cells forming free-floating tumor spheres (3D culture). Then, we compared the activation of the ERK kinases in the 2D and 3D cultures. Just like the mouse NB508 cell line containing a sub-population of low p-Erk stem cell-like cells, both human cancer cell lines showed lower levels of p-ERK in the 3D culture (Figure S17D, E). These results thus support the idea that cancer cells with low p-ERK levels may represent CSC-like cells.

Metformin targets reprogrammed cancer cells with low p-ERK levels

Although the role of CSCs in cancer is still under debate, these cells are thought to contribute to resistance to several therapies and to the process of metastasis. Also, their highly tumorigenic potential is now well established (176). Hence, a clinical need to target these cells

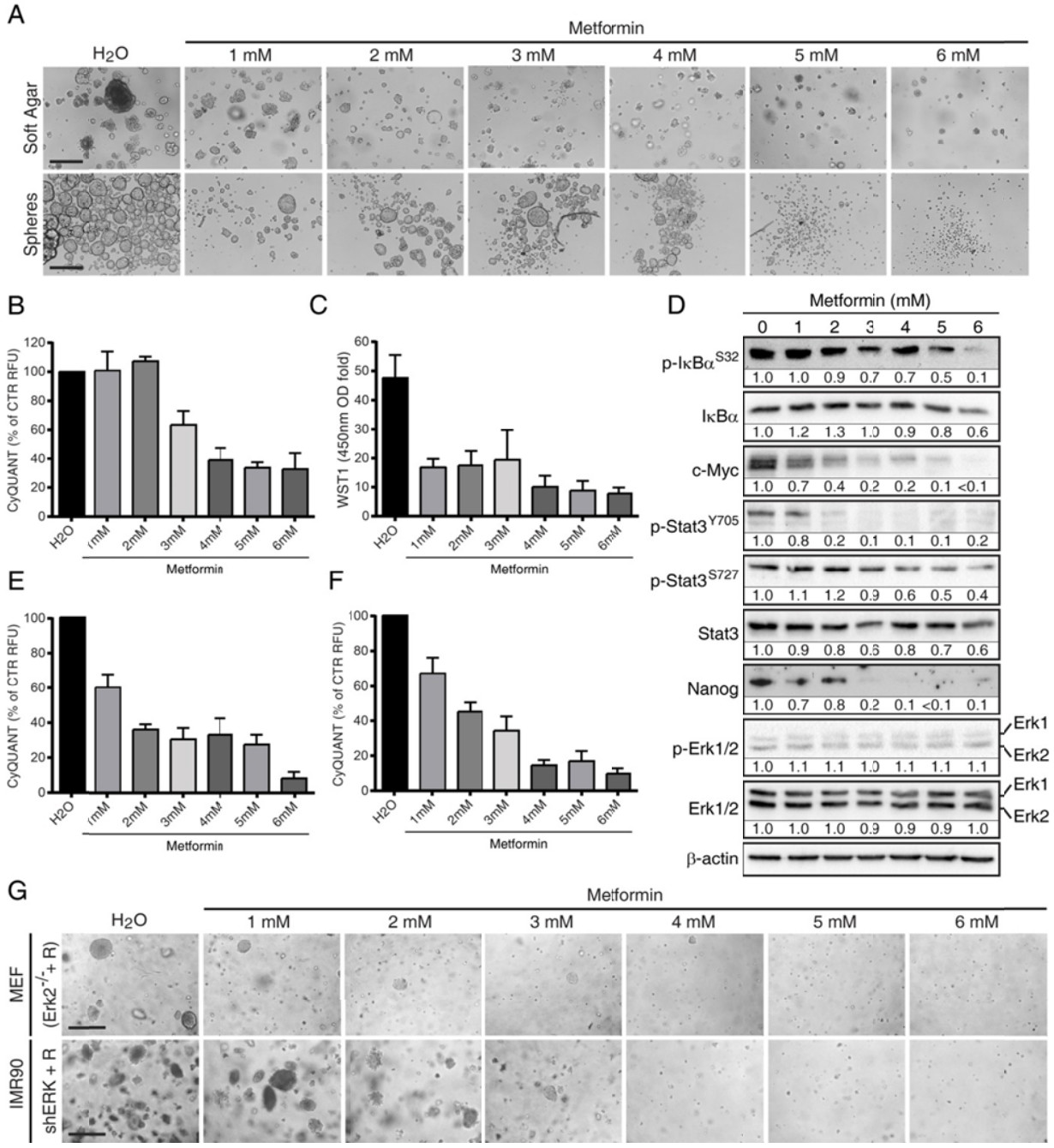

Figure 27. Metformin targets CSC-like cells with low p-ERK levels

(***A***) Metformin inhibits the capacity of AH375 cells to form colonies in soft agar (*top*) and tumor spheres (*bottom*). Scale bar = 200μm. (***B***) Quantification of proliferation over a 7-days period in soft agar of cells as in (*A*) using the CyQuant GR dye. The relative fluorescence unit (RFU) at 520 nm of the control (H_2O) is expressed as 100% and the other results are expressed as the percent of control. Average of triplicates ± SD. (***C***) Proliferation of tumor spheres in (*A*) over a period of 7 days is expressed as the fold of absorbance at 450 nm after coloration with the WST-1 cell proliferation assay.

Average of triplicates ± SD. (***D***) Immunoblots for the indicated proteins in extracts from AH375 cells treated with the indicated concentrations of metformin. (***E, F***) Quantification of proliferation over a period of 7 days in soft agar as in (*B*) of MEF (*E*) and IMR90 (*F*) shown in (*G*). Average of triplicates ± SD. (***G***) Metformin inhibits the capacity of $HRas^{G12V}$ (R)-transformed Erk2-null MEF and IMR90 (hTERT+shERK) to form colonies in soft agar. Scale bar = 400μm. See also Figure S18.

is emerging. Earlier studies suggested that biguanides, such as metformin, selectively deplete the pool of CSCs (441, 446). We thus tested whether metformin interferes with the expansion of the CSC-like cells with low p-ERK levels, and if such an effect could depend on the activation of the ERK pathway. We found that metformin has a potent inhibitory effect on the formation of AH375 cell colonies in soft agar (Figure 27A, B), and even more on tumor sphere formation (Figure 27A, C). This effect occurs in conjunction with reduction of the stem cell marker Nanog, decrease of c-Myc levels and reduction of activated (phosphorylated) but not total levels of STAT3 (Figure 27D). An inhibition of the NF-κB pathway was also observed at higher concentrations, as seen by a decrease of IκBα phosphorylation (Figure 27D). However, metformin had no effects on p-ERK levels, suggesting that the effect of metformin is independent of the ERK signaling pathway (Figure 27D). Further strengthening this hypothesis, metformin still has a profound effect on tumorigenicity when used on transformed MEF and IMR90 cells where ERK activity is attenuated by genetic interventions (Figure 27E-G). Of note, the effect of metformin on CSC-like cells is also seen in human cancer cell lines, where it inhibits tumor sphere formation or greatly reduces the size of the spheres depending on the cell line (Figure S18A, B). Collectively, these results suggest that metformin could be a valuable tool to target CSCs, without the adverse effect of increasing ERK signaling in the other cells of the tumor.

3.3.5 Discussion

Our results define a novel anti-tumor effect of ERK signaling and suggest that processes attenuating ERK activity may promote reprogramming into CSC-like cells, thereby contributing to tumor initiation, therapy resistance and metastasis. To reconcile this function of the ERK pathway with its well-known role in tumor growth (Deschênes-Simard et al., 2014) and the contribution of its hyperactivation in cellular senescence (390), we propose a model where the outcome of the pathway depends on signaling strength (Figure 28).

According to this model, low levels of activated ERK promote dedifferentiation, whereas moderate levels promote proliferation of the bulk tumor cells. Then, higher levels limit cancer initiation and maintenance by activating cellular senescence, a potent tumor-suppressor mechanism (73, 349).

ERK signaling, reprogramming and senescence: is there a link?

Reprogramming tumor cells into CSC-like cells is reminiscent of the *in vitro* generation of iPSCs. This implies that similar mechanisms can be shared between both processes. *In vitro* reprogramming of somatic cells is a stepwise and stochastic phenomenon, with a very low efficiency. Interestingly, the induction of cellular senescence has been shown to counteract the process (804-808). Accordingly, the selection of mechanisms allowing a bypass of senescence is a rate-limiting step towards the establishment of iPSCs (809).

Similarly to somatic cell reprogramming, the initiation of tumorigenesis by oncogenic hits is a multistep process. Also, classical oncogenes have been shown to promote reprogramming (434), and cellular senescence is a well-established tumor-suppressive barrier (67). We and others thus extrapolate that cellular senescence activated by aberrant oncogenic signaling, such as hyperactivation of the ERK/MAPK pathway, could suppress tumor formation by limiting the generation of CSCs (67). Hence, decreasing ERK activity in senescent cells may overcome this barrier, allowing the completion of the reprogramming process into "dedifferentiated" and tumorigenic cancer cells (Figure 28A).

Beyond p-ERK levels: what are the mechanisms?

Up to now, neither what regulates ERK signaling during reprogramming, nor the mechanisms by which high ERK signals circumvent the process are clear. The regulation of ERK activity is complex and involves several phosphatases and negative regulators acting upstream of the pathway. These can have redundant effects and context-dependent importance depending on the cell type. Thus, much more investigation is required to evaluate the respective contribution of the ERK pathway regulators in reprogramming. Nevertheless, studies in ESCs suggest potential candidates. Indeed, many DUSPs have been shown to restrict ERK activity in these cells (810-812). Interestingly, DUSP2 and 7 have been shown to

be regulated by c-MYC, which is thought to play an important role in CSCs (788, 812). However, although we found several DUSPs that are regulated at the mRNA level in our microarray analyses (data not shown), it is not yet clear whether they play a significant role in the ERK pathway activity during reprogramming. Also, DUSPs could be regulated post-translationally and this effect does not appear in our microarray data. Another family of ERK negative modulators that could play a role in CSCs is suggested by the biology of progenitor cells. Sprouty Homolog 1 (SPRY1) and Sprouty-related protein with EVH-1 (SPRED1) have been shown to negatively regulate the ERK/MAPK pathway at the level of RAF, thereby suppressing differentiation (813, 814). Interestingly, both SPRY1 and SPRED1 are upregulated at the mRNA level in AH375 cells compared to 1499 cells (data not shown). Also, despite the fact that the downregulation of ERK signaling in the mouse PDAC-derived cell lines is more evident at the level of MEK, a visible decrease in RAF phosphorylation is visible (Figure 23F).

The other major challenge we face is to determine how ERK signaling opposes reprogramming. According to the broad range of ERK targets and functions, much more investigation is again required in order to have a clear answer. High ERK signals have been shown to target c-MYC and STAT3 for degradation during cellular senescence (390), and this mechanism could play a role in other contexts where ERK signaling is sustained, such as during differentiation. Notably, bypassing senescence by downregulating ERK signaling promotes the stabilization of these transcription factors and facilitates reprogramming into CSC-like cells (Figures 26 and S16). Consistent with a mechanism involving ERK-induced degradation of multiple factors associated with reprogramming, the ERK1/2 kinases have been shown to drive the degradation of KLF4, thereby inducing ESC differentiation (815). However, it is not excluded that ERK also regulates stem cell factors by transcriptional or post-transcriptional mechanisms as reported for the control of NANOG expression (816, 817).

Clinical implication of CSC-like cells with low p–ERK levels

CSCs are associated with tumor initiation, tumor recurrence, resistance to several cancer therapies and the process of metastatic tumor formation (176). These cells actually

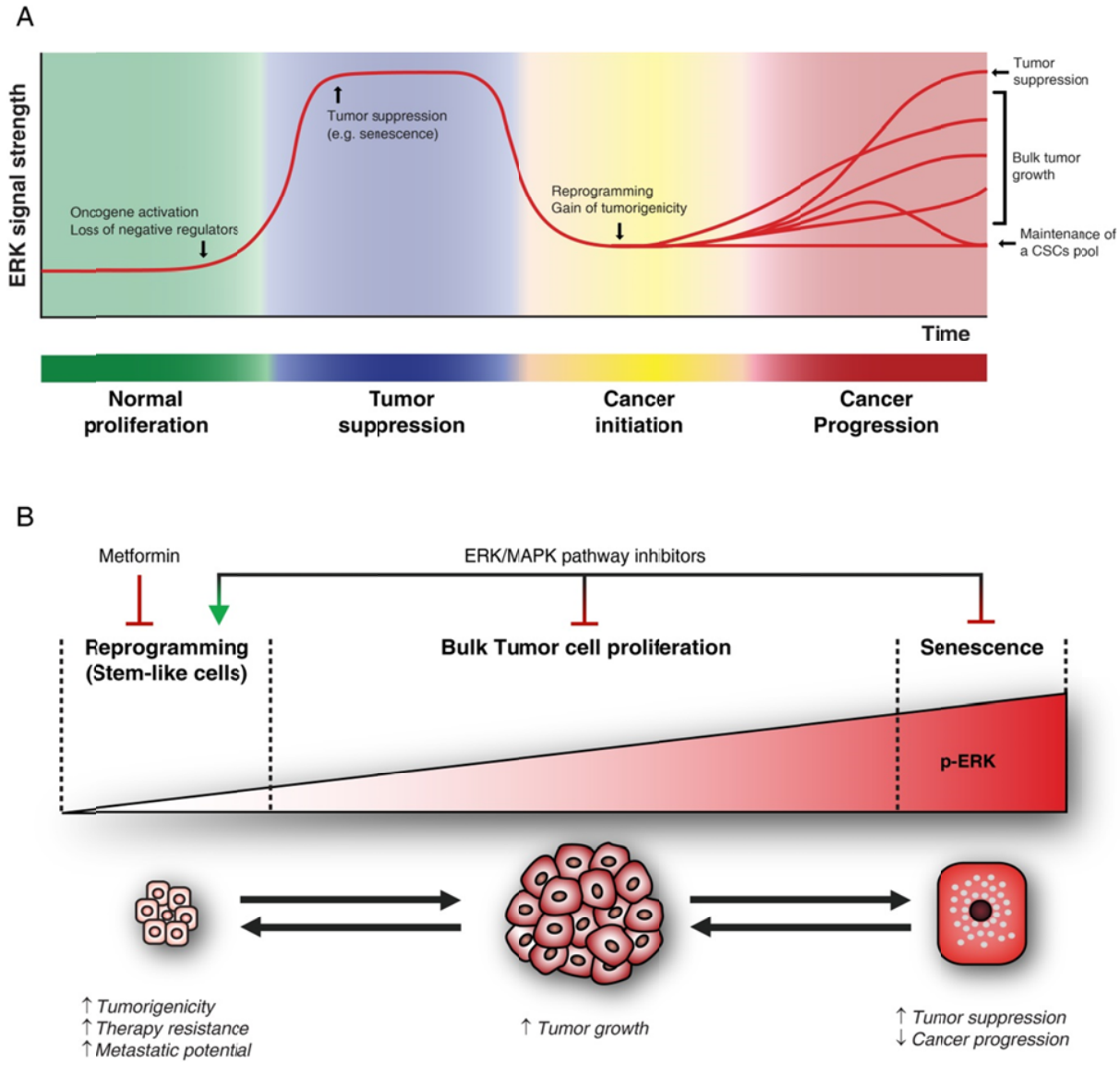

Figure 28. Models of ERK signaling in cancer initiation and maintenance

(***A***) Model of ERK signaling during cancer initiation and progression. Following oncogene activation or loss of negative regulators of the ERK/MAPK pathway, strong ERK signals trigger tumor-suppressive responses, such as cellular senescence. Then, negative regulators of the pathway reduce its activation, allowing a bypass of tumor suppression and reprogramming into cancer stem cells (CSCs). Following "differentiation", the CSCs promote a heterogeneous tumor, where the more differentiated cells constitute to the bulk of the tumor and depend on higher ERK signaling. Although it is not depicted in the model, there is the possibility that oncogenic lesions hit normal stem cells with low ERK activity. Cellular senescence could not be induced in this case and additional mutations could be required for tumor growth. (***B***). Model of the outcome of the ERK/MAPK pathway within an established tumor. Cancer cell plasticity depends on ERK signaling strength. The bulk tumor consists

of "differentiated" cancer cells, and their maintenance depends on moderate ERK activity. Nevertheless, low ERK signaling is critical to maintain a subpopulation of CSCs, whereas hyperactivation of the pathway reactivate tumor-suppressive barriers. The modulation of the pathway allows the cells to move from one state to another. This model suggest that the use of ERK/MAPK pathway inhibitors could be a good strategy to target the bulk tumor cells, but adversely circumvents cellular senescence and promotes reprogramming into CSCs. Metformin targets the latter and could be combined with ERK/MAPK pathway inhibitors.

challenge our current therapeutic strategies and may explain several cases of therapeutic failure. This is especially true concerning the use of ERK/MAPK pathway inhibitors. Multiple groups have shown that resistance to RAF and MEK inhibitors, which are upstream regulators of the ERK pathway, could be caused by reactivation of ERK activity (349). This effect could actually contribute to proliferation of residual "differentiated" cancer cells from the initial bulk tumor, explaining several relapses and clinical trial failures after treatments which such inhibitors (349). However, our work suggests another possibility, complementary to the latter. Indeed, we hypothesize that these inhibitors could have an effect as reported for the reprogramming of somatic cells into iPSCs. In this situation, inhibition of the ERK pathway prevents proliferation of normal cells, but promotes their reprogramming into iPSCs and allows the expansion of the latter (818). Hence, targeting the ERK/MAPK pathway may be a valuable strategy to inhibit the maintenance of the bulk tumor cells when they depend on aberrant signaling through this pathway (Figure 28). However, perhaps this approach does not affect the CSCs. Even worse, such a treatment could have the adverse effect of promoting dedifferentiation, thereby increasing the pool of CSCs (Figure 28B). The subsisting CSCs could thus give rise to a new tumor.

Metformin: a promising drug to fight CSC-like cells

Our results highlight the importance of targeting cells with low p-ERK levels within a tumor. We suggest that the use of metformin, with its reported anti-CSCs activities (441), could be an interesting avenue (Figure 28B). Despite the fact that the exact mechanisms by which metformin inhibits CSCs expansion are still largely unknown, these could involve the direct inhibition of STAT3 (Figure 27D) (447, 448). A previous report showed that a positive feedback loop between NF-κB and STAT3 activation could be required for the self-renewal of

CSCs (801). Interestingly, our work has shown that metformin also inhibits the NF-κB pathway at higher concentrations (Figure 27D) (819), and this effect possibly contributes to the inhibition of CSCs growth (447). Finally, metformin may interfere with c-MYC expression (Figure 27D) (449, 450). Taken together, these observations suggest that metformin could be a powerful drug to eliminate CSCs by acting at multiple levels. Considering this effect of metformin and previous reports on tumor recurrence after its combination with chemotherapeutic agents, the addition of this drug to conventional therapies targeting the bulk tumor cells could be a promising strategy to reduce cancer relapses (446, 820). This could be particularly true with inhibitors of the ERK/MAPK pathway, where a predicted side effect is an increased reprogramming of cancer cells into CSCs. The depletion of a pool of CSCs could thus be another explanation for the therapeutic benefit of phenformin, a metformin analogue, when combined with a RAF inhibitor (821). Such a strategy may inhibit the proliferation of the bulk tumor cells driven by aberrant ERK signaling, while preventing cellular reprogramming into CSCs able to generate a new tumor (Figure 28B). Importantly, combination therapies with metformin could target CSCs without increasing ERK signaling, which may have undesirable effects on proliferation of the other, more differentiated cancer cells.

3.3.6 Experimental Procedures

Mouse Experiments

All mouse experiments were approved by the University of Montreal animal ethics committee (CDEA) or the subcommittee on research animal care of the Massachusetts General Hospital. For *immunohistochemical studies* of the multistage initiation of pancreatic cancer, *Pdx1-Cre;LSL-KRas*^{G12D} mice were sacrificed at 9 (n = 3), 24 (n = 7) or 50 (n = 4) weeks after birth and pancreas were collected and fixed in formalin for paraffin embedding. For *subcutaneous xenografts*, 5 x 10^5 or 1 x 10^6 of the specified cells were suspended in 50 µL PBS mixed with 50 µL Matrigel (#356234, BD Biosciences), and then injected subcutaneously into the lower flank of SCID mice (C3SnSmn.CB17-*Prkdc*^{scid}/J, Jackson Labs) or BALB/c nude mice (CAnN.Cg-*Foxn1*^{nu}/Crl, Charles River) under sterile condition and using a 30-gauge needle. Both flanks were used as injection sites. Mice were euthanized after

the indicated time, tumors were weighed and their volumes were calculated according to the formula (length x width^2)/2. Tumors were fixed in formalin for paraffin embedding. For *orthotopic xenografts* into the pancreas, SCID mice were subjected to general anesthesia with intraperitoneal injection of Avertin (0.5 mg/g). A left lateral laparotomy was performed in order to visualize the spleen and then mobilize the distal pancreas. Approximately 100 µL of cell suspension (50 µL PBS and 50 µL Matrigel) containing 5 x 10^5 AH375 cells were injected into the pancreas. The abdominal incision was closed using silk suture 3/0 (K943H, Ethicon) for the peritoneum and the skin. The mice were inspected daily for a week for any health complication and were examined for tumor formation by palpation. Mice were euthanized after a maximum of 21 days and pancreas were fixed in formalin for paraffin embedding. For *tail vein assay of cancer metastasis*, SCID mice were injected as described previously (Elkin and Vlodavsky, 2001). Briefly, a suspension of 1.25 x 10^6 cells/mL was prepared in divalent cation-free PBS. The mice were placed in a restrainer and the tails were immerged in warm water (50-60^{o}C) for 2 minutes in order to dilate the veins. Then, 200 µL of the cell suspension were injected into the lateral tail vein using a 3/10 cc syringe with a 29G ½'' needle. Mice were euthanized 3 weeks after injection and lungs were collected and fixed in formalin for paraffin embedding.

Histology and Immunohistochemical Analyses

Pancreatic tissue samples from 16 patients diagnosed with PDAC and/or pre-malignant lesions, including ADM and PanINs, were analysed for p-ERK levels and KI-67 expression. Specimens were obtained from consenting patients and the experiments were performed in accordance with the Partners Healthcare Institutional Review Board (IRB) policies. Pancreatic tissue samples from 14 *Pdx1-Cre;LSL-KRas^{G12D}* mice were also analysed for p-Erk levels and Ki-67 expression. The protocol and details on the antibodies used are given in the Supplemental Experimental Procedures. H&E and immunostained slides were analysed with an Olympus DP72 microscope. Lesions and colorations have been validated by a pathologist. For KI-67, the percentage of stained epithelial cells was evaluated in the different types of lesions. For p-ERK, a grading system based on a scale of 4 staining intensities was used (0 for

no staining to 3 for strong staining). The percentage of epithelial cells for each intensity was evaluated in the different types of lesions

Cell Culture and Viral-mediated Gene Transfer

Human cancer cell lines were obtained from the American Type Culture Collection (ATCC) or from the Massachusetts General Hospital Center for Molecular Therapeutics (CMT). IMR90 cells were obtained from ATCC, HMEC are from Lonza and the immortalized HPDE cells were established and characterized previously (822). Erk2-null MEFs were a kind gift of Dr. Sylvain Meloche (IRIC, University of Montréal, Qc, Canada) and their preparation was previously described (257). 1497, 1498 and 1499 pancreatic ductal cell lines were isolated from 9-week-old *Pdx1-Cre;LSL-KRas*^{G12D} mice as reported previously (200). The transformed AH375 pancreatic ductal cell line was established from a 52-week-old *Pdx1-Cre;LSL-KRas*^{G12D} mouse. The procedure used for isolation of 1497, 1498, 1499 and AH375 cells is detailed in the Supplemental Experimental Procedures. The NB508 PDAC cell line was established from the *Pdx1-Cre;LSL-Kras*^{G12D}*;p53*$^{Lox/+}$*;p16*$^{+/-}$ mouse model as described previously (823). Cells were cultured in the following conditions: IMR90, HPAF-II, MEF and NCI-H1299 in DMEM (#319-015-CL,Wisent) supplemented with 10% fetal bovine serum (FBS; Wisent) and 1% penicillin G/streptomycin sulfate (P/S; Wisent); HMEC in 90% MEGM completed with bovine pituitary extract (BPE), human recombinant Epidermal Growth Factor (hEGF), insulin, hydrocortisone and Gentamicin/Amphotericin as provided in the MEGM Bullet kit (CC-3150; Lonza) and 10% DMEM supplemented with 10% FBS and 1% P/S; NB508 in RPMI (#350-000-CL, Wisent) supplemented with 10% FBS and 1% P/S; 1497, 1498, 1499 and AH375 cells were propagated on surfaces coated with laminin (#354239, BD Biosciences) in pancreatic medium, consisting of DMEM-F12 (#11330-032, Gibco) supplemented with 5 mg/mL D-glucose, 1.22 mg/mL Nicotinamide (N-3376, Sigma), 5 nM 3,3',5-triiodo-L-thyronine (#91990, Sigma), 1 µM Dexamethasone (D1756, Sigma), 100 ng/mL Cholera toxin (C8052, Sigma), 5 mL/L ITS+ (#354352, BD Biosciences), 0.1 mg/mL Soybean Trypsin Inhibitor type 1 (T6522, Sigma), 20 ng/mL EGF (#5331-LF, Cell Signaling Technology), 5% Nu-Serum IV (#355104, BD Biosciences), 25 µg/mL Bovine Pituitary Extract (13028-014, Gibco) and 1% P/S. Adherent cells were trypsinized using

trypsine-EDTA 1X (Stock 10X; 325-052-EL, Wisent) except for mouse pancreatic ductal cells. For the latter, cell dissociation was carried out using TrypleE (#12604-013, Gibco). Retroviral and lentiviral-mediated gene transfers were done as described previously (390).

Cell proliferation assays, soft agar assays, sphere-forming assays, immunoblotting procedure, immunofluorescence staining protocol, reagents and plasmids are described in the Supplemental Experimental Procedures

Microarray gene expression analysis

Total mRNA extracts were prepared in TRIzol (#15596-026, Ambion), and their purification was performed according to the manufacturer's instructions. The mRNA solution was further purified using the RNeasy MinElute Cleanup Kit (#74204, Qiagen). Solutions of 100 ng/µL mRNA were sent to the Génome Québec Innovation Centre for RNA processing, hybridation on GeneChip® Human Gene 1.0 ST Array or GeneChip® Mouse Gene 2.0 ST Array (Affymetrix) and data acquisition. The microarray data discussed were deposited in NCBI's Gene Expression Omnibus (GEO) and are accessible through GEO Series accession numbers GSE33613 and GSE57566. More details on the procedure and bioinformatic analyses are presented in the Supplemental Experimental Procedures.

3.3.7 Author contributions

X. Deschênes-Simard performed the immunohistochemical experiments, most cellular and biochemical experiments, subcutaneous xenografts, microarray experiments and conducted data analysis. F. Kottakis helped with xenografts and with IHC scoring on Figures 22, 23 and 24. E. Saint-Germain helped with tumor sphere assays on Figures 26 and S17. K. Moineau-Vallée helped with experiments involving metformin treatments on Figures 27 and S18 and IHC scoring on Figures 22 and 23. R.M. Perera obtained tissues from *Pdx1-Cre;LSL-KRas*^{G12D} mice. Y. Mizukami helped with orthotopic injections on Figure 24. J. Fitamant helped with tail vein injections on Figure 24. M.-F. Gaumont-Leclerc performed the IHC presented on Figure 26D. F. Lessard contributed by conceptual and technical input. X. Deschênes-Simard, F. Kottakis, N. Bardeesy and G. Ferbeyre participated in experimental

design. X. Deschênes-Simard wrote the manuscript and the latter was reviewed by M.-F. Gaumont-Leclerc, F. Lessard, F. Kottakis, N. Bardeesy and G. Ferbeyre.

3.3.8 Acknowledgments

We thank Sylvain Meloche for Erk2-null MEF and Sylvie Mader for breast cancer cell lines. This work was supported by the Vanier Canada Graduate Scholarships Program and Michael Smith Foreign Study Supplements Program to X. Deschênes-Simard. N. Bardeesy is supported by grants from the National Institutes of Health (R01 CA133557-05 and P01 CA117969-07) and the Linda J. Verville Cancer Research Foundation. G. Ferbeyre is a FRSQ national research fellow and is supported by grants from the Canadian Institute of Heath and Research (CIHR MOP11151).

3.3.9 Supplemental Material

3.3.9.1 Supplemental Data

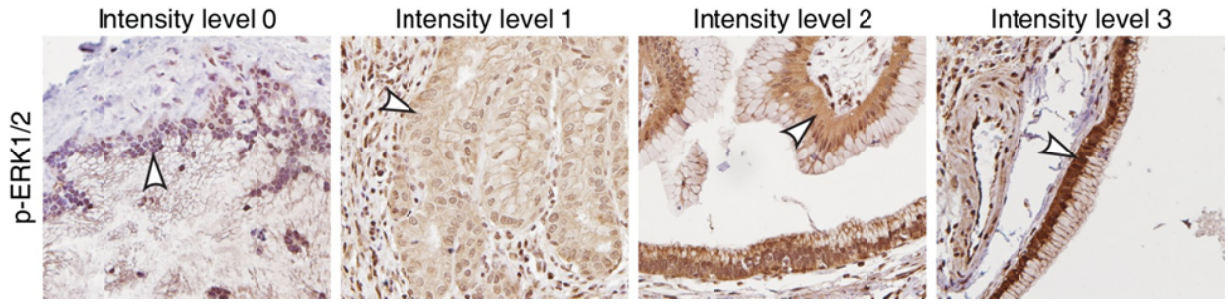

Figure S12. Scoring key for human tissues stained by immunochemistry against p-ERK, Related to Figure 22

Intensity levels used as references for scoring p-ERK staining of human pancreatic tissues. White arrows, epithelial cells considered for staining intensity.

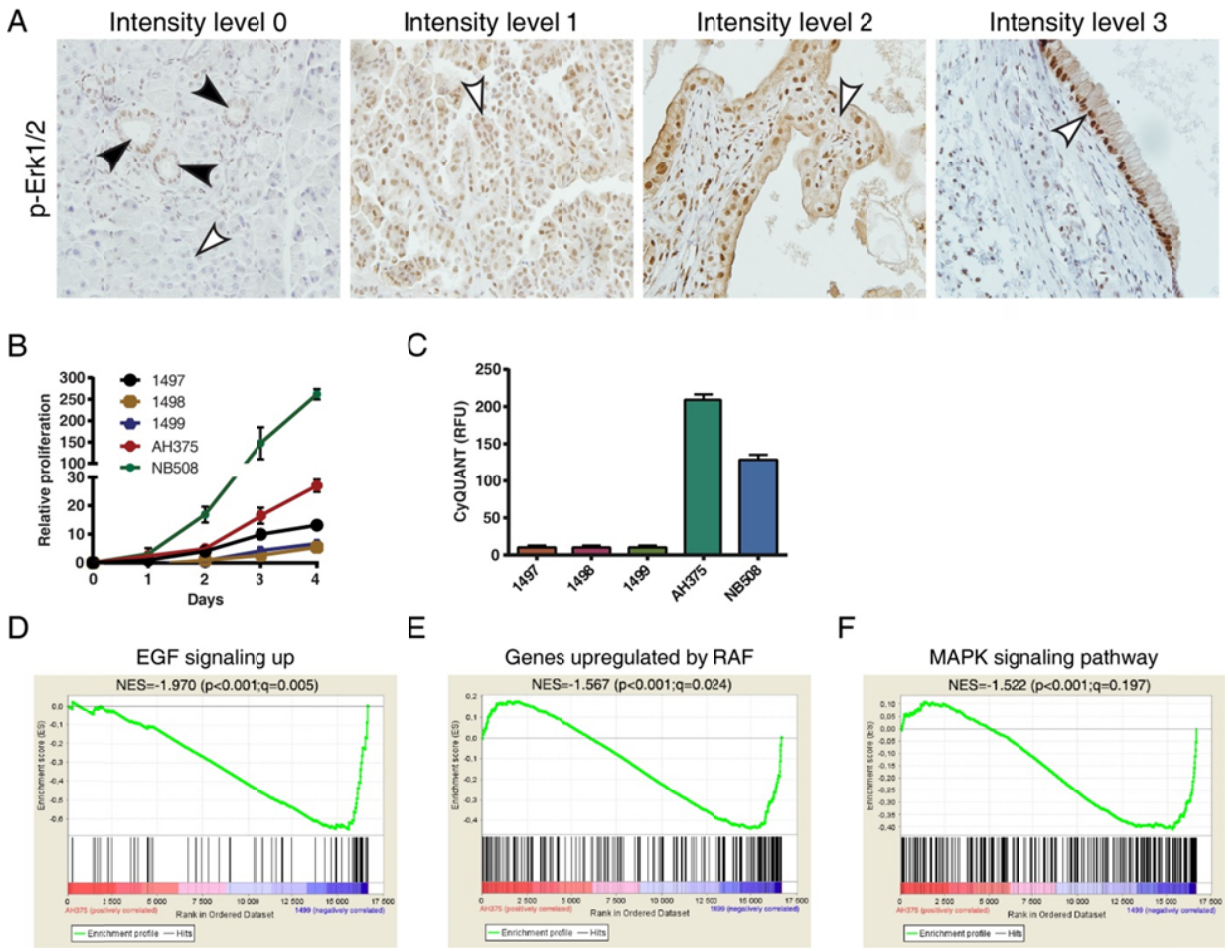

Figure S13. Additional characterization of mouse cells established from KRas-driven pancreatic lesions, Related to Figure 23

(***A***) Intensity levels used as references for scoring p-ERK staining of human pancreatic tissues. White arrows, epithelial cells considered for staining intensity; black arrows, cells to exclude from intensity level 0. (***B***) Proliferation of the indicated mouse cell lines measured by MTT. The relative proliferation represents the fold of OD at 500 nm over the indicated period of time. Each point represents the average of triplicates ± SD. (***C***) Quantification of proliferation in soft agar over a period of 7 days for the indicated cell lines. Results were obtained using the CyQuant GR dye and are expressed as relative fluorescence unit (RFU) at 520 nm. Average of triplicates ± SD. (***D-F***) Microarray data analysis (GEO accession number: GSE57566) by GSEA showing gene expression signatures of EGF signaling (NAGASHIMA_ EGF_SIGNALING_UP; M16311) (*D*), RAF activation (RAF_UP.V1_UP; M2728) (*E*) and MAPK activation (MAP_KINASE_ ACTIVITY; M4513) (*F*) in 1499 cells.

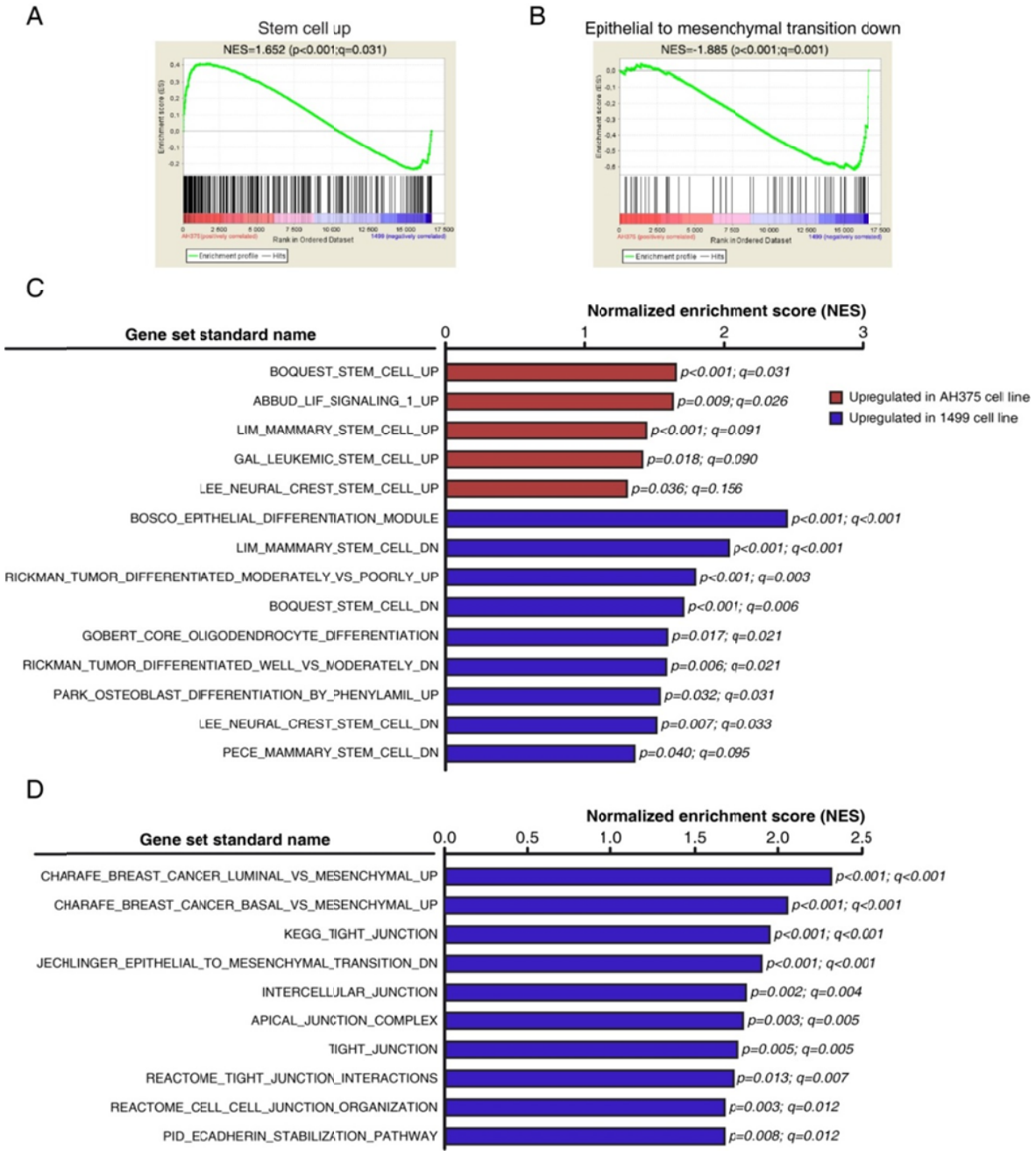

Figure S14. Additional characterization of reprogramming during pancreatic cancer initiation, Related to Figure 24

(***A, B***) Additional gene expression signatures showing stem cell-like properties (BOQUEST_ STEM_CELL_UP; M1834) (*A*) and EMT (ECHLINGER_EPITHELIAL_TO_MESENCHYMAL_ TRANSITION_DN; M1417) (*B*) in AH375 cells. (***C, D***) Compilation of significant gene expression signatures suggesting stem cell-like properties (*C*) and EMT (*D*) in AH375 cells. Red, gene expression module enriched in AH375 cells; Blue, gene expression module enriched in 1499 cells.

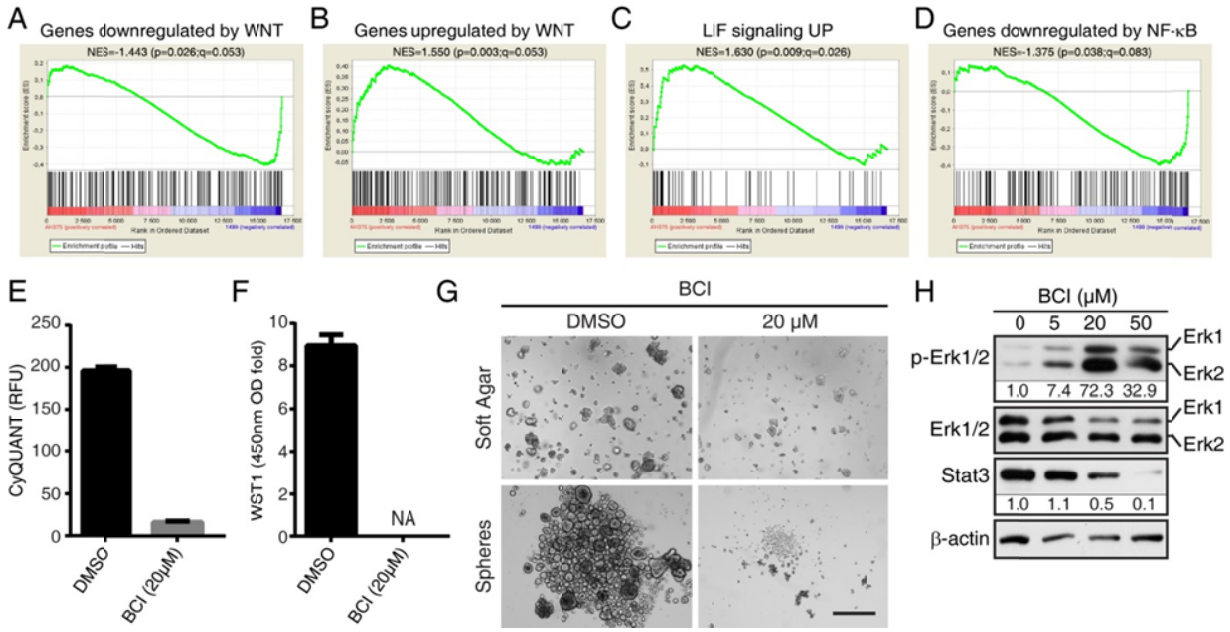

Figure S15. The stem cell-like phenotype and p-ERK levels, Related to Figures 24 and 25 (***A-D***) Gene expression signatures suggesting WNT pathway activation (WNT_ UP.V1_DN; M2689, and WNT_UP.V1_UP; M2690) (*A, B*), LIF signaling (ABBUD_LIF_SIGNALING_ 1_UP; M1458) (*C*) and NF-κB activation (RELA_ DN.V1_UP; M2696) (*D*) in AH375 cells. (***E***) Quantification of the effect of BCI on proliferation in soft agar as in Figure 25E, but for NB508 cells. Average of triplicates ± SD. (***F***) Quantification of proliferation in tumor-sphere forming conditions with BCI as in Figure 25F, but for NB508 cells. Average of triplicates ± SD. (***G***) Phenotype of colonies in soft agar and tumor spheres of cells in (*B-C*). Scale bar = 400μm. (***H***) Immunoblots for the indicated proteins in extracts from NB508 cells treated with the indicated concentration of BCI.

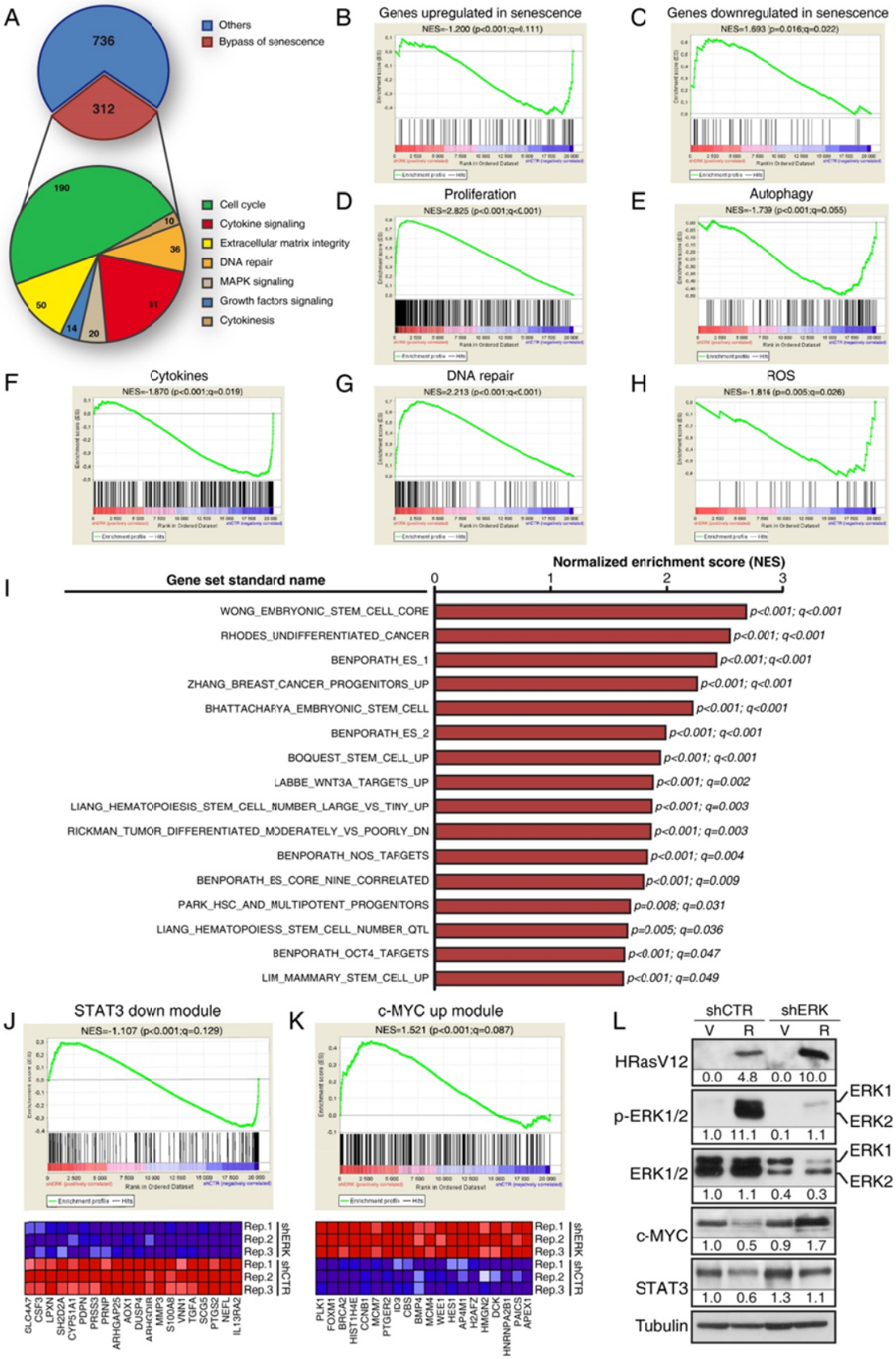
A
736
312
190
10
36
81
20
14
50
Others
Bypass of senescence
Cell cycle
Cytokine signaling
Extracellular matrix integrity
DNA repair
MAPK signaling
Growth factors signaling
Cytokinesis
B
Genes upregulated in senescence
NES=-1.200 (p<0.001;q=0.111)
C
Genes downregulated in senescence
NES=1.693 (p=0.016;q=0.022)
D
Proliferation
NES=2.825 (p<0.001;q<0.001)
E
Autophagy
NES=-1.739 (p<0.001;q=0.055)
F
Cytokines
NES=-1.870 (p<0.001;q=0.019)
G
DNA repair
NES=2.213 (p<0.001;q<0.001)
H
ROS
NES=-1.816 (p=0.005;q=0.026)
I
Gene set standard name
Normalized enrichment score (NES)
0
1
2
3
WONG_EMBRYONIC_STEM_CELL_CORE p<0.001; q<0.001
RHODES_UNDIFFERENTIATED_CANCER p<0.001; q<0.001
BENPORATH_ES_1 p<0.001; q<0.001
ZHANG_BREAST_CANCER_PROGENITORS_UP p<0.001; q<0.001
BHATTACHARYA_EMBRYONIC_STEM_CELL p<0.001; q<0.001
BENPORATH_ES_2 p<0.001; q<0.001
BOQUEST_STEM_CELL_UP p<0.001; q<0.001
LABBE_WNT3A_TARGETS_UP p<0.001; q=0.002
LIANG_HEMATOPOIESIS_STEM_CELL_NUMBER_LARGE_VS_TINY_UP p<0.001; q=0.003
RICKMAN_TUMOR_DIFFERENTIATED_MODERATELY_VS_POORLY_DN p<0.001; q=0.003
BENPORATH_NOS_TARGETS p<0.001; q=0.004
BENPORATH_ES_CORE_NINE_CORRELATED p<0.001; q=0.009
PARK_HSC_AND_MULTIPOTENT_PROGENITORS p=0.008; q=0.031
LIANG_HEMATOPOIESS_STEM_CELL_NUMBER_QTL p=0.005; q=0.036
BENPORATH_OCT4_TARGETS p<0.001; q=0.047
LIM_MAMMARY_STEM_CELL_UP p<0.001; q=0.049
J
STAT3 down module
NES=-1.107 (p<0.001;q=0.129)
Rep.1
Rep.2
Rep.3
shERK
shCTR
GLC4A7
CSF3
LPXN
SH2D2A
CYP51A1
PDPN
PRSS3
PRNP
ARHGAP25
AOX1
DUSP4
ARHGDIB
MMP3
S100A8
VNN1
TGFA
SCG5
PTGS2
NEFL
IL13RA2
K
c-MYC up module
NES=1.521 (p<0.001;q=0.087)
PLK1
FOXM1
BRCA2
HIST1H4E
CCNB1
MCM7
PTGER2
ID3
CBS
BMP4
MCM4
WEE1
HES1
AP4M1
H2AFZ
HMGN2
ZDK
HNRNPA2B1
PAICS
APEX1
L
shCTR
shERK
V
R
V
R
HRasV12
0.0
4.8
0.0
10.0
p-ERK1/2
ERK1
ERK2
1.0
11.1
0.1
1.1
ERK1/2
ERK1
ERK2
1.0
1.1
0.4
0.3
c-MYC
1.0
0.5
0.9
1.7
STAT3
1.0
0.6
1.3
1.1
Tubulin

Figure S16. Low p-ERK levels bypass Ras-induced senescence and promote stemness, Related to figure 26

(***A***) Microarray data as in Figure 26 (GEO accession number: GSE33613) were analysed by a FatiGo single enrichment analysis with the Babelomics 4.3 platform. The terms obtained showing that IMR90 hTERT/HRas^{G12V}/shERK-expressing cells bypass Ras-induced senescence are grouped into the indicated general categories. The number of transcripts in each category is indicated. (***B, C***) Gene expression signatures indicating a bypass of senescence in IMR90 hTERT/HRas^{G12V}/shERK-expressing cells [FRIDMAN_ SENESCENCE_UP; M9143 (*B*), and KAMMINGA_SENESCENCE; M2037 (*C*)]. (***D-H***) The most significant gene expression signatures indicating a bypass of several senescence-associated phenotypes in IMR90 hTERT/HRas^{G12V}/shERK-expressing cells; rescue of proliferation (REACTOME_ CELL_CYCLE; M543) (*D*), decreased lysosomal activity associated to autophagy (KEGG_LYSOSOME; M11266) (*E*), decreased cytokine activity suggesting a bypass of the senescence-associated secretory phenotype (SASP) (KEGG_CYTOKINE_ CYTOKINE_ RECEPTOR_INTERACTION; M9809) (*F*), increased DNA repair (REACTOME_ DNA_REPAIR; M15434) (*G*), decreased generation of reactive oxygen species (HOUSTIS_ROS; M6891) (*H*). (***I***) Compilation of significant gene expression signatures suggesting stem cell-like properties in IMR90 hTERT/HRas^{G12V}/shERK-expressing cells. (***J, K***) Gene expression signatures suggesting upregulation of STAT3 (AZARE_ NEOPLASTIC_TRANSFORMATION_BY_STAT3_DN; M2311) (*J*) and c-MYC (BENPORATH_MYC_TARGETS_WITH_EBOX; M27) (*K*) in IMR90 hTERT/HRas^{G12V}/ shERK-expressing cells. (***L***) Immunoblots for the indicated proteins in extracts from IMR90 cells expressing hTERT and the indicated vectors. shCTR, non-targeting shRNA; shERK, shRNA targeting ERK2; V, empty vector; R, vector expressing HRas^{G12V}. Of note, a condition has been eliminated between shCTR and shERK samples.

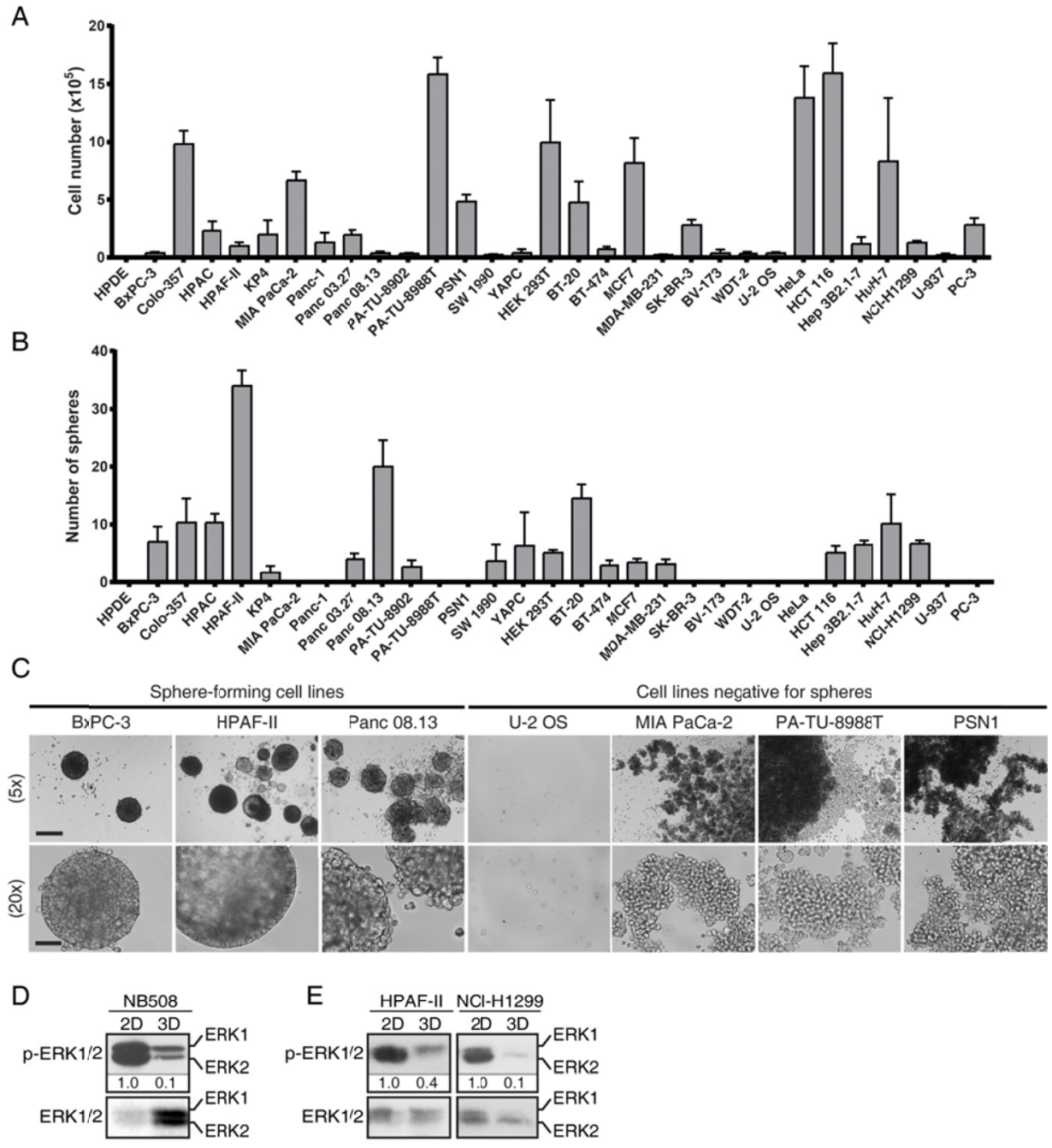
A
Cell number (x10^5)
20
15
10
5
0
HPDE
BxPC-3
Colo-357
HPAC
HPAF-II
KP4
MIA PaCa-2
Panc-1
Panc 03.27
Panc 08.13
PA-TU-8902
PA-TU-8988T
PSN1
SW 1990
YAPC
HEK 293T
BT-20
BT-474
MCF7
MDA-MB-231
SK-BR-3
BV-173
WDT-2
U-2 OS
HeLa
HCT 116
Hep 3B2.1-7
HuH-7
NCI-H1299
U-937
PC-3
B
Number of spheres
40
30
20
10
0
C
Sphere-forming cell lines
Cell lines negative for spheres
BxPC-3
HPAF-II
Panc 08.13
U-2 OS
MIA PaCa-2
PA-TU-8988T
PSN1
(5x)
(20x)
D
NB508
2D
3D
p-ERK1/2
ERK1
ERK2
1.0
0.1
ERK1/2
E
HPAF-II
NCI-H1299
1.0
0.4
0.1

Figure S17. Cancer cell lines with stem cell-like subpopulations associated with low p-ERK levels, Related to Figure 26

(***A***) Proliferation of several human cancer cell lines in tumor sphere-forming conditions. Immortal human pancreatic duct epithelial (HPDE) cells were used as a control of normal cells. Proliferation is expressed as the total of cells per well (24-wells plate) 10 days following an initial plating of 1000 cells. Average of triplicates ± SD. (***B***) Number of spheres for cells and conditions as in (*A*). Average of triplicates ± SD. (***C***) Representative examples of cell lines forming spheres versus cell lines negative for sphere formation. U-2 OS cells do not proliferate while the three other sphere-negative cell lines proliferate in sphere-forming conditions. Scale bar for 5X = 400μm; scale bar for 20X = 100μm. (***D, E***) Immunoblots for the indicated proteins in extracts from NB508 mouse cells (*D*) and the indicated human cancer cell lines (*E*) cultured in the same medium, but in adherent conditions (2D culture) or in non-adherent condition to allow free-floating tumor sphere formation (3D culture). ERK activity is downregulated in tumor-spheres.

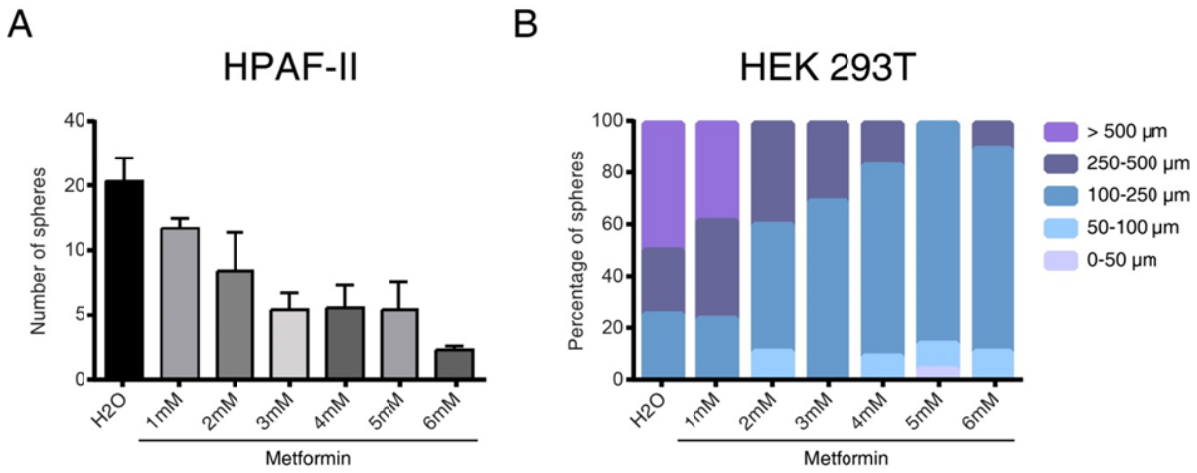

Figure S18. Effect of metformin on cells with low p-ERK levels and properties of stem cells, Related to figure 27

(***A***) Number of spheres formed by HPAF-II cells after treatment for 7 days with the indicated concentration of metformin. Average of triplicates ± SD. (***B***) The size of spheres formed by HEK 293T cells after treatment for 7 days with the indicated concentration of metformin. The percentage of cells for each size category is shown.

Table SV. List of cancer cell lines evaluated for their ability to proliferate in sphere formation conditions and for the presence of a sphere-forming cell subpopulation, Related to Figure 26

Cell line	Origin	Morphology	Tumor Source	Histology	Proliferation 3D	Spheres	Mutation/alteration
HPDE	Pancreas	Epithelial	NA	NA	-	-	NA
BxPC-3	Pancreas	Epithelial	Primary	Adenocarcinoma	+	++	SMAD4;TP53;CDKN2A;MAP2K4
Colo-357	Pancreas	Epithelial	Lymph node metastasis	Adenocarcinoma	+++	++	KRAS;SMAD4;CDKN2A
HPAC	Pancreas	Epithelial	Primary	Adenocarcinoma	++	++	KRAS;CDKN2A
HPAF-II	Pancreas	Epithelial	Ascites	Adenocarcinoma	+	+++	KRAS;TP53;CDKN2A
KP4	Pancreas	Epithelial	Ascites	ductal carcinoma	++	+	KRAS;SMAD4;CDKN2A
MIA PaCa-2	Pancreas	Epithelial	Primary	carcinoma	++	-	KRAS;TP53;CDKN2A
Panc-1	Pancreas	Epithelial	Primary	Epithelioid carcinoma	++	-	KRAS;AKT2;TP53;CDKN2A
Panc 03.27	Pancreas	Epithelial	Primary	Adenocarcinoma	++	+	KRAS;TP53;SMAD4;CDKN2A
Panc 08.13	Pancreas	Epithelial	Primary	Adenocarcinoma	+	+++	KRAS;SMAD4;CDKN2A
PA-TU-8902	Pancreas	Epithelial	Primary	Adenocarcinoma	+	+	KRAS;TP53
PA-TU-8988T	Pancreas	Epithelial	Liver metastasis	Adenocarcinoma	+++	-	KRAS;TP53
PSN1	Pancreas	Epithelial	Primary	Adenocarcinoma	++	-	KRAS;C-MYC;TP53
SW 1990	Pancreas	Epithelial	Spleen metastasis	Adenocarcinoma	+	+	KRAS;CDKN2A
YAPC	Pancreas	Epithelial	Ascites	Adenocarcinoma	+	++	KRAS;TP53;SMAD4;CDKN2A
HEK 293T	Kidney	Epithelial	NA	NA	+++	++	Express SV40 T antigen
BT-20	Breast	Epithelial	Primary	Ductal carcinoma	++	++	PIK3CA;TP53;CDKN2A
BT-474	Breast	Epithelial	Primary	Ductal carcinoma	+	+	PIK3CA;ERBB2;TP53
MCF7	Breast	Epithelial	Pleural effusion	Adenocarcinoma	++	+	PIK3CA;CDKN2A
MDA-MB-231	Breast	Epithelial	Pleural effusion	Adenocarcinoma	+	+	KRAS;BRAF;NF2;TP53;CDKN2A
SK-BR-3	Breast	Epithelial	Pleural effusion	Adenocarcinoma	++	-	ERBB2;TP53
BV-173	Blood	B cell precursor	Primary	Chronic myeloid leukemia	-	-	BCR-ABL
WDT-2	Blood	Myeloid	Primary	Chronic myeloid leukemia	-	-	BCR-ABL
U-2 OS	Bone	Epithelial	Primary	Osteosarcoma	-	-	Unknown
HeLa	Cervix	Epithelial	Primary	Adenocarcinoma	+++	-	STK11
HCT 116	Colon	Epithelial	Primary	Carcinoma	+++	++	KRAS;PIK3CA;CTNNB1;CDKN2A;BRCA2;MLH1
Hep 3B2.1-7	Liver	Epithelial	Primary	Carcinoma	+	++	FGF19; TP53
HuH-7	Liver	Epithelial	Primary	Carcinoma	++	++	TP53
NCI-H1299	Lung	Epithelial	Lymph node metastasis	Non-small cell carcinoma	+	++	NRAS;TP53
U-937	Lymphoid tissue	Monocyte	Pleural effusion	Histiocytic lymphoma	-	-	PTEN;TP53
PC-3	Prostate	Epithelial	Bone metastasis	Adenocarcinoma	++	-	PTEN;TP53

Mutation/alteration; RED = activating mutation, amplification; GREEN = deactivating mutation, gene methylation, deletion,incorrect splicing, etc; BLUE = Fusion gene

3.3.9.2 Supplemental Experimental Procedures

Immunohistochemical Analyses

Tissue samples were melted at 55°C for 1 hour and then deparaffinized and rehydrated by sequential incubation in xylenes (2 x 5 min), 100% ethanol (1 x 5 min), 95% ethanol (1 x 3 min), 75% ethanol (1 x 3 min) and 40% ethanol (1 x 3 min). Samples were washed in PBX/0.3% Triton X-100 5 min and then in dH_2O 3 min. Heat-induced epitope retrieval was performed using a pressure cooker for 20 min in citrate-based buffer (H-3300, Vector Labs). Samples were cooled down for at least 1 hour and then washed 3 times during 3 min with PBS/0.3% Triton X-100. Endogenous peroxidase was inactivated by incubation for 10 min at room temperature in a solution of 1% H_2O_2. Samples were washed 3 times for 3 min in PBS/0.3% Triton X-100 and tissues were delimited using a hydrophobic barrier pen. Tissues were blocked 1 hour at room temperature with 5% goat serum in PBS/0.3% Triton X-100, and then incubated with primary antibodies diluted in the same buffer overnight at 4°C. The following primary antibodies were used: anti-phospho-ERK1/2$^{T202/Y204}$ (1:400; clone D13.14.4E, #4370, Cell Signaling Technology) for mouse tissues, anti-phospho-ERK1/2$^{T202/Y204}$ (1:400; clone E10, #9106, Cell Signaling Technology) for human tissues and anti-KI-67 (1:200; ab15580, Abcam) for both human and mouse tissues. Tissues were washed 3 times for 3 min in PBS/0.3% Triton X-100 and then incubated with secondary antibodies diluted in PBS/0.3% Triton X-100 + 5% goat serum during 1 hour at room temperature. The following secondary antibodies were used: biotinylated goat anti-rabbit IgG (1:200; BA-1000, Vector Labs) or biotinylated goat anti-mouse IgG (1:200; BA-9200, Vector Labs). Slides were incubated with ABC Elite reagent (PK-6100, Vector Labs) 30 min at room temperature (prepared 30 min before incubation), and then washed 3 times for 3 min with PBS/0.3% Triton X-100. Finally, the specimens were stained for peroxidase with Di-amine-benzidine (DAB) substrate kit (SK-4100, Vector Labs). The reaction was stopped by washing with water when the coloration was sufficient; the same incubation time was applied to all samples. Tissues were counterstained with hematoxylin (H9627, Sigma) and dehydrated by sequential incubation in 40% ethanol (1 x 1 min), 75% ethanol (1 x 1 min), 95% ethanol (1 x 1 min),

100% ethanol (1 x 1 min) and xylenes (2 x 5 min). Finally, slides were mounted with Sub-X Mounting Medium (#13519, EMS).

Additional Information on Cell Culture

Cell used for the screen presented in Figure S17 were cultured in the following media: BT-474, HCT 116, HEK 293T, HeLa, Hep 3B2.1-7, HPAC, HPAF-II, HuH-7, KP4, MCF7, MDA-MB-231, MIA PaCa-2, NCI-H1299, Panc-1, PA-TU-8902, PA-TU-8988T, PC-3, SK-BR-3, SW 1990, U-2 OS in DMEM supplemented with 10% FBS and 1% P/S; BxPC-3, BV-173, Colo-357, Panc 03.27, Panc 08.13, U-937, PSN1, WDT-2, YAPC in RPMI supplemented with 10% FBS and 1% P/S; BT-20 in AMEM supplemented with 10% FBS and 1% P/S; HPDE in Keratinocyte-SFM media (10724-011, Gibco) supplemented with 30 µg/mL Bovine Pituitary Extract (BPE) (#13028-014, Gibco), 0.2 ng/mL EGF (#10450-013, Gibco), 4 mM L-glutamine (550-065-EG, Wisent) and 1% P/S.

Pancreatic Ductal Cell Isolation

The protocol for isolation of 1497, 1498, 1499 and AH375 cells was adapted from a previously published method (824). Briefly, mice were euthanized, the pancreas was gently resected, minced and digested in 10 mL of Hank's balanced salt solution (HBSS) containing 2 mg/mL collagenase D (#11088858001, Roche Applied Science) during 25 min at 37^{o}C with agitation by magnetic stir. The cell suspension was pelleted by centrifugation at 1200 rpm for 5 min and cells were washed once with PBS. Then, cells were resuspended in 3 mL of 0.05% trypsin-EDTA (#25300-054, Gibco) and incubated for 3 min at 37^{o}C. Three volumes of DMEM + 10% FBS were added to neutralize trypsin, the cell suspension was filtered through a 85 µM nylon mesh and then pelleted by centrifugation at 1200 rpm for 5 min. Cells were resuspended in a small volume of PBS pH 7.2 + 0.5% BSA + 2 mM EDTA and counted. A suspension of 1 to 1.5 x 10^6 cells/mL was made in the same buffer and Fluorescein-conjugated DBA (FITC-DBA) lectin (FL-1031, Vector Labs) was added at a dilution 1:400. Cells were incubated at 4^{o}C for 10 min on a rotor and then pelleted by centrifugation at 1200 rpm for 5 min. Cells were washed once with PBS pH 7.2 + 0.5% BSA + 2 mM EDTA and then resuspended in 3 mL of the same buffer. FITC-positive cells were sorted by FACS at low

pressure and seeded in wells of a 48-well plate precoated with laminin and containing pancreatic medium.

Cell Proliferation Assays

Cells were plated in 48-well plates at 5000 cells per well in 0.5 mL of media. At the indicated time points, 50 µL of 12 mM MTT reagent (M-6494, Molecular Probes) was added to each well and cells were incubated 3 hours at 37°C. After incubation, the medium was aspirated and the cells dried for conservation at room temperature. At the end of the experiment, the formazan was solubilised with 200µL DMSO and the absorbance at 540 nm was measured using a microplate reader. The relative proliferation is expressed as the fold of absorbance between a specific time point and the beginning of the experiment (day 0).

Soft Agar Assays

Soft agar assays with MEF and IMR90 cells were done on 96-well flat-bottom microplate with 5000 cells seeded per well by using the CytoSelect™ 96-Well Cell Transformation Assay kit (CBA-130, Cell Biolabs) as described previously (390). For mouse pancreatic cells, the protocol was adapted to substitute the required specific culture medium. Agar was directly solubilized in the culture medium by incubating at 95°C to obtain a concentrated 2.4% agar solution. This solution was cooled to 37°C in a water bath and then medium was added to obtain a final solution of 0.6% agar. The latter solution was used for the base agar layer and to mix with cell suspensions. The normal protocol was then followed, but with the specific medium.

Sphere-Forming Assays

To examine the capacity of tumor sphere formation, the cells of interest were trypsinized and washed with PBS to remove FBS. Cells were cultured in ultra-low attachment 24-well plates (#3473, Corning) (1000 cells/well) and in 1 mL of CSC medium, consisting of DMEM-F12 (#11039-021, Gibco) supplemented with B-27 Supplement (#17504-044, Gibco), 20 ng/mL EGF (mouse cells: #5331-LF, human cells: #8916-LF, Cell Signaling Technology) and 20 ng/mL βFGF (mouse cells: #5414-LF, human cells: #8910-LF, Cell Signaling

Technology). The cells were incubated in a humidified atmosphere with 5% CO_2 at 37°C for the indicated period of time and supplements (B-27, EGF, βFGF) were added every 4 days at the above concentration. Spheroids were counted using a microscope. The sphere size was evaluated by an automated analysis of pictures with the software CellProfiler (Broad Institute). To evaluate cell proliferation two methods were used: (1) cells (one day after seeding) and spheroids (at the experiment end point) were incubated with 100 µL of premixed WST-1 reagent (#630118, Clontech) for 3 hours at 37°C. The absorbance at 450 nm was measured using a microplate reader and the results are expressed as the fold of absorbance. (2) Spheroids were collected by centrifugation and dissociated into single cells by trypsinization. When cells were well dissociated, they were pelleted by gentle centrifugation, resuspended in 1 mL culture medium and counted using a Countess automated cell counter (Invitrogen) or a TC20 automated cell counter (Bio-Rad) depending on the experiment.

Immunoblotting

Adherent cells were washed with PBS and then scraped on ice into 250 to 500 µL of ice cold RIPA buffer (50 mM Tris-Hcl pH8.0, 150 mM NaCl, 1% Triton X-100, 0.1% SDS, 0.5% Na-deoxycholate, 1 mM EDTA, 1 mM EGTA) containing 1X Complete-EDTA free Protease Inhibitor Cocktail (#11 873 580 001, Roche Applied Science) and 1X PhosSTOP Phosphatase Inhibitor Cocktail (#04 906 837 001, Roche Applied Science). Cell lysates were kept on ice for 15 min, sonicated 40 seconds at a low intensity and then cleared by centrifugation at 13 000 RPM for 20 min. Protein concentration was evaluated using the Micro BCA Protein Assay Kit (#23235, Thermo Scientific) and the concentration of samples was normalized by adding appropriated quantity of RIPA buffer. The samples were completed with 1X laemmli buffer (Stock of 6X: 12% SDS, 47% glycerol, 60 mM Tris pH6.8, 0.06% bromophenol blue) and 10% β-mercaptoethanol. Then the lysates were boiled 5 min and conserved at -80°C until migration. Proteins were separated by SDS-PAGE and to Immobilon-P PVDF membrane (IPVH00010, Millipore). Membranes were blocked 1 hour at room temperature in Tris-buffered saline containing 0.1% Tween 20 (TBS-T) and 5% dry milk and then washed 3 times 5 min with TBS-T. The membranes were incubated with the primary antibodies diluted in TBS-T + 3% BSA + 0.05% Na-azide overnight at 4°C or 1 hour at room

temperature. The following primary antibodies were used: anti-c-MYC (1:1000; clone D84C12, #5605, Cell Signaling Technology), anti-phospho-c-RAF^{S338} (1:1000; clone 56A6, #9427, Cell Signaling Technology), anti-ERK1/2 (1:400; Sc-94 (K-23), Santa Cruz Biotechnology), anti-ERK1/2 (1:1000; clone 137F5, #4695, Cell Signaling Technology), anti-phospho-ERK1/2$^{T202/Y204}$ (1:2000; clone D13.14.4E, #4370, Cell Signaling Technology), anti-phospho-ERK1/2$^{T202/Y204}$ (1:1000; #9101, Cell Signaling Technology), anti-H-Ras (1:250; clone F235, Sc-29, Santa Cruz Biotechnology), anti-IκBα (1:1000; #9242, Cell Signaling Technology), anti-phospho-IκBα^{S32} (1:1000; clone 14D4, #2859, Cell Signaling Technology), anti-phospho-MEK1/2$^{S217/S221}$ (1:1000; clone 41G9, #9154, Cell Signaling Technology), anti-Nanog (1:2000; clone D73G4, #4903, Cell Signaling Technology), anti-STAT3 (1:1000; clone 124H6, #9139, Cell Signaling Technology), anti-phospho-STAT3^{S727} (1:1000; #9134, Cell Signaling Technology), anti-phospho-STAT3^{Y705} (1:1000; #9131, Cell Signaling Technology), anti-α-Tubulin (1:20000; clone B-5-1-2, T6074, Sigma-Aldrich), anti-β-actin (1:10000; clone 8H10D10, #3700, Cell Signaling Technology). Membranes were washed 3 times 5 min with TBS-T and then incubated with the secondary antibodies diluted in TBS-T + 5% dry milk 1 hour at room temperature. The following secondary antibodies were used: goat anti-rabbit IgG conjugated to HRP (1:3000, #170-6515, Bio-Rad) or goat anti-mouse IgG conjugated to HRP (1:3000, #170-6516, Bio-Rad). Finally, the membranes were washed 3 times 5 min with TBS-T. Immunoblots were visualised using enhanced chemiluminescence (ECL) detection systems and Super RX X-Ray films (Fujifilm) or a ChemiDoc^{TM} MP system (Bio-Rad). Band quantification was carried out using ImageJ or Image Lab 4.0 (Bio-Rad).

Immunofluorescence

Indirect immunofluorescence staining was performed on slides from paraffin-embedded tissues. Tissue samples were deparaffinized and rehydrated by sequential incubation in xylenes (3 x 5 min), 100% ethanol (2 x 2 min), 95% ethanol (1 x 2 min), 70% ethanol (1 x 2 min) and dH_2O (2 x 2 min). Heat-induced epitope retrieval was performed using a pressure cooker for 20 min in Tris-EDTA-based buffer pH 9.0 (ab93684, Abcam). Slides were cooled down for at least 1 hour, washed 1 time during 5 min with PBS, washed 1 time during 5 min with PBS + Tween 20 (PBS-T) and tissues were delimited using a hydrophobic

barrier pen. Tissues were blocked 1 hour at room temperature with PBS-T + 2% BSA and then incubated with primary antibodies diluted in the same buffer overnight at 4°C. The following primary antibodies were used: anti-c-MYC (1:800; clone D84C12, #5605, Cell Signaling Technology), anti-phospho-ERK1/2$^{T202/Y204}$ (1:200; clone E10, #9106, Cell Signaling Technology). Slides were rinsed 3 times for 3 min in PBS-T and then incubated with secondary antibodies diluted in PBS-T + 2% BSA for 45 min at room temperature. The following secondary antibodies were used: donkey anti-mouse AlexaFluor 555 (1:400; A-31570, Molecular Probes) and donkey anti-rabbit AlexaFluor 488 (1:400; A-21206, Molecular Probes). Slides were washed 3 times for 5 min in PBS-T and then mounted with Vectashield Mounting Medium with DAPI (H-1200, Vector Labs). Images were captured with a Nikon Eclipse 80i upright microscope.

Reagents and Plasmids

The DUSP1/6 inhibitor BCI (#317496, Calbiochem) was resuspended in DMSO and directly added to the cell media at the indicated concentrations. Metformin hydrochloride (#1396309, Sigma) was diluted in H_2O and added to cell media at the indicated concentrations. Fresh media containing BCI or metformin was added after 4 days of starting treatments. pFG12-CMV-hTERT-IRES-GFP, pWZL-hygro and pWZL-hygro/HRas^{G12V} were described before (100, 492). pLPC-puro/E1A and pLPC-puro/c-MYC-HA is a kind gift from Dr. Scott W. Lowe (Memorial Sloan-Kettering Cancer Center, New-York, NY). The pLKO-puro lentiviral vectors used to express a non-targeting shRNA (shCTR) or an shRNA against ERK2 (shERK) were from Sigma (SHC002, TRCN0000010041). The pMLPX-puro retroviral vectors used to express a non-targeting shRNA (shCTR) or an shRNA against ERK2 (shERK) were previously described (390).

Microarrays

RNA quality, cDNA synthesis and data acquisition

The Eukaryote Total RNA Nano assay of the Agilent 2100 Bioanalyzer (Agilent Technologies) was used to validate total RNA integrity. The protocol from the Ambion® WT Expression kit for Affymettrix® GeneChip®Whole Transcript (WT) Expression Arrays

(Applied Biosystems) was followed to prepare cDNAs. The single-stranded cDNAs were treated with Uracil DNA glycosylase, fragmented with APE1 enzyme and labelled with Biotin Allonamide Triphosphate according to the instructions of the GeneChip® WT Terminal Labeling Kit (Applied Biosystems). Labelled cDNAs were hybridized for 16 hours at 45^{o}C with rotation at 60 rpm on the appropriated DNA Gene Chip. The DNA chips were washed and stained in the Affymetrix Fluidics Station 400 according to the manufacturer's instructions and then scanned on a GeneChip® Scanner 3000 7G/4 Color Early Access (Affymetrix).

Data normalization and analysis

Data from triplicates of each condition were analyzed with the FlexArray 1.6.3 software (825) using Affymetrix default analysis settings. Raw data were normalized with a Robust Multi-array Average (RMA) algorithm, the mean fold change in the signal intensity between conditions was determined for all transcripts and a two-sample student's t-test was used to identify significant changes. Transcripts with a fold changes greater than ± 2 and a p-value <0.05 were considered for further analysis.

Bioinformatic analyses

Inferring biological functions

A FatiGO single enrichment analysis with the Babelomics 4.3 platform (493) was performed to infer biological functions affected between experimental conditions. The Gene Ontology (GO) and Kyoto Encyclopedia of Genes and Genomes (KEGG) terms significantly enriched among transcripts when compared with the rest of genome were identified. These terms and their associated transcripts were grouped in general categories as indicated.

Prediction of regulated transcription factors

The Distant Regulatory Elements of Co-regulated genes (DIRE) web-based application (826) was used to predict regulated transcription factors (TF). A random set of 5000 genes was used as the source of background genes.

Gene set enrichment analysis

An unbiased global analysis of gene set enrichment with The Gene set Enrichment Analysis (GSEA) 2.0.14 software (827) was used to identify the relevant phenotypes significantly over represented in the experimental conditions of interest. A positive NES indicates a correlation with the phenotype that is compared to the phenotype used as a reference, while a negative NES indicates correlation with the opposite phenotype (the reference). The significance of NES values is determined by the False Discovery Rate (FDR; q-value) and by a nominal p-value calculated by using an empirical phenotype-based permutation test procedure. The threshold of significance was set at a p-value ≤ 0.05 and a q-value ≤ 0.25. The ranking metric used was the signal-to-noise ratio and 1000 permutations were performed.

4. La metformine inhibe le facteur de transcription NF-κB et les effets délétères d'une activation aberrante de la voie ERK/MAPK

4.1 Mise en contexte de l'article 5

Au cours du précédent chapitre, nous avons proposé la metformine afin de cibler les CSC. Également, nous avons pu apprécier sa capacité potentielle à interférer avec l'activation de la voie de NF-κB. L'objectif principal de cet article était de confirmer la capacité de la metformine à inhiber cette voie de signalisation. Pour ce faire, nous avons tiré avantage du SASP, lequel est un phénotype facilement mesurable et intimement lié à l'activation du facteur de transcription NF-κB (140, 144). Nous avons ainsi mesuré l'impact de la metformine sur le phénotype sécrétoire associé à l'OIS induite par l'oncogène *RAS*.

La voie de NF-κB permet la transduction du signal suite à l'activation des récepteurs de type Toll (*Toll-like receptors*; TLR) en présence de motifs moléculaires associés aux pathogènes (*pathogen-associated molecular patterns*; PAMP) (828, 829). Par conséquent, afin de montrer la capacité de la metformine à inhiber la voie dans un contexte n'impliquant pas la surexpression de RAS, nous avons évalué son effet sur différents types cellulaires traités avec des lipopolysaccharides (LPS), lesquels sont des endotoxines servant de ligan au TLR4 (830).

Globalement, nos résultats montrent que la metformine interfère avec la production de cytokines pro-inflammatoires en inhibant l'activation de NF-κB.

4.2 Contribution à l'article 5

Pour cet article, j'ai partagé la gestion du projet avec Olga Moiseeva. Cette dernière a préparé les échantillons pour l'expérience par puce à ADN, puis j'ai effectué l'analyse des résultats obtenus pour les figures 1B, C; 3A-C; S1; S2; S3 et le tableau I. J'ai effectué l'ensemble des travaux pour les figures 1A; 5F et 6. Olga Moiseeva a obtenu les résultats des Figures 3D-F et a préparé les échantillons pour les analyses par PCR quantitatif, lesquelles ont été effectuées par Véronique Bourdeau. Emmanuelle Saint-Germain a obtenu les résultats de la Figure 5C-E. Sebastian Igelmann a produit les résultats de la Figure 5A, B. Enfin, Geneviève Huot a effectué l'expérience de la Figure 1M.

Concernant le manuscrit, j'ai conçu l'ensemble des figures et rédigé les légendes, la section matériel et méthodes et le matériel supplémentaire. Gerardo Ferbeyre a rédigé les autres sections. Conjointement avec Olga Moiseeva et Gerardo Ferbeyre, j'ai contribué à la révision de l'ensemble du manuscrit.

4.3 Article 5

Metformin inhibits the senescence-associated secretory phenotype by interfering with IKK/NF-κB activation

Olga Moiseeva[1]*, Xavier Deschênes-Simard[1]*, Emmanuelle Saint-Germain[1], Sebastian Igelmann[1], Geneviève Huot[1], Alexandra E. Cadar[1], Véronique Bourdeau[1], Michael N. Pollak[2] and Gerardo Ferbeyre[1]

Aging Cell, 2013 May 13, 12 (3): 489-98

1) Département de Biochimie, Université de Montréal, Pavillon Roger-Gaudry 2900 boul. Édouard Montpetit, Montréal, Qc H3C 3J7, Canada
2) Division of Experimental Medicine, McGill University and Segal Cancer Centre of Jewish General Hospital, 3755 Côte Ste Catherine, Montréal, Qc H3T 1E2, Canada

* Both authors contributed equally to this work.

Running title: Metformin and senescent cytokines

Keywords: NF-κB; cellular senescence; cytokines; metformin; senescence

Correspondence to: Gerardo Ferbeyre and Michael N. Pollak

4.3.1 Summary

We show that the antidiabetic drug metformin inhibits the expression of genes coding for multiple inflammatory cytokines seen during cellular senescence. Conditioned medium (CM) from senescent cells stimulates the growth of prostate cancer cells but treatment of senescent cells with metfomin inhibited this effect. Bioinformatic analysis of genes downregulated by metformin suggests that the drug blocks the activity of the transcription factor NF-κB. In agreement, metformin prevented the translocation of NF-κB to the nucleus and inhibited the phosphorylation of IκB and IKKα/β, events required for activation of the NF-κB pathway. These effects were not dependent on AMPK activation or on the context of cellular senescence, as metformin inhibited the NF-κB pathway stimulated by lipopolysaccharide (LPS) in *ampk* null fibroblasts and in macrophages. Taken together, our results provide a novel mechanism for the antiaging and anti-neoplastic effects of metformin reported in animal models and in diabetic patients taking this drug.

4.3.2 Introduction

Aging is characterized by a general decline in the functions of all tissues and an increased incidence of chronic disease. A large body of evidence has correlated age-associated diseases with chronic inflammation leading to an aging theory known as inflammaging (831). Alzheimer disease, cancer, sarcopenia, atherosclerosis and diabetes are common diagnoses in the aging population associated to chronic inflammation (831, 832).

It has been proposed that the process of cellular senescence represents a general response to various forms of damage that may accumulate with age. Senescence is a permanent cell cycle arrest triggered by a variety of stressors, including short telomeres, oncogenes, DNA damage, and reactive oxygen species (147). The evidence correlating cellular senescence with aging and age-related diseases is abundant (147). Remarkably, elimination of senescent cells attenuates signs of accelerated aging in mice (166). The mechanisms by which senescent cells accelerate organismal aging are not known but senescent cells secrete a large variety of inflammatory cytokines that can impair tissue homeostasis and promote chronic inflammation (147).

Cellular senescence is also a tumor suppressor mechanism and inhibiting key mediators of senescence such as p53, and the retinoblastoma protein leads to accelerated tumor formation (455). It has been proposed that cellular senescence was selected during evolution for tumor suppression and that its pro-aging effect was not eliminated by natural selection because it mainly acts after reproduction (833). High cytokine gene expression by senescent cells is associated with persistent DNA damage signals (834), and in some situations, it can promote tumorigenesis in neighboring cells (155, 835). Retrospective studies have suggested that the antidiabetic drug metformin has unanticipated cancer prevention activity in patients (836, 837) and inhibits the generation of reactive oxygen species and DNA damage in normal cells expressing oncogenic *ras* or treated with paraquat (445). However, metformin did not prevent RAS-induced growth arrest (445). We thus decided to investigate whether metformin could suppress the production of inflammatory cytokines by senescent cells.

4.3.3 Results

Effects of metformin on the gene expression profile of oncogene-induced senescence

To study the effects of metformin on the gene expression profile of oncogene-induced senescence, we infected normal human diploid fibroblasts IMR90 with a retroviral vector pBABE or its derivative expressing oncogenic *ras* (Ha-RAS-V12). In this protocol, cells expressing RASV12 entered a hyperproliferative phase quickly after selection but arrested their growth and senesced 4 days after, as shown by the increase in the percentage of flat blue cells positive for senescence-associated β-galactosidase (SA-β-Gal) (Figure 29A). We treated a fraction of RAS-expressing cells with 5 mM metformin 1 day postinfection during the hyperproliferative phase. Metformin arrested the growth of the cells (not shown) and both metformin-treated and untreated cells entered senescence at day four postinfection. We collected RNA from both cell populations at day six postinfection, when more than 90% of the cells were positive for SA-β-Gal (Figure 29A). The RNA was then used to prepare probes for Affymetrix microarrays. Data from three independent experiments were analyzed with Flexarray 1.6.1.1 using robust multiarray average (RMA) as normalization method. The data discussed were deposited in NCBI's Gene Expression Omnibus and are accessible through GEO Series accession number GSE33612 (http://www.ncbi.nlm.nih.gov/geo/query/acc.cgi?acc=GSE33612). All gene expression changes showing 2 or more fold differences were considered for a pathway analysis using FatiGO single enrichment from the bioinformatics platform Babelomics 4.3 (493). We found that metformin mostly inhibited gene expression with its largest effect being on genes controlling immunity and metabolism (Figure 29B). The drug affected the expression of genes controlling hypoxia and oxidative stress, extracellular matrix, regulation of cell death, ion homeostasis, cell cycle, cell migration, cell signaling, metabolism, and immunity (Table II). These global categories were derived from the most significant Gene Ontology (GO) and Kyoto Encyclopedia of Genes and Genomes (KEGG) term names (Figure S19).

We previously showed that metformin may prevent RAS-expressing cells from escaping senescence by reinforcing growth arrest (445) and this can be explained by the

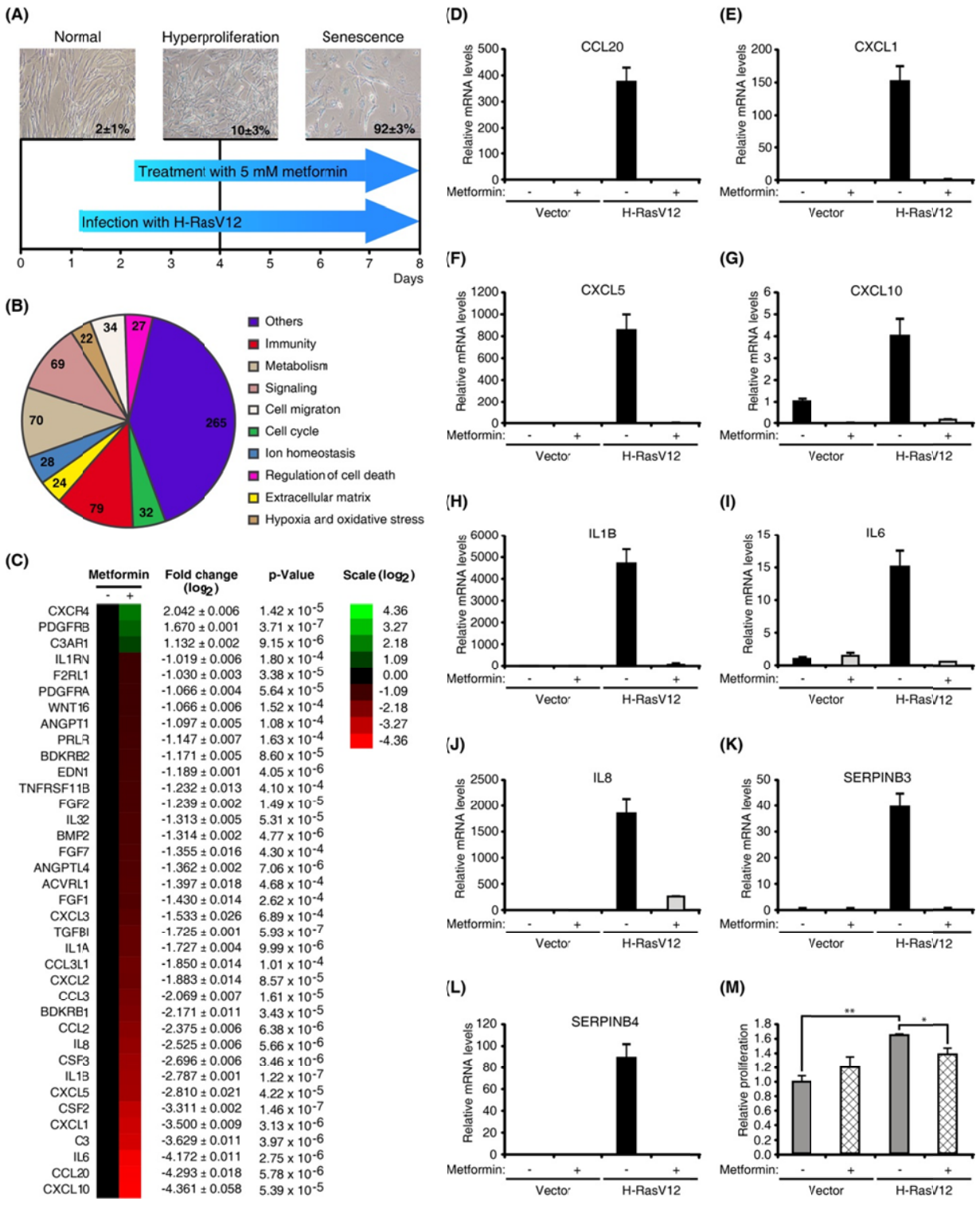
(A)
Normal
Hyperproliferation
Senescence
2±1%
10±3%
92±3%
Treatment with 5 mM metformin
Infection with H-RasV12
0 1 2 3 4 5 6 7 8
Days
(B)
Others
Immunity
Metabolism
Signaling
Cell migraton
Cell cycle
Ion homeostasis
Regulation of cell death
Extracellular matrix
Hypoxia and oxidative stress
265
32
79
24
28
70
69
22
34
27
(C)
Metformin
- +
Fold change (log2)
p-Value
Scale (log2)
4.36
3.27
2.18
1.09
0.00
-1.09
-2.18
-3.27
-4.36
CXCR4 2.042 ± 0.006 1.42 x 10-5
PDGFRB 1.670 ± 0.001 3.71 x 10-7
C3AR1 1.132 ± 0.002 9.15 x 10-6
IL1RN -1.019 ± 0.006 1.80 x 10-4
F2RL1 -1.030 ± 0.003 3.38 x 10-5
PDGFRA -1.066 ± 0.004 5.64 x 10-5
WNT16 -1.066 ± 0.006 1.52 x 10-4
ANGPT1 -1.097 ± 0.005 1.08 x 10-4
PRLR -1.147 ± 0.007 1.63 x 10-4
BDKRB2 -1.171 ± 0.005 8.60 x 10-5
EDN1 -1.189 ± 0.001 4.05 x 10-6
TNFRSF11B -1.232 ± 0.013 4.10 x 10-4
FGF2 -1.239 ± 0.002 1.49 x 10-5
IL32 -1.313 ± 0.005 5.31 x 10-5
BMP2 -1.314 ± 0.002 4.77 x 10-6
FGF7 -1.355 ± 0.016 4.30 x 10-4
ANGPTL4 -1.362 ± 0.002 7.06 x 10-6
ACVRL1 -1.397 ± 0.018 4.68 x 10-4
FGF1 -1.430 ± 0.014 2.62 x 10-4
CXCL3 -1.533 ± 0.026 6.89 x 10-4
TGFBI -1.725 ± 0.001 5.93 x 10-7
IL1A -1.727 ± 0.004 9.99 x 10-6
CCL3L1 -1.850 ± 0.014 1.01 x 10-4
CXCL2 -1.883 ± 0.014 8.57 x 10-5
CCL3 -2.069 ± 0.007 1.61 x 10-5
BDKRB1 -2.171 ± 0.011 3.43 x 10-5
CCL2 -2.375 ± 0.006 6.38 x 10-6
IL8 -2.525 ± 0.006 5.66 x 10-6
CSF3 -2.696 ± 0.006 3.46 x 10-6
IL1B -2.787 ± 0.001 1.22 x 10-7
CXCL5 -2.810 ± 0.021 4.22 x 10-5
CSF2 -3.311 ± 0.002 1.46 x 10-7
CXCL1 -3.500 ± 0.009 3.13 x 10-6
C3 -3.629 ± 0.011 3.97 x 10-6
IL6 -4.172 ± 0.011 2.75 x 10-6
CCL20 -4.293 ± 0.018 5.78 x 10-6
CXCL10 -4.361 ± 0.058 5.39 x 10-5
(D)
CCL20
(E)
CXCL1
(F)
CXCL5
(G)
CXCL10
(H)
IL1B
(I)
IL6
(J)
IL8
(K)
SERPINB3
(L)
SERPINB4
(M)
Relative mRNA levels
Relative proliferation
Metformin: - + - +
Vector
H-RasV12
**
*

Figure 29. Effect of metformin on gene expression in RAS-expressing cells

(***A***) Time course of RAS-induced senescence and treatment with metformin. IMR90 cells were infected with retroviruses allowing expression of H-RASV12. Twenty-four hours after infection, cells were treated with 5.0 mM metformin or vehicle for 6 days. RNA was collected at day 7 for microarray gene expression analysis (GEO accession number: GSE33612). (***B***) Pie chart of most important biological functions affected by metformin in senescent H-RASV12-expressing cells. A FatiGO single enrichment analysis was performed using transcripts with a fold change higher or equal to 2 and a *P*-value < 0.05 according to the two-sample Student's *t*-test. (***C***) Heat Map of fold change ($\log_2$) of genes coding for cytokines and their receptors identified by a combination of Gene Ontology (GO) analysis and literature-based curation. The fold change and standard deviation (SD) are calculated from the mean expression values of three replicates of each condition. The *P*-value is determined according to the two-sample Student's *t*-test. (***D-L***) qPCR validation of several cytokine genes that are highly expressed in senescent cells expressing oncogenic *ras* and are repressed by metformin. RNA extracts from IMR90 fibroblasts expressing H-RASV12 or an empty vector and treated with 5 mM metformin or vehicle for 6 days were obtained 7 days after infection. Error bars represent ± SD of replicates. (***M***) Conditioned medium from senescent fibroblasts promote the growth of PC3 prostate cancer cells but pretreatment of senescent cells with metformin decreased the effect: * $P < 0.05$ and ** $P < 0.005$ according to a two-sample Student's *t*-test, $n = 3$.

repression of cell cycle, cell signaling, cell migration, and metabolic genes (Figure S19). For example, metformin represses the expression of growth factor receptors such as PDGFRA, ACVRL1, and BDKRB1, which can transduce signals from extracellular factors that stimulate cell proliferation (838), the cell cycle enzyme CDK6 (839), and the key signaling enzyme PDK1, which acts in the AKT signaling pathway (840). Metformin also suppresses the expression of kynureninase (KYNU) and quinolinate phosphorybosyl transferase (QPRT), enzymes important for *de novo* NAD biosynthesis (841). Limiting NAD levels may make cells more susceptible to metabolic stress and limit the use of NAD as a source of ADP-ribosylation reactions that control many signaling pathways (841). The drug also inhibited the expression of PTGS2 (also known as COX-2), an enzyme that links inflammation to cancer considered to be a potential target for cancer chemoprevention (842). Another intriguing downregulated gene is GPAM (also known as GPAT), coding for the mitochondrial enzyme glycerol-3-phosphate acyltransferase, critical for the synthesis of triglycerides and phospholipids (843). However, the most dramatic effect of metformin on gene expression involved genes controlling inflammatory cytokines (Figure 29C). We confirmed by qPCR that metformin

Table II. Biological functions and genes affected by metformin in oncogenic *ras* expressing cells

Categories	Genes
Immunity	ACVRL1, ADM, ANGPT1, ANGPTL4, BDKRB1, BDKRB2, BIRC3, BMP2, C3, C3AR1, CCL2, CCL20, CCL3, CCL3L1, CD36, CDK6, CFH, COL1A1, CSF2, CSF3, CXCL1, CXCL10, CXCL2, CXCL3, CXCL5, CXCR4, DPP4, EDN1, EREG, F2RL1, F3, FABP4, FGF1, FGF2, FGF7, GCH1, GGCX, HIST2H2BE, ICAM1, ID3, IKBKE, IL1A, IL1B, IL1RN, IL32, IL6, IL8, IRAK2, KYNU, MAP3K8, NFKBIZ, NRG1, OLR1, PAPSS2, PDGFRA, PDGFRB, PIK3R3, PLD1, PLXDC2, PRLR, PSG4, PSG7, PTGS2, SERPINA1, SERPIND1, SERPINF1, SNCA, SOD2, STAT4, TGFBI, THBS1, THY1, TNFAIP3, TNFRSF11B, TNIP1, UACA, VCAN, VNN1
Metabolism	ADM, AMPD3, ANGPT1, ANGPTL4, APLP1, BDKRB1, BDKRB2, BMP2, CCL2, CD36, COL1A1, CSF2, CYB5R2, DHRS1, EDN1, EGR2, ENO2, ENTPD3, EREG, F3, FABP4, FGD4, FGF2, FGF7, GALNT5, GCH1, GDPD3, GPAM, HMGB2, HMOX1, IL1B, IL1RN, IL6, IRS2, KYNU, LPAR1, LPCAT3, LRRN3, MMP10, MMP8, NRG1, NRK, PDE5A, PDGFRA, PDPK1, PIK3R3, PLCXD1, PLD1, PPARG, PRKD3, PRLR, PTGS2, PTPRN, QPRT, RDH8, RETSAT, SERPINA1, SERPINB4, SLC25A20, SNCA, SOD2, SPP1, SULT1B1, TACR1, THBS1, THY1, TNFRSF11B, UACA, VGF, VLDLR
Signaling	ACVRL1, ADM, ANGPT1, ANGPTL4, BDKRB2, BDNF, BIRC3, BMP2, CCL2, CCL20, CCL3, CD36, CDK6, CHRNA1, COL1A2, CSF2, CXCL1, CXCL10, CXCL5, DCN, DDIT4, EDN1, EDNRA, EREG, F3, FABP4, FGD4, FGF1, FGF2, FGF7, FST, GABRA2, HIST1H4C, HMGB2, HOMER1, ID1, ID3, IKBKE, IL1B, IL1RN, IL6, IL8, IRAK2, JUP, L1CAM, LPAR1, LRRN3, NRG1, NRK, OLR1, PDGFRA, PDPK1, PIK3CG, PIK3R3, PLD1, PRLR, PTGS2, RAB3A, ROS1, RPS6KA2, SNCA, STAT4, TACR1, THBS1, THY1, TNFAIP3, TRAF3IP2, ULK2, WNT16
Cell Cycle	ACVRL1, ADM, BDKRB2, BDNF, BMP2, CCL2, CCL3L1, CDK6, COL8A1, CSF2, CSF3, CXADR, CXCL1, CXCL10, CXCL5, EDN1, EREG, F3, FABP4, FGF1, FGF2, FGF7, ID3, IL1A, IL1B, IL6, IL8, MMP12, MYOCD, PDGFRA, PTGS2, SOD2, THBS1
Cell migration	ACVRL1, BDKRB1, C3, CCL2, CCL20, CCL3, CCL3L1, CXCL1, CXCL10, CXCL2, CXCL3, CXCL5, EDN1, F2RL1, F3, FABP4, FGF2, ICAM1, ID1, IL1B, IL6, IL8, NRG1, PDGFRA, PLD1, PSG2, PTGS2, SEMA3C, SERPIND1, SERPINF1, SNCA, THBS1, THY1, UACA
Ion homeostasis	ADCY3, ADM, BDKRB1, BDKRB2, CCL2, CCL3, CHRNA1, EDN1, EDNRA, F2RL1, IL1B, IL6, ITPKA, ITPR3, LPAR1, NRG1, PDGFRB, PTGS2, SERPINA1, SLC11A2, SLC5A3, SLC8A3, SNCA, SOD2, TACR1, THBS1, THY1, TNFRSF11B
Regulation of cell death	ADM, ANGPT1, ANGPTL4, BDKRB2, BDNF, BIRC3, CCL2, CSF2, F3, FGF2, GCH1, ID3, IL1A, IL1B, IL1RN, IL6, IRAK2, PIK3R3, PRLR, PTGS2, SNCA, SOD2, THBS1, TMEM132A, TNFAIP3, UACA, VNN1
Extracellular matrix	ADAMTS9, ANGPTL4, APLP1, CD248, COL1A1, COL1A2, COL6A1, COL8A1, DCN, F3, FGF1, LUM, MMP10, MMP12, MMP8, NID2, PDGFRA, PI3, SERPINA1, TGFBI, THBS1, TNFRSF11B, VCAN, WNT16
Hypoxia and oxydative stress	ADM, ANGPT1, ANGPTL4, CCL2, COL1A1, DPP4, EDN1, GCH1, ICAM1, IL1B, IL6, OLR1, PDE5A, PDGFRA, PDLIM1, PTGS2, SERPINA1, SNCA, SOD2, THBS1, TRPA1, VNN1

inhibited the expression of multiple cytokines, chemokines, and serpin genes in the context of RAS-induced senescence (Figure 29D-L). These changes in gene expression were translated into a reduction in the ability of the supernatant of metformin-treated senescent cells to stimulate the growth of the PC3 prostate cancer cells (Figure 29M) as recently reported (844). A dose-response experiment indicated that metformin inhibited cytokine expression at doses of 1 mM or higher (Figure 30). Intriguingly, at doses of 1 mM, metformin reduced cytokine gene expression in cells expressing oncogenic *ras* but did not affect cell proliferation in the control cells (Figure 30). At 0.5 mM, the effects of metformin on RASV12 expressing cells were moderately stimulatory on IL6 and IL8 and inhibitory on CXCL5. Taken together, the results suggest that high doses of metformin can block potentially maladaptive effects of the senescence program without compromising its anticancer effects.

Analysis of downregulated genes with the algorithm SPEED (Signaling Pathway Enrichment using Experimental Datasets) identified genes in Toll-like receptor (TLR), IL-1 and TNFα signaling pathways as the most downregulated genes in cells treated with metformin (Figure S20A, B). TLR signaling regulates the expression of inflammatory cytokines via the transcription factors AP1/Jun and NF-κB but also the antiviral and antiproliferative interferon pathway through the transcription factors IRF3 and IRF7 (845). Using gene set enrichment analysis (GSEA), we found that genes regulated by AP1/JUN and NF-κB were significantly enriched among the downregulated genes in metformin-treated cells but not in the control (Figure S20C, D). In contrast, genes regulated by the interferon pathway (IRF3/7) were not significantly altered by metformin (Figure S20E). Next, we analyzed the gene expression data with the bioinformatics programs TFacTS and DIRE to look for transcription factors that can regulate the affected genes. The transcription factors TCF4, NFKB1, and RELA were the most important associated with gene expression changes caused by metformin (Figure S21A, B). When we considered only downregulated cytokine genes, gene set enrichment analysis (GSEA) indicated a significant enrichment of cytokines genes targeted by NF-κB (Figure 31A) and as shown in heat maps (Figure 31B), this downregulation was consistent in three replicas of the same experiment. When we used this list of cytokine

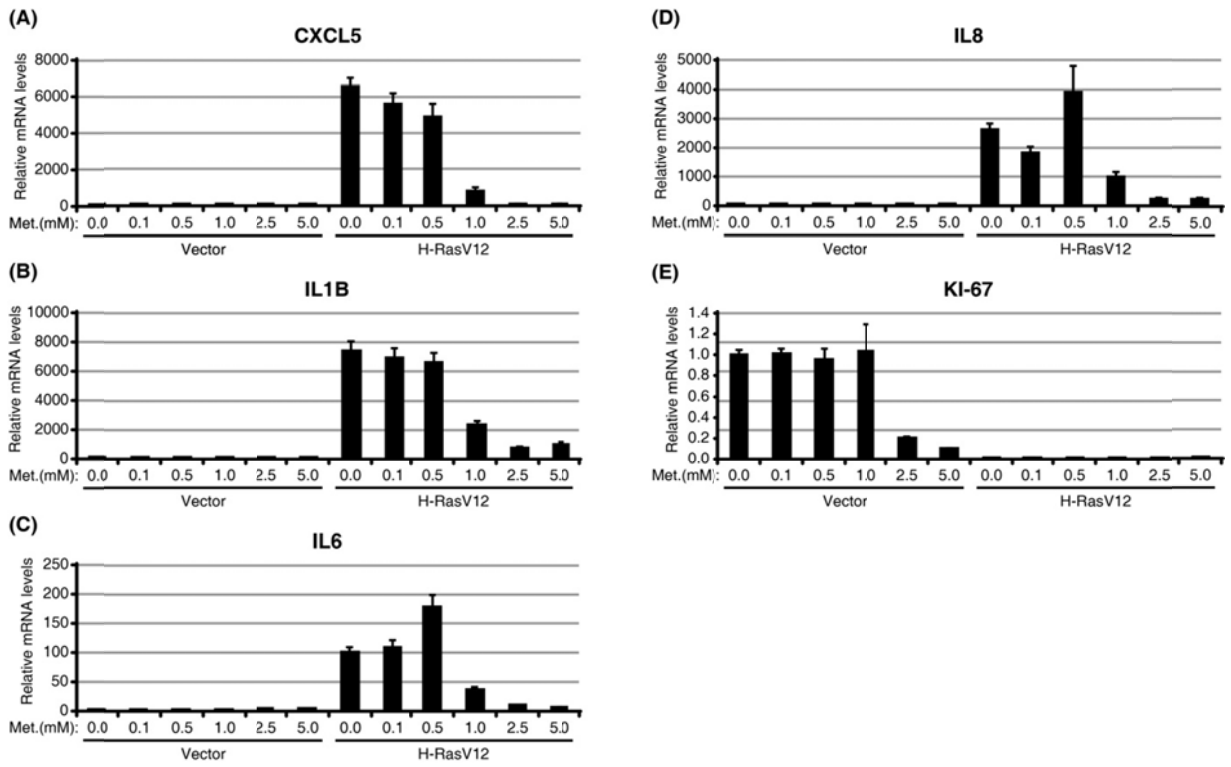

Figure 30. Metformin inhibits the senescence-associated secretory phenotype at concentrations that do not affect the growth of normal cells

(***A-D***) qPCR validation of several cytokine genes that are highly expressed in senescent cells expressing oncogenic *ras* and are repressed by 1.0, 2.5 and 5.0 mM metformin. RNA extracts from IMR90 fibroblasts expressing H-RASV12 or an empty vector and treated with metformin at the indicated concentrations or vehicle for 6 days. (***E***) qPCR for the proliferation marker KI-67. Error bars represent ± SD of replicates.

genes downregulated by metformin with the programs TFacTS and DIRE, NFKB and C/EBPδ were the most common transcription factors regulating those genes (Figures 31C and S21C). NF-κB is recognized as a master regulator of cytokine gene expression in senescent cells (140, 141, 846) and aging (847, 848). Therefore, we hypothesized that metformin inhibited cytokine gene expression in senescent cells by inhibiting NF-κB activation.

Effects of metformin on the NF-κB pathway

NF-κB is a transcription factor formed by homo or heterodimers of five distinct subunits RELA (p65), RELB, c-REL, NFKB1, and NFKB2 and is sequestered in the

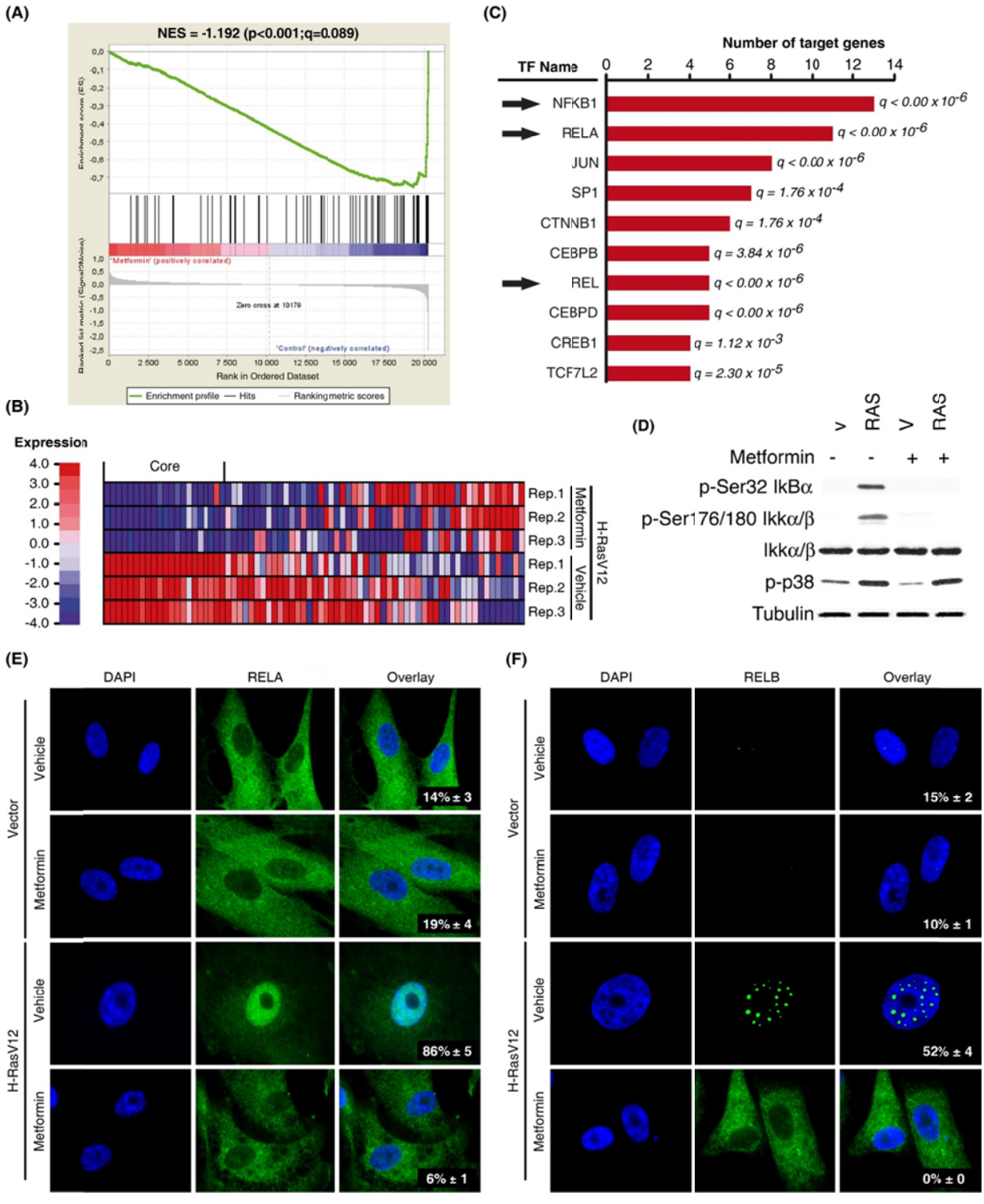
(A)
NES = -1.192 (p<0.001;q=0.089)
Enrichment score (ES)
'Metformin' (positively correlated)
Zero cross at 10179
'Control' (negatively correlated)
Ranked list metric (Signal2Noise)
Rank in Ordered Dataset
Enrichment profile
Hits
Ranking metric scores
(B)
Expression
Core
Rep.1
Rep.2
Rep.3
Metformin
Rep.1
Rep.2
Rep.3
Vehicle
H-RasV12
(C)
Number of target genes
TF Name
NFKB1
RELA
JUN
SP1
CTNNB1
CEBPB
REL
CEBPD
CREB1
TCF7L2
q < 0.00 x 10-6
q < 0.00 x 10-6
q < 0.00 x 10-6
q = 1.76 x 10-4
q = 1.76 x 10-4
q = 3.84 x 10-6
q < 0.00 x 10-6
q < 0.00 x 10-6
q = 1.12 x 10-3
q = 2.30 x 10-5
(D)
V
RAS
V
RAS
Metformin
p-Ser32 IkBα
p-Ser176/180 Ikkα/β
Ikkα/β
p-p38
Tubulin
(E)
DAPI
RELA
Overlay
Vector
Vehicle
Metformin
H-RasV12
Vehicle
Metformin
14% ± 3
19% ± 4
86% ± 5
6% ± 1
(F)
DAPI
RELB
Overlay
Vector
Vehicle
Metformin
H-RasV12
Vehicle
Metformin
15% ± 2
10% ± 1
52% ± 4
0% ± 0

Figure 31. Metformin inhibits the IKK/NF-κB signal transduction pathway

(***A***) Gene Set Enrichment analysis (GSEA) revealed that a gene set related to cytokines regulated by NF-κB was significantly decreased following treatment of H-RASV12 expressing cells with 5.0 mM metformin. The Normalized Enrichment Score (NES), the nominal *P*-value determined by an empirical phenotype-based permutation test procedure and the False Discovery Rate (FDR; q-value) are indicated. (***B***) Heat map of relative expression levels of the genes used in the GSEA analysis (Red = upregulated, blue = downregulated). The microarrays data obtained from three replicates are shown. (***C***) TFactS prediction of downregulated transcription factors in H-RASV12 expressing cells treated with 5.0 mM metformin for genes coding for cytokines and their receptors as identified in figure 29C. For each transcription factor, the number of target genes found in the list of 26 submitted genes present in the TFactS database is shown. The minimum False Discovery Rate (FDR) is indicated (q-value). (***D***) Immunoblots for the indicated proteins from extracts of IMR90 cells expressing an empty vector (V) or oncogneic *ras* (RAS) and treated with 5 mM metformin or vehicle for 6 days. (***E-F***) Indirect immunofluorescence against RELA (*E*) or RELB (*F*) of cells as in (*D*). The percent of cells with RELA or RELB in the nucleus is indicated at the bottom right of the overlay panel, standard deviations of three counts of a 100 cells each is indicated, $n = 3$.

cytoplasm by the ankyrin repeat containing IκB proteins (849). During senescence, both canonical and noncanonical NF-κB pathways are activated because DNA binding by RELA, RELB, NFKB1, and NFKB2 was found increased (846). A key event in the activation of the NF-κB pathway is the phosphorylation of the cytoplasmic inhibitor IκB (850) and metformin dramatically inhibited this event in RAS-expressing cells (Figure 31D). IκB is phosphorylated by the IκB kinase, a complex of two catalytic subunits (IKKα and IKKβ) and one regulatory subunit (IKKγ also known as NEMO). This complex is activated by a mechanism involving several protein kinases including the ubiquitin-dependent kinase TAK1 (851) and the serine/threonine kinase RIP1 (852) that phosphorylate IKKα/β in their activation loop at S176/177 and S180/181, respectively. Metformin also inhibited the phosphorylation of IKKα/β in RAS-senescent cells (Figure 31D), suggesting that oncogenic *ras* activates the IKK kinases in primary cells but these kinases are inactive in metformin-treated cells. Of note, metformin did not prevent the activation of p38 MAP kinase in RAS-expressing cells (Figure 31D), suggesting that its activity is confined to the NF-κB pathway. Finally, we found that oncogenic *ras* induced the nuclear translocation of RELA and RELB and metformin

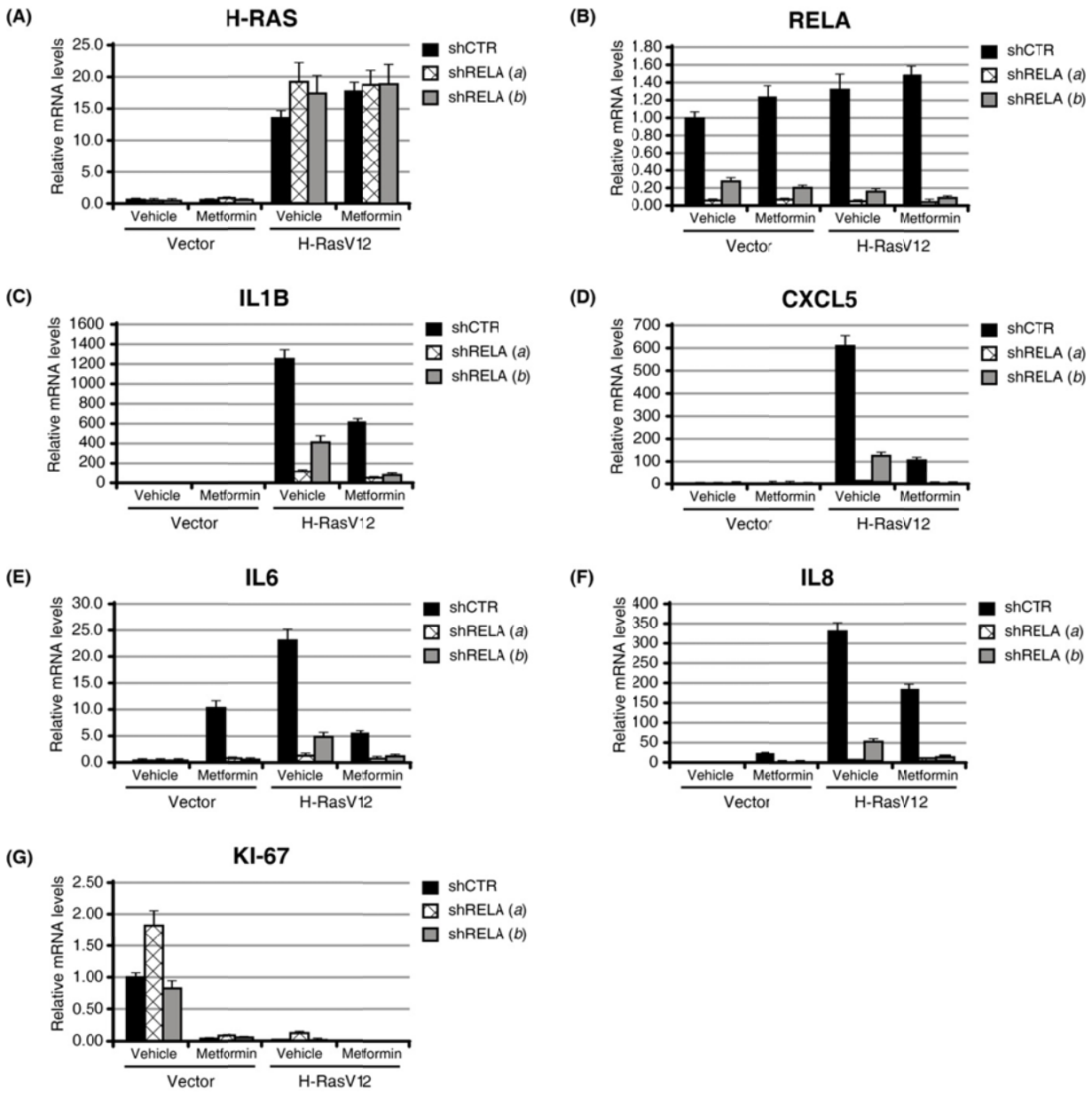

Figure 32. Metformin and RELA act on the same pathway to control the SASP

qPCR of HRAS, RELA and several cytokine genes that are highly expressed in senescent cells expressing oncogenic *ras* and are repressed by shRELA(a), shRELA(b) or shRELA (a or b) plus 5.0 mM metformin for 6 days. Error bars represent ± SD of replicates.

dramatically inhibited this effect (Figure 31E, F). Of note, RELB localized to distinct nuclear foci in senescent fibroblasts and metformin reduced the intensity of staining of these foci.

Next, we investigated whether the main effect of metformin inhibiting the senescence-associated secretory phenotype (SASP) depended on NF-κB inhibition. We introduced previously validated shRNAs against RELA (140) into primary human fibroblasts IMR90 together with oncogenic *ras* to induce cell senescence. Of note, neither metformin nor shRNAs against RELA reduced RAS mRNA expression (Figure 32A). However, the two shRNAs used did efficiently reduced RELA mRNA: shRELA(a) more than shRELA(b) (Figure 32B). Then, we measured the expression of several cytokines genes in these cells after treatment with metformin or vehicle. We found that knocking down RELA inhibited the expression of all tested cytokines and that metformin did not significantly further this effect in cells with shRELA(a) (Figure 32C-F). Metformin did improve the ability of shRELA(b) to inhibit cytokine gene expression (Figure 32C-F) and this can be explained because this shRNA was not as efficient as shRELA(a) on knocking down RELA levels. Notably, shRNAs against RELA did not affect growth as seen with the levels of the KI67 cell cycle gene, and RAS did induce growth arrest independently of their presence (Figure 32G). Taken together, these results strongly suggest that metformin and the shRNAs against RELA are targeting the same pathway.

The exact activation mechanism of the IKK/NF-κB pathway during RAS-induced senescence is not yet fully characterized. For this reason, we investigated whether metformin could inhibit NF-κB activation in cells treated with lipopolysaccharide (LPS), which activate NF-κB by a pathway starting from Toll-like receptors leading to activation of the ubiquitin-dependent kinase TAK1 (853). We found that metformin also inhibited RelA nuclear translocation in response to LPS in the murine macrophage cell line RAW264.7 (Figures 33A, B). We also measured the phosphorylation of IκB in response to LPS in MEFs from *ampk* wild-type and *ampk* null animals and observed a similar inhibition of NF-κB pathway by metformin (Figure 33C, D). We thus conclude that the inhibition of the TLR/NF-κB signaling pathway by metformin is independent of AMPK.

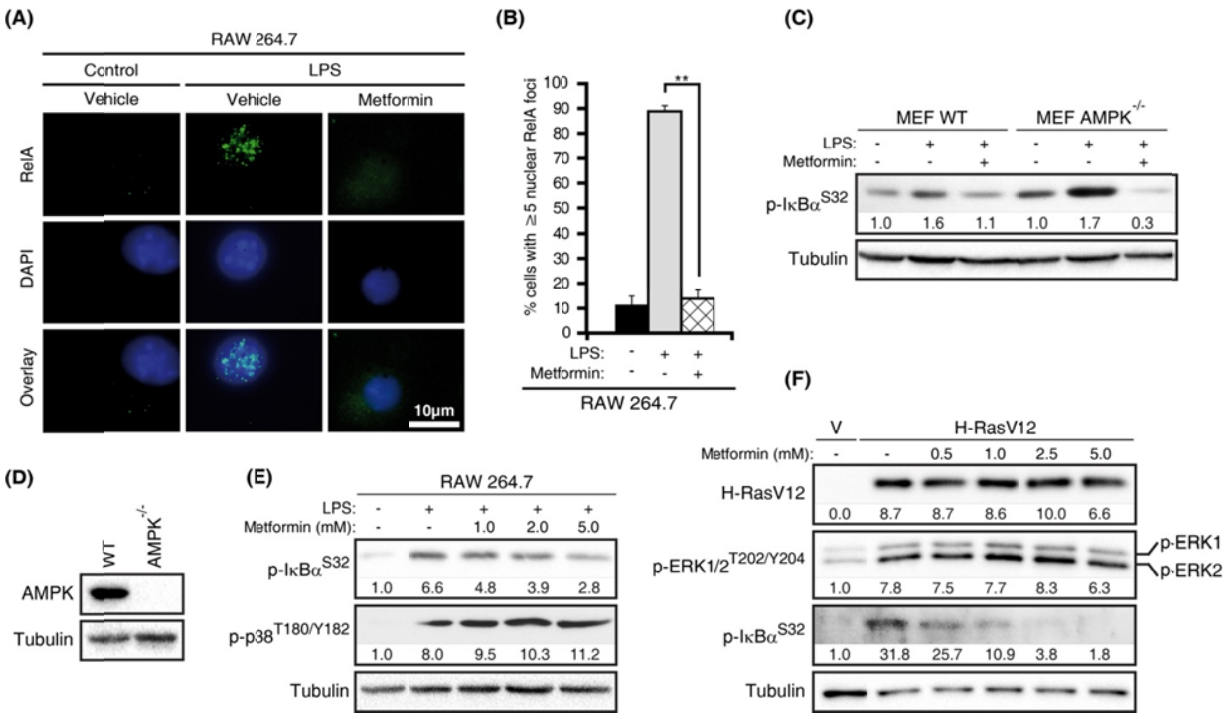

Figure 33. Metformin inhibits NF-κB activation by lipopolysaccharide (LPS) in fibroblasts and macrophages

(***A***) Indirect immunofluorescence against RelA in murine machophages (RAW 264.7) treated with LPS (500 ng/mL) and 5.0 mM metformin or vehicle for 24 h. (***B***) Quantitation of immunofluorescence data in (*A*), the percentage of cells and the standard deviation were calculated with three independent counts of 100 cells; $^{**}P < 0.005$ according to a two-sample Student's *t*-test. (***C***) Immunoblots for phospho-IκBα from extracts with wild-type and *ampk* null MEFs treated with LPS as in (*A*) and 5.0 mM metformin or vehicle for 48 h. (***D***) Immunoblots for Ampk from extracts with wild-type and *ampk* null MEFs. (***E***) Immunoblots for phospho-IκBα and phospho-p38 MAPK in RAW 264.7 macrophages treated with LPS or vehicle and metformin for 24 h at the indicated concentrations. (***F***) Immunoblots for phospho-IκBα and RAS/ERK signaling proteins in fibroblasts expressing RASV12 or an empty vector (V) control treated with the indicated concentrations of metformin for 6 days.

We previously used metformin at a dose of 5 mM to inhibit production of ROS in human and rodent primary cells (445). We treated RAW264.7 cells with 1, 2, and 5 mM metformin and observed a dose-dependent inhibition of LPS-stimulated phosphorylation of IκB (Figure 33E). A similar result was also obtained in senescent IMR90 cells expressing oncogenic *ras* (Figure 33F) where we previously showed that a dose of 1 mM was sufficient to reduce cytokine gene expression (Figure 30). These concentrations are considerably higher

than serum concentration achieved in the treatment of diabetes (~16 μM) (854). However, dose-response relationships relating serum level to activity are complex as different cell types concentrate metformin to different extents based on expression of cell surface transporters such as OCT-1 (854). Thus, it will be necessary to investigate *in vivo* inflammatory endpoints in relationship to administered metformin dose to determine the clinical relevance of our findings.

4.3.4 Discussion

Epidemiological and laboratory studies have suggested that metformin has antineoplastic activity (443, 836, 855, 856). These findings are intriguing but require further study, as the population studies are retrospective, and thus hypothesis-generating rather than definitive, and the laboratory evidence does not fully take into account pharmacokinetic factors in humans.

One major risk factor in cancer is age and at the cellular level aging has been linked to the process of cellular senescence (166). Paradoxically, cellular senescence is a tumor suppressor mechanism (455) and inhibiting cellular senescence may increase overall cancer incidence as seen in animals with disabled mutations in senescent regulators such as p16INK4a and p53 (455). One important question in the aging field is whether it is possible to reduce the pro-aging effects of cellular senescence without compromising tumor suppression. It was recently reported that glucocorticoids reduced the secretion of some but not all cytokines produced by senescence cells without interfering with the growth arrest program (857), suggesting that the pro-aging and anticancer effects of senescence can be experimentally dissociated.

Here, we report that metformin decrease the production of inflammatory cytokines in senescent cells and in response to LPS by interfering with the master regulator of inflammatory gene expression, the transcription factor NF-κB. In fact, analysis of the gene expression data in metformin-treated senescent cells indicates that the drug reduced the expression of proinflammatory cytokines mostly regulated by NF-κB but did not affect the

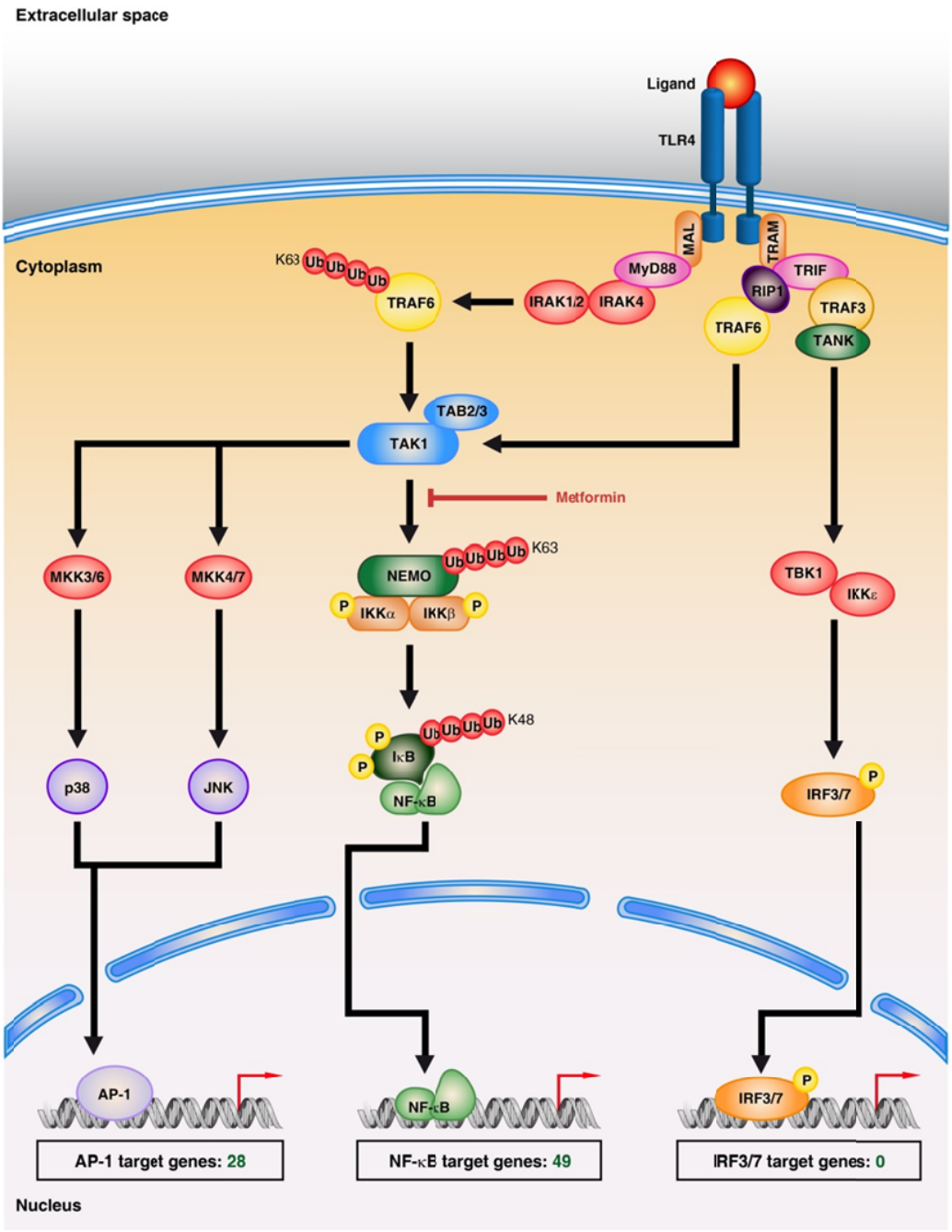

Figure 34. Model of metformin action of the TLR signaling pathway

The drug blocks the proinflammatory NF-κB but does not affect the antiproliferative interferon pathway. In addition, as p38MAPK is not affected by metformin, its site of action must be between TAK1 and IKK kinases. Number of genes affected by AP-1, NF-κB and IRF3/IRF7 are shown at the bottom. Interferon genes were not affected by metformin, while multiple NF-κB and AP-1 genes were affected. However, 16 of 28 AP-1-affected genes were also NF-κB target genes.

expression of anticancer cytokines such as interferons and interferon target genes (Figure 34). Consistent with this explanation, it was found in an experimental model of uveitis in rats that metformin prevented the production of inflammatory cytokines and the phosphorylation of RelA (858). There is evidence that metformin can inhibit the production of ROS in senescent cells (445) and mitochondrial ROS have been implicated in NF-κB activation (837). The exact mechanism by which ROS may activate the NF-κB pathway is unknown. Metformin inhibits IKKα/β kinases but not the p38MAPK, and as these two pathways are downstream of TAK1, it seems that the drug interferes only with the IKK activation pathway (Figure 34). Also, metformin does not affect the expression of interferon target genes in RAS-expressing cells, suggesting that it does not interfere with NEMO functions, which are required for activation of both NF-κB and IRF3/7 in response to viral RNA (859).

NF-κB, ROS, and inflammatory cytokines have all been implicated in the physiopathology of aging. In fact, bioinformatic analysis of microarray data from several aged tissues indicated that NF-κB was the transcription factor most associated to changes in gene expression during aging (847) and reducing NF-kB activity attenuated the accelerated aging phenotype of a mouse model of progeria (860). Metformin can extend life span in rodents (861) and worms (862). In patients with impaired fasting glucose, high doses of metformin (3 g/day for 90 days) reduced the levels of several inflammatory cytokines accompanied by an improvement in insulin sensitivity and a reduction of blood free fatty acids (863). Our data suggest that these beneficial clinical effects can be explained by metformin-mediated inhibition of NF-κB. In addition, the secretion of cytokines by senescent cells may have pro-cancer effects (155) and inhibit the action of anticancer chemotherapy (864). Hence, anti-inflammatory actions of metformin may provide novel opportunities for cancer prevention or treatment. However, the dose of metformin used for the treatment of diabetes was chosen to improve hyperglycemia, and this exposure level may or may not be optimal for antineoplastic or anti-inflammatory effects. Thus, our work motivates study of metformin pharmacokinetics in the context of endpoints beyond glycemic control.

4.3.5 Materials and methods

Cell Growth and retroviral infection

Normal lung human diploid fibroblasts IMR90 (CCL-186, ATCC, Manassas, VA, USA) and the murine macrophage cell line RAW264.7 (ATCC) were cultured in DMEM (Invitrogen, Logan UT, USA) supplemented with 10% FBS (Wisent, Montreal, QC, Canada) and 1% penicillin G/streptomycin sulfate (Wisent). AMP-activated protein kinase α (AMPKα)+/+ and AMPKα-/- mouse embryonic fibroblasts (MEFs) were provided by Dr. Russell Jones (McGill University) and were cultured in 10% FBS DMEM (Wisent) with glutamine. LPS (Sigma, Oakville, ON, Canada) was used at 500 ng/mL. Retroviral vector pBabe, pWZL, pBabe H-RASV12, pWZLH-RASV12, and shRNAs RELA(a) and (b) were from S.W. Lowe (140). IMR90 cells were infected with retroviruses expressing RASV12 and selected during 2 days with 2.5μg/mL puromycin or 75 μg/mL hygromycin depending on the vecotrs. Twenty-four hours after infection, cells were treated with five different concentrations of metformin (Sigma) or water (vehicle) for 6 days. Infection and senescence protocols were described in (110).

Effects of conditioned medium from senescent cells on prostate cancer cells

Senescent IMR90 (H-RASV12) or control IMR90 (vector) were treated with 5 mM metformin for 48 h. Fresh medium without metformin was used the last 24 h to generate conditioned medium (CM). CM was then filtered (with 45-μm, to prevent cell transfer and added on PC3 cells (8 x 10^4 cells per 6 cm plates). PC3 cells were then grown for 3 days and fixed in 1% glutaraldehyde. Relative cell number was estimated using a crystal violet incorporation assay as previously described (100). Each condition was carried out in triplicate.

RNA analysis

Total mRNA extracts were prepared in TRIzol (Invitrogen), and their purification was performed according to the manufacturer's instructions. For cDNA preparation, 2 μg of total RNA was reverse transcribed using the RevertAid H minus first strand cDNA synthesis kit (Fermentas, Burlington, ON, Canada). Reverse transcription products were amplified by real-

time quantitative PCR using TaqMan PCR Master Mix (Applied Biosystems, Foster City, CA, USA) with TBP gene as endogenous control in figure 29 or with SyberGreen for all other figures with both TBP and HMBS as endogenous controls as previously described (103). The lightCycler 480 Real-Time PCR System (Roche Applied Science, Laval, QC, Canada) was used to detect the amplification level and was programmed to an initial step of 10 min at 95°C, followed by 40 cycles of 15 seconds at 95°C and 1 minute at 60°C. The TBP (TATA-binding protein) was used as endogenous control (Applied Biosystems, #4326322E-0705006). The relative quantification of target genes was determined using the ΔΔCT method. Primers used for qPCR and detailed procedure for microarrays and bioinformatics are presented in the supplementary data.

Western blot

For Western blot analysis, total protein extracts were separated on SDS-PAGE and transferred to Immobilon-P membranes (Millipore, Billerica, MA, USA). Membranes were incubated with the primary antibodies: anti-AMPKα (#2532, 1:1000, Cell Signaling Technology, Pickering, ON, Canada), antiphosphoThr202/Tyr204 ERK1/2 (1:2000; clone D13.14.4E, #4370, Cell Signaling), anti-H-RAS (1:250; clone F235, Sc-29, Santa Cruz Biotechnology, Santa Cruz, CA, USA), antiphosphoSer32 IkBα (1:1000, (#2859 Cell Signaling), antiphospho-Ser176/180 Ikkα/β (1:1000 #2694 Cell Signaling), antiphospho Thr180/Tyr182 p38MAPK (1:1000, #9211 Cell Signaling), antitubulin (1:5000, T5168, Sigma). Signals were revealed after incubation with anti-mouse or anti-rabbit secondary antibodies, coupled to peroxidase (BioRad, Hercules, CA, USA) using enhanced chemiluminescence (ECL, Amersham, Baie d'Urfe, QC, Canada).

Immunofluorescence

Cells were fixed as described (103). After washing with PBS and 3% bovine serum albumin (BSA) coverslips were incubated with anti-p65 RELA antibody (1:200, #8242 Cell Signaling) for 2 h at room temperature. Then, coverslips were washed with PBS and incubated with goat anti-mouse AlexaFluor 488 (1:1000; A-11001, Molecular Probes, Invitrogen, Logan, UT, USA) for 1 h at room temperature. Finally, coverslips were rinsed with PBS and

incubated with 300 nM DAPI for 10 min. Images were acquired with an inverted microscope Nikon TE2000U and processed with the software Metamorph.

4.3.6 Acknowledgements

This work was supported by a grant from Prostate Cancer Canada to G.F. and M.P. G.F. is a FRSQ national fellow. X.D.-S. is a fellow of the Vanier Canada Graduate Scholarships Program.

4.3.7 Supplemental Material

4.3.7.1 Supplemental Results

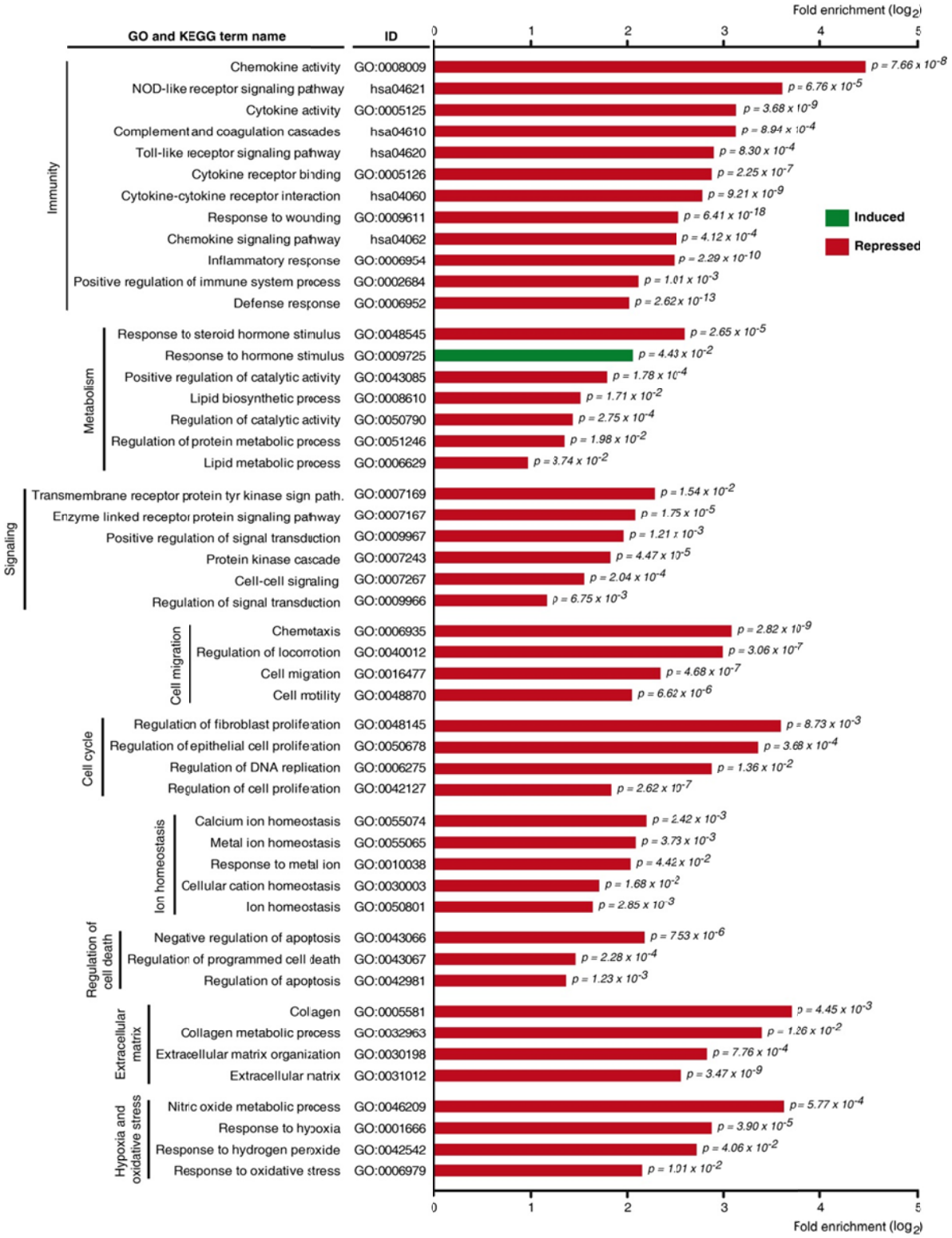

Figure S19. Biological function analysis of microarrays data obtained from oncogenic *ras*-expressing cells treated with metformin

Summary of the significant Gene Ontology (GO) and Kyoto Encyclopedia of Genes and Genomes (KEGG) term names used to associate the genes to general biological functions. These terms were identified by a FatiGO single enrichment analysis using Affymetrix microarrays data for conditions as in Figure 29. This analysis was carried out using transcripts with a fold change ≥2 and a *P*-value < 0.05 calculated according to the two-sample student's *t*-test. For each term, an adjusted *P*-value was calculated by the methodology implemented in the Babelomics 4.3 platform.

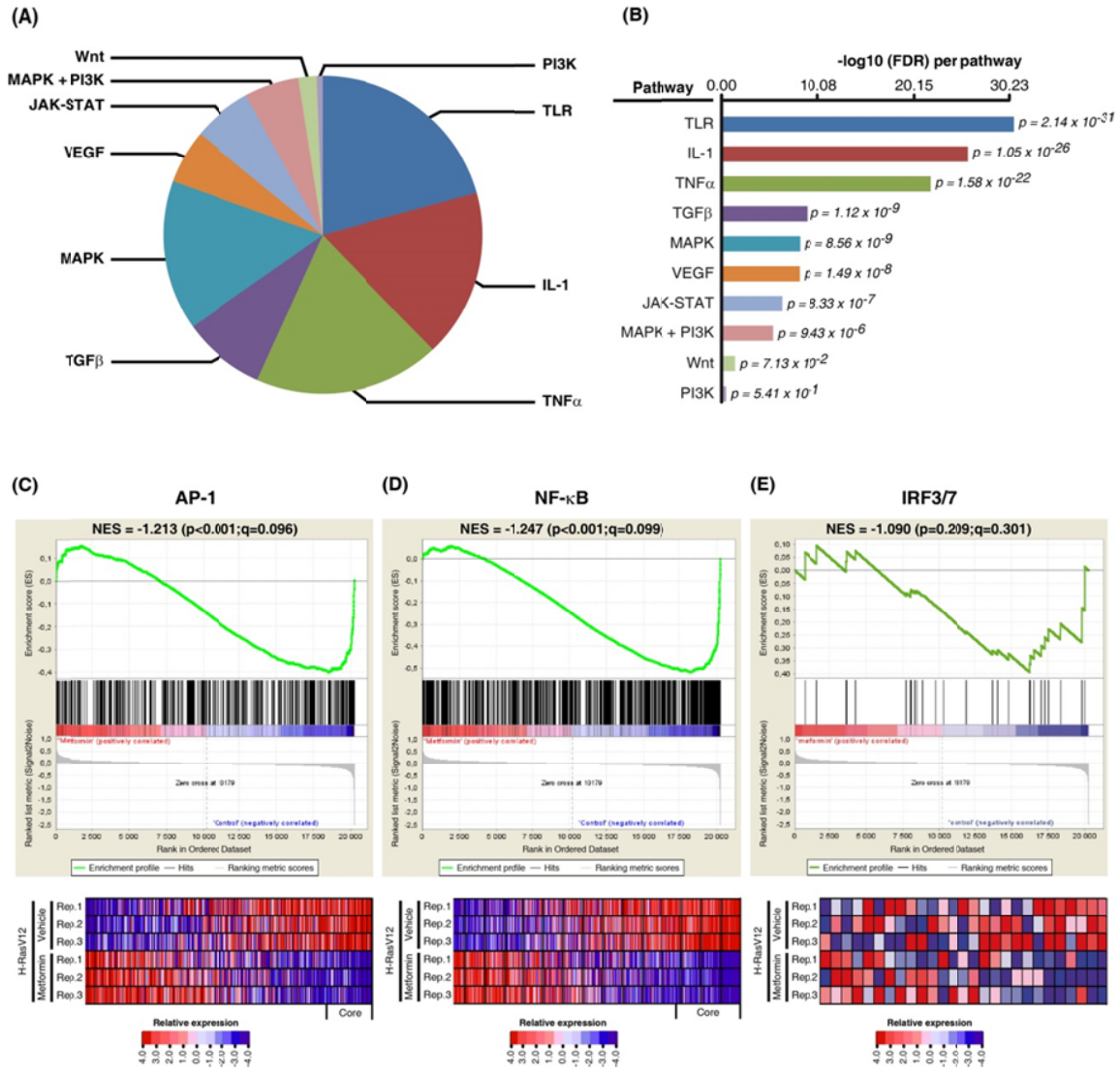

Figure S20. Metformin inhibits Toll-like receptors (TLRs) signaling to NF-κB

(***A***) Prediction of downregulated signaling pathways in H-RASV12-expressing cells treated with 5 mM metformin with the SPEED (Signaling Pathway Enrichment using Experimental Datasets) bioinformatics tool. The microarrays data as in Figure 29 were used. The analysis was carried out using transcripts with a decrease ≥2 and a *P*-value < 0.05 (two-sample student's *t*-test). For each pathway, the proportion of genes found in the SPEED database is shown. (***B***) Statistics for each pathway identified; the FDR in $\log_{10}$ and the *P*-value (Fisher's exact test) are shown. (***C-E, top***) GSEA revealed that gene sets related to AP-1 and NF-κB target genes, but not IRF3/7 target genes, were significantly decreased following treatments of H-RASV12-expressing cells with 5.0 mM metformin. The Normalized Enrichment Score (NES), the False Discovery Rate (FDR; q-value), and the nominal *P*-value, which is determined by an empirical phenotype-based permutation test procedure, are indicated. (***C-E, bottom***) Heat map of relative expression levels of the genes used in the GSEA (n = 3) (red, upregulated; blue, downregulated).

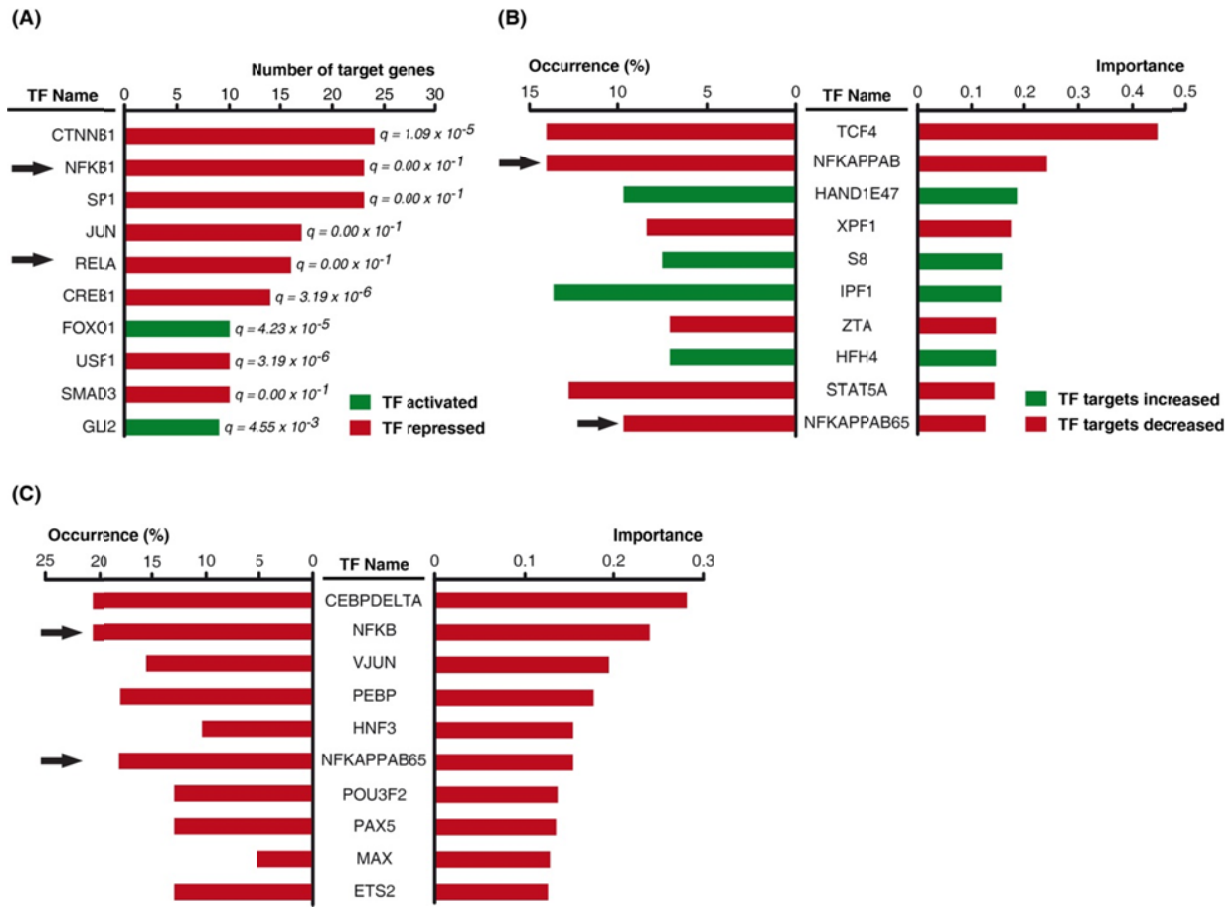

Figure S21. Metformin inhibits genes regulated by NF-κB and C/EBPδ

(***A***) TFactS prediction of regulated transcription factors (TFs) in H-RASV12-expressing cells treated with 5.0 mM metformin, using microarrays data as in Figure 29 (red, downregulated; green, upregulated). For each TF, the number of target genes found in the TFactS database is shown (from a list of 108 submitted genes). The FDR (q-value) is indicated. (***B***) DIRE prediction of regulated TFs in conditions as in the previous panel (red, the TF target genes identified are in majority downregulated; green, these genes are in majority upregulated). The percentage of target genes found in a list of 388 recognized submitted genes (input gene set) is shown for each potential TF (occurrence). The importance is the product of a TF occurrence and his weight, which is a measure of its association with the input gene set. (***C***) DIRE prediction for TFs regulating cytokine genes downregulated by metformin. The percentage of target genes found in the list of 37 recognized submitted genes is shown for each potential TF (occurrence).

4.3.7.2 Supplemental materials and methods

Real-time PCR

The primers used are presented in the Supplemental Table SVI.

Table SVI. List of primers used for qPCR with the TaqMan technology

Target	Forward (5'→3')	Reverse (5'→3')
CCL20	ATGTGCTGTACCAAGAGTTTGC	TCAAAGTTGCTTGCTGCTTC
CXCL1	TCCTGCATCCCCCATAGTTA	CTTCAGGAACAGCCACCAGT
CXCL5	TCTGCTATGCTATTGAAGTTTTGG	TCACCTACAATTCAAGACACTTTGA
CXCL10	GAAAGCAGTTAGCAAGGAAAGGT	GACATATACTCCATGTAGGGAAGTGA
IL1B	CTGTCCTGCGTGTTGAAAGA	TTGGGTAATTTTTGGGATCTACA
IL6	GATGAGTACAAAAGTCCTGATCCA	CTGCAGCCACTGGTTCTGT
IL8	AGACAGCAGAGCACACAAGC	ATGGTTCCTTCCGGTGGT
KI-67	AGAAGACAGTACCGCAGATGA	CGGCTCACTAATTTAACGCTGG
SERPINB3	AGAACACCACAGGAAAAGCTG	TGCATCAGTGGATTTGTTGAA
SERPINB4	CACAGACACACACAGCCTCTC	TTCATGGTGAACTCGATGTGA

Microarrays

RNA quality and cDNA synthesis

Total RNA integrity was evaluated with the Eukaryote Total RNA Nano assay of the Agilent 2100 Bioanalyzer (Agilent Technologies, Palo Alto, CA). All RNA samples had a RNA Integrity Number (RIN) ≥ 9.5, a 28S and 18S rRNA ratio > 1.8 and an A260/A280 ratio in the range of 1.9 to 2.1. cDNAs were prepared according to the protocol from the Ambion® WT Expression kit for Affymettrix® GeneChip®Whole Transcript (WT) Expression Arrays (Applied Biosystems, Foster City, CA). The resulting single-stranded cDNAs containing the unnatural uracil base are treated with Uracil DNA glycosylase which removes the uracil residue. Then the cDNAs are fragmented by a treatment with the APE1 enzyme which cleaves

the phosphodiester backbone where the uracil is missing and leaves 3'-OH and 5'-deoxyribose phosphate ends. The majority of the fragments range from 20 to 200 bases with a peak around 40 to 70 bases. These fragments are labeled with Biotin Allonamide Triphosphate as described in the instructions of the GeneChip® WT Terminal Labeling Kit (Applied Biosystems).

Following fragmentation and labeling, 10 µg of cDNAs were hybridized for 16 h at 45°C with rotation (60 RPM) on GeneChips® Human Gene 1.0 ST array (Affymetrix, Santa Clara, CA). GeneChips were washed and stained in the Affymetrix Fluidics Station 400 according to the manufacturer's instructions. GeneChips were scanned on a GeneChip® Scanner 3000 7G/4 Color Early Access (Affymetrix).

Data normalization and analysis

The microarray data files from triplicates of both conditions (control and metformin-treated cells) were analyzed with the FlexArray 1.6.1.1 software (http://genomequebec.mcgill.ca/FlexArray; Génome Québec Innovation Centre) using Affymetrix default analysis settings. Raw data were normalized with a Robust Multi-array Average (RMA) algorithm. Probeset IDs were assigned to their respective transcript names with the metadata file furnished for GeneChips® Human Gene 1.0 ST array on the Affymetrix website. The mean fold change in the signal intensity between conditions was calculated for all transcripts and the significance (*P*-value) was evaluated with the two-sample student's *t*-test. Transcripts with a fold change ≥2 and a *P*-value < 0.05 were considered for further analysis.

Bioinformatic analyses

Inferring biological functions

To infer biological functions from modulated genes, we performed a FatiGO single enrichment analysis with the Babelomics 4.3 platform (493). This platform was used to identify Gene Ontology (GO) and Kyoto Encyclopedia of Genes and Genomes (KEGG) terms significantly enriched among transcripts with a fold changes ≥2 when compared with the rest of genome. For each term, an adjusted *P*-value was calculated by the methodology implemented in the Babelomics 4.3 platform.

Inferring regulated signaling pathways

We used the SPEED (Signaling Pathway Enrichment using Experimental Datasets) algorithm (865) to predict regulated signaling pathways from transcripts with a decrease ≥2 fold. For each potential regulated signaling pathway, the significance was determined by the False Discovery Rate (FDR; q-value) and a *P*-value calculated by a Fisher's exact test. We used the default settings of the application.

Prediction of regulated transcription factors (TFs)

The TFactS web-based application (866) was used to predict TFs from transcripts with a fold change ≥2. TFactS relies on catalogues of TF signatures established from the literature and many databases. The Sign-Less catalogue was used to find relationships between TFs and their target genes present in our gene lists. The type of regulation (up or down) of a specific TF was determined with the Sign-Sensitive catalogue. For our analyses, we used 1000 random genes as negative control and the other default parameters of the application. The significance for each TF is determined by many statistical parameters. A *P*-value is computed using the Fisher's exact test, an E-value is determined, the minimum False Discovery Rate (q-value) is evaluated according to the Storey *et al.* methodology (867), and a False Discovery Rate control (FDR-control) is calculated as described in Benjamini and Hochberg (868).

We used also the Distant Regulatory Elements of Co-regulated genes (DIRE) web-based application (826) to predict regulated TFs. DIRE calculates the percentage of candidate transcripts containing a conserved binding site for a particular TF (occurence). The application also calculates a weight for each TF (importance) as a measure of its association with the input gene set, and it is therefore able to give an estimation of the importance of a specific TF. In this purpose, it does the product of TF occurrence and TF weight. We used a random set of 5000 genes as the source of background genes.

Gene set enrichment analysis

The Gene Set Enrichment Analysis (GSEA) software (827) was used to determine whether a priori defined set of genes showed statistically significant differences between our two biological conditions. The software uses raw microarray expression datasets to calculate a Normalized Enrichment Score (NES). This NES reflects the degree to which a gene set is overrepresented in upregulated or downregulated genes, and it accounts for differences in the gene set sizes and in correlations between gene sets and the expression dataset. A positive NES indicates gene set enrichment in upregulated genes, while a negative NES indicates gene set enrichment in downregulated genes. The significance of NES values is determined by the False Discovery Rate (FDR; q-value), and by a nominal *P*-value, which is calculated by an empirical phenotype-based permutation test procedure as described (827). Only enriched gene sets with a *P*-value ≤ 0.05 and a q-value ≤ 0.25 were considered significant. The signal-to-noise ratio was the ranking metric used for ranking genes in the expression dataset, and we run 1000 permutations. The values of the ranking metric for all genes in the microarray dataset and the distribution of the enrichment scores for each gene in a gene set are shown in the default plot of the software. The expression values of all genes in a gene set are represented in a heat map.

We used the TRANSFAC® 7.0 Public database (869), the TFacTs catalogue (866) and the Transcriptional Regulatory Element Database (TRED) (870) to create gene sets associated to AP-1 target genes, NF-κB target genes, or IRF3/7 target genes. The databases as before, Gene Ontology, and the literature were used for the gene set associated to NF-κB-regulated cytokines (871).

4.4 Mise en contexte de l'article 6

Tel que présenté dans les sections précédentes, le facteur de transcription NF-κB semble impliqué dans les effets protumoraux associés à la fois à une inhibition de la voie ERK/MAPK et à son hyperactivation. En d'autres mots, il contribuerait à la reprogrammation cellulaire et à la production soutenue de cytokines pro-inflammatoires suite à une accumulation de cellules sénescentes. Ainsi, les résultats présentés suggèrent un potentiel thérapeutique à la metformine dans divers contextes.

Les résultats présentés dans l'article 5 montrent également que la metformine n'affecte pas l'arrêt de la prolifération caractérisant la sénescence cellulaire et n'inhibe pas la production des interférons, soit des cytokines possédant un pouvoir antitumoral (872). Globalement, ces observations suggèrent que la metformine pourrait avoir un potentiel en médecine préventive. En n'affectant pas la capacité de suppression tumorale conférée par la sénescence cellulaire, mais en inhibant les effets néfastes du SASP, la metformine pourrait non seulement limiter le développement de cancers, mais aussi restreindre le développement des pathologies associées au vieillissement. L'article 6 introduit la discussion à ce sujet, ce qui est approfondi dans la discussion de la thèse.

4.5 Contribution à l'article 6

L'article a été rédigé par Gerardo Ferbeyre. J'ai conçu la Figure, rédigé la légende et révisé le manuscrit.

4.6 Article 6

Metformin, aging and cancer

Olga Moiseeva[1], Xavier Deschênes-Simard[1], Michael N. Pollak[2] and Gerardo Ferbeyre[1]

Aging, 2013 May 9, 5 (5): 330-31

1) Département de Biochimie, Université de Montréal, Pavillon Roger-Gaudry 2900 boul. Édouard Montpetit, Montréal, Qc H3C 3J7, Canada
2) Division of Experimental Medicine, McGill University and Segal Cancer Centre of Jewish General Hospital, 3755 Côte Ste Catherine, Montréal, Qc H3T 1E2, Canada

Keywords: Aging; cancer; cytokines; NF-κB; metformin

Correspondence to: Gerardo Ferbeyre and Michael N. Pollak

4.6.1 Summary

Many cancers are associated with aging (873). Metformin, a widely used antidiabetic drug, has been linked to a reduced cancer incidence in some retrospective, hypothesis-generating studies (443). Since cancer and aging may share certain molecular processes, it is plausible that metformin may prevent cancer by acting on the aging process. Consistent with this idea, several studies report a life span extension in animal models after treatment with metformin (861).

4.6.2 Main text

What is the mechanism by which aging may increase cancer incidence? Although many molecular changes correlate with aging, the presence of senescent cells capable of secreting inflammatory cytokines may be involved. This senescence associated secretory phenotype (SASP) consists of multiple cytokines, chemokines, growth factors and extracellular matrix degrading enzymes that can potentially affect normal tissue structure (147). The SASP probably evolved as a gene expression program to assist the senescent tumor suppression response and tissue repair after damage and should be viewed as an initial adaptive response (151). However, like acute inflammation, the SASP should be turned off to avoid maladaptive consequences. In some contexts, senescent cells are cleared by professional phagocytic cells (89) and this mechanism avoids any further complications. On the other hand, if senescent cells escape clearance, mechanisms that prevent the SASP should operate to avoid chronic inflammation and tissue disruption. Such endogenous mechanisms for clearing senescent cells or suppressing the SASP may fail with age. As a consequence, chronic SASP may cause a microenvironment in old tissues that facilitates tumor initiation and then stimulates cancer cell growth, motility and angiogenic activity. This unfortunate interaction between senescent cells and cancer cells has been reproduced in experimental mouse models where senescent fibroblasts stimulated tumor progression (147). The mechanisms of senescent cell clearance and SASP control are not yet known. However, during experiments to study the potential cancer prevention activity of metformin, we found serendipitously that the drug prevented the expression of many proteases, cytokines and chemokines in senescent cells (819).

At the molecular level, we found that metformin interfered with the activation of protein kinases IKK α and β, which are responsible for activating NF-κB, an essential transcription factor for SASP activation. Intriguingly, metformin did not reduce the expression of anticancer cytokines such as interferon and interferon target genes in senescent cells, suggesting that it modulates SASP to reduce its inflammatory potential but retaining its antitumor activity. In addition, metformin did not affect the senescent cell cycle arrest caused

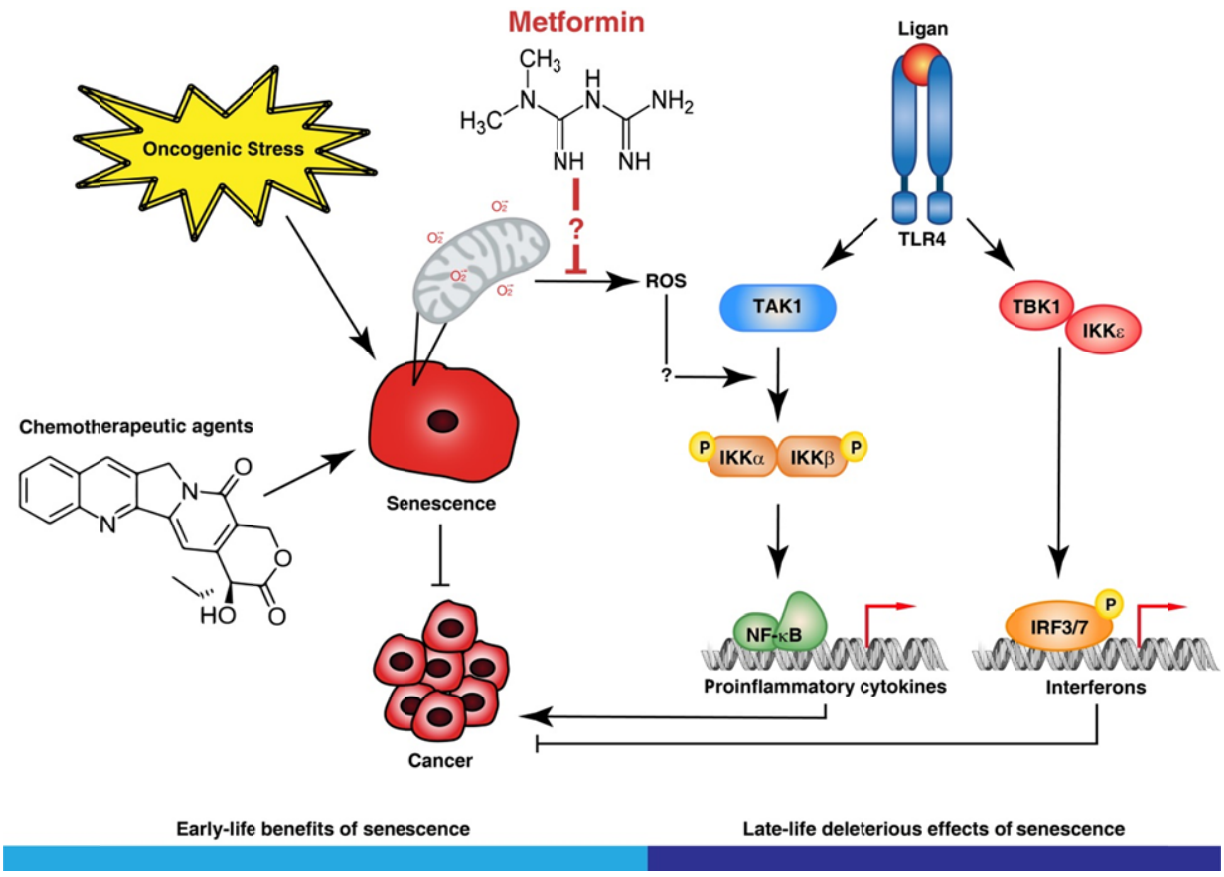

Figure 35. Metformin inhibits the activation of IKK kinases in senescent cells
The model proposes that metformin reduces ROS generation by mitochondria preventing the activation of IKK kinases a step that is ROS-sensitive. Metformin does not affect the activation of the interferon response in senescent cells suggesting that it modulates the senescence associated secretory phenotype in a way that reduces chronic inflammation but not tumor suppression.

by oncogenic *ras* in primary human cells, suggesting again that it can modulate the SASP without allowing proliferation of potentially malignant cells. The primary site of action of metformin is considered to be the complex I of the electron transport chain (443). However, molecular details of the interaction between metformin and complex I remain to be identified. Complex I is one of the main cellular sources for reactive oxygen species (ROS) and we have shown that metformin can prevent ROS production by senescent cells (445). It is thus plausible that ROS links senescence to NF-kB activation and that metformin interferes with this mechanism by acting on complex I (Figure 35). Metformin is not immunosuppressive so its ability to inhibit NF-κB is likely confined to certain proinflammatory contexts such as

senescence. We thus propose that metformin prevents cancer by modulating the SASP in tissues where senescent cells were not naturally cleared.

Many questions remain to be addressed in order to fully characterize metformin actions. Our results were obtained using cultured senescent fibroblasts and macrophages; other cell types should be studied as well. In addition, it remains to be determined if metformin can achieve this anti-SASP activity in vivo or whether it can influence the clearance of senescent cells by modulating the SASP. Anisimov and colleagues reported that metformin extends life span in female mice but not males (861) and it would be interesting to study whether NF-κB and SASP inhibition by metformin is gender dependent. Additional epidemiological data and laboratory experiments may justify well-designed clinical studies to evaluate metformin as a cancer preventive agent in specific contexts where its recently described actions would be hypothesized to be useful.

5. Discussion générale

5.1 Vue d'ensemble

L'activité de la voie ERK/MAPK implique un vaste réseau de protéines régulatrices et les fonctions qu'elle régule dépendent de plusieurs paramètres spatio-temporels (273). Étant donné la fréquence élevée des mutations activatrices au sein de régulateurs positifs de la voie dans les cellules cancéreuses, les kinases ERK sont considérées comme des composantes critiques de la réponse à de nombreux oncogènes (44, 255, 301, 302). Plusieurs mécanismes favorisant la progression tumorale sont attribués à leur activation et, par conséquent, la voie ERK/MAPK a pendant longtemps été considérée comme essentiellement oncogénique. Au fil du temps, une accumulation d'observations a cependant confronté cette vision unilatérale, suggérant de possibles fonctions antitumorales.

L'objectif général des travaux présentés au sein de cette thèse était de mettre en évidence la capacité des kinases ERK à activer des mécanismes de suppression tumorale. Considérant l'engouement pour le développement d'inhibiteurs de la voie ERK/MAPK afin de traiter divers cancers, le but de la thèse était également d'intégrer nos observations dans le contexte des efforts déployés et ce, afin de proposer des avenues thérapeutiques.

Les résultats présentés tout au long de la thèse montrent que l'impact de la voie ERK/MAPK sur la progression tumorale est intimement lié à l'intensité de son activation (Figure 36). Alors qu'une activation modérée de la voie pourrait contribuer à la prolifération des cellules formant le corps d'une tumeur, une hyperactivation de la voie induirait plutôt la sénescence cellulaire et donc, contribuerait à la suppression tumorale. De même, l'activation de la voie ERK/MAPK pourrait s'opposer à la reprogrammation cellulaire nécessaire à l'initiation d'un cancer et à la présence d'une sous-population de CSC au sein des tumeurs malignes. Ces observations suggèrent une certaine prudence à adopter face à l'utilisation des inhibiteurs de la voie ERK/MAPK en clinique.

Les résultats présentés au chapitre 2 de la thèse ont montré que la sénescence cellulaire induite par l'hyperactivation des kinases ERK implique la dégradation de nombreuses protéines. L'impact de ce phénotype, le SAPD, et sa contribution à l'établissement de la sénescence ont été discutés en profondeur dans le second article de la thèse. De même, les

mécanismes qui pourraient expliquer le contournement de la sénescence cellulaire induite par la voie ERK/MAPK lors de l'initiation du cancer ont été abordés dans le troisième article de la thèse. Nous profiterons donc de la section qui suit pour résumer les principales questions auxquelles nous sommes aujourd'hui confrontés et l'importance que pourrait avoir le SAPD quant à l'accomplissement de la fonction des cellules sénescentes. Nous approfondirons ensuite la discussion sur l'impact et les limites des résultats présentés au chapitre 3, lesquels concernent le rôle de la voie ERK/MAPK dans la reprogrammation cellulaire. Enfin, nous proposerons une série de stratégies thérapeutiques en tenant compte des résultats des chapitres 2 et 3 et ceci, en considérant la capacité de la metformine à inhiber la voie de signalisation de NF-κB telle que démontrée au chapitre 4.

5.2 ERK et SAPD : un bref retour

Comme ce fut détaillé dans le second article du chapitre 2, le SAPD induit par l'hyperactivation de la voie ERK/MAPK pourrait jouer un rôle déterminant dans l'établissement de la sénescence cellulaire (Figure 36). Nous avons d'ailleurs montré que la déplétion de certaines cibles du SAPD suite à l'expression d'ARN interférents est suffisante pour induire le phénotype sénescent (390). Cependant, notre démonstration demeure corrélative et le lien de causalité sera difficile à démontrer. En effet, il n'est pas envisageable que l'inhibition du protéasome puisse contourner la sénescence cellulaire. Un certain nombre de protéines E3 ubiquitines ligases ont un rôle clairement oncogénique puisqu'elles induisent la dégradation de suppresseurs de tumeurs (692). L'inhibition du protéasome causerait la stabilisation de leurs cibles, tel p53. Une accumulation de p53 favorise la sénescence et, au-delà d'un certain seuil, conduit à l'apoptose (620, 692). L'impact du patron de dégradation protéique à un instant donné, que nous pourrions qualifier de «dégradome», semble donc dépendre d'un fin équilibre entre la dégradation de protéines ayant des fonctions antitumorales versus oncogéniques (Figure 19). Peut-être existe-t-il une unique E3 ubiquitine ligase, spécifiquement impliquée dans l'induction de la sénescence, au niveau de laquelle nous pourrions intervenir pour contourner le phénotype. Cependant, nous n'avons pour le moment aucune évidence suggérant une telle possibilité. De plus, étant donné le nombre important de protéines E3 ubiquitines ligases dans le protéome humain (691), il est plus probable que le

SAPD implique diverses E3 ubiquitines ligases. Dans ce cas, nous devrons identifier celles qui catalysent la dégradation de différentes cibles du SAPD et démontrer leur implication dans les mécanismes effecteurs de la sénescence cellulaire (97). Seule une accumulation de telles démonstrations pourra renforcer le lien de causalité entre le SAPD et le phénotype sénescent.

Un autre défi auquel nous sommes confrontés consiste à déterminer quel est le mécanisme qui permet de sélectionner spécifiquement certaines protéines à dégrader (97). Ce mécanisme ne semble pas s'expliquer par une régulation de l'activité du protéasome (Figure 15D). Est-ce qu'il implique le ciblage des protéines à des structures spécialisées pour la dégradation des protéines? Nécessite-t-il la régulation de l'activité de certaines E3 ubiquitines ligases? Implique-t-il une série de modifications post-traductionnelles? Malgré le fait que toutes ces possibilités ne soient pas mutuellement exclusives, la littérature ainsi que nos données actuelles suggèrent que la phosphorylation serait un signal important afin de catalyser la dégradation de bon nombre de cibles du SAPD (97, 281, 390). Ainsi, puisque différentes voies de signalisation impliquent une phosphorylation de nombreux substrats, nous posons l'hypothèse que la dégradation de protéines hyperphosphorylées serait un mécanisme commun afin de mettre fin à une signalisation aberrante. En d'autres mots, le SAPD pourrait être la réponse appropriée à un tel stress, lequel pourrait être qualifié de «stress de phosphorylation», et avoir comme conséquence l'établissement de la sénescence cellulaire. Un tel processus pourrait impliquer la reconnaissance des protéines maintenues de manière prolongée dans un état phosphorylé par des E3 ubiquitines ligases ou l'activation de phosphodégrons (281).

Les deux paragraphes précédents s'attardent à décortiquer à la fois comment le SAPD pourrait contribuer au phénotype sénescent et les mécanismes qui seraient responsables de la spécificité de la dégradation protéique. Cependant, la réflexion sur le rôle du SAPD au sein des cellules sénescentes peut s'étendre au-delà de la fine mécanistique (97). Globalement, quelle pourrait être la contribution du SAPD afin que les cellules sénescentes puissent accomplir leur fonction? Il est vrai que le SAPD pourrait contribuer à freiner le cycle cellulaire et ainsi empêcher la propagation de cellules anormales (Figure 20) (97). Néanmoins, il semble de plus en plus évident que ces cellules soient destinées à l'élimination par le système immunitaire (89, 151, 152, 154). Ainsi, de manière similaire à l'apoptose, la

sénescence permettrait l'élimination des cellules portant des aberrations génétiques prédisposant au cancer. Afin d'activer les cellules du système immunitaire et d'assurer la reconnaissance des cellules sénescentes, le SASP semble jouer un rôle critique (Figure 20) (97, 140). Cependant, il s'agit d'un processus anabolique coûteux et les cellules sénescentes doivent faire face à la disponibilité limitée des ressources et de l'énergie. Ainsi, elles doivent réorganiser l'attribution des ressources afin d'assurer la production de cytokines et, par conséquent, mener à bien leur fonction ultime, c'est-à-dire leur propre élimination. L'autophagie a déjà été suggérée comme un processus assurant une augmentation des ressources disponibles (109, 502, 527). Toutefois, le SAPD pourrait contribuer de manière ciblée à la redistribution des ressources. En inactivant des fonctions coûteuses en énergie, telles que la synthèse des ribosomes, la synthèse de l'ADN et la réparation de l'ADN, il pourrait assurer une plus grande disponibilité de l'énergie pour soutenir le SASP (Figure 20) (97). En résumé, l'autophagie, le SAPD et le SASP pourraient travailler en étroite collaboration afin de réorganiser le protéome d'une manière à supporter l'élimination des cellules sénescentes.

5.3 ERK : une barrière à la reprogrammation

5.3.1 Limites de nos résultats actuels et orientation du projet

Les résultats présentés au chapitre 3 suggèrent que la voie ERK/MAPK s'oppose à la reprogrammation cellulaire permettant l'acquisition de la tumorigénicité et des caractéristiques normalement attribuables aux cellules souches (Figure 36). Cette affirmation est supportée par des corrélations avec l'évolution des niveaux de p-ERK durant la progression tumorale qui conduit à l'initiation du PDAC (Figures 22 et 23). Effectivement, l'acquisition de la malignité corrèle avec une diminution marquée de la signalisation par la voie ERK/MAPK. De plus, des niveaux faibles de p-ERK sont associés avec la présence de phénotypes cellulaires et de patrons d'expression génique associés aux CSC (Figures 24, 24 et 26). Un lien de causalité est également suggéré puisque la diminution de l'activité des kinases ERK par différentes interventions génétiques permet l'acquisition de ces phénotypes (Figure 26).

Il est important de mentionner que malgré les observations que nous venons d'aborder, le projet n'a pas encore été soumis à un comité de pairs et laisse place à un certain nombre d'améliorations. Bien entendu, les signatures d'expression génique observées suite aux analyses par puce à ADN sont en cours de validation par une série de réactions de PCR quantitatif. De même, nous voulons clarifier le lien de causalité entre une diminution de la voie ERK/MAPK et la reprogrammation des cellules cancéreuses. Pour le moment, nos résultats se limitent largement à un système de transformation de cellules normales suite à l'expression de transgènes. Pour pallier aux limites qu'impose ce système sur l'extrapolation des résultats à un contexte physiologique, nous avons effectué un criblage de nombreuses lignées de cellules cancéreuses humaines afin d'identifier celles possédant des sous-populations de CSC (Tableau SV et Figure S17). Nous cherchons à évaluer par cytométrie en flux si les sous-populations de CSC possèdent des niveaux diminués de p-ERK. Ensuite, l'idée est de manipuler l'activité de la voie ERK/MAPK au sein des lignées cellulaires sélectionnées afin d'évaluer l'impact sur l'importance des sous-populations de CSC. Les résultats envisagés sont qu'une inhibition de la voie devrait augmenter la taille des sous-populations, alors qu'une augmentation de l'activation de la voie devrait avoir l'effet inverse. Étant donné que la tumorigénicité est un aspect caractérisant les cellules cancéreuses reprogrammées, nous chercherons également à mesurer cette capacité suite à un enrichissement des cellules avec de faibles niveaux de p-ERK versus la lignée cellulaire d'origine. Pour ce faire, nous envisageons l'évaluation de la formation de tumeurs suite à l'injection sous-cutanée de dilutions sérielles de préparations cellulaires à des souris immunodéprimées SCID (*severe combined immunodeficiency*).

Pour étendre la pertinence *in vivo* de nos résultats, nous envisageons deux approches complémentaires aux résultats des Figures 22 et 23. D'abord, nous avons obtenu une série de lignées cellulaires primaires établies suite à l'extraction de l'ascite de patients atteints du PDAC. Nous évaluerons par cytométrie en flux si ces lignées possèdent des sous-populations de CSC et le statut de p-ERK dans ces sous-populations versus les autres cellules. Ensuite, nous avons obtenu des puces à tissus (*tissue micro arrays*; TMA) portant des échantillons représentatifs de nombreux cas de PDAC. À l'aide de marquages avec des anticorps fluorescents, nous vérifierons la présence de cellules arborant des marqueurs de CSC et les

niveaux de p-ERK au sein de telles cellules. Dans l'éventualité où des CSC avec de faibles niveaux de p-ERK sont observées, nous pourrons estimer leur abondance et la corréler avec des paramètres cliniques des patients.

En résumé, nos résultats proposent que la voie ERK/MAPK s'oppose à la reprogrammation des cellules cancéreuses, comme le suggérait la biologie des cellules souches normales et les expériences de reprogrammation des cellules somatiques *in vitro* (418-423, 435-440). Cependant, il importait de mettre en évidence les forces et les faiblesses des résultats actuels afin de nuancer l'interprétation de la discussion qui suivra.

5.3.2 Impacts du modèle proposé

L'acquisition de la tumorigénicité est une étape critique de la transformation maligne et, par conséquent, à l'apparition des TIC (175-177). De même, les CSC sont associées avec la résistance à diverses thérapies, les rechutes thérapeutiques et la formation de métastases (176). Dans les deux cas, un certain niveau de perte d'identité cellulaire, laquelle nous qualifions de reprogrammation, est requise. En conséquence, la compréhension des mécanismes soutenant la reprogrammation cellulaire revêt une grande importance afin de développer de nouveaux outils thérapeutiques et d'adapter les thérapies actuelles.

La démonstration de l'opposition de la voie ERK/MAPK face à la dédifférenciation des cellules cancéreuses vient remettre en question l'usage des inhibiteurs de cette voie de signalisation. Il faut distinguer les cellules formant le corps d'une tumeur, lesquelles pourraient nécessiter l'activation de la voie ERK/MAPK afin de proliférer et de contribuer à la progression tumorale, et les sous-populations de CSC qui assureraient la maintenance de la tumeur en conservant un potentiel tumorigénique (Figure 36) (202, 213). Ainsi, l'inhibition des kinases ERK pourrait avoir un effet bénéfique en ciblant la majorité des cellules formant une tumeur. Cependant, cette stratégie pourrait ne pas affecter les CSC, voire pire, augmenter leur nombre en favorisant la reprogrammation cellulaire (Figure 28). Un tel scénario serait conforme à ce qui est observé lors de la reprogrammation des cellules somatiques en iPSC. Dans ce contexte, les inhibiteurs de la voie ERK/MAPK freinent la prolifération des cellules normales, mais permettent la reprogrammation en iPSC et favorisent l'expansion de la sous-

population formée de ces cellules (818). Ainsi, la subsistance de CSC pourrait être une nouvelle explication au développement d'une résistance aux inhibiteurs de la voie ERK/MAPK. Ce phénomène fréquemment rapporté était, jusqu'à maintenant, généralement expliqué par des mécanismes permettant la réactivation des kinases ERK (243, 349). La reprogrammation cellulaire induite par l'inhibition de la voie ERK/MAPK pourrait également être une explication aux cas rapportés de cancers secondaires portant des mutations de *RAS*, tels que des SCC et des leucémies, suite aux traitements avec des inhibiteurs de RAF (349, 736, 737). De plus, le même phénomène pourrait expliquer pourquoi les inhibiteurs de RAF accélèrent la formation de tumeurs dans un modèle murin destiné à l'étude des cancers de la peau induits par l'oncogène *Ras* (736).

Outre une prudence à adopter face à l'utilisation des inhibiteurs de la voie ERK/MAPK, nos résultats proposent de nouvelles avenues à investiguer afin d'identifier les vulnérabilités des cellules cancéreuses reprogrammées. Comment les kinases ERK s'opposent-elles à la reprogrammation; quelles sont les cibles impliquées? Des réponses à ces questions pourraient suggérer des stratégies thérapeutiques que nous pourrions utiliser en combinaison avec les inhibiteurs de la voie ERK/MAPK et ce, afin de cibler à la fois les cellules constituant le corps de la tumeur et les cellules cancéreuses dédifférenciées.

Étant donné la grande diversité de substrats que possèdent ces kinases et les nombreuses fonctions qu'elles contrôlent, différentes hypothèses devront être testées afin d'obtenir des réponses claires aux questions que nous venons d'énoncer. Néanmoins, nous pouvons suggérer divers éléments de réponse en s'inspirant de la biologie des cellules souches et des iPSC. D'abord, la voie ERK/MAPK pourrait réprimer l'expression de facteurs clefs de la reprogrammation cellulaire, tel que le facteur de transcription NANOG, ce qui fut rapporté pour les cellules souches (816, 817).

Pourrions-nous supposer que les kinases ERK induisent la dégradation de facteurs requis pour la reprogrammation des cellules cancéreuses? Encore une fois, une telle hypothèse est appuyée par des observations au niveau des cellules souches normales. Par exemple, les kinases ERK phosphorylent le facteur KLF4, ce qui conduit à sa dégradation et à la différenciation cellulaire (815). En outre, lors de nos expériences de phosphoprotéomique afin

d'identifier les cibles potentielles du SAPD, nous avons trouvé un certain nombre de protéines ayant des rôles connus dans l'acquisition de propriétés attribuables aux cellules souches, telles que c-MYC (40), STAT3 (795), TRIM28/KAP1 (*Tripartite motif-containing 28*/ *KRAB-associated protein 1*) (874) et YAP1 (*Yes-associated protein 1*) (875-877). Il est donc envisageable que le patron de dégradation évolue selon l'intensité de la signalisation par la voie ERK/MAPK. Par exemple, des substrats requis pour la reprogrammation pourraient être sensibles à la dégradation suite à leur phosphorylation, alors que d'autres substrats, tels que ceux assurant la prolifération et le maintien de l'homéostasie cellulaire, pourraient être plus résistants. Un tel principe pourrait s'expliquer par la présence de différents phosphodégrons assurant un fin réglage de la dégradation selon l'intensité de la signalisation.

Enfin, la reprogrammation cellulaire implique des changements épigénétiques importants (175, 178, 180). L'activation de la voie ERK/MAPK pourrait peut-être avoir un impact direct sur des régulateurs de l'état de la chromatine (878). Alors que l'activation de la voie favoriserait l'adoption et le maintien des changements au niveau de la chromatine requis pour la différenciation, l'inhibition de la voie pourrait permettre un remodelage compatible avec un état dédifférencié.

5.4 ERK et l'initiation du cancer : un modèle privilégié

Dans leur ensemble, les résultats présentés aux chapitres 2 et 3 suggèrent que le modèle de la voie ERK/MAPK «tamponnée» pourrait être privilégié lors de la progression tumorale en présence d'oncogènes en amont de la voie (Figures 21B et 28A) (349). En bref, ce modèle suggère que suite à l'activation de tels oncogènes, une augmentation de l'activité des kinases ERK freine la progression tumorale. Une forte activation de ces kinases empêcherait la reprogrammation nécessaire à l'acquisition de la tumorigénicité, voire induirait la sénescence cellulaire si l'intensité de la signalisation dépasse un certain seuil (Figures 28 et 36). Bien que les résultats présentés au sein de cette thèse ne démontrent pas cette possibilité, il n'est pas exclu qu'une hyperactivation de la voie ERK/MAPK puisse aussi conduire à l'apoptose dans certains contextes. En effet, l'hyperactivation des kinases ERK a été associée à l'induction de l'apoptose dans un certain nombre de systèmes *in vitro* et *in vivo* (340, 879, 880). Enfin, la

sélection de mécanismes permettant d'atténuer l'activité de la voie ERK/MAPK semble requise afin de progresser d'une lésion bénigne à une tumeur maligne.

Sans exclure les autres modèles potentiels décrits à l'article 3 de cette thèse, le modèle que nous venons de décrire pourrait-il s'appliquer à l'initiation de la plupart des cancers? Pour le moment, nous pouvons affirmer que l'évolution des niveaux de p-ERK au cours de la progression tumorale menant au PDAC reflète ce modèle (Figures 22 et 23). De même, une telle cinétique des niveaux de p-ERK a déjà été rapportée lors de la progression tumorale menant au cancer de la prostate (389, 390).

Nos observations au niveau de l'initiation du cancer pancréatique soulèvent cependant certaines questions supplémentaires face au modèle. Comment se fait-il que lors de la première étape de la progression tumorale, soit lors de l'ADM, les niveaux de p-ERK sont modérés et que les cellules prolifèrent? Ainsi, il semble y avoir des mécanismes autres que l'activation de l'oncogène *RAS* qui contribuent à l'augmentation de la signalisation par la voie ERK/MAPK. Ces mécanismes permettraient un rétrocontrôle positif sur la voie conduisant à la suppression tumorale.

Pourquoi ces mécanismes sont-ils enclenchés; pourquoi seraient-ils sélectionnés durant les premières étapes de la progression tumorale? En interprétant la littérature, nous pouvons proposer une hypothèse. Plusieurs avantages contribuant à la progression tumorale peuvent être conférés par d'autres voies de signalisation, lesquelles sont activées par les mêmes régulateurs en amont de la voie ERK/MAPK. De même, la reprogrammation cellulaire nécessaire à l'acquisition de la tumorigénicité ne requiert pas seulement une diminution de l'activation de la voie ERK/MAPK. Le processus implique d'autres voies de signalisation, dont certaines potentiellement en aval de RAS. En effet, alors que la voie ERK/MAPK favorise la différenciation, la voie RALGEFs/RAL s'oppose à ce processus (881-883) et la voie PI3K/AKT régule positivement c-MYC (40), STAT3 (884, 885) et NF-κB (886, 887), lesquels ont des rôles connus dans la reprogrammation cellulaire (40, 201, 795, 796). Il est d'ailleurs à noter que ces deux voies de signalisation sont critiques à la transformation par l'oncogène *RAS* dans certains contextes (888-893). Plus particulièrement, la voie PI3K/AKT semble jouer un rôle de premier plan dans une multitude de cancers (voir l'article 3 du

chapitre 2), incluant le PDAC (753). Nous pouvons donc supposer que des mécanismes favorisant l'activation des diverses voies de signalisation requises à la progression tumorale auraient comme effet secondaire d'augmenter l'activité de la voie ERK/MAPK. Par exemple, l'activation de *RAS* pourrait initier la reprogrammation cellulaire, conduisant à l'ADM, et stimuler la prolifération. Par contre, l'activité initiale de RAS suite à une mutation oncogénique pourrait s'avérer insuffisante pour conduire à la transformation cellulaire. Ainsi, des processus permettant d'augmenter davantage son activité pourraient être favorisés au début de la progression tumorale. Ceux-ci pourraient inclure la surexpression du gène codant pour *RAS*, tel que suggéré pour l'initiation de certains cancers du sein (894). La sécrétion de facteurs inflammatoires suite à l'activation de NF-κB par l'oncogène RAS pourrait également contribuer, via une signalisation auto/paracrine, à une boucle de rétroaction positive (895). L'activité augmentée de RAS conduirait à une plus grande activation de NF-κB, et ainsi un cycle de renforcement entre l'activation de RAS et de NF-κB se mettrait en place. Un tel phénomène a été montré critique à l'initiation du PDAC (196). L'augmentation de l'activité de RAS pourrait donc avoir des effets profitables pour la progression tumorale, mais ce, jusqu'au moment où l'activation de la voie ERK/MAPK dépasserait un certain seuil, lequel enclencherait des mécanismes de suppression tumorale comme la sénescence et la différenciation. Des mécanismes limitant spécifiquement l'activation de la voie ERK/MAPK devraient donc être sélectionnés afin de conserver les avantages conférés par les autres voies de signalisation et ce, tout en éliminant la barrière à la transformation maligne que crée une hyperactivation des kinases ERK.

Quels sont les mécanismes qui pourraient permettre aux cellules précancéreuses d'éviter la suppression tumorale imposée par les kinases ERK? Les possibilités sont nombreuses et probablement dépendantes du contexte. Néanmoins, étant donné leur capacité à inhiber préférentiellement la voie ERK/MAPK au niveau de MEK, les phosphatases DUSP sont des candidates de choix. D'ailleurs, plusieurs membres de cette grande famille sont surexprimés dans divers cancers et sont suspectés de contribuer à la progression tumorale (312, 393-402). Ces phosphatases sont aussi connues pour contribuer à maintenir une faible activité des kinases ERK dans les ESC (810-812). D'autres candidats, soit les membres de la

famille des protéines SPRY, peuvent réguler la voie de différentes manières, entre autres en interférant avec l'activation de RAF (290).

Concernant RAF, si la voie ERK/MAPK joue un rôle important dans l'induction de mécanismes suppresseurs de tumeurs, comment se fait-il que les mutations oncogéniques au niveau des gènes codant pour les protéines RAF sont fréquentes dans les cancers? Cette question découle du fait que la voie ERK/MAPK est perçue comme essentiellement linéaire entre RAF et ERK. Cependant, une accumulation d'observations suggèrent que les kinases RAF auraient d'autres substrats que les kinases MEK (234). Entre autres, RAF conduit à l'activation de NF-κB d'une manière indépendante de l'activation de MEK (896-898), ce qui pourrait être essentiel à son pouvoir transformant (898, 899). Comme expliqué plus tôt, l'activation de NF-κB pourrait enclencher la production de facteurs activant RAS de manière auto/paracrine et, par conséquent, engager la signalisation par d'autres voies favorisant la progression tumorale et l'initiation du cancer. En d'autres mots, les oncogènes RAF auraient la même capacité que les oncogènes RAS à enclencher un cycle de renforcement positif de l'activation de NF-κB et de la signalisation par RAS. Les kinases MEK et ERK ne posséderaient pas cette capacité, ce qui pourrait expliquer pourquoi les mutations de MEK sont rares dans les cancers humains (900-903) et qu'aucune mutation dans les kinases ERK n'a été identifiée. De plus, puisque les oncogènes RAF activent plus directement la voie ERK/MAPK que les oncogènes RAS, les mécanismes pouvant diminuer l'activation des kinases ERK seraient plus limités. Cette situation pourrait expliquer pourquoi les protéines RAF constitutivement actives provoquent surtout la formation de lésions bénignes chez la souris, qui dérivent rarement vers des tumeurs malignes (86, 87, 340, 414-417).

En conclusion, le facteur de transcription NF-κB semble être le point de convergence de plusieurs voies de signalisation favorisant l'initiation du cancer. La voie PI3K/AKT, la voie RALGEFs/RAL et les kinases RAF conduisent à son activation (883, 886, 887, 896-898). La voie ERK/MAPK pourrait non seulement s'opposer à son effet transformant par l'induction de mécanismes de suppression tumorale, mais aussi par l'activation de mécanismes de rétrocontrôle négatif qui agissent sur les voies mentionnées ci-haut. À titre d'exemple, les protéines SPRY limitent également l'activation de RAS par les RTK (291-293). En plus d'éliminer une barrière à la transformation maligne, une diminution spécifique de l'activité

des kinases ERK potentialiserait la boucle de rétrocontrôle positif entre NF-κB et la signalisation par RAS. Enfin, étant donné le rôle central que semble jouer NF-κB et son activation constitutive dans une majorité de cancers (904-906), il apparait comme une cible de choix dans le développement de nouvelles thérapies (907).

5.5 Sénescence, reprogrammation et metformine : repenser les stratégies thérapeutiques

5.5.1 Combiner la metformine aux inhibiteurs de la voie ERK/MAPK

Comme nous l'avons détaillé précédemment, les tumeurs sont généralement hétérogènes. Il n'est donc pas exclu qu'une activation modérée de la voie ERK/MAPK, sous le seuil requis pour l'induction de la sénescence cellulaire, puisse contribuer à la prolifération des cellules «différenciées» formant le corps d'une tumeur. Les inhibiteurs de la voie auraient donc un effet bénéfique en limitant l'expansion de ces cellules. Cependant, ces inhibiteurs pourraient avoir deux effets secondaires importants (Figures 28 et 36). Effectivement, ils pourraient limiter l'entrée en sénescence des cellules faisant le gain de mutations oncogéniques. Pire, ils pourraient favoriser la reprogrammation de cellules cancéreuses en CSC, lesquelles résisteraient à la thérapie. De même, ils pourraient contribuer à la reprogrammation de cellules précancéreuses, initiant ainsi des cancers secondaires. L'idée qui en découle ne serait pas nécessairement de proscrire les inhibiteurs de la voie ERK/MAPK, mais plutôt d'adapter leur utilisation afin d'en optimiser les avantages.

Tout d'abord, afin d'éviter la prolifération des cellules qui pourraient échapper à la sénescence, il semble crucial d'assurer une inhibition forte et généralisée de la voie au sein des cellules portant des mutations oncogéniques. Ensuite, une thérapie avec des inhibiteurs de la voie ERK/MAPK devrait se faire en combinaison avec une stratégie permettant d'éliminer des cellules cancéreuses «dédifférenciés», lesquelles pourraient bénéficier ou même résulter de l'inactivation des kinases ERK.

La littérature récente et nos résultats suggèrent que la metformine a le potentiel de cibler les CSC, voire même d'interférer avec la reprogrammation cellulaire. En effet, elle

inhibe des effecteurs reconnus de la reprogrammation, tels que STAT3 et c-MYC (447-450). Nos travaux montrent qu'elle inhibe également l'activation du facteur de transcription NF-κB (Figure 36). Cette observation a d'ailleurs été confirmée par deux groupes indépendants (447, 908). Non seulement l'activation de NF-κB peut contribuer directement à la reprogrammation (201, 796), mais elle semble impliquée dans l'établissement d'un mécanisme de rétrocontrôle positif assurant une robustesse au processus (801). En effet, NF-κB induit la production de l'IL6, laquelle active davantage NF-κB et STAT3 suite à une signalisation autocrine (801). Ainsi, la capacité de la metformine à inhiber NF-κB, qui s'additionne à ses autres effets mentionnés ci-haut, suggère qu'elle aurait un potentiel thérapeutique non négligeable en combinaison avec les inhibiteurs de la voie ERK/MAPK et d'autres agents thérapeutiques (Figures 28 et 36).

La stratégie que nous venons de proposer trouve un appui dans une étude récente. En effet, la phenformine, un analogue de la metformine, augmente les bénéfices thérapeutiques d'un traitement avec des inhibiteurs de la voie ERK/MAPK (821). Les auteurs de cette étude ont observé que l'usage de ces inhibiteurs n'affecte pas toutes les cellules des mélanomes. Au sein de ces cellules, une sous-population se caractérise par l'expression de KDM5B (*Lysine-specific demethylase 5B*), aussi connu sous le nom de JARID1B (*Jumonji AT-rich interactive domain 1B*), lequel est une histone H3K4 déméthylase pouvant s'opposer à la différenciation cellulaire (909). Bien que les cellules de mélanomes exprimant ce marqueur démontrent un faible potentiel prolifératif, elles possèdent une capacité d'auto-renouvellement et sont critiques pour le maintien des tumeurs (910). Elles pourraient donc représenter une sous-population de cellules reprogrammées, voire de CSC (821, 910). Les travaux de Yuan et ses collègues ont montré que les inhibiteurs de la voie ERK/MAPK ciblent les cellules qui n'expriment pas JARID1B, alors qu'ils augmentent la sous-population de cellules positives pour l'expression de ce marqueur (821). La phenformine cible spécifiquement cette sous-population, coopérant ainsi avec l'effet des inhibiteurs de la voie ERK/MAPK (821). Non seulement ces travaux supportent notre hypothèse selon laquelle l'inhibition des kinases ERK favoriserait la reprogrammation des cellules cancéreuses, mais démontrent les avantages que pourrait conférer une thérapie combinant la metformine aux inhibiteurs de la voie ERK/MAPK.

5.5.2 Combiner la metformine aux agents thérapeutiques qui induisent la sénescence

Nos résultats laissent sous-entendre que des stratégies visant à augmenter la signalisation par la voie ERK/MAPK seraient envisageables afin de freiner la progression tumorale (Figure 36). Elles pourraient forcer la différenciation des CSC et induire la sénescence cellulaire. Cependant, une telle approche pourrait avoir divers effets indésirables. Selon le contexte, elle pourrait contribuer à la prolifération des cellules formant le corps d'une tumeur si les niveaux nécessaires à la sénescence ne peuvent être atteints. Elle pourrait stimuler la prolifération de diverses cellules normales, créant des hyperplasies et d'autres lésions bénignes. De même, elle pourrait forcer la différenciation des cellules progénitrices, ce qui pourrait compromettre la maintenance de nombreux tissus.

Cependant, la radiothérapie et plusieurs agents chimiothérapeuthiques induisent la sénescence des cellules cancéreuses par des mécanismes qui ciblent certaines de leurs vulnérabilités (911-913). Cette observation et la mise en évidence du potentiel antitumoral du phénotype sénescent ont suscité un intérêt dans le développement de nouveaux outils visant à forcer l'établissement de la sénescence cellulaire au niveau des cellules cancéreuses (912, 913). Bien que cette stratégie ait démontré son potentiel (913), il ne faut pas perdre de vue les effets néfastes conférés par le SASP. En plus de stimuler la prolifération des cellules cancéreuses, les facteurs sécrétés par le SASP pourraient contribuer à leur reprogrammation (72, 147, 155-157, 914). Un tel effet secondaire résultant de l'accumulation de cellules sénescentes pourrait conduire au développement d'une résistance et à une éventuelle rechute thérapeutique.

La metformine serait donc une option envisageable pour cibler le processus de la reprogrammation favorisé par le contexte inflammatoire résultant du SASP. De plus, puisque NF-κB est un régulateur clef du SASP, la metformine pourrait limiter les effets secondaires de l'accumulation de cellules sénescentes en interférant avec la source du problème, soit la production des cytokines pro-inflammatoires (819). En bref, une thérapie combinant la metformine à des stratégies visant l'induction de la sénescence pourrait permettre de tirer avantage du pouvoir antitumoral des cellules sénescentes et ce, tout en éliminant les effets protumoraux indirects de ces cellules (Figure 36).

Néanmoins, une question importante s'impose face à la stratégie que nous venons de proposer. L'élimination des cellules sénescentes par le système immunitaire est un phénomène aujourd'hui bien documenté (89, 151-154). Ce processus contribuerait aux bénéfices découlant d'une thérapie qui induit la sénescence cellulaire au niveau des cellules cancéreuses (912, 913). Ainsi, est-ce qu'interférer avec le SASP en inhibant NF-κB pourrait limiter le recrutement des cellules du système immunitaire? En conséquence, est-ce que l'élimination des cellules sénescentes serait compromise? Une telle possibilité ferait en sorte que, suite au traitement, les effets délétères du SASP pourraient à nouveau contribuer à une rechute thérapeutique. Nous serions alors confrontés à l'obligation de prolonger le traitement à la metformine, voire traiter le cancer comme une maladie chronique.

Les résultats présentés au chapitre 4 suggèrent que la metformine n'inhibe pas significativement la production des interférons (Figure 33). Étant donné que ces cytokines jouent un rôle central dans la réponse du système immunitaire aux cellules cancéreuses (872), nous pouvons poser l'hypothèse qu'elles jouent un rôle tout aussi important en ce qui concerne l'élimination des cellules sénescentes. De même, la metformine, en combinaison avec des agents connus pour induire la sénescence, a été montrée en mesure de prolonger la rémission suite à une chimiothérapie (446, 820). Ainsi, le potentiel thérapeutique de la metformine en combinaison avec divers agents prosénescents suscite un intérêt pour de futures investigations.

5.5.3 Metformine : prévenir plutôt que guérir?

La question posée peut sembler loufoque, voire propice à la controverse. Néanmoins, il faut penser à l'origine du cancer et considérer les facteurs qui contribuent à l'acquisition de la tumorigénicité. Afin de gagner la capacité d'initier un cancer, les cellules précancéreuses doivent subir une certaine reprogrammation, laquelle peut être favorisée par le microenvironnement, tel qu'un contexte inflammatoire chronique (184-188). Un défaut au niveau de l'élimination des cellules sénescentes par le système immunitaire et, conséquemment, leur accumulation dans les tissus, pourrait peut-être participer à un tel contexte inflammatoire pathologique (72, 161, 915). Du moins, une série d'observations suggèrent que l'accumulation de cellules sénescentes et la présence du SASP contribueraient à

l'inflammation chronique qui sous-tend diverses pathologies associées au vieillissement (72, 159, 161).

Une constatation intéressante est que le facteur de transcription NF-κB semble jouer un rôle central à la fois dans le processus de la reprogrammation cellulaire et dans l'induction du SASP (Figure 36) (73, 201, 796). Ainsi, en ciblant l'activité de NF-κB, un traitement prophylactique avec la metformine pourrait-il prévenir la reprogrammation à l'origine des cancers? Pourrait-il également limiter l'inflammation chronique induite par les cellules sénescentes qui résultent, par exemple, d'une hyperactivation de la voie ERK/MAPK? Dans l'affirmative, la metformine pourrait non seulement limiter les risques de développer un cancer, mais également prévenir certaines pathologies associées au vieillissement. Évidemment, avant d'offrir une telle approche de médecine préventive, bon nombre de questions devront être répondues. Parmi celles-ci, nous devrons nous interroger sur l'impact d'un usage prolongé de la metformine sur les fonctions du système immunitaire. De même, la metformine affecte divers processus, incluant le métabolisme cellulaire (441, 444). Il faudra déterminer si ces effets peuvent être dommageables pour le fonctionnement d'un organisme sain à long terme.

Malgré tout, des études sur des modèles murins ont montré qu'un traitement prolongé à la metformine réduit l'incidence des cancers et prolonge la durée de vie (861, 908, 916, 917). De plus, une série d'études épidémiologiques chez l'humain suggèrent une association entre l'usage de la metformine et une diminution du risque de développer un cancer (441-443). Étant donné l'engouement suscité par ces observations et les nombreuses études cliniques qui en découlent (918), les prochaines années devraient apporter de nombreuses réponses aux questions concernant un usage prophylactique de la metformine.

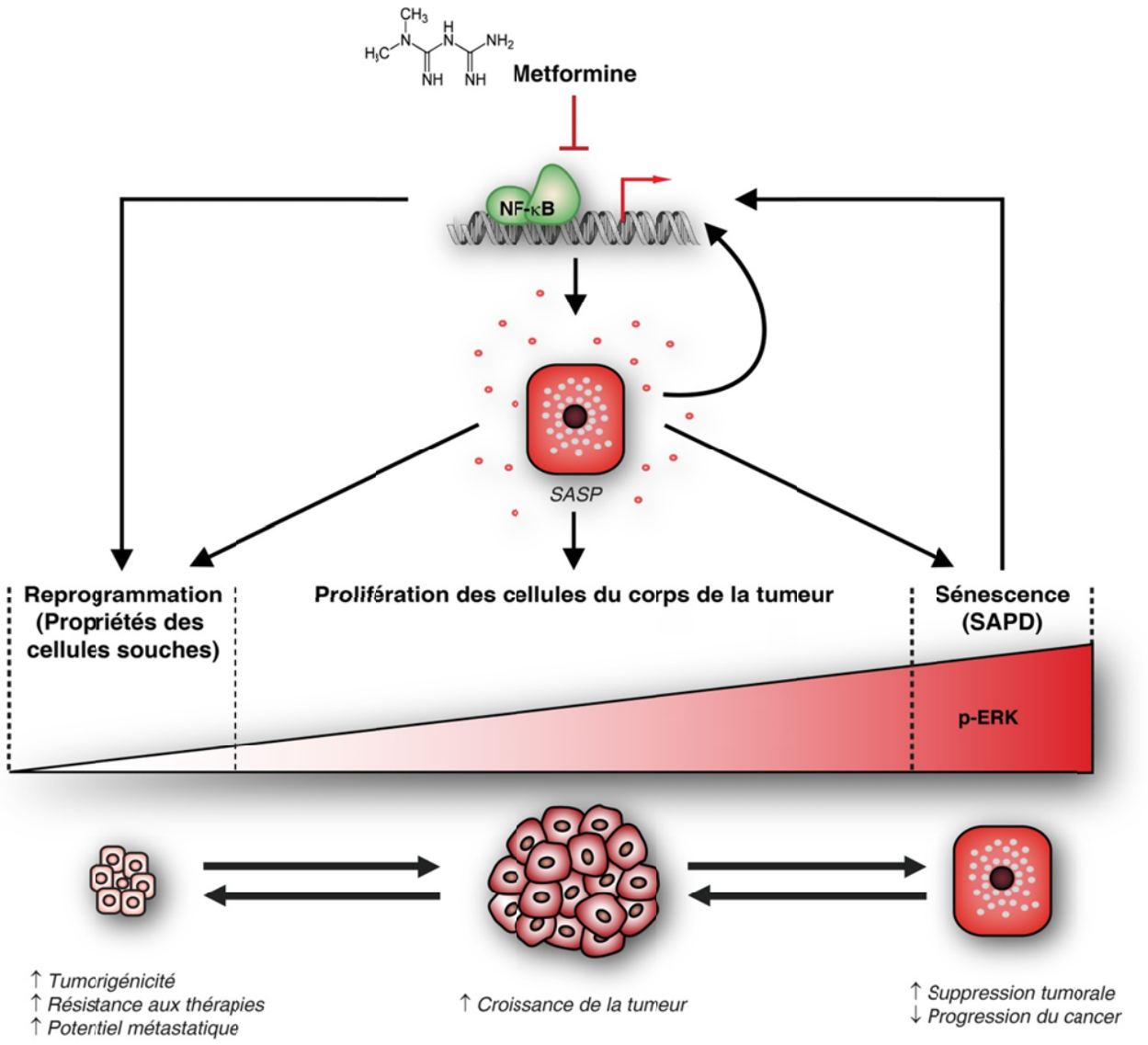

Figure 36. Modèle récapitulatif de la thèse

L'effet de la voie ERK/MAPK sur la progression tumorale dépend de l'intensité de son activation. Une faible activité permettrait la reprogrammation cellulaire nécessaire à l'acquisition de la tumorigénicité et l'initiation du cancer (formation des cellules initiatrices de tumeurs; TIC). De même, elle permettrait à des cellules cancéreuses au sein d'une tumeur de se dédifférencier (cellules souches cancéreuses; CSC). Une activation modérée de la voie favoriserait plutôt la prolifération des cellules «différenciées» de la tumeur. Enfin, une forte activation de la voie favoriserait l'établissement de la sénescence cellulaire. Ceci impliquerait la dégradation dépendante du protéasome de nombreuses protéines (SAPD). La metformine inhibe le facteur de transcription NF-κB, lequel contribue à la reprogrammation cellulaire et au phénotype sécrétoire associé à la sénescence (SASP). La metformine pourrait donc freiner à la fois les effets procancéreux d'une inhibition et d'une hyperactivation de la voie ERK/MAPK.

6. Conclusion

Les résultats présentés au sein de cette thèse mettent au clair le potentiel antitumoral de la voie ERK/MAPK, laquelle était jusqu'alors essentiellement perçue comme une composante clef de la progression tumorale. Ils démontrent ainsi que le rôle joué par cette voie dans la physiopathologie du cancer est complexe, à l'image de la multitude de fonctions qu'elle peut contrôler. L'idée fortement enracinée du rôle unidirectionnel de la voie ERK/MAPK dans la progression du cancer découle probablement de tout l'engouement suivant sa caractérisation, ainsi que de la démonstration de son activation par l'oncogène RAS au début des années 1990. Nous avions enfin un mécanisme moléculaire pouvant expliquer l'effet de cet oncogène, ce qui offrait une panoplie de possibilités thérapeutiques. La motivation de trouver une cure au cancer a forcément encouragé l'étude des fonctions protumorales de la voie. Néanmoins, les deux dernières décennies ont montré la complexité de la signalisation induite par RAS, de même que la diversité des fonctions régulées par la voie ERK/MAPK. Il semblait nécessaire de faire l'exercice et de revoir le modèle initial.

Ainsi, au-delà des aspects purement factuels et théoriques, les résultats de cette thèse démontrent également l'importance de remettre en question les modèles, surtout ceux faisant preuve d'un large consensus, mais qui ne s'appuient pas toujours sur une revue récente de la littérature. Aristote ne défendait-il pas le géocentrisme; Les travaux de Copernic et de Galilée n'ont-ils pas été condamnés par leurs pairs? Telle est la science, tel est l'humain, et parfois faut-il se le rappeler.

Nos résultats ne permettent pas de conclure sur l'impact que peuvent avoir plusieurs paramètres contribuant à déterminer les fonctions de la voie ERK/MAPK. Cependant, l'intensité de son activation semble jouer un rôle critique afin de discriminer entre l'induction de fonctions protumorales et antitumorales. Alors qu'une hyperactivation conduirait à la sénescence cellulaire, une activation modérée pourrait favoriser la prolifération de la plupart des cellules d'une tumeur. De plus, une faible activation de la voie pourrait être requise pour la reprogrammation cellulaire nécessaire à l'initiation du cancer et contribuant à l'apparition de cellules résistantes aux outils thérapeutiques conventionnels. D'un autre côté, l'hyperactivation de la voie et la sénescence cellulaire pourraient participer à un contexte inflammatoire chronique, lequel favoriserait le cancer. L'activité de la voie semble donc trop,

juste assez ou pas assez, de même que bonne ou mauvaise, tout dépendamment du contexte dans lequel se place l'observateur. Cette polyvalence justifie la prudence à adopter face à l'utilisation des inhibiteurs de la voie pour traiter le cancer, mais surtout, motive à trouver de nouvelles stratégies plus appropriées.

Nous n'avons pas la recette pour pallier aux défis que nous impose la voie ERK/MAPK dans le traitement du cancer. Nos résultats offrent néanmoins un cadre de travail afin d'orienter les efforts de recherche vers des solutions mieux adaptées à la complexité de la voie et donc, plus efficaces. Nous pouvons également proposer des pistes de solution. Les travaux de cette thèse, mis en contexte avec la littérature, montrent le potentiel de la metformine. Cette molécule semble à la fois bloquer les effets néfastes d'une inhibition et d'une hyperactivation des kinases ERK. La metformine est une petite molécule polyvalente, qui semble avoir de nombreuses cibles et de nombreux effets cellulaires. Confrontant la volonté généralement prônée de développer des molécules spécifiques à des cibles données, est-ce que la metformine serait une molécule non spécifique, mais bénéfique? S'agirait-il d'une non-spécificité, qui dans son ensemble, serait tout à notre avantage?

7. Bibliographie

1. Stratton MR (2011) Exploring the genomes of cancer cells: progress and promise. *Science* 331(6024):1553-1558.
2. Boveri T (1914) Zur Frage der Entstehung Maligner Tumoren. *Gustav Fischer*:1–64.
3. Boveri T (2008) Concerning the origin of malignant tumours by Theodor Boveri. Translated and annotated by Henry Harris. *J Cell Sci* 121 Suppl 1:1-84.
4. Nowell PC (1976) The clonal evolution of tumor cell populations. *Science* 194(4260):23-28.
5. Alexandrov LB*, et al.* (2013) Signatures of mutational processes in human cancer. *Nature* 500(7463):415-421.
6. Baer CF, Miyamoto MM, & Denver DR (2007) Mutation rate variation in multicellular eukaryotes: causes and consequences. *Nat Rev Genet* 8(8):619-631.
7. Stratton MR, Campbell PJ, & Futreal PA (2009) The cancer genome. *Nature* 458(7239):719-724.
8. Talbot SJ & Crawford DH (2004) Viruses and tumours--an update. *Eur J Cancer* 40(13):1998-2005.
9. Egger G, Liang G, Aparicio A, & Jones PA (2004) Epigenetics in human disease and prospects for epigenetic therapy. *Nature* 429(6990):457-463.
10. Feinberg AP, Ohlsson R, & Henikoff S (2006) The epigenetic progenitor origin of human cancer. *Nat Rev Genet* 7(1):21-33.
11. Merlo LM, Pepper JW, Reid BJ, & Maley CC (2006) Cancer as an evolutionary and ecological process. *Nat Rev Cancer* 6(12):924-935.
12. Greaves M & Maley CC (2012) Clonal evolution in cancer. *Nature* 481(7381):306-313.
13. Visvader JE (2011) Cells of origin in cancer. *Nature* 469(7330):314-322.
14. Hanahan D & Weinberg RA (2011) Hallmarks of cancer: the next generation. *Cell* 144(5):646-674.
15. Hruban RH, Goggins M, Parsons J, & Kern SE (2000) Progression model for pancreatic cancer. *Clinical cancer research : an official journal of the American Association for Cancer Research* 6(8):2969-2972.
16. Grippo PJ, Nowlin PS, Demeure MJ, Longnecker DS, & Sandgren EP (2003) Preinvasive pancreatic neoplasia of ductal phenotype induced by acinar cell targeting of mutant Kras in transgenic mice. *Cancer Res* 63(9):2016-2019.
17. Hruban RH*, et al.* (2006) Pathology of genetically engineered mouse models of pancreatic exocrine cancer: consensus report and recommendations. *Cancer Res* 66(1):95-106.
18. Guerra C*, et al.* (2007) Chronic pancreatitis is essential for induction of pancreatic ductal adenocarcinoma by K-Ras oncogenes in adult mice. *Cancer Cell* 11(3):291-302.

19. Hruban RH*, et al.* (2001) Pancreatic intraepithelial neoplasia: a new nomenclature and classification system for pancreatic duct lesions. *The American journal of surgical pathology* 25(5):579-586.

20. Sipos B, Frank S, Gress T, Hahn S, & Kloppel G (2009) Pancreatic intraepithelial neoplasia revisited and updated. *Pancreatology : official journal of the International Association of Pancreatology* 9(1-2):45-54.

21. Hingorani SR*, et al.* (2003) Preinvasive and invasive ductal pancreatic cancer and its early detection in the mouse. *Cancer Cell* 4(6):437-450.

22. Morris JPt, Wang SC, & Hebrok M (2010) KRAS, Hedgehog, Wnt and the twisted developmental biology of pancreatic ductal adenocarcinoma. *Nat Rev Cancer* 10(10):683-695.

23. Hezel AF, Kimmelman AC, Stanger BZ, Bardeesy N, & Depinho RA (2006) Genetics and biology of pancreatic ductal adenocarcinoma. *Genes Dev* 20(10):1218-1249.

24. Vincent A, Herman J, Schulick R, Hruban RH, & Goggins M (2011) Pancreatic cancer. *Lancet* 378(9791):607-620.

25. Martin GS (2001) The hunting of the Src. *Nat Rev Mol Cell Biol* 2(6):467-475.

26. Duesberg PH & Vogt PK (1970) Differences between the ribonucleic acids of transforming and nontransforming avian tumor viruses. *Proc Natl Acad Sci U S A* 67(4):1673-1680.

27. Stehelin D, Varmus HE, Bishop JM, & Vogt PK (1976) DNA related to the transforming gene(s) of avian sarcoma viruses is present in normal avian DNA. *Nature* 260(5547):170-173.

28. Karnoub AE & Weinberg RA (2008) Ras oncogenes: split personalities. *Nat Rev Mol Cell Biol* 9(7):517-531.

29. Malumbres M & Barbacid M (2003) RAS oncogenes: the first 30 years. *Nat Rev Cancer* 3(6):459-465.

30. Shih C & Weinberg RA (1982) Isolation of a transforming sequence from a human bladder carcinoma cell line. *Cell* 29(1):161-169.

31. Goldfarb M, Shimizu K, Perucho M, & Wigler M (1982) Isolation and preliminary characterization of a human transforming gene from T24 bladder carcinoma cells. *Nature* 296(5856):404-409.

32. Pulciani S*, et al.* (1982) Oncogenes in human tumor cell lines: molecular cloning of a transforming gene from human bladder carcinoma cells. *Proc Natl Acad Sci U S A* 79(9):2845-2849.

33. Der CJ, Krontiris TG, & Cooper GM (1982) Transforming genes of human bladder and lung carcinoma cell lines are homologous to the ras genes of Harvey and Kirsten sarcoma viruses. *Proc Natl Acad Sci U S A* 79(11):3637-3640.

34. Cooper GM (1982) Cellular transforming genes. *Science* 217(4562):801-806.

35. Parada LF, Tabin CJ, Shih C, & Weinberg RA (1982) Human EJ bladder carcinoma oncogene is homologue of Harvey sarcoma virus ras gene. *Nature* 297(5866):474-478.

36. Santos E, Tronick SR, Aaronson SA, Pulciani S, & Barbacid M (1982) T24 human bladder carcinoma oncogene is an activated form of the normal human homologue of BALB- and Harvey-MSV transforming genes. *Nature* 298(5872):343-347.

37. Taparowsky E*, et al.* (1982) Activation of the T24 bladder carcinoma transforming gene is linked to a single amino acid change. *Nature* 300(5894):762-765.

38. Reddy EP, Reynolds RK, Santos E, & Barbacid M (1982) A point mutation is responsible for the acquisition of transforming properties by the T24 human bladder carcinoma oncogene. *Nature* 300(5888):149-152.

39. Tabin CJ*, et al.* (1982) Mechanism of activation of a human oncogene. *Nature* 300(5888):143-149.

40. Dang CV (2012) MYC on the path to cancer. *Cell* 149(1):22-35.

41. Taub R*, et al.* (1982) Translocation of the c-myc gene into the immunoglobulin heavy chain locus in human Burkitt lymphoma and murine plasmacytoma cells. *Proc Natl Acad Sci U S A* 79(24):7837-7841.

42. Dalla-Favera R*, et al.* (1982) Human c-myc onc gene is located on the region of chromosome 8 that is translocated in Burkitt lymphoma cells. *Proc Natl Acad Sci U S A* 79(24):7824-7827.

43. Croce CM (2008) Oncogenes and cancer. *The New England journal of medicine* 358(5):502-511.

44. Schubbert S, Shannon K, & Bollag G (2007) Hyperactive Ras in developmental disorders and cancer. *Nat Rev Cancer* 7(4):295-308.

45. Jones S*, et al.* (2008) Core signaling pathways in human pancreatic cancers revealed by global genomic analyses. *Science* 321(5897):1801-1806.

46. Hancock JF (2003) Ras proteins: different signals from different locations. *Nat Rev Mol Cell Biol* 4(5):373-384.

47. Vigil D, Cherfils J, Rossman KL, & Der CJ (Ras superfamily GEFs and GAPs: validated and tractable targets for cancer therapy? *Nat Rev Cancer* 10(12):842-857.

48. Cherfils J & Zeghouf M (2013) Regulation of small GTPases by GEFs, GAPs, and GDIs. *Physiological reviews* 93(1):269-309.

49. Pylayeva-Gupta Y, Grabocka E, & Bar-Sagi D (2011) RAS oncogenes: weaving a tumorigenic web. *Nat Rev Cancer* 11(11):761-774.

50. Haigis KM*, et al.* (2008) Differential effects of oncogenic K-Ras and N-Ras on proliferation, differentiation and tumor progression in the colon. *Nat Genet* 40(5):600-608.

51. Michor F, Iwasa Y, & Nowak MA (2004) Dynamics of cancer progression. *Nat Rev Cancer* 4(3):197-205.

52. Kinzler KW & Vogelstein B (1997) Cancer-susceptibility genes. Gatekeepers and caretakers. *Nature* 386(6627):761, 763.

53. Campisi J (2005) Senescent cells, tumor suppression, and organismal aging: good citizens, bad neighbors. *Cell* 120(4):513-522.

54. van Heemst D, den Reijer PM, & Westendorp RG (2007) Ageing or cancer: a review on the role of caretakers and gatekeepers. *Eur J Cancer* 43(15):2144-2152.

55. Levitt NC & Hickson ID (2002) Caretaker tumour suppressor genes that defend genome integrity. *Trends in molecular medicine* 8(4):179-186.

56. Vousden KH & Prives C (2009) Blinded by the Light: The Growing Complexity of p53. *Cell* 137(3):413-431.

57. Burkhart DL & Sage J (2008) Cellular mechanisms of tumour suppression by the retinoblastoma gene. *Nat Rev Cancer* 8(9):671-682.

58. Song MS, Salmena L, & Pandolfi PP (2012) The functions and regulation of the PTEN tumour suppressor. *Nat Rev Mol Cell Biol* 13(5):283-296.

59. Lowe SW, Cepero E, & Evan G (2004) Intrinsic tumour suppression. *Nature* 432(7015):307-315.

60. Bieging KT, Mello SS, & Attardi LD (2014) Unravelling mechanisms of p53-mediated tumour suppression. *Nat Rev Cancer* 14(5):359-370.

61. Levine AJ & Oren M (2009) The first 30 years of p53: growing ever more complex. *Nat Rev Cancer* 9(10):749-758.

62. Brosh R & Rotter V (2009) When mutants gain new powers: news from the mutant p53 field. *Nat Rev Cancer* 9(10):701-713.

63. Hayflick L & Moorhead PS (1961) The serial cultivation of human diploid cell strains. *Experimental cell research* 25:585-621.

64. Hayflick L (1965) The Limited in Vitro Lifetime of Human Diploid Cell Strains. *Experimental cell research* 37:614-636.

65. Harley CB, Futcher AB, & Greider CW (1990) Telomeres shorten during ageing of human fibroblasts. *Nature* 345(6274):458-460.

66. Wright WE, Piatyszek MA, Rainey WE, Byrd W, & Shay JW (1996) Telomerase activity in human germline and embryonic tissues and cells. *Developmental genetics* 18(2):173-179.

67. Kuilman T, Michaloglou C, Mooi WJ, & Peeper DS (2010) The essence of senescence. *Genes Dev* 24(22):2463-2479.

68. Bodnar AG*, et al.* (1998) Extension of life-span by introduction of telomerase into normal human cells. *Science* 279(5349):349-352.

69. Campisi J & d'Adda di Fagagna F (2007) Cellular senescence: when bad things happen to good cells. *Nat Rev Mol Cell Biol* 8(9):729-740.

70. Rodier F & Campisi J (2011) Four faces of cellular senescence. *J Cell Biol* 192(4):547-556.

71. Collado M & Serrano M (2010) Senescence in tumours: evidence from mice and humans. *Nat Rev Cancer* 10(1):51-57.

72. Freund A, Orjalo AV, Desprez PY, & Campisi J (2010) Inflammatory networks during cellular senescence: causes and consequences. *Trends in molecular medicine* 16(5):238-246.

73. Salama R, Sadaie M, Hoare M, & Narita M (2014) Cellular senescence and its effector programs. *Genes Dev* 28(2):99-114.

74. Choi J*, et al.* (2000) Expression of senescence-associated beta-galactosidase in enlarged prostates from men with benign prostatic hyperplasia. *Urology* 56(1):160-166.

75. Castro P, Giri D, Lamb D, & Ittmann M (2003) Cellular senescence in the pathogenesis of benign prostatic hyperplasia. *The Prostate* 55(1):30-38.

76. Dimri GP*, et al.* (1995) A biomarker that identifies senescent human cells in culture and in aging skin in vivo. *Proc Natl Acad Sci U S A* 92(20):9363-9367.

77. Jeyapalan JC, Ferreira M, Sedivy JM, & Herbig U (2007) Accumulation of senescent cells in mitotic tissue of aging primates. *Mechanisms of ageing and development* 128(1):36-44.

78. Yamakoshi K*, et al.* (2009) Real-time in vivo imaging of p16Ink4a reveals cross talk with p53. *J Cell Biol* 186(3):393-407.

79. Burd CE*, et al.* (2013) Monitoring tumorigenesis and senescence in vivo with a p16(INK4a)-luciferase model. *Cell* 152(1-2):340-351.

80. Michaloglou C*, et al.* (2005) BRAFE600-associated senescence-like cell cycle arrest of human naevi. *Nature* 436(7051):720-724.

81. Guerra C*, et al.* (2011) Pancreatitis-induced inflammation contributes to pancreatic cancer by inhibiting oncogene-induced senescence. *Cancer Cell* 19(6):728-739.

82. Collado M*, et al.* (2005) Tumour biology: senescence in premalignant tumours. *Nature* 436(7051):642.

83. Chin L*, et al.* (1997) Cooperative effects of INK4a and ras in melanoma susceptibility in vivo. *Genes Dev* 11(21):2822-2834.

84. Ackermann J*, et al.* (2005) Metastasizing melanoma formation caused by expression of activated N-RasQ61K on an INK4a-deficient background. *Cancer Res* 65(10):4005-4011.

85. Braig M*, et al.* (2005) Oncogene-induced senescence as an initial barrier in lymphoma development. *Nature* 436(7051):660-665.

86. Dankort D*, et al.* (2007) A new mouse model to explore the initiation, progression, and therapy of BRAFV600E-induced lung tumors. *Genes Dev* 21(4):379-384.

87. Carragher LA, *et al.* (2010) V600EBraf induces gastrointestinal crypt senescence and promotes tumour progression through enhanced CpG methylation of p16INK4a. *EMBO molecular medicine* 2(11):458-471.

88. Kwong LN, *et al.* (2012) Oncogenic NRAS signaling differentially regulates survival and proliferation in melanoma. *Nature medicine* 18(10):1503-1510.

89. Xue W, *et al.* (2007) Senescence and tumour clearance is triggered by p53 restoration in murine liver carcinomas. *Nature* 445(7128):656-660.

90. Ventura A, *et al.* (2007) Restoration of p53 function leads to tumour regression in vivo. *Nature* 445(7128):661-665.

91. Denoyelle C, *et al.* (2006) Anti-oncogenic role of the endoplasmic reticulum differentially activated by mutations in the MAPK pathway. *Nat Cell Biol* 8(10):1053-1063.

92. Kurz DJ, Decary S, Hong Y, & Erusalimsky JD (2000) Senescence-associated (beta)-galactosidase reflects an increase in lysosomal mass during replicative ageing of human endothelial cells. *J Cell Sci* 113 (Pt 20):3613-3622.

93. Lee BY, *et al.* (2006) Senescence-associated beta-galactosidase is lysosomal beta-galactosidase. *Aging cell* 5(2):187-195.

94. Debacq-Chainiaux F, Erusalimsky JD, Campisi J, & Toussaint O (2009) Protocols to detect senescence-associated beta-galactosidase (SA-betagal) activity, a biomarker of senescent cells in culture and in vivo. *Nature protocols* 4(12):1798-1806.

95. Gerland LM, *et al.* (2003) Association of increased autophagic inclusions labeled for beta-galactosidase with fibroblastic aging. *Experimental gerontology* 38(8):887-895.

96. Young AR, *et al.* (2009) Autophagy mediates the mitotic senescence transition. *Genes Dev* 23(7):798-803.

97. Deschênes-Simard X, Lessard F, Gaumont-Leclerc MF, Bardeesy N, & Ferbeyre G (2014) Cellular senescence and protein degradation: Breaking down cancer. *Cell Cycle* 13(12):Epub.

98. Narita M, *et al.* (2003) Rb-mediated heterochromatin formation and silencing of E2F target genes during cellular senescence. *Cell* 113(6):703-716.

99. Zhang R, *et al.* (2005) Formation of MacroH2A-containing senescence-associated heterochromatin foci and senescence driven by ASF1a and HIRA. *Developmental cell* 8(1):19-30.

100. Ferbeyre G, *et al.* (2000) PML is induced by oncogenic ras and promotes premature senescence. *Genes Dev* 14(16):2015-2027.

101. Pearson M, *et al.* (2000) PML regulates p53 acetylation and premature senescence induced by oncogenic Ras. *Nature* 406(6792):207-210.

102. Bischof O, *et al.* (2002) Deconstructing PML-induced premature senescence. *EMBO J* 21(13):3358-3369.

103. Vernier M*, et al.* (2011) Regulation of E2Fs and senescence by PML nuclear bodies. *Genes Dev* 25(1):41-50.

104. Zhang R, Chen W, & Adams PD (2007) Molecular dissection of formation of senescence-associated heterochromatin foci. *Mol Cell Biol* 27(6):2343-2358.

105. Seeler JS, Marchio A, Sitterlin D, Transy C, & Dejean A (1998) Interaction of SP100 with HP1 proteins: a link between the promyelocytic leukemia-associated nuclear bodies and the chromatin compartment. *Proc Natl Acad Sci U S A* 95(13):7316-7321.

106. Wu WS*, et al.* (2001) The growth suppressor PML represses transcription by functionally and physically interacting with histone deacetylases. *Mol Cell Biol* 21(7):2259-2268.

107. Alcalay M*, et al.* (1998) The promyelocytic leukemia gene product (PML) forms stable complexes with the retinoblastoma protein. *Mol Cell Biol* 18(2):1084-1093.

108. Kaplon J*, et al.* (2013) A key role for mitochondrial gatekeeper pyruvate dehydrogenase in oncogene-induced senescence. *Nature* 498(7452):109-112.

109. Dorr JR*, et al.* (2013) Synthetic lethal metabolic targeting of cellular senescence in cancer therapy. *Nature* 501(7467):421-425.

110. Moiseeva O, Bourdeau V, Roux A, Deschênes-Simard X, & Ferbeyre G (2009) Mitochondrial dysfunction contributes to oncogene-induced senescence. *Mol Cell Biol* 29(16):4495-4507.

111. Passos JF*, et al.* (2007) Mitochondrial dysfunction accounts for the stochastic heterogeneity in telomere-dependent senescence. *PLoS Biol* 5(5):e110.

112. Lee AC*, et al.* (1999) Ras proteins induce senescence by altering the intracellular levels of reactive oxygen species. *J Biol Chem* 274(12):7936-7940.

113. Lu T & Finkel T (2008) Free radicals and senescence. *Experimental cell research* 314(9):1918-1922.

114. Passos JF*, et al.* (2010) Feedback between p21 and reactive oxygen production is necessary for cell senescence. *Molecular systems biology* 6:347.

115. Di Micco R*, et al.* (2006) Oncogene-induced senescence is a DNA damage response triggered by DNA hyper-replication. *Nature* 444(7119):638-642.

116. Bartkova J*, et al.* (2006) Oncogene-induced senescence is part of the tumorigenesis barrier imposed by DNA damage checkpoints. *Nature* 444(7119):633-637.

117. Takai H, Smogorzewska A, & de Lange T (2003) DNA damage foci at dysfunctional telomeres. *Curr Biol* 13(17):1549-1556.

118. d'Adda di Fagagna F*, et al.* (2003) A DNA damage checkpoint response in telomere-initiated senescence. *Nature* 426(6963):194-198.

119. Herbig U, Jobling WA, Chen BP, Chen DJ, & Sedivy JM (2004) Telomere shortening triggers senescence of human cells through a pathway involving ATM, p53, and p21(CIP1), but not p16(INK4a). *Mol Cell* 14(4):501-513.

120. Mallette FA, Gaumont-Leclerc MF, & Ferbeyre G (2007) The DNA damage signaling pathway is a critical mediator of oncogene-induced senescence. *Genes Dev* 21(1):43-48.

121. Mallette FA & Ferbeyre G (2007) The DNA damage signaling pathway connects oncogenic stress to cellular senescence. *Cell Cycle* 6(15):1831-1836.

122. d'Adda di Fagagna F (2008) Living on a break: cellular senescence as a DNA-damage response. *Nat Rev Cancer* 8(7):512-522.

123. Rodier F*, et al.* (2011) DNA-SCARS: distinct nuclear structures that sustain damage-induced senescence growth arrest and inflammatory cytokine secretion. *J Cell Sci* 124(Pt 1):68-81.

124. Fumagalli M*, et al.* (2012) Telomeric DNA damage is irreparable and causes persistent DNA-damage-response activation. *Nat Cell Biol* 14(4):355-365.

125. de Stanchina E*, et al.* (2004) PML is a direct p53 target that modulates p53 effector functions. *Mol Cell* 13(4):523-535.

126. Kortlever RM, Higgins PJ, & Bernards R (2006) Plasminogen activator inhibitor-1 is a critical downstream target of p53 in the induction of replicative senescence. *Nat Cell Biol* 8(8):877-884.

127. Tront JS, Hoffman B, & Liebermann DA (2006) Gadd45a suppresses Ras-driven mammary tumorigenesis by activation of c-Jun NH2-terminal kinase and p38 stress signaling resulting in apoptosis and senescence. *Cancer Res* 66(17):8448-8454.

128. Qian Y, Zhang J, Yan B, & Chen X (2008) DEC1, a basic helix-loop-helix transcription factor and a novel target gene of the p53 family, mediates p53-dependent premature senescence. *J Biol Chem* 283(5):2896-2905.

129. Aksoy O*, et al.* (2012) The atypical E2F family member E2F7 couples the p53 and RB pathways during cellular senescence. *Genes Dev* 26(14):1546-1557.

130. Brown JP, Wei W, & Sedivy JM (1997) Bypass of senescence after disruption of p21CIP1/WAF1 gene in normal diploid human fibroblasts. *Science* 277(5327):831-834.

131. Jackson JG & Pereira-Smith OM (2006) p53 is preferentially recruited to the promoters of growth arrest genes p21 and GADD45 during replicative senescence of normal human fibroblasts. *Cancer Res* 66(17):8356-8360.

132. McConnell BB, Starborg M, Brookes S, & Peters G (1998) Inhibitors of cyclin-dependent kinases induce features of replicative senescence in early passage human diploid fibroblasts. *Curr Biol* 8(6):351-354.

133. Gil J & Peters G (2006) Regulation of the INK4b-ARF-INK4a tumour suppressor locus: all for one or one for all. *Nat Rev Mol Cell Biol* 7(9):667-677.

134. Malumbres M & Barbacid M (2009) Cell cycle, CDKs and cancer: a changing paradigm. *Nat Rev Cancer* 9(3):153-166.

135. Bertoli C, Skotheim JM, & de Bruin RA (2013) Control of cell cycle transcription during G1 and S phases. *Nat Rev Mol Cell Biol* 14(8):518-528.

136. Shelton DN, Chang E, Whittier PS, Choi D, & Funk WD (1999) Microarray analysis of replicative senescence. *Curr Biol* 9(17):939-945.

137. Zhang H, Pan KH, & Cohen SN (2003) Senescence-specific gene expression fingerprints reveal cell-type-dependent physical clustering of up-regulated chromosomal loci. *Proc Natl Acad Sci U S A* 100(6):3251-3256.

138. Chicas A*, et al.* (2010) Dissecting the unique role of the retinoblastoma tumor suppressor during cellular senescence. *Cancer Cell* 17(4):376-387.

139. Coppe JP*, et al.* (2008) Senescence-associated secretory phenotypes reveal cell-nonautonomous functions of oncogenic RAS and the p53 tumor suppressor. *PLoS biology* 6(12):2853-2868.

140. Chien Y*, et al.* (2011) Control of the senescence-associated secretory phenotype by NF-kappaB promotes senescence and enhances chemosensitivity. *Genes Dev* 25(20):2125-2136.

141. Ohanna M*, et al.* (2011) Senescent cells develop a PARP-1 and nuclear factor-{kappa}B-associated secretome (PNAS). *Genes Dev* 25(12):1245-1261.

142. Murano S*, et al.* (1991) Diverse gene sequences are overexpressed in werner syndrome fibroblasts undergoing premature replicative senescence. *Mol Cell Biol* 11(8):3905-3914.

143. Cristofalo VJ & Pignolo RJ (1996) Molecular markers of senescence in fibroblast-like cultures. *Experimental gerontology* 31(1-2):111-123.

144. Acosta JC*, et al.* (2008) Chemokine signaling via the CXCR2 receptor reinforces senescence. *Cell* 133(6):1006-1018.

145. Kuilman T*, et al.* (2008) Oncogene-induced senescence relayed by an interleukin-dependent inflammatory network. *Cell* 133(6):1019-1031.

146. Kuilman T & Peeper DS (2009) Senescence-messaging secretome: SMS-ing cellular stress. *Nat Rev Cancer* 9(2):81-94.

147. Coppe JP, Desprez PY, Krtolica A, & Campisi J (2010) The senescence-associated secretory phenotype: the dark side of tumor suppression. *Annual review of pathology* 5:99-118.

148. Calabrese V*, et al.* (2009) SOCS1 links cytokine signaling to p53 and senescence. *Mol Cell* 36(5):754-767.

149. Hubackova S, Krejcikova K, Bartek J, & Hodny Z (2012) IL1- and TGFbeta-Nox4 signaling, oxidative stress and DNA damage response are shared features of replicative, oncogene-induced, and drug-induced paracrine 'bystander senescence'. *Aging* 4(12):932-951.

150. Acosta JC*, et al.* (2013) A complex secretory program orchestrated by the inflammasome controls paracrine senescence. *Nat Cell Biol* 15(8):978-990.

151. Krizhanovsky V*, et al.* (2008) Senescence of activated stellate cells limits liver fibrosis. *Cell* 134(4):657-667.

152. Kang TW*, et al.* (2011) Senescence surveillance of pre-malignant hepatocytes limits liver cancer development. *Nature* 479(7374):547-551.

153. Iannello A, Thompson TW, Ardolino M, Lowe SW, & Raulet DH (2013) p53-dependent chemokine production by senescent tumor cells supports NKG2D-dependent tumor elimination by natural killer cells. *The Journal of experimental medicine* 210(10):2057-2069.

154. Lujambio A*, et al.* (2013) Non-cell-autonomous tumor suppression by p53. *Cell* 153(2):449-460.

155. Krtolica A, Parrinello S, Lockett S, Desprez PY, & Campisi J (2001) Senescent fibroblasts promote epithelial cell growth and tumorigenesis: a link between cancer and aging. *Proc Natl Acad Sci U S A* 98(21):12072-12077.

156. Bavik C*, et al.* (2006) The gene expression program of prostate fibroblast senescence modulates neoplastic epithelial cell proliferation through paracrine mechanisms. *Cancer Res* 66(2):794-802.

157. Liu D & Hornsby PJ (2007) Senescent human fibroblasts increase the early growth of xenograft tumors via matrix metalloproteinase secretion. *Cancer Res* 67(7):3117-3126.

158. Coppe JP, Kauser K, Campisi J, & Beausejour CM (2006) Secretion of vascular endothelial growth factor by primary human fibroblasts at senescence. *J Biol Chem* 281(40):29568-29574.

159. van Deursen JM (2014) The role of senescent cells in ageing. *Nature* 509(7501):439-446.

160. Collado M, Blasco MA, & Serrano M (2007) Cellular senescence in cancer and aging. *Cell* 130(2):223-233.

161. Campisi J (2013) Aging, cellular senescence, and cancer. *Annual review of physiology* 75:685-705.

162. Janzen V*, et al.* (2006) Stem-cell ageing modified by the cyclin-dependent kinase inhibitor p16INK4a. *Nature* 443(7110):421-426.

163. Krishnamurthy J*, et al.* (2006) p16INK4a induces an age-dependent decline in islet regenerative potential. *Nature* 443(7110):453-457.

164. Molofsky AV*, et al.* (2006) Increasing p16INK4a expression decreases forebrain progenitors and neurogenesis during ageing. *Nature* 443(7110):448-452.

165. Baker DJ*, et al.* (2008) Opposing roles for p16Ink4a and p19Arf in senescence and ageing caused by BubR1 insufficiency. *Nat Cell Biol* 10(7):825-836.

166. Baker DJ*, et al.* (2011) Clearance of p16Ink4a-positive senescent cells delays ageing-associated disorders. *Nature* 479(7372):232-236.

167. Franceschi C*, et al.* (2000) Inflamm-aging. An evolutionary perspective on immunosenescence. *Annals of the New York Academy of Sciences* 908:244-254.

168. Vasto S*, et al.* (2007) Inflammatory networks in ageing, age-related diseases and longevity. *Mechanisms of ageing and development* 128(1):83-91.

169. Vasile E, Tomita Y, Brown LF, Kocher O, & Dvorak HF (2001) Differential expression of thymosin beta-10 by early passage and senescent vascular endothelium is modulated by VPF/VEGF: evidence for senescent endothelial cells in vivo at sites of atherosclerosis. *FASEB J* 15(2):458-466.

170. Price JS*, et al.* (2002) The role of chondrocyte senescence in osteoarthritis. *Aging cell* 1(1):57-65.

171. Sone H & Kagawa Y (2005) Pancreatic beta cell senescence contributes to the pathogenesis of type 2 diabetes in high-fat diet-induced diabetic mice. *Diabetologia* 48(1):58-67.

172. Williams GC (1957) Pleiotropy, natural Selection, and the evolution of senescence. *Evolution* 11(398-411).

173. Kirkwood TB & Austad SN (2000) Why do we age? *Nature* 408(6809):233-238.

174. Campisi J (2003) Cancer and ageing: rival demons? *Nat Rev Cancer* 3(5):339-349.

175. Baylin SB & Jones PA (2011) A decade of exploring the cancer epigenome - biological and translational implications. *Nat Rev Cancer* 11(10):726-734.

176. Baccelli I & Trumpp A (2012) The evolving concept of cancer and metastasis stem cells. *J Cell Biol* 198(3):281-293.

177. Munoz P, Iliou MS, & Esteller M (2012) Epigenetic alterations involved in cancer stem cell reprogramming. *Molecular oncology* 6(6):620-636.

178. Suva ML, Riggi N, & Bernstein BE (2013) Epigenetic reprogramming in cancer. *Science* 339(6127):1567-1570.

179. Schwitalla S*, et al.* (2013) Intestinal tumorigenesis initiated by dedifferentiation and acquisition of stem-cell-like properties. *Cell* 152(1-2):25-38.

180. You JS & Jones PA (2012) Cancer genetics and epigenetics: two sides of the same coin? *Cancer Cell* 22(1):9-20.

181. Dawson MA & Kouzarides T (2012) Cancer epigenetics: from mechanism to therapy. *Cell* 150(1):12-27.

182. Suzuki H*, et al.* (2004) Epigenetic inactivation of SFRP genes allows constitutive WNT signaling in colorectal cancer. *Nat Genet* 36(4):417-422.

183. Clevers H & Nusse R (2012) Wnt/beta-catenin signaling and disease. *Cell* 149(6):1192-1205.

184. Kreso A & Dick JE (2014) Evolution of the cancer stem cell model. *Cell stem cell* 14(3):275-291.

185. Hanahan D & Coussens LM (2012) Accessories to the crime: functions of cells recruited to the tumor microenvironment. *Cancer Cell* 21(3):309-322.

186. Futscher BW (2013) Epigenetic changes during cell transformation. *Advances in experimental medicine and biology* 754:179-194.

187. Grivennikov SI, Greten FR, & Karin M (2010) Immunity, inflammation, and cancer. *Cell* 140(6):883-899.

188. Elinav E*, et al.* (2013) Inflammation-induced cancer: crosstalk between tumours, immune cells and microorganisms. *Nat Rev Cancer* 13(11):759-771.

189. Yu H, Pardoll D, & Jove R (2009) STATs in cancer inflammation and immunity: a leading role for STAT3. *Nat Rev Cancer* 9(11):798-809.

190. Grivennikov SI & Karin M (2010) Dangerous liaisons: STAT3 and NF-kappaB collaboration and crosstalk in cancer. *Cytokine & growth factor reviews* 21(1):11-19.

191. Yadav D & Lowenfels AB (2013) The epidemiology of pancreatitis and pancreatic cancer. *Gastroenterology* 144(6):1252-1261.

192. Deschênes-Simard X, Mizukami Y, & Bardeesy N (2013) Macrophages in pancreatic cancer: starting things off on the wrong track. *J Cell Biol* 202(3):403-405.

193. Kopp JL*, et al.* (2012) Identification of Sox9-dependent acinar-to-ductal reprogramming as the principal mechanism for initiation of pancreatic ductal adenocarcinoma. *Cancer Cell* 22(6):737-750.

194. Miyatsuka T*, et al.* (2006) Persistent expression of PDX-1 in the pancreas causes acinar-to-ductal metaplasia through Stat3 activation. *Genes Dev* 20(11):1435-1440.

195. Fukuda A*, et al.* (2011) Stat3 and MMP7 contribute to pancreatic ductal adenocarcinoma initiation and progression. *Cancer Cell* 19(4):441-455.

196. Ling J*, et al.* (2012) KrasG12D-induced IKK2/beta/NF-kappaB activation by IL-1alpha and p62 feedforward loops is required for development of pancreatic ductal adenocarcinoma. *Cancer Cell* 21(1):105-120.

197. Liou GY*, et al.* (2013) Macrophage-secreted cytokines drive pancreatic acinar-to-ductal metaplasia through NF-kappaB and MMPs. *J Cell Biol* 202(3):563-577.

198. Lesina M*, et al.* (2011) Stat3/Socs3 activation by IL-6 transsignaling promotes progression of pancreatic intraepithelial neoplasia and development of pancreatic cancer. *Cancer Cell* 19(4):456-469.

199. Maniati E*, et al.* (2011) Crosstalk between the canonical NF-kappaB and Notch signaling pathways inhibits Ppargamma expression and promotes pancreatic cancer progression in mice. *The Journal of clinical investigation* 121(12):4685-4699.

200. Corcoran RB*, et al.* (2011) STAT3 plays a critical role in KRAS-induced pancreatic tumorigenesis. *Cancer Res* 71(14):5020-5029.

201. Sun L*, et al.* (2013) Epigenetic Regulation of SOX9 by the NF-kappaB Signaling Pathway in Pancreatic Cancer Stem Cells. *Stem cells* 31(8):1454-1466.

202. Magee JA, Piskounova E, & Morrison SJ (2012) Cancer stem cells: impact, heterogeneity, and uncertainty. *Cancer Cell* 21(3):283-296.

203. Burrell RA, McGranahan N, Bartek J, & Swanton C (2013) The causes and consequences of genetic heterogeneity in cancer evolution. *Nature* 501(7467):338-345.

204. Marusyk A, Almendro V, & Polyak K (2012) Intra-tumour heterogeneity: a looking glass for cancer? *Nat Rev Cancer* 12(5):323-334.

205. Cahill DP, Kinzler KW, Vogelstein B, & Lengauer C (1999) Genetic instability and darwinian selection in tumours. *Trends in cell biology* 9(12):M57-60.

206. Polyak K, Haviv I, & Campbell IG (2009) Co-evolution of tumor cells and their microenvironment. *Trends in genetics : TIG* 25(1):30-38.

207. Junttila MR & de Sauvage FJ (2013) Influence of tumour micro-environment heterogeneity on therapeutic response. *Nature* 501(7467):346-354.

208. Bonnet D & Dick JE (1997) Human acute myeloid leukemia is organized as a hierarchy that originates from a primitive hematopoietic cell. *Nature medicine* 3(7):730-737.

209. Lapidot T*, et al.* (1994) A cell initiating human acute myeloid leukaemia after transplantation into SCID mice. *Nature* 367(6464):645-648.

210. Visvader JE & Lindeman GJ (2008) Cancer stem cells in solid tumours: accumulating evidence and unresolved questions. *Nat Rev Cancer* 8(10):755-768.

211. Meacham CE & Morrison SJ (2013) Tumour heterogeneity and cancer cell plasticity. *Nature* 501(7467):328-337.

212. Ishizawa K*, et al.* (2010) Tumor-initiating cells are rare in many human tumors. *Cell stem cell* 7(3):279-282.

213. Friedmann-Morvinski D & Verma IM (2014) Dedifferentiation and reprogramming: origins of cancer stem cells. *EMBO Rep* 15(3):244-253.

214. Visvader JE & Lindeman GJ (2012) Cancer stem cells: current status and evolving complexities. *Cell stem cell* 10(6):717-728.

215. Chaffer CL*, et al.* (2011) Normal and neoplastic nonstem cells can spontaneously convert to a stem-like state. *Proc Natl Acad Sci U S A* 108(19):7950-7955.

216. Lobo NA, Shimono Y, Qian D, & Clarke MF (2007) The biology of cancer stem cells. *Annual review of cell and developmental biology* 23:675-699.

217. Aguirre AJ*, et al.* (2003) Activated Kras and Ink4a/Arf deficiency cooperate to produce metastatic pancreatic ductal adenocarcinoma. *Genes Dev* 17(24):3112-3126.

218. Jones PA & Baylin SB (2007) The epigenomics of cancer. *Cell* 128(4):683-692.

219. Avruch J (2007) MAP kinase pathways: the first twenty years. *Biochim Biophys Acta* 1773(8):1150-1160.

220. Sturgill TW & Ray LB (1986) Muscle proteins related to microtubule associated protein-2 are substrates for an insulin-stimulatable kinase. *Biochem Biophys Res Commun* 134(2):565-571.

221. Ahn NG, *et al.* (1991) Multiple components in an epidermal growth factor-stimulated protein kinase cascade. In vitro activation of a myelin basic protein/microtubule-associated protein 2 kinase. *J Biol Chem* 266(7):4220-4227.

222. Gomez N & Cohen P (1991) Dissection of the protein kinase cascade by which nerve growth factor activates MAP kinases. *Nature* 353(6340):170-173.

223. Kyriakis JM, *et al.* (1992) Raf-1 activates MAP kinase-kinase. *Nature* 358(6385):417-421.

224. Dent P, *et al.* (1992) Activation of mitogen-activated protein kinase kinase by v-Raf in NIH 3T3 cells and in vitro. *Science* 257(5075):1404-1407.

225. Howe LR, *et al.* (1992) Activation of the MAP kinase pathway by the protein kinase raf. *Cell* 71(2):335-342.

226. Wood KW, Sarnecki C, Roberts TM, & Blenis J (1992) ras mediates nerve growth factor receptor modulation of three signal-transducing protein kinases: MAP kinase, Raf-1, and RSK. *Cell* 68(6):1041-1050.

227. Leevers SJ & Marshall CJ (1992) Activation of extracellular signal-regulated kinase, ERK2, by p21ras oncoprotein. *EMBO J* 11(2):569-574.

228. de Vries-Smits AM, Burgering BM, Leevers SJ, Marshall CJ, & Bos JL (1992) Involvement of p21ras in activation of extracellular signal-regulated kinase 2. *Nature* 357(6379):602-604.

229. Robbins DJ, *et al.* (1992) Evidence for a Ras-dependent extracellular signal-regulated protein kinase (ERK) cascade. *Proc Natl Acad Sci U S A* 89(15):6924-6928.

230. Hattori S, *et al.* (1992) Activation of mitogen-activated protein kinase and its activator by ras in intact cells and in a cell-free system. *J Biol Chem* 267(28):20346-20351.

231. Shibuya EK, Polverino AJ, Chang E, Wigler M, & Ruderman JV (1992) Oncogenic ras triggers the activation of 42-kDa mitogen-activated protein kinase in extracts of quiescent Xenopus oocytes. *Proc Natl Acad Sci U S A* 89(20):9831-9835.

232. Chang L & Karin M (2001) Mammalian MAP kinase signalling cascades. *Nature* 410(6824):37-40.

233. Raman M & Cobb MH (2003) MAP kinase modules: many roads home. *Curr Biol* 13(22):R886-888.

234. Wellbrock C, Karasarides M, & Marais R (2004) The RAF proteins take centre stage. *Nat Rev Mol Cell Biol* 5(11):875-885.

235. Koide H, Satoh T, Nakafuku M, & Kaziro Y (1993) GTP-dependent association of Raf-1 with Ha-Ras: identification of Raf as a target downstream of Ras in mammalian cells. *Proc Natl Acad Sci U S A* 90(18):8683-8686.

236. Warne PH, Viciana PR, & Downward J (1993) Direct interaction of Ras and the amino-terminal region of Raf-1 in vitro. *Nature* 364(6435):352-355.

237. Vojtek AB, Hollenberg SM, & Cooper JA (1993) Mammalian Ras interacts directly with the serine/threonine kinase Raf. *Cell* 74(1):205-214.

238. Van Aelst L, Barr M, Marcus S, Polverino A, & Wigler M (1993) Complex formation between RAS and RAF and other protein kinases. *Proc Natl Acad Sci U S A* 90(13):6213-6217.

239. Zhang XF*, et al.* (1993) Normal and oncogenic p21ras proteins bind to the amino-terminal regulatory domain of c-Raf-1. *Nature* 364(6435):308-313.

240. Moodie SA, Willumsen BM, Weber MJ, & Wolfman A (1993) Complexes of Ras.GTP with Raf-1 and mitogen-activated protein kinase kinase. *Science* 260(5114):1658-1661.

241. Stokoe D, Macdonald SG, Cadwallader K, Symons M, & Hancock JF (1994) Activation of Raf as a result of recruitment to the plasma membrane. *Science* 264(5164):1463-1467.

242. McCubrey JA*, et al.* (2007) Roles of the Raf/MEK/ERK pathway in cell growth, malignant transformation and drug resistance. *Biochim Biophys Acta* 1773(8):1263-1284.

243. Lito P, Rosen N, & Solit DB (2013) Tumor adaptation and resistance to RAF inhibitors. *Nature medicine* 19(11):1401-1409.

244. Udell CM, Rajakulendran T, Sicheri F, & Therrien M (2011) Mechanistic principles of RAF kinase signaling. *Cell Mol Life Sci* 68(4):553-565.

245. Yeung K*, et al.* (1999) Suppression of Raf-1 kinase activity and MAP kinase signalling by RKIP. *Nature* 401(6749):173-177.

246. Farrar MA, Alberol-Ila J, & Perlmutter RM (1996) Activation of the Raf-1 kinase cascade by coumermycin-induced dimerization. *Nature* 383(6596):178-181.

247. Luo Z*, et al.* (1996) Oligomerization activates c-Raf-1 through a Ras-dependent mechanism. *Nature* 383(6596):181-185.

248. Rushworth LK, Hindley AD, O'Neill E, & Kolch W (2006) Regulation and role of Raf-1/B-Raf heterodimerization. *Mol Cell Biol* 26(6):2262-2272.

249. Rajakulendran T, Sahmi M, Lefrancois M, Sicheri F, & Therrien M (2009) A dimerization-dependent mechanism drives RAF catalytic activation. *Nature* 461(7263):542-545.

250. Douziech M, Sahmi M, Laberge G, & Therrien M (2006) A KSR/CNK complex mediated by HYP, a novel SAM domain-containing protein, regulates RAS-dependent RAF activation in Drosophila. *Genes Dev* 20(7):807-819.

251. Payne DM*, et al.* (1991) Identification of the regulatory phosphorylation sites in pp42/mitogen-activated protein kinase (MAP kinase). *EMBO J* 10(4):885-892.

252. Roux PP & Blenis J (2004) ERK and p38 MAPK-activated protein kinases: a family of protein kinases with diverse biological functions. *Microbiology and molecular biology reviews : MMBR* 68(2):320-344.

253. Cargnello M & Roux PP (2011) Activation and function of the MAPKs and their substrates, the MAPK-activated protein kinases. *Microbiology and molecular biology reviews : MMBR* 75(1):50-83.

254. Shaul YD & Seger R (2007) The MEK/ERK cascade: from signaling specificity to diverse functions. *Biochim Biophys Acta* 1773(8):1213-1226.

255. Roskoski R, Jr. (2012) ERK1/2 MAP kinases: structure, function, and regulation. *Pharmacological research : the official journal of the Italian Pharmacological Society* 66(2):105-143.

256. Lefloch R, Pouyssegur J, & Lenormand P (2008) Single and combined silencing of ERK1 and ERK2 reveals their positive contribution to growth signaling depending on their expression levels. *Mol Cell Biol* 28(1):511-527.

257. Voisin L, Saba-El-Leil MK, Julien C, Fremin C, & Meloche S (2010) Genetic demonstration of a redundant role of extracellular signal-regulated kinase 1 (ERK1) and ERK2 mitogen-activated protein kinases in promoting fibroblast proliferation. *Mol Cell Biol* 30(12):2918-2932.

258. Lefloch R, Pouyssegur J, & Lenormand P (2009) Total ERK1/2 activity regulates cell proliferation. *Cell Cycle* 8(5):705-711.

259. Yoon S & Seger R (2006) The extracellular signal-regulated kinase: multiple substrates regulate diverse cellular functions. *Growth Factors* 24(1):21-44.

260. Kosako H*, et al.* (2009) Phosphoproteomics reveals new ERK MAP kinase targets and links ERK to nucleoporin-mediated nuclear transport. *Nat Struct Mol Biol* 16(10):1026-1035.

261. Old WM*, et al.* (2009) Functional proteomics identifies targets of phosphorylation by B-Raf signaling in melanoma. *Mol Cell* 34(1):115-131.

262. Pan C, Olsen JV, Daub H, & Mann M (2009) Global effects of kinase inhibitors on signaling networks revealed by quantitative phosphoproteomics. *Molecular & cellular proteomics : MCP* 8(12):2796-2808.

263. Carlson SM*, et al.* (2011) Large-scale discovery of ERK2 substrates identifies ERK-mediated transcriptional regulation by ETV3. *Science signaling* 4(196):rs11.

264. Courcelles M*, et al.* (2013) Phosphoproteome dynamics reveal novel ERK1/2 MAP kinase substrates with broad spectrum of functions. *Molecular systems biology* 9:669.

265. Gonzalez FA, Raden DL, & Davis RJ (1991) Identification of substrate recognition determinants for human ERK1 and ERK2 protein kinases. *J Biol Chem* 266(33):22159-22163.

266. Songyang Z*, et al.* (1996) A structural basis for substrate specificities of protein Ser/Thr kinases: primary sequence preference of casein kinases I and II, NIMA, phosphorylase kinase, calmodulin-dependent kinase II, CDK5, and Erk1. *Mol Cell Biol* 16(11):6486-6493.

267. Yang SH, Yates PR, Whitmarsh AJ, Davis RJ, & Sharrocks AD (1998) The Elk-1 ETS-domain transcription factor contains a mitogen-activated protein kinase targeting motif. *Mol Cell Biol* 18(2):710-720.

268. Jacobs D, Glossip D, Xing H, Muslin AJ, & Kornfeld K (1999) Multiple docking sites on substrate proteins form a modular system that mediates recognition by ERK MAP kinase. *Genes Dev* 13(2):163-175.

269. Casar B*, et al.* (2009) Ras subcellular localization defines extracellular signal-regulated kinase 1 and 2 substrate specificity through distinct utilization of scaffold proteins. *Mol Cell Biol* 29(5):1338-1353.

270. Kolch W (2005) Coordinating ERK/MAPK signalling through scaffolds and inhibitors. *Nat Rev Mol Cell Biol* 6(11):827-837.

271. Ramos JW (2008) The regulation of extracellular signal-regulated kinase (ERK) in mammalian cells. *The international journal of biochemistry & cell biology* 40(12):2707-2719.

272. Brown MD & Sacks DB (2009) Protein scaffolds in MAP kinase signalling. *Cell Signal* 21(4):462-469.

273. Kholodenko BN, Hancock JF, & Kolch W (2010) Signalling ballet in space and time. *Nat Rev Mol Cell Biol* 11(6):414-426.

274. Chuderland D & Seger R (2005) Protein-protein interactions in the regulation of the extracellular signal-regulated kinase. *Molecular biotechnology* 29(1):57-74.

275. Dhanasekaran DN, Kashef K, Lee CM, Xu H, & Reddy EP (2007) Scaffold proteins of MAP-kinase modules. *Oncogene* 26(22):3185-3202.

276. Meister M, Tomasovic A, Banning A, & Tikkanen R (2013) Mitogen-Activated Protein (MAP) Kinase Scaffolding Proteins: A Recount. *International journal of molecular sciences* 14(3):4854-4884.

277. Murphy LO & Blenis J (2006) MAPK signal specificity: the right place at the right time. *Trends Biochem Sci* 31(5):268-275.

278. Murphy LO, Smith S, Chen RH, Fingar DC, & Blenis J (2002) Molecular interpretation of ERK signal duration by immediate early gene products. *Nat Cell Biol* 4(8):556-564.

279. Murphy LO, MacKeigan JP, & Blenis J (2004) A network of immediate early gene products propagates subtle differences in mitogen-activated protein kinase signal amplitude and duration. *Mol Cell Biol* 24(1):144-153.

280. Ebisuya M, Kondoh K, & Nishida E (2005) The duration, magnitude and compartmentalization of ERK MAP kinase activity: mechanisms for providing signaling specificity. *J Cell Sci* 118(Pt 14):2997-3002.

281. Hunter T (2007) The age of crosstalk: phosphorylation, ubiquitination, and beyond. *Mol Cell* 28(5):730-738.

282. Skaar JR, Pagan JK, & Pagano M (2013) Mechanisms and function of substrate recruitment by F-box proteins. *Nat Rev Mol Cell Biol* 14(6):369-381.

283. Jeffrey KL, Camps M, Rommel C, & Mackay CR (2007) Targeting dual-specificity phosphatases: manipulating MAP kinase signalling and immune responses. *Nat Rev Drug Discov* 6(5):391-403.

284. Huang CY & Tan TH (2012) DUSPs, to MAP kinases and beyond. *Cell & bioscience* 2(1):24.

285. Kondoh K & Nishida E (2007) Regulation of MAP kinases by MAP kinase phosphatases. *Biochim Biophys Acta* 1773(8):1227-1237.

286. Brondello JM, Brunet A, Pouyssegur J, & McKenzie FR (1997) The dual specificity mitogen-activated protein kinase phosphatase-1 and -2 are induced by the p42/p44MAPK cascade. *J Biol Chem* 272(2):1368-1376.

287. Amit I*, et al.* (2007) A module of negative feedback regulators defines growth factor signaling. *Nat Genet* 39(4):503-512.

288. Hacohen N, Kramer S, Sutherland D, Hiromi Y, & Krasnow MA (1998) sprouty encodes a novel antagonist of FGF signaling that patterns apical branching of the Drosophila airways. *Cell* 92(2):253-263.

289. Kim HJ & Bar-Sagi D (2004) Modulation of signalling by Sprouty: a developing story. *Nat Rev Mol Cell Biol* 5(6):441-450.

290. Mason JM, Morrison DJ, Basson MA, & Licht JD (2006) Sprouty proteins: multifaceted negative-feedback regulators of receptor tyrosine kinase signaling. *Trends in cell biology* 16(1):45-54.

291. Reich A, Sapir A, & Shilo B (1999) Sprouty is a general inhibitor of receptor tyrosine kinase signaling. *Development* 126(18):4139-4147.

292. Impagnatiello MA*, et al.* (2001) Mammalian sprouty-1 and -2 are membrane-anchored phosphoprotein inhibitors of growth factor signaling in endothelial cells. *J Cell Biol* 152(5):1087-1098.

293. Hanafusa H, Torii S, Yasunaga T, & Nishida E (2002) Sprouty1 and Sprouty2 provide a control mechanism for the Ras/MAPK signalling pathway. *Nat Cell Biol* 4(11):850-858.

294. Gross I, Bassit B, Benezra M, & Licht JD (2001) Mammalian sprouty proteins inhibit cell growth and differentiation by preventing ras activation. *J Biol Chem* 276(49):46460-46468.

295. Yusoff P*, et al.* (2002) Sprouty2 inhibits the Ras/MAP kinase pathway by inhibiting the activation of Raf. *J Biol Chem* 277(5):3195-3201.

296. Sasaki A*, et al.* (2003) Mammalian Sprouty4 suppresses Ras-independent ERK activation by binding to Raf1. *Nat Cell Biol* 5(5):427-432.

297. Rubin C*, et al.* (2003) Sprouty fine-tunes EGF signaling through interlinked positive and negative feedback loops. *Curr Biol* 13(4):297-307.

298. Wong ES*, et al.* (2002) Sprouty2 attenuates epidermal growth factor receptor ubiquitylation and endocytosis, and consequently enhances Ras/ERK signalling. *EMBO J* 21(18):4796-4808.

299. Egan JE, Hall AB, Yatsula BA, & Bar-Sagi D (2002) The bimodal regulation of epidermal growth factor signaling by human Sprouty proteins. *Proc Natl Acad Sci U S A* 99(9):6041-6046.

300. Levkowitz G*, et al.* (1998) c-Cbl/Sli-1 regulates endocytic sorting and ubiquitination of the epidermal growth factor receptor. *Genes Dev* 12(23):3663-3674.

301. Maurer G, Tarkowski B, & Baccarini M (2011) Raf kinases in cancer-roles and therapeutic opportunities. *Oncogene* 30(32):3477-3488.

302. Davies H*, et al.* (2002) Mutations of the BRAF gene in human cancer. *Nature* 417(6892):949-954.

303. Tsao H, Chin L, Garraway LA, & Fisher DE (2012) Melanoma: from mutations to medicine. *Genes Dev* 26(11):1131-1155.

304. Citri A & Yarden Y (2006) EGF-ERBB signalling: towards the systems level. *Nat Rev Mol Cell Biol* 7(7):505-516.

305. Sharma SV, Bell DW, Settleman J, & Haber DA (2007) Epidermal growth factor receptor mutations in lung cancer. *Nat Rev Cancer* 7(3):169-181.

306. da Cunha Santos G, Shepherd FA, & Tsao MS (2011) EGFR mutations and lung cancer. *Annual review of pathology* 6:49-69.

307. Arteaga CL*, et al.* (2012) Treatment of HER2-positive breast cancer: current status and future perspectives. *Nature reviews. Clinical oncology* 9(1):16-32.

308. Cancer Genome Atlas Research N (2008) Comprehensive genomic characterization defines human glioblastoma genes and core pathways. *Nature* 455(7216):1061-1068.

309. Parsons DW*, et al.* (2008) An integrated genomic analysis of human glioblastoma multiforme. *Science* 321(5897):1807-1812.

310. Laycock-van Spyk S, Thomas N, Cooper DN, & Upadhyaya M (2011) Neurofibromatosis type 1-associated tumours: their somatic mutational spectrum and pathogenesis. *Human genomics* 5(6):623-690.

311. Masoumi-Moghaddam S, Amini A, & Morris DL (2014) The developing story of Sprouty and cancer. *Cancer metastasis reviews*.

312. Bermudez O, Pages G, & Gimond C (2010) The dual-specificity MAP kinase phosphatases: critical roles in development and cancer. *American journal of physiology. Cell physiology* 299(2):C189-202.

313. Julien SG, Dube N, Hardy S, & Tremblay ML (2011) Inside the human cancer tyrosine phosphatome. *Nat Rev Cancer* 11(1):35-49.

314. Hoshino R*, et al.* (1999) Constitutive activation of the 41-/43-kDa mitogen-activated protein kinase signaling pathway in human tumors. *Oncogene* 18(3):813-822.

315. Downward J (2003) Targeting RAS signalling pathways in cancer therapy. *Nat Rev Cancer* 3(1):11-22.

316. Meloche S & Pouyssegur J (2007) The ERK1/2 mitogen-activated protein kinase pathway as a master regulator of the G1- to S-phase transition. *Oncogene* 26(22):3227-3239.

317. Graves LM*, et al.* (2000) Regulation of carbamoyl phosphate synthetase by MAP kinase. *Nature* 403(6767):328-332.

318. Grassian AR, Metallo CM, Coloff JL, Stephanopoulos G, & Brugge JS (2011) Erk regulation of pyruvate dehydrogenase flux through PDK4 modulates cell proliferation. *Genes Dev* 25(16):1716-1733.

319. Ying H*, et al.* (2012) Oncogenic Kras maintains pancreatic tumors through regulation of anabolic glucose metabolism. *Cell* 149(3):656-670.

320. Roux PP, Ballif BA, Anjum R, Gygi SP, & Blenis J (2004) Tumor-promoting phorbol esters and activated Ras inactivate the tuberous sclerosis tumor suppressor complex via p90 ribosomal S6 kinase. *Proc Natl Acad Sci U S A* 101(37):13489-13494.

321. Ma L, Chen Z, Erdjument-Bromage H, Tempst P, & Pandolfi PP (2005) Phosphorylation and functional inactivation of TSC2 by Erk implications for tuberous sclerosis and cancer pathogenesis. *Cell* 121(2):179-193.

322. Wullschleger S, Loewith R, & Hall MN (2006) TOR signaling in growth and metabolism. *Cell* 124(3):471-484.

323. Stefanovsky VY*, et al.* (2001) An immediate response of ribosomal transcription to growth factor stimulation in mammals is mediated by ERK phosphorylation of UBF. *Mol Cell* 8(5):1063-1073.

324. Barna M*, et al.* (2008) Suppression of Myc oncogenic activity by ribosomal protein haploinsufficiency. *Nature* 456(7224):971-975.

325. Sears R, Leone G, DeGregori J, & Nevins JR (1999) Ras enhances Myc protein stability. *Mol Cell* 3(2):169-179.

326. Sears R*, et al.* (2000) Multiple Ras-dependent phosphorylation pathways regulate Myc protein stability. *Genes Dev* 14(19):2501-2514.

327. Vial E, Sahai E, & Marshall CJ (2003) ERK-MAPK signaling coordinately regulates activity of Rac1 and RhoA for tumor cell motility. *Cancer Cell* 4(1):67-79.

328. Huang C, Jacobson K, & Schaller MD (2004) MAP kinases and cell migration. *J Cell Sci* 117(Pt 20):4619-4628.

329. Rasola A*, et al.* (2010) Activation of mitochondrial ERK protects cancer cells from death through inhibition of the permeability transition. *Proc Natl Acad Sci U S A* 107(2):726-731.

330. Gille H, Sharrocks AD, & Shaw PE (1992) Phosphorylation of transcription factor p62TCF by MAP kinase stimulates ternary complex formation at c-fos promoter. *Nature* 358(6385):414-417.

331. Morton S, Davis RJ, McLaren A, & Cohen P (2003) A reinvestigation of the multisite phosphorylation of the transcription factor c-Jun. *EMBO J* 22(15):3876-3886.

332. Albanese C*, et al.* (1995) Transforming p21ras mutants and c-Ets-2 activate the cyclin D1 promoter through distinguishable regions. *J Biol Chem* 270(40):23589-23597.

333. Lavoie JN, L'Allemain G, Brunet A, Muller R, & Pouyssegur J (1996) Cyclin D1 expression is regulated positively by the p42/p44MAPK and negatively by the p38/HOGMAPK pathway. *J Biol Chem* 271(34):20608-20616.

334. Topisirovic I, Ruiz-Gutierrez M, & Borden KL (2004) Phosphorylation of the eukaryotic translation initiation factor eIF4E contributes to its transformation and mRNA transport activities. *Cancer Res* 64(23):8639-8642.

335. Bouchard C*, et al.* (1999) Direct induction of cyclin D2 by Myc contributes to cell cycle progression and sequestration of p27. *EMBO J* 18(19):5321-5333.

336. Hermeking H*, et al.* (2000) Identification of CDK4 as a target of c-MYC. *Proc Natl Acad Sci U S A* 97(5):2229-2234.

337. Galaktionov K, Chen X, & Beach D (1996) Cdc25 cell-cycle phosphatase as a target of c-myc. *Nature* 382(6591):511-517.

338. Chambard JC, Lefloch R, Pouyssegur J, & Lenormand P (2007) ERK implication in cell cycle regulation. *Biochim Biophys Acta* 1773(8):1299-1310.

339. Yamamoto T*, et al.* (2006) Continuous ERK activation downregulates antiproliferative genes throughout G1 phase to allow cell-cycle progression. *Curr Biol* 16(12):1171-1182.

340. Mercer K*, et al.* (2005) Expression of endogenous oncogenic V600EB-raf induces proliferation and developmental defects in mice and transformation of primary fibroblasts. *Cancer Res* 65(24):11493-11500.

341. Cowley S, Paterson H, Kemp P, & Marshall CJ (1994) Activation of MAP kinase kinase is necessary and sufficient for PC12 differentiation and for transformation of NIH 3T3 cells. *Cell* 77(6):841-852.

342. Mansour SJ*, et al.* (1994) Transformation of mammalian cells by constitutively active MAP kinase kinase. *Science* 265(5174):966-970.

343. Brunet A, Pages G, & Pouyssegur J (1994) Constitutively active mutants of MAP kinase kinase (MEK1) induce growth factor-relaxation and oncogenicity when expressed in fibroblasts. *Oncogene* 9(11):3379-3387.

344. Robinson MJ, Stippec SA, Goldsmith E, White MA, & Cobb MH (1998) A constitutively active and nuclear form of the MAP kinase ERK2 is sufficient for neurite outgrowth and cell transformation. *Curr Biol* 8(21):1141-1150.

345. Troppmair J*, et al.* (1994) Mitogen-activated protein kinase/extracellular signal-regulated protein kinase activation by oncogenes, serum, and 12-O-tetradecanoylphorbol-13-acetate requires Raf and is necessary for transformation. *J Biol Chem* 269(9):7030-7035.

346. Heinicke T*, et al.* (2000) Retroviral gene transfer of dominant negative raf-1 mutants suppresses ha-ras-induced transformation and delays tumor formation. *Cancer gene therapy* 7(5):697-706.

347. Okazaki K & Sagata N (1995) MAP kinase activation is essential for oncogenic transformation of NIH3T3 cells by Mos. *Oncogene* 10(6):1149-1157.

348. Khosravi-Far R, Solski PA, Clark GJ, Kinch MS, & Der CJ (1995) Activation of Rac1, RhoA, and mitogen-activated protein kinases is required for Ras transformation. *Mol Cell Biol* 15(11):6443-6453.

349. Deschênes-Simard X, Kottakis F, Meloche S, & Ferbeyre G (2014) ERKs in Cancer: Friends or Foes? *Cancer Res* 74(2):412-419.

350. Blasco RB*, et al.* (2011) c-Raf, but not B-Raf, is essential for development of K-Ras oncogene-driven non-small cell lung carcinoma. *Cancer Cell* 19(5):652-663.

351. Zhang Z*, et al.* (2005) Induction of invasive mouse skin carcinomas in transgenic mice with mutations in both H-ras and p53. *Molecular cancer research : MCR* 3(10):563-574.

352. Ahmad I*, et al.* (2011) Ras mutation cooperates with beta-catenin activation to drive bladder tumourigenesis. *Cell death & disease* 2:e124.

353. Li Q*, et al.* (2011) Hematopoiesis and leukemogenesis in mice expressing oncogenic NrasG12D from the endogenous locus. *Blood* 117(6):2022-2032.

354. Parikh C, Subrahmanyam R, & Ren R (2006) Oncogenic NRAS rapidly and efficiently induces CMML- and AML-like diseases in mice. *Blood* 108(7):2349-2357.

355. Knauf JA*, et al.* (2005) Targeted expression of BRAFV600E in thyroid cells of transgenic mice results in papillary thyroid cancers that undergo dedifferentiation. *Cancer Res* 65(10):4238-4245.

356. Shields JM, Pruitt K, McFall A, Shaub A, & Der CJ (2000) Understanding Ras: 'it ain't over 'til it's over'. *Trends in cell biology* 10(4):147-154.

357. Hahn WC*, et al.* (1999) Creation of human tumour cells with defined genetic elements. *Nature* 400(6743):464-468.

358. Elenbaas B*, et al.* (2001) Human breast cancer cells generated by oncogenic transformation of primary mammary epithelial cells. *Genes Dev* 15(1):50-65.

359. Rich JN*, et al.* (2001) A genetically tractable model of human glioma formation. *Cancer Res* 61(9):3556-3560.

360. Roberts PJ & Der CJ (2007) Targeting the Raf-MEK-ERK mitogen-activated protein kinase cascade for the treatment of cancer. *Oncogene* 26(22):3291-3310.

361. Gee JM, Barroso AF, Ellis IO, Robertson JF, & Nicholson RI (2000) Biological and clinical associations of c-jun activation in human breast cancer. *Int J Cancer* 89(2):177-186.

362. Mueller H, *et al.* (2000) Potential prognostic value of mitogen-activated protein kinase activity for disease-free survival of primary breast cancer patients. *Int J Cancer* 89(4):384-388.

363. Svensson S, *et al.* (2005) ERK phosphorylation is linked to VEGFR2 expression and Ets-2 phosphorylation in breast cancer and is associated with tamoxifen treatment resistance and small tumours with good prognosis. *Oncogene* 24(27):4370-4379.

364. Milde-Langosch K, *et al.* (2005) Expression and prognostic relevance of activated extracellular-regulated kinases (ERK1/2) in breast cancer. *Br J Cancer* 92(12):2206-2215.

365. Pelloski CE, *et al.* (2006) Prognostic associations of activated mitogen-activated protein kinase and Akt pathways in glioblastoma. *Clin Cancer Res* 12(13):3935-3941.

366. El-Habr EA, *et al.* (2010) Analysis of PIK3CA and B-RAF gene mutations in human astrocytomas: association with activation of ERK and AKT. *Clin Neuropathol* 29(4):239-245.

367. Antonelli M, *et al.* (2012) Expression of pERK and pAKT in pediatric high grade astrocytomas: correlation with YKL40 and prognostic significance. *Neuropathology* 32(2):133-138.

368. Oka H, *et al.* (1995) Constitutive activation of mitogen-activated protein (MAP) kinases in human renal cell carcinoma. *Cancer Res* 55(18):4182-4187.

369. Lee HJ, *et al.* (2009) Phosphorylation of ERK1/2 and prognosis of clear cell renal cell carcinoma. *Urology* 73(2):394-399.

370. Campbell L, Nuttall R, Griffiths D, & Gumbleton M (2009) Activated extracellular signal-regulated kinase is an independent prognostic factor in clinically confined renal cell carcinoma. *Cancer* 115(15):3457-3467.

371. Schmitz KJ, *et al.* (2008) Activation of the ERK and AKT signalling pathway predicts poor prognosis in hepatocellular carcinoma and ERK activation in cancer tissue is associated with hepatitis C virus infection. *J Hepatol* 48(1):83-90.

372. Ito Y, *et al.* (1998) Activation of mitogen-activated protein kinases/extracellular signal-regulated kinases in human hepatocellular carcinoma. *Hepatology* 27(4):951-958.

373. Schmitz KJ, *et al.* (2007) Activation of extracellular regulated kinases (ERK1/2) but not AKT predicts poor prognosis in colorectal carcinoma and is associated with k-ras mutations. *Virchows Arch* 450(2):151-159.

374. Davies JM, *et al.* (2011) Phospho-ERK and AKT status, but not KRAS mutation status, are associated with outcomes in rectal cancer treated with chemoradiotherapy. *Radiat Oncol* 6:114.

375. Eggstein S, *et al.* (1999) Expression and activity of mitogen activated protein kinases in human colorectal carcinoma. *Gut* 44(6):834-838.

376. Vicent S, *et al.* (2004) ERK1/2 is activated in non-small-cell lung cancer and associated with advanced tumours. *Br J Cancer* 90(5):1047-1052.

377. Ricciardi MR, *et al.* (2005) Quantitative single cell determination of ERK phosphorylation and regulation in relapsed and refractory primary acute myeloid leukemia. *Leukemia* 19(9):1543-1549.

378. Towatari M, *et al.* (1997) Constitutive activation of mitogen-activated protein kinase pathway in acute leukemia cells. *Leukemia* 11(4):479-484.

379. Iida M, *et al.* (1999) Lack of constitutive activation of MAP kinase pathway in human acute myeloid leukemia cells with N-Ras mutation. *Leukemia* 13(4):585-589.

380. Cohen C, *et al.* (2002) Mitogen-actived protein kinase activation is an early event in melanoma progression. *Clin Cancer Res* 8(12):3728-3733.

381. Satyamoorthy K, *et al.* (2003) Constitutive mitogen-activated protein kinase activation in melanoma is mediated by both BRAF mutations and autocrine growth factor stimulation. *Cancer Res* 63(4):756-759.

382. Zhuang L, *et al.* (2005) Activation of the extracellular signal regulated kinase (ERK) pathway in human melanoma. *J Clin Pathol* 58(11):1163-1169.

383. Yip-Schneider MT, Lin A, Barnard D, Sweeney CJ, & Marshall MS (1999) Lack of elevated MAP kinase (Erk) activity in pancreatic carcinomas despite oncogenic K-ras expression. *Int J Oncol* 15(2):271-279.

384. Yip-Schneider MT, Lin A, & Marshall MS (2001) Pancreatic tumor cells with mutant K-ras suppress ERK activity by MEK-dependent induction of MAP kinase phosphatase-2. *Biochem Biophys Res Commun* 280(4):992-997.

385. Pham NA, *et al.* (2008) Immunohistochemical analysis of changes in signaling pathway activation downstream of growth factor receptors in pancreatic duct cell carcinogenesis. *BMC Cancer* 8:43.

386. Yamamoto S, *et al.* (2004) Prognostic significance of activated Akt expression in pancreatic ductal adenocarcinoma. *Clinical cancer research : an official journal of the American Association for Cancer Research* 10(8):2846-2850.

387. Price DT, *et al.* (1999) Activation of extracellular signal-regulated kinase in human prostate cancer. *J Urol* 162(4):1537-1542.

388. Gioeli D, Mandell JW, Petroni GR, Frierson HF, Jr., & Weber MJ (1999) Activation of mitogen-activated protein kinase associated with prostate cancer progression. *Cancer Res* 59(2):279-284.

389. Malik SN, *et al.* (2002) Immunohistochemical demonstration of phospho-Akt in high Gleason grade prostate cancer. *Clin Cancer Res* 8(4):1168-1171.

390. Deschênes-Simard X, *et al.* (2013) Tumor suppressor activity of the ERK/MAPK pathway by promoting selective protein degradation. *Genes Dev* 27(8):900-915.

391. Wang XS, *et al.* (2011) Characterization of KRAS rearrangements in metastatic prostate cancer. *Cancer Discov* 1(1):35-43.

392. Chen X & Ruiz-Echevarria MJ (2013) TMEFF2 modulates the AKT and ERK signaling pathways. *Int J Biochem Mol Biol* 4(2):83-94.

393. Magi-Galluzzi C, *et al.* (1997) Mitogen-activated protein kinase phosphatase 1 is overexpressed in prostate cancers and is inversely related to apoptosis. *Laboratory investigation; a journal of technical methods and pathology* 76(1):37-51.

394. Denkert C, *et al.* (2002) Expression of mitogen-activated protein kinase phosphatase-1 (MKP-1) in primary human ovarian carcinoma. *International journal of cancer. Journal international du cancer* 102(5):507-513.

395. Levy-Nissenbaum O, *et al.* (2003) Dual-specificity phosphatase Pyst2-L is constitutively highly expressed in myeloid leukemia and other malignant cells. *Oncogene* 22(48):7649-7660.

396. Vicent S, *et al.* (2004) Mitogen-activated protein kinase phosphatase-1 is overexpressed in non-small cell lung cancer and is an independent predictor of outcome in patients. *Clinical cancer research : an official journal of the American Association for Cancer Research* 10(11):3639-3649.

397. Cui Y, *et al.* (2006) Elevated expression of mitogen-activated protein kinase phosphatase 3 in breast tumors: a mechanism of tamoxifen resistance. *Cancer Res* 66(11):5950-5959.

398. Small GW, Shi YY, Higgins LS, & Orlowski RZ (2007) Mitogen-activated protein kinase phosphatase-1 is a mediator of breast cancer chemoresistance. *Cancer Res* 67(9):4459-4466.

399. Messina S, *et al.* (2011) Dual-specificity phosphatase DUSP6 has tumor-promoting properties in human glioblastomas. *Oncogene* 30(35):3813-3820.

400. Degl'Innocenti D, *et al.* (2013) DUSP6/MKP3 is overexpressed in papillary and poorly differentiated thyroid carcinoma and contributes to neoplastic properties of thyroid cancer cells. *Endocrine-related cancer* 20(1):23-37.

401. De Vriendt V, *et al.* (2013) DUSP 4 expression identifies a subset of colorectal cancer tumors that differ in MAPK activation, regardless of the genotype. *Biomarkers : biochemical indicators of exposure, response, and susceptibility to chemicals* 18(6):516-524.

402. Groschl B, *et al.* (2013) Expression of the MAP kinase phosphatase DUSP4 is associated with microsatellite instability in colorectal cancer (CRC) and causes increased cell proliferation. *International journal of cancer. Journal international du cancer* 132(7):1537-1546.

403. Liao Q, *et al.* (2003) Down-regulation of the dual-specificity phosphatase MKP-1 suppresses tumorigenicity of pancreatic cancer cells. *Gastroenterology* 124(7):1830-1845.

404. Guerra C, *et al.* (2003) Tumor induction by an endogenous K-ras oncogene is highly dependent on cellular context. *Cancer Cell* 4(2):111-120.

405. Tuveson DA, *et al.* (2004) Endogenous oncogenic K-ras(G12D) stimulates proliferation and widespread neoplastic and developmental defects. *Cancer Cell* 5(4):375-387.

406. Maldonado JL, Timmerman L, Fridlyand J, & Bastian BC (2004) Mechanisms of cell-cycle arrest in Spitz nevi with constitutive activation of the MAP-kinase pathway. *Am J Pathol* 164(5):1783-1787.

407. Jacob K*, et al.* (2011) Genetic aberrations leading to MAPK pathway activation mediate oncogene-induced senescence in sporadic pilocytic astrocytomas. *Clin Cancer Res* 17(14):4650-4660.

408. Raabe EH*, et al.* (2011) BRAF activation induces transformation and then senescence in human neural stem cells: a pilocytic astrocytoma model. *Clin Cancer Res* 17(11):3590-3599.

409. Serrano M, Lin AW, McCurrach ME, Beach D, & Lowe SW (1997) Oncogenic ras provokes premature cell senescence associated with accumulation of p53 and p16INK4a. *Cell* 88(5):593-602.

410. Lin AW*, et al.* (1998) Premature senescence involving p53 and p16 is activated in response to constitutive MEK/MAPK mitogenic signaling. *Genes Dev* 12(19):3008-3019.

411. Zhu J, Woods D, McMahon M, & Bishop JM (1998) Senescence of human fibroblasts induced by oncogenic Raf. *Genes Dev* 12(19):2997-3007.

412. Boucher MJ, Jean D, Vezina A, & Rivard N (2004) Dual role of MEK/ERK signaling in senescence and transformation of intestinal epithelial cells. *American journal of physiology. Gastrointestinal and liver physiology* 286(5):G736-746.

413. Powell MB*, et al.* (1995) Hyperpigmentation and melanocytic hyperplasia in transgenic mice expressing the human T24 Ha-ras gene regulated by a mouse tyrosinase promoter. *Molecular carcinogenesis* 12(2):82-90.

414. Kerkhoff E*, et al.* (2000) Lung-targeted expression of the c-Raf-1 kinase in transgenic mice exposes a novel oncogenic character of the wild-type protein. *Cell Growth Differ* 11(4):185-190.

415. Lyustikman Y, Momota H, Pao W, & Holland EC (2008) Constitutive activation of Raf-1 induces glioma formation in mice. *Neoplasia* 10(5):501-510.

416. Dankort D*, et al.* (2009) Braf(V600E) cooperates with Pten loss to induce metastatic melanoma. *Nat Genet* 41(5):544-552.

417. Dhomen N*, et al.* (2009) Oncogenic Braf induces melanocyte senescence and melanoma in mice. *Cancer Cell* 15(4):294-303.

418. Burdon T, Stracey C, Chambers I, Nichols J, & Smith A (1999) Suppression of SHP-2 and ERK signalling promotes self-renewal of mouse embryonic stem cells. *Developmental biology* 210(1):30-43.

419. Ying QL*, et al.* (2008) The ground state of embryonic stem cell self-renewal. *Nature* 453(7194):519-523.

420. Buehr M*, et al.* (2008) Capture of authentic embryonic stem cells from rat blastocysts. *Cell* 135(7):1287-1298.

421. Li P, *et al.* (2008) Germline competent embryonic stem cells derived from rat blastocysts. *Cell* 135(7):1299-1310.

422. Gafni O, *et al.* (2013) Derivation of novel human ground state naive pluripotent stem cells. *Nature* 504(7479):282-286.

423. Ware CB, *et al.* (2014) Derivation of naive human embryonic stem cells. *Proc Natl Acad Sci U S A* 111(12):4484-4489.

424. Marshall CJ (1995) Specificity of receptor tyrosine kinase signaling: transient versus sustained extracellular signal-regulated kinase activation. *Cell* 80(2):179-185.

425. Kunath T, *et al.* (2007) FGF stimulation of the Erk1/2 signalling cascade triggers transition of pluripotent embryonic stem cells from self-renewal to lineage commitment. *Development* 134(16):2895-2902.

426. Chazaud C, Yamanaka Y, Pawson T, & Rossant J (2006) Early lineage segregation between epiblast and primitive endoderm in mouse blastocysts through the Grb2-MAPK pathway. *Developmental cell* 10(5):615-624.

427. Nichols J & Smith A (2009) Naive and primed pluripotent states. *Cell stem cell* 4(6):487-492.

428. Stavridis MP, Lunn JS, Collins BJ, & Storey KG (2007) A discrete period of FGF-induced Erk1/2 signalling is required for vertebrate neural specification. *Development* 134(16):2889-2894.

429. Lu CW, *et al.* (2008) Ras-MAPK signaling promotes trophectoderm formation from embryonic stem cells and mouse embryos. *Nat Genet* 40(7):921-926.

430. Nichols J, Silva J, Roode M, & Smith A (2009) Suppression of Erk signalling promotes ground state pluripotency in the mouse embryo. *Development* 136(19):3215-3222.

431. Takahashi K, *et al.* (2007) Induction of pluripotent stem cells from adult human fibroblasts by defined factors. *Cell* 131(5):861-872.

432. Takahashi K & Yamanaka S (2006) Induction of pluripotent stem cells from mouse embryonic and adult fibroblast cultures by defined factors. *Cell* 126(4):663-676.

433. Yu J, *et al.* (2007) Induced pluripotent stem cell lines derived from human somatic cells. *Science* 318(5858):1917-1920.

434. Ischenko I, Zhi J, Moll UM, Nemajerova A, & Petrenko O (2013) Direct reprogramming by oncogenic Ras and Myc. *Proc Natl Acad Sci U S A* 110(10):3937-3942.

435. Lin T, *et al.* (2009) A chemical platform for improved induction of human iPSCs. *Nature methods* 6(11):805-808.

436. Rais Y, *et al.* (2013) Deterministic direct reprogramming of somatic cells to pluripotency. *Nature* 502(7469):65-70.

437. Silva J, *et al.* (2008) Promotion of reprogramming to ground state pluripotency by signal inhibition. *PLoS biology* 6(10):e253.

438. Li W, *et al.* (2009) Generation of rat and human induced pluripotent stem cells by combining genetic reprogramming and chemical inhibitors. *Cell stem cell* 4(1):16-19.

439. Zhu S, *et al.* (2010) Reprogramming of human primary somatic cells by OCT4 and chemical compounds. *Cell stem cell* 7(6):651-655.

440. Hou P, *et al.* (2013) Pluripotent stem cells induced from mouse somatic cells by small-molecule compounds. *Science* 341(6146):651-654.

441. Pernicova I & Korbonits M (2014) Metformin--mode of action and clinical implications for diabetes and cancer. *Nature reviews. Endocrinology* 10(3):143-156.

442. Giovannucci E, *et al.* (2010) Diabetes and cancer: a consensus report. *Diabetes care* 33(7):1674-1685.

443. Pollak MN (2012) Investigating metformin for cancer prevention and treatment: the end of the beginning. *Cancer discovery* 2(9):778-790.

444. Gronich N & Rennert G (2013) Beyond aspirin-cancer prevention with statins, metformin and bisphosphonates. *Nature reviews. Clinical oncology* 10(11):625-642.

445. Algire C, *et al.* (2012) Metformin reduces endogenous reactive oxygen species and associated DNA damage. *Cancer Prev Res (Phila)* 5(4):536-543.

446. Hirsch HA, Iliopoulos D, Tsichlis PN, & Struhl K (2009) Metformin selectively targets cancer stem cells, and acts together with chemotherapy to block tumor growth and prolong remission. *Cancer Res* 69(19):7507-7511.

447. Hirsch HA, Iliopoulos D, & Struhl K (2013) Metformin inhibits the inflammatory response associated with cellular transformation and cancer stem cell growth. *Proc Natl Acad Sci U S A* 110(3):972-977.

448. Deng XS, *et al.* (2012) Metformin targets Stat3 to inhibit cell growth and induce apoptosis in triple-negative breast cancers. *Cell Cycle* 11(2):367-376.

449. Akinyeke T, *et al.* (2013) Metformin targets c-MYC oncogene to prevent prostate cancer. *Carcinogenesis* 34(12):2823-2832.

450. Blandino G, *et al.* (2012) Metformin elicits anticancer effects through the sequential modulation of DICER and c-MYC. *Nature communications* 3:865.

451. Satyanarayana A, *et al.* (2004) Mitogen stimulation cooperates with telomere shortening to activate DNA damage responses and senescence signaling. *Mol Cell Biol* 24(12):5459-5474.

452. Bostwick DG, *et al.* (2004) Human prostate cancer risk factors. *Cancer* 101(10 Suppl):2371-2490.

453. Orsted DD & Bojesen SE (2013) The link between benign prostatic hyperplasia and prostate cancer. *Nature reviews. Urology* 10(1):49-54.

454. Evan GI, *et al.* (1992) Induction of apoptosis in fibroblasts by c-myc protein. *Cell* 69(1):119-128.

455. Serrano M, Lin AW, McCurrach ME, Beach D, & Lowe SW (1997) Oncogenic ras provokes premature cell senescence associated with accumulation of p53 and p16INK4a. *Cell* 88(5):593-602.

456. Murphy DJ*, et al.* (2008) Distinct thresholds govern Myc's biological output in vivo. *Cancer Cell* 14(6):447-457.

457. Chen Z*, et al.* (2005) Crucial role of p53-dependent cellular senescence in suppression of Pten-deficient tumorigenesis. *Nature* 436(7051):725-730.

458. DeNicola GM*, et al.* (2011) Oncogene-induced Nrf2 transcription promotes ROS detoxification and tumorigenesis. *Nature* 475(7354):106-109.

459. Leist M & Jaattela M (2001) Four deaths and a funeral: from caspases to alternative mechanisms. *Nat Rev Mol Cell Biol* 2(8):589-598.

460. Efeyan A*, et al.* (2009) Limited role of murine ATM in oncogene-induced senescence and p53-dependent tumor suppression. *PloS one* 4(5):e5475.

461. Ferbeyre G*, et al.* (2002) Oncogenic ras and p53 cooperate to induce cellular senescence. *Mol Cell Biol* 22(10):3497-3508.

462. Narita M*, et al.* (2003) Rb-mediated heterochromatin formation and silencing of E2F target genes during cellular senescence. *Cell* 113(6):703-716.

463. Pratilas CA*, et al.* (2009) (V600E)BRAF is associated with disabled feedback inhibition of RAF-MEK signaling and elevated transcriptional output of the pathway. *Proc Natl Acad Sci U S A* 106(11):4519-4524.

464. Lin AW*, et al.* (1998) Premature senescence involving p53 and p16 is activated in response to constitutive MEK/MAPK mitogenic signaling. *Genes Dev.* 12(19):2997-3007.

465. Hahn WC*, et al.* (2002) Enumeration of the simian virus 40 early region elements necessary for human cell transformation. *Mol Cell Biol* 22(7):2111-2123.

466. He J, Kallin EM, Tsukada Y, & Zhang Y (2008) The H3K36 demethylase Jhdm1b/Kdm2b regulates cell proliferation and senescence through p15(Ink4b). *Nat Struct Mol Biol* 15(11):1169-1175.

467. Gabai VL, Yaglom JA, Waldman T, & Sherman MY (2009) Heat shock protein Hsp72 controls oncogene-induced senescence pathways in cancer cells. *Mol Cell Biol* 29(2):559-569.

468. Ma L*, et al.* (2008) CSIG inhibits PTEN translation in replicative senescence. *Mol Cell Biol* 28(20):6290-6301.

469. Martin N*, et al.* (2012) Physical and functional interaction between PML and TBX2 in the establishment of cellular senescence. *EMBO J* 31(1):95-109.

470. Yeh E*, et al.* (2004) A signalling pathway controlling c-Myc degradation that impacts oncogenic transformation of human cells. *Nat Cell Biol* 6(4):308-318.

471. Choi J, *et al.* (2000) Expression of senescence-associated beta-galactosidase in enlarged prostates from men with benign prostatic hyperplasia [In Process Citation]. *Urology* 56(1):160-166.

472. Bric A, *et al.* (2009) Functional identification of tumor-suppressor genes through an in vivo RNA interference screen in a mouse lymphoma model. *Cancer Cell* 16(4):324-335.

473. Olsen JV, *et al.* (2010) Quantitative phosphoproteomics reveals widespread full phosphorylation site occupancy during mitosis. *Sci Signal* 3(104):ra3.

474. Guney I, Wu S, & Sedivy JM (2006) Reduced c-Myc signaling triggers telomere-independent senescence by regulating Bmi-1 and p16(INK4a). *Proc Natl Acad Sci U S A* 103(10):3645-3650.

475. Wu CH, *et al.* (2007) Cellular senescence is an important mechanism of tumor regression upon c-Myc inactivation. *Proc Natl Acad Sci U S A* 104(32):13028-13033.

476. Gough DJ, *et al.* (2009) Mitochondrial STAT3 supports Ras-dependent oncogenic transformation. *Science* 324(5935):1713-1716.

477. Land H, Parada LF, & Weinberg RA (1983) Tumorigenic conversion of primary embryo fibroblasts requires at least two cooperating oncogenes. *Nature* 304(5927):596-602.

478. Callejas-Valera JL, *et al.* (2008) E1a gene expression blocks the ERK1/2 signaling pathway by promoting nuclear localization and MKP up-regulation: implication in v-H-Ras-induced senescence. *J Biol Chem* 283(19):13450-13458.

479. Sahin E & Depinho RA (2010) Linking functional decline of telomeres, mitochondria and stem cells during ageing. *Nature* 464(7288):520-528.

480. Tomas-Loba A, *et al.* (2008) Telomerase reverse transcriptase delays aging in cancer-resistant mice. *Cell* 135(4):609-622.

481. Jaskelioff M, *et al.* (2011) Telomerase reactivation reverses tissue degeneration in aged telomerase-deficient mice. *Nature* 469(7328):102-106.

482. Chadha KS, *et al.* (2006) Activated Akt and Erk expression and survival after surgery in pancreatic carcinoma. *Annals of surgical oncology* 13(7):933-939.

483. Mawrin C, *et al.* (2005) Different activation of mitogen-activated protein kinase and Akt signaling is associated with aggressive phenotype of human meningiomas. *Clin Cancer Res* 11(11):4074-4082.

484. Mawrin C, *et al.* (2003) Prognostic relevance of MAPK expression in glioblastoma multiforme. *Int J Oncol* 23(3):641-648.

485. Sebolt-Leopold JS (2008) Advances in the development of cancer therapeutics directed against the RAS-mitogen-activated protein kinase pathway. *Clin Cancer Res* 14(12):3651-3656.

486. Bostwick DG, *et al.* (1992) The association of benign prostatic hyperplasia and cancer of the prostate. *Cancer* 70(1 Suppl):291-301.

487. Bostwick DG (1996) Prospective origins of prostate carcinoma. Prostatic intraepithelial neoplasia and atypical adenomatous hyperplasia. *Cancer* 78(2):330-336.

488. Hayashi S, Lewis P, Pevny L, & McMahon AP (2002) Efficient gene modulation in mouse epiblast using a Sox2Cre transgenic mouse strain. *Mech Dev* 119 Suppl 1:S97-S101.

489. Diallo JS*, et al.* (2007) NOXA and PUMA expression add to clinical markers in predicting biochemical recurrence of prostate cancer patients in a survival tree model. *Clin Cancer Res* 13(23):7044-7052.

490. Schwartz D & Gygi SP (2005) An iterative statistical approach to the identification of protein phosphorylation motifs from large-scale data sets. *Nat Biotechnol* 23(11):1391-1398.

491. Deng Q, Liao R, Wu BL, & Sun P (2004) High intensity ras signaling induces premature senescence by activating p38 pathway in primary human fibroblasts. *J Biol Chem* 279(2):1050-1059.

492. Voghel G*, et al.* (2010) Endogenous oxidative stress prevents telomerase-dependent immortalization of human endothelial cells. *Mechanisms of ageing and development* 131(5):354-363.

493. Medina I*, et al.* (2010) Babelomics: an integrative platform for the analysis of transcriptomics, proteomics and genomic data with advanced functional profiling. *Nucleic acids research* 38(Web Server issue):W210-213.

494. Engelbrecht Y*, et al.* (2003) Glucocorticoids induce rapid up-regulation of mitogen-activated protein kinase phosphatase-1 and dephosphorylation of extracellular signal-regulated kinase and impair proliferation in human and mouse osteoblast cell lines. *Endocrinology* 144(2):412-422.

495. Beausejour CM*, et al.* (2003) Reversal of human cellular senescence: roles of the p53 and p16 pathways. *EMBO J* 22(16):4212-4222.

496. Burns DM & Richter JD (2008) CPEB regulation of human cellular senescence, energy metabolism, and p53 mRNA translation. *Genes Dev* 22(24):3449-3460.

497. Manfredi JJ (2010) The Mdm2-p53 relationship evolves: Mdm2 swings both ways as an oncogene and a tumor suppressor. *Genes Dev* 24(15):1580-1589.

498. Petroulakis E*, et al.* (2009) p53-dependent translational control of senescence and transformation via 4E-BPs. *Cancer Cell* 16(5):439-446.

499. Scaglioni PP*, et al.* (2012) Translation-dependent mechanisms lead to PML upregulation and mediate oncogenic K-RAS-induced cellular senescence. *EMBO molecular medicine* 4(7):594-602.

500. Salomoni P, Dvorkina M, & Michod D (2012) Role of the promyelocytic leukaemia protein in cell death regulation. *Cell death & disease* 3:e247.

501. Louria-Hayon I*, et al.* (2009) E6AP promotes the degradation of the PML tumor suppressor. *Cell death and differentiation* 16(8):1156-1166.

502. Mizushima N & Komatsu M (2011) Autophagy: renovation of cells and tissues. *Cell* 147(4):728-741.

503. Guo JY*, et al.* (2011) Activated Ras requires autophagy to maintain oxidative metabolism and tumorigenesis. *Genes Dev* 25(5):460-470.

504. Yang S*, et al.* (2011) Pancreatic cancers require autophagy for tumor growth. *Genes Dev* 25(7):717-729.

505. Maclean KH, Dorsey FC, Cleveland JL, & Kastan MB (2008) Targeting lysosomal degradation induces p53-dependent cell death and prevents cancer in mouse models of lymphomagenesis. *The Journal of clinical investigation* 118(1):79-88.

506. Wei H*, et al.* (2011) Suppression of autophagy by FIP200 deletion inhibits mammary tumorigenesis. *Genes Dev* 25(14):1510-1527.

507. Mathew R, Karantza-Wadsworth V, & White E (2007) Role of autophagy in cancer. *Nat Rev Cancer* 7(12):961-967.

508. Liang XH*, et al.* (1999) Induction of autophagy and inhibition of tumorigenesis by beclin 1. *Nature* 402(6762):672-676.

509. Takamura A*, et al.* (2011) Autophagy-deficient mice develop multiple liver tumors. *Genes Dev* 25(8):795-800.

510. Inami Y*, et al.* (2011) Persistent activation of Nrf2 through p62 in hepatocellular carcinoma cells. *J Cell Biol* 193(2):275-284.

511. Marino G*, et al.* (2007) Tissue-specific autophagy alterations and increased tumorigenesis in mice deficient in Atg4C/autophagin-3. *J Biol Chem* 282(25):18573-18583.

512. Takahashi Y*, et al.* (2007) Bif-1 interacts with Beclin 1 through UVRAG and regulates autophagy and tumorigenesis. *Nat Cell Biol* 9(10):1142-1151.

513. Liang C*, et al.* (2006) Autophagic and tumour suppressor activity of a novel Beclin1-binding protein UVRAG. *Nat Cell Biol* 8(7):688-699.

514. Kim MS*, et al.* (2008) Frameshift mutation of UVRAG, an autophagy-related gene, in gastric carcinomas with microsatellite instability. *Human pathology* 39(7):1059-1063.

515. Elgendy M, Sheridan C, Brumatti G, & Martin SJ (2011) Oncogenic Ras-induced expression of Noxa and Beclin-1 promotes autophagic cell death and limits clonogenic survival. *Mol Cell* 42(1):23-35.

516. Cuervo AM & Dice JF (2000) Age-related decline in chaperone-mediated autophagy. *J Biol Chem* 275(40):31505-31513.

517. Wang Y*, et al.* (2012) Autophagic activity dictates the cellular response to oncogenic RAS. *Proc Natl Acad Sci U S A* 109(33):13325-13330.

518. Capparelli C*, et al.* (2012) CDK inhibitors (p16/p19/p21) induce senescence and autophagy in cancer-associated fibroblasts, "fueling" tumor growth via paracrine interactions, without an increase in neo-angiogenesis. *Cell Cycle* 11(19):3599-3610.

519. Gamerdinger M*, et al.* (2009) Protein quality control during aging involves recruitment of the macroautophagy pathway by BAG3. *EMBO J* 28(7):889-901.

520. Singh K, Matsuyama S, Drazba JA, & Almasan A (2012) Autophagy-dependent senescence in response to DNA damage and chronic apoptotic stress. *Autophagy* 8(2):236-251.

521. Sasaki M, Miyakoshi M, Sato Y, & Nakanuma Y (2010) Autophagy mediates the process of cellular senescence characterizing bile duct damages in primary biliary cirrhosis. *Laboratory investigation; a journal of technical methods and pathology* 90(6):835-843.

522. Mosieniak G*, et al.* (2012) Curcumin induces permanent growth arrest of human colon cancer cells: link between senescence and autophagy. *Mechanisms of ageing and development* 133(6):444-455.

523. Patschan S*, et al.* (2008) Lipid mediators of autophagy in stress-induced premature senescence of endothelial cells. *American journal of physiology. Heart and circulatory physiology* 294(3):H1119-1129.

524. Leidal AM, Cyr DP, Hill RJ, Lee PW, & McCormick C (2012) Subversion of autophagy by Kaposi's sarcoma-associated herpesvirus impairs oncogene-induced senescence. *Cell host & microbe* 11(2):167-180.

525. Ivanov A*, et al.* (2013) Lysosome-mediated processing of chromatin in senescence. *J Cell Biol* 202(1):129-143.

526. Narita M*, et al.* (2011) Spatial coupling of mTOR and autophagy augments secretory phenotypes. *Science* 332(6032):966-970.

527. Mizushima N (2007) Autophagy: process and function. *Genes Dev* 21(22):2861-2873.

528. Wajapeyee N, Serra RW, Zhu X, Mahalingam M, & Green MR (2008) Oncogenic BRAF induces senescence and apoptosis through pathways mediated by the secreted protein IGFBP7. *Cell* 132(3):363-374.

529. de Jong A, Schuurman KG, Rodenko B, Ovaa H, & Berkers CR (2012) Fluorescence-based proteasome activity profiling. *Methods in molecular biology* 803:183-204.

530. von Ballmoos C, Wiedenmann A, & Dimroth P (2009) Essentials for ATP synthesis by F1F0 ATP synthases. *Annual review of biochemistry* 78:649-672.

531. Wegrzyn J*, et al.* (2009) Function of mitochondrial Stat3 in cellular respiration. *Science* 323(5915):793-797.

532. Tammineni P*, et al.* (2013) The import of the transcription factor STAT3 into mitochondria depends on GRIM-19, a component of the electron transport chain. *J Biol Chem* 288(7):4723-4732.

533. Faou P & Hoogenraad NJ (2012) Tom34: a cytosolic cochaperone of the Hsp90/Hsp70 protein complex involved in mitochondrial protein import. *Biochim Biophys Acta* 1823(2):348-357.

534. Dai C, Dai S, & Cao J (2012) Proteotoxic stress of cancer: implication of the heat-shock response in oncogenesis. *Journal of cellular physiology* 227(8):2982-2987.

535. Kalmar B & Greensmith L (2009) Induction of heat shock proteins for protection against oxidative stress. *Advanced drug delivery reviews* 61(4):310-318.

536. O'Callaghan-Sunol C, Gabai VL, & Sherman MY (2007) Hsp27 modulates p53 signaling and suppresses cellular senescence. *Cancer Res* 67(24):11779-11788.

537. Merolla F*, et al.* (2007) Involvement of H4(D10S170) protein in ATM-dependent response to DNA damage. *Oncogene* 26(42):6167-6175.

538. Zhao J, Tang J, Men W, & Ren K (2012) FBXW7-mediated degradation of CCDC6 is impaired by ATM during DNA damage response in lung cancer cells. *FEBS Lett* 586(24):4257-4263.

539. Cui H, Kong Y, & Zhang H (2012) Oxidative stress, mitochondrial dysfunction, and aging. *Journal of signal transduction* 2012:646354.

540. Wang JC (2002) Cellular roles of DNA topoisomerases: a molecular perspective. *Nat Rev Mol Cell Biol* 3(6):430-440.

541. Crabbe L, Cesare AJ, Kasuboski JM, Fitzpatrick JA, & Karlseder J (2012) Human telomeres are tethered to the nuclear envelope during postmitotic nuclear assembly. *Cell reports* 2(6):1521-1529.

542. de Lange T (2005) Shelterin: the protein complex that shapes and safeguards human telomeres. *Genes Dev* 19(18):2100-2110.

543. Li B, Oestreich S, & de Lange T (2000) Identification of human Rap1: implications for telomere evolution. *Cell* 101(5):471-483.

544. Sarthy J, Bae NS, Scrafford J, & Baumann P (2009) Human RAP1 inhibits non-homologous end joining at telomeres. *EMBO J* 28(21):3390-3399.

545. Sfeir A, Kabir S, van Overbeek M, Celli GB, & de Lange T (2010) Loss of Rap1 induces telomere recombination in the absence of NHEJ or a DNA damage signal. *Science* 327(5973):1657-1661.

546. Martinez P*, et al.* (2010) Mammalian Rap1 controls telomere function and gene expression through binding to telomeric and extratelomeric sites. *Nat Cell Biol* 12(8):768-780.

547. Yang Y*, et al.* (2000) Conserved composition of mammalian box H/ACA and box C/D small nucleolar ribonucleoprotein particles and their interaction with the common factor Nopp140. *Mol Biol Cell* 11(2):567-577.

548. Tsai YT*, et al.* (2008) Chromatin tethering effects of hNopp140 are involved in the spatial organization of nucleolus and the rRNA gene transcription. *Journal of biomedical science* 15(4):471-486.

549. Lechertier T, Grob A, Hernandez-Verdun D, & Roussel P (2009) Fibrillarin and Nop56 interact before being co-assembled in box C/D snoRNPs. *Exp Cell Res* 315(6):928-942.

550. Srivastava L, Lapik YR, Wang M, & Pestov DG (2010) Mammalian DEAD box protein Ddx51 acts in 3' end maturation of 28S rRNA by promoting the release of U8 snoRNA. *Mol Cell Biol* 30(12):2947-2956.

551. Utama B, Kennedy D, Ru K, & Mattick JS (2002) Isolation and characterization of a new nucleolar protein, Nrap, that is conserved from yeast to humans. *Genes Cells* 7(2):115-132.

552. Wu J*, et al.* (2012) Transcriptional repressor NIR functions in the ribosome RNA processing of both 40S and 60S subunits. *PloS one* 7(2):e31692.

553. Abdelmohsen K & Gorospe M (2012) RNA-binding protein nucleolin in disease. *RNA biology* 9(6):799-808.

554. Artero-Castro A*, et al.* (2009) Rplp1 bypasses replicative senescence and contributes to transformation. *Exp Cell Res* 315(8):1372-1383.

555. Meng L, Yasumoto H, & Tsai RY (2006) Multiple controls regulate nucleostemin partitioning between nucleolus and nucleoplasm. *J Cell Sci* 119(Pt 24):5124-5136.

556. Tafforeau L*, et al.* (2013) The complexity of human ribosome biogenesis revealed by systematic nucleolar screening of Pre-rRNA processing factors. *Mol Cell* 51(4):539-551.

557. Itahana K*, et al.* (2003) Tumor suppressor ARF degrades B23, a nucleolar protein involved in ribosome biogenesis and cell proliferation. *Mol Cell* 12(5):1151-1164.

558. Tago K, Chiocca S, & Sherr CJ (2005) Sumoylation induced by the Arf tumor suppressor: a p53-independent function. *Proc Natl Acad Sci U S A* 102(21):7689-7694.

559. Lapi E*, et al.* (2008) PML, YAP, and p73 are components of a proapoptotic autoregulatory feedback loop. *Mol Cell* 32(6):803-814.

560. Hu C*, et al.* (2008) Analysis of ABCG2 expression and side population identifies intrinsic drug efflux in the HCC cell line MHCC-97L and its modulation by Akt signaling. *Carcinogenesis* 29(12):2289-2297.

561. Labib K, Tercero JA, & Diffley JF (2000) Uninterrupted MCM2-7 function required for DNA replication fork progression. *Science* 288(5471):1643-1647.

562. Shen Z*, et al.* (2010) A WD-repeat protein stabilizes ORC binding to chromatin. *Mol Cell* 40(1):99-111.

563. Eferl R & Wagner EF (2003) AP-1: a double-edged sword in tumorigenesis. *Nat Rev Cancer* 3(11):859-868.

564. Hatakeyama S (2011) TRIM proteins and cancer. *Nat Rev Cancer* 11(11):792-804.

565. Wang C*, et al.* (2005) MDM2 interaction with nuclear corepressor KAP1 contributes to p53 inactivation. *EMBO J* 24(18):3279-3290.

566. Doyle JM, Gao J, Wang J, Yang M, & Potts PR (2010) MAGE-RING protein complexes comprise a family of E3 ubiquitin ligases. *Mol Cell* 39(6):963-974.

567. Jacobs JJ, *et al.* (2000) Senescence bypass screen identifies TBX2, which represses Cdkn2a (p19(ARF)) and is amplified in a subset of human breast cancers. *Nat Genet* 26(3):291-299.

568. Vance KW, Carreira S, Brosch G, & Goding CR (2005) Tbx2 is overexpressed and plays an important role in maintaining proliferation and suppression of senescence in melanomas. *Cancer Res* 65(6):2260-2268.

569. Ludtke TH, *et al.* (2013) Tbx2 controls lung growth by direct repression of the cell cycle inhibitor genes Cdkn1a and Cdkn1b. *PLoS genetics* 9(1):e1003189.

570. Dolfini D & Mantovani R (2013) Targeting the Y/CCAAT box in cancer: YB-1 (YBX1) or NF-Y? *Cell death and differentiation* 20(5):676-685.

571. Lyabin DN, Eliseeva IA, & Ovchinnikov LP (2014) YB-1 protein: functions and regulation. *Wiley interdisciplinary reviews. RNA* 5(1):95-110.

572. Blencowe BJ, Issner R, Nickerson JA, & Sharp PA (1998) A coactivator of pre-mRNA splicing. *Genes Dev* 12(7):996-1009.

573. Blencowe BJ, *et al.* (2000) The SRm160/300 splicing coactivator subunits. *Rna* 6(1):111-120.

574. Eldridge AG, Li Y, Sharp PA, & Blencowe BJ (1999) The SRm160/300 splicing coactivator is required for exon-enhancer function. *Proc Natl Acad Sci U S A* 96(11):6125-6130.

575. Szymczyna BR, *et al.* (2003) Structure and function of the PWI motif: a novel nucleic acid-binding domain that facilitates pre-mRNA processing. *Genes Dev* 17(4):461-475.

576. Zwerschke W, *et al.* (2003) Metabolic analysis of senescent human fibroblasts reveals a role for AMP in cellular senescence. *Biochem J* 376(Pt 2):403-411.

577. Hutter E, *et al.* (2004) Senescence-associated changes in respiration and oxidative phosphorylation in primary human fibroblasts. *Biochem J* 380(Pt 3):919-928.

578. Elschami M, Scherr M, Philippens B, & Gerardy-Schahn R (2013) Reduction of STAT3 expression induces mitochondrial dysfunction and autophagy in cardiac HL-1 cells. *European journal of cell biology* 92(1):21-29.

579. Zhang Q, *et al.* (2013) Mitochondrial localized Stat3 promotes breast cancer growth via phosphorylation of serine 727. *J Biol Chem* 288(43):31280-31288.

580. Rao S, *et al.* (2011) Signaling at the gate: phosphorylation of the mitochondrial protein import machinery. *Cell Cycle* 10(13):2083-2090.

581. Morimoto RI (2008) Proteotoxic stress and inducible chaperone networks in neurodegenerative disease and aging. *Genes Dev* 22(11):1427-1438.

582. Passos JF, Saretzki G, & von Zglinicki T (2007) DNA damage in telomeres and mitochondria during cellular senescence: is there a connection? *Nucleic acids research* 35(22):7505-7513.

583. Berlett BS & Stadtman ER (1997) Protein oxidation in aging, disease, and oxidative stress. *J Biol Chem* 272(33):20313-20316.

584. Davies MJ (2005) The oxidative environment and protein damage. *Biochim Biophys Acta* 1703(2):93-109.

585. Sherman M (2010) Major heat shock protein Hsp72 controls oncogene-induced senescence. *Annals of the New York Academy of Sciences* 1197:152-157.

586. Rohde M*, et al.* (2005) Members of the heat-shock protein 70 family promote cancer cell growth by distinct mechanisms. *Genes Dev* 19(5):570-582.

587. Yaglom JA, Gabai VL, & Sherman MY (2007) High levels of heat shock protein Hsp72 in cancer cells suppress default senescence pathways. *Cancer Res* 67(5):2373-2381.

588. Kim G*, et al.* (2012) The heat shock transcription factor Hsf1 is downregulated in DNA damage-associated senescence, contributing to the maintenance of senescence phenotype. *Aging cell* 11(4):617-627.

589. Bonelli MA*, et al.* (1999) Attenuated expression of 70-kDa heat shock protein in WI-38 human fibroblasts during aging in vitro. *Experimental cell research* 252(1):20-32.

590. Dai C, Whitesell L, Rogers AB, & Lindquist S (2007) Heat shock factor 1 is a powerful multifaceted modifier of carcinogenesis. *Cell* 130(6):1005-1018.

591. De Raedt T*, et al.* (2011) Exploiting cancer cell vulnerabilities to develop a combination therapy for ras-driven tumors. *Cancer Cell* 20(3):400-413.

592. Murphy ME (2013) The HSP70 family and cancer. *Carcinogenesis* 34(6):1181-1188.

593. Whitesell L & Lindquist SL (2005) HSP90 and the chaperoning of cancer. *Nat Rev Cancer* 5(10):761-772.

594. Lamark T & Johansen T (2012) Aggrephagy: selective disposal of protein aggregates by macroautophagy. *International journal of cell biology* 2012:736905.

595. Goldberg AL (2003) Protein degradation and protection against misfolded or damaged proteins. *Nature* 426(6968):895-899.

596. Marques C*, et al.* (2006) The triage of damaged proteins: degradation by the ubiquitin-proteasome pathway or repair by molecular chaperones. *FASEB J* 20(6):741-743.

597. Sisoula C & Gonos ES (2011) CHIP E3 ligase regulates mammalian senescence by modulating the levels of oxidized proteins. *Mechanisms of ageing and development* 132(5):269-272.

598. Aiken CT, Kaake RM, Wang X, & Huang L (2011) Oxidative stress-mediated regulation of proteasome complexes. *Molecular & cellular proteomics : MCP* 10(5):R110 006924.

599. Moiseeva O, Bourdeau V, Roux A, Deschenes-Simard X, & Ferbeyre G (2009) Mitochondrial dysfunction contributes to oncogene-induced senescence. *Mol Cell Biol*.

600. Elchuri S*, et al.* (2005) CuZnSOD deficiency leads to persistent and widespread oxidative damage and hepatocarcinogenesis later in life. *Oncogene* 24(3):367-380.

601. Blander G, de Oliveira RM, Conboy CM, Haigis M, & Guarente L (2003) Superoxide dismutase 1 knock-down induces senescence in human fibroblasts. *J Biol Chem* 278(40):38966-38969.

602. Bermejo R, *et al.* (2007) Top1- and Top2-mediated topological transitions at replication forks ensure fork progression and stability and prevent DNA damage checkpoint activation. *Genes Dev* 21(15):1921-1936.

603. Cuvier O, Stanojcic S, Lemaitre JM, & Mechali M (2008) A topoisomerase II-dependent mechanism for resetting replicons at the S-M-phase transition. *Genes Dev* 22(7):860-865.

604. Fachinetti D, *et al.* (2010) Replication termination at eukaryotic chromosomes is mediated by Top2 and occurs at genomic loci containing pausing elements. *Mol Cell* 39(4):595-605.

605. Baxter J & Diffley JF (2008) Topoisomerase II inactivation prevents the completion of DNA replication in budding yeast. *Mol Cell* 30(6):790-802.

606. Holm C, Stearns T, & Botstein D (1989) DNA topoisomerase II must act at mitosis to prevent nondisjunction and chromosome breakage. *Mol Cell Biol* 9(1):159-168.

607. Bermejo R, *et al.* (2009) Genome-organizing factors Top2 and Hmo1 prevent chromosome fragility at sites of S phase transcription. *Cell* 138(5):870-884.

608. Bae NS & Baumann P (2007) A RAP1/TRF2 complex inhibits nonhomologous end-joining at human telomeric DNA ends. *Mol Cell* 26(3):323-334.

609. Hewitt G, *et al.* (2012) Telomeres are favoured targets of a persistent DNA damage response in ageing and stress-induced senescence. *Nature communications* 3:708.

610. Suram A, *et al.* (2012) Oncogene-induced telomere dysfunction enforces cellular senescence in human cancer precursor lesions. *EMBO J* 31(13):2839-2851.

611. Lee OH, *et al.* (2011) Genome-wide YFP fluorescence complementation screen identifies new regulators for telomere signaling in human cells. *Mol Cell Proteomics* 10(2):M110 001628.

612. Lallemand-Breitenbach V, *et al.* (2001) Role of promyelocytic leukemia (PML) sumolation in nuclear body formation, 11S proteasome recruitment, and As2O3-induced PML or PML/retinoic acid receptor alpha degradation. *J Exp Med* 193(12):1361-1371.

613. Buschbeck M, *et al.* (2007) PML4 induces differentiation by Myc destabilization. *Oncogene* 26(23):3415-3422.

614. Vennemann A & Hofmann TG (2013) SUMO regulates proteasome-dependent degradation of FLASH/Casp8AP2. *Cell Cycle* 12(12):1914-1921.

615. Sharma P, Murillas R, Zhang H, & Kuehn MR (2010) N4BP1 is a newly identified nucleolar protein that undergoes SUMO-regulated polyubiquitylation and proteasomal turnover at promyelocytic leukemia nuclear bodies. *J Cell Sci* 123(Pt 8):1227-1234.

616. Moss T (2004) At the crossroads of growth control; making ribosomal RNA. *Curr Opin Genet Dev* 14(2):210-217.

617. Romanova L*, et al.* (2009) Critical role of nucleostemin in pre-rRNA processing. *J Biol Chem* 284(8):4968-4977.

618. Mialon A*, et al.* (2008) Identification of nucleolar effects in JNK-deficient cells. *FEBS Lett* 582(20):3145-3151.

619. Sherr CJ (2001) The INK4a/ARF network in tumour suppression. *Nat Rev Mol Cell Biol* 2(10):731-737.

620. Wade M, Li YC, & Wahl GM (2013) MDM2, MDMX and p53 in oncogenesis and cancer therapy. *Nat Rev Cancer* 13(2):83-96.

621. Lessard F*, et al.* (2010) The ARF tumor suppressor controls ribosome biogenesis by regulating the RNA polymerase I transcription factor TTF-I. *Mol Cell* 38(4):539-550.

622. Drygin D*, et al.* (2011) Targeting RNA polymerase I with an oral small molecule CX-5461 inhibits ribosomal RNA synthesis and solid tumor growth. *Cancer Res* 71(4):1418-1430.

623. Quin JE*, et al.* (2014) Targeting the nucleolus for cancer intervention. *Biochim Biophys Acta*.

624. Laplante M & Sabatini DM (2012) mTOR signaling in growth control and disease. *Cell* 149(2):274-293.

625. Demidenko ZN*, et al.* (2009) Rapamycin decelerates cellular senescence. *Cell Cycle* 8(12):1888-1895.

626. Leontieva OV*, et al.* (2012) Hypoxia suppresses conversion from proliferative arrest to cellular senescence. *Proc Natl Acad Sci U S A* 109(33):13314-13318.

627. Leontieva OV, Demidenko ZN, & Blagosklonny MV (2013) MEK drives cyclin D1 hyperelevation during geroconversion. *Cell death and differentiation* 20(9):1241-1249.

628. Blagosklonny MV (2013) Hypoxia, MTOR and autophagy: converging on senescence or quiescence. *Autophagy* 9(2):260-262.

629. Blagosklonny MV (2012) Cell cycle arrest is not yet senescence, which is not just cell cycle arrest: terminology for TOR-driven aging. *Aging* 4(3):159-165.

630. Kolesnichenko M, Hong L, Liao R, Vogt PK, & Sun P (2012) Attenuation of TORC1 signaling delays replicative and oncogenic RAS-induced senescence. *Cell Cycle* 11(12):2391-2401.

631. Xie Q*, et al.* (2013) YAP/TEAD-mediated transcription controls cellular senescence. *Cancer Res* 73(12):3615-3624.

632. Zhou D*, et al.* (2009) Mst1 and Mst2 maintain hepatocyte quiescence and suppress hepatocellular carcinoma development through inactivation of the Yap1 oncogene. *Cancer Cell* 16(5):425-438.

633. Zhao B, Li L, Tumaneng K, Wang CY, & Guan KL (2010) A coordinated phosphorylation by Lats and CK1 regulates YAP stability through SCF(beta-TRCP). *Genes Dev* 24(1):72-85.

634. Gulshan K, Thommandru B, & Moye-Rowley WS (2012) Proteolytic degradation of the Yap1 transcription factor is regulated by subcellular localization and the E3 ubiquitin ligase Not4. *J Biol Chem* 287(32):26796-26805.

635. Fernandez-Cid A*, et al.* (2013) An ORC/Cdc6/MCM2-7 complex is formed in a multistep reaction to serve as a platform for MCM double-hexamer assembly. *Mol Cell* 50(4):577-588.

636. Shen Z & Prasanth SG (2012) Orc2 protects ORCA from ubiquitin-mediated degradation. *Cell Cycle* 11(19):3578-3589.

637. Kotake Y, Zeng Y, & Xiong Y (2009) DDB1-CUL4 and MLL1 mediate oncogene-induced p16INK4a activation. *Cancer Res* 69(5):1809-1814.

638. Choi SH, Wright JB, Gerber SA, & Cole MD (2010) Myc protein is stabilized by suppression of a novel E3 ligase complex in cancer cells. *Genes Dev* 24(12):1236-1241.

639. Mallette FA, Gaumont-Leclerc MF, Huot G, & Ferbeyre G (2007) Myc down-regulation as a mechanism to activate the Rb pathway in STAT5A-induced senescence. *J Biol Chem* 282(48):34938-34944.

640. Hydbring P*, et al.* (2010) Phosphorylation by Cdk2 is required for Myc to repress Ras-induced senescence in cotransformation. *Proc Natl Acad Sci U S A* 107(1):58-63.

641. Zhuang D*, et al.* (2008) C-MYC overexpression is required for continuous suppression of oncogene-induced senescence in melanoma cells. *Oncogene* 27(52):6623-6634.

642. Yada M*, et al.* (2004) Phosphorylation-dependent degradation of c-Myc is mediated by the F-box protein Fbw7. *EMBO J* 23(10):2116-2125.

643. Welcker M*, et al.* (2004) The Fbw7 tumor suppressor regulates glycogen synthase kinase 3 phosphorylation-dependent c-Myc protein degradation. *Proc Natl Acad Sci U S A* 101(24):9085-9090.

644. von der Lehr N*, et al.* (2003) The F-box protein Skp2 participates in c-Myc proteosomal degradation and acts as a cofactor for c-Myc-regulated transcription. *Mol Cell* 11(5):1189-1200.

645. Kim SY, Herbst A, Tworkowski KA, Salghetti SE, & Tansey WP (2003) Skp2 regulates Myc protein stability and activity. *Mol Cell* 11(5):1177-1188.

646. Paul I, Ahmed SF, Bhowmik A, Deb S, & Ghosh MK (2013) The ubiquitin ligase CHIP regulates c-Myc stability and transcriptional activity. *Oncogene* 32(10):1284-1295.

647. Inoue S*, et al.* (2013) Mule/Huwe1/Arf-BP1 suppresses Ras-driven tumorigenesis by preventing c-Myc/Miz1-mediated down-regulation of p21 and p15. *Genes Dev* 27(10):1101-1114.

648. Kimura Y, *et al.* (2007) MM-1 facilitates degradation of c-Myc by recruiting proteasome and a novel ubiquitin E3 ligase. *International journal of oncology* 31(4):829-836.

649. Wisdom R, Johnson RS, & Moore C (1999) c-Jun regulates cell cycle progression and apoptosis by distinct mechanisms. *EMBO J* 18(1):188-197.

650. Schreiber M, *et al.* (1999) Control of cell cycle progression by c-Jun is p53 dependent. *Genes Dev* 13(5):607-619.

651. Riley T, Sontag E, Chen P, & Levine A (2008) Transcriptional control of human p53-regulated genes. *Nat Rev Mol Cell Biol* 9(5):402-412.

652. Li X, *et al.* (2007) Role for KAP1 serine 824 phosphorylation and sumoylation/desumoylation switch in regulating KAP1-mediated transcriptional repression. *J Biol Chem* 282(50):36177-36189.

653. Lee YK, Thomas SN, Yang AJ, & Ann DK (2007) Doxorubicin down-regulates Kruppel-associated box domain-associated protein 1 sumoylation that relieves its transcription repression on p21WAF1/CIP1 in breast cancer MCF-7 cells. *J Biol Chem* 282(3):1595-1606.

654. Kepkay R, Attwood KM, Ziv Y, Shiloh Y, & Dellaire G (2011) KAP1 depletion increases PML nuclear body number in concert with ultrastructural changes in chromatin. *Cell Cycle* 10(2):308-322.

655. Lu ZH, Books JT, & Ley TJ (2005) YB-1 is important for late-stage embryonic development, optimal cellular stress responses, and the prevention of premature senescence. *Mol Cell Biol* 25(11):4625-4637.

656. Lasham A, *et al.* (2012) YB-1, the E2F pathway, and regulation of tumor cell growth. *Journal of the National Cancer Institute* 104(2):133-146.

657. Lasham A, *et al.* (2003) The Y-box-binding protein, YB1, is a potential negative regulator of the p53 tumor suppressor. *J Biol Chem* 278(37):35516-35523.

658. Dutertre M, *et al.* (2010) Cotranscriptional exon skipping in the genotoxic stress response. *Nat Struct Mol Biol* 17(11):1358-1366.

659. Chibi M, *et al.* (2008) RBBP6 interacts with multifunctional protein YB-1 through its RING finger domain, leading to ubiquitination and proteosomal degradation of YB-1. *Journal of molecular biology* 384(4):908-916.

660. Wojcik C & DeMartino GN (2003) Intracellular localization of proteasomes. *The international journal of biochemistry & cell biology* 35(5):579-589.

661. Wigley WC, *et al.* (1999) Dynamic association of proteasomal machinery with the centrosome. *J Cell Biol* 145(3):481-490.

662. Fabunmi RP, Wigley WC, Thomas PJ, & DeMartino GN (2000) Activity and regulation of the centrosome-associated proteasome. *J Biol Chem* 275(1):409-413.

663. Fabunmi RP, Wigley WC, Thomas PJ, & DeMartino GN (2001) Interferon gamma regulates accumulation of the proteasome activator PA28 and immunoproteasomes at nuclear PML bodies. *J Cell Sci* 114(Pt 1):29-36.

664. Mattsson K, Pokrovskaja K, Kiss C, Klein G, & Szekely L (2001) Proteins associated with the promyelocytic leukemia gene product (PML)-containing nuclear body move to the nucleolus upon inhibition of proteasome-dependent protein degradation. *Proc Natl Acad Sci U S A* 98(3):1012-1017.

665. von Mikecz A (2006) The nuclear ubiquitin-proteasome system. *J Cell Sci* 119(Pt 10):1977-1984.

666. Bernardi R & Pandolfi PP (2007) Structure, dynamics and functions of promyelocytic leukaemia nuclear bodies. *Nat Rev Mol Cell Biol* 8(12):1006-1016.

667. Chen M*, et al.* (2002) Subcellular recruitment of fibrillarin to nucleoplasmic proteasomes: implications for processing of a nucleolar autoantigen. *Molecular biology of the cell* 13(10):3576-3587.

668. Rockel TD, Stuhlmann D, & von Mikecz A (2005) Proteasomes degrade proteins in focal subdomains of the human cell nucleus. *J Cell Sci* 118(Pt 22):5231-5242.

669. Arabi A, Rustum C, Hallberg E, & Wright AP (2003) Accumulation of c-Myc and proteasomes at the nucleoli of cells containing elevated c-Myc protein levels. *J Cell Sci* 116(Pt 9):1707-1717.

670. Lamond AI & Spector DL (2003) Nuclear speckles: a model for nuclear organelles. *Nat Rev Mol Cell Biol* 4(8):605-612.

671. Baldin V*, et al.* (2008) A novel role for PA28gamma-proteasome in nuclear speckle organization and SR protein trafficking. *Molecular biology of the cell* 19(4):1706-1716.

672. Lafarga M*, et al.* (2002) Clastosome: a subtype of nuclear body enriched in 19S and 20S proteasomes, ubiquitin, and protein substrates of proteasome. *Molecular biology of the cell* 13(8):2771-2782.

673. Smith KP*, et al.* (2004) c-Myc localization within the nucleus: evidence for association with the PML nuclear body. *Journal of cellular biochemistry* 93(6):1282-1296.

674. Herrmann A*, et al.* (2004) STAT3 is enriched in nuclear bodies. *J Cell Sci* 117(Pt 2):339-349.

675. Kawasaki A*, et al.* (2003) Opposing effects of PML and PML/RAR alpha on STAT3 activity. *Blood* 101(9):3668-3673.

676. St-Germain JR, Chen J, & Li Q (2008) Involvement of PML nuclear bodies in CBP degradation through the ubiquitin-proteasome pathway. *Epigenetics : official journal of the DNA Methylation Society* 3(6):342-349.

677. Bandyopadhyay D*, et al.* (2002) Down-regulation of p300/CBP histone acetyltransferase activates a senescence checkpoint in human melanocytes. *Cancer Res* 62(21):6231-6239.

678. Shima Y*, et al.* (2008) PML activates transcription by protecting HIPK2 and p300 from SCFFbx3-mediated degradation. *Mol Cell Biol* 28(23):7126-7138.

679. Bernassola F*, et al.* (2004) Ubiquitin-dependent degradation of p73 is inhibited by PML. *The Journal of experimental medicine* 199(11):1545-1557.

680. Xu ZX, Timanova-Atanasova A, Zhao RX, & Chang KS (2003) PML colocalizes with and stabilizes the DNA damage response protein TopBP1. *Mol Cell Biol* 23(12):4247-4256.

681. Bernardi R*, et al.* (2004) PML regulates p53 stability by sequestering Mdm2 to the nucleolus. *Nat Cell Biol* 6(7):665-672.

682. Miteva M, Keusekotten K, Hofmann K, Praefcke GJ, & Dohmen RJ (2010) Sumoylation as a signal for polyubiquitylation and proteasomal degradation. *Sub-cellular biochemistry* 54:195-214.

683. Praefcke GJ, Hofmann K, & Dohmen RJ (2012) SUMO playing tag with ubiquitin. *Trends Biochem Sci* 37(1):23-31.

684. Malloy MT*, et al.* (2013) Trafficking of the transcription factor Nrf2 to promyelocytic leukemia-nuclear bodies: implications for degradation of NRF2 in the nucleus. *J Biol Chem* 288(20):14569-14583.

685. Nystrom T (2005) Role of oxidative carbonylation in protein quality control and senescence. *EMBO J* 24(7):1311-1317.

686. Davies KJ (2001) Degradation of oxidized proteins by the 20S proteasome. *Biochimie* 83(3-4):301-310.

687. Welcker M & Clurman BE (2008) FBW7 ubiquitin ligase: a tumour suppressor at the crossroads of cell division, growth and differentiation. *Nat Rev Cancer* 8(2):83-93.

688. Vredeveld LC*, et al.* (2012) Abrogation of BRAFV600E-induced senescence by PI3K pathway activation contributes to melanomagenesis. *Genes Dev* 26(10):1055-1069.

689. Kennedy AL*, et al.* (2011) Activation of the PIK3CA/AKT pathway suppresses senescence induced by an activated RAS oncogene to promote tumorigenesis. *Mol Cell* 42(1):36-49.

690. Malleshaiah MK, Shahrezaei V, Swain PS, & Michnick SW (2010) The scaffold protein Ste5 directly controls a switch-like mating decision in yeast. *Nature* 465(7294):101-105.

691. Nakayama KI & Nakayama K (2006) Ubiquitin ligases: cell-cycle control and cancer. *Nat Rev Cancer* 6(5):369-381.

692. Lipkowitz S & Weissman AM (2011) RINGs of good and evil: RING finger ubiquitin ligases at the crossroads of tumour suppression and oncogenesis. *Nat Rev Cancer* 11(9):629-643.

693. Deshaies RJ & Joazeiro CA (2009) RING domain E3 ubiquitin ligases. *Annual review of biochemistry* 78:399-434.

694. Bernassola F, Karin M, Ciechanover A, & Melino G (2008) The HECT family of E3 ubiquitin ligases: multiple players in cancer development. *Cancer Cell* 14(1):10-21.

695. Hatakeyama S & Nakayama KI (2003) U-box proteins as a new family of ubiquitin ligases. *Biochem Biophys Res Commun* 302(4):635-645.

696. Aravind L & Koonin EV (2000) The U box is a modified RING finger - a common domain in ubiquitination. *Curr Biol* 10(4):R132-134.

697. Coscoy L & Ganem D (2003) PHD domains and E3 ubiquitin ligases: viruses make the connection. *Trends in cell biology* 13(1):7-12.

698. Kamura T*, et al.* (2004) VHL-box and SOCS-box domains determine binding specificity for Cul2-Rbx1 and Cul5-Rbx2 modules of ubiquitin ligases. *Genes Dev* 18(24):3055-3065.

699. Petroski MD & Deshaies RJ (2005) Function and regulation of cullin-RING ubiquitin ligases. *Nat Rev Mol Cell Biol* 6(1):9-20.

700. Ishikawa Y*, et al.* (2013) Opposing functions of Fbxw7 in keratinocyte growth, differentiation and skin tumorigenesis mediated through negative regulation of c-Myc and Notch. *Oncogene* 32(15):1921-1932.

701. Roy N*, et al.* (2010) DDB2, an essential mediator of premature senescence. *Mol Cell Biol* 30(11):2681-2692.

702. Prudden J*, et al.* (2007) SUMO-targeted ubiquitin ligases in genome stability. *EMBO J* 26(18):4089-4101.

703. Sun H, Leverson JD, & Hunter T (2007) Conserved function of RNF4 family proteins in eukaryotes: targeting a ubiquitin ligase to SUMOylated proteins. *EMBO J* 26(18):4102-4112.

704. Lin HK*, et al.* (2010) Skp2 targeting suppresses tumorigenesis by Arf-p53-independent cellular senescence. *Nature* 464(7287):374-379.

705. Munoz-Espin D*, et al.* (2013) Programmed cell senescence during mammalian embryonic development. *Cell* 155(5):1104-1118.

706. Storer M*, et al.* (2013) Senescence is a developmental mechanism that contributes to embryonic growth and patterning. *Cell* 155(5):1119-1130.

707. Rock KL & Goldberg AL (1999) Degradation of cell proteins and the generation of MHC class I-presented peptides. *Annual review of immunology* 17:739-779.

708. Vyas JM, Van der Veen AG, & Ploegh HL (2008) The known unknowns of antigen processing and presentation. *Nature reviews. Immunology* 8(8):607-618.

709. Bedford L, Lowe J, Dick LR, Mayer RJ, & Brownell JE (2011) Ubiquitin-like protein conjugation and the ubiquitin-proteasome system as drug targets. *Nat Rev Drug Discov* 10(1):29-46.

710. Duhamel S*, et al.* (2012) Sef downregulation by Ras causes MEK1/2 to become aberrantly nuclear localized leading to polyploidy and neoplastic transformation. *Cancer Res* 72(3):626-635.

711. Mandell JW (2008) Immunohistochemical assessment of protein phosphorylation state: the dream and the reality. *Histochem Cell Biol* 130(3):465-471.

712. Ehrenreiter K, *et al.* (2009) Raf-1 addiction in Ras-induced skin carcinogenesis. *Cancer Cell* 16(2):149-160.

713. Zmajkovicova K, *et al.* (2013) MEK1 is required for PTEN membrane recruitment, AKT regulation, and the maintenance of peripheral tolerance. *Mol Cell* 50(1):43-55.

714. Yeh TC, *et al.* (2007) Biological characterization of ARRY-142886 (AZD6244), a potent, highly selective mitogen-activated protein kinase kinase 1/2 inhibitor. *Clin Cancer Res* 13(5):1576-1583.

715. Adjei AA, *et al.* (2008) Phase I pharmacokinetic and pharmacodynamic study of the oral, small-molecule mitogen-activated protein kinase kinase 1/2 inhibitor AZD6244 (ARRY-142886) in patients with advanced cancers. *J Clin Oncol* 26(13):2139-2146.

716. Bekaii-Saab T, *et al.* (2011) Multi-institutional phase II study of selumetinib in patients with metastatic biliary cancers. *J Clin Oncol* 29(17):2357-2363.

717. Kirkwood JM, *et al.* (2012) Phase II, open-label, randomized trial of the MEK1/2 inhibitor selumetinib as monotherapy versus temozolomide in patients with advanced melanoma. *Clin Cancer Res* 18(2):555-567.

718. O'Neil BH, *et al.* (2011) Phase II study of the mitogen-activated protein kinase 1/2 inhibitor selumetinib in patients with advanced hepatocellular carcinoma. *J Clin Oncol* 29(17):2350-2356.

719. Yeh JJ, *et al.* (2009) KRAS/BRAF mutation status and ERK1/2 activation as biomarkers for MEK1/2 inhibitor therapy in colorectal cancer. *Mol Cancer Ther* 8(4):834-843.

720. Solit DB, *et al.* (2006) BRAF mutation predicts sensitivity to MEK inhibition. *Nature* 439(7074):358-362.

721. Catalanotti F, *et al.* (2013) Phase II trial of MEK inhibitor selumetinib (AZD6244, ARRY-142886) in patients with BRAFV600E/K-mutated melanoma. *Clin Cancer Res* 19(8):2257-2264.

722. Turke AB, *et al.* (2012) MEK inhibition leads to PI3K/AKT activation by relieving a negative feedback on ERBB receptors. *Cancer Res* 72(13):3228-3237.

723. Gopal YN, *et al.* (2010) Basal and treatment-induced activation of AKT mediates resistance to cell death by AZD6244 (ARRY-142886) in Braf-mutant human cutaneous melanoma cells. *Cancer Res* 70(21):8736-8747.

724. Duncan JS, *et al.* (2012) Dynamic reprogramming of the kinome in response to targeted MEK inhibition in triple-negative breast cancer. *Cell* 149(2):307-321.

725. Roberts PJ, *et al.* (2012) Combined PI3K/mTOR and MEK inhibition provides broad antitumor activity in faithful murine cancer models. *Clin Cancer Res* 18(19):5290-5303.

726. Bollag G, *et al.* (2010) Clinical efficacy of a RAF inhibitor needs broad target blockade in BRAF-mutant melanoma. *Nature* 467(7315):596-599.

727. Poulikakos PI & Rosen N (2011) Mutant BRAF melanomas--dependence and resistance. *Cancer Cell* 19(1):11-15.

728. Nazarian R, *et al.* (2010) Melanomas acquire resistance to B-RAF(V600E) inhibition by RTK or N-RAS upregulation. *Nature* 468(7326):973-977.

729. Lito P, *et al.* (2012) Relief of profound feedback inhibition of mitogenic signaling by RAF inhibitors attenuates their activity in BRAFV600E melanomas. *Cancer Cell* 22(5):668-682.

730. Flaherty KT, *et al.* (2012) Combined BRAF and MEK inhibition in melanoma with BRAF V600 mutations. *N Engl J Med* 367(18):1694-1703.

731. Flaherty KT, *et al.* (2012) Improved survival with MEK inhibition in BRAF-mutated melanoma. *N Engl J Med* 367(2):107-114.

732. Shi H, *et al.* (2012) Preexisting MEK1 exon 3 mutations in V600E/KBRAF melanomas do not confer resistance to BRAF inhibitors. *Cancer Discov* 2(5):414-424.

733. Johannessen CM, *et al.* (2010) COT drives resistance to RAF inhibition through MAP kinase pathway reactivation. *Nature* 468(7326):968-972.

734. Hatzivassiliou G, *et al.* (2012) ERK inhibition overcomes acquired resistance to MEK inhibitors. *Molecular cancer therapeutics* 11(5):1143-1154.

735. Atefi M, *et al.* (2011) Reversing melanoma cross-resistance to BRAF and MEK inhibitors by co-targeting the AKT/mTOR pathway. *PLoS One* 6(12):e28973.

736. Su F, *et al.* (2012) RAS mutations in cutaneous squamous-cell carcinomas in patients treated with BRAF inhibitors. *N Engl J Med* 366(3):207-215.

737. Callahan MK, *et al.* (2012) Progression of RAS-mutant leukemia during RAF inhibitor treatment. *N Engl J Med* 367(24):2316-2321.

738. Heidorn SJ, *et al.* (2010) Kinase-dead BRAF and oncogenic RAS cooperate to drive tumor progression through CRAF. *Cell* 140(2):209-221.

739. O'Hagan RC & Heyer J (2011) KRAS Mouse Models: Modeling Cancer Harboring KRAS Mutations. *Genes & cancer* 2(3):335-343.

740. Parikh N, Shuck RL, Nguyen TA, Herron A, & Donehower LA (2012) Mouse tissues that undergo neoplastic progression after K-Ras activation are distinguished by nuclear translocation of phospho-Erk1/2 and robust tumor suppressor responses. *Molecular cancer research : MCR* 10(6):845-855.

741. Bennecke M, *et al.* (2010) Ink4a/Arf and oncogene-induced senescence prevent tumor progression during alternative colorectal tumorigenesis. *Cancer Cell* 18(2):135-146.

742. Jackson EL, *et al.* (2001) Analysis of lung tumor initiation and progression using conditional expression of oncogenic K-ras. *Genes Dev* 15(24):3243-3248.

743. Jackson EL, *et al.* (2005) The differential effects of mutant p53 alleles on advanced murine lung cancer. *Cancer Res* 65(22):10280-10288.

744. Junttila MR, *et al.* (2010) Selective activation of p53-mediated tumour suppression in high-grade tumours. *Nature* 468(7323):567-571.

745. Karreth FA, Frese KK, DeNicola GM, Baccarini M, & Tuveson DA (2011) C-Raf is required for the initiation of lung cancer by K-Ras(G12D). *Cancer discovery* 1(2):128-136.

746. Sansom OJ, *et al.* (2006) Loss of Apc allows phenotypic manifestation of the transforming properties of an endogenous K-ras oncogene in vivo. *Proc Natl Acad Sci U S A* 103(38):14122-14127.

747. Braun BS, *et al.* (2004) Somatic activation of oncogenic Kras in hematopoietic cells initiates a rapidly fatal myeloproliferative disorder. *Proc Natl Acad Sci U S A* 101(2):597-602.

748. Ji B, *et al.* (2009) Ras activity levels control the development of pancreatic diseases. *Gastroenterology* 137(3):1072-1082, 1082 e1071-1076.

749. Collins MA, *et al.* (2012) Oncogenic Kras is required for both the initiation and maintenance of pancreatic cancer in mice. *The Journal of clinical investigation* 122(2):639-653.

750. Collisson EA, *et al.* (2012) A central role for RAF-->MEK-->ERK signaling in the genesis of pancreatic ductal adenocarcinoma. *Cancer discovery* 2(8):685-693.

751. Ardito CM, *et al.* (2012) EGF receptor is required for KRAS-induced pancreatic tumorigenesis. *Cancer Cell* 22(3):304-317.

752. Navas C, *et al.* (2012) EGF receptor signaling is essential for k-ras oncogene-driven pancreatic ductal adenocarcinoma. *Cancer Cell* 22(3):318-330.

753. Eser S, *et al.* (2013) Selective requirement of PI3K/PDK1 signaling for Kras oncogene-driven pancreatic cell plasticity and cancer. *Cancer Cell* 23(3):406-420.

754. Caldwell ME, *et al.* (2012) Cellular features of senescence during the evolution of human and murine ductal pancreatic cancer. *Oncogene* 31(12):1599-1608.

755. Hill R, *et al.* (2010) PTEN loss accelerates KrasG12D-induced pancreatic cancer development. *Cancer Res* 70(18):7114-7124.

756. Iwanaga K, *et al.* (2008) Pten inactivation accelerates oncogenic K-ras-initiated tumorigenesis in a mouse model of lung cancer. *Cancer Res* 68(4):1119-1127.

757. Gupta S, *et al.* (2007) Binding of ras to phosphoinositide 3-kinase p110alpha is required for ras-driven tumorigenesis in mice. *Cell* 129(5):957-968.

758. Engelman JA, *et al.* (2008) Effective use of PI3K and MEK inhibitors to treat mutant Kras G12D and PIK3CA H1047R murine lung cancers. *Nature medicine* 14(12):1351-1356.

759. Schutzman JL & Martin GR (2012) Sprouty genes function in suppression of prostate tumorigenesis. *Proc Natl Acad Sci U S A* 109(49):20023-20028.

760. Salmena L, Carracedo A, & Pandolfi PP (2008) Tenets of PTEN tumor suppression. *Cell* 133(3):403-414.

761. Cichowski K*, et al.* (1999) Mouse models of tumor development in neurofibromatosis type 1. *Science* 286(5447):2172-2176.

762. Lin L, Chen J, Richardson JA, & Parada LF (2009) Mice lacking neurofibromin develop gastric hyperplasia. *American journal of physiology. Gastrointestinal and liver physiology* 297(4):G751-761.

763. King D, Yang G, Thompson MA, & Hiebert SW (2002) Loss of neurofibromatosis-1 and p19(ARF) cooperate to induce a multiple tumor phenotype. *Oncogene* 21(32):4978-4982.

764. Vogel KS*, et al.* (1999) Mouse tumor model for neurofibromatosis type 1. *Science* 286(5447):2176-2179.

765. Reilly KM, Loisel DA, Bronson RT, McLaughlin ME, & Jacks T (2000) Nf1;Trp53 mutant mice develop glioblastoma with evidence of strain-specific effects. *Nat Genet* 26(1):109-113.

766. Johnson L*, et al.* (2001) Somatic activation of the K-ras oncogene causes early onset lung cancer in mice. *Nature* 410(6832):1111-1116.

767. Courtois-Cox S*, et al.* (2006) A negative feedback signaling network underlies oncogene-induced senescence. *Cancer Cell* 10(6):459-472.

768. Shin S, Dimitri CA, Yoon SO, Dowdle W, & Blenis J (2010) ERK2 but not ERK1 induces epithelial-to-mesenchymal transformation via DEF motif-dependent signaling events. *Mol Cell* 38(1):114-127.

769. Bonito NA*, et al.* (2013) Control of gp130 expression by the mitogen-activated protein kinase ERK2. *Oncogene*.

770. Shin J, Yang J, Lee J, & Baek KH (2013) Depletion of ERK2 but not ERK1 abrogates oncogenic Ras-induced senescence. *Cell Signal*.

771. Hermann PC*, et al.* (2007) Distinct populations of cancer stem cells determine tumor growth and metastatic activity in human pancreatic cancer. *Cell stem cell* 1(3):313-323.

772. Simeone DM (2008) Pancreatic cancer stem cells: implications for the treatment of pancreatic cancer. *Clinical cancer research : an official journal of the American Association for Cancer Research* 14(18):5646-5648.

773. Dorado J, Lonardo E, Miranda-Lorenzo I, & Heeschen C (2011) Pancreatic cancer stem cells: new insights and perspectives. *Journal of gastroenterology* 46(8):966-973.

774. Thomson JA*, et al.* (1998) Embryonic stem cell lines derived from human blastocysts. *Science* 282(5391):1145-1147.

775. Greber B*, et al.* (2011) FGF signalling inhibits neural induction in human embryonic stem cells. *EMBO J* 30(24):4874-4884.

776. Li J, *et al.* (2007) MEK/ERK signaling contributes to the maintenance of human embryonic stem cell self-renewal. *Differentiation; research in biological diversity* 75(4):299-307.

777. Greber B, *et al.* (2010) Conserved and divergent roles of FGF signaling in mouse epiblast stem cells and human embryonic stem cells. *Cell stem cell* 6(3):215-226.

778. Brons IG, *et al.* (2007) Derivation of pluripotent epiblast stem cells from mammalian embryos. *Nature* 448(7150):191-195.

779. Rossant J (2008) Stem cells and early lineage development. *Cell* 132(4):527-531.

780. Tesar PJ, *et al.* (2007) New cell lines from mouse epiblast share defining features with human embryonic stem cells. *Nature* 448(7150):196-199.

781. Guo G, *et al.* (2009) Klf4 reverts developmentally programmed restriction of ground state pluripotency. *Development* 136(7):1063-1069.

782. Hanna J, *et al.* (2009) Metastable pluripotent states in NOD-mouse-derived ESCs. *Cell stem cell* 4(6):513-524.

783. Hanna J, *et al.* (2010) Human embryonic stem cells with biological and epigenetic characteristics similar to those of mouse ESCs. *Proc Natl Acad Sci U S A* 107(20):9222-9227.

784. Xu Y, *et al.* (2010) Revealing a core signaling regulatory mechanism for pluripotent stem cell survival and self-renewal by small molecules. *Proc Natl Acad Sci U S A* 107(18):8129-8134.

785. Al-Hajj M, Wicha MS, Benito-Hernandez A, Morrison SJ, & Clarke MF (2003) Prospective identification of tumorigenic breast cancer cells. *Proc Natl Acad Sci U S A* 100(7):3983-3988.

786. Singh SK, *et al.* (2004) Identification of human brain tumour initiating cells. *Nature* 432(7015):396-401.

787. Ben-Porath I, *et al.* (2008) An embryonic stem cell-like gene expression signature in poorly differentiated aggressive human tumors. *Nat Genet* 40(5):499-507.

788. Wong DJ, *et al.* (2008) Module map of stem cell genes guides creation of epithelial cancer stem cells. *Cell stem cell* 2(4):333-344.

789. Li C, *et al.* (2007) Identification of pancreatic cancer stem cells. *Cancer Res* 67(3):1030-1037.

790. Hruban RH, *et al.* (2004) An illustrated consensus on the classification of pancreatic intraepithelial neoplasia and intraductal papillary mucinous neoplasms. *The American journal of surgical pathology* 28(8):977-987.

791. Polyak K & Weinberg RA (2009) Transitions between epithelial and mesenchymal states: acquisition of malignant and stem cell traits. *Nat Rev Cancer* 9(4):265-273.

792. Tsai JH & Yang J (2013) Epithelial-mesenchymal plasticity in carcinoma metastasis. *Genes Dev* 27(20):2192-2206.

793. Malanchi I, *et al.* (2012) Interactions between cancer stem cells and their niche govern metastatic colonization. *Nature* 481(7379):85-89.

794. Todaro M, *et al.* (2014) CD44v6 is a marker of constitutive and reprogrammed cancer stem cells driving colon cancer metastasis. *Cell stem cell* 14(3):342-356.

795. Yang J, *et al.* (2010) Stat3 activation is limiting for reprogramming to ground state pluripotency. *Cell stem cell* 7(3):319-328.

796. Myant KB, *et al.* (2013) ROS production and NF-kappaB activation triggered by RAC1 facilitate WNT-driven intestinal stem cell proliferation and colorectal cancer initiation. *Cell stem cell* 12(6):761-773.

797. Maddox J, *et al.* (2012) Transcription factor Oct1 is a somatic and cancer stem cell determinant. *PLoS genetics* 8(11):e1003048.

798. Fournier M, Lebert-Ghali CE, Krosl G, & Bijl JJ (2012) HOXA4 induces expansion of hematopoietic stem cells in vitro and confers enhancement of pro-B-cells in vivo. *Stem cells and development* 21(1):133-142.

799. Kim J, *et al.* (2013) An iPSC line from human pancreatic ductal adenocarcinoma undergoes early to invasive stages of pancreatic cancer progression. *Cell reports* 3(6):2088-2099.

800. Willert K & Jones KA (2006) Wnt signaling: is the party in the nucleus? *Genes Dev* 20(11):1394-1404.

801. Iliopoulos D, Hirsch HA, & Struhl K (2009) An epigenetic switch involving NF-kappaB, Lin28, Let-7 MicroRNA, and IL6 links inflammation to cell transformation. *Cell* 139(4):693-706.

802. Molina G, *et al.* (2009) Zebrafish chemical screening reveals an inhibitor of Dusp6 that expands cardiac cell lineages. *Nature chemical biology* 5(9):680-687.

803. Scaffidi P & Misteli T (2011) In vitro generation of human cells with cancer stem cell properties. *Nat Cell Biol* 13(9):1051-1061.

804. Banito A, *et al.* (2009) Senescence impairs successful reprogramming to pluripotent stem cells. *Genes Dev* 23(18):2134-2139.

805. Hong H, *et al.* (2009) Suppression of induced pluripotent stem cell generation by the p53-p21 pathway. *Nature* 460(7259):1132-1135.

806. Li H, *et al.* (2009) The Ink4/Arf locus is a barrier for iPS cell reprogramming. *Nature* 460(7259):1136-1139.

807. Kawamura T, *et al.* (2009) Linking the p53 tumour suppressor pathway to somatic cell reprogramming. *Nature* 460(7259):1140-1144.

808. Marion RM, *et al.* (2009) A p53-mediated DNA damage response limits reprogramming to ensure iPS cell genomic integrity. *Nature* 460(7259):1149-1153.

809. Utikal J, *et al.* (2009) Immortalization eliminates a roadblock during cellular reprogramming into iPS cells. *Nature* 460(7259):1145-1148.

810. Zhang J, *et al.* (2009) Identification of an ES cell pluripotent state-specific DUSP6 enhancer. *Biochem Biophys Res Commun* 378(2):319-323.

811. Li Z, *et al.* (2012) BMP4 Signaling Acts via dual-specificity phosphatase 9 to control ERK activity in mouse embryonic stem cells. *Cell stem cell* 10(2):171-182.

812. Chappell J, Sun Y, Singh A, & Dalton S (2013) MYC/MAX control ERK signaling and pluripotency by regulation of dual-specificity phosphatases 2 and 7. *Genes Dev* 27(7):725-733.

813. Jung JE, *et al.* (2012) Sprouty1 regulates neural and endothelial differentiation of mouse embryonic stem cells. *Stem cells and development* 21(4):554-561.

814. Wakioka T, *et al.* (2001) Spred is a Sprouty-related suppressor of Ras signalling. *Nature* 412(6847):647-651.

815. Kim MO, *et al.* (2012) ERK1 and ERK2 regulate embryonic stem cell self-renewal through phosphorylation of Klf4. *Nat Struct Mol Biol* 19(3):283-290.

816. Tan FE & Elowitz MB (2014) Brf1 posttranscriptionally regulates pluripotency and differentiation responses downstream of Erk MAP kinase. *Proc Natl Acad Sci U S A* 111(17):E1740-1748.

817. Hamazaki T, Kehoe SM, Nakano T, & Terada N (2006) The Grb2/Mek pathway represses Nanog in murine embryonic stem cells. *Mol Cell Biol* 26(20):7539-7549.

818. Shi Y, *et al.* (2008) A combined chemical and genetic approach for the generation of induced pluripotent stem cells. *Cell stem cell* 2(6):525-528.

819. Moiseeva O, *et al.* (2013) Metformin inhibits the senescence-associated secretory phenotype by interfering with IKK/NF-kappaB activation. *Aging cell* 12(3):489-498.

820. Iliopoulos D, Hirsch HA, & Struhl K (2011) Metformin decreases the dose of chemotherapy for prolonging tumor remission in mouse xenografts involving multiple cancer cell types. *Cancer Res* 71(9):3196-3201.

821. Yuan P, *et al.* (2013) Phenformin enhances the therapeutic benefit of BRAF(V600E) inhibition in melanoma. *Proc Natl Acad Sci U S A* 110(45):18226-18231.

822. Furukawa T, *et al.* (1996) Long-term culture and immortalization of epithelial cells from normal adult human pancreatic ducts transfected by the E6E7 gene of human papilloma virus 16. *The American journal of pathology* 148(6):1763-1770.

823. Bardeesy N, *et al.* (2006) Both p16(Ink4a) and the p19(Arf)-p53 pathway constrain progression of pancreatic adenocarcinoma in the mouse. *Proc Natl Acad Sci U S A* 103(15):5947-5952.

824. Schreiber FS, *et al.* (2004) Successful growth and characterization of mouse pancreatic ductal cells: functional properties of the Ki-RAS(G12V) oncogene. *Gastroenterology* 127(1):250-260.

825. Blazejczyk M, Miron M, & Nadon R (2007) FlexArray: A statistical data analysis software for gene expression microarrays. *Genome Quebec, Montreal, Canada* http://genomequebec.mcgill.ca/FlexArray.

826. Gotea V & Ovcharenko I (2008) DiRE: identifying distant regulatory elements of co-expressed genes. *Nucleic acids research* 36(Web Server issue):W133-139.

827. Subramanian A*, et al.* (2005) Gene set enrichment analysis: a knowledge-based approach for interpreting genome-wide expression profiles. *Proc Natl Acad Sci U S A* 102(43):15545-15550.

828. Kawai T & Akira S (2007) Signaling to NF-kappaB by Toll-like receptors. *Trends in molecular medicine* 13(11):460-469.

829. Napetschnig J & Wu H (2013) Molecular basis of NF-kappaB signaling. *Annual review of biophysics* 42:443-468.

830. Miller SI, Ernst RK, & Bader MW (2005) LPS, TLR4 and infectious disease diversity. *Nature reviews. Microbiology* 3(1):36-46.

831. Bonafe M, Storci G, & Franceschi C (2012) Inflamm-aging of the stem cell niche: breast cancer as a paradigmatic example: breakdown of the multi-shell cytokine network fuels cancer in aged people. *Bioessays* 34(1):40-49.

832. Cesari M*, et al.* (2003) Inflammatory markers and onset of cardiovascular events: results from the Health ABC study. *Circulation* 108(19):2317-2322.

833. Ferbeyre G & Lowe SW (2002) The price of tumour suppression? *Nature* 415(6867):26-27.

834. Rodier F*, et al.* (2009) Persistent DNA damage signalling triggers senescence-associated inflammatory cytokine secretion. *Nat Cell Biol* 11(8):973-979.

835. Gilbert LA & Hemann MT (2010) DNA damage-mediated induction of a chemoresistant niche. *Cell* 143(3):355-366.

836. Pollak M (2010) Metformin and other biguanides in oncology: advancing the research agenda. *Cancer prevention research* 3(9):1060-1065.

837. Formentini L, Sanchez-Arago M, Sanchez-Cenizo L, & Cuezva JM (2012) The mitochondrial ATPase inhibitory factor 1 triggers a ROS-mediated retrograde prosurvival and proliferative response. *Mol Cell* 45(6):731-742.

838. Pietras K, Sjoblom T, Rubin K, Heldin CH, & Ostman A (2003) PDGF receptors as cancer drug targets. *Cancer Cell* 3(5):439-443.

839. Malumbres M*, et al.* (2000) Cellular response to oncogenic ras involves induction of the Cdk4 and Cdk6 inhibitor p15(INK4b). *Mol Cell Biol* 20(8):2915-2925.

840. Raimondi C & Falasca M (2011) Targeting PDK1 in cancer. *Curr Med Chem* 18(18):2763-2769.

841. Rongvaux A, Andris F, Van Gool F, & Leo O (2003) Reconstructing eukaryotic NAD metabolism. *Bioessays* 25(7):683-690.

842. Fischer SM, Hawk ET, & Lubet RA (2011) Coxibs and other nonsteroidal anti-inflammatory drugs in animal models of cancer chemoprevention. *Cancer Prev Res (Phila)* 4(11):1728-1735.

843. Ericsson J, Jackson SM, Kim JB, Spiegelman BM, & Edwards PA (1997) Identification of glycerol-3-phosphate acyltransferase as an adipocyte determination and differentiation factor 1- and sterol regulatory element-binding protein-responsive gene. *J Biol Chem* 272(11):7298-7305.

844. Sun Y, *et al.* (2012) Treatment-induced damage to the tumor microenvironment promotes prostate cancer therapy resistance through WNT16B. *Nature medicine* 18(9):1359-1368.

845. Hacker H, *et al.* (2006) Specificity in Toll-like receptor signalling through distinct effector functions of TRAF3 and TRAF6. *Nature* 439(7073):204-207.

846. Jing H, *et al.* (2011) Opposing roles of NF-kappaB in anti-cancer treatment outcome unveiled by cross-species investigations. *Genes Dev* 25(20):2137-2146.

847. Adler AS, *et al.* (2007) Motif module map reveals enforcement of aging by continual NF-kappaB activity. *Genes Dev* 21(24):3244-3257.

848. Donato AJ, Black AD, Jablonski KL, Gano LB, & Seals DR (2008) Aging is associated with greater nuclear NF kappa B, reduced I kappa B alpha, and increased expression of proinflammatory cytokines in vascular endothelial cells of healthy humans. *Aging Cell* 7(6):805-812.

849. Hoffmann A, Levchenko A, Scott ML, & Baltimore D (2002) The IkappaB-NF-kappaB signaling module: temporal control and selective gene activation. *Science* 298(5596):1241-1245.

850. Mercurio F, *et al.* (1997) IKK-1 and IKK-2: cytokine-activated IkappaB kinases essential for NF-kappaB activation. *Science* 278(5339):860-866.

851. Wang C, *et al.* (2001) TAK1 is a ubiquitin-dependent kinase of MKK and IKK. *Nature* 412(6844):346-351.

852. Meylan E, *et al.* (2004) RIP1 is an essential mediator of Toll-like receptor 3-induced NF-kappa B activation. *Nat Immunol* 5(5):503-507.

853. Dong W, *et al.* (2006) The IRAK-1-BCL10-MALT1-TRAF6-TAK1 cascade mediates signaling to NF-kappaB from Toll-like receptor 4. *J Biol Chem* 281(36):26029-26040.

854. Graham GG, *et al.* (2011) Clinical pharmacokinetics of metformin. *Clin Pharmacokinet* 50(2):81-98.

855. Memmott RM, *et al.* (2010) Metformin prevents tobacco carcinogen--induced lung tumorigenesis. *Cancer Prev Res (Phila)* 3(9):1066-1076.

856. Bhalla K, *et al.* (2012) Metformin prevents liver tumorigenesis by inhibiting pathways driving hepatic lipogenesis. *Cancer Prev Res (Phila)* 5(4):544-552.

857. Laberge RM, *et al.* (2012) Glucocorticoids suppress selected components of the senescence-associated secretory phenotype. *Aging Cell* 11(4):569-578.

858. Kalariya NM, Shoeb M, Ansari NH, Srivastava SK, & Ramana KV (2012) Antidiabetic drug metformin suppresses endotoxin-induced uveitis in rats. *Invest Ophthalmol Vis Sci* 53(7):3431-3440.

859. Zhao T, *et al.* (2007) The NEMO adaptor bridges the nuclear factor-kappaB and interferon regulatory factor signaling pathways. *Nat Immunol* 8(6):592-600.

860. Tilstra JS, *et al.* (2012) NF-kappaB inhibition delays DNA damage-induced senescence and aging in mice. *J Clin Invest* 122(7):2601-2612.

861. Anisimov VN, *et al.* (2011) If started early in life, metformin treatment increases life span and postpones tumors in female SHR mice. *Aging* 3(2):148-157.

862. Onken B & Driscoll M (2010) Metformin induces a dietary restriction-like state and the oxidative stress response to extend C. elegans Healthspan via AMPK, LKB1, and SKN-1. *PLoS One* 5(1):e8758.

863. Krysiak R & Okopien B (2012) Lymphocyte-suppressing and systemic anti-inflammatory effects of high-dose metformin in simvastatin-treated patients with impaired fasting glucose. *Atherosclerosis*.

864. Sun Y, *et al.* (2012) Treatment-induced damage to the tumor microenvironment promotes prostate cancer therapy resistance through WNT16B. *Nat Med*.

865. Parikh JR, Klinger B, Xia Y, Marto JA, & Bluthgen N (2010) Discovering causal signaling pathways through gene-expression patterns. *Nucleic Acids Res* 38(Web Server issue):W109-117.

866. Essaghir A, *et al.* (2010) Transcription factor regulation can be accurately predicted from the presence of target gene signatures in microarray gene expression data. *Nucleic Acids Res* 38(11):e120.

867. Storey JD & Tibshirani R (2003) Statistical significance for genomewide studies. *Proc Natl Acad Sci U S A* 100(16):9440-9445.

868. Reiner A, Yekutieli D, & Benjamini Y (2003) Identifying differentially expressed genes using false discovery rate controlling procedures. *Bioinformatics* 19(3):368-375.

869. Wingender E, *et al.* (2000) TRANSFAC: an integrated system for gene expression regulation. *Nucleic Acids Res* 28(1):316-319.

870. Jiang C, Xuan Z, Zhao F, & Zhang MQ (2007) TRED: a transcriptional regulatory element database, new entries and other development. *Nucleic Acids Res* 35(Database issue):D137-140.

871. Hayden MS, West AP, & Ghosh S (2006) NF-kappaB and the immune response. *Oncogene* 25(51):6758-6780.

872. Dunn GP, Koebel CM, & Schreiber RD (2006) Interferons, immunity and cancer immunoediting. *Nature reviews. Immunology* 6(11):836-848.

873. Balducci L & Ershler WB (2005) Cancer and ageing: a nexus at several levels. *Nat Rev Cancer* 5(8):655-662.

874. Rowe HM, *et al.* (2013) TRIM28 repression of retrotransposon-based enhancers is necessary to preserve transcriptional dynamics in embryonic stem cells. *Genome research* 23(3):452-461.

875. Camargo FD, *et al.* (2007) YAP1 increases organ size and expands undifferentiated progenitor cells. *Curr Biol* 17(23):2054-2060.

876. Lian I, *et al.* (2010) The role of YAP transcription coactivator in regulating stem cell self-renewal and differentiation. *Genes Dev* 24(11):1106-1118.

877. Seo E, *et al.* (2013) SOX2 regulates YAP1 to maintain stemness and determine cell fate in the osteo-adipo lineage. *Cell reports* 3(6):2075-2087.

878. Ficz G, *et al.* (2013) FGF signaling inhibition in ESCs drives rapid genome-wide demethylation to the epigenetic ground state of pluripotency. *Cell stem cell* 13(3):351-359.

879. Omidvar N, *et al.* (2007) BCL-2 and mutant NRAS interact physically and functionally in a mouse model of progressive myelodysplasia. *Cancer Res* 67(24):11657-11667.

880. Cagnol S & Chambard JC (2010) ERK and cell death: mechanisms of ERK-induced cell death--apoptosis, autophagy and senescence. *The FEBS journal* 277(1):2-21.

881. Goi T, Rusanescu G, Urano T, & Feig LA (1999) Ral-specific guanine nucleotide exchange factor activity opposes other Ras effectors in PC12 cells by inhibiting neurite outgrowth. *Mol Cell Biol* 19(3):1731-1741.

882. Omidvar N, Pearn L, Burnett AK, & Darley RL (2006) Ral is both necessary and sufficient for the inhibition of myeloid differentiation mediated by Ras. *Mol Cell Biol* 26(10):3966-3975.

883. Seguin L, *et al.* (2014) An integrin beta3-KRAS-RalB complex drives tumour stemness and resistance to EGFR inhibition. *Nat Cell Biol* 16(5):457-468.

884. Hart JR, Liao L, Yates JR, 3rd, & Vogt PK (2011) Essential role of Stat3 in PI3K-induced oncogenic transformation. *Proc Natl Acad Sci U S A* 108(32):13247-13252.

885. Vogt PK & Hart JR (2011) PI3K and STAT3: a new alliance. *Cancer discovery* 1(6):481-486.

886. Agarwal A, *et al.* (2005) The AKT/I kappa B kinase pathway promotes angiogenic/metastatic gene expression in colorectal cancer by activating nuclear factor-kappa B and beta-catenin. *Oncogene* 24(6):1021-1031.

887. Dan HC, *et al.* (2008) Akt-dependent regulation of NF-{kappa}B is controlled by mTOR and Raptor in association with IKK. *Genes Dev* 22(11):1490-1500.

888. Rodriguez-Viciana P, *et al.* (1997) Role of phosphoinositide 3-OH kinase in cell transformation and control of the actin cytoskeleton by Ras. *Cell* 89(3):457-467.

889. Osada M, *et al.* (1999) Differential roles of Akt, Rac, and Ral in R-Ras-mediated cellular transformation, adhesion, and survival. *Mol Cell Biol* 19(9):6333-6344.

890. Hamad NM, *et al.* (2002) Distinct requirements for Ras oncogenesis in human versus mouse cells. *Genes Dev* 16(16):2045-2057.

891. Nguyen KT, Wang WJ, Chan JL, & Wang LH (2000) Differential requirements of the MAP kinase and PI3 kinase signaling pathways in Src- versus insulin and IGF-1

receptors-induced growth and transformation of rat intestinal epithelial cells. *Oncogene* 19(47):5385-5397.

892. Rangarajan A, Hong SJ, Gifford A, & Weinberg RA (2004) Species- and cell type-specific requirements for cellular transformation. *Cancer Cell* 6(2):171-183.

893. Lim KH*, et al.* (2005) Activation of RalA is critical for Ras-induced tumorigenesis of human cells. *Cancer Cell* 7(6):533-545.

894. Sarkisian CJ*, et al.* (2007) Dose-dependent oncogene-induced senescence in vivo and its evasion during mammary tumorigenesis. *Nat Cell Biol* 9(5):493-505.

895. Daniluk J*, et al.* (2012) An NF-kappaB pathway-mediated positive feedback loop amplifies Ras activity to pathological levels in mice. *The Journal of clinical investigation* 122(4):1519-1528.

896. Ikenoue T*, et al.* (2003) Functional analysis of mutations within the kinase activation segment of B-Raf in human colorectal tumors. *Cancer Res* 63(23):8132-8137.

897. Li S & Sedivy JM (1993) Raf-1 protein kinase activates the NF-kappa B transcription factor by dissociating the cytoplasmic NF-kappa B-I kappa B complex. *Proc Natl Acad Sci U S A* 90(20):9247-9251.

898. Baumann B*, et al.* (2000) Raf induces NF-kappaB by membrane shuttle kinase MEKK1, a signaling pathway critical for transformation. *Proc Natl Acad Sci U S A* 97(9):4615-4620.

899. Finco TS*, et al.* (1997) Oncogenic Ha-Ras-induced signaling activates NF-kappaB transcriptional activity, which is required for cellular transformation. *J Biol Chem* 272(39):24113-24116.

900. Bansal A, Ramirez RD, & Minna JD (1997) Mutation analysis of the coding sequences of MEK-1 and MEK-2 genes in human lung cancer cell lines. *Oncogene* 14(10):1231-1234.

901. Estep AL, Palmer C, McCormick F, & Rauen KA (2007) Mutation analysis of BRAF, MEK1 and MEK2 in 15 ovarian cancer cell lines: implications for therapy. *PLoS One* 2(12):e1279.

902. Marks JL*, et al.* (2008) Novel MEK1 mutation identified by mutational analysis of epidermal growth factor receptor signaling pathway genes in lung adenocarcinoma. *Cancer Res* 68(14):5524-5528.

903. Murugan AK, Dong J, Xie J, & Xing M (2009) MEK1 mutations, but not ERK2 mutations, occur in melanomas and colon carcinomas, but none in thyroid carcinomas. *Cell Cycle* 8(13):2122-2124.

904. Karin M, Cao Y, Greten FR, & Li ZW (2002) NF-kappaB in cancer: from innocent bystander to major culprit. *Nat Rev Cancer* 2(4):301-310.

905. Courtois G & Gilmore TD (2006) Mutations in the NF-kappaB signaling pathway: implications for human disease. *Oncogene* 25(51):6831-6843.

906. Prasad S, Ravindran J, & Aggarwal BB (2010) NF-kappaB and cancer: how intimate is this relationship. *Molecular and cellular biochemistry* 336(1-2):25-37.

907. Baud V & Karin M (2009) Is NF-kappaB a good target for cancer therapy? Hopes and pitfalls. *Nat Rev Drug Discov* 8(1):33-40.

908. Martin-Montalvo A*, et al.* (2013) Metformin improves healthspan and lifespan in mice. *Nature communications* 4:2192.

909. Dey BK*, et al.* (2008) The histone demethylase KDM5b/JARID1b plays a role in cell fate decisions by blocking terminal differentiation. *Mol Cell Biol* 28(17):5312-5327.

910. Roesch A*, et al.* (2010) A temporarily distinct subpopulation of slow-cycling melanoma cells is required for continuous tumor growth. *Cell* 141(4):583-594.

911. Ewald JA, Desotelle JA, Wilding G, & Jarrard DF (2010) Therapy-induced senescence in cancer. *Journal of the National Cancer Institute* 102(20):1536-1546.

912. Nardella C, Clohessy JG, Alimonti A, & Pandolfi PP (2011) Pro-senescence therapy for cancer treatment. *Nat Rev Cancer* 11(7):503-511.

913. Acosta JC & Gil J (2012) Senescence: a new weapon for cancer therapy. *Trends in cell biology* 22(4):211-219.

914. Parrinello S, Coppe JP, Krtolica A, & Campisi J (2005) Stromal-epithelial interactions in aging and cancer: senescent fibroblasts alter epithelial cell differentiation. *J Cell Sci* 118(Pt 3):485-496.

915. Moiseeva O, Deschênes-Simard X, Pollak M, & Ferbeyre G (2013) Metformin, aging and cancer. *Aging* 5(5):330-331.

916. Anisimov VN*, et al.* (2005) Metformin decelerates aging and development of mammary tumors in HER-2/neu transgenic mice. *Bulletin of experimental biology and medicine* 139(6):721-723.

917. Anisimov VN*, et al.* (2008) Metformin slows down aging and extends life span of female SHR mice. *Cell Cycle* 7(17):2769-2773.

918. Quinn BJ, Kitagawa H, Memmott RM, Gills JJ, & Dennis PA (2013) Repositioning metformin for cancer prevention and treatment. *Trends in endocrinology and metabolism: TEM* 24(9):469-480.

L’argent donne, la religion croit, la philosophie pense et la science dit…

mais n’oublions jamais que d’abord et avant tout, l’humain aime et espère.